U.S. DEPARTMENT OF ENERGY

Characterization, Leaching, and Filtration Testing for Bismuth Phosphate Sludge (Group 1) and Bismuth Phosphate Saltcake (Group 2) Actual Waste Sample Composites

GJ Lumetta   MK Edwards   ED Jenson   RW Shimskey
EC Buck   SK Fiskum   AE Kozelisky   SI Sinkov
RC Daniel   RT Hallen   PJ MacFarlan   LA Snow
K Draper   LK Jagoda   RA Peterson

February 2009

Pacific Northwest
NATIONAL LABORATORY

Characterization, Leaching, and Filtration Testing for Bismuth Phosphate Sludge (Group 1) and Bismuth Phosphate Saltcake (Group 2) Actual Waste Sample Composites

GJ Lumetta	MK Edwards	ED Jenson	RW Shimskey
EC Buck	SK Fiskum	AE Kozelisky	SI Sinkov
RC Daniel	RT Hallen	PJ MacFarlan	LA Snow
K Draper	LK Jagoda	RA Peterson	

February 2009

Pacific Northwest National Laboratory
Richland, Washington 99352

COMPLETENESS OF TESTING

This report describes the results of work and testing specified by Test Specification 24590-PTF-TSP-RT-06-003, Rev. 1 and Test Plans TP-RPP-WTP-467, Rev. 1 7/31/07 and TP-RPP-WTP-456, Rev. 0 11/29/06. The work and any associated testing followed the quality assurance requirements outlined in the Test Specification/Plan. The descriptions provided in this test report are an accurate account of both the conduct of the work and the data collected. Test plan results are reported. Also reported are any unusual or anomalous occurrences that are different from expected results. The test results and this report have been reviewed and verified.

Approved:

Gordon H. Beeman, Manager
WTP R&T Support Project

2/19/09
Date

Contents

Figures

Figure No.	Caption	Page No.

Figure No.	Caption	Page No.

Tables

Abbreviation/Acronym List

AEA	alpha energy analysis
ASO	Analytical Support Organization
ASR	Analytical Service Request
ATL	Advanced Technologies and Laboratories, International Inc.
AV	Axial Velocity
BBI	Best Basis Inventory
BET	(Brunauer, Emmett, and Teller) surface area analysis technique
BNI	Bechtel National, Incorporated
BS	blank spike
CCD	charge coupled device
CCN	corporate correspondence number (BNI)
CUF	cell unit filter
CWP	PUREX cladding waste
CWR	REDOX cladding waste
DACS	data acquisition collection system
DI	deionized
DOE	U.S. Department of Energy
ED	electron diffraction
EDS	energy-dispersive spectroscopy
EELS	electron energy-loss spectroscopy
EFRT	external flowsheet review team
EQL	estimated quantitation limit
FTIR	Fourier transform infrared
GEA	gamma energy analysis
GIF	Gatan Imaging Filter
HAADF	High Angle Annular Dark-Field Detector
HDPE	high-density polypropylene
HLRF	High-Level Radiochemistry Facility
HLW	high-level waste
HP	hot persulfate
IC	ion chromatography
ICDD	International Centre for Diffraction Data
ICP-OES	inductively coupled plasma-optical emission spectroscopy
ICSD	Inorganic Crystal Structure Database
KOH	potassium hydroxide
KPA	kinetic phosphorescence analysis
LAW	low activity waste
LCS	laboratory control sample
LEPS	Low-Energy Photon Spectroscopy
MDL	minimum detection limit
MRQ	minimum reportable quantity
MS	matrix spike
M&TE	measuring and test equipment

NIST	National Institute of Standards and Technology
OES	optical emission spectroscopy
ORP	Office of River Protection
PB	preparation blank
PNNL	Pacific Northwest National Laboratory
PSD	particle-size distribution
PTF	Pretreatment Facility
PUREX	plutonium-uranium extraction
QA	quality assurance
QAM	Quality Assurance Manual
QAPjP	quality assurance project plan
QARD	Quality Assurance Requirements and Descriptions
QC	quality control
REDOX	reduction oxidation
RIR	relative intensity ratio
RPD	relative percent difference
RPL	Radiochemical Processing Laboratory
RPP	River Protection Project
RSD	relative standard deviation
R&T	research and technology
TBP	tributyl phosphate
TGA	thermogravimetric analysis
TIC	total inorganic carbon
TMP	transmembrane pressure
TOC	total organic carbon
TRU	transuranics
SBMS	Standards Based Management System
SEM	scanning electron microscopy
STEM	scanning transmission electron microscopy
TEM	transmission electron microscopy
TP	test plan
TWINS	Tank-Waste Information Network System
UDS	undissolved solids
UFP	ultrafiltration process
WCS	wet centrifuged solids
WTP	Hanford Tank Waste Treatment and Immobilization Plant
XRD	X-ray diffraction

References

Barnes HA, and NQ Dzuy. 2001. "Rotating Vane Rheometry - A Review." *Journal of Non-Newtonian Fluid Mechanics* 98(1):1-14.

Cleveland JM. 1970. *The Chemistry of Plutonium*. Gordon and Breach Science Publishers, New York.

CRC. 1978. *CRC Handbook of Chemistry and Physics, 59th Edition*, CRC Press, West Palm Beach, Florida.

de Barry Barnett E, and CL Wilson. 1953. *Inorganic Chemistry: A Text-Book for Advanced Students*, Longmans Green and Co, London.

Fiskum SK, EC Buck, RC Daniel, K Draper, MK Edwards, TL Hubler, LK Jagoda, ED Jenson, GJ Lumetta, BK McNamara, RA Peterson, SI Sinkov, and LA Snow. 2008. *Characterization and Leach Testing for REDOX Sludge and S-Saltcake Actual Waste Sample Composites*. PNNL-17368 (WTP-RPT-157), Pacific Northwest National Laboratory, Richland, Washington.

Li H, J Addai-Mensah, JC Thomas, and AR Gerson. 2005. "The Influence of Al(III) Supersaturation and NaOH Concentration on the Rate of Crystallization of $Al(OH)_3$ Precursor Particles From Sodium Aluminate Solutions*." J. Colloid and Interface Science* 286:511-519.

Li J, CA Prestidge, and J Addai-Mensah. 2000. "Viscosity, Density, and Refractive Index of Aqueous Sodium and Potassium Aluminate Solutions." *J. Chem. Eng. Data* 45:665-671.

Liu Q, H Xu, and A Navrostsky. 2005. "Nitrate cancrinite: Synthesis, characterization, and determination of enthalpy of formation." *Microporous and Mesoporous Materials* 87:146-152.

Lumetta GJ. 2008. *Mechanism of Phosphorus Removal from Hanford Tank Sludge by Caustic Leaching*. PNNL-17257, Pacific Northwest National Laboratory, Richland, Washington.

Lumetta GJ, LP Darnell, PA Garza, LR Greenwood, BM Oliver, DE Rinehart, DR Sanders, CZ Soderquist, T Trang-Le, MW Urie, JJ Wagner. 2002. *Caustic Leaching of Hanford Tank T-110 Sludge*. PNNL-13956, Pacific Northwest National Laboratory, Richland, Washington.

Lumetta GJ, KJ Carson, LP Darnell, LR Greenwood, FV Hoopes, RL Sell, SI Sinkov, CZ Soderquist, MW Urie, JJ Wagner. 2001. *Caustic Leaching of Hanford Tank S-110 Sludge*, PNNL-13702, Pacific Northwest National Laboratory, Richland, Washington.

Lumetta GJ and BM Rapko. 1999. "Removal of Chromium from Hanford Tank Sludges." *Sep. Sci. Technol.* 34:1495-1506.

Lumetta GJ, BM Rapko, J Liu, DJ Temer, and RD Hunt. 1998. *Washing and Caustic Leaching of Hanford Tank Sludges: Results of FY 1998 Studies*. PNNL-12026, Pacific Northwest National Laboratory, Richland, Washington.

Malvern Instruments Ltd. 1997. *Sample Dispersion and Refractive Index Guide*. MAN 0079, Version 3.1, Worcestershire, England.

Rapko BM, GJ Lumetta, JD Vienna, and SK Fiskum. 2005. *Oxidative Alkaline Leaching of SX-101 and SY-102 and Its Impact on Immobilized High Level Waste.* PNWD-3600 (WTP-RPT-137), Battelle—Pacific Northwest Division, Richland, Washington. (WTP Doc. No. 24590-101-TSA-W000-0004-168-00002 Rev 00A.)

Rapko BM, JGH Geeting, SI Sinkov, and JD Vienna. 2004. *Oxidative-Alkaline Leaching of Washed 241-SY-102 and 241-SX-101 Tank Sludges.* PNWD-3512 (WTP-RPT-117), Battelle—Pacific Northwest Division, Richland, Washington. (WTP Doc. No. 24590-101-TSA-W000-0004-99-00012 Rev 00A.)

Rapko BM, and JD Vienna. 2002. *Selective Leaching of Chromium from Hanford Tank Sludge 241-U-108.* PNNL-14019, Pacific Northwest National Laboratory, Richland, Washington.

Rapko BM, JD Vienna, SI Sinkov, J Kim, and AJ Cisar. 2002. *Alkaline Leaching of Key, Non-Radioactive Components from Simulants and Hanford Tank Sludge 241-S-110: Results of FY 01 Studies.* PNNL-14018, Pacific Northwest National Laboratory, Richland, Washington.

Rapko BM. 1998. *Oxidative Alkaline Dissolution of Chromium from Hanford Tank Sludges: Results of FY 98 Studies.* PNNL-11908, Pacific Northwest National Laboratory, Richland, Washington.

Rector DR, and BC Bunker. 1995. *Effect of Colloidal Aggregation on the Sedimentation and Rheological Properties of Tank Waste.* PNL-10761, Pacific Northwest Laboratory, Richland, Washington.

Templeton DH, HW Ruben, and A Zalkin. 1990. "Entropy and Crystal Structure of Hydrates of Disodium Hydrogen Phosphate." *J. Phys. Chem.* 94:7830-7834.

Wefers K, and C Misra. 1987. *Oxides and Hydroxides of Aluminum.* Alcoa Technical Paper No. 19 Revised, Alcoa Laboratories, Alcoa Center, Pittsburg, Pennsylvania.

Wellman DM, JG Catlano, JP Icenhower, and AP Gamerdinger. 2005. "Synthesis and Characterization of Sodium meta-Autunite, $Na[UO_2PO_4]\cdot3H_2O$." *Radiochim. Acta*, 93:393-399.

Zhukhlistov AP, and BB Zvyagin. 1977. "Determination of Crystal-Structures of Chapmanite and Bismuthoferrite by High-Voltage Neutron-Diffraction Method." *Soviet Physics Crystallography* 22:419-423.

Testing Summary

A testing program evaluating actual tank waste was developed in response to Task 4 from the M-12 External Flowsheet Review Team (EFRT) issue response plan.[a] The test program was subdivided into logical increments. The bulk water-insoluble solid wastes that are anticipated to be delivered to the Hanford Tank Waste Treatment and Immobilization Plant (WTP) were identified according to type such that the actual waste testing could be targeted to the relevant categories. Eight broad waste groupings were defined. Samples available from the 222S archive were identified and obtained for testing. The actual waste-testing program included homogenizing the samples by group, characterizing the solids and aqueous phases, and performing parametric leaching tests.

Two of the eight defined groups—bismuth phosphate sludge (Group 1) and bismuth phosphate saltcake (Group 2)—are the subjects of this report. The Group 1 waste was anticipated to be high in phosphorus and was implicitly assumed to be present as $BiPO_4$ (however, results presented here indicate that the phosphate in Group 1 is actually present as amorphous iron(III) phosphate). The Group 2 waste was also anticipated to be high in phosphorus, but because of the relatively low bismuth content and higher aluminum content, it was anticipated that the Group 2 waste would contain a mixture of gibbsite, sodium phosphate, and aluminum phosphate. Thus, the focus of the Group 1 testing was on determining the behavior of P removal during caustic leaching, and the focus of the Group 2 testing was on the removal of both P and Al. This report discusses the waste-type definition, archived sample conditions, homogenization activities, characterization (physical, chemical, radioisotope, and crystal habit), and caustic leaching behavior as functions of time, temperature, and hydroxide concentration. Testing was conducted according to TP-RPP-WTP-467.[b]

Objectives

The test objectives are summarized in Table S.1 along with a discussion of how the objectives were met. Several objectives (in gray shading lighter than header shading) did not specifically apply to the scope provided in this report; they will be reported in companion reports as indicated in the controlling test plan.

(a) SM Barnes, and R Voke. 2006. "Issue Response Plan for Implementation of External Flowsheet Review Team (EFRT) Recommendations - M12: Undemonstrated Leaching Process." 24590-WTP-PL-ENG-06-0024 Rev. 0.

(b) SK Fiskum. 2007. *Characterization and Small Scale Testing of Hanford Wastes to Support the Development and Demonstration of Leaching and Ultrafiltration Pretreatment Processes*. TP-RPP-WTP-467, Rev. 0, 2/2/07 and Rev. 1, 7/31/07.

Table S.1. Test Objectives

Test Objective	Objective Met? (Y/N)	Discussion
1) Determine the physical and chemical characteristics (summarized in Section 6.2.2 of the test plan) relevant to leaching and ultrafiltration behaviors of actual waste samples required for the validation of simulants.	Y	The following characterizations were conducted on the washed solids for Group 1 and Group 2: • solids chemical composition • mineral composition • particle-size distribution • crystal habit and morphology • slurry density • slurry rheology, flow curve, and shear strength • settling rate, fraction of settled solids, fraction of centrifuged solids. The results are summarized in Sections 3 and 4.
2) Determine the dissolution rate of aluminum in the actual waste samples, present predominantly as gibbsite, as a function of temperature, free hydroxide concentration, and over a range of sodium concentrations of interest to the caustic leaching process.	Y	A significant portion of the Al in the Group 2 waste was present in the form of gibbsite. The behavior of this component during caustic leaching could be reasonably discerned because most of the remaining Al was present as aluminosilicate materials (which are not leachable). These results are discussed in Section 4.4.
3) Determine the dissolution rate of aluminum in the actual waste samples, present predominantly as boehmite, as a function of temperature, free hydroxide concentration, and over a range of sodium concentrations of interest to the caustic leaching process.	NA	Neither Group 1 nor Group 2 was expected to contain significant quantities of boehmite and indeed this was found to be the case. Aluminum was only a minor component of the Group 1 solids constituting only ~3 wt% of the washed Group 1 solids (Table 3.6). XRD and microscopy analyses revealed no boehmite in the Group 1 solids (Section 3.2.6). The washed Group 2 solids contained ~12 wt% Al (Table 4.6), but XRD and microscopy analyses indicated the Al to be primarily in the forms of gibbsite and aluminosilicate (Section 4.2.6).
4) Determine the dissolution rate of chromium and the extent of dissolution of plutonium and other safety-related constituents (U, Fe, Mn, Ni, and Zn) in the actual waste samples as functions of temperature and over a range of NaOH concentrations of interest for oxidative leaching. (The NaMnO$_4$ dosage will be predetermined for the oxidation of the chromium in the waste solids.)	NA	Oxidative leaching was not an objective of the Group 1 and Group 2 testing because neither of these was anticipated to be a high-Cr waste. Parametric oxidative leaching tests were performed on the Group 1/2 composite solids that had been caustic-leached in the CUF apparatus. The parameters examined included NaOH concentration (0.25 and 1.25 M), and the Mn/Cr molar ratio (0.75, 1.0, 1.25, and 1.5). Temperature was not a parameter examined in these experiments; all oxidative leaching measurements were made at 45°C. These results are discussed in Section 6.
5) Determine the dissolution/reaction rate of phosphates in the actual waste samples as a function of temperature	Y	Both Group 1 and Group 2 contained significant amounts of P. The P behavior for the Group 1 and Group 2 composites during caustic leaching was

Table S.1 (Contd)

Test Objective	Objective Met? (Y/N)	Discussion
and over a range of NaOH concentrations of interest for the caustic leaching process as well as the extent of dissolution during post-leaching wash.		characterized as a function of time, temperature, and free hydroxide concentration. However, for Group 2, the P behavior was only tracked opportunistically (without full quality assurance [QA] review of the analytical data). The P results can be found in Sections 3 (Group 1), 4 (Group 2), and 6 (Group 1/2).
6) Determine ultrafiltration flux before and after caustic and oxidative leaching over the operating range of solids concentrations during the leaching processes at 25°C when sufficient actual waste sample is available for testing of the filtration behavior.	Y	Ultrafiltration (CUF) testing was performed on a blended composite of the Group 1 and Group 2 solids. The CUF testing was performed before leaching using slurries with both low- and high-solids contents. Further CUF testing was performed after caustic leaching, and after oxidative leaching. During these tests, the ultrafiltration flux was determined as a function of transmembrane pressure and axial velocity. The CUF tests were conducted at ambient temperature. All the CUF testing results are discussed in Section 5.
7) Scanning electron microscopy (SEM), transmission electron microscopy (TEM), energy dispersive spectroscopy (EDS), and X-ray diffraction (XRD) will be used to determine the primary mineral forms present for Al, Cr, and P and provide information to enable the correlation of these mineral forms to dissolution behavior.	Y	SEM, TEM, EDS, and XRD were performed on the washed Group 1 and Group 2 solids both before and after caustic leaching. In addition, preliminary application of vibrational spectroscopy [Fourier-transform infrared (FTIR) and Raman spectroscopies] to the characterization of tank sludge solids was performed for these two waste samples. The solids characterization results are distributed throughout the report, at the specific relevant sections.

Test Exceptions

No test exceptions applied to this work.

Results and Performance Against Success Criteria

The test plan delineated several success criteria, which are listed in Table S.2. Selected criteria were relevant to the test scope included in this report; the other criteria that are outside of the reported scope are shaded.

Table S.2. Results and Performance Against Success Criteria

List Success Criteria	Explain How the Tests Did or Did Not Meet the Success Criteria
1) A summary (letter report format) of the available information (including published literature) is provided on the characteristics (both known characteristics and those needed to be determined) relevant to leaching and filtration behaviors of the tank farm waste groupings identified for testing.	Letter report number RPP-WTP-07-705 (GJ Lumetta and RT Hallen, WTP-RPT-151, *Review of Caustic Leaching Testing With Hanford Tank Waste Sludges*) which addressed this success criterion, was delivered to BNI-WTP on 1/24/2007.
2) The physical and chemical characteristics for each of the actual waste-sample composites selected for testing are provided (including a format in conformance with the presentation protocols [24590-WTP-GPG-RTD-001]). The relevant physical and chemical characteristics are elaborated in Test Conditions, Section 6.0, of the test plan.	All physical and chemical characterization testing as defined in the test plan was completed. This included extensive physical and chemical characterization of the homogenized slurry materials and extensive chemical characterization of selected leach solids. The analytical results for each test group are reported in the appropriate report sections.
3) The dissolution rate and the extent of dissolution of aluminum present predominantly as gibbsite in actual waste solids are determined as a function of temperature, free-hydroxide, and sodium concentrations. The associated uncertainties in test results are provided.	Dissolution of the gibbsite fraction of the Group 2 washed solids was evaluated by measuring the Al in the leaching solution as a function of time (1, 2, 4, 8, and 24 h). The effects of free hydroxide concentration and temperature were assessed. Testing was conducted at three free hydroxide concentrations (1, 3, and 5 M) and at three temperatures (60, 80, and 100°C). One test condition (3 M free hydroxide at 80°C) was conducted in triplicate to assess overall test precision. The dissolution of the (presumed) gibbsite fraction of the Group 2 solids was rapid, with steady state reached in 4 to 8 h under all conditions examined. The steady-state Al concentrations in these experiments represented 60 to 70% Al dissolution, suggesting that 30 to 40% of the Al in the Group 2 solids was present as an aluminosilicate (nitrate cancrinite, as identified by XRD and FTIR). Detailed results are presented in Section 4.0. The Group 1 solids did not have any significant fraction of gibbsite present, so this success criterion is not applicable to the Group 1 test.
4) The dissolution rate and the extent of dissolution of aluminum present predominantly as boehmite in actual waste solids are determined as a function of temperature, free-hydroxide, and sodium concentrations. The associated uncertainties in test results are provided.	Not applicable. Neither Group 1 nor Group 2 samples had significant amounts of boehmite.
5) The dissolution rate and the extent of dissolution of chromium in the actual waste solids are determined as a function of temperature and over a range of	For the Group 1/2 caustic-leached solids, Cr reaction with the MnO_4^- was rapid, with near-steady state Cr concentration reached within 1 h of leaching. The

Table S.2 (Contd)

List Success Criteria	Explain How the Tests Did or Did Not Meet the Success Criteria
NaOH concentrations of interest to oxidative leaching. The NaMnO$_4$ dosage will be predetermined for the oxidation of the chromium in the waste solids. The associated uncertainties in the test results are provided.	amount of Cr removed from the Group 1/2 solids was dependent upon the Mn/Cr ratio, with most impact observed in going from Mn/Cr = 0.75 to Mn/Cr = 1.0. About 65% of the Cr from the caustic-leached Group 1/2 solids was removed by treatment with 1 molar equivalent of Mn(VII) in 0.25 M NaOH at 45°C. No improvement in Cr removal was observed when the NaOH concentration was raised from 0.25 to 1.25 M.
	Under all conditions examined, the U concentrations in the oxidative leaching solutions remained low, with the U concentration typically ~3 µg/mL after leaching for 24 h. The exception was during leaching in 1.25 M NaOH at a Mn/Cr ratio of 1.25; in that case the U concentration in solution reached a level of ~8 µg/mL. The Fe, Ni, Cd, and B concentrations in the oxidative leaching solutions were also very low, generally below the detection limit or < 1 µg/mL. Manganese was observed to be in the leachate solutions at Mn/Cr = 1.25 or higher, but the amount in solution decreased with time and was below the detection limit at 24 h.
	The Pu concentration was measured for each leaching condition and at each sampling time. The Pu dissolution was strongly dependent on the free-hydroxide concentration. Increasing the NaOH concentration from 0.25 M to 1.25 M resulted in a large (~6×) increase in the Pu concentration. As a consequence, low free-hydroxide concentrations will need to be maintained to minimize Pu mobilization during oxidative leaching of Cr.
6) The dissolution rate and the extent of dissolution of phosphates in the actual waste solids are determined as a function of temperature and NaOH concentration along with the uncertainty in these estimates.	Phosphorus removal from the Group 1 washed solids was evaluated by measuring the P in the leaching solution as a function of time (1, 2, 4, 8, and 24 h). The effects of free hydroxide concentration and temperature were assessed. Testing was conducted at two free-hydroxide concentrations (1 and 3 M) and at three temperatures (40, 60, and 80°C). One test condition (3 M free hydroxide at 40°C) was conducted in triplicate to assess overall test precision.
	The P removal from the Group 1 solids was rapid, with steady state reached within 4 h under all conditions examined. Near quantitative P removal was achieved for nearly all conditions examined. Detailed results are presented in Section 3.0.
	Phosphorus removal from the Group 2 solids was opportunistically evaluated as a function of time (1, 2, 4,

Table S.2 (Contd)

List Success Criteria	Explain How the Tests Did or Did Not Meet the Success Criteria
	8, and 24 h), temperature (60, 80, and 100°C), and free hydroxide concentration (1, 3, and 5 M). Phosphorus removal from the Group 2 solids was much lower than that observed for Group 1. Only about 25% of the P was removed from the Group 2 solids under the most ideal conditions. This can be attributed to P in the form of hydroxyapatite.
7) The ultrafiltration flux before and after caustic and, as applicable, oxidative leaching (re-concentration, if sufficient solids are available) over the operating range of solids concentrations with the actual waste samples at 25°C is defined when available sample size is adequate for the testing.	During CUF testing using the Group 1/2 slurry with an undissolved solids (UDS) concentration of 8 wt%, the filter flux decayed rapidly at each test condition examined. Although the flux could be mostly restored by back-pulsing, some irreversible fouling of the membrane occurred during the course of the low-solids slurry tests. The filter flux was dependent upon the transmembrane pressure (TMP), but had no apparent dependency upon the axial velocity (AV). Similar observations were made with the high-solids (16 wt% UDS) concentration, except that the initial filter flux was considerably less that that observed for the low-solids slurry. Furthermore, there appeared to be a small irreversible fouling of the filter with the high-solids Group 1/2 slurry. At initiation of the dewatering step following caustic leaching, it was discovered that the pump head was clogged with a gel. This gel is hypothesized to be caused by precipitation of $Na_3PO_4 \cdot 12H_2O$ from the caustic-leaching solution. The gel could be cleared by flushing with water. The filter flux during dewatering of the caustic leachate was low (~0.01 GPM/ft^2) and declined approximately 2% during the course of the 5-h filtration test. The filter flux increased with successive washing of the caustic-leached slurry. During the first two washings of the oxidative-leached slurry, the temperature was above ambient because the chiller was inadvertently not turned on. Corrections to the filter flux were made to account for elevated temperature during these experiments. With this correction made, the flux was essentially constant at ~0.04 GPM/ft^2 during the three washes of the oxidatively-leached solids. The filter flux was dependent upon the TMP during the final dewatering of the Group 1/2 slurry, but also showed an apparent dependence on the AV. So simple classification of the final slurry into a membrane-resistance or cake-resistance model is not obvious.

Table S.2 (Contd)

List Success Criteria	Explain How the Tests Did or Did Not Meet the Success Criteria
	Comparison of the initial clean water flux measurements suggests an irreversible fouling of the membrane following the leaching and filtration tests. Iron present in the waste was suspected because it was believed not to be impacted by the leaching operations or by the 2 M nitric acid cleaning. Cleaning the filter with 0.5 M oxalic acid before the next test significantly improved the flux. This supports the theory of iron present in the slurry solid fouling the filter because oxalic acid is very effective in dissolving iron into solution.
8) Determination of the primary mineral forms present for Al, Cr, and P, and a qualitative correlation of the dissolution behavior of these waste elements to the mineral forms identified.	Determination of specific phases present in the Group 1 composite sample was vitiated by the fact that the material was largely an amorphous solid. However, through a combination of SEM, FTIR spectroscopy, and chemical observations, it could be concluded that the P in the Group 1 sample is present mainly as amorphous $FePO_4 \bullet xH_2O$. The P behavior for caustic leaching of the Group 1 solids can be explained by rapid metathesis of this amorphous phase to ferric hydroxide and sodium phosphate. This explains the rapid color change of the solids from beige to rusty red (characteristic of ferric hydroxide) upon addition of NaOH solution. Note: When a commercially procured sample of $FePO_4 \bullet xH_2O$ (pale pink) was mixed with 3 M NaOH, an immediate rust-colored solid formed; the liquid phase gelled after standing for ~15 min (indicative of precipitation of $Na_3PO_4 \bullet 12H_2O$). Also it should be noted that $FePO_4 \bullet \times H_2O$ prepared by mixing aqueous ferric nitrate solution with aqueous Na_3PO_4 solution was beige-colored, with an appearance quite similar to the actual Group 1 solids. As mainly determined by XRD and FTIR, the Group 2 solids contained gibbsite, nitrate cancrinite $Na_{7.92}(AlSiO_4)_6(NO_3)_{1.7}(H_2O)_{2.34}$, and urancalcarite $Ca(UO_2)_3CO_3(OH)(H_2O)_3$. The Al removal behavior during caustic leaching can be correlated with this observation, assuming 60 to 70% of the Al as gibbsite and the remaining as primarily nitrate cancrinite. The forms of P in the water-insoluble Group 2 solids could not be definitively determined. However, the P in the caustic-leached Group 2 solids appeared to be in the form of hydroxyapatite, based on FTIR analysis and the measure Ca/P mole ratio.

Quality Requirements

Pacific Northwest National Laboratory (PNNL) is operated for the U.S. Department of Energy (DOE) by Battelle under Contract DE-AC05-76RL01830. PNNL implements a Quality Assurance Program that is based upon the requirements as defined in DOE Order 414.1C, "Quality Assurance," and 10 CFR 830, "Energy/Nuclear Safety Management," Subpart A—"Quality Assurance Requirements." PNNL has chosen to implement the requirements of DOE Order 414.1C and 10 CFR 830, Subpart A by integrating them into the laboratory's management systems and daily operating processes. The procedures necessary to implement the requirements are documented through the laboratory's Standards-Based Management System (SBMS).

PNNL implemented the RPP-WTP quality requirements by performing work in accordance with the *River Protection Project – Waste Treatment Plant Support Program (RPP-WTP) Quality Assurance Plan (*RPP-WTP-QA-001, QAP*).* Work was performed to the quality requirements of NQA-1-1989 Part I, "Basic and Supplementary Requirements," NQA-2a-1990, Part 2.7, and DOE/RW-0333P, Rev 13, *Quality Assurance Requirements and Descriptions (QARD).* These quality requirements were implemented through the *River Protection Project – Waste Treatment Plant Support Program (RPP-WTP) Quality Assurance Manual* (RPP-WTP-QA-003, QAM). The analytical requirements were implemented through RPP-WTP's Statement of Work (RPP-WTP-QA-005) with the Radiochemical Processing Laboratory (RPL) Analytical Service Operations (ASO).

A matrix that cross-references the NQA-1, NQA-2a, and QARD requirements with the procedures for RPP-WTP work was provided in the test plan TP-RPP-WTP-467. It included justification for those requirements not implemented.

Experiments that were not method-specific were performed in accordance with RPP-WTP's procedures QA-RPP-WTP-1101 "Scientific Investigations" and QA-RPP-WTP-1201 "Calibration and Control of Measuring and Testing Equipment" so that sufficient data were taken with properly calibrated measuring and test equipment (M&TE) to obtain quality results.

RPP-WTP addressed internal verification and validation activities by conducting an Independent Technical Review of the final data report in accordance with RPP-WTP's procedure QA-RPP-WTP-604. This review verified that the reported results were traceable, that inferences and conclusions were soundly based, and the reported work satisfied the Test Plan objectives. This review procedure is part of PNNL's *RPP-WTP Quality Assurance Manual*.

R&T Test Conditions

The R&T test conditions, as defined in the Test Specification,[a] are summarized in Table S.3.

Table S.3. R&T Test Conditions

List R&T Test Conditions	Were Test Conditions Followed?
1) Selection of actual wastes for testing: the waste samples selected for testing will be from the groupings identified in the resolution of Issue M4.	Yes. Two of the eight waste groupings identified in resolution to Issue M4 were tested: Group 1 (bismuth phosphate sludge) and Group 2 (bismuth phosphate saltcake).
2) Physical and chemical characterization properties shall be stated and carried out according to the Guideline document 24590-WTP-GPG-RTD-001.	Yes. Physical characterizations, including specific gravity (density), settling rate, rheology, volume-percent settled solids, and volume-percent centrifuged solids, were determined for both test groups according to the requirements document. Chemical characterization was conducted on the supernatant (water used to dissolve and slurry the solids into a workable homogenized composite) on the solids rinsed with three contacts of 1:1 volume ratios of 0.01 M NaOH and on the rinse solution composite.
3) Actual determinations of waste leach kinetics will be carried out in well-mixed conditions. A test matrix will be forwarded to the research and technology (R&T) M12 Issue manager for concurrence before testing. Residual leached and washed solids will be characterized.	Yes. Test matrices for both the Group 1 and Group 2 waste samples were forwarded to, and approved by, the R&T M12 Issue Manager. Actual test conditions are given in Sections 3.0 and 4.0 and were compliant with the test matrices.
4) Testing for filtration behavior will be performed.	Yes. Cross-flow filtration testing was performed on a mixture of solids from Groups 1 and 2. CUF testing matrices were applied to a low-solids slurry, a high-solids slurry, post-caustic leaching, and post-oxidative leaching. Rheology and particle size distribution measurements were made before and after the various process steps.

(a) PS Sundar. Nov. 2006. *Characterization and Small Scale Testing of Hanford Wastes to Support the Development and Demonstration of Leaching and Ultrafiltration Pretreatment Processes.* 24590-PTF-TSP-RT-06-003, Rev. 1.

Simulant Use

The testing used actual Hanford tank wastes; simulant usage does not apply.

Discrepancies and Follow-on Tests

None.

1.0   Introduction

This report is one in a series that defines the characterization, parametric leaching, and filtration testing of actual Hanford tank wastes in support of the Hanford Tank Waste Treatment and Immobilization Plant (WTP) pretreatment process development and demonstration. The tests reported here were conducted according to test plan TP-RPP-WTP-467,[a] which was written in response to Test Specification 24590-PTF-TSP-RT-06-003 Rev. 1.[b]

1.1 Tank Waste Pretreatment Operations at the WTP

Figure 1.1 provides a schematic illustration of the primary functions to be performed in the WTP. Initially, the low-activity waste (LAW) liquid stream will be removed from the high-level waste (HLW) solids phase by ultrafiltration in the Pretreatment Facility (PTF). The concentrated HLW solids will be pretreated with caustic and, in some cases, oxidative leaching processes to dissolve and remove components (specifically, aluminum, chromium, phosphates, and sulfates) that would otherwise limit HLW loading in the immobilized waste glass. The current plant design calls for the pretreatment leaching processes to be carried out in the ultrafiltration feed vessels. The function of caustic leaching is to solubilize the aluminum, phosphorus, and sulfur in the HLW solids, thereby removing these components from the HLW vitrification feed. The function of oxidative leaching is to oxidize the chromium [from Cr(III) to Cr(VI)] with a sodium permanganate ($NaMnO_4$) solution, so that the Cr can be routed to the LAW stream. The HLW solids will be re-concentrated after each leaching and washing operation in the ultrafilter.

The current design of the PTF was based on aluminum dissolution results from earlier small, bench-scale, caustic leaching tests that were provided to Bechtel National, Incorporated (BNI) by the U.S. Department of Energy's (DOE's) Office of River Protection (ORP). Only a limited number of small bench-scale oxidative leaching tests using two selected actual waste tank samples (SX-101 and SY-102) with the preferred oxidant $NaMnO_4$ were carried out to estimate the oxidant dosage and the efficacy of the oxidative leaching process (Rapko et al. 2004; Rapko et al. 2005), but a number of previous studies demonstrated the technical feasibility of the oxidative leaching process (Rapko 1998; Lumetta and Rapko 1999; Rapko and Vienna 2002; Rapko et al. 2002). The testing with actual radioactive wastes has been generally limited to small-scale testing (typically 1 to 10 g) because of limited sample availability and personnel safety associated with sample handling.

(a) SK Fiskum, TP-RPP-WTP-467, Rev. 0, 2/2/07 and Rev. 1 7/31/07, *Characterization and Small Scale Testing of Hanford Wastes to Support the Development and Demonstration of Leaching and Ultrafiltration Pretreatment Processes*.

(b) PS Sundar. 2006. 24590-PTF-TSP-RT-06-003 Rev. 1, *Characterization and Small Scale Testing of Hanford Wastes to Support the Development and Demonstration of Leaching and Ultrafiltration Pretreatment Processes*.
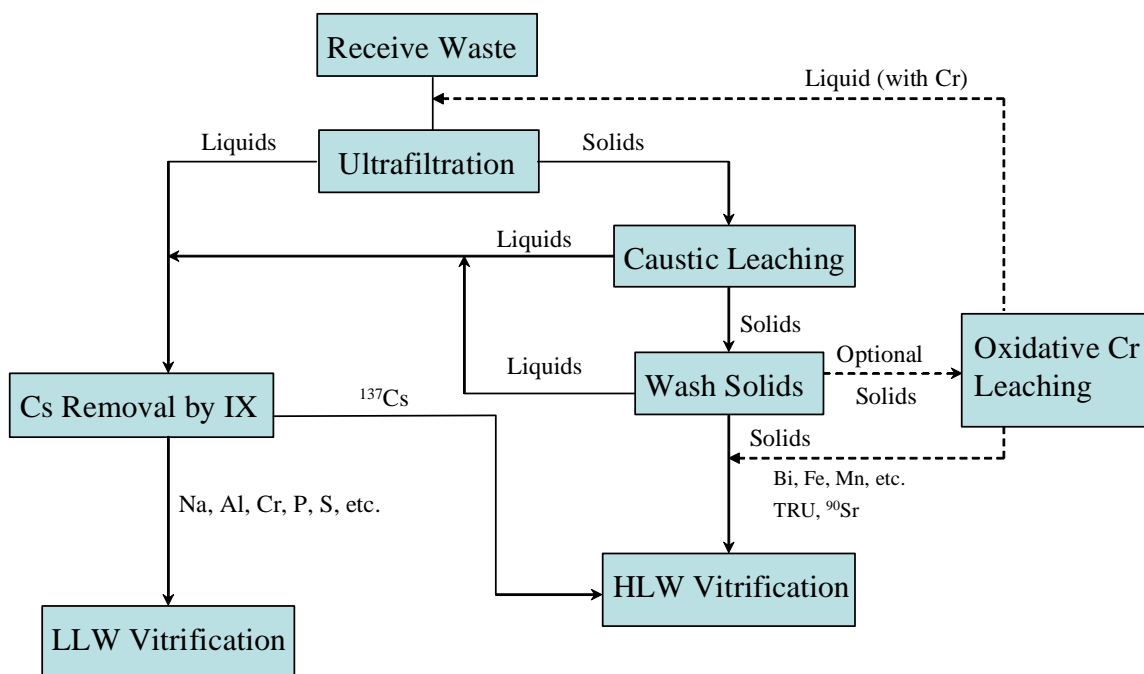
Figure 1.1. Schematic Representation of the Key Processes to be Performed in the WTP (Note: This is for illustrative purposes only, it is not meant to be a comprehensive view of the functions performed within the WTP)

1.2 Issues Identified by the External Flowsheet Review Team

A team of foremost experts from industry, national laboratories, and universities (referred to as the External Flowsheet Review Team or EFRT) was assembled by BNI in October of 2005 to conduct an in-depth review of the process flowsheet supporting the design of the WTP. The EFRT identified several issues from the critical review of the process flowsheet,[a,b] including

- Issue M4: The WTP has not demonstrated that its design is sufficiently flexible to reliably process all of the Hanford tank farm wastes at the design throughputs.

- Issue M12: Neither the caustic leaching nor the oxidative leaching process has been demonstrated at greater than bench scale. The small-scale experiments are capable of defining the leaching chemistry. However, they are limited in their capability to predict the effectiveness of these processes without a scale-up demonstration.

- Issue M13: For wastes requiring leaching, a combination of inadequate filter flux and area will likely limit throughput to the HLW or LAW vitrification facilities.

(a) WTP Doc. No. 24590-WTP-PL-ENG-06-0008, Rev 0, "Hanford Waste Treatment and Immobilization Plant (WTP) Project Response Plan for Resolution of Issues Identified by the Comprehensive Review of the WTP Flowsheet and Throughput." L Lucas, March 2006.

(b) WTP Project Doc. No. CCN 132846 "Comprehensive Review of the Hanford Waste Treatment Plant Flowsheet and Throughput - Assessment Conducted by an Independent Team of External Experts." March 2006, chartered by the Hanford Waste Treatment and Immobilization Plant Project at the Direction of the U.S. Department of Energy, Office of Environmental Management, Washington DC.

The work scope defined in the TP-RPP-WTP-467 represented the initial actual waste-testing part of Task 4 from the M-12 EFRT issue response plan.[a] The actual tank waste testing was based on responses developed to resolve EFRT Issue M4. In this case, a family of waste groupings representing the behavior of ~75% of the tank-farm inventory was developed to assist in designing subsequent tests that will assess the adequacy of the overall flowsheet design in treating the tank-farm wastes. These waste groupings were the basis for selecting actual wastes for the current scope of testing.

The results from the actual waste testing reported herein also support the resolution of following related EFRT issues:

- Issue M1: Piping that transports slurries will plug unless it is properly designed to minimize this risk. This design approach has not been followed consistently, which will lead to frequent shutdowns due to line plugging.

- Issue M2: Large, dense particles will accelerate erosive wear in mixing vessels. The effects of such particles on vessel life must be re-evaluated.

- Issue M3: Issues were identified related to mixing-system designs that will result in insufficient mixing and/or extended mixing times. These issues include a design basis that discounts the effects of large particles and of rapidly settling Newtonian slurries. There is also insufficient testing of the selected designs.

- Issue M6: Many of the process operating limits have not been defined. Further testing is required to define process limits for WTP unit operations. Without this more complete understanding of each process, it will be difficult or impossible to define a practical operating range for each unit operation.

1.3 Waste Groupings

The available information regarding tank history and tank waste characterization was analyzed. This analysis revealed eight groupings of waste tanks that represent ~75% of the inventory of those components that are most significant with respect to leaching in the WTP; i.e., Al, Cr, phosphate, and sulfate (Fiskum et al. 2008). Table 1.1 summarizes the eight waste groups along with the estimated water-insoluble fractions (with respect to the entire tank farm inventory) of selected components contained in each one. To support the actual waste testing, samples were obtained from the archives at the Hanford 222S Laboratory. Composites of these archived samples were made to obtain the most representative samples of each group as practical. The details of the sample selection for Groups 1 and 2 are provided in Section 2.0.

(a) SM Barnes, and R Voke, September 2006, 24590-WTP-PL-ENG-06-0024 Rev. 0, "Issue Response Plan for Implementation of External Flowsheet Review Team (EFRT) Recommendations - M12: Undemonstrated Leaching Process."

Table 1.1. Projected Distribution of Water-Insoluble Components in the Tank Waste Groupings (Fiskum et al. 2008)

Group ID	Type	Al (%)	Cr (%)	F (%)	Fe (%)	Oxalate (%)	Phosphate (%)	Sulfate (%)
1	Bi Phosphate sludge	4	4	22	22	0.5	36	7
2	Bi Phosphate saltcake (BY, T)	13	18	24	8	37	23	42
3	CWP, PUREX Cladding Waste sludge	17	1	1.3	5	1	2	0.4
4	CWR, REDOX Cladding Waste sludge	10	1	<0.1	1	0.4	0.1	<0.1
5	REDOX sludge	29	6	0.1	4	3	1	0.4
6	S - Saltcake (S)	8	46	0.6	4	27	4	14
7	TBP Waste sludge	1	0.4	0.5	7	0.1	17	3
8	FeCN Waste sludge	1	1	0.4	7	1	6	1
	Balance	17	24	51	41	30	10	32
Note: The component values were rounded off; therefore, the sums may not add to exactly 100%. CWP = PUREX cladding waste CWR = REDOX cladding waste FeCN = ferrocyanide PUREX = plutonium uranium extraction REDOX = reduction oxidation TBP = tributyl phosphate								

1.4 Simulant Development

BNI plans to carry out process development and scale-up testing to demonstrate the design effectiveness of both the caustic- and the oxidative-leaching processes over the entire applicable range of Hanford tank farm wastes.[a] Scale-up testing will require substantial volumes of feed. Therefore, the development of simulants that mimic the chemical, leaching, and ultrafiltration behaviors over the range observed for actual waste groups is necessary to the process development and demonstration. The characterization and leaching performance data obtained from the actual waste testing will serve as benchmarks for defining the simulant characteristics and behaviors for revising the parameters used in process models for evaluating WTP process performance using the appropriate process models.

1.5 Testing of Groups 1 and 2

The characterization and parametric leaching of two of the eight defined groups, bismuth phosphate sludge (Group 1) and bismuth phosphate saltcake (Group 2), are the subject of this report. In the case of the bismuth phosphate sludge, the phosphate behavior is of particular interest, as this is the major component targeted to be removed by caustic leaching (Table 1.1). Phosphate is also of interest for the

---

(a) WTP Doc. No. 24590-WTP-PL-ENG-06-0008, Rev 0, "Hanford Waste Treatment and Immobilization Plant (WTP) Project Response Plan for Resolution of Issues Identified by the Comprehensive Review of the WTP Flowsheet and Throughput." L Lucas, March 2006.

bismuth phosphate saltcake, but the behaviors of aluminum, chromium, and sulfate are also expected of significance (Table 1.1).

The waste-type definition, sample identification, archived sample conditions, and homogenization activities are discussed in this report. The caustic leaching experiments and results are described for the Group 1 and Group 2 solids. The physical, chemical, radioisotope, and crystal morphology characterization in the waste before and after leach processing are also discussed. Crossflow ultrafiltration tests using a blend of the Group 1 and Group 2 solids are described and the results presented.

The results from these tests will refine the knowledge base of the tank waste chemical and mineralogical characteristics. Parametric leach testing will provide the leaching kinetics of gibbsite, phosphorus, and chromium and support follow-on leach and filtration testing.

2.0   Test Sample Selection, Compositing, and Homogenization

This section describes the rationale for selecting bismuth phosphate sludge (Group 1) and saltcake (Group 2) test materials from the Hanford tank waste sample archive located in the 222S building of the Hanford Site. Retrieval of new sample materials from the tanks was deemed to be prohibitively expensive and time intensive and therefore was not considered. Also described is the homogenization and sub-sampling of Group 1 and Group 2 composite samples.

2.1 Group 1—Bismuth Phosphate Sludge Sample Selection

Bismuth phosphate first and second cycle (1C and 2C, respectively) tank waste sludge samples with high bismuth content were targeted to construct the Group 1 composite. The 1C and 2C wastes originated from neutralization of acidic process solutions from the bismuth phosphate process used to separate plutonium from irradiated fuel in the 1940s and 1950s (Cleveland 1970, pp. 500-503). The Tank-Waste Information Network System (TWINS) database[a] was queried to identify the tanks containing >95% 1C and/or 2C waste type. These tank wastes were queried in the Best Basis Inventory (BBI)[a] for the major inorganic components (phosphate, Bi, Al, Fe, Cr, Si, and U) in the solid and sludge phases. Figure 2.1 shows the relative mass distributions of these analytes; mass fraction variation between these components in the tank wastes was relatively minor. (Note that major elemental and anionic contributions from Na, nitrate, nitrite, and oxalate are excluded from the data in Figure 2.1.)

The decision process flowchart for selecting tank waste samples from the sample archive is summarized in Figure 2.2. The 222S archive sample inventory[b] was searched for sludge samples from the tanks identified as containing first (1C) and second (2C) cycle bismuth phosphate waste (Figure 2.2). The samples were then cross-referenced to the TWINS database to determine if analytical data from the specific samples were available; samples identified as containing >10 mg Bi per g sludge (reported on a wet mass basis) were carried forward in the selection process. It was assumed that samples high in Bi were also high in phosphate. Of these samples, those with <5 g material were omitted. The final list of samples was submitted to CH2MHill personnel[c] for a two-step evaluation process: 1) the samples were confirmed to represent the bismuth phosphate sludge waste stream based on the tank strata, core segment, and corresponding characterization results, and 2) the samples were not held for other activities and could be released from the archive.

Table 2.1 summarizes the tank sources evaluated and shows whether the tank met or failed the selection criteria. Samples highlighted in bold in the table were those determined to meet all of the selection criteria.

(a) The TWINS database and the BBI are DOE-owned resources.
(b) Personal communication of the inventory database, file "Vials May18," provided from P Brackenbury, Bechtel, June 2006.
(c) David Place and Bruce Higley, Process Engineers, Process Analysis Organization, CH2MHill.
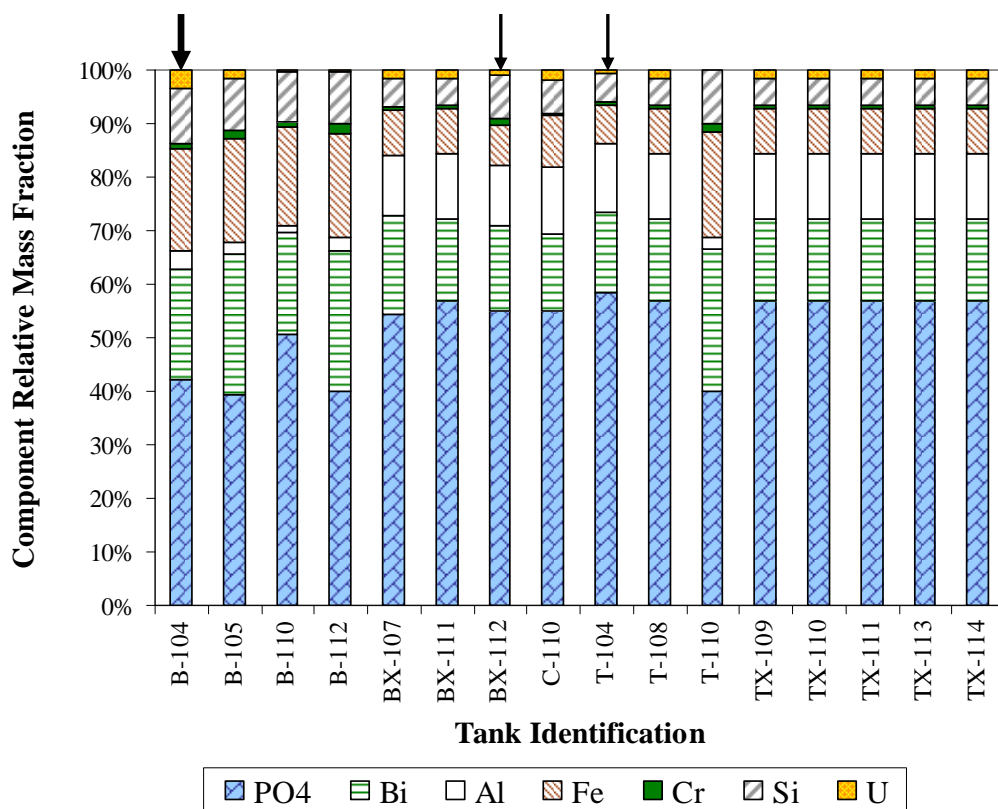
Figure 2.1. Estimated Tank Waste Composition of Selected Analytes for 1C and 2C Sludge Wastes in the Hanford Tank Farm (BBI Source). Note: arrows point to the tanks actually used to prepare the Group 1 composite; B-104 dominated the composite mass (see text).

Table 2.2 summarizes the individual samples (sample date, tank ID, sample core, and segment) from the archive that met the selection criteria. These samples had been in storage at 222-S for ~12 to 15 years. The long storage time could potentially cause the sample characteristics to be altered relative to the as-retrieved sample condition through aging and drying. But, as stated previously, obtaining fresh core samples from the Hanford waste tanks was outside the scope of the project budget and schedule. Also shown in Table 2.2 are the anticipated bismuth concentrations (wet sample basis) and the mass assumed available based on the archive inventory in ~2002. A total of 2.28 kg of bismuth phosphate sludge was assumed to be available and sufficient for the complete testing scope.

The Group 1 sample set was heavily represented by one tank, B-104. The potential impact of the Group 1 composite representation primarily by B-104 was evaluated. As seen in Figure 2.1, gross deviations in the elemental compositions within this suite of tank wastes were relatively minor, so it was concluded that B-104 would be reasonably representative of the group.

```
            ┌─────────────────────────┐
            │ Identify BiPO₄ 1C and 2C Tank │
            │  Waste Samples from TWINS │
            └─────────────────────────┘
                        │
                        ▼
                    ╱ >95 wt% ╲        no
                   ⟨  1C or 2C  ⟩ ─────────▶  [ Not selected ]
                    ╲  waste? ╱
                        │ yes
                        ▼
                 ╱ Sludge sample ╲     no
                ⟨ available in 222S ⟩ ─────▶  [ Not selected ]
                 ╲    archive?   ╱
                        │ yes
                        ▼
                   ╱ Analytical ╲      no
                  ⟨ data available ⟩ ───────▶  [ Not selected ]
                   ╲      ?      ╱
                        │ yes
                        ▼
                     ╱  [Bi]  ╲        no
                    ⟨ >10 mg/g  ⟩ ─────────▶  [ Not selected ]
                     ╲    ?   ╱
                        │ yes
                        ▼
                    ╱ Sample ╲         no
                   ⟨   >5g?   ⟩ ───────────▶  [ Not selected ]
                    ╲        ╱
                        │ yes
                        ▼
                   ╱ Confirmed ╲       no
                  ⟨  1C and 2C  ⟩ ─────────▶  [ Not selected ]
                   ╲  waste ?  ╱
                        │ yes
                        ▼
                   ╱ Approve ╲         no
                  ⟨ release from ⟩ ────────▶  [ Not selected ]
                   ╲  archive? ╱
                        │ yes
                        ▼
                ┌──────────────┐
                │ Sample selected │
                │  for testing  │
                └──────────────┘
```

Figure 2.2. Selection Decision Process 1C and 2C Sludge Samples

Table 2.1. Selection of Bismuth Phosphate Sludge Tanks

Tank	1C or 2C Sludge, kL	Total Sludge, kL	Fraction 1C or 2C Sludge	222S Archive		
				Available Samples	Identified as Sludge	Analytical Results
241-B-104	1170	1170	1			
241-B-105	106	106	1	no		
241-B-110	914	925	0.99	no		
241-B-112	56	56	1	no		
241-BX-107	1313	1313	1	no		
241-BX-111	121	121	1	no		
241-BX-112	**617**	**617**	**1**			
241-C-108	27.3	27.3	1			no[b]
241-C-110	670	670	1	no		
241-T-104	**1199**	**1199**	**1**			
241-T-108	20	20	1	no		
241-T-110	1360	1397	0.97			no[b]
241-TX-109	1375	1375	1	no		
241-TX-110	140	140	1	no		
241-TX-111	163	163	1	no		
241-TX-113	351	351	1		no[a]	
241-TX-114	15	15	1	no		
(a) The available TX-113 samples in the 222S inventory were identified as saltcake in the TWINS database.						
(b) Bismuth analytical data were not available from TWINS.						
Bold highlighted text indicates tank wastes were represented in the composite suite for Group 1.						

2.2 Group 2—Bismuth Phosphate Saltcake Sample Selection

In the Best-Basis Inventory (BBI), saltcake is generally divided into six main groupings as a function of waste source: A, B, BY,R, S, and T (in general, these designations refer to the tank farm at the Hanford Site from which these saltcake wastes originate). Saltcake tank wastes high in phosphate and chromium concentrations were targeted for testing. The TWINS database was queried to identify the tanks containing 100% BY and T saltcake waste types, which were derived from evaporation of neutralized solutions from the bismuth phosphate process and were expected to have high phosphate and chromium content based on a previous evalutation (Fiskum et al. 2008). These tank wastes were queried in the BBI for major inorganic components (phosphate, Bi, Al, Fe, Cr, Si, and U) in the saltcake phase. Figure 2.3 shows the relative mass distributions of these analytes. (Note that major elemental and anionic contributions from Na, nitrate, nitrite, and oxalate are excluded from the data in Figure 2.3.) The disparate fractionation of all components is evident.

The decision process flowchart for selecting tank waste samples is summarized in Figure 2.4. The 222S archive sample inventory was searched for samples from the identified tanks; those defined as a saltcake matrix were retained for consideration. These samples were then cross-referenced to the TWINS database to determine if analytical data from the specific samples were available; samples containing >20 mg PO_4^{3-}/g saltcake were carried forward. Of these samples, those with >20 g material as identified in the 222S archive inventory were selected. The final list of samples was submitted to CH2MHill

personnel for a two-step evaluation process: 1) the samples were confirmed to represent the BY or T saltcake waste based on strata from tank and corresponding characterization results, and 2) the samples were not held for other activities and could be released from the archive.

Table 2.2. Group 1 Targeted Samples and Masses from 222S Archive

Tank Sampling Date[a]	Jar #	Tank	Core	Segment	Estimated Bi, mg/g[b]	Net Sample Weight (g)[c]
8/20/1992	13518	T-104	45	Comp	18	62.41
6/1/1995	7197	B-104	88	1	13	54.8
	7190	B-104	88	2	16	62.1
	8427	B-104	88	2	16	46.15
	8428	B-104	88	2	16	49.48
	7200	B-104	88	3	14	62.4
	8421	B-104	88	3	14	64.04
	8423	B-104	88	4	12	60.89
	7206	B-104	88	4	12	57.19
	7205	B-104	88	4	12	58.67
	7207	B-104	88	5	12	56.98
	7208	B-104	88	5	12	57.4
	8425	B-104	88	5	12	60.16
	10113	B-104	88	5	12	101.66
	7373	B-104	88	Comp	10	78
6/9/1995	11843	B-104	89	1	11	172.1
	7228	B-104	89	5	12	59.99
	7227	B-104	89	5	12	60.92
	13164	B-104	89	5	12	77.52
	17523	B-104	89	5	12	94
	7231	B-104	89	6	11	58.48
	7229	B-104	89	6	11	59.77
	8419	B-104	89	6	11	60.13
	8418	B-104	89	6	11	62.11
	7232	B-104	89	7	11	60.44
	7233	B-104	89	7	11	60.68
	9018	B-104	89	7	11	79.46
	9028	B-104	89	7	11	81.34
	13442	B-104	89	Comp	11	81.82
11/30/1995	9151	BX-112	118	1	17	60.28
	9152	BX-112	118	1	17	66.52
					Sum	2128
(a) Sample date is defined in TWINS database.						
(b) Wet mass basis, as defined in TWINS database.						
The anticipated mass was determined based on the sample mass inventory in database "Vials May 18" provided by P Brackenbury.						
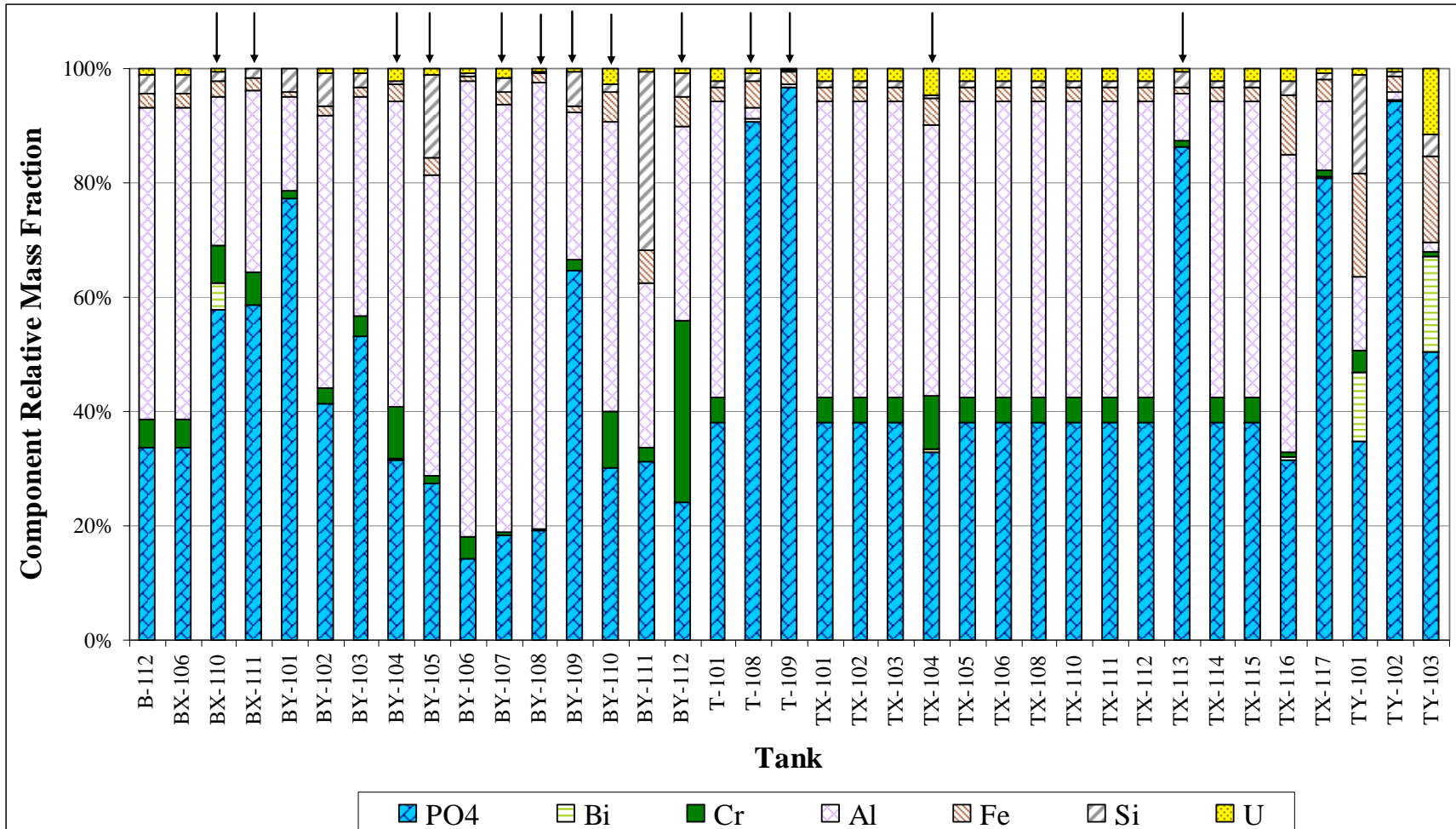
Figure 2.3. Estimated Tank Waste Composition of Selected Analytes for Bismuth Phosphate (BY and T) Saltcake Wastes in the Hanford Tank Farm (BBI Source). Note: arrows point to tank wastes actually used to prepare the Group 2 composite.

```
┌─────────────────────────────┐
│ Identify BY and T Saltcake Waste │
│ Tank Samples from TWINS      │
└─────────────────────────────┘
              │
              ▼
        ◇ 100 wt%              no    ┌──────────────┐
        BY or T-Saltcake  ────────▶  │ Not selected │
        waste? ◇                     └──────────────┘
              │ yes
              ▼
        ◇ Samples              no    ┌──────────────┐
        available in 222S ────────▶  │ Not selected │
        archive? ◇                   └──────────────┘
              │ yes
              ▼
        ◇ Analytical           no    ┌──────────────┐
        data available  ────────▶    │ Not selected │
        ? ◇                          └──────────────┘
              │ yes
              ▼
        ◇ [PO₄³⁻]              no    ┌──────────────┐
        >20 mg/g ────────────────▶   │ Not selected │
        ? ◇                          └──────────────┘
              │ yes
              ▼
        ◇ Sample               no    ┌──────────────┐
        >20g? ◇ ─────────────────▶   │ Not selected │
              │ yes
              ▼
        ◇ Confirmed            no    ┌──────────────┐
        BY or T-Saltcake ────────▶   │ Not selected │
        waste? ◇                     └──────────────┘
              │ yes
              ▼
        ◇ Approve              no    ┌──────────────┐
        release from  ───────────▶   │ Not selected │
        archive? ◇                   └──────────────┘
              │ yes
              ▼
       ┌──────────────┐
       │ Sample selected │
       │ for testing   │
       └──────────────┘
```

Figure 2.4. Selection Decision Process for the Bismuth Phosphate Saltcake Samples

Table 2.3 summarizes the evaluated BY and T saltcake tank sources and shows whether the tank met or failed the selection criteria. Samples highlighted in bold in the table were those determined to meet all of the selection criteria.

Table 2.4 summarizes the specific samples selected from the 222S archive that met the selection criteria. These samples had been in storage at 222-S for ~8 to 12 years. Again, the aging and probable desiccation processes could result in changes to the waste mineralogical forms, but these were deemed to be the best samples available given the project budget and schedule.

The BBI-predicted BY and T saltcake compositions varied widely (refer to Figure 2.3). The source tanks used to generate the Group 2 composite, shown with arrows in Figure 2.3, were chosen to provide a reasonable approximation of the overall waste type, based on the constrained set of archive samples that were available.

2.3 Group 1 Sample Homogenization and Sub-Sampling

The homogenization vessel and mixing system used to homogenize the Group 1 bismuth phosphate sludge sample was designed and fabricated for use at the Pacific Northwest National Laboratory (PNNL) in the High-Level Radiochemistry Facility (HLRF). This stainless steel equipment was specifically designed to composite tank wastes and divide them into homogeneous sub-samples. The homogenization vessel was designed to hold and effectively mix a variable volume of 1 to 5 L of waste. A set of removable baffles was designed and added to enhance mixing. Industry experience shows that the best mixing is achieved when a tank height to diameter ratio is 1:1. For a fixed volume batch tank, this is easy to achieve. For a variable volume tank, this presents a challenge usually solved by making the tank conical. Height restrictions and volume requirements made it unfeasible to make the entire homogenization vessel conical, so to optimize mixing, a compromise tank design was devised. The bottom of the tank with a volume capacity of ~1.5 to 2.0 L was conical. At low volumes, the mixing assistance from the baffles was less than at larger volumes. Therefore, the need to rigorously maintain the 1:1 ratio was achieved in this section of the tank. When the volumes are above 2 L, the baffles combined with a down-sweeping mixer blade were shown to be sufficient to maintain a good mixing profile in the non-conical portion of the tank. The bottom of the conical section slopes toward the side to facilitate good subdivision of the samples.

Figure 2.5 shows photographs of the homogenization vessel along with a schematic representation of its design. The Group 1 sample material was loaded into the vessel through a Tyler sieve mounted to the top of the vessel (see right side of Figure 2.5). This was done so that no chunks of material greater than 3.2 mm in diameter were included in the composite, which was necessary for forming a uniform composite and protecting the crossflow ultra filtration (CUF) equipment during later testing. This vessel was used to composite several groups of tank samples. Extensive cleaning was done between each group with water, 0.01 M NaOH, and 0.01 M HNO_3.

Before the actual tank waste samples were homogenized, non-radioactive testing of this system with various simulants was performed to establish the best operating conditions and procedures and to verify the uniformity of the sub-samples obtained with this tank. Simulants with high yield stress values (Figure 2.6) and simulants with the capability to settle rapidly (Figure 2.7) were tested to verify that good mixing could be maintained and uniform sub-samples removed. Operating conditions and guidelines that

resulted in a composite with homogeneous sub-samples of the most challenging simulants were then incorporated into the test instructions for the actual waste testing.

Table 2.3. Selection of Group 2 Bismuth Phosphate Saltcake Tanks

Tank ID	BY Saltcake, kL	Total, kL	Fraction of BY	222S Archive		
				Available Samples	Samples >20 mg PO_4^{3-}/g	Samples >20 g?
B-112	49	49	1.0	no		
BX-106	80	80	1.0	no		
BX-110	**433**	**433**	**1.0**			
BX-111	**538**	**538**	**1.0**			
BY-101	1208	1208	1.0			no
BY-102	**897**	**897**	**1.0**			
BY-103	1316	1316	1.0	no		
BY-104	**1208**	**1208**	**1.0**			
BY-105	**1481**	**1481**	**1.0**			
BY-106	1365	1365	1.0		no	
BY-107	**835**	**835**	**1.0**			
BY-108	**587**	**587**	**1.0**			
BY-109	**851**	**851**	**1.0**			
BY-110	**1123**	**1123**	**1.0**			
BY-111	1378	1378	1.0		no	
BY-112	**996**	**996**	**1.0**			
				222S Archive		
Tank ID	T Saltcake, kL	Total, kL	Fraction of T	Available Samples	Samples >20 mg PO_4^{3-}/g	Samples >20 g?
T-101	179	179	1.0	no		
T-108	**30**	**30**	**1.0**			
T-109	**197**	**197**	**1.0**			
TX-101	49	49	1.0	no		
TX-102	692	692	1.0	no		
TX-103	454	454	1.0	no		
TX-104	**93**	**93**	**1.0**			
TX-105	2044	2044	1.0	no		
TX-106	1147	1147	1.0	no		
TX-108	415	415	1.0	no		
TX-110	1580	1580	1.0	no		
TX-111	1194	1194	1.0	no		
TX-112	2290	2290	1.0	no		
TX-113	**2045**	**2045**	**1.0**			
TX-114	1923	1923	1.0	no		
TX-115	1960	1960	1.0	no		
TX-116	1903	1903	1.0	no		
TX-117	1659	1659	1.0	no		
TY-101	159	159	1.0	no		
TY-102	199	199	1.0	no		
TY-103	150	150	1.0	no		
Bold highlighted text indicates tank wastes were represented in the composite suite for Group 2.						

2.9

Table 2.4. Group 2 Targeted Samples and Masses from 222S Archive

Tank Sample Date[a]	Jar #	Tank	Core	Segment	Estimated PO_4^{3-}, mg/g[b]	Net Sample Weight (g)[c]
5/19/1997	19298	BX-110	197	1	45	54.5
	12694	BX-110	197	1	45	87.77
	12744	BX-110	197	2	38	55.12
	13021	BX-111	200	1	51	67.5
	12647	BX-111	200	2	42	78.5
	13022	BX-111	200	2A	27	92.77
	13031	BX-111	202	1	45	59.1
10/31/1995	8410	BY-104	116	2	25	20.2
	8757	BY-104	116	3	35	29
	8758	BY-104	116	3	35	69.9
8/30/1995	8643	BY-105	108	2AR	27	79.87
6/12/1996	18632	BY-107	151	4	25	38.7
	10544	BY-107	151	4	25	51.5
	10545	BY-107	151	4	25	109.3
7/25/1996	10848	BY-107	161	1	30	30.9
8/16/1995	15622	BY-108	104	1	75	48.8
	16950	BY-108	104	2	32	27.2
	15570	BY-108	104	2	32	29.5
	7686	BY-108	104	2	32	49.57
	7679	BY-108	104	2	32	60.22
	7689	BY-108	104	3	67	24.5
	7687	BY-108	104	3	67	58.79
	13525	BY-108	104	4	32	27.78
	7690	BY-108	104	4	32	33
	7691	BY-108	104	4	32	67.3
	7692	BY-108	104	4	32	67.3
6/6/1997	13040	BY-109	203	3	36	69.9
	13039	BY-109	203	3	36	72.3
	19086	BY-109	203	3	36	95.9
9/25/1995	8375	BY-110	96	1	65	49.89
8/15/1995	13472	BY-110	103	1	57	33.5
8/22/1995	7655	BY-110	106	1	25	39.5
9/13/1995	7972	BY-110	109	1	30	41.47
10/2/1996	11799	BY-112	174	1	38	29.3
10/3/1996	11793	BY-112	177	1	106	20.3
7/19/1995	7428	T-108	Riser 5	Auger-35	25	27.32
8/21/1995	7467	T-109	Riser 2	Auger-41	270	34.7
2/18/1998	13856	TX-104	230	1	35	100.9
2/18/1998	14021	TX-104	231	2A	25	26.75
10/22/1998	19272	TX-113	253	5	40	23.3
4/15/1999	18801	TX-113	258	5	29	143.5
					Sum	2227

(a) Sample date is defined in TWINS database.

(b) Wet mass basis, as defined in TWINS database.

(c) The anticipated mass was determined based on the sample mass inventory in database "Vials May 18" provided by P Brackenbury.

Clay simulants were prepared with high Bingham yield stresses and cohesive properties that would make them sticky. These consisted primarily of kaolin and bentonite clay mixtures. These simulants mixed well and delivered uniform samples while the homogenization vessel was tested (Figure 2.6, left and center). However, they did leave a thick film of material coating the tank, mixer, and baffle surfaces (Figure 2.6, right). In compositing the actual tank waste samples, solids materials with these characteristics would need to be recovered for CUF testing with extra rinses of de-ionized (DI) water after completing homogenization and sub-sampling of the bulk material.
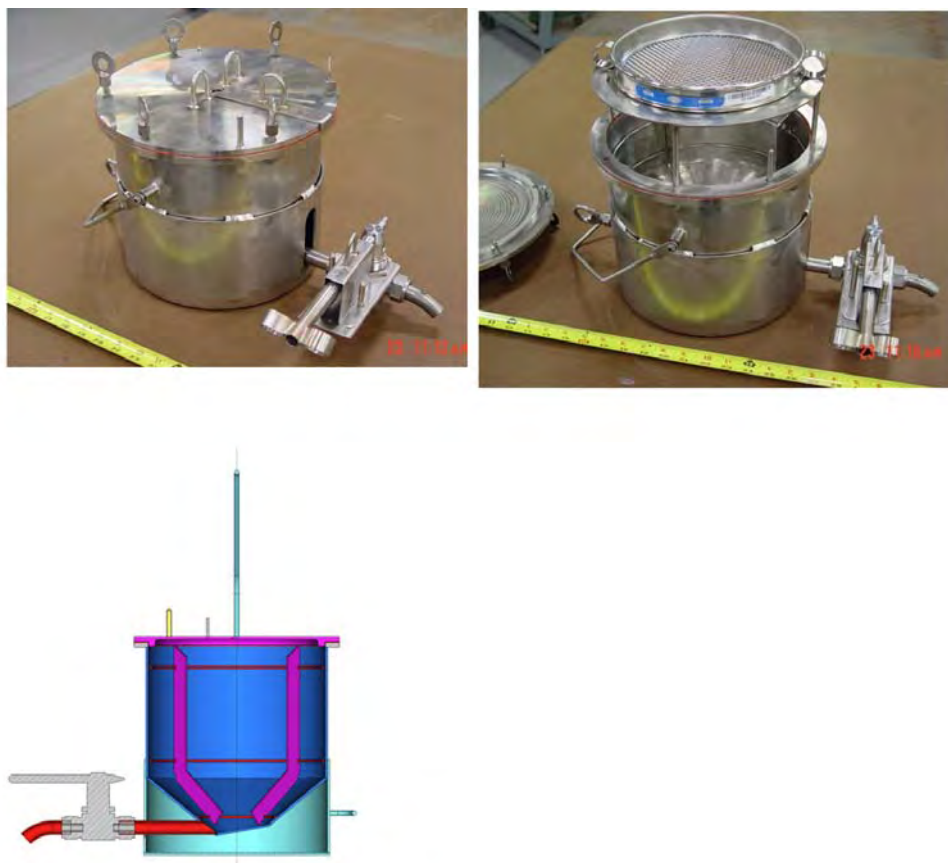
Figure 2.5. Homogenization Vessel Used to Prepare and Sub-Sample the Group 1 Composite Slurry

Figure 2.6. Photographs of a High Yield Stress Clay Simulant in the Homogenization Vessel Used for Group 1

Min-u-sil®-based simulants were used to test variable mixing speeds and propeller placement because of their tendency to settle swiftly when mixing is not sufficient. Figure 2.7 shows that these simulant types could usually be cleanly and completely recovered from the tanks. However, the sub-samples were often non-uniform with the Min-u-sil® simulants. Figure 2.8 shows an example of non-uniform settling results for sub-samples taken when the mixer speed was too low. Based on these results, a hold point was inserted into the compositing test instructions such that after 3 days of settling, the settled solids of all the composite samples would be compared and statistically analyzed to verify that good homogenization of the composite had been achieved and maintained during the sub-sampling process.

Figure 2.7. Photographs of the Mixing of a Min-u-sil® Simulant that Settles Rapidly in the Homogenization Vessel Used for Group 1 (left) and the Vessel After Draining of the Material (right)
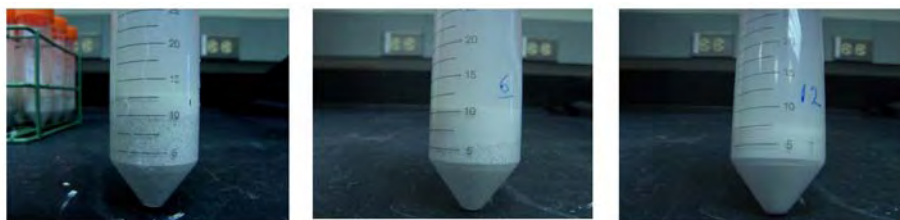
Figure 2.8. Photographs of Three Different Sub-Samples Taken from the Homogenization Vessel During Non-Radioactive Testing with a Min-u-sil® Simulant. Note the different degrees of settling, which indicates in-homogeneity in the slurry.

The 31 Group 1 bismuth phosphate sludge samples were shipped from the Hanford 222-S laboratory to PNNL. Masses for these archived samples were provided by Advanced Technologies and Laboratories International (ATL) in the shipping letter report. Many of the samples had dried out during the time spent in archived storage. Photographs, as received weights, and detailed sample descriptions were all recorded in TI-RPP-WTP-508. There were crystallized deposits on the outsides of many of the jars. Efforts were made to get this material into the composite, provided it was immediately around the threads of the jar. However, if the crystals were further down on the jar and were potentially contaminated with unknown materials, they were left intact, and the loss accounted for in the mass balance done after sample transfer from the jar was completed. The samples' appearance and color ranged from white dry crystals, to grey pastes, to brownish yellow sludge. The supernate liquid was yellow on the samples that still had standing liquid. Figure 2.9 shows some representative photographs of the as-received samples.

The Group 1 sample material fell into the following general categories:

   a. Dry powdery sample—added directly to the homogenizer though the screen.

   b. Dry solid sample—added water to soak sample so it could be broken up and removed from the jar for addition to the homogenizer.

   c. Semi-solid—sample was added to homogenizer without soaking sample with water first.

   d. Clearly visible supernate liquid in jar.

Figure 2.9. Representative Photographs of As-Received Group 1 Waste Samples

Table 2.5 lists the individual samples added to the composite sample, along with gross mass (expected and found), the mass of the empty container, and the net mass of waste transferred to the homogenizer. Samples that appeared to be fine solids were added first and easily passed through the sieve. If foreign material such as pieces of broken caps were present, those were picked out with stainless steel tweezers and weighed when possible (there were very few instances of this for these samples). In some cases, the thin Teflon® liner pieces often disintegrated in the tweezers, so no weights could be obtained for these. For wet samples, the solids were removed from the sample jar by a process of scraping and rinsing with DI water using a squirt bottle. In this fashion, nearly all residues were removed from the sample jars. These samples were originally placed in secondary containment and removed from their smaller jars into larger jars to minimize evaporative losses that sitting in the larger tank might have allowed over the several days required to empty the smaller jars. Three of the larger transfer jars were used for Group 1; the contents of all of these were transferred into the homogenizer on the morning the final mixing was done.

Solids and semi-solids were forced through the sieve using DI water, rubber spatulas, and a stainless steel mashing tool that also was used in breaking up some chunks of solid materials so they could pass though the sieve. To the maximum extent possible, all sample materials were placed into the homogenizer; there was very little loss of actual sample due to splattering or spillage. Water was used conservatively during the entire process of removing the samples from the jars so as to have enough water to remove all sample residues and come close to the desired total solution added to reach the desired Na concentration.

Table 2.5. Bi Phosphate Sludge Samples (Group 1)

Hanford Tank ID	222-S ID	222S Expected Gross Mass (g)	PNNL As-found Gross Mass (g)	PNNL Jar and Lid Condition	PNNL Empty Container Mass (g)	PNNL Mass Transferred (g)
B-104	7190	86.8	86.83	Good	27.69	59.14
B-104	7197	80	75.76	Good	30.26	45.50
B-104	7200	87.6	87.95	Good	29.34	58.61
B-104	7205	83.5	84.00	Good	27.61	56.39
B-104	7206	82.4	83.89	Good	27.82	56.07
B-104	7207	82.3	82.46	Good	28.07	54.39
B-104	7208	82.8	83.15	Good	29.91	53.24
B-104	7227	86.3	83.95	Good	27.27	56.68
B-104	7228	85.4	82.16	Good	27.59	54.57
B-104	7229	85.1	85.65	Good	28.02	57.63
B-104	7231	83.7	82.65	Good	27.68	54.97
B-104	7232	85.7	83.84	Good	28.89	54.95
B-104	7233	86.2	86.40	Good	28.53	57.87
B-104	7373	202.2	199.32	Good	128.3	71.02
B-104	8418	87.8	86.32	Good	28.92	57.40
B-104	8419	85.8	86.33	Good	28.73	57.60
B-104	8421	89.7	87.93	Good	27.96	59.97
B-104	8423	86.7	87.25	Good	29.32	57.93
B-104	8425	85.8	86.42	Good	29.53	56.89
B-104	8427	71.6	71.53	Good	28.49	43.04
B-104	8428	75.4	70.86	Good	28.84	42.02
B-104	9018	165.3	166.01	Good	95.12	70.89
B-104	9028	167.2	168.1	Good	95.49	72.61
BX-112	9151	151.8	151.96	Good	98.22	53.74
BX-112	9152	157.7	119.74	Good	93.35	26.39
B-104	10113	189.6	190.58	Good	95.59	94.99
B-104	11843	292.4	225.18	Lid Loose Sample loss	93.55	131.63
B-104	13164	163.4	166.13	Good	94.11	72.02
B-104	13442	166.5	163.11	Good	92.54	70.57
T-104	13518	151.0	146.94	Good	95.20	51.74
B-104	17523	176.4	169.86	Good	90.41	79.45

After all of the recoverable sample materials were transferred to the homogenizer tank, the sample jars were allowed to dry, and they were then reweighed. These values were used to calculate sample recovery and actual amount of sample added to the homogenizer (Table 2.5). A few jars had significant differences between the expected gross mass and the as-found gross mass. These larger differences are probably due to loss of water from the sample over time during storage at 222S and/or sample loss in

shipping. The jar lids tend to become brittle in the radiological environment over time, so some of these likely cracked, and the water evaporated. Some tare masses were based on vials with blue lids; lids had been replaced with green lids for shipping. The mass difference associated with the change in lids was ~4.6 g and this was taken into account for the samples this applied to. New lids were placed on the jars before shipping. One of the B-104 samples (11843) had a loose lid during shipping. This was noted by moisture in the double containment bag when unloading the cask after shipping. Weight of sample lost due to this leak was 67.22 grams.

There was an 11.2% mass loss from the expected mass, archive records, and the received mass. A total of 94.7% of the received mass was recovered from the sample jars and put into the composite. The received mass was calculated by subtracting the 222S supplied tare weights for the sample jars from the total mass measured in HLRF before transferring the sample materials. The recovered mass was determined by subtracting the mass of the jars after being emptied of sample from the total mass obtained beforehand. Approximately 5.3% of the material could not be removed from the jars. The final tank composite based on the mass balance was primarily made of B-104 tank waste as can be seen in Figure 2.10.
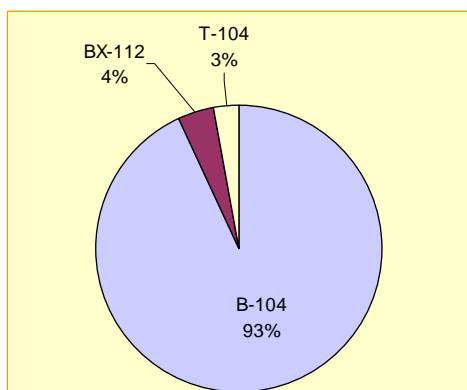
Figure 2.10. Contribution of the Individual Tanks to the Composition of the Group 1 Composite Sample

After all samples had been added to the homogenizer tank, and all equipment (spatula, sieve, mashing tool) had been rinsed free of sample, the sieve screen was removed. A total of 742.97 g of DI water was added during the compositing process. A mechanical stirrer with stainless steel impeller was lowered into the tank, the fitted lid was placed on the tank, and the material was mixed thoroughly. The temperature in the hot cell was 35°C at the start of mixing. The goal of this step was to homogenize the sample using as little force as possible. The stirrer speed was slowly increased until the solids were mobilized. The positions and arrangements for the height of the mixer relative to the support rod and impeller were predetermined during the preliminary non-radioactive testing, and the proper alignments marked onto the impeller and support rod correctly aligned. While operating the vessel agitator, material was extracted from the collection port at the bottom of the tank and returned through the top of the vessel to so that all the material was mixed well.

The test plan defined a minimum required mixing time of 1 hour. The total mixing time for the Group 1 composite slurry was 1 hour and 40 minutes before sub-sampling began. Sub-sampling took 40 minutes, and the mixer continued to mix during this time. The consistency of the Group 1 composite was about that of a light milkshake and remained that way throughout all the subsamples. The sub-samples were

removed in a specific order to pre-determined target volumes. Pre-weighed and labeled jars and centrifuge tubes were staged in collection vessels in the order provided in Table 2.6.

At the start of sub-sampling, while operating the vessel agitator, one sub-sample of sufficient size (minimum of 100 mL) was extracted through the sample valve into **TI508-G1-AR-J1** to clear material from the lowest portion of the vessel. This was then added back to the mixing vessel before sub-sampling began. Approximately 10 to 20 mL of composite was lost from the spigot because surface tension kept the sample in the nozzle initially but cleared after the jar was filled. The S-1 test tube over-filled, losing ~10 mL, and also several of the test tubes missed the target volume. The excess was decanted as quickly as possible to AR-J6. A video was taken of the homogenized samples showing the settled solids after 3 days settling time.

Table 2.6. Group 1 Sub-Sample Mass Density and Settling Data

Sample ID in Order of Collection	Target Collection Volume	Sample Net Wt, g	Total Slurry Volume, mL	Settled Solids Volume, mL	Gross Slurry Density	Vol % Settled Solids
TI508-G1-AR-J1	300–400 mL	331.199	280	170	1.18	60.7%
TI508-G1-AR-S1	10–15 mL	9.745	8.3	5.2	1.17	62.7%
TI508-G1-AR-C1	25 mL	29.162	22.5	14.5	1.30	64.4%
TI508-G1-AR-J2	300–400 mL	325.810	275	170	1.18	61.8%
TI508-G1-AR-RH1	50 mL	113.315	85	50	1.33	58.8%
TI508-G1-AR-C2	25 mL	48.513	37.5	22	1.29	58.7%
TI508-G1-AR-S3	50 mL	19.785	16.5	9.6	1.20	58.2%
TI508-G1-AR-P1	150 mL	180.760	145	75	1.25	51.7%
TI508-G1-AR-J3	300–400 mL	343.648	285	175	1.21	61.4%
TI508-G1-AR-J4	300–400 mL	339.914	280	165	1.21	58.9%
TI508-G1-AR-S2	10–15 mL	15.818	13	7.5	1.22	57.7%
TI508-G1-AR-C3	25 mL	36.071	28.5	16.5	1.27	57.9%
TI508-G1-AR-J5	300–400 mL	354.478	295	170	1.20	57.6%
TI508-G1-AR-J7	300–400 mL	315.525	255	155	1.24	60.8%
TI508-G1-AR-J6	300–400 mL	168.138	135	75	1.25	55.6%

For compositing to be considered successful, the sample density and settled solids data standard deviation had to be less than ± 5%, and there had to be no statistically significant trend in settled solids and density variation due to subsample removal order. Figure 2.11 shows that the Group 1 composting and sub-sampling successfully met these criteria.

Following is a summary of Group 1 sample homogenization and sub-sampling:

- The total mass of Group 1 bismuth phosphate sludge samples homogenized together was 1889 g.

- The total mixing time after all Group 1 bismuth phosphate sludge samples had been added to the homogenizer tank, including a sufficient volume of water to bring the total volume to about 2.3 L, was 1 hr and 40 minutes at 35°C, after which the material was sub-sampled.

- The total mass of water used in this test was 968 g based on the difference between the starting amount stored in the DI water containers and the amount remaining at the end of the test. The actual amount of water that actually was mixed in the tank was somewhat less because of the loss of water by spillage and evaporation.

- The total gross mass of the entire homogenized sample collected was 2632 g with a total slurry volume of 2161 mL. The volume of insoluble solids (gravity-settled) as described above was determined to be 849 mL.

The total gross mass of the entire homogenized Group 1 bismuth phosphate saltcake sample collected was 1889 g sample + 968 g water = 2857 g. The difference between that total mass and that actually collected in the final sample jars is 2857 – 2632 g = 225 g (8% loss). The difference is likely due to evaporative losses of water, followed by loss of water through spilling during manipulations using the squirt bottle and dispensing water from the water-storage bottles. About 30 to 40 mL of sample was lost during problems dispensing the sample from the homogenizer tank.

2.4 Group 2 Sample Homogenization and Sub-Sampling

The Group 2 composite was prepared at the Hanford 222S laboratory using equipment that had previously been installed in the hot cell facility. This equipment was somewhat different than that used for Group 1 homogenization. It had a conical bottom, but its outlet valve was straight down, and the baffles were not removable. Modifications to the vessel were proposed and tested with a non-radioactive duplicate system out of the cell.

Before homogenizing the actual tank waste sample in the 222-S hot cell facility, non-radioactive testing and preparation of equipment was carried out at PNNL. A homogenizer that was an exact replica of the one to be used in the hot cell was obtained from ATL staff to design and fit the new components. The new components specifically fitted for the tank were a new stainless steel valve and spout at the base of the tank for dispensing of samples, a stainless steel lid with manipulator rings to prevent contamination and evaporation of water from the samples, a device to hold a stainless steel rod for placement of a stainless steel impeller/electrical stirring device, a stainless steel funnel and special lid with a slit and slit hole cover for use during the actual homogenization/mixing process, and a mounting for a video camera to record pictures of the samples and the process.
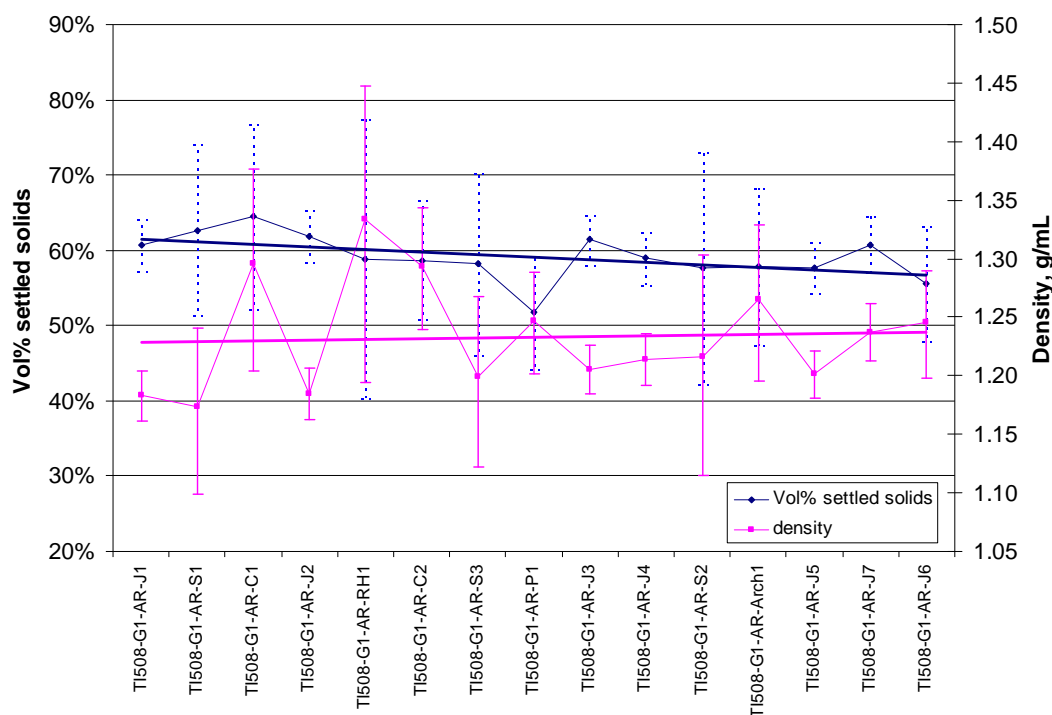
Figure 2.11. Group 1 Confirmation of Successful Material Composite Based on Density and Settled Solids

Additional equipment that was fabricated and/or supplied for this test was a heavy stainless steel "mashing" tool to help force sample through the stainless steel sieve (all samples went through a sieve so that no rocks or other foreign objects that were larger than 3.2 mm were a part of the final homogenized samples). Stainless steel manipulator rings were fabricated onto the stainless steel sieve, stainless steel spatulas, and a stainless steel "probe" to work loose the solids that settled to the bottom of the tank after homogenization so that the final samples could be dispensed. A few additional items were supplied in the form of plastic trays for secondary containment to recover any samples that may have been spilled during the test and stainless steel tweezers with manipulator rings for removing foreign matter.

Non-radioactive testing with a saltcake stimulant solution on the "cold test" tank at PNNL resulted in some areas of corrosion (Figure 2.12). After consulting other experts about corrosion and the potential causes, it was decided to proceed with the test as conceived, but to minimize the homogenizer tank residence time for the saltcake samples as much as reasonably possible to minimize the opportunity for corrosion. No corrosion was observed in the in hot cell homogenization tank before or after compositing the actual Group 2 samples.

The actual homogenizer tank that was used for the test in the 222S hotcell 11A5 was the one that appeared to be the cleanest of the three tanks in that hot cell. This tank was fitted with the new stainless steel ball valve/spout. To verify that the tank was clean and would not result in cross-contamination, it was cleaned with the following order of rinse solutions: NaOH, DI water, HNO₃, and finally with copious amounts of DI water according to Test Procedure TPR-RPP-WTP-489. The order of the cleaning procedure was to first release the water that had been sitting in the tank since the last homogenization procedure for Group 6 S-Saltcake was completed. A liter of 0.1 M NaOH was poured into the tank and down the sides of the wall, then the mixing apparatus was attached to the support rod, and the stainless

steel impeller was immersed in the solution. Some additional DI water was added to fill the level up to a sufficient level to immerse all the stirring vanes. After stirring for about 30 minutes, this solution was released through the bottom valve, and the entire apparatus was rinsed with copious amounts of DI water. Three liters of 0.1 M HNO$_3$ were then added to the tank, and the apparatus was stirred for about 30 minutes. The acid solution was released through the bottom valve, and the entire apparatus was rinsed with copious amounts of DI water, including the lids and ancillary parts of the homogenizer. The entire apparatus was well rinsed and then dried before beginning work with the Group 2 tank waste samples. There was no noticeable residue in the tank, on the impeller, or the ancillary lids.
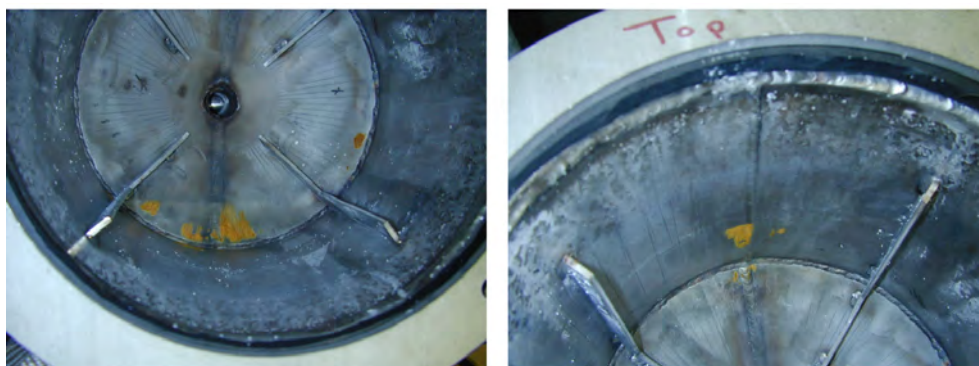
Figure 2.12. Corrosion Seen in Non-Radioactive Homogenization Tank After Saltcake Simulant Testing

During the sample homogenization, the temperature in hot cell 11A5, where the work was carried out, varied from 26.9 to 27.7°C. All original sample jars were weighed and the masses recorded (Table 2.7), and lids were removed to inspect the contents inside. Water was added to some of the samples, and the lids were replaced (to minimize evaporation) so that the samples could soak and the solids could be broken up and added to the homogenizer. A triage of the samples was performed, and the general procedure was to first add all samples that appeared to be fine-grain dry solids since those should travel easily through the sieve without the need to add water to transfer the contents.

The sample jars fell into the following general categories:

    a. Semi-solid—sample was added to homogenizer without soaking sample with water first. 222-S sample jars 19298, 12694, 13021, 8643, 18632, 10544, 10545, 10848, 16950, 15570, 7686, 7689, 13040, and 8375.

    b. Dry solid sample—added water to soak sample so it could be broken up and removed from the jar for addition to the homogenizer. 222-S sample jars 12744, 12647, 8410, 13039, and 14021.

    c. Dry solid sample—no water added for sample soaking. Was fairly easy to remove from container and place in homogenizer. In the case of 222-S sample Jar 13472, there was a single hard chunk of solid that was returned to the container for soaking to break it up after the majority of this sample was added to the tank as a dry solid. 222-S sample jars 13031, 8757, 8758, 15622, 13525, 7690, 13472, 7655, 7972, 11799, 11793, 7428, 7467, 19272, and 18801.

    d. Clearly visible supernate liquid in jar. 222-S sample jars 13022, 7679, 7687, 7691, 7692, 19086, and 13856.

The sample jars that had caps that broke or chipped during operations to remove the samples from the jars included 12744, 10545, 10848, 7689, 7691, 13040, 13856, and 18801. The mass of water added to the samples were as follows: 12744 (10.932 g), 13021 (10.711 g), 12647 (13.457), 8410 (16.141 g), 13039

(14.428 g), 13472 (12.224 g), and 14021 (11.294) g. Roughly half the samples had the appearance of a dark gray-brown solid, either dry or moist, while the other half had a whitish or tan (light) coloration—most of the latter samples tended to be fine dry samples and had perhaps been homogenized previously. Two jars, 19298 and 12694, appeared to be a blackish-green color and were sticky semisolids (19298 did have some specks of light material in it). Figure 2.13 presents some representative photographs of the Group 2 samples.

All samples were added to the top of the homogenizer, which was fitted with a stainless steel sieve that would not allow passage of particles of a size greater than 3.2 mm. Samples that appeared to be fine solids were added first and easily passed through the sieve. No water was added to the tank for those samples in order to minimize the chance for corrosion of the tank during the entire homogenization operation. Sample jars were placed inside a plastic tray for secondary containment, the lids were removed, and using a stainless steel spatula (wood handle, blade size ¾ inch wide by 5 inches long), the contents were thoroughly mixed to a consistency such that most of the contents could be poured or scraped out onto the sieve with the spatula for semi-solids. If foreign material such as pieces of broken caps were present, those were picked out with stainless steel tweezers; there were only a few instances of this for these samples.

The remaining residues were then removed from the sample jar by a process of scraping and rinsing with DI water (using a squirt bottle). In this fashion, nearly all residues were removed from the sample jars. Solids (or semi-solids) were forced through the sieve with the stainless steel mashing tool, which was very effective in breaking up some chunks of solid materials that otherwise would not have easily gone through the sieve. Figure 2.14 provides a typical illustration of semi-solid material on the sieve. To the maximum extent possible, all sample materials were placed into the homogenizer; there was very little loss of actual sample due to splattering or spillage for this group of samples. During the entire process of transferring the samples from the jars to the homogenizer, the use of water was conservative so as to have enough water to remove all sample residues and come close to the desired total solution volume for the homogenized material of 3 L.

After transferring all sample materials to the homogenizer tank, the sample jars were allowed to dry and were reweighed (Table 2.7, Final Gross Mass). These values were used to calculate the amount of sample added to the homogenizer (Table 2.7, Sample Mass Transferred to Homogenizer). The total mass of Group 2 tank waste sample added to the homogenizer was 1,966.1 g.

222-S Sample Jar 12647
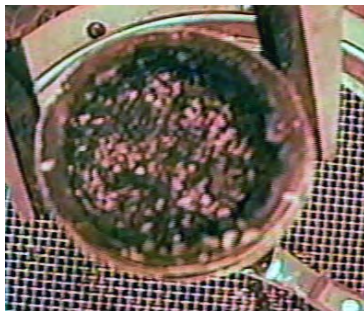
222-S Sample Jar 12694

222-S Sample Jar 10545
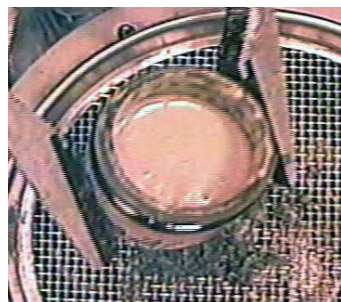
222-S Sample Jar 13021

222-S Sample Jar 15570

222-S Sample Jar 13022

222-S Sample Jar 11799
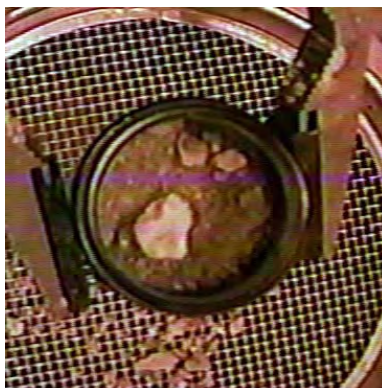
222-S Sample Jar 11793

222-S Sample Jar 7428

Figure 2.13. Representative Photographs of the Group 2 Bismuth Phosphate Saltcake Samples
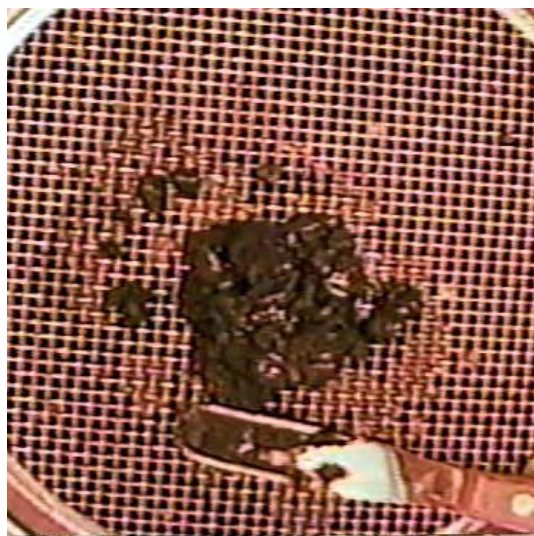
Figure 2.14. Example of Group 2 Waste Transfer into the Homogenizer

The following jars had fairly significant differences between the Expected Gross Mass and the As-Found Gross Mass (greater than 20 g): 12694 (31.47 g), 12744 (28.93 g), 13021 (21.9 g), 12647 (28.1 g), 13031 (21.7 g), and 13856 (21.3 g). These larger differences are probably due to loss of water from the sample over time during storage and/or a change in the cap at sometime during storage sample.

During the course of adding samples to the homogenizer, it was noticed that a small leak had developed where the valve at the bottom of the homogenizer connects to the tank. The leak probably occurred as a result of a poor seal due to decomposing Teflon® tape used on the thread. A small finger of bright yellow solid was noticed forming at this juncture. The solid was recovered and placed back in the tank. Also, it was possible to recover (minus evaporated water) the leaked liquid because a clean tray had been placed under the bottom of the tank. The valve-to-tank connection was tightened several times, but eventually there was inevitably a small leak that occurred within a few days. All solid material was recovered, and the losses here consisted primarily of water loss due to evaporation. This situation had to be managed because there was a delay of several days in the homogenization operation when some of the bands on the manipulator broke and required repair.

After all samples had been added to the homogenizer tank, and all equipment (spatula, sieve, mashing tool) had been rinsed free of sample, the sieve screen was removed and sufficient DI water was added to the tank to bring the volume to approximately 3 L. An electrical stirrer with stainless steel impeller was lowered into the tank, and the solution was mixed thoroughly. A special lid, which had a slot cut out radially so as to fit the stirring apparatus, was placed on the tank. Another small lid with a manipulator ring covered up the open space left by the slot to prevent cross contamination of the sample and to minimize evaporation and/or splattering losses during mixing. These pieces were made from stainless steel.

Table 2.7. Group 2 Bismuth Phosphate Saltcake Sample Masses

Hanford Tank ID	222-S Jar #	Expected Gross Mass (g)	As-Found Gross Mass (g)	Final Gross Mass (g)	Sample Mass Transfer'd to Homogenizer (g)	Mass Loss Between Expected and As-Found (g)
BX-110	19298	138.2	137.879	83.397	54.482	0.3
BX-110	12694	175.17	143.697	86.146	57.551	31.47
BX-110	12744	141.22	112.292	86.522	25.770	28.93
BX-111	13021	154.9	133.013	87.765	45.248	21.9
BX-111	12647	164.6	136.534	84.553	51.981	28.1
BX-111	13022	179.87	178.638	88.085	90.553	1.23
BX-111	13031	146.9	125.229	87.891	37.338	21.7
BY-104	8410	105.4	103.325	84.884	18.441	2.1
BY-104	8757	113.8	113.535	85.418	28.117	0.3
BY-104	8758	155.2	154.129	85.582	68.547	1.1
BY-105	8643	165.35	164.453	86.677	77.776	0.90
BY-107	18632	122.5	122.799	91.189	31.610	-0.3
BY-107	10544	139.9	139.774	94.285	45.489	0.1
BY-107	10545	197.9	183.202	87.835	95.367	14.7
BY-107	10848	118.9	117.576	88.820	28.756	1.3
BY-108	15622	132.2	131.784	83.433	48.351	0.4
BY-108	16950	112.3	111.943	84.706	27.237	0.4
BY-108	15570	113.2	112.903	84.094	28.809	0.3
BY-108	7686	75.27	74.982	25.719	49.263	0.29
BY-108	7679	85.92	85.636	25.693	59.943	0.28
BY-108	7689	50	49.134	25.469	23.665	1
BY-108	7687	84.48	83.684	26.772	56.912	0.80
BY-108	13525	115.78	114.519	88.096	26.423	1.26
BY-108	7690	58.6	54.219	25.424	28.795	4.4
BY-108	7691	92.9	92.355	25.334	67.021	0.5
BY-108	7692	93.1	92.983	25.626	67.357	0.1
BY-109	13040	156.7	150.817	89.017	61.800	5.9
BY-109	13039	159.6	145.048	87.807	57.241	14.6
BY-109	19086	180	179.670	84.324	95.346	<1
BY-110	8375	135.49	135.027	85.798	49.229	0.46
BY-110	13472	117	117.101	83.969	33.132	<1
BY-110	7655	65.3	65.206	26.030	39.176	0.1
BY-110	7972	66.97	64.305	26.144	38.161	2.66
BY-112	11799	117.7	116.636	88.449	28.187	1.1
BY-112	11793	106.5	104.385	86.254	18.131	2.1
T-108	7428	52.6	44.722	25.358	19.364	7.9
T-109	7467	59.6	59.886	25.714	34.172	-0.3
TX-104	13856	184.2	162.858	85.000	77.858	21.3
TX-104	14021	112.1	111.722	85.784	25.938	0.378
TX-113	19272	106.6	88.522	83.359	5.163	18.1
TX-113	18801	267.6	266.574	124.176	142.398	1.0

The positions and arrangements for the height of the mixer relative to the support rod and impeller were predetermined using the cold testing tank (done at PNNL), and the proper alignments were marked onto the impeller and support rod using a marking pen. The impeller itself was composed of three separate blade units. The bottom unit was situated as close as reasonably possible to the bottom of the funnel/cone shaped tank to maximize stirring/mixing of the solids. There was another blade unit situated roughly in the center of the slurry (based on a volume of 3 L) while the final mixing blade was situated just below the highest level of the liquid (again based on a volume of 3 L).

The temperature of the hot cell during the mixing period was 27.1°C, and the total mixing time was 1 hour and 56 minutes. After the solution had been mixed for about 50 minutes, mixing was briefly stopped, and the valve at the bottom of the tank was opened to collect some of the sample into a jar. The purpose of this procedure was to make sure that the solids in the bottom neck of the homogenizer tank were actually being thoroughly mixed to obtain a homogeneous solution. About 100 mL of solid and liquids were collected and recycled into the top of the tank. A small amount of additional DI water was used to rinse out this jar back into the vessel. The valve was firmly closed, and mixing was restarted. Upon completion of the mixing time, the mixing apparatus was first clamped above the slurry in the tank, and the impeller blades were washed carefully with DI water to recover as much sample as possible. Then the mixing apparatus was completely removed from the support rod, and the solid tank lid was placed on the tank to allow the solids to settle in the tank.

The amount of water used in compositing and homogenizing the Group 2 sample is listed in Table 2.8. Water usage was determined by tracking the masses of the stock water bottles used during the course of the compositing and homogenization work. The total mass of water used as determined in this manner was 2973.6 g. The actual amount was undoubtedly somewhat less due to minor losses of water through spillage and evaporation.

Table 2.8. Mass of DI Water Used in Compositing/Homogenization of Group 2 Bismuth Phosphate Saltcake Samples

Water Container	Tare of Container (g)	Tare and Wt of Water (g)	Mass of Water (g)	Mass of Residual Water (g)	Total Mass of Water Used (g)
Bottle 1	103.80	1056.11	952.31	0.41	951.90
Bottle 2	103.64	1052.49	948.85	0.93	947.92
Bottle 3	104.31	1065.50	961.19	6.77	954.42
Bottle 4	104.6	1047.1	942.5	767.8	174.7
Squirt Bottle	39.19	39.19	0	55.34	-55.34

For the Group 2 sample, the goal was to separate the settled solids after homogenization, rather than to collect a uniform composite. Thus, the entire lot of material was allowed to settle for about 91 hours (over the weekend).

Upon removing the lid covering the tank, it did appear that the mixture consisted of insoluble material in the bottom of the homogenizer tank with a clear supernatant as the fixed baffles of the tank interior could be seen clearly towards the bottom of the tank. There was also a very minor dark ring of material noted at the top of the liquid level, and the material appeared to be a dark bluish black color. Some very minor pieces of material were also floating on the top of the solution.

The intended procedure was to dispense the samples into the collection jars such that essentially all of the insoluble materials would be collected in the first three jars (volume to be about 600 mL total). As it turned out, this was not possible as the solids were quite fine and easily re-suspended. The procedure used to dispense the samples was to place a collection jar directly under the spout with the top lip of the jar close to the bottom of the spout so as to minimize any spattering/loss of sample. The operation was conducted with a secondary containment tray in place in case there was any sample spilled. The capacity of the collection jars was 250 mL, and the jars were marked with volume calibrations on the side and included matching bar codes on the lids and jars along with regular markings to clearly identify each cap and jar unit.

Dispensing of the sample into the first jar proved difficult. The solids that had settled to the bottom of the homogenizer tank plugged the ball valve so that there was very little flow of material initially, which had been considered a possibility. In anticipation of this possibility, a stainless steel probe was fabricated for this specific issue. The probe was used to prod the solids at the bottom of the tank to get flow of the material started. This proved to be successful.

It proved to be critically important to use a clean tray to serve as secondary containment. When trying to get the solids collected in the bottom neck of the homogenizer to loosen up so the material could flow freely out of the tank, the stainless steel probe became stuck in the valve, forcing it to stay open and thus overfilling the collection jar. About five jars worth of solution was spilled into the secondary containment tray before the probe was removed and the valve closed. However, all but about 20 mL of the homogenized sample solution was recovered from the containment tray, and the tray had been clean, so the integrity of the samples was not compromised. It was decided to let the rest of the sample in the tank settle for another day since the solids in the solution in the tank had become resuspended; during this course of action, the stainless steel spatula was also dropped into the tank with the remaining solution. Part of the wood handle on this spatula was submerged below the liquid level in the tank, but it was decided to leave this as it was in the tank rather than risk any further potential for contamination.

The remaining slurry of solids was moved out of the tank easily. Even though the probe, essentially a stainless steel rod of small diameter, was used primarily in a downward probing manner to minimize stirring and mixing of the solids, it become clear that the insoluble materials did become re-suspended into the solution. All the jars had some insoluble solids collected in them by the time the tank had been emptied, although the amounts of the solids did decrease steadily.

Data on the homogenized sample collection vessels are given in Table 2.9. Viewing the tank after all sample had been dispensed showed that essentially the entire sample had been dispensed to the sample jars, and there was a clear view through the opened ball valve to the floor of the hot cell; there was nothing entrained in the valve area (Figure 2.15). There was also no evidence of tank corrosion.

Table 2.9. Tare Weight, Sample Gross Mass, Slurry Volumes, and Settled Solids Volumes for Group 2 Bismuth Phosphate Saltcake Homogenized Samples

Jar ID	Tare (g)	Gross Mass (g)	Net Sample Mass (g)	Total Slurry Volume, mL	Settled Solids Volume, mL
TI487-G2-AR-J1	255.750	519.514	263.76	197	72
TI487-G2-AR-J2	253.220	494.993	241.77	200	40
TI487-G2-AR-J3	250.788	510.648	259.86	215	42
TI487-G2-AR-J4	254.067	513.114	259.05	208	35
TI487-G2-AR-J5	251.586	519.300	267.71	210	70
TI487-G2-AR-J6	251.830	489.416	237.59	187	53
TI487-G2-AR-J7	251.972	489.970	238.00	185	40
TI487-G2-AR-J8	252.269	497.419	245.15	190	50
TI487-G2-AR-J9	251.160	498.814	247.65	204	48
TI487-G2-AR-J10	249.120	496.972	247.85	200	47
TI487-G2-AR-J11	250.692	492.631	241.94	195	42
TI487-G2-AR-J12	249.218	494.290	245.07	200	35
TI487-G2-AR-J13	251.822	501.340	249.52	200	35
TI487-G2-AR-J14	249.745	488.428	238.68	200	30
TI487-G2-AR-J15	248.403	488.623	240.22	200	17
TI487-G2-AR-J16	249.847	499.055	249.21	200	45
TI487-G2-AR-J17	252.499	508.867	256.37	205	63
TI487-G2-AR-J18	252.740	464.437	211.70	175	45
TI487-G2-AR-J19	250.850	336.101	85.25	70	35
TI487-G2-AR-J20	249.823	265.610	15.79	15	5

Figure 2.15. Homogenizer Tank after Dispensing Composite Group 2 Sample

Sample jar TI487-G2-AR-J20A was used to collect the minor amount of dark ring material that had collected at the high solution mark in the homogenizer tank. Collection of this material showed that it would not settle after 3 days, and some of the insoluble material that had dried out looked very similar in coloration to the blue jar lids that were used on the sample storage jars in the hot cells in 222S. Because the appearance of several of the Group 2 samples seemed to suggest that they may have been previously

homogenized using a tissue homogenizer, it seems likely that these are pieces of jar lid that were also finely ground up during a previous homogenizing procedure. This would also explain the tendency of the fine bluish residue to float on top of the sample solution (density of the plastic would be less than the salt solution).

The solids in the jars were allowed to settle for 3 days, and then the volume of solids in each jar was determined using the graduated markings on the jars. The insoluble solids were dark brown while the supernate liquid was bright yellow. Even after settling for 3 days, it could be seen that the interface between the insoluble fraction and the supernate liquid was not rigid, although solids were not re-suspended by careful movement of the jars. The solids had a fair amount of the sample liquid entrained in that volume, and a process such as centrifugation would likely be required to get a more accurate assessment of the true volume of the insoluble fraction.

Following is a summary of Group 2 sample homogenization and sub-sampling:

- The total mass of Group 2 bismuth phosphate saltcake samples homogenized together was 1966 g.

- The total mixing time after all Group 2 bismuth phosphate saltcake samples had been added to the homogenizer tank, including a sufficient volume of water to bring the total volume to about 3 L, was 1 hour and 56 minutes at 27.1°C.

- The total mass of water used in this test was 2974 g based on the difference between the starting amount stored in the DI water containers and the amount remaining at the end of the test. The actual amount of water that actually was mixed in the tank was somewhat less because of the loss of water by spillage and evaporation.

- The total gross mass of the entire homogenized sample collected was 4542 g with a total slurry volume of 3656 mL. The volume of insoluble solids (gravity-settled) as described above was determined to be 849 mL.

- Sample overflowed the first collection jar while it was dispensed from the homogenizer tank, but it was recovered from a clean secondary containment tray that had been used in the procedure. All but about 20 mL of the sample solution was recovered.

- Sample jar TI487-G2-AR-J20A was used to collect the minor amount of dark ring material that had collected at the high solution mark in the homogenizer tank. Because the appearance of several of the Group 2 samples seemed to suggest that they may have been previously homogenized using a tissue homogenizer, it seems likely that these are pieces of jar lid that were also finely ground up during a previous homogenization procedure. This would also explain the tendency of the fine bluish residue to float on top of the sample solution (the density of the plastic would be less than the salt solution).

The total gross mass of the entire homogenized Group 2 bismuth phosphate saltcake sample collected was 1966 g sample + 2974 g water = 4940 g. The difference between that total mass and that actually collected in the final sample jars is 4940 - 4542 g = 398 g (8 % difference). The difference is likely due to evaporative losses of water, followed by loss of water through spilling during manipulations using the squirt bottle and dispensing water from the water-storage bottles. About 20 mL of sample was lost during problems dispensing sample from the homogenizer tank.

3.0 Group 1 Characterization and Leaching

This section reports on and discusses the characterization activities, analytical results, parametric leach testing, and leaching results for the Group 1 bismuth phosphate sludge slurry composite.

3.1 Group 1 Characterization Experimental

Table 3.1 lists the Group 1 characterization samples that were taken during the homogenization and sample splitting activities described in Section 2. Figure 3.1 summarizes the sample processing performed to characterize the Group 1 sample, and Figure 3.2 shows the specific washing scheme for the Group 1 sludge solids.

Table 3.1. Group 1 Characterization Samples

Sample ID	Characterization Activity	Slurry Volume, mL	Slurry Mass, g
TI508-G1-AR-S1	Physical Properties	8.3	9.745
TI508-G1-AR-S2	Physical Properties	13.0	15.818
TI508-G1-AR-S3	Physical Properties	16.5	19.785
TI508-G1-AR-C1	Chemical characterization and crystal habit	22.5	29.162
TI508-G1-AR-C2	Chemical characterization and crystal habit	37.5	48.513
TI508-G1-AR-RH1	Rheology	85	113.315
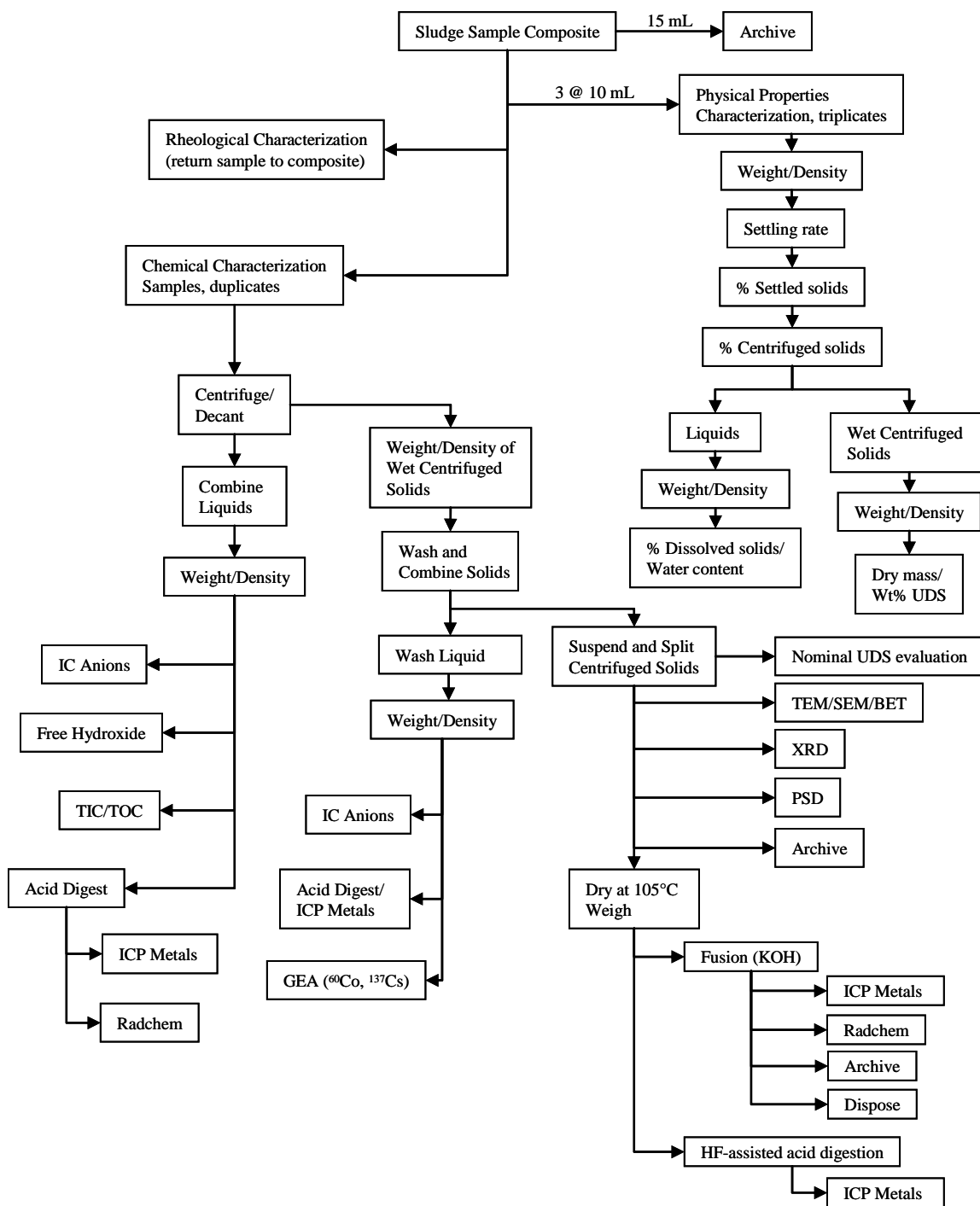
Figure 3.1. Group 1 Characterization Process Flowchart
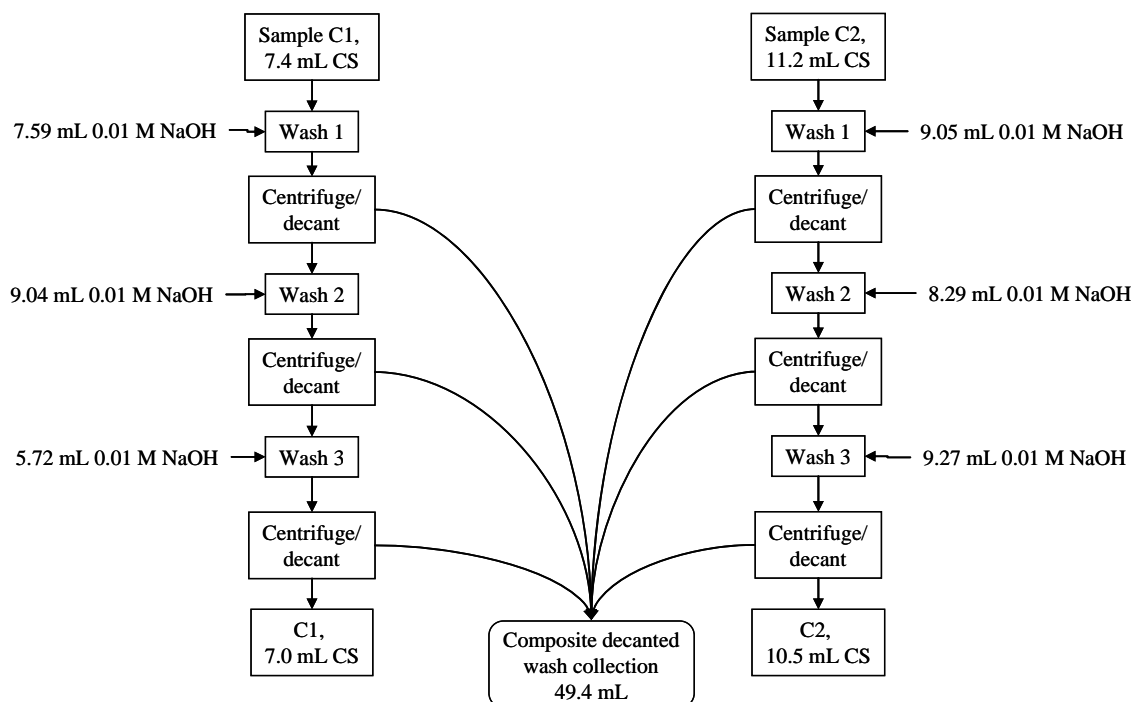
Figure 3.2. Wash Sequence of Group 1 Sludge Supporting Initial Characterization

(CS = centrifuged solids)

After each successive washing step, the wet centrifuged solids were stratified in three layers (see Figure 3.3). The whitest layer was apparently the densest layer. The middle layer was the darkest color. The top layer appeared light brown or tan.

3.2 Characterization Results

3.2.1 Physical Properties of the Composite Slurry

Figure 3.4 shows the settling curves for the Group 1 samples in two different manners: the volume percent of the settled solids as a function of time and the solids height as function of time. Precision between the triplicate tests was good. The solids settled rapidly during the first 6 h, but the settling rate slowed beyond that point. The initial settling rate was ~0.6 cm/h. The solids appeared to be completely settled after 48 h. The observed settling behavior is consistent with a slurry in which the initial solids loading is below the gel point, i.e., the

Figure 3.3. Centrifuged Solids for Chemical Characterization Sample of Group 1

point at which agglomerates interconnect to form a network (Rector and Bunker 1995). The change in the slope of the settling curve is approximately at a settled-solids volume of 70%. Based on an initial

undissolved solids loading of 9 wt% (Table 3.2), the gel point for this slurry is estimated to be 13 wt% (9 wt% ÷ 0.7).[a]
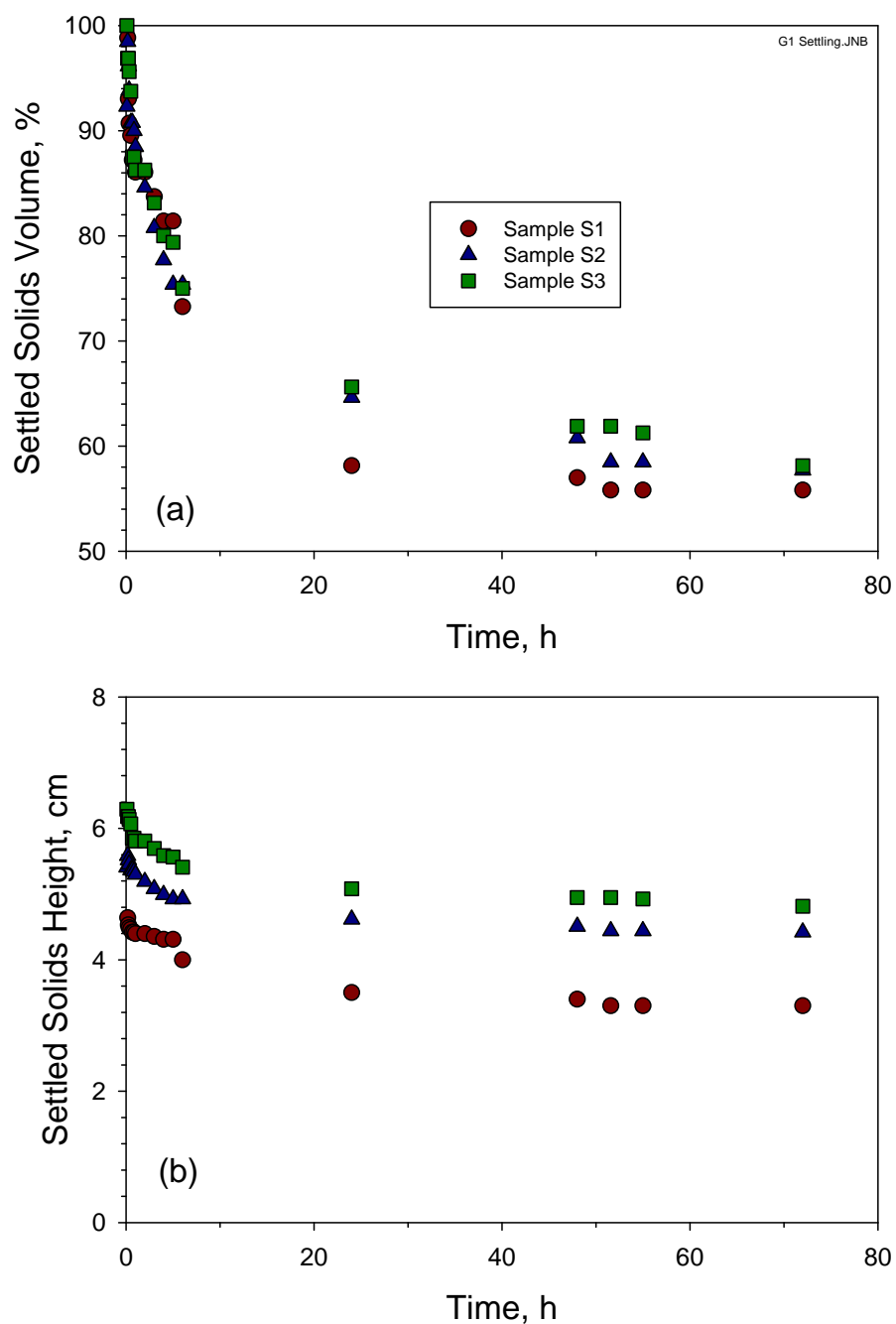
Figure 3.4. Group 1 Settling Curves: a) Volume Percent Settled Solids vs Time and b) Settled Solids Height vs Time

---

(a) This estimate of the gel point does not take into account the increasing density of the settled-solids layer as settling progresses.

Table 3.2 presents the physical properties of the Group 1 samples, including the propagated 1-σ error, the average values of the triplicate measurements, and the relative standard deviation. Good precision was obtained for the sample set.

Table 3.2. Physical Properties of Homogenized Group 1 Sludge

Description	AR-S1	AR-S2	AR-S3	Nominal 1σ error	Avg.	RSD[a] (%)
Bulk Sample						
Density (g/mL)	1.29	1.33	1.32	0.17	1.31	1.2
Total Solids (wt%)	31.5	34.7	32.5	0.047	32.9	5.0
Total Undissolved Solids (wt%)	7.1	11.4	8.4	0.05	9.0	25
Settled Solids						
Density (g/mL)	1.31	1.39	1.38	0.25	1.36	3.6
Vol% relative to the total sample volume	57	57.7	58.1	9.0	57.4	0.97
Wt% relative to the total sample weight	52.5	57.9	58.9	13	56.4	6.1
Total Undissolved Solids (wt%)	10.9	17.3	12.9	2.9	13.7	24
Wet Centrifuged Solids						
Density (g/mL)	1.36	1.43	1.46	0.22	1.41	2.1
Vol% relative to the total sample volume	37.3	37.8	34.9	7.4	36.7	4.1
Wt% relative to the total sample weight	39.4	40.8	38.8	0.04	39.6	2.6
Total Undissolved Solids (wt%)	18.1	26.4	20.8	7.2	21.8	19
Total Solids (wt%)	39.5	46.9	42.3	0.082	42.9	8.7
Supernatant						
Density (g/mL)	1.25	1.21	1.21	0.032	1.22	0
Total Dissolved Solids (wt%)	26.1	26.2	26.2	0.06	26.2	0.22
Water Content (g/g)	0.739	0.738	0.738	0.738	0.001	0.08
(a) RSD = relative standard deviation						

3.2.2 Rheology of the Composite Slurry

3.2.2.1 Shear Strength

A single measurement of shear strength was made on the settled solids in sample jar TI508-G1-AR-RH1. It was not possible to satisfy the geometric constraints for vane immersion because of the limited volume of settled solids (< 100 mL) in the test sample. As a consequence, the shear strength result is not independent of container geometry and may not even be representative of the actual shear strength of the settled solids. For this reason, no duplicate measurements were taken. The single value reported herein should be taken as a rough estimate of the shear strength of the settled Group 1 solids.

The settled solids in test jar TI508-G1-AR-RH1 were fully dispersed and allowed to settle undisturbed for 67 h before performing the shear strength measurement. The shear strength test was performed directly in the 250-mL Qorpak sample jars in which the slurry was provided. The shear strength was tested as follows (the measurements were conducted at the ambient cell temperature of ~24°C):

1. A 16 × 16 mm (diameter by height) shear vane tool was installed on the measuring head.

2. The sample jar being tested was opened and positioned on a laboratory jack stand directly beneath the measuring head/vane.

3. The laboratory jack was slowly raised until the top of the vane blades were just below the surface of the settled solids. For this sample, the volume of settled solids was just barely sufficient to fully immerse the vane without contacting the bottom of the container.

4. The vane was slowly rotated at 0.3 revolutions per minute (RPM) for 240 seconds. For the entire duration of rotation, the time, rotational rate, and vane torque were continuously monitored and recorded.

At the completion of testing, the vane was removed from the settled solids, rinsed clean of residual solids with deionzied (DI) water, and allowed to air dry before the next test. The sample jar was closed and set aside.

At the end of the measurement, the software parsed the shear stress versus time data and determined and reported the maximum measured shear stress (i.e., the material's shear strength). The curve of shear stress versus time was visually inspected using the RheoWin software to verify that the appropriate stress maximum was selected.

The single observation at 67 hours of settling time indicated that the shear strength of the settled Group 1 slurry was 15 Pa. Because the geometric constraints required for shear strength testing could not be met given the low settled solids volume, this result is an order-of-magnitude estimate only. The measured 15-Pa shear strength is relatively low. For comparison, Group 5 solids attained shear strengths of 72 Pa after 52 hours of settling (Fiskum et al. 2008). It should be noted that only the transient shear-strength behavior was observed for 2 to 3 days in accordance with the test plan. Again, the limited solids volume for the Group 1 sample prevented examining the shear strength at longer settling periods.

3.2.2.2 Flow Curve

Flow curve testing for both slurry and supernatant samples employed an MV1 cup and rotor (see Appendix B). Each flow curve measurement was accomplished as follows:

1. The MV1 rotor was installed on the measuring head.

2. The temperature jacket was installed and the recirculator turned on and set to 25°C. The jacket was allowed to achieve temperature equilibrium.

3. The test sample was transferred from its source jar into the MV1 measurement cup. The sample was added to the cup until the fluid level was above the first (i.e., lowest) cup level marker but still below the second level marker. This typically required 40 to 50 mL of sample. Gross material transfer was accomplished by pouring the sample into the test container until a rough estimate of the required sample volume was obtained. Fine-level adjustments were made by adding and removing material to and from the measuring cup using a plastic transfer pipette.

4. The measuring cup was installed into the water jacket by slowly raising it on a laboratory jack stand. The cup was raised until the test material was observed to spill over the top of the rotor. Before continuing, excess material was removed from the top of the rotor (to the extent possible) using a plastic transfer pipette. In most cases, there was approximately 1 to 3 mL of excess material that could not be removed from the upper rotor recess.

5. A moisture barrier was wetted and installed over the opening at the top of the temperature jacket. This barrier is a stainless steel clamshell collar lined with a sponge. It serves to minimize sample evaporation by blocking openings at the top of the water jacket (where the sample is exposed to air) and by humidifying the air space above the sample.

6. The sample was left undisturbed in the measuring system for 5 minutes to allow temperature equilibration.

7. The sample was sheared for 3 minutes to break the sample structure, to attempt to re-suspend any settled slurry particles, and to verify that the rotor was properly centered.

8. The material flow curve data were measured. Rheological analysis was performed over a 15-minute period, split into three 5-minute intervals. Over the first 5 minutes, the shear rate was smoothly increased from zero to 1000 s^{-1}. For the second 5 minutes, the shear rate was held constant at 1000 s^{-1}. For the final 5-minutes, the shear rate was smoothly reduced back to zero. During this time, the resisting torque and rotational rate were continuously monitored and recorded.

9. The flow curve data for 25°C were saved using the RheoWin file format and a unique filename identifier. Sample information and the associated RheoWin filename were entered into the laboratory record book (LRB).

10. The cup was raised so that fresh sludge/slurry filled the gap. Excess sludge was pipetted from the top. The moisture guard was removed, re-wetted, and then re-installed.

11. The flow curve measurement at 25°C was repeated as per steps 7 through 9.

12. The temperature set point was set to 40°C. Once the jacket had reached the temperature set point, the sample was allowed an additional 5 minutes to reach temperature equilibrium. The cup was raised so that fresh sludge/slurry filled the gap. Excess sludge was removed from the top using a pipette. The moisture guard was removed, re-wetted, and then re-installed.

13. The flow curve at 40°C was measured as per steps 7 through 9.

14. The temperature set point was set to 60°C. Once the jacket had reached the temperature set point, the sample was allowed an additional 5 minutes to reach temperature equilibrium. The cup was raised so that fresh sludge/slurry filled the gap. Excess sludge was removed from the top using a pipette. The moisture guard was removed, re-wetted, and then re-installed.

15. The flow curve at 60°C was measured as per steps 7 through 9.

At the end of testing, the measuring cup was removed from the system. The test material was returned to its original container. The measuring system was disassembled. Any slurry or precipitated salt solids remaining in the cup or rotor were cleaned-off by rinsing with copious amounts of water and by wiping down the instrument with a damp cloth.

Visual inspection of the Group 1 slurry before testing found no observable solids settling during transfer from sample jar to rheometer measurement cup. In addition, when performing Step 7, the rotor torques that were measured while mixing were constant. This indicated that for short periods of time, such as the

3-minute mixing step or the time required to transfer the sample to the measuring cup (~5 minutes), settling and shear history effects were minimal for the Group 1 slurry sample.

The RheoWin Pro Data Manager software, Version 2.96, was used for post-measurement analysis and review of flow-curve data. For each set of measurement data, the flow curve data were characterized by determining the best-fit parameters for the constitutive equation outlined in Appendix B of this report (i.e., the Newtonian, Power-Law, Bingham-Plastic, and Herschel-Bulkley flow models). This analysis used the least-squares data regression routine native to the RheoWin 2.96 software. Each regression included both up- and down-ramp portions of the flow curve, resulting in an "average" set of model parameters for the total flow curve. In certain cases, model fits were limited to specific shear rate ranges to avoid flow curve anomalies such as Taylor Vortices (at high shear rates) and slip (at low shear rates).

Figure 3.5 shows the results of flow curve testing for the Group 1 initial characterization slurry sample, TI508-G1-AR-RH1. The flow behavior is somewhat difficult to characterize. In some respects, this slurry appears to show slight non-Newtonian behavior. The basis for this conclusion is the small but finite yield stresses (~0.5 Pa) and the downward curvature in the 0 to 100 s^{-1} region observed in the flow curve at each temperature set point studied. On the other hand, the stress versus strain rate response is linear over 100 to 1000 s^{-1}. In addition, the yield stress is at the instrument sensitivity limit of 0.5 Pa (i.e., the yield stress may not be significantly different than zero) and the low shear curvature may be an artifact of poor sampling. Based on the latter arguments, it may be more appropriate to classify the flow behavior Newtonian. For the purposes of reporting herein, the flow behavior was treated using a Bingham-Plastic model to obtain parametric estimates for yield stress and consistency (or Newtonian viscosity, if the yield point was not significantly different than zero). A Herschel-Bulkley analysis of the flow curve data was also done to determine the degree of shear thinning or thickening.

Table 3.3 summarizes the best-fit rheological parameters for flow curve data for sample TI508-G1-AR-RH1. Bingham-Plastic fits consider shear rates from 200 to 1000 s^{-1} to avoid the strong downward curvature in the flow curve data from 0 to 100 s^{-1}. Herschel-Bulkley fits consider the entire range of shear rate studied. An example of the quality of the data fit that these parameters provide is shown in Figure 3.6, which shows both Bingham-Plastic and Herschel-Bulkley flow curve fits at 40°C. In terms of capturing the range of magnitude, curvature, slope, and yield, both Herschel-Bulkley and Bingham-Plastic equations provide roughly the same fit. Additionally, the fitting parameters confirm the observations made in the preceding paragraphs. Specifically, they show that, at 9 wt% UDS (Table 3.2):

- The Bingham-Plastic yield stresses typically range from 0.0 to 0.5 Pa. Given the typically ±0.5 Pa measurement limit for the M5 system, the measured yield stress is likely not significantly different than zero. Overall, this suggests that Group 1 waste slurries are Newtonian fluids with regards to our measurement capability.

The Herschel-Bulkley flow indices fall between 1.0 and 1.2, indicating that the flow curve curvature is minor and that the stress response to increased shear is linear (i.e., consistent with the Bingham-Plastic model).
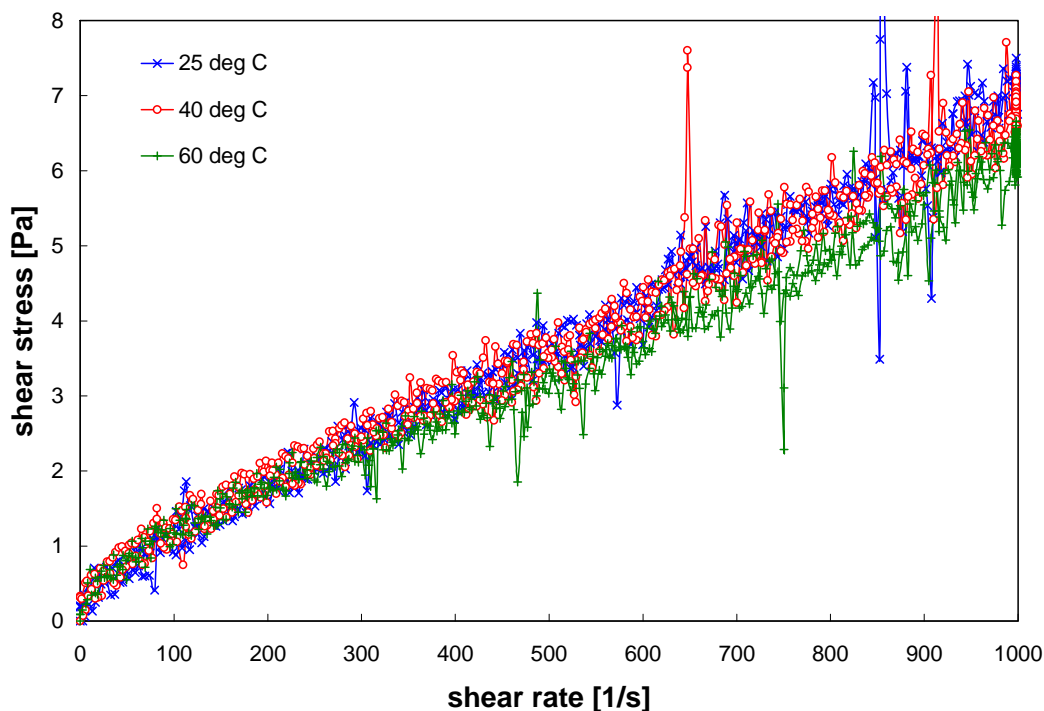
Figure 3.5. Flow Curve (shear stress versus shear rate) for the Group 1 Initial Characterization Slurry Sample TI508-G1-AR-RH1 at 25° C, 40° C, and 60° C. Note: the second repeat measurement for 25°C is shown here, as it is the closest to the 40° and 60°C measurements in time.

Table 3.3. Results of Fitting Analysis for Rheology Sample TI508-G1-AR-RH1

Model	Temperature [°C]	Yield Stress [Pa]	Consistency [Pa·s^n]	Flow Index	R
Bingham-Plastic (200 – 1000 s^{-1})	25 (1 of 2)	0.0	0.0064	n/a	0.992
	25 (2 of 2)	0.3	0.0067	n/a	0.993
	40	0.5	0.0063	n/a	0.989
	60	0.5	0.0056	n/a	0.991
Herschel-Bulkley (0 – 1000 s^{-1})	25 (1 of 2)	0.4	0.0014	1.2	0.994
	25 (2 of 2)	0.5	0.0044	1.1	0.993
	40	0.6	0.0056	1.0	0.989
	60	0.7	0.0027	1.1	0.991

In addition, the fitting results provide qualitative information on the stress response of the fluid and how it changes with temperature:

- The fluid consistency decreases from 6.7 cP to 5.6 cP as the temperature is increased from 25° to 60°C. Figure 3.5 confirms this observation, as the slope of the flow curve for the 60°C temperature is less than that at 25°C. This decrease is consistent with a decrease in suspending phase viscosity; however, changes in suspending phase viscosity with temperature are not necessarily the only physical mechanism by which the slurry consistency can be decreased.

- The apparent Bingham fluid yield stress increases with 0.0 to 0.5 Pa throughout the course of testing. This change may be the result of shearing effects, suspending phase evaporation, temperature increases, or some combination thereof. However, the final estimated yield stress of 0.5 Pa is still not significant.

Both Bingham yield and consistency of the replicate measurement at 25°C are within the ±0.5 Pa and ±0.5 cP stress and consistency fitting limits for the instrument. In other words, the replicate measurement confirms the primary measurement. This, combined with the absence of flow curve hysteresis (even at 60°C, where hysteresis is typically observed for slurry samples), indicates that evaporation does not significantly impact the Group 1 rheological properties.
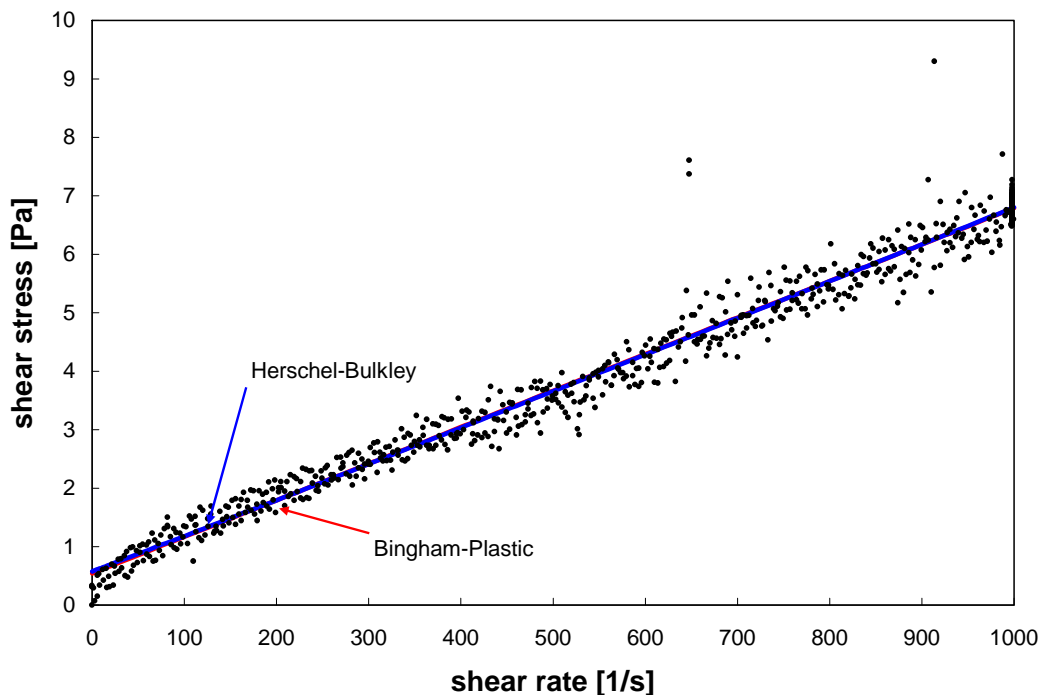
Figure 3.6. Model Fits of Flow Curve Data for Group 1 Initial Characterization Slurry Sample TI508-G1-AR-RH1 at 40 °C. Both model fits consider the full shear rate range of 0 to 1000 s^{-1}.

For ease of reference, apparent viscosities at 33 s^{-1}, 100 s^{-1}, 500 s^{-1}, and 1000 s^{-1} were derived from each measurement. For each temperature, the 33 s^{-1}, 100 s^{-1}, and 500 s^{-1} reference viscosities were determined from the average of up-ramp and down-ramp flow curve data. The apparent viscosity at 1000 s^{-1} averages apparent viscosity measurements over the period of constant rotation at 1000 s^{-1}. As a point of comparison, apparent viscosities at 33 s^{-1}, 100 s^{-1}, 500 s^{-1}, and 1000 s^{-1} were also calculated using the Bingham-Plastic and Herschel-Bulkley fitting parameters in Table 3.3. The results of these analyses are provided in Table 3.4 and show that apparent viscosities typically range from 6.7 to 26 cP at 33 s^{-1}, 6.5 to 12 cP at 100 s^{-1}, 5.5 to 7.4 cP at 500 s^{-1}, and 6.2 to 7.1 cP at 1000 s^{-1}.

Table 3.4. Apparent Viscosity of Sample TI508-G1-AR-RH1

Source	Temperature [°C]	Apparent Viscosity [cP]			
		@ 33 s⁻¹	@ 100 s⁻¹	@ 500 s⁻¹	@ 1000 s⁻¹
Measured	25 (1 of 2)	13	8.5	5.5	6.5
	25 (2 of 2)	16	11	7.2	7.1
	40	22	12	7.1	6.8
	60	20	11	6.4	6.2
Bingham-Plastic	25 (1 of 2)	6.7	6.5	6.4	6.4
	25 (2 of 2)	17	10	7.4	7.0
	40	23	12	7.3	6.8
	60	21	11	6.7	6.2
Herschel-Bulkley	25 (1 of 2)	16	8.1	6.1	6.5
	25 (2 of 2)	20	11	7.3	7.1
	40	23	12	7.3	6.8
	60	26	12	6.5	6.2

In summary, visual inspection of flow curves for Group 1 initial characterization slurry sample, TI508-G1-AR-RH1, suggests rheological properties consistent with a Bingham Plastic model; however, the yield stress is sufficiently low that the rheometer used for the current measurements cannot qualitatively distinguish the rheology from that of a Newtonian fluid. Regression analysis of the flow curve data finds Bingham-Plastic yield stresses that range from 0.0 to 0.5 Pa with an associated uncertainly of ±0.5 Pa, indicating that they are not distinguishable from zero. Bingham-Plastic consistencies for the slurry range from 6.4 cP at 25°C to 5.6 cP at 60°C. Flow curve hysteresis effects were not observed, which indicates that evaporation of the suspending phase does not noticeably increase slurry viscosity over time.

3.2.3 Chemical and Radiochemical Composition

The two samples of the Group 1 composite taken for chemical characterization were evaluated for volume-percent centrifuged solids as part of the initial phase separation. In this case, the volume-percent centrifuged solids duplicated well at 31 vol%, but was slightly less than the 37% centrifuged solids found with the physical-property testing samples. Centrifuging conditions were the same in each case; however, the centrifuge cones were constructed of different materials: polypropylene for the characterization samples and glass for the physical-property test samples.

The supernatant density was determined to be 1.193 g/mL (T = 28°C) based on the average masses of four 1-mL volume deliveries. This compared well with the density determined as part of the physical-property testing procedure (density = 1.2 g/mL). The density of the composite washing solution was 1.063 g/mL. The volumes of the supernatant liquid and the washing solution were 41.91 and 49.46 mL, respectively, and the mass of the washed solids on a dry weight basis was 6.387 g.

The average radioanalytical results for the supernatant, composited wash solution, and washed solids are provided in Table 3.5 along with the applicable relative percent differences (RPD, measure of precision between duplicates). The gross-beta results showed good agreement with the sum of beta emitters: ^{137}Cs and ^{90}Sr (in secular equilibrium with ^{90}Y) thus indicating that no other major source of beta-gamma activity was present. The gross-alpha activity in the supernatant liquid was below the method detection limit. The gross-alpha activity measured in the solids agreed with the summation of alpha emitters (^{238}Pu,

$^{239+240}$Pu, and ^{241}Am). The fusion blank processed with the washed solids contained ^{60}Co and ^{238}Pu contamination. The ^{60}Co contamination in the blank was equivalent to the sample concentration and should be considered an upper bound. The ^{60}Co concentration was 3 times lower than the detection limit defined in the test plan (3.0E-2 μCi/g). The ^{238}Pu activity concentration in the process blank represented 40% of the sample activity; because sample contamination could not be ruled out, the reported value is provided for information only and should be considered an upper bound.

Table 3.5. Radionuclide Characterization of the Group 1 Sludge

	Supernatant		Wash Composite		Washed Solids	
Sample ID>	07-01714		07-01715		07-01716	
Analyte	μCi/mL	RPD	μCi/mL	RPD[a]	μCi/g[b]	RPD
^{137}Cs	3.56E+0	1.69	8.07E-1	na	2.19E+1	1.4
^{60}Co	<6.E-5	na	5.31E-5	na	9.59E-3[c]	25
^{241}Am	<3.E-3	na	<3.E-4	na	5.87E-2	24
^{238}Pu	<1.E-6	na			1.02E-2[d]	44
$^{239+240}$Pu	3.90E-5	14			5.64E-1	0.71
^{90}Sr	8.40E-4	4.9			3.95E+1	1.0
Gross alpha	<7.E-4	na	na		6.31E-1	8.7
Sum of alpha	na	na			6.33E-1	0.87
Gross beta	3.64E+0	3.6			1.07E+2	0.94
Sum of beta	3.56E+0	1.7			1.01E+2	1.09
Opportunistic						
^{154}Eu	<2.E-4	na	<9.E-6	na	<5.E-3	na
^{155}Eu	<2.E-3	na	<2.E-4	na	<2.E-2	na

ASR 7985; Reference date is July 15, 2007.
(a) This sample was not required to be run in duplicate; therefore, an RPD was not calculated.
(b) Analyte concentrations are calculated on a dry-mass basis.
(c) High analyte activity was found in the process blank; the ^{60}Co in the blank was equal to the sample concentration. The sample concentration was a factor of three lower than contracted detection limit, and thus, it is reported for information only and should be considered an upper bound.
(d) High analyte activity was found in the process blank; the ^{238}Pu in the blank was 40% of the sample concentration. The sample concentration was a factor of 10 higher than the contracted detection limit, and thus is reported for information only and should be considered an upper bound.
Notes: na = not applicable

The chemical composition of the washed Group 1 solids is provided in Table 3.6. The supernatant liquid consisted primarily of sodium nitrate with minor contributions of other sodium salts (sulfate, phosphate, and nitrite). The free-hydroxide concentration in the supernatant liquid was very low. The anionic and cationic charge balance was evaluated for the supernatant, resulting in a relative 6.0% difference, well within analytical uncertainties. Agreement between the total S and P values (determined by inductively coupled plasma-optical emission spectrometry [ICP-OES]) and SO_4^{2-} and PO_4^{3-} (determined by ion chromatrography [IC]) were well within the analytical uncertainties.

Table 3.6. Chemical Characterization of the Group 1 Test Material

	Supernatant			Wash Composite			Washed Solids[a]			
Sample ID:	**07-01714**			**07-01715**			**07-01716**			
	Acid Digestion			**Acid Digestion**			**KOH Fusion**		**Acid Digestion**[b]	
Analyte	µg/mL	M	RPD	µg/mL	M	RPD	µg/g	RPD	µg/g	RPD
Al	<3.77	<1.4E-4	na	<3.75	<1.4E-4		26,350	0.4	28,450	2.5
B	[9.4]	[8.7E-4]	[8.5]	[5.1]	[4.7E-4]		[130]	[31]	na	na
Bi	<2.29	<1.1E-5	na	<2.28	<1.1E-5		98,200	1.0	108,000	1.9
Cd	<0.24	<2.2E-6	na	<0.24	<2.1E-6		<7	11	<3	na
Cr	26.0	4.99E-4	1	8.46	1.63E-4		4,260	0.5	5,905	17.8
Fe	<2.05	<3.7E-5	na	<2.04	<3.6E-5		85,550	0.8	105,500	10.4
K	[85]	2.16E-3	6	[22]	[5.6E-4]		na		<350	na
Mn	<0.21	<3.8E-6	na	<0.20	<3.7E-6	na	373	20	482	21.0
Na	89,300	3.88E+0	2.46	27,400	1.19E+0		146,000	0	151,500	3.3
Ni	<0.58	<9.9E-6	na	<0.58	<9.9E-6		na		892	44.5
S	5,360	1.67E-1	0.9	1,620	5.05E-2		[3,250]	[9]	[2,950]	[3]
Si	12.6	4.5E-4	2	[7.1]	[2.5E-4]		42,850	5	na	na
Sr	<0.017	<1.9E-7	na	<0.017	<1.9E-7		888	0.5	980	3.1
U	<8.41	<3.5E-5	na	<8.35	<3.5E-5		[7,800]	[3]	10,850	8.3
Zn	[2.51]	[3.8E-5]	[151]	[0.69]	[1.1E-5]		[380]	[0]	536	32.7
Zr	<0.81	<8.9E-6	na	<0.81	<8.8E-6		[205]	[24]	373	7.0
U KPA			na				11,400	2	na	na
nitrite	2,820	6.13E-2	0.7	822	1.79E-2					
nitrate	198,500	3.20E+0	0.50	57,900	9.34E-1					
phosphate	14,800	1.56E-1	0.0	5,870	6.18E-2	na			na	
sulfate	14,800	1.54E-1	0.00	4,490	4.67E-2					
oxalate	[36]	[4.1E-4]	na	[12]	[1.4E-4]					
free OH⁻	<160	<1.E-3	na							
TOC as C	66	5.5E-3	6.1				na			
TIC as C	140	1.2E-2	14.3							
Opportunistic										
fluoride	521	2.74E-2	1.34	482	2.54E-2	na			na	

Table 3.6 (Contd)

Analyte	Supernatant 07-01714 Acid Digestion µg/mL	M	RPD	Wash Composite 07-01715 Acid Digestion µg/mL	M	RPD	Washed Solids[a] 07-01716 KOH Fusion µg/g	RPD	Acid Digestion[b] µg/g	RPD
chloride	1515	4.27E-2	0.66	445	1.26E-2					
Ag	<0.42	<3.9E-6	na	<0.42	<3.9E-6		<14	na	<5	na
As	<7.0	<9.3E-5	na	<7.0	<9.3E-5		<230	na	<85	na
Ba	<0.34	<2.5E-6	na	<0.34	<2.5E-6		[54]	[4]	60.7	4.0
Be	<0.012	<1.3E-6	na	<0.012	<1.3E-6		<1	na	<0.2	na
Ca	[2.6]	[6.5E-5]	[38]	<2.1	<5.2E-5		<2600	na	1,790	7.3
Ce	<1.2	<8.6E-6	na	<1.2	<8.5E-6		<170	na	175	[74]
Co	[0.58]	[9.8E-6]	[12]	<0.39	<6.5E-6		<18	na	[18]	[33]
Cu	<0.49	<7.6E-6	na	<0.48	<7.6E-6		[59]	[39]	82.1	10.1
Dy	<0.35	<2.2E-6	na	<0.35	<2.2E-6		<44	na	<4	na
Eu	<0.11	<7.2E-7	na	<0.11	<7.1E-7		<14	na	<5	na
La	<0.13	<9.6E-7	na	<0.13	<9.5E-7		<9	na	<2	na
Li	[3.95]	[5.7E-4]	[13]	[2.5]	3.60E-4		<27	na	[60]	[13]
Mg	[0.78]	[3.2E-5]	[20]	<0.70	<2.9E-5		[900]	[2]	942	5.1
Mo	[1.55]	[1.6E-5]	[19]	<0.65	<6.8E-6		<25	11	[15]	[21]
Nd	<1.7	<1.2E-5	na	<1.7	<1.2E-5		<260	na	[28]	[4]
P	4,720	1.52E-1	1.27	1,870	6.04E-2		81,300	na	90,700	4.2
Pb	<3.7	<1.8E-5	na	<3.7	<1.8E-5		[285]	[4]	579	0.9
Pd	<1.3	<1.2E-5	na	<1.3	<1.2E-5		<160	na	<15	na
Rh	<2.5	<2.5E-5	na	<2.5	<2.4E-5	na	<100	na	<31	na
Ru	<0.82	<8.1E-6	na	<0.82	<8.1E-6		<44	na	<10	na
Sb	<3.2	<2.6E-5	na	<3.1	<2.6E-5		<150	na	<38	na
Se	<4.9	<6.2E-5	na	<4.9	<6.2E-5		<250	na	<60	na
Sn	<2.0	<1.7E-5	na	<2.0	<1.7E-5		<230	na	[26]	na
Ta	<1.3	<7.4E-6	na	<1.3	<7.3E-6		<50	na	<16	na
Te	<3.2	<2.5E-5	na	<3.1	<2.5E-5		<200	na	<39	na
Th	<1.2	<5.1E-6	na	<1.2	<5.1E-6		<150	na	<14	na
Ti	<0.10	<2.0E-6	na	<0.10	<2.0E-6		[45]	na	64.1	11.4
Tl	<6.1	<3.2E-5	na	<6.5	<3.2E-5		<180	na	<79	na
V	<0.32	<6.2E-6	na	<0.31	<6.1E-6		<12	na	<4	na
W	<1.5	<8.2E-6	na	<1.5	<8.1E-6		<78	na	<18	na
Y	<0.08	<9.6E-7	na	<0.08	<9.5E-7		<17	na	<1	na

(a) Analyte concentrations are calculated on a dry-mass basis.

(b) The solids acid digestion results were "J" flagged or estimated because of uncertainties associated with the dry-mass measurement. ASR 7985.

Analyte uncertainties were typically within ±15% (2-σ); results in brackets indicate that the analyte concentrations were less than the minimum detection limit (MDL) and greater than the estimated quantitation limit (EQL), and uncertainties were >15%.

Opportunistic analytes are reported for information only; QC requirements did not apply to these analytes.

3.14

Major constituents in the washed solids were sodium, iron, phosphorus, and bismuth. Aluminum, uranium, and chromium provided minor contributions to the mass of the washed solids. Overall good agreement was obtained between the two different sample preparation methods (potassium hydroxide [KOH] fusion and acid digestion). The U results between kinetic phosphorescence analysis (KPA) of the fusion preparation and the ICP-OES analysis of the acid digestion agreed well.

The fractional distribution of selected analytes between the supernatant, wash, and solids phases is shown in Table 3.7 and Figure 3.7. A large portion of the Na (85%) and S (as sulfate, 94%) partitioned to the aqueous phase as a result of the initial contact with water during homogenization and the continued water washing. The Al and Cr remained primarily in the solids phase. Phosphorus was split between the aqueous and solids phases.

The total P concentrations in the supernatant and wash solutions determined by ICP-OES were equivalent to the phosphate concentrations determined by IC. Likewise, the total S concentrations were equivalent to the sulfate concentrations. Therefore, the mobilized forms represented the water-soluble sulfate and phosphate salts. The forms of S and P in the solids were not determined. For most analytes, the concentration in the wash composite was ~30% of that in the supernatant. However, the phosphate (and total P) concentration in the wash composite was ~40% of that in the supernatant liquid, indicating that some phosphate was further dissolved as a result of water washing.

The Cr, Na, Al, P, and S water-wash factors (analyte fraction in combined aqueous phases) obtained from the current testing were compared with B-104 water-wash factors obtained from the TWINS database. The experimental wash factors generally agreed with those provided in the TWINS database.

Table 3.7. Phase Distribution of Selected Analytes in Group 1

Analyte	Supernatant %	Wash Solution %	Solids %	Water-Wash Factor %	TWINS Water-Wash Factor[a] %
Cr	3.8	1.5	94.8	5.2	3
Al	<0.1	<0.1	99.8	0.2	1.6
Na	62.1	22.5	15.5	84.5	93
P	24.4	11.4	64.1	35.9	45[b]
S	69.0	24.6	6.4	93.6	92[c]
(a) The water-wash factors are represented by B-104 (2/29/08 query of TWINS database).					
(b) Phosphate water-wash factor.					
(c) Sulfate water-wash factor.					
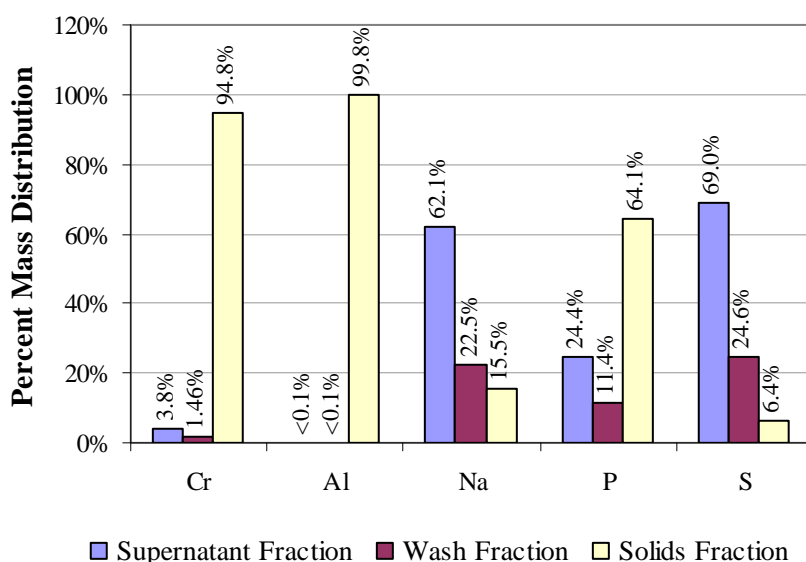
Figure 3.7. Selected Analyte Phase Distribution for Group 1

3.2.4 Particle Size

Figure 3.8 through Figure 3.10 and Table 3.8 and Table 3.9 present the results of Group 1 initial characterization particle-size analysis as a function of test conditions. Figure 3.8 through Figure 3.10 show the differential volume population distribution for the primary Group 1 initial characterization sample (see Appendix E for the duplicate sample results) and allow a qualitative examination of the particle-size distribution (PSD) behavior with respect to pump speed and sonication. Table 3.8 is a summary of the measured oversize diameter percentiles (by volume/weight) for the primary, TI483-G1-S-WL-PSD-1. Table 3.9 presents the analogous data for the duplicate standard, TI483-G1-S-WL-PSD-2. Both tables present cumulative oversize diameters corresponding to the 10th, 50th, and 90th volume/weight percentiles, hereafter referred to as d(10), d(50), and d(90), respectively. More extensive percentile results are provided in Appendix F. These tables will be used to quantitatively examine reproducibility and changes in particle size.

Figure 3.8 shows the PSD for the primary Group 1 initial characterization sample as a function of pump speed before sonication. The distribution of particles is broad, ranging from 0.3 to 100 μm and peaks near 10 μm. Although a small shoulder is visible near 2 μm, the distribution is relatively continuous. The size distribution of particles and particle aggregates before sonication is not significantly affected by changes in pump speed. From this, we may conclude that Group 1 solids are stable with respect to transient effects, such as shear-induced agglomeration, and mechanical effects, such as shear break-up of particle aggregates. Because a significant increase in the population of very large particles (10 to 100 μm) does not occur as pump speed is increased, it may be tentatively concluded that most (if not all) Group 1 solids are dispersed by the analyzer pump and sampled in the current set of analyses.
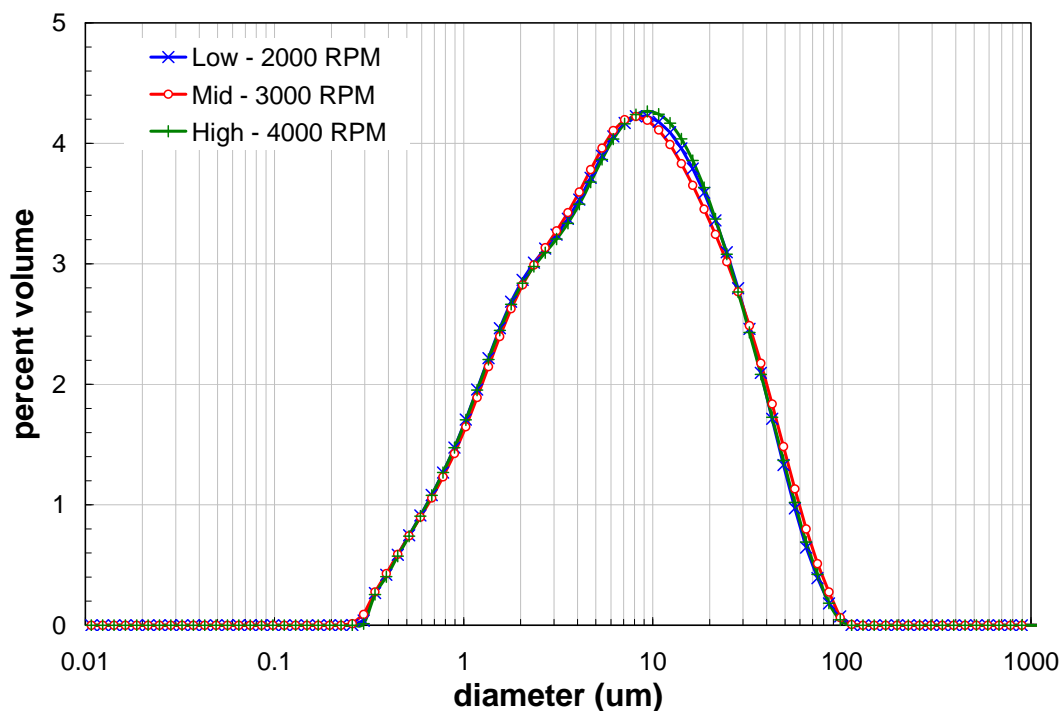
Figure 3.8. Pre-Sonication Volume Distribution Result for the Primary Group 1 Initial Characterization
Sample as a Function of Pump Speed

Figure 3.9 shows the PSD for the washed Group 1 solids as a function of sonication. This figure indicates
that sonication does not alter the range of the PSD, as it still spans 0.3 to 100 μm, but does shift the
population to smaller diameters. Specifically, sonication decreases the volume of 10- to 100-μm particles
while increasing the volume of the "shoulder" (i.e., 0.3 to 4 μm) particles. This change could result from
sonic disruption (breakup) of particle aggregates.

Figure 3.10 shows the primary Group 1 initial characterization PSD as a function of pump speed after
being sonicated. As with the distribution before sonication, changes in pump speed to not appear to
significantly change the distribution. Based on this observation, it can be concluded that the particles are
still stable with respect to mechanical (shear-induced) break-up even after sonication. Transient changes
in the PSD are also minor. Indeed, the disruption of large particles as a result of sonication is permanent
within the time scale of the measurement as the 10- to 100-μm particle population does not recover in any
of the post-sonication distributions.
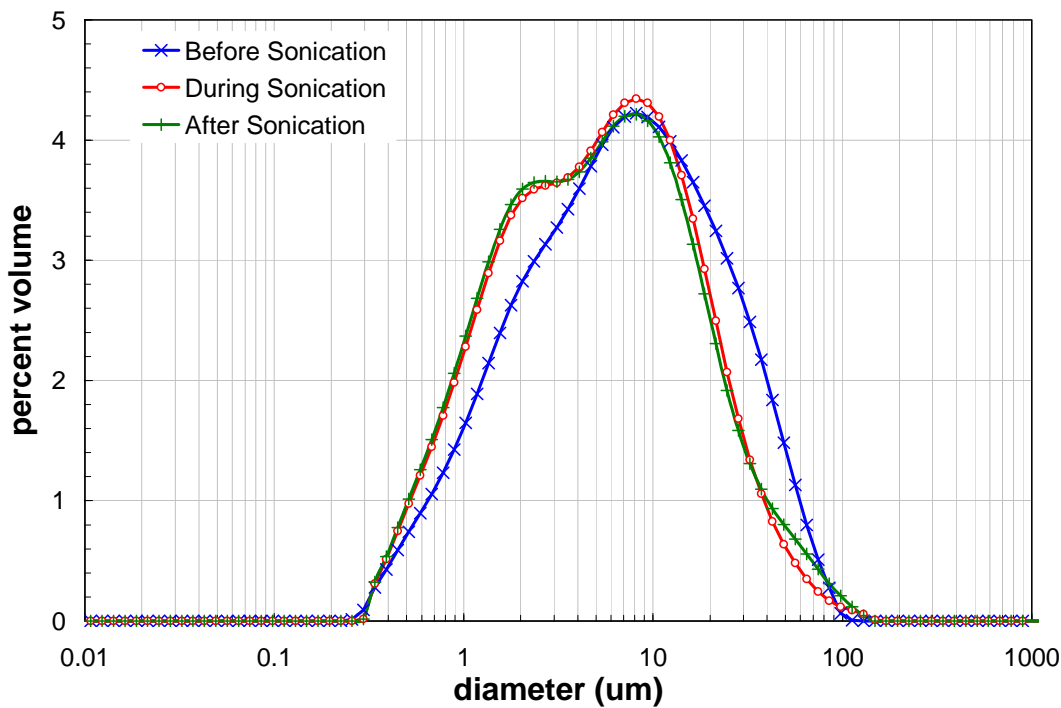
Figure 3.9. Volume Distribution Result for the Primary Group 1 Initial Characterization Sample as a Function of Sonication (75% power)
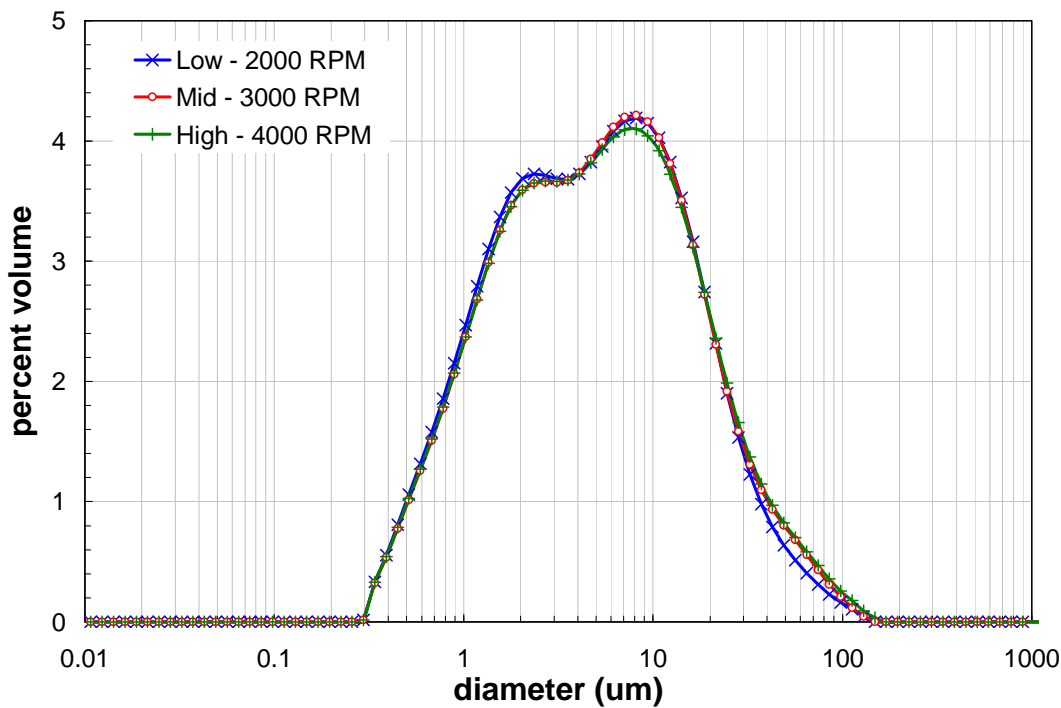
Figure 3.10. Post-Sonication Volume Distribution Result for the Primary Group 1 Initial Characterization Sample as a Function of Pump Speed

Using the results in Table 3.8 (i.e., those of the primary sample) as a reference, the behavior of Group 1 initial characterization particle size as a function of pump speed and sonication can be quantitatively evaluated. Specifically, the following observations can be made:

- In general, the d(10) falls between 0.97 and 1.2 μm, the d(50) between 5.0 and 7.0 μm, and the d(90) between 21 and 31 μm.

- The listed diameter percentiles appear to be relatively insensitive to changes in pump speed, both before and after sonication. Changes in the distribution that occur as flow rate is first decreased from 3,000 to 2,000 RPM and subsequently increased to 4,000 RPM are below the limit of accuracy (10%) for the measurement.

Sonication of the Group 1 solids dispersion decreases particle size. With reference to the measurements at 3,000 RPM, sonication lowers the mean particle size [i.e., the d(50)] from 6.9 to 5.0 μm. This represents a decrease of ~27% in the mean particle size as a result of sonication.

Table 3.8. Particle-Size Analysis Percentile Results of the Primary Group 1 Initial Characterization Sample, TI483-G1-S-WL-PSD-1

Measurement Condition	Pump Speed	Sonication	d(10) [μm]	d(50) [μm]	d(90) [μm]
1	3000	pre-sonic	1.2	6.9	31
2	2000	pre-sonic	1.2	6.9	30
3	4000	pre-sonic	1.2	7.0	30
4	3000	25%	1.2	6.4	26
5	3000	50%	1.1	5.8	24
6	3000	75%	1.0	5.2	22
7	3000	post-sonic	1.0	5.0	23
8	2000	post-sonic	0.97	4.8	21
9	4000	post-sonic	0.99	5.0	24

Table 3.9. Particle Size Analysis Percentile Results of the Duplicate Group 1 Initial Characterization Sample, TI483-G1-S-WL-PSD-2

Measurement Condition	Pump Speed	Sonication	d(10) [μm]	d(50) [μm]	d(90) [μm]
1	3000	pre-sonic	1.1	5.7	28
2	2000	pre-sonic	1.1	5.7	26
3	4000	pre-sonic	1.1	6.0	29
4	3000	25%	1.0	5.3	22
5	3000	50%	0.99	5.0	21
6	3000	75%	0.94	4.6	19
7	3000	post-sonic	0.92	4.5	21
8	2000	post-sonic	0.90	4.3	20
9	4000	post-sonic	0.92	4.6	24

The behavior of the duplicate sample PSD with respect to pump speed and sonication mirrors and confirms that of the primary sample. However, the PSD of the duplicate sample is consistently lower than that of the primary at equivalent measurement conditions. Table 3.10 shows the absolute relative percent difference between the d(10), d(50), and d(90) values determined for the primary and duplicate Group 1 initial characterization samples. Here, absolute relative percent difference is determined using the following equation:

$$RPD = \left| \frac{d_d(n) - d_p(n)}{d_p(n)} \right|$$
(3.1)

where $d_p(n)$ and $d_d(n)$ are the primary and duplicate cumulative oversize diameters corresponding to the nth percentile. The listed RPDs indicate that there is a slight difference between samples.

Table 3.10. Absolute Relative Percent Difference Between Primary and Duplicate Group 1 Initial Characterization Samples

Measurement Condition	Pump Speed	Sonication	Absolute RPD		
			d(10)	d(50)	d(90)
1	3000	pre-sonic	12%	17%	12%
2	2000	pre-sonic	12%	18%	13%
3	4000	pre-sonic	10%	14%	4.1%
4	3000	25%	11%	16%	13%
5	3000	50%	9.4%	14%	12%
6	3000	75%	8.4%	12%	13%
7	3000	post-sonic	7.9%	10%	6.8%
8	2000	post-sonic	8.0%	11%	7.9%
9	4000	post-sonic	7.5%	8.3%	2.3%

For particle-size measurements on the Malvern Mastersizer 2000, RPDs of up to 10% are generally expected given the accuracy of the instrument. The results for Group 1 initial characterization samples show RPDs that range from 2 to 18%, depending on the measurement condition and percentile examined. Based on the large number of RPDs greater than 10% in Table 3.10, it is likely that there is a significant size difference in the solids species in the primary and duplicate sample. It should be noted, however, that the largest differences affect only the before- and during-sonication measurement conditions. In contrast, post-sonication RPDs generally fall below 10%, indicating that sonication eliminates any size difference between the samples. As such, it can be postulated that the differences in particle size observed before sonication derive from differences in the state of solid particle aggregation (i.e., apparent particle size) between the primary and duplicate sample rather than an actual difference in the actual size of the solids sampled.

Figure 3.11 and Figure 3.12 show how the differences in the primary and duplicate PSDs described in the preceding paragraphs manifest in the differential volume distributions. The primary and duplicate samples, both before and after sonication (Figure 3.11 and Figure 3.12, respectively), show roughly the same distribution of particles. Specifically, both pre-sonication samples show distributions ranging from 0.3 to 100 μm with peak populations between 6 and 10 μm and a shoulder over 2 to 3 μm. Both post-sonication distributions show a more strongly bimodal distribution with peaks at ~2 and ~8 μm.
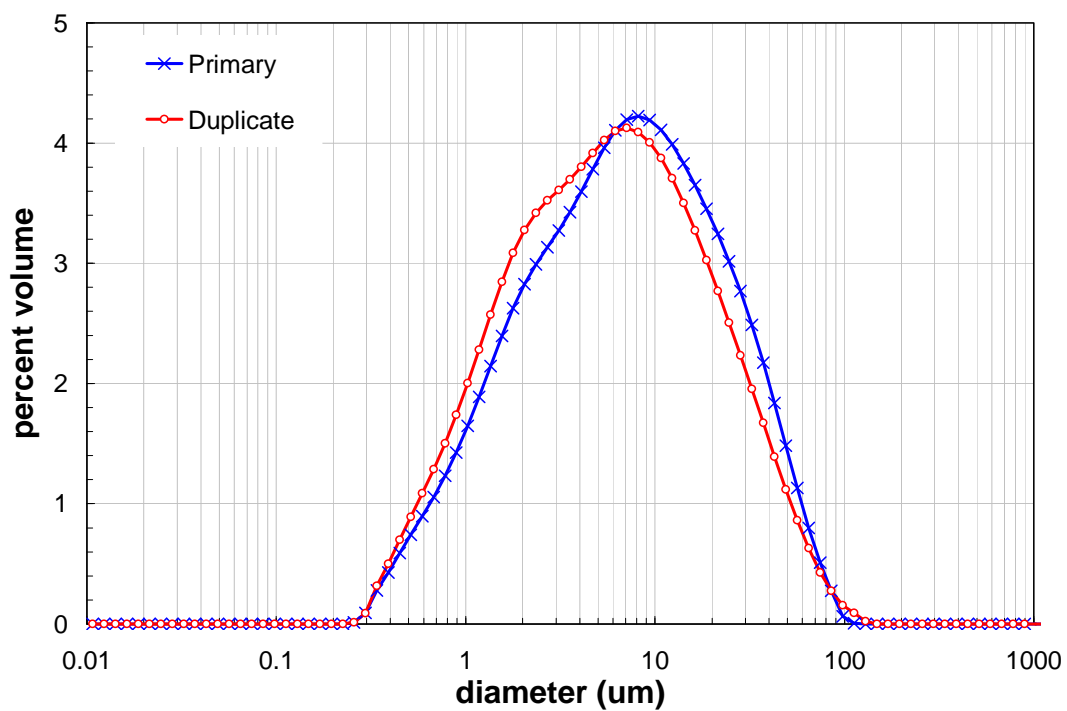
Figure 3.11. Comparison of Primary and Duplicate Sample Differential Volume PSD at 3,000 RPM Before Sonication for the Group 1 Solids
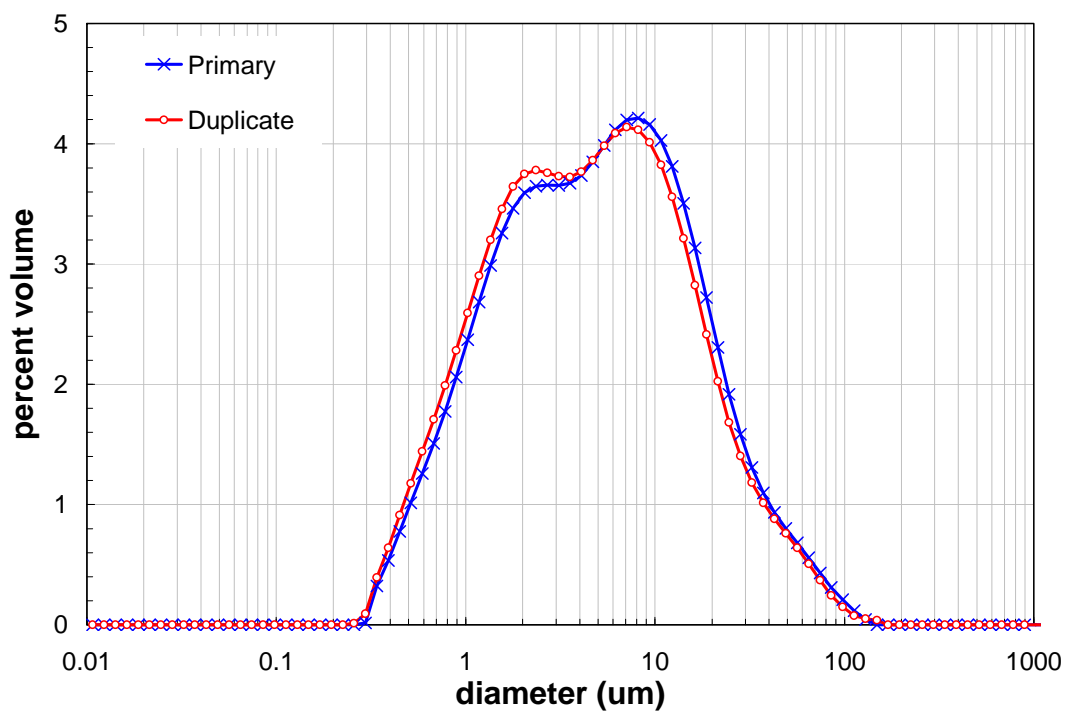
Figure 3.12. Comparison of Primary and Duplicate Sample Differential Volume PSD at 3,000 RPM After Sonication for the Group 1 Solids

In summary, particle-size analysis of Group 1 bismuth phosphate sludge samples derived from initial characterization efforts indicates a broad distribution of solids particle sizes ranging from 0.3 μm to 100 μm. The initial distribution of solids is nearly uni-modal, with a peak population near 10 μm and a small shoulder at 4 μm. Changes in the pump speed used to disperse the solids during analysis did not significantly change the PSD observed, indicating 1) that the state of particle aggregation for Group 1 solids is stable with respect to shear and 2) that most of the Group 1 solids were adequately dispersed (and as such, well-sampled) by the measurement apparatus. The application of sonic energy to the dispersion significantly reduced the particle size, affecting an ~27% reduction in the mean diameter of the dispersion. This reduction is likely caused by the break-up of 10- to 100-μm particle aggregates. This break-up appears to be irreversible, as a recovery of the 10- to 100-μm particle population was not observed after dispersion sonication was stopped. After sonication, the distribution is more strongly bimodal with population peaks at 2 and 8 μm.

3.2.5   Surface Area

Samples were analyzed in duplicate for surface area by Brunauer, Emmett, and Teller (BET), each with a nominal ~0.11-g sample size. The results, 96 and 93 m^2/g, demonstrated excellent precision.

3.2.6   Crystal Form and Habit

The X-ray diffraction (XRD) pattern for Group 1 washed solids is provided in Figure 3.13; the background-subtracted XRD pattern with stick-figure phase identification is shown in Figure 3.14. The raised background associated with the raw data diffraction pattern indicated the material had a significant amorphous component. The sample material was difficult to grind (sample grinding is required for powder XRD analysis), indicative of a hard, dense material. The final sample mount showed some granular particles, indicating incomplete pulverization of the sample. For the best results in power XRD, the final sample must have roughly equal numbers of crystallites oriented in every possible direction. The presence of visible grains leads to preferred orientation for that phase, resulting in large variations in peak intensities, and, in extreme cases, may result in some peak intensities being reduced to near zero. However, these specific granular particles should have no significant effect on other phases in the sample.

Identification of the phases present in the washed Group 1 solids sample was difficult because of the large number of peaks and the low intensity of many of them. Identification by XRD is dependent on the pattern of peaks present, not just their location. This includes the spacing of peaks as well as their relative intensities. Many phases identified in Table 3.11 showed one strong peak and then several much-less-intense peaks. These lower intensity peaks are, in many cases, close to the same count rate as the observed background statistical variation. This results in some identifications being based on one peak, or the pattern resulting from very few peaks. Additional indications of whether a phase is present come from the chemistry restrictions. Failure to meet both requirements, pattern and chemistry, eliminates many phases, but meeting these requirements based on a pattern of 1 or 2 peak positions is also questionable. Because of these considerations, the following designations are used in Table 3.11. Phases identified based on a limited pattern are designated as "possible" to emphasize the weakness of the identification. Phases for which identification may be based on a better pattern, but far from ideal, have been labeled "probable." Phases showing good pattern matching and meeting chemistry requirements have been labeled "excellent" or "good."

[071016b_G1-S-WL-XRD-1_raw_sum7.dif] Log# 082807b, SCAN: 5.0/65.0/0.02/2(sec), Cu, I(max)=22368, 11/05/07 09:31a
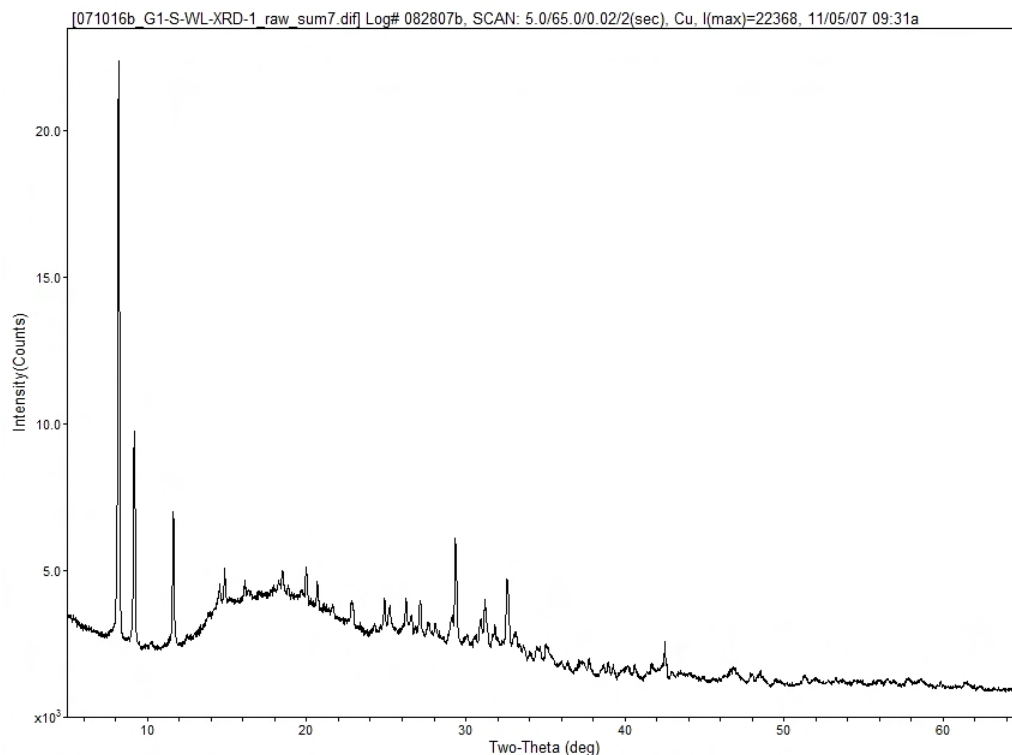
Figure 3.13. Raw X-ray Diffraction Pattern of Washed Group 1 Solids

The strongest peaks present in the sample were in the 8 to 10° 2-θ range. The 8.26 and 9.24° 2-θ peaks could potentially be due to a form of silicon oxide (crystal density 3.56 g/cm^3, JADE Version 8.0), vauxite [$FeAl_2(PO_4)_2 \cdot 6H_2O$] (crystal density 2.39 g/cm^3, JADE Version 8.0), beyerite [$CaBi_2(CO_3)_2O_2$] (crystal density 6.55 g/cm^3, JADE Version 8.0, calculated value), uranyl hydrogen phosphate acetone [$C_3H_6O \cdot UO_2HPO_4$], or combinations of these phases. Except for beyerite, each of these phases shows the characteristics mentioned above, i.e., one major peak followed by a series of peaks of intensity too low to confirm the identification. That is, these species are considered to possibly be present.

SiO_2 (silicon oxide, ICDD card 74-3423), shows a good fit to the 9.24 ° 2-θ line. However, this is a theoretical zeolite structure; the actual phase was not in existence in 2003, the time the paper was published. This phase is not quartz. The only other phase matching this diffraction line and the appropriate chemistry conditions was $C_3H_6O \cdot UO_2HPO_4$. The phase uranyl hydrogen phosphate acetone ($C_3H_6O \cdot UO_2HPO_4$, ICDD card 37-1501) is a good match to the observed strong peak at 9.24° 2-θ if the organic database is searched. Other lines from the card are too low intensity to be observed, so this phase cannot be confirmed. Based on the processing history it is highly unlikely that such an acetone adduct would form in the Hanford tank waste. Indeed, the quality of these card data is listed as "doubtful," but it is the only phase representing material actually in existence giving a good match to this peak. Other potential matches to organic phases were dismissed on the basis of chemistry or overall card pattern.
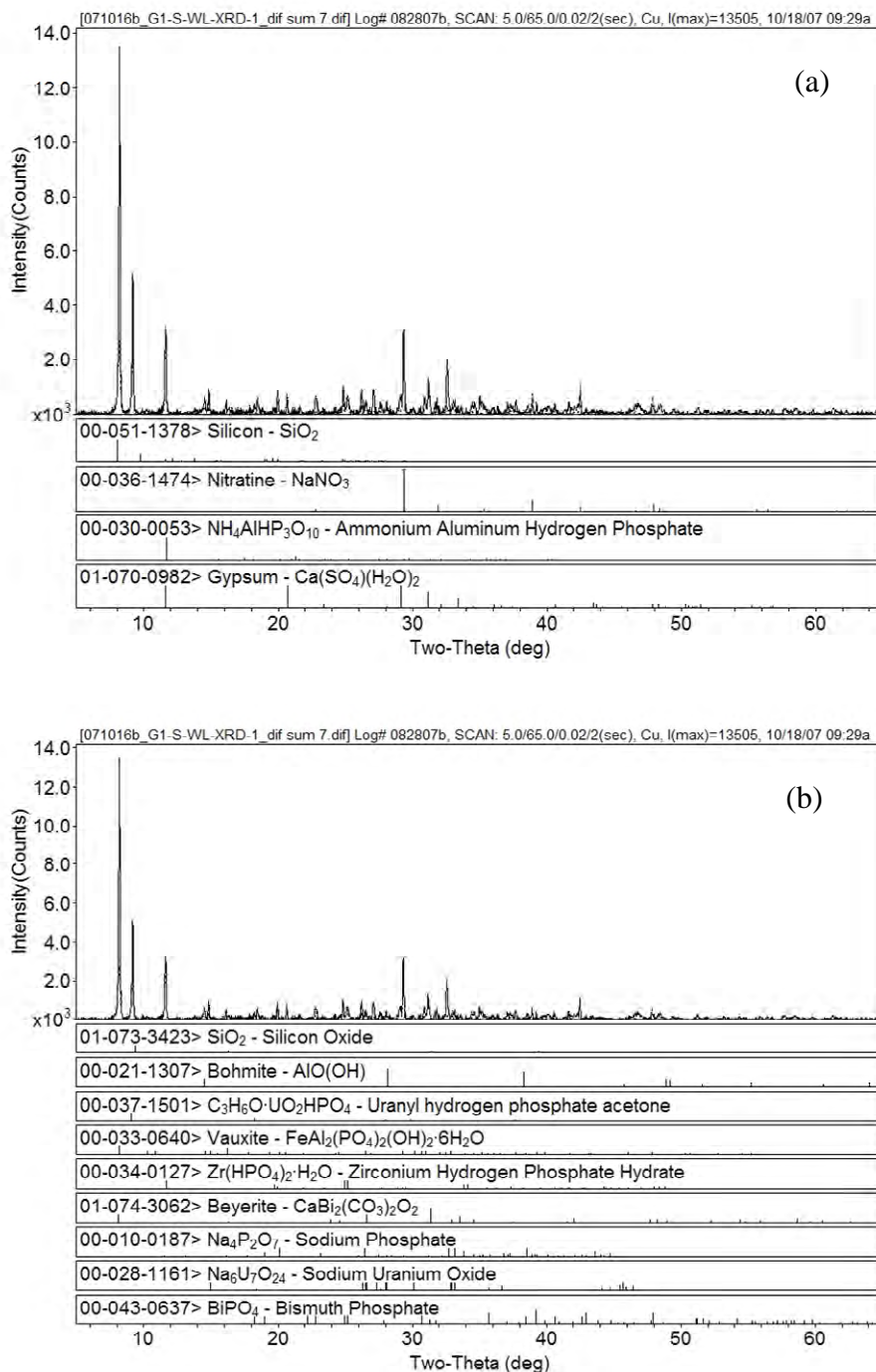
Figure 3.14. XRD Pattern of Washed Group 1 Solids, Background-Subtracted with Stick-Figure Peak Identification: a) Probable Phases Present and b) Possible Phases Present

Calcium sulfate [$Ca(SO_4)(H_2O)_2$] was identified in some of the replicate sample preparations. Since these samples were dried over "Drierite," which is calcium sulfate, the source of this phase (sample or "Drierite") cannot be definitively determined. However, the Fourier transform infrared (FTIR) spectrum taken on a separate sample of the washed Group 1 solids did not display any evidence of calcium sulfate, so the Drierite is the suspected source of this.

Table 3.11. Possible Phase Identification of Group 1 Water-Insoluble Solids

Crystalline Phase	Chemical Structure	Phase Match Description
Silicon oxide (ITQ-9)	SiO_2	Possible[a]
Nitratine (sodium nitrate)	$NaNO_3$	Excellent[b]
Ammonium aluminum hydrogen phosphate	$NH_4AlHP_3O_{10}$	Probable[c]
Calcium sulfate	$Ca(SO_4)(H_2O)_2$	Good[d]
Bismuth phosphate	$BiPO_4$	Probable[e]
Silicon oxide	SiO_2	Possible[f]
Boehmite	$AlO(OH)$	Possible[g]
Vauxite	$FeAl_2(PO_4)_2(OH)_2 \cdot 6H_2O$	Possible[h]
Zirconium hydrogen phosphate hydrate	$Zr(HPO_4)_2 \cdot H_2O$	Questionable[i]
Beyerite	$CaBi_2(CO_3)_2O_2$	Possible[j]
Sodium phosphate	$Na_4P_2O_7$	Possible[k]
Sodium uranium oxide	$Na_6U_7O_{24}$	Possible[l]
Uranyl hydrogen phosphate acetone	$C_3H_6O \cdot UO_2HPO_4$	Questionable[m]

(a) SiO_2, (ICDD card 51-1378) not confirmed. Intensity of confirming lines is too low. Lattice parameter "a" drifts by 1.6%, "b" and "c" drift by 1%. Delta 2-θ was high, but was the best fit to the observed strong peak at 8.24° 2-θ. Appears to be a zeolite.

(b) $NaNO_3$, excellent match to card data and associated with supernatant entrainment.

(c) $NH_4AlHP_3O_{10}$, not confirmed; confirming lines too low intensity to detect.

(d) $Ca(SO_4)(H_2O)_2$, excellent match to card data. However, the presence of gypsum is likely attributable to contamination of the sample during drying over the Drierite desicant.

(e) $BiPO_4$ confirming lines were good matches.

(f) SiO_2 (ICDD card 73-3423), one fair confirming line, but low intensity. From study of theoretical structure of zeolites.

(g) $AlO(OH)$, one good confirming line, others too low intensity.

(h) $FeAl_2(PO_4)_2(OH)_2 \cdot 6H_2O$, fair match to strong 8.24° 2-θ peak. Fair match to confirming lines, some missed.

(i) $Zr(HPO_4)_2 \cdot H_2O$, good match to moderate intensity lines. Although this provides an excellent match to the observed data, it does not fit the chemistry constraints since the Group 1 solids contain little Zr.

(j) $CaBi_2(CO_3)_2O_2$, good match to 8.24° 2-θ line. Good match to moderate intensity lines. Misses some lower intensity lines.

(k) $Na_4P_2O_7$, fair match to major peak and stronger confirming lines.

(l) $Na_6U_7O_{24}$, fair match to major peak. Matches some confirming lines, misses some.

(m) $C_3H_6O \cdot UO_2HPO_4$, fair match to major peak and one confirming line. Other confirming line intensities (ICDD card 37-1501) too low to be observed in this pattern. Furthermore, this phase is not reasonable based on tank history.

Sodium nitrate (crystal density 2.26 g/cm^3, CRC 1978) was found in the XRD mount and was a constituent of entrained supernatant. The following phases were excluded because no match to the XRD pattern could be defined: gibbsite [γ-Al(OH)$_3$], sodium phosphate (Na$_3$PO$_4$), quartz (SiO$_2$), and sodium oxalate (Na$_2$C$_2$O$_4$). It is interesting to note that with the possible exception of vauxite, no major iron-containing phases were identified in the XRD pattern. This would be consistent with the bulk of the iron and phosphate being present in an amorphous form of iron(III) phosphate, which is supported by other evidence (see Section 3.4.1). Furthermore, although bismuth phosphate (crystal density 6.75 g/cm^3,

JADE Version 8.0) was identified as a possible phase by the XRD analysis, the intensities of the lines for $BiPO_4$ are very weak. So at best, $BiPO_4$ is only a minor constituent of the Group 1 solids (again consistent with the FTIR spectral data presented in Section 3.4.1).

Scanning electron microscopy (SEM), coupled with energy dispersive spectroscopy (EDS), was used to obtain information regarding the particle morphology and elemental distribution within the Group 1 solid phases. Several SEM images of the washed solids are shown in Figure 3.15 and Figure 3.16. Highly variable particle morphologies are apparent in these figures. Spheroids with a primary size of <1 μm appeared to form aggregates that are 1 to 3 μm (e.g., see the upper left hand image in Figure 3.17). Needle-like structures were visible in lengths up to 40 μm (see the bottom images in Figure 3.17). Rod structures, possibly tetragonal, are shown prominently in Figure 3.16.

The EDS spectra of selected solids phases are shown in Figure 3.17 through Figure 3.19. In virtually all cases, Na, Si, P, Fe, and Bi were present in significant quantities, as would be expected based on the ICP-OES analysis of the bulk material. Aluminum was also evident in most of the EDS spectra. The EDS elemental mapping is particularly useful in interpreting the results of the SEM examination of the washed Group 1 solids. Figure 3.20 shows an example elemental map for the washed Group 1 solids. The most striking feature of this map is the close association of Fe and P; the patterns displayed for these two elements are nearly identical. Sodium (and to some degree, Sr) also appears to track with the Fe and P. The other major components appear to be evenly distributed across the image, suggesting that these are likely present as the individual oxides or hydroxides that are intermingled together. Similar results are seen in other areas within the SEM image (Figure 3.21). Thus, the SEM results suggest that most of the phosphorus in the Group 1 solids is present in the form of an iron phosphate phase. Further evidence for this is presented in Section 3.4.1. The XRD analysis suggested one possible crystalline iron phosphate species—vauxite, $FeAl_2(PO_4)_2(OH)_2 \cdot 6H_2O$. However, the EDS mapping in Figure 3.20 and Figure 3.21 do not support the notion that vauxite is the primary iron phosphate phase because Al does not map closely with the Fe and P. So the bulk of the iron phosphate material is likely an amorphous material.
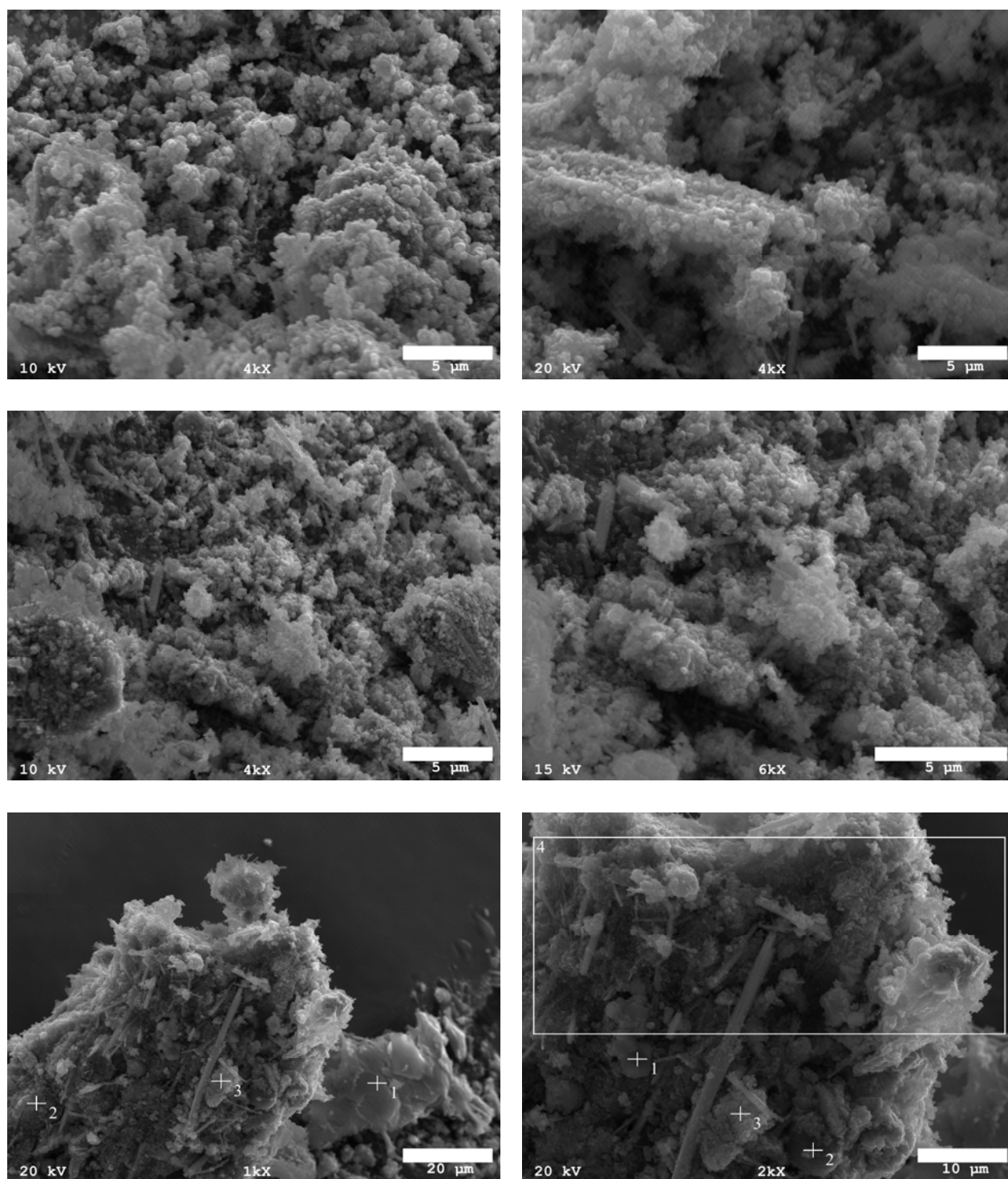
Figure 3.15. SEM Images of Group 1 Initial Characterization Solids
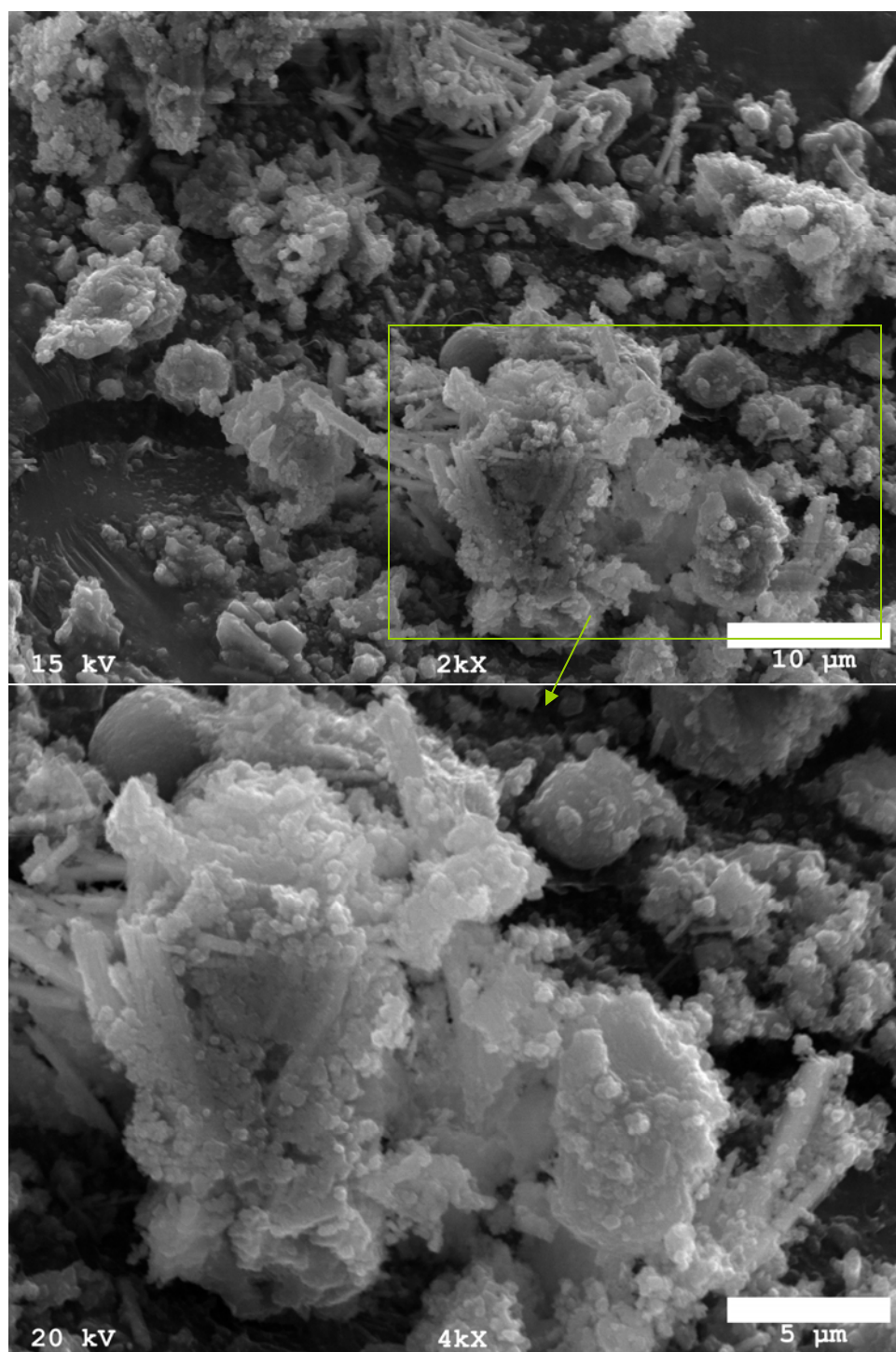
Figure 3.16. Additional SEM Images of Group 1 Initial Characterization Solids
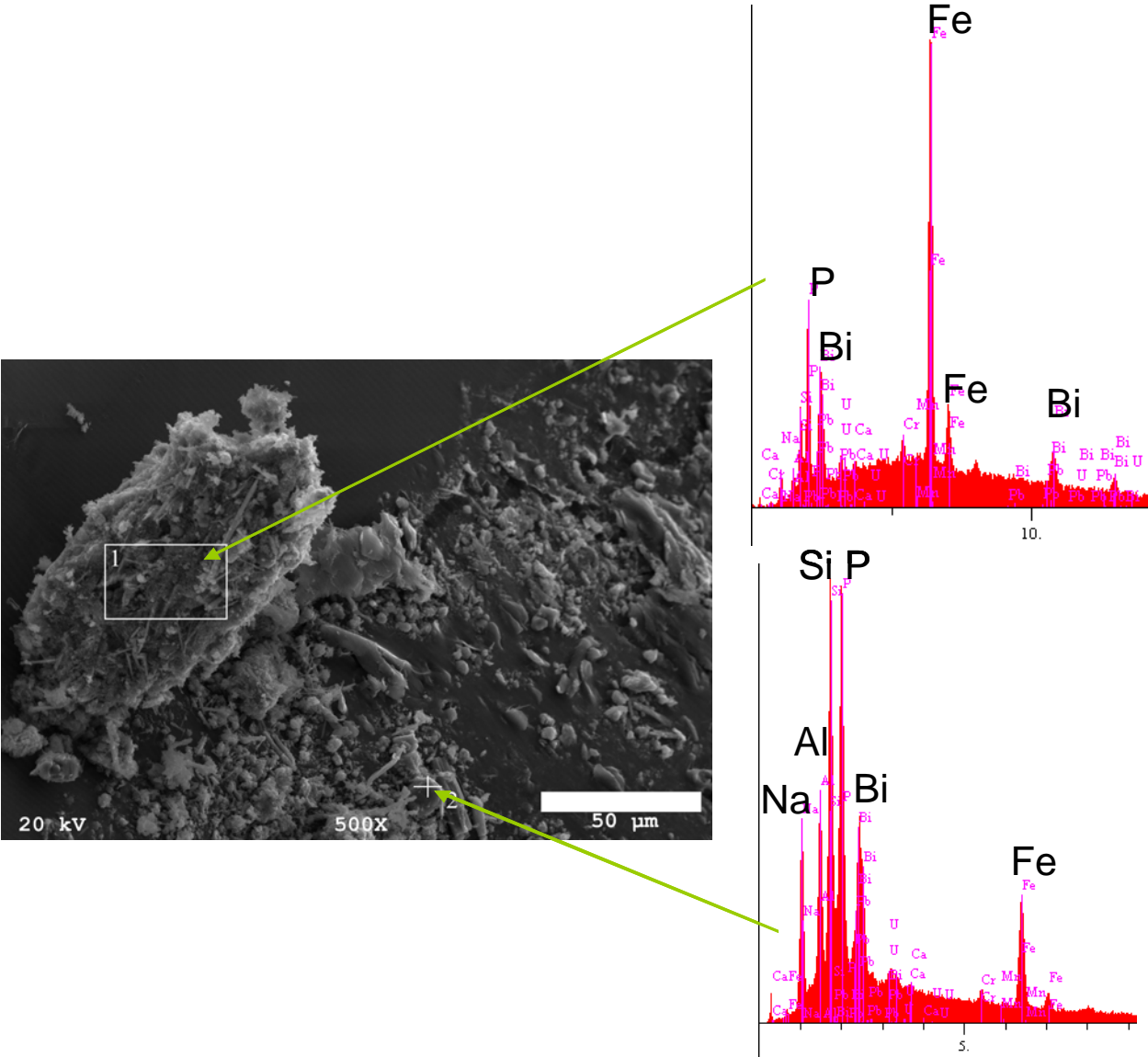
Figure 3.17. SEM-EDS Image 1
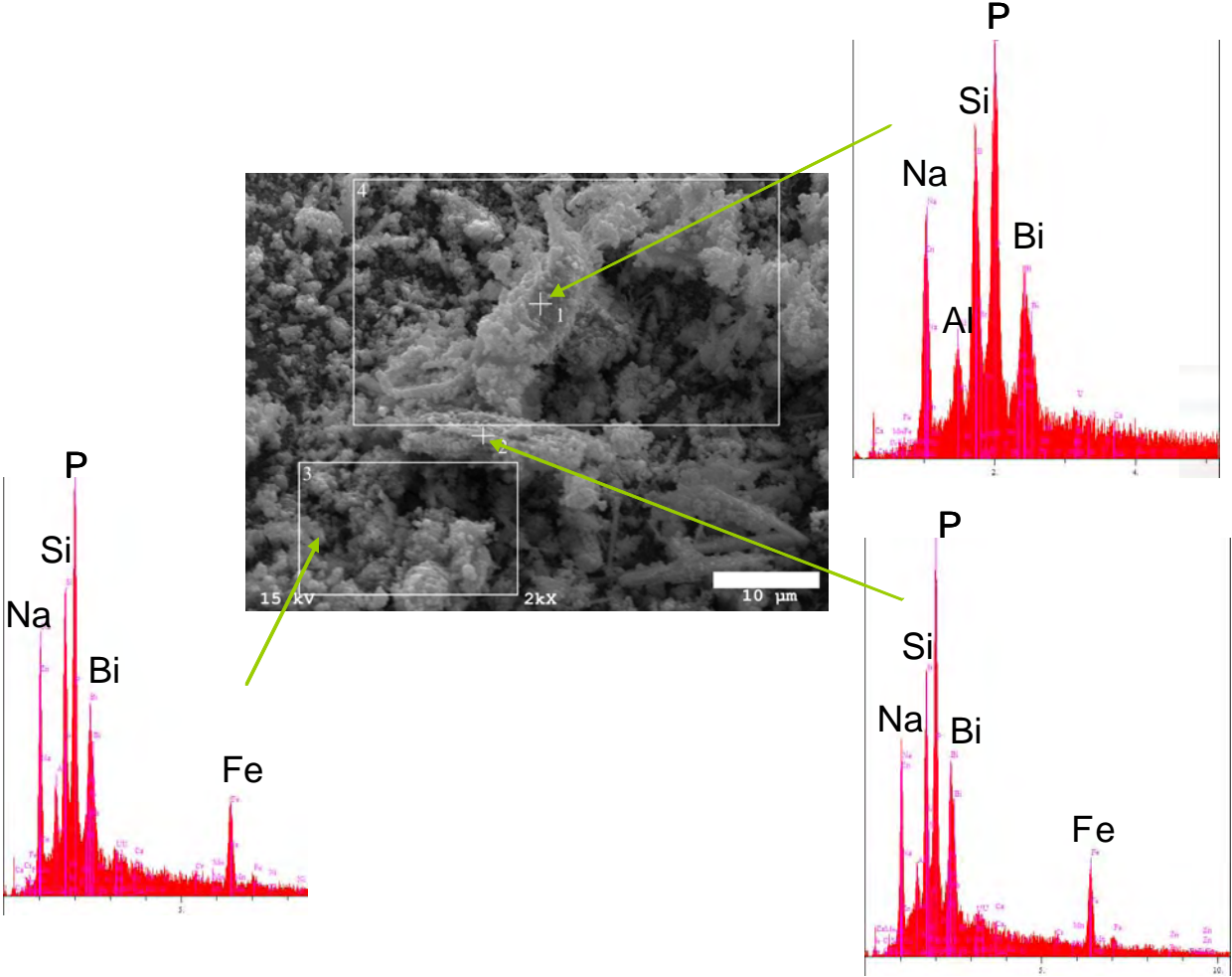
Figure 3.18. SEM-EDS Image 2
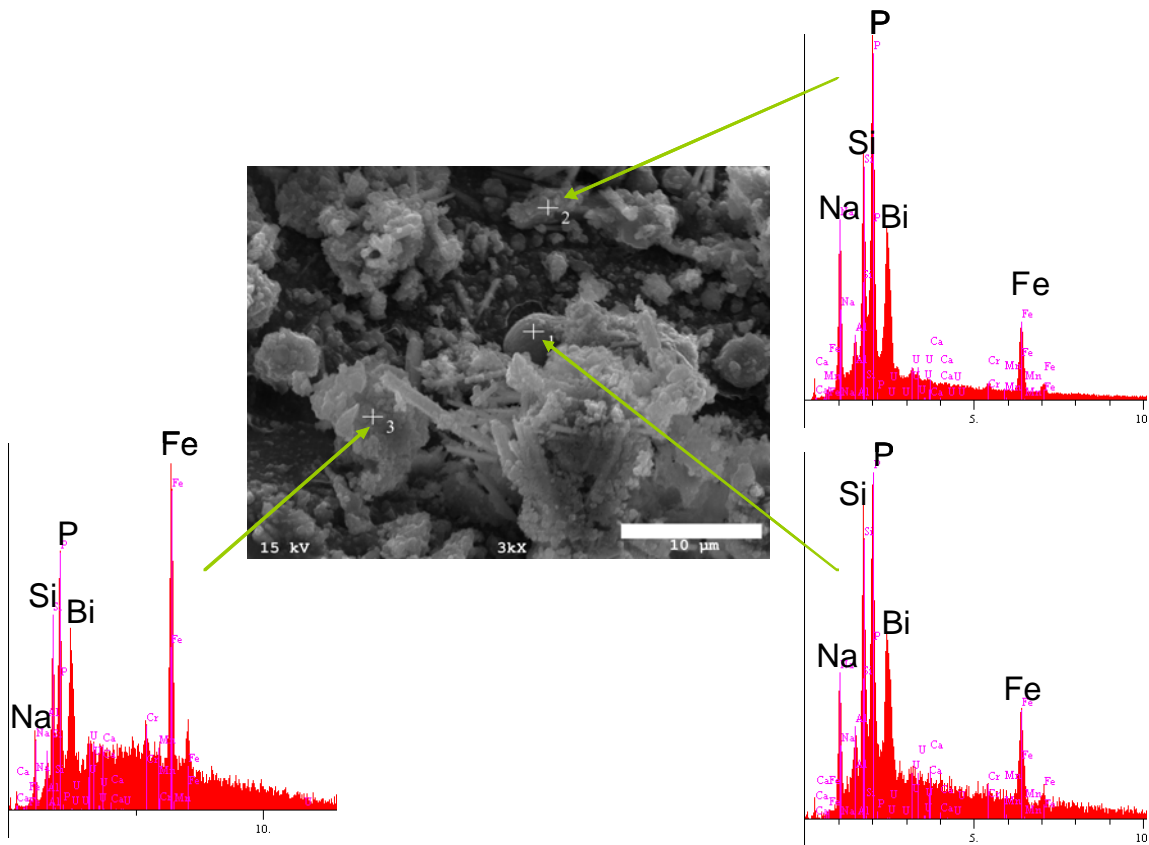
Figure 3.19. SEM-EDS Image 3
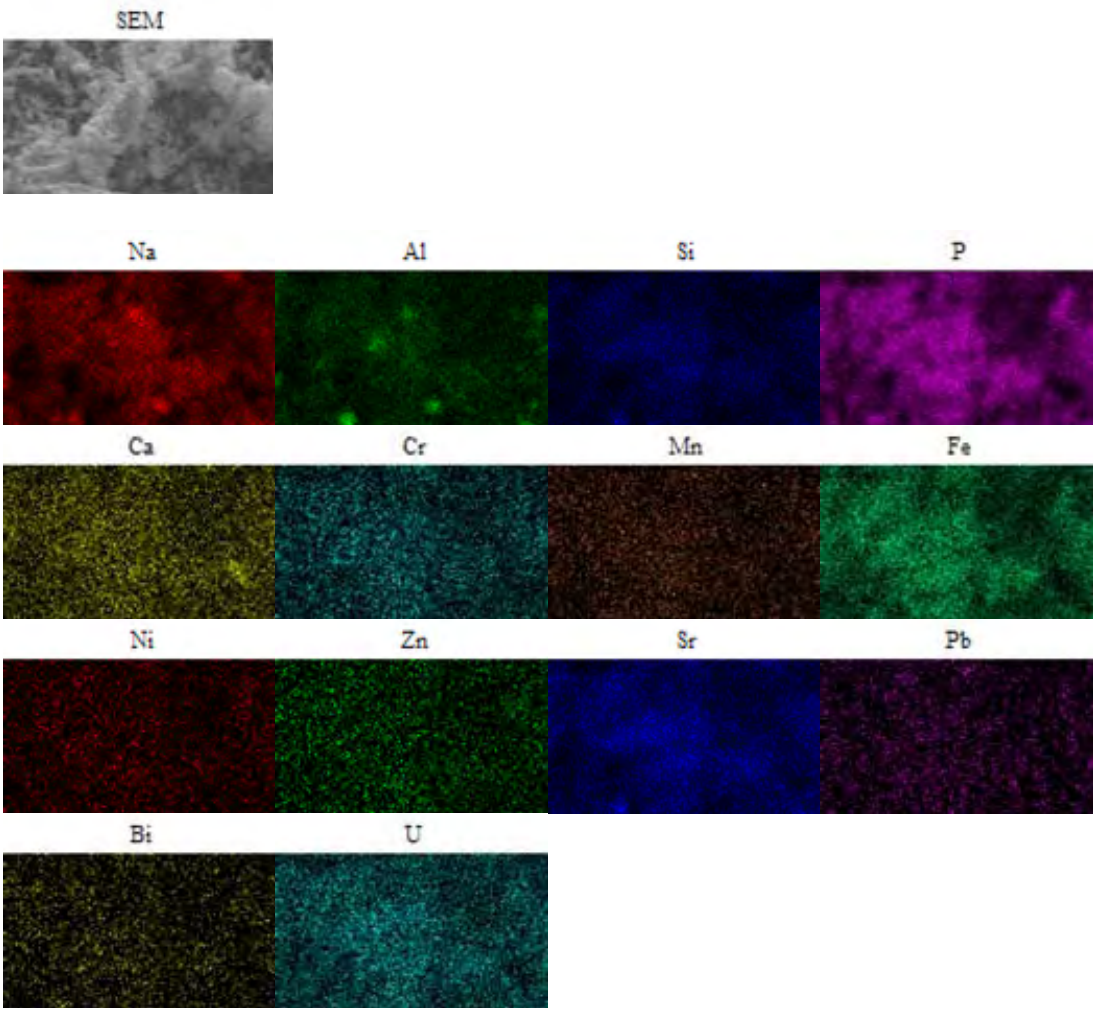
Figure 3.20. EDS Elemental Map of Group 1 Solids (1)
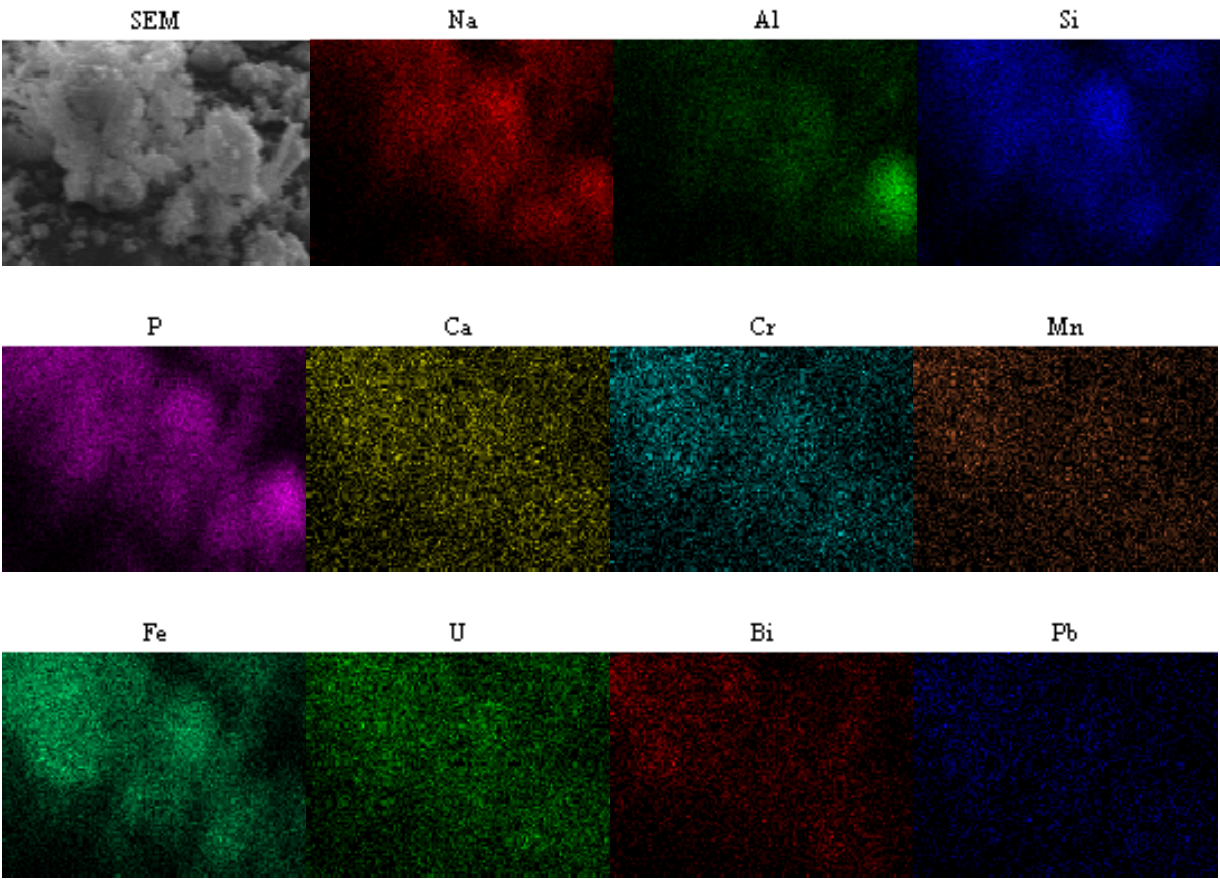
Figure 3.21. EDS Elemental Map of Group 1 Solids (2)

The TEM micrographs of the solids phase are shown in Figure 3.22, and STEM micrographs with EDS are shown in Figure 3.23. As the particles were too thick to allow viewing of diffraction spots, it was not possible to determine if the particles in this region were crystalline. The material had a relatively high surface area with small particles and was dominated by Bi, Fe, P, and Si phases (as was found by SEM-EDS).
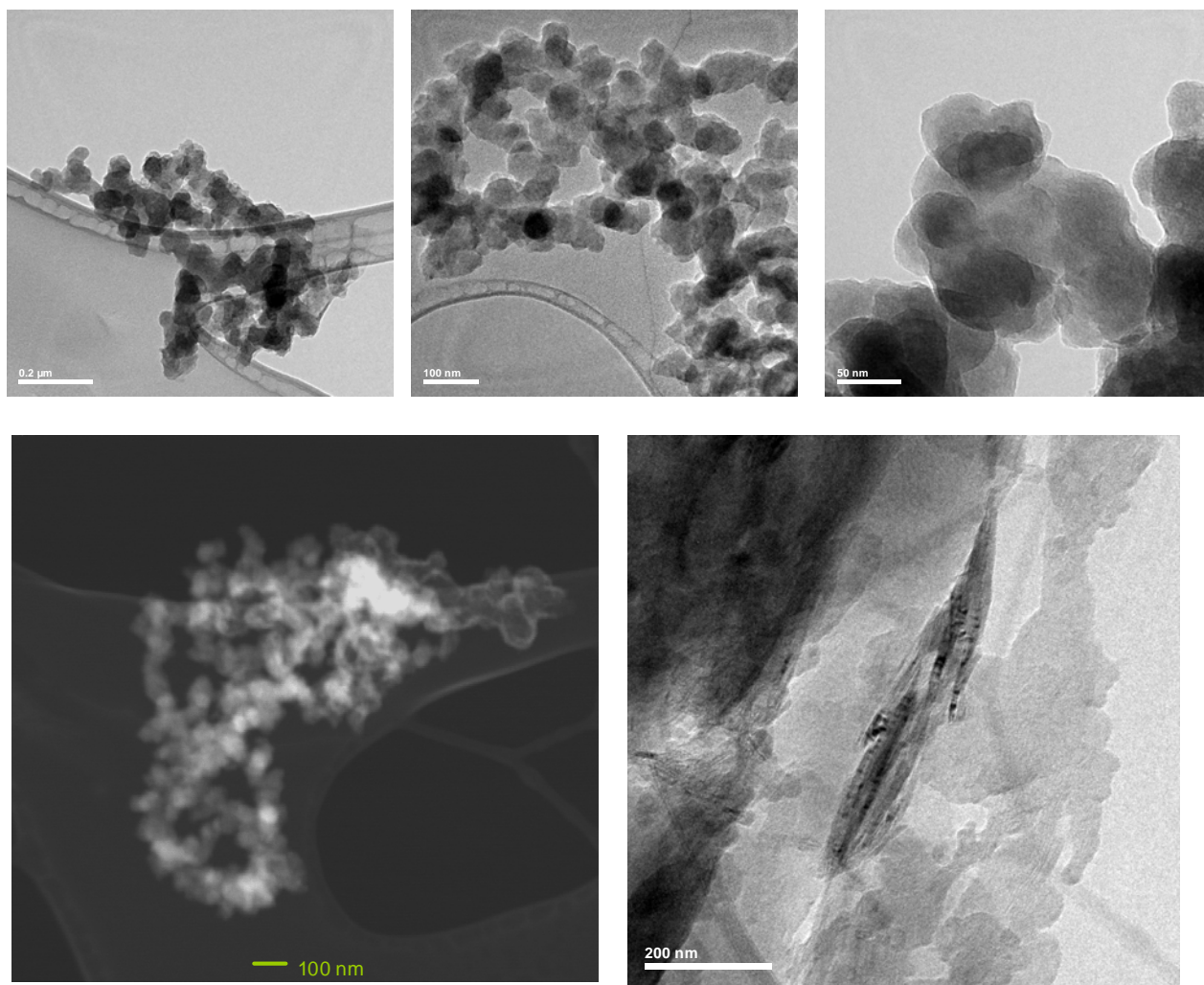
Figure 3.22. TEM Images of Group 1 Washed Solids
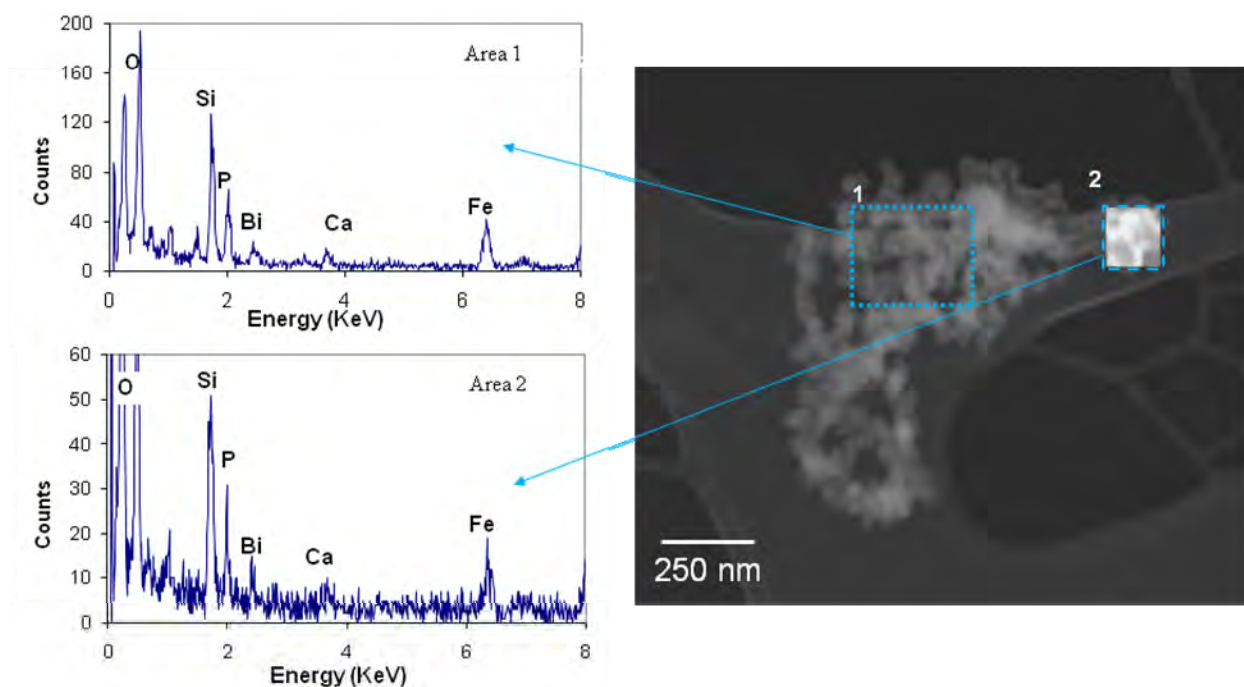
Figure 3.23. STEM-EDS Image of Nano-Agglomerates

3.3 Group 1 Batch Parametric Leaching: Experimental

Parametric caustic leaching tests were performed on the Group 1 bismuth phosphate sludge sample to determine the behavior of phosphate and other components during leaching at different conditions. The composite Group 1 sample material was rinsed with 0.01 M NaOH, subdivided, and subjected to a parametric test matrix for caustic leach testing as discussed in the following sections.[a]

3.3.1 Initial Washing of the Group 1 Solids

The Group 1 composite sample was mixed with an overhead stirrer fitted with a bladed stainless steel impeller. A 122-g aliquot was removed with a large transfer pipet and transferred to a 200-mL centrifuge bottle. At a concentration of 0.082 g dry water-insoluble solids per gram of slurry, the 122-g slurry contained ~10 g of water-insoluble solids. The slurry aliquot was centrifuged at ~2500 RPM (1200 G) for 15 min, and then the supernatant was removed. The volume of centrifuged solids was estimated to be ~20 mL based on volume graduations on the sample bottle. Approximately 60 mL (3× the centrifuged solids volume) of 0.01 M NaOH was added to wash the solids, and the slurry was mixed for 15 minutes with an overhead mixer. The slurry was centrifuged at ~1200 G for 15 min, and then the supernatant was removed. The washing steps were repeated twice for a total of three washes.

(a) Testing was conducted according to TI-RPP-WTP-555, *Parametric Caustic Leach Test of Group 1 Hanford Bi-Phosphate Sludge Waste*, L Snow, November, 2007.

3.3.2 Division of the Washed Group 1 Solids

To conduct a successful sample subdivision, the washed centrifuged solids needed to be thinned. DI water (60 mL) was added to the solids, resulting in a final volume of ~85 mL (or 10 g solids in 87 g of slurry, equivalent to 11.5 wt% undissolved solids [UDS]).

An overhead mixer equipped with a 3-bladed stainless steel impeller was used to homogenize the thinned slurry. Eight ~9.9-g slurry samples were transferred to 125-mL high-density polyethylene (HDPE) bottles with a large disposable polyethylene pipet. Each sample contained ~0.95 g UDS. The samples were removed from the hot cell for follow-on processing at the fume hood workstation.

One additional sample (G1-WL-Solids) containing approximately 6.5 g of slurry (equivalent to 0.75 g dry solids) was transferred to a 60-mL HDPE bottle. A portion of this sample was submitted for a potassium hydroxide (KOH) fusion and the following subsequent analyses: inductively coupled plasma-optical emission spectroscopy (ICP-OES) metals, gamma energy analysis (GEA), Pu, total alpha, total beta, ^{90}Sr, and U by KPA. These analyses were performed to establish the starting composition of the washed solids.

3.3.3 Caustic Leaching of the Washed Group 1 Solids

The leaching test matrix for each of the eight samples is summarized in Table 3.12. The test matrix evaluated the effects of free-hydroxide concentration (1 to 3 M NaOH) and temperature (40 to 80°C) on phosphate leaching kinetics.

Table 3.12. Group 1 Caustic Leaching Conditions

Bottle ID	Free OH, M		Na, M		Temperature, °C[b]
	Target	Measured[a]	Target	Measured[a]	
G1-40-1	1	1.10	1	1.14	40
G1-40-3a	3	3.28	3	3.26	40
G1-40-3b	3	3.23	3	3.31	40
G1-40-3c	3	3.14	3	3.18	40
G1-60-1	1	1.03	1	1.17	60
G1-60-3	3	3.20	3	3.27	60
G1-80-1	1	1.07	1	1.17	80
G1-80-3	3	3.23	3	3.25	80
(a) The measured analyte concentrations represent the equilibrium concentration obtained after a 24-h contact time. (b) The temperature uncertainty was ±2.5°C Analytical Service Request (ASR): 8060					

The NaOH concentration in each leaching mixture was adjusted to support the test matrix. Sodium hydroxide (19 M) was added to each aliquot of the washed solids slurry in the following amounts: 5.3 mL to yield 1 M NaOH and 15.8 mL to yield 3 M NaOH. The leaching mixtures were then diluted to a final volume of 100 mL (with an estimated uncertainty of 2 mL) with DI water. The contact time with the concentrated NaOH was brief (<5 min). The sample bottles were weighed after each addition of reagents (NaOH and water). Each leaching vessel was closed with a cap equipped with a tube condenser. The

condenser was used to eliminate pressurization and minimize water loss, while at the same time minimizing the spread of contamination.

The sample slurries were transferred to a temperature-controlled shaker table. The temperature was controlled with an aluminum heating block (J-KEM Scientific, Inc.) equipped with a Type T thermocouple. The heating block was supported on a J-KEM BTS-3500 digital bench-top shaker (Figure 3.24). The shaking speed was digitally controlled to 200 RPM; based on visual inspection, the solids were well suspended in solution. The samples were grouped according to the leaching temperature, and one group was leach-tested at a time. The heating block was pre-heated to the appropriate temperature before leach testing.

Figure 3.24. Aluminum Heating Block and Shaker Table Used in Parametric Leaching Tests

The leaching mixtures were shaken at temperature for 24 hours, and solution samples were withdrawn at 0 (taken before insertion into heating block), 1, 2, 4, 8, and 24 hours. At each sampling time, the shaker was stopped, and the solids were allowed to settle for ~5 to 10 min, resulting in sufficient clarification of the aqueous portion to support sampling without removing any solids. Approximately 1.5-mL of the clarified leachate solution was withdrawn with a transfer pipette and filtered through a 0.45-μm pore size nylon syringe filter; the syringe filter and the syringe had been pre-heated in an oven to the sample temperature (40, 60, or 80°C) before filtering in an effort to minimize temperature changes impacting the sample. One 0.5-mL sample of filtered solution was acidified with 15 mL of 0.3 M HNO_3 for analysis by ICP-OES; another 0.5-mL sample of filtered solution was added to 2.5 mL of 1×10^{-4} M NaOH for analysis by ion chromatography. The remaining filtered solution was returned to the leaching vessel, and the leaching process was continued. The new liquid level was marked after each sample was taken. Evaporation was minimal during the course of the experiment, but when evaporation was observed, DI water was added to restore the volume to the previously marked liquid level. After 24 hours, additional leachate samples were taken to determine the free-hydroxide ion concentration and gamma-emitting isotopes by GEA.

After the final samples were taken at temperature, the slurries were removed from the mixing/heating block and cooled to ambient (~22°C) temperature. The slurries were centrifuged, and half of the leachate was decanted.[a]

The equilibrium concentration values for free hydroxide and sodium are shown in Table 3.12 and were based on results from the samples taken at 24 hours.

3.3.4 Washing of Caustic-Leached Group 1 Solids for Analysis

The solids from the triplicate samples (G1-40-3a, -3b, -3c, leached at 40°C in 3 M NaOH) were prepared for characterization as shown in Figure 3.25. One of the solids samples was slurried in 15 mL of 0.01 M NaOH and divided between the remaining two solids samples. The leaching bottle was then rinsed with 10 mL of 0.01 M NaOH, and the wash was split between the remaining two solids samples. The solids were mixed on a shaker table for 15 minutes. The slurry was centrifuged for 5 min and the supernatant removed. Dilute sodium hydroxide solution (0.01 M; 15 mL) was added to the solids, the compacted solids were broken up with disposable pipet, and the slurry was mixed on a shaker table for 15 minutes. The slurry was centrifuged for 5 min and the supernatant removed. The wash steps were repeated once more for a total of three washes. After the final wash, the solids were slurried in ~2 mL of DI water and sub-divided for analysis by particle-size distribution (PSD), X-ray diffraction (XRD), transmission electron microscopy (TEM), scanning electron microscopy (SEM), Brunauer, Emmett, and Teller (surface area analysis technique) (BET) surface area, and a KOH fusion with subsequent analysis for ICP-OES metals, GEA, Pu, total alpha, total beta, ^{90}Sr, and U by KPA.

(a) The contact dose rates of the leached solids were too high to safely conduct transfer to volume-graduated centrifuge tubes to assess the volume of centrifuged solids.
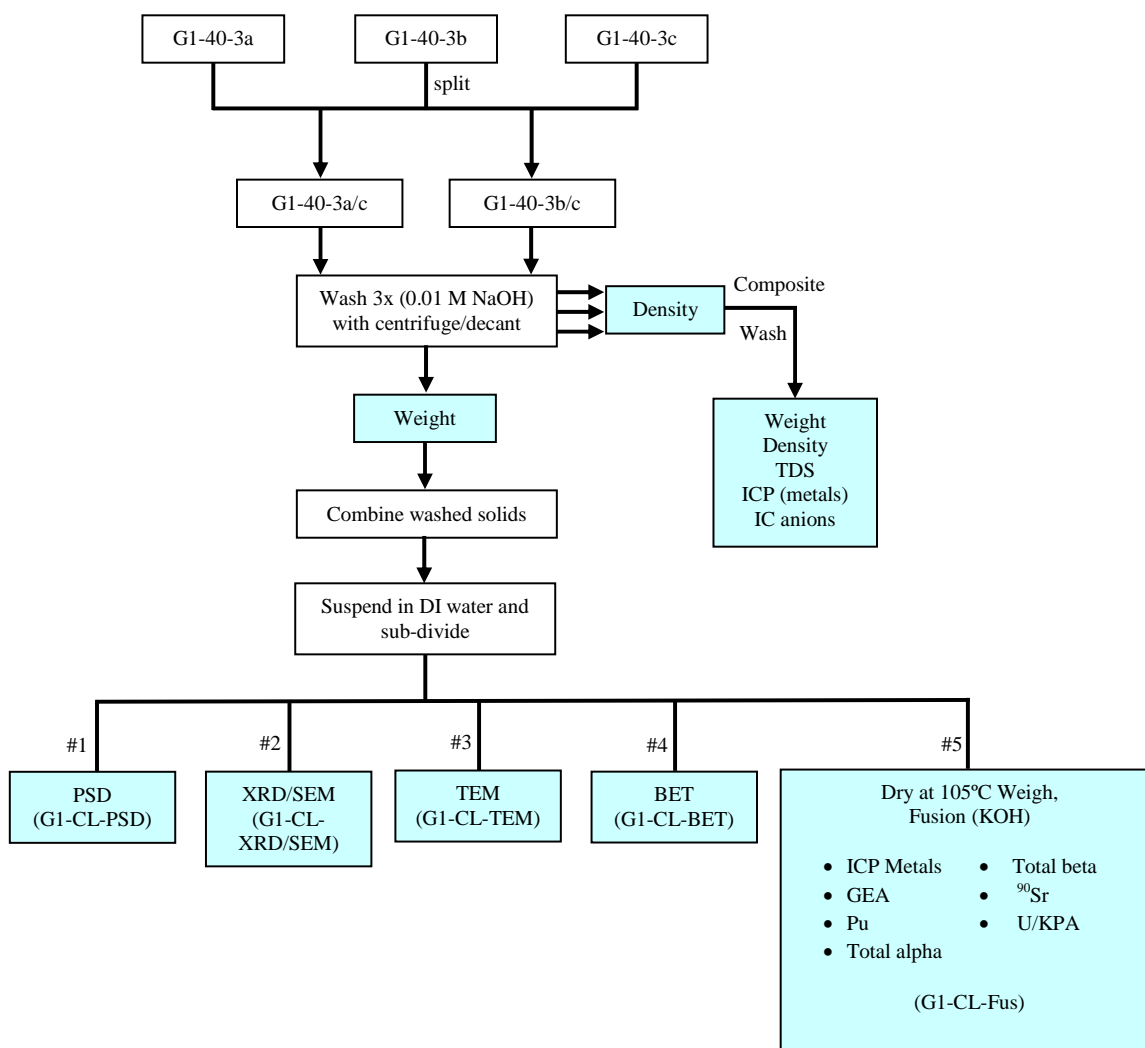
Figure 3.25. Washing, Subdivision, and Analysis Scheme for the Group 1 Caustic Leached Solids

3.4 Group 1 Bi-Phosphate Sludge Waste Parametric Caustic-Leaching Test Results

Phosphorus is the most important component in the water-insoluble Group 1 bismuth phosphate sludge solids with respect to caustic leaching. Aluminum is present at a relatively low concentration (2.7 wt%), so the behavior of this element is less important for this particular waste group. However, the behavior of Cr (0.51 wt%) is of interest because this can become a glass-limiting component if sufficient P is removed by caustic leaching. The parametric leach testing of this sample was primarily directed at understanding the phosphorus dissolution in the actual tank waste in order to understand and subsequently match the dissolution properties to a simulant material. But the behaviors of Al and Cr were also determined. The parametric leaching results and residual solids composition are discussed in the following sub-sections.

3.4.1 Time, Temperature, and Hydroxide Effects on Phosphorus Dissolution from the Group 1 Solids

The P dissolution behavior for the washed Group 1 solids was evaluated as a function of time, temperature, and free-hydroxide concentration. Based on the total P concentration in the solids material (0.101 g P/g), and the wt% UDS of the starting slurry (9.62%), the complete dissolution of P would result in a concentration of 0.96 mg P/mL or 0.031 M. This expected maximum concentration is about 24% less than the value of 0.038 M P, which was actually determined in the liquid samples. This difference can be attributed to the experimental uncertainty in the solids analysis and to the uncertainty in determining wt% UDS. The reported wt% of P dissolved at each sampling point was calculated based on the final concentration in the triplicate solids samples, as discussed in Section 3.4.6.2.

Figure 3.26 summarizes the P behavior during leaching of the washed Group 1 solids in 1 M and 3 M NaOH at 40°C. In 1 M NaOH, there was rapid transfer of P to the liquid phase. Even before heating was applied (i.e., at t = 0), ~60% of the P was removed from the solid phase. It should be noted that this was accompanied by the visual observation of a dramatic color change from the initial beige color of the solids to rusty-red after adding NaOH (this was seen for all conditions examined) as shown in Figure 3.27. This result points to a rapid metathesis of an iron(III) phosphate phase to sodium phosphate and ferric hydroxide (*vide infra*). After 1 h at 40°C, 97% of the P had dissolved, and 99% had dissolved after 2 h. For the triplicate runs done at 40°C and 3 M NaOH, there is considerable scatter in the data. The reason for this scatter is not clear, but it appears to be dominated by lower P concentrations in the 1- and 2-h sampling points for Trials b and c (the data for Trial a are more similar to that observed for 1 M NaOH). Regardless, complete P removal is achieved after 4 h of leaching in 3 M NaOH at 40°C.

Figure 3.28 and Figure 3.29 show the P behavior for leaching of the Group 1 solids at 60 and 80°C, respectively. Within the experimental uncertainty, the P behavior in 1 M NaOH is essentially the same as that in 3 M NaOH at 60°C; the same can be said for the results at 80°C. Figure 3.30 compares the P leaching behaviors at the three different temperatures examined at the individual NaOH concentrations investigated. Generally, the temperature had little influence on the P leaching kinetics. Rapid P removal was observed in all cases, typically with essentially complete removal being achieved after 2 h. Again, the final P concentrations observed were essentially the same, within the experimental uncertainty.
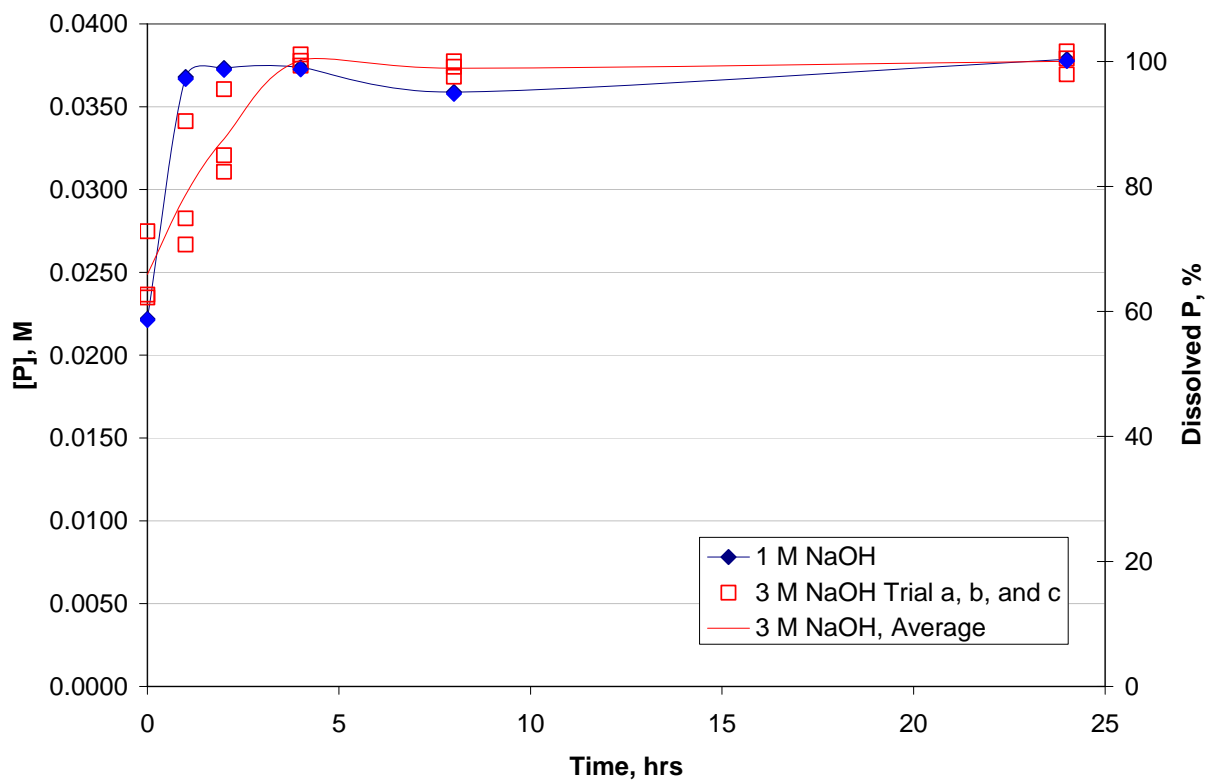
Figure 3.26. Phosphorus Concentration and Percent Removed Versus Time at 40°C for Leaching of the Group 1 Washed Solids in 1 and 3 M NaOH
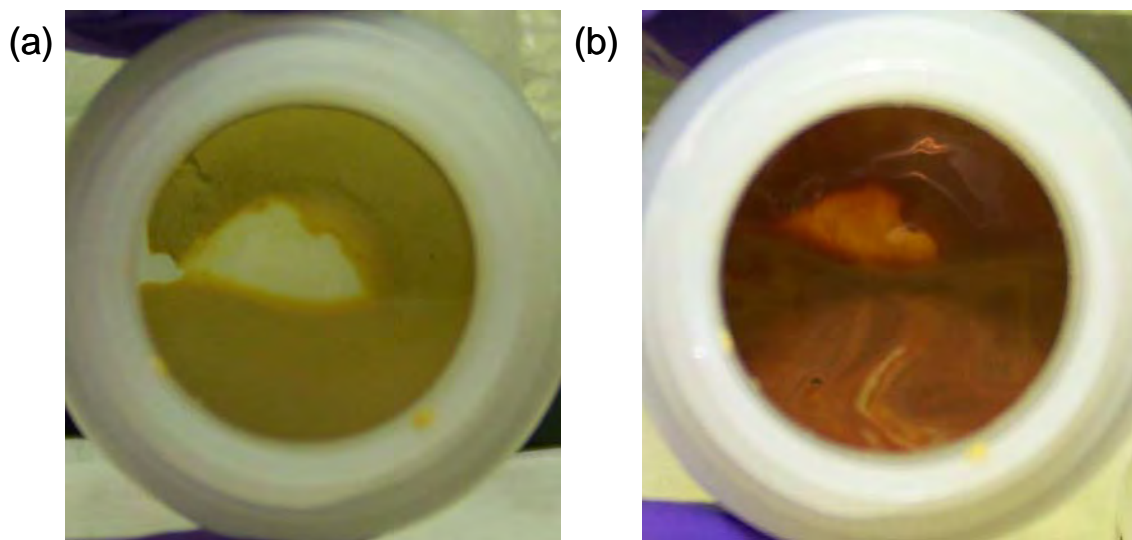
Figure 3.27. Color Change Observed in Group 1 Solids upon Addition of NaOH: (a) Initial Solids; (b) Solids After Addition of NaOH
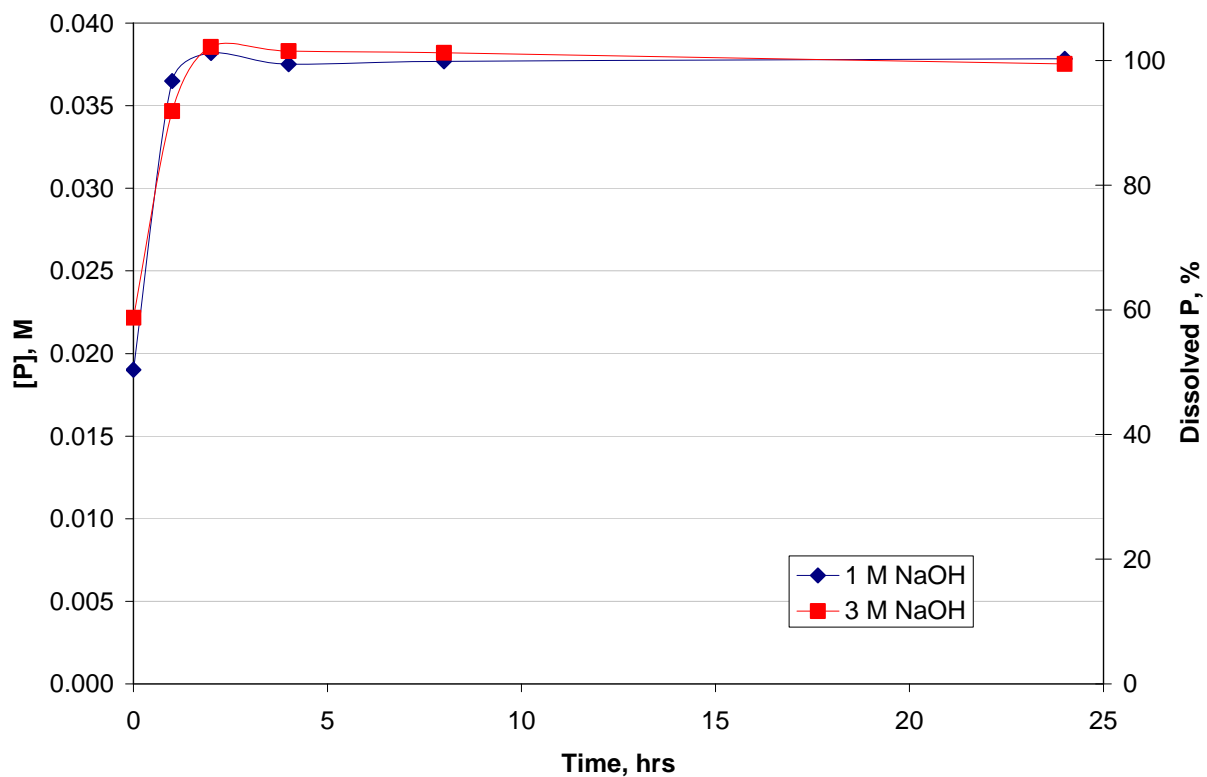
Figure 3.28. Phosphorus Concentration and Percent Removed Versus Time at 60°C for Leaching of the Group 1 Washed Solids in 1 and 3 M NaOH
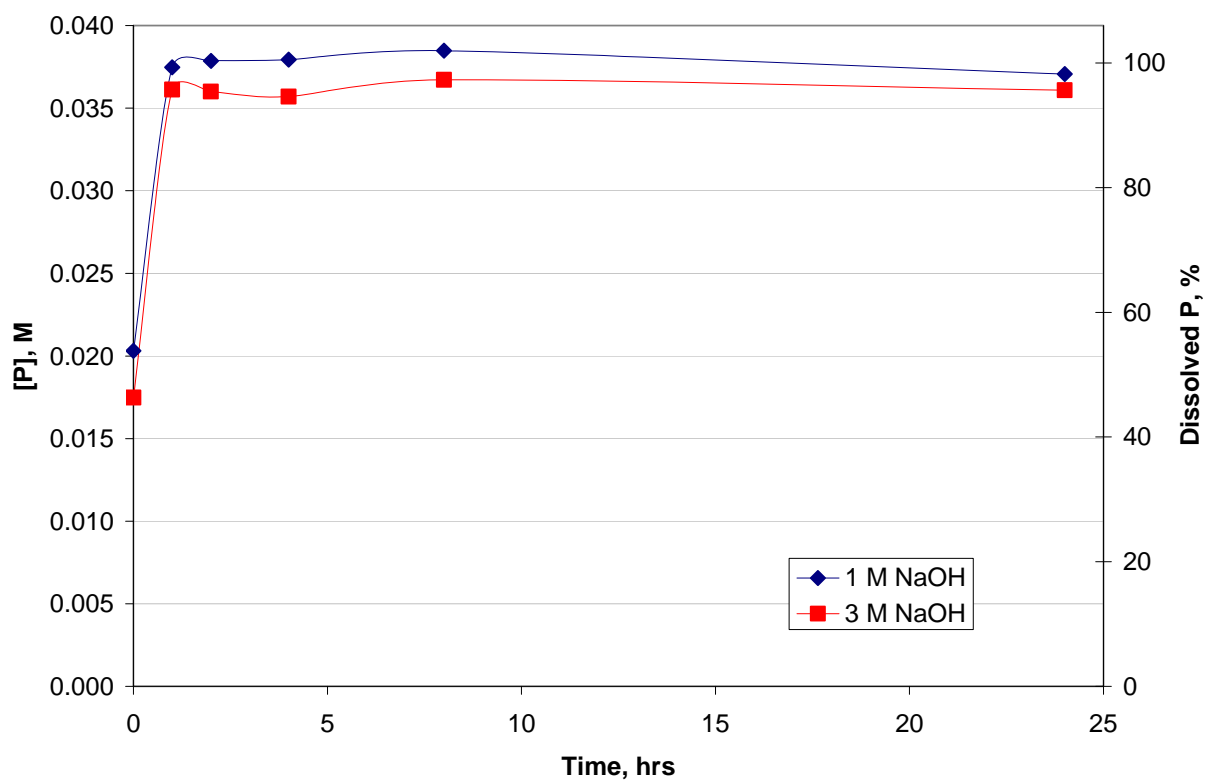
Figure 3.29. Phosphorus Concentration and Percent Removed Versus Time at 80°C for Leaching of the Group 1 Washed Solids in 1 and 3 M NaOH
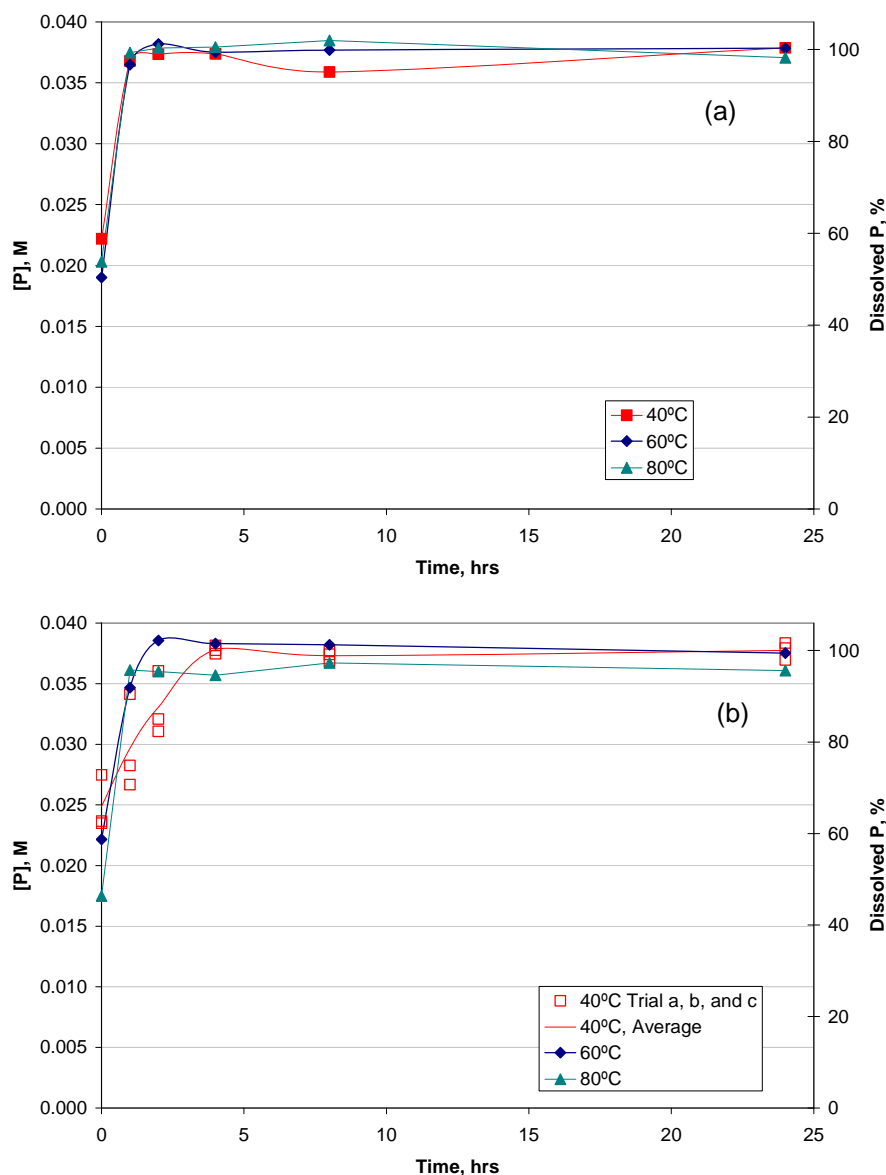
Figure 3.30. Phosphorus Concentration and Percent Removed Versus Time at a) 1 M NaOH, 40, 60, and 80°C and b) 3 M NaOH, 40, 60, and 80°C for Leaching of the Group 1 Washed Solids

Based on the observations described above, it was hypothesized that the phosphorus in the washed Group 1 solids was primarily in the form of an iron(III) phosphate phase. To test this hypothesis, the Raman spectrum[a] of a portion of the washed Group 1 solids was recorded and compared to that of commercially procured $FePO_4 \cdot \times H_2O$. The latter material displayed distinct PO_4^{3-} bands at 997 and 1034 cm^{-1}. On the other hand, the Raman spectrum of the Group 1 solids was featureless. A second "$FePO_4$" material was prepared in-house by adding ferric nitrate solution to an aqueous solution of Na_3PO_4. This resulted in a beige precipitate that was quite different in appearance from the commercially procured $FePO_4 \cdot \times H_2O$ (which was a pale pink crystalline solid). On the other hand, this beige precipitate

---

(a) All Raman and FTIR spectroscopic work discussed here is for indication only.

was visually very similar to the actual Group 1 tank waste sample (Figure 3.31). Indeed, the SEM-EDS elemental mapping for the beige iron(III) phosphate product (Figure 3.32) was similar to that seen for the Group 1 sample (Figure 3.20 and Figure 3.21), with Na, Fe, and P mapping very closely together. It is unclear whether the Na is entrained sodium nitrate or phosphate or whether it is actually incorporated into the iron phosphate solid structure.

The Raman spectrum of the beige $FePO_4$ product displayed a weak phosphate band at 1069 cm^{-1}. Because the Group 1 solids did not display any Raman bands, the FTIR spectrum was recorded. Figure 3.33 shows the FTIR spectrum of the washed Group 1 solids along with the spectra of beige iron(III) phosphate product, the commercially procured $FePO_4 \cdot \times H_2O$, and $BiPO_4$. The FTIR spectrum of Group 1 solids is consistent with an iron(III) phosphate species, although there is not a perfect match with the material formed by mixing ferric nitrate solution to an aqueous solution of Na_3PO_4. This is not surprising since the product formed by reacting ferric ion with aqueous sodium phosphate can only approximately be considered to be $FePO_4 \cdot \times H_2O$ (amorphous), and its composition depends upon the pH of the solution during precipitation (de Barry Barnett and Wilson 1953, p. 202). The amorphous iron(III) phosphate product prepared in this work was undoubtedly formed under conditions that were different from that for the actual tank waste, so slight differences in their FTIR spectra should be expected. It can be definitively concluded, however, that the phosphate present in "bismuth phosphate" sludge (i.e., Group 1) is *not* in the form of $BiPO_4$.

Figure 3.31. Visual Comparison of the Washed Group 1 Solids (right) with Iron(III) Phosphate Prepared by Mixing $Fe(NO_3)_3$ Solution with Na_3PO_4 Solution (left)

Iron   *Phosphorus*   *Sodium*
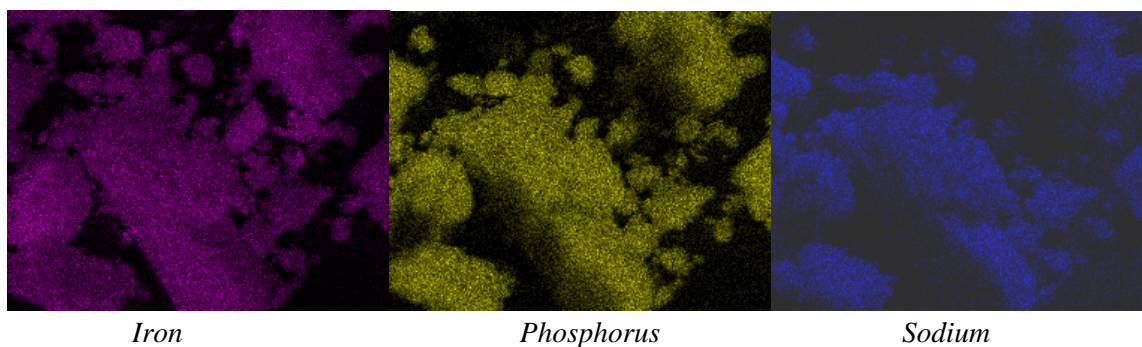
Figure 3.32. SEM-EDS Elemental Mapping for Iron(III) Phosphate Prepared by Mixing $Fe(NO_3)_3$ Solution with Na_3PO_4 Solution
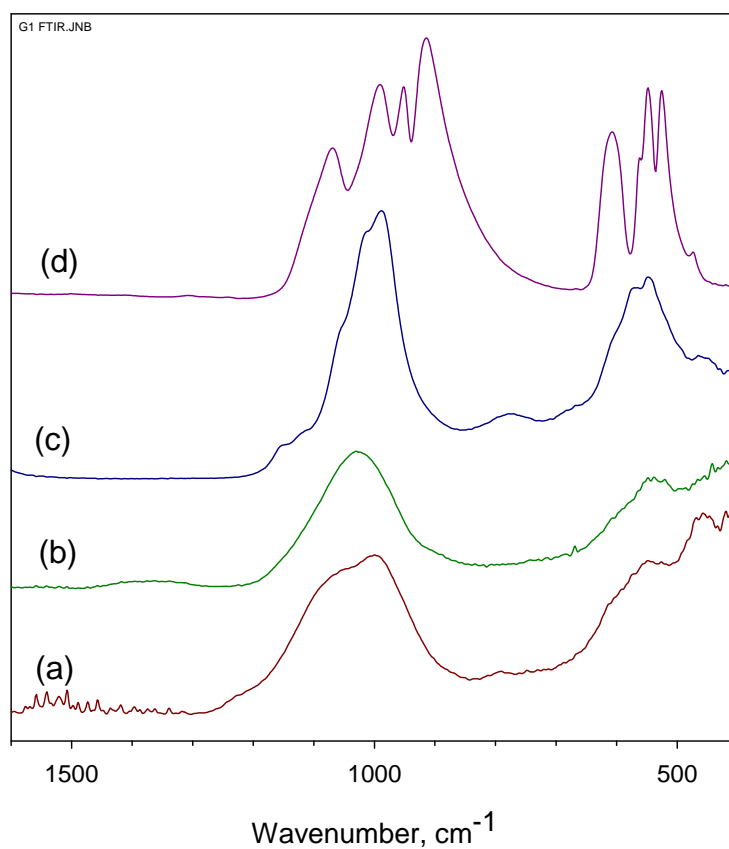
Figure 3.33. FTIR Spectrum (taken on diamond ATR plate) of a) the Washed Group 1 solids, b) the Iron(III) Phosphate Prepared by Mixing $Fe(NO_3)_3$ Solution with Na_3PO_4 Solution, c) Commercially Procured $Fe(PO_4)\cdot xH_2O$, and d) $BiPO_4$

Heating of the Group 1 solids in air would not change their elemental form but rather would alter their chemical speciation. Four thermal gravimetric (TG) scans were acquired for washed Group 1 solids. The samples would be best represented by the elemental concentrations in the 2nd column of Table 3.15. In each case, the samples lost between 20 and 24 wt% of their initial mass. The majority of the mass loss occurred below 200°C. No other large thermal signature was apparent between 200 and 500°C but slow mass loss was observed over this range. Heating the washed Group 1 solids to 830°C in quartz pans produced a dark red-brown slag.

Bismuth as Bi_2O_3 melts at 824°C. The phosphate ($BiPO_4$) melts at 350°C and decomposes at high temperature to Bi_2O_3. Melting of $BiPO_4$ was not observed in the TG scans of the four samples. It is also fairly certain that the melting of Bi_2O_3 was not observed in the TG analysis of the Group 1 solids, but rather was precluded by vitrification of the sample near 800°C in air.

TG scans of the commercially procured $FePO_4 \cdot \times H_2O$ indicated that this material had a dehydration pattern different from that observed in the Group 1 samples. The TG scan of the amorphous iron phosphate obtained by precipitation from Na_3PO_4 solution (i.e., the material shown in Figure 3.31) displayed mass loss and dehydration pattern very similar to that seen for the Group 1 samples. This material also formed a glass, with a transition temperature near 660°C. In the four tank waste samples, the observed glass transition temperatures were consistently higher; between 710°C and 794°C. The red-brown surfaces of the slags were scrapped with a needle and this exposed a shiny-looking material just below the surface. The shiny material appeared to be a bismuth phosphate glass. The presence of the exterior red-brown material indicates that the stoichiometry of the glass that formed partially excluded some iron. The TG analysis was consistent with the conclusion from the FTIR that the phosphate in the Group 1 solids is not in the form of distinct crystalline $FePO_4 \cdot \times H_2O$ or $BiPO_4$, but probably more resembles the amorphous material precipitated from Na_3PO_4 solution. The degree of Bi inclusion into this phase is not clear.

3.4.2   Time, Temperature, and Hydroxide Effects on Aluminum Dissolution from the Group 1 Solids

The aluminum leaching data at 40, 60, and 80°C are plotted in Figure 3.34 through Figure 3.36, respectively. There was some variability in the initial (t = 0) Al concentrations; this might have been due to variability in the initial sub-sampling or from differences introduced when the NaOH solution was first added to the sample (e.g., slight differences in the time interval between NaOH addition and dilution to 100 mL). As expected, the amount of Al removed increased with increasing concentration of NaOH, although effective Al removal (> 70%) was achieved in 1 M NaOH at all temperatures examined. That is, only 5 to 10% more Al was removed by going from 1 M to 3 M NaOH. Furthermore, the Al was removed fairly rapidly, reaching maximum removal for each leaching condition within 2 h. Figure 3.37 compares the Al leaching behaviors at the three different temperatures examined at the individual NaOH concentrations investigated. Only a weak temperature dependence was observed, which was most pronounced at 1 M NaOH. These observations indicate that 75 to 85% of the Al present in the washed Group 1 solids was present in a form that is readily dissolved in caustic media. Candidate phases that would explain this behavior include gibbsite (or amorphous aluminum hydroxide) and aluminum phosphate (Lumetta 2008). Definitive identification of the specific Al-containing phases was vitiated by the relatively low concentration of Al in the sample.
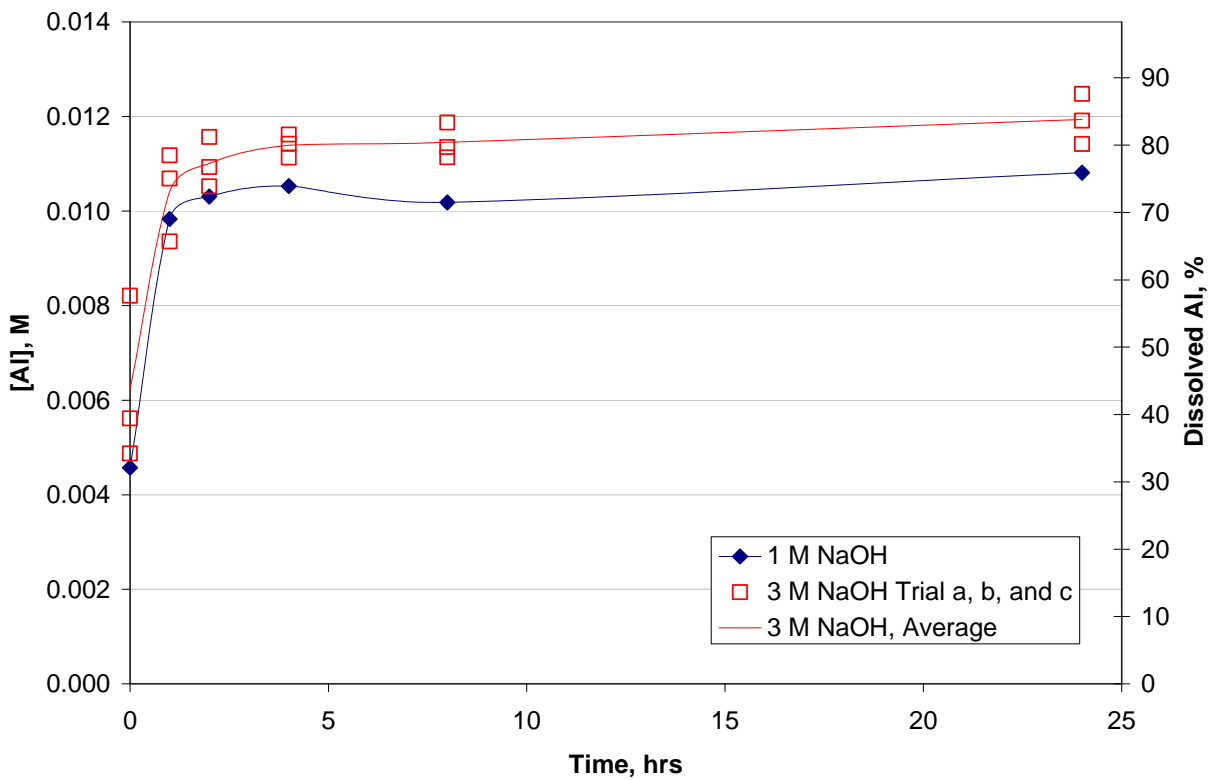
Figure 3.34. Aluminum Concentration and Percent Removed Versus Time at 40°C for Leaching of the Group 1 Washed Solids in 1 and 3 M NaOH
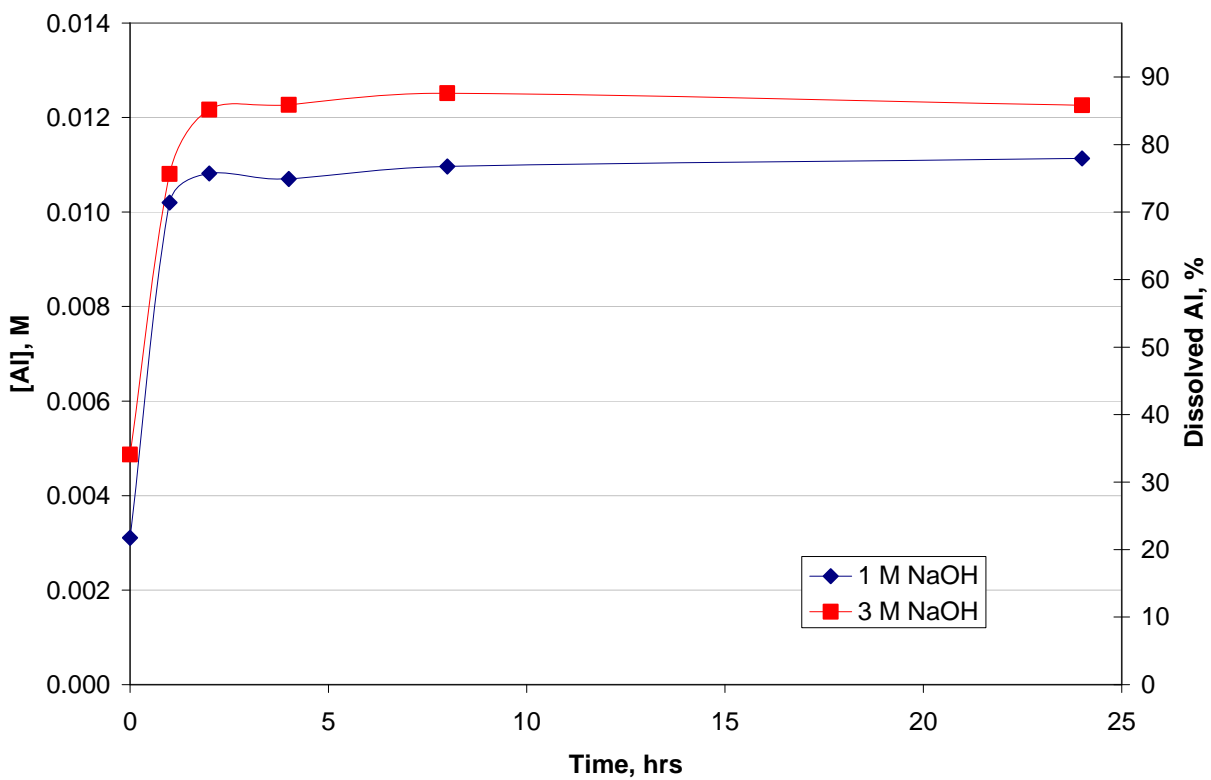
Figure 3.35. Aluminum Concentration and Percent Removed Versus Time at 60°C for Leaching of the Group 1 Washed Solids in 1 and 3 M NaOH
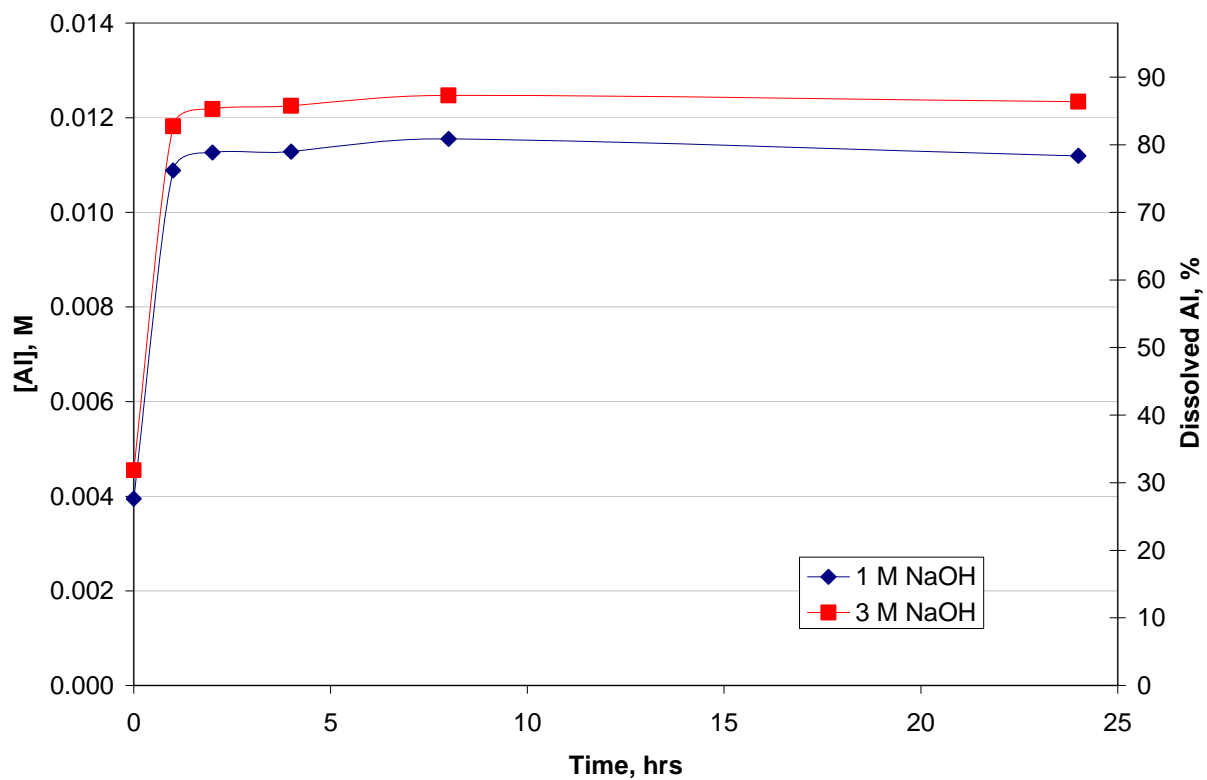
Figure 3.36. Aluminum Concentration and Percent Removed Versus Time at 80°C for Leaching of the Group 1 Washed Solids in 1 and 3 M NaOH
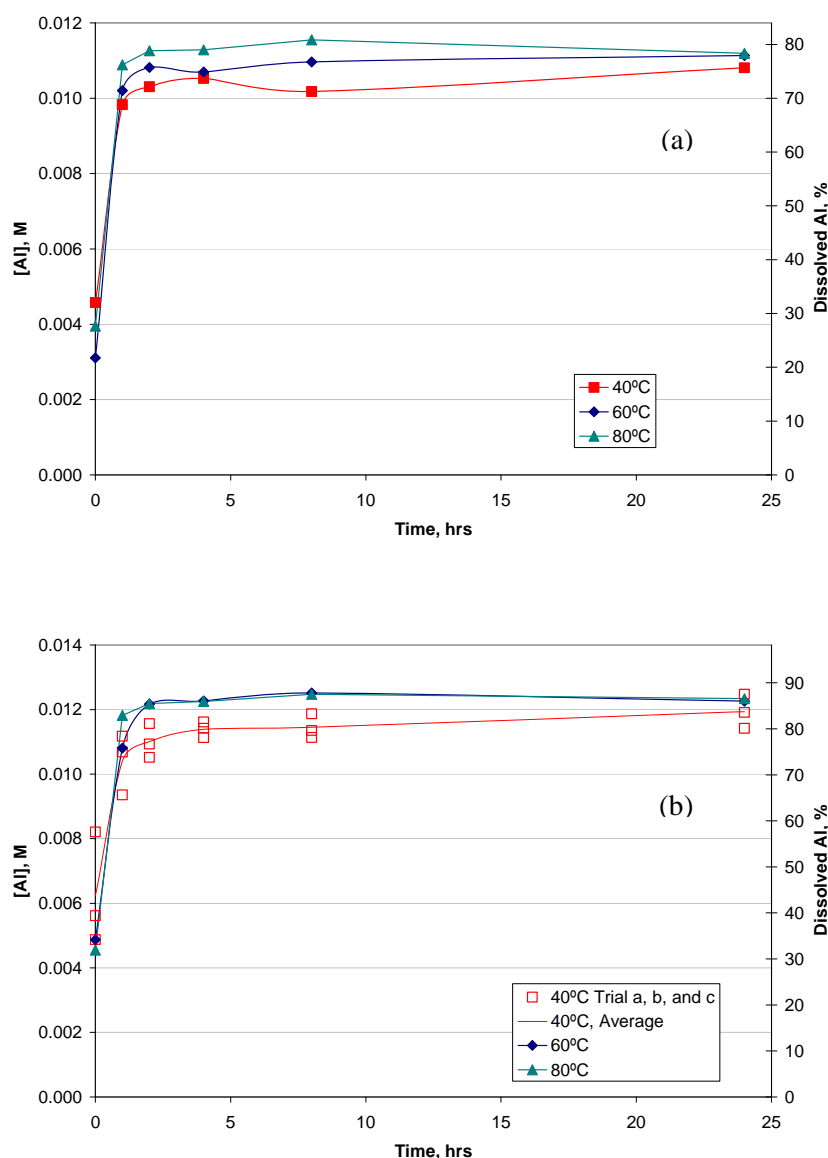
Figure 3.37. Aluminum Concentration and Percent Removed Versus Time at a) 1 M NaOH, 40, 60, and 80°C, and b) 3 M NaOH, 40, 60, and 80°C, for Leaching of the Group 1 Washed Solids

3.4.3 Time, Temperature, and Hydroxide Effects on Chromium Dissolution from the Group 1 Solids

The rate and extent of Cr removal from the washed Group 1 solids were investigated as a function of time, temperature, and free-hydroxide concentration. Based on the total Cr concentration in the washed Group 1 solids (5.37 mg/g—free of residual supernatant), the complete dissolution of Cr would result in a concentration of 0.051 mg Cr/mL or 0.0010 M.

The chromium leaching data at 40, 60, and 80°C are plotted in Figure 3.38 through Figure 3.40, respectively. Figure 3.41 compares the Cr leaching behaviors at the three different temperatures

examined at the individual NaOH concentrations investigated. Under all temperature conditions, the amount of Cr in solution increased with increasing NaOH concentration. Similarly, at a given NaOH concentration, the amount of Cr removed during caustic leaching increased with increasing temperature. However, even under the most rigorous leaching conditions examined (3 M NaOH at 80°C), only 22% of the Cr was removed after 24 h of leaching. These observations are consistent with previous parametric caustic-leaching tests with Hanford tank sludges (Lumetta et al. 1998, 2001, 2002).

At 40 and 60°C and 3 M NaOH, the Cr concentration at 1 h of leaching appeared to be lower than expected based on the shape of the rest of the curve (Figure 3.38 and Figure 3.39). This might suggest an initial partial reduction of the Cr(VI) present [leading to precipitation of Cr(III)]. Based on the experimental uncertainty, it is not entirely clear that this phenomenon is real, but given the reproducibility of the observation in the triplicate 40°C runs and the similar observation at 60°C, the lower than expected Cr concentration at 1 h does appear to be real. A similar observation is not observed at 80°C. Perhaps with the higher rate of Cr(III) oxidation at higher temperature, any Cr(III) initially formed was rapidly oxidized back to Cr(VI) at 80°C.
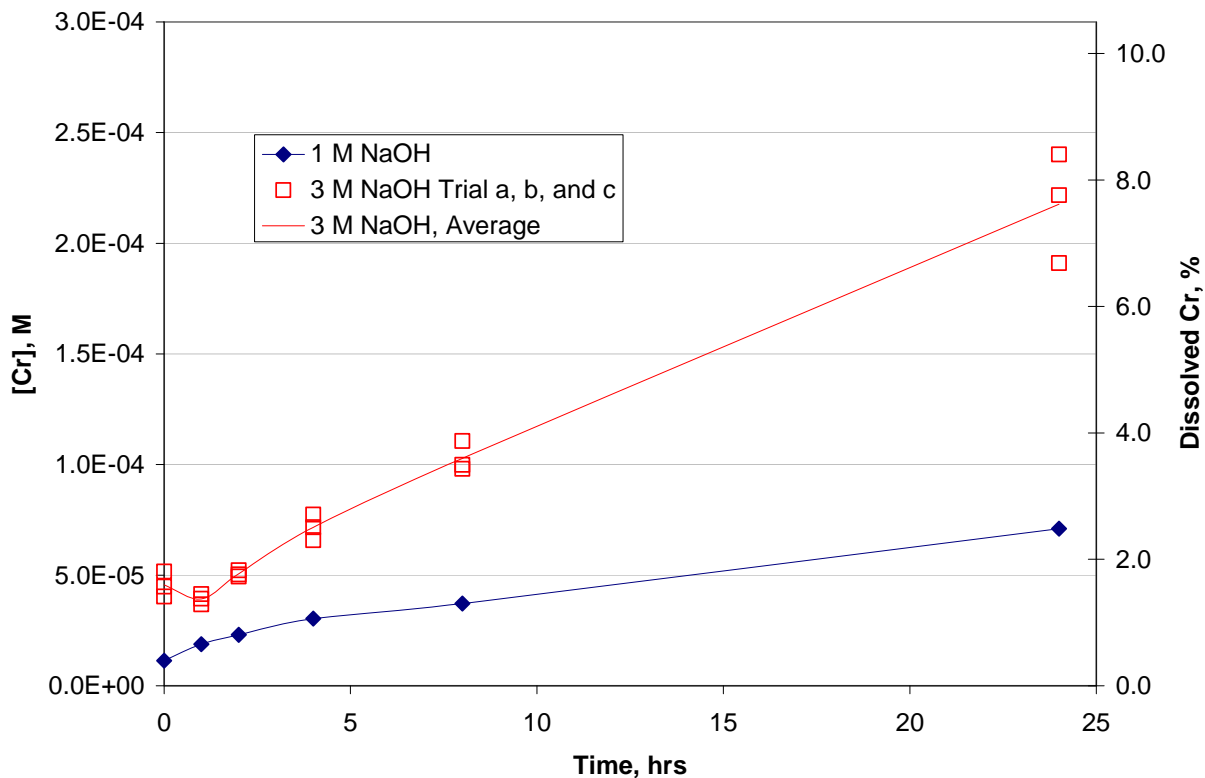
Figure 3.38. Chromium Concentration and Percent Removed Versus Time at 40°C for Leaching of the Group 1 Washed Solids in 1 and 3 M NaOH
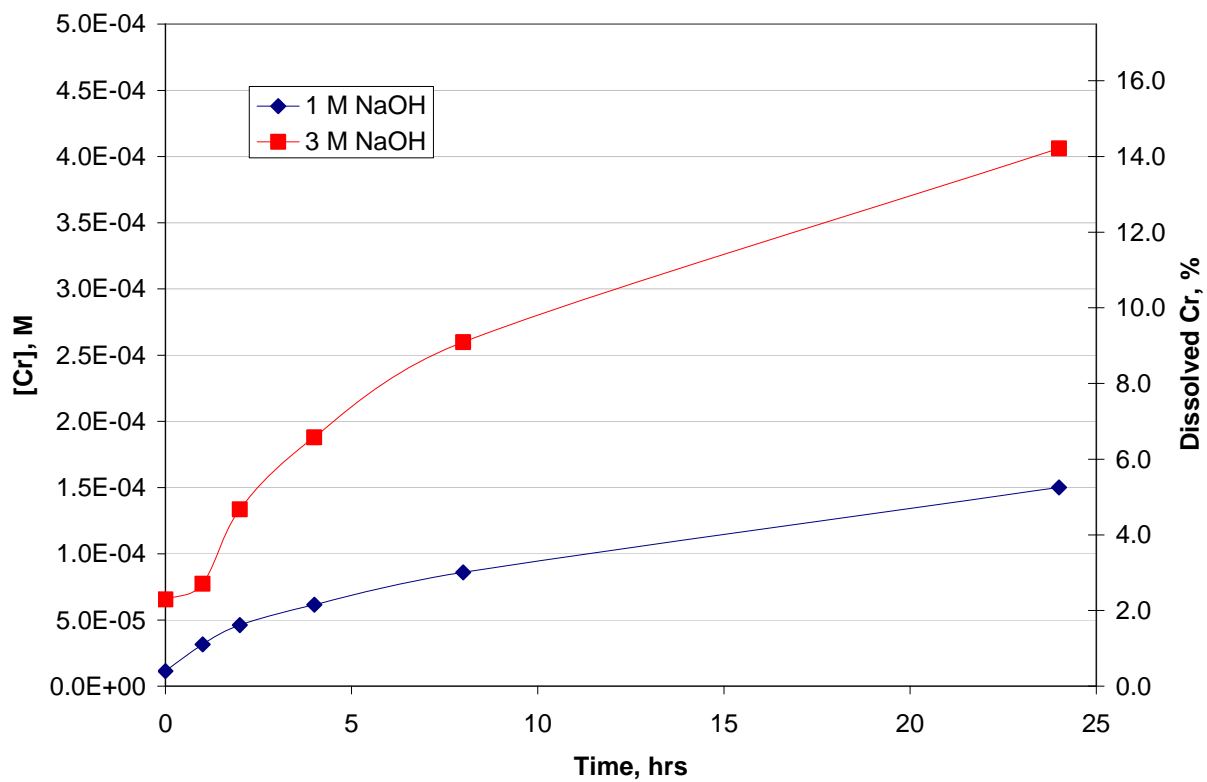
Figure 3.39. Chromium Concentration and Percent Removed Versus Time at 60°C for Leaching of the Group 1 Washed Solids in 1 and 3 M NaOH
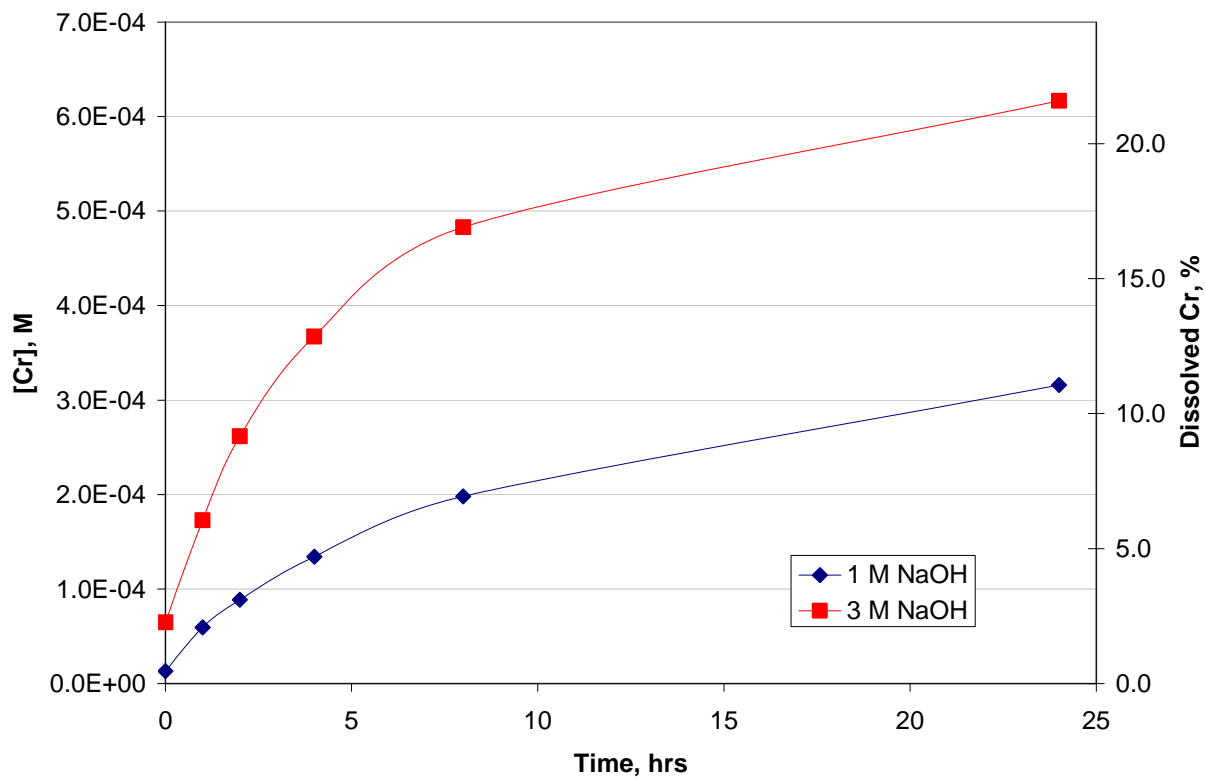
Figure 3.40. Chromium Concentration and Percent Removed Versus Time at 80°C for Leaching of the
Group 1 Washed Solids in 1 and 3 M NaOH
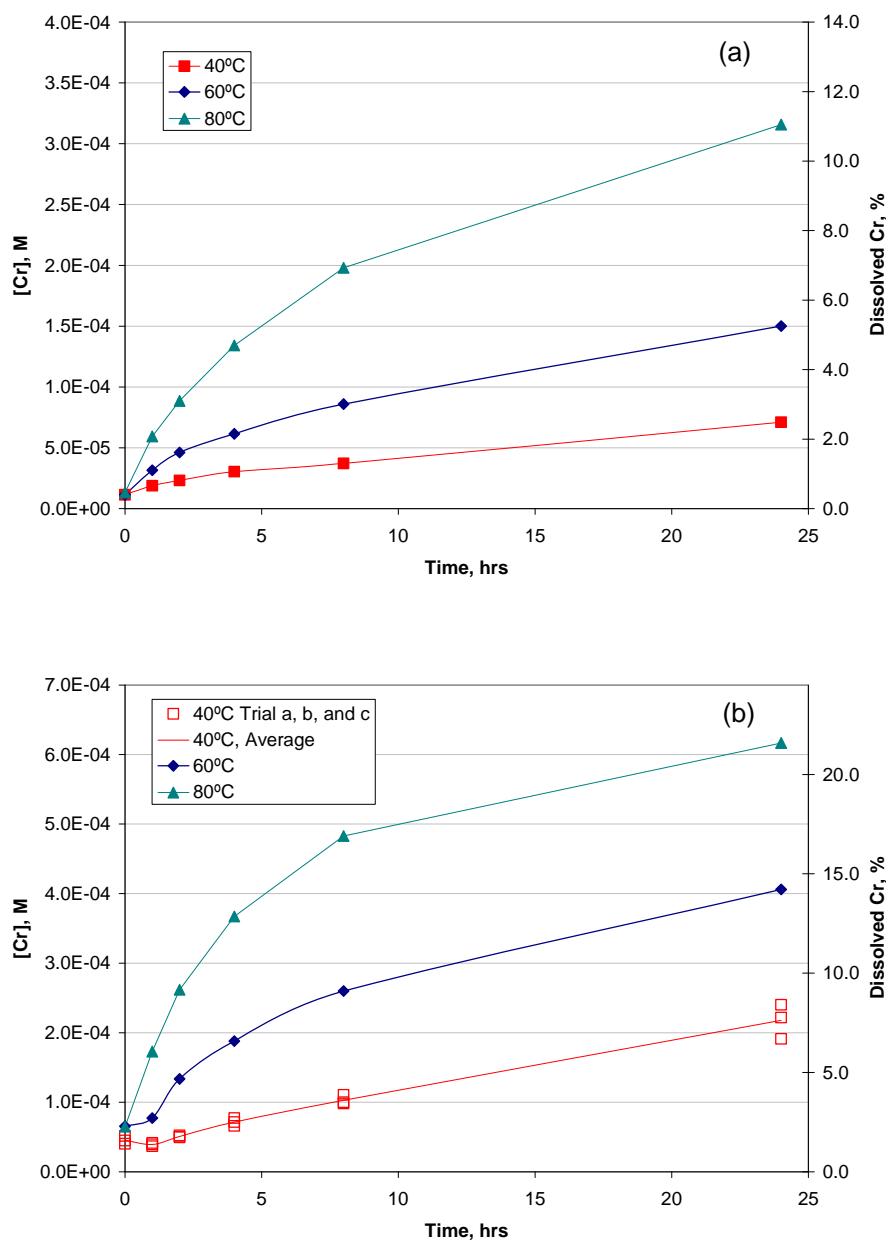
Figure 3.41. Chromium Concentration and Percent Removed Versus Time at a) 1 M NaOH, 40, 60, and 80°C, and b) 3 M NaOH, 40, 60, and 80°C, for Leaching of the Group 1 Washed Solids

3.4.4   Anion, Silicon, and Iron Leaching Behavior

The concentration of Si was measured opportunistically by ICP-OES. The anionic compositions were also assessed at each sampling period. Anion and Si concentrations in the leachate did not significantly change during the leach testing. The results are summarized in Appendix G.

Iron concentrations were also measured opportunistically by ICP-OES. The Fe concentrations in the leachates decreased relative to the first sampling period at 0 hr (4.85×10^{-4} M Fe) to the 24-hr sampling

period ($<2.23 \times 10^{-4}$ M Fe) for the triplicate samples treated at 40°C in 3 M NaOH. Concentrations were lower ($\sim 7 \times 10^{-5}$ M) for samples treated in 1 M NaOH.

3.4.5   Assessment of Final Leaching Conditions

A summary of the final (24-h) leach solution chemistry and physical parameters is shown in Table 3.13. The final free-hydroxide and sodium concentrations were at the targeted values within the uncertainty of the analytical methods ($\pm 15\%$). The calculated percentage of phosphorus and aluminum that was removed at each leaching condition is also shown. Appendix G provides a compilation of the concentrations of Al, Cr, Fe, Na, P, Si, nitrite, nitrate, phosphate, and sulfate in the final leaching solutions. The GEA results for ^{60}Co and ^{241}Am were <MDL; the GEA results are also provided in Appendix G.

Table 3.13. Group 1 Bi-Phosphate Sludge Leaching Final Aqueous Phase Conditions

Temp., °C	Density, g/mL	Free OH, M	Na, M	P, M	Wt % P Removed	Al, M	Wt % Al Removed
40	1.05	1.10	1.14	0.0379	100.0	0.0108	75.9
40 trial a	1.14	3.28	3.26	0.0383	100.0	0.0125	87.6
40 trial b	1.14	3.23	3.31	0.0379	100.0	0.0119	83.6
40 trial c	1.13	3.14	3.18	0.0370	97.6	0.0114	80.1
60	1.05	1.03	1.17	0.0378	100.0	0.0111	78.1
60	1.14	3.20	3.27	0.0375	99.2	0.0123	86.0
80	1.05	1.07	1.17	0.0371	97.9	0.0112	78.5
80	1.14	3.23	3.25	0.0361	95.3	0.0123	86.6
ASR 8060							

3.4.6   Comparison of Initial and Caustic-Leached and Washed Solids Properties

The Group 1 solids that had been caustic leached at 40°C in 3 M NaOH for 24 hrs were combined and washed in preparation for analysis. The wash solution composition and the washed solids chemical, radiochemical, particle size, and crystal habit are discussed.

3.4.6.1 Leached Solids Wash Solution

After the third washing of the caustic-leached Group 1 solids, the wet centrifuged solids mass was 7.644 g. The densities of the three sequential wash solutions were 1.012 g/mL, 1.006 g/mL, and 1.004 g/mL, respectively. The composite wash solution (132.7 mL volume) density, ICP metals, and anion composition are shown in Table 3.14.

Table 3.14. Group 1 Solids Wash Solution Composition and Density

Analyte	µg/mL	Analyte	µg/mL	Density Measurement	Value
Al	[4.73]	Si	6.32	Density	1.009 g/mL
Cr	1.23	nitrate	86.6		
Na	1,542	phosphate	16.1		
P	[5.61]	sulfate	[2.75]		

3.4.6.2 Chemical and Radiochemical Composition

The initial composition of washed solids (before caustic leaching) is provided in Table 3.15 along with selected results from the initial characterization study. The solids composition after leaching in 3 M NaOH at 40°C for 24 hours and washing is also shown in Table 3.15. The solids used for the initial characterization had been washed three times, resulting in an estimated 14 wt% salt entrainment from the supernatant phase. The "before leaching" material had been more extensively washed, i.e., little or no salt entrainment was expected (except for NaOH from the washing liquid). The composition of the initial characterization sample was generally consistent with that for the "before leaching" material. This can be discerned by normalizing the major component concentrations to the iron content. For example, the Bi/Fe ratio was 1.15 for the initial characterization sample versus 1.12 for the material used for parametric leaching. Similarly, the P/Fe ratio of 0.95 for the initial characterization sample agreed well with the value of 0.93 for the material used for parametric leaching. On the other hand, the Na/Fe ratio for the initial characterization sample was 1.71 compared to 1.23 for the parametric leaching sample. This is consistent with the more extensive washing procedure that was performed on the latter sample.

Because the maximum P concentration projected to be in the caustic leachate solutions (based on the P in the initial solids) was 24% less than that found in the final 3 M NaOH leachate solutions, three methods of determining the percent leached were performed. Method 1 used the concentration of each analyte experimentally determined in the initial solids and the concentration of the analytes determined in the final leachate solutions. Method 2 used the concentration of the analytes in the final leachate solutions and the concentration in the final leached solids. Method 3 used the concentrations in the initial and final solids and the "concentration factor" method.

For the first method, the total amount (on a dry solids basis) of solids that went into each sample was determined based on the measurement of the UDS in the sample slurry and the mass of slurry added to each leaching bottle. The mass of solids in each leaching bottle was multiplied by the concentration of each of the analytes (i.e., Al, Cr, and P) in the initial solids to determine the total mass (in µg) of Al, Cr, and P in each sample. The total mass of Al, Cr, and P in the final leachate solutions was calculated by multiplying the concentration of each analyte (µg/mL) determined to be in solution at 24 h by 100 mL (the total volume of leaching solution). The leach factor was then taken as the mass of each component in the leachate solution at 24 hrs (W_L) divided by the mass of that component in the initial sample (W_{IS}) (Equation 3.2).

$$LF_1 = \left(\frac{W_L}{W_{IS}} \right)$$

(3.2)

Table 3.15. Group 1 Bi-Phosphate Sludge Leached Solids Composition and Leach Factors (Dry Mass Basis)

Analyte	Avg. Initial Charac. µg/g (ASR 7985)	Avg. Before Leaching, µg/g (ASR 8060)	Avg. After Leaching, µg/g (ASR 8060)	Observed Leach Factor
Al	26,350	26,400	[11,500]	0.84
B	[130]	[160]	[240]	0.44
Bi	98,200	121,000	314,500	0.03
Cd	<6.6	[120]	<12.1	0.96
Cr	4,260	5,370	13,300	0.08
Fe	85,550	108,500	304,500	--
Mn	373	441	1,290	--
Na	146,000	133,500	[14,000]	0.96
P	81,300	101,000	[795]	1.00
S	[3,250]	[1,700]	[840]	0.82
Si	42,850	60,000	19,850	0.88
Sr	888	1,215	3,160	0.03
U	[7,800]	13,300	8,580	0.76
Zn	[380]	522	193	0.86
Zr	[205]	745	723	0.64
U (KPA)	11,400	10,400	7,900	0.72
	µCi/g	µCi/g	µCi/g	
^{60}Co	9.59×10^{-3}	1.18×10^{-3}	7.15×10^{-3}	--
^{90}Sr	3.95×10^{1}	4.45×10^{1}	1.35×10^{2}	--
^{137}Cs	2.19×10^{1}	3.00×10^{1}	1.25×10^{0}	0.98
^{154}Eu	$<5.0 \times 10^{-3}$	2.73×10^{-3}	8.51×10^{-3}	--
^{155}Eu	$<2.0 \times 10^{-2}$	1.65×10^{-2}	1.29×10^{-2}	0.71
$^{239+240}$Pu	5.64×10^{-1}	6.88×10^{-1}	1.86×10^{0}	--
^{241}Am	5.87×10^{-2}	6.80×10^{-2}	1.74×10^{-1}	0.05
total alpha	6.31×10^{-1}	6.78×10^{-1}	1.99×10^{0}	--
total beta	1.07×10^{2}	1.22×10^{2}	2.70×10^{2}	0.17
^{238}Pu	1.02×10^{-2}	6.79×10^{-3}	1.51×10^{-2}	0.17
Opportunistic				
Ag	<14	<6.44	<6.25	0.64
As	<230	<167.6	<162.6	--
Ba	[54]	106	203	0.29
Be	<1	<0.21	<0.20	0.63
Ca	<2600	<4726	[5,800]	--
Ce	<170	452	[275]	0.77
Co	<18	[17]	[53]	--
Cu	[59]	211	193	0.66
Dy	<44	<12.5	<12.1	0.64
Eu	<14	[4.95]	<2.54	--
La	<9	[74]	<11.3	0.94
Li	<27	[48]	[56]	0.56

Table 3.15 (Contd)

Analyte	Avg. Initial Charac. µg/g (ASR 7874)	Avg. Before Leaching, µg/g (ASR 8032)	Avg. After Leaching, µg/g (ASR 8032)	Observed Leach Factor
Mg	[900]	1,050	2,950	--
Mo	<25	<30.9	[39]	--
Nd	<260	[58]	<26	0.83
Pb	[285]	[635]	[1,150]	0.32
Pd	<160	<27.5	<26.7	--
Rh	<100	<55.9	<54.2	--
Ru	<44	[40]	[95]	0.11
Sb	<150	<134	<130	--
Se	<250	<473	<459	--
Sn	<230	<108	<105	--
Ta	<50	<85.9	<83.4	--
Te	<200	<112	[108]	--
Th	<150	[50]	[69]	0.49
Ti	[45]	59.7	199	--
Tl	<180	[190]	<125	0.75
V	<12	<13.8	[22]	--
W	<78	<90.3	<87.6	--
Y	<17	[3.45]	[4.75]	0.49

For the second method, the mass of residual solids in each of the three samples treated at 40°C in 3 M NaOH was first determined. These three solids samples were combined, washed, and then slurried in water. A sample of this slurry was dried to determine the wt % UDS. The total mass of solids was determined from the slurry mass and wt% UDS. This number was then divided by three to obtain the average mass of dried solids in each of the three samples of leached solids. This mass was then multiplied by the concentration of each of the analytes in the final solids to determine the mass (in µg) of Al, Cr, and P in each leached sample. The leach factor was then calculated by dividing the mass of the component in the leachate solution (W_L) by the total mass of the analyte in each sample, calculated from the mass of each in the final solids and leachate solution (sum of W_L and weight in the final samples [W_{FS}]) as shown in Equation 3.3.

$$LF_{triplicate\_samples} = \left(\frac{W_L}{W_L + W_{FS}} \right)$$

(3.3)

As is done with the "concentration factor" method, the average leach factor from the three samples for each analyte was calculated. The average of the concentration of each analyte in the final leachates from the triplicate runs was divided by the average leach factor of the triplicate samples to obtain an average corrected concentration (CC) that corresponds to the concentration that would be obtained if 100% of the sample had dissolved. The weight of each analyte in the leachate solutions is divided by the average corrected concentration to determine the leach factors as shown in Equation 3.4.

$$LF_2 = \left(\frac{W_L}{CC}\right) \tag{3.4}$$

The third method is the same that was previously reported in Fiskum et al. (2008). The analysis of the leachate solutions showed that Bi, Cr, Fe, Mn, and Sr were not dissolved by caustic leaching. The average ratio of the concentration of these components in the leached solids divided by the concentration in the solids before leaching (referred to as the relative concentration factor or CF) was 2.68. This term was used to determine the specific analyte leach factors according to Equation 3.5:

$$LF_3 = 1 - \left(\frac{C_L}{C_W \times 2.68}\right) \tag{3.5}$$

where LF_3 is the caustic-leach factor, C_L is the analyte concentration in the leached solids, and C_W is the analyte concentration in the initial washed solids.

Results from all three methods are given in Table 3.16. The results from the first method are higher than those obtained from the second two methods. Reasonably good agreement is seen between methods two and three. This would indicate an error in the initial solids data, either in the wt% UDS or in the ICP-OES data. This error is not seen in the third method of calculating the leach factor because, although this method also uses the initial solids data, the absolute weights of the various analytes are not used, only the concentration, which is normalized with the concentrations in the final solids by using the concentration factor. All values of percent leached plotted in this section and shown in Table 3.13 and Table 3.15 were calculated using method three, the "concentration factor" method.

Figure 3.42 presents the mass fraction for selected components of the Group 1 waste in the initial water-insoluble solids and in the leached and washed material. As can be seen from the figure, approximately 45% of the metals mass dissolved within a 24-hr leaching time (3 M NaOH at 40°C).

Table 3.16. Group 1 Bi-Phosphate Sludge Leach Factors

Temp., °C	Free [OH], M	Na, M	Fraction Removed Based on Initial Solids/Leachate Solution			Fraction Removed Based on Final Solids/Leachate Solution			Fraction Removed Based on Initial/ Final Solids ("concentration factor" method)		
			Al	Cr	P	Al	Cr	P	Al	Cr	P
40	1.10	1.14	1.16	0.07	1.22	0.81	0.07	1.00	0.76	0.02	1.00
40: trial a	3.28	3.26	1.34	0.24	1.24	0.90	0.22	1.00	0.88	0.08	1.01
40: trial b	3.23	3.31	1.30	0.23	1.24	0.89	0.21	1.00	0.84	0.08	1.00
40: trial c	3.14	3.18	1.22	0.19	1.18	0.89	0.18	1.00	0.80	0.07	0.98
60	1.03	1.17	1.21	0.15	1.23	0.83	0.14	1.00	0.78	0.05	1.00
60	3.20	3.27	1.33	0.42	1.22	0.92	0.38	0.99	0.86	0.14	0.99
80	1.07	1.17	1.21	0.32	1.20	0.84	0.30	0.98	0.79	0.07	0.98
80	3.23	3.25	1.34	0.63	1.17	0.92	0.58	0.95	0.87	0.17	0.95
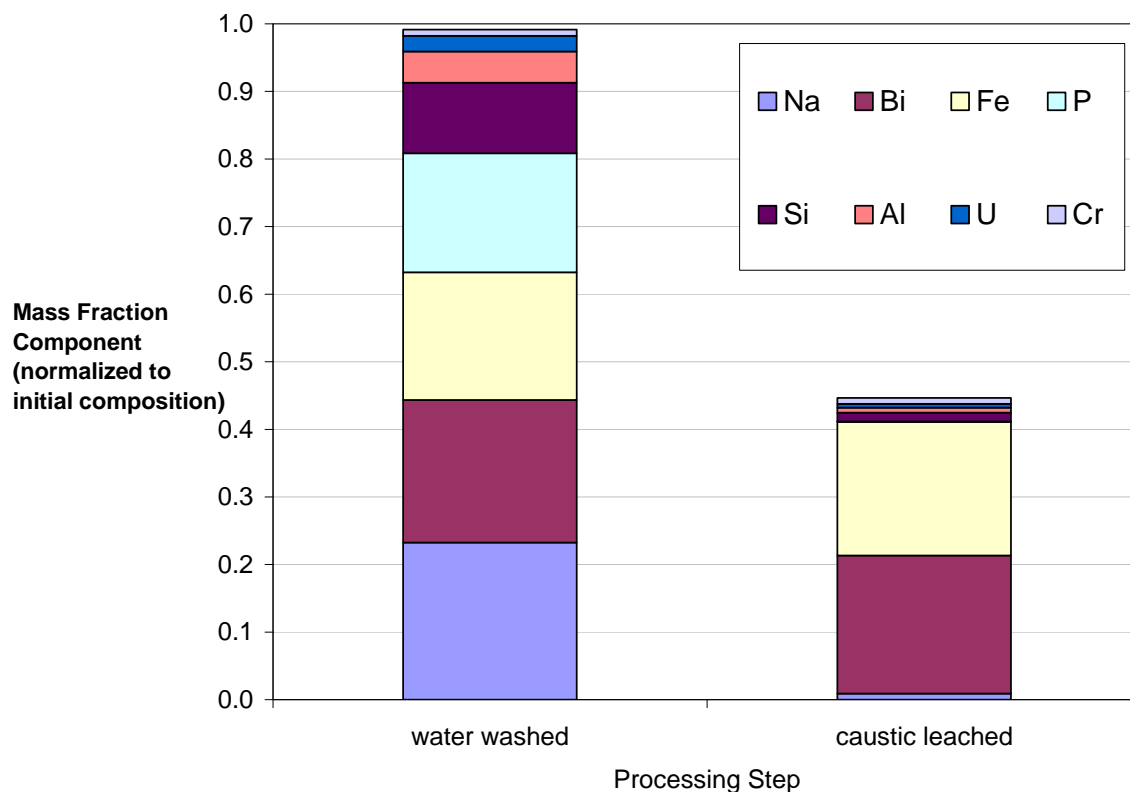
Figure 3.42. Group 1 Bi-Phosphate Sludge Reduction in Solid Mass with Water Washing and Caustic Leaching

3.4.6.3 Particle-Size Distribution

PSD measurements were performed on a sample of the caustic-leached solids (sample ID 555-G1-CL-PSD). Table 3.17 shows selected cumulative undersize percentiles for this sample. Here, the d(10) ranges from 2.2 to 8.3 μm, the d(50) ranges from 14 to 42 μm, and the d(90) ranges from 76 to 130 μm. All percentiles, regardless of measurement condition, are significantly (>10%) larger than those observed in the Group 1 source material (sample ID TI483-G1-S-WL-PSD). The increase observed in percentiles for the leached material compared to the starting material could be attributed to either dissolution of the smaller particles originally present (with the larger particles being insoluble in caustic) or to the formation of agglomerates in the leached material. A combination of both of these is also possible.

Before sonication, the PSD appears to shift towards smaller particles at high pump speed (4000 RPM). This could indicate possible breakage of weak agglomerates through shearing action; this conclusion is supported by increased obscuration at 4000 RPM (i.e., more particles in the dispersion). Applying sonic energy causes a dramatic decrease in obscuration accompanied by an increase in particle size. Both trends suggest sonication-induced agglomeration. The rapid agglomeration upon sonication appears to be unique to caustic-leached and washed Group 1 solids. The post-sonication PSD behaves in a similar manner to that of the pre-sonic distribution. A high pump speed (4000 RPM) causes significant reductions in d(10) and d(50). A low pump speed (2000 RPM) causes increases in both d(50) and d(90).

Overall, the dispersion appears to be unstable, as evidenced by the decreasing obscuration and increasing values for cumulative percent undersize as the measurement progresses.

Table 3.17. Particle-Size Analysis Percentile Results for the Caustic-Leached and Washed Group 1 Solids (sample 555-G1-CL-PSD). Also reported is the laser obscuration (i.e., the percent laser blocked/scatted by the dispersion) for the measurement.

Measurement Condition	Pump Speed	Sonication	Obscuration [%]	d(10) [μm]	d(50) [μm]	d(90) [μm]
1	3000	pre-sonic	9.4	2.9	25	99
2	4000	pre-sonic	10.2	2.2	14	76
3	2000	pre-sonic	9.2	2.2	18	110
4	3000	25%	7.2	2.2	20	87
5	3000	50%	5.1	3.0	27	96
6	3000	75%	3.9	4.5	30	100
7	3000	post-sonic	3.4	8.3	36	100
8	4000	post-sonic	4.3	3.6	31	100
9	2000	post-sonic	4.2	3.1	42	130

Figure 3.43 shows the PSD in the caustic-leached and washed Group 1 solids before sonication. The distributions are broad, spanning 0.3 to 300 μm, and multimodal. At 3000 RPM, the distribution is dominated by a peak with a maximum population at 30 to 40 μm. A secondary population of particles spans 0.3 to 8 μm and has a peak population over 4 to 5 μm. Increasing the pump speed decreases the relative contribution of particles in the range of 20 to 200 μm and correspondingly increases the relative contribution of particles from 0.3 to 8 μm. Again, this trend suggests shear breakage of agglomerates. At low pump speeds (2000 RPM), the PSD suggests agglomerate reformation through an increase in the contribution of particles in the range of 80 to 200 μm. On the other hand, this behavior could also result from decreased suspension of dense particles from 10 to 50 μm. However, for this behavior to hold, flocculates in the 50- to 200-μm range must be very loose (i.e., low-density) and easy to suspend. Considering all of these observations, the state of pre-sonication particle aggregation/flocculation appears to be highly sensitive to changes in pump speed.
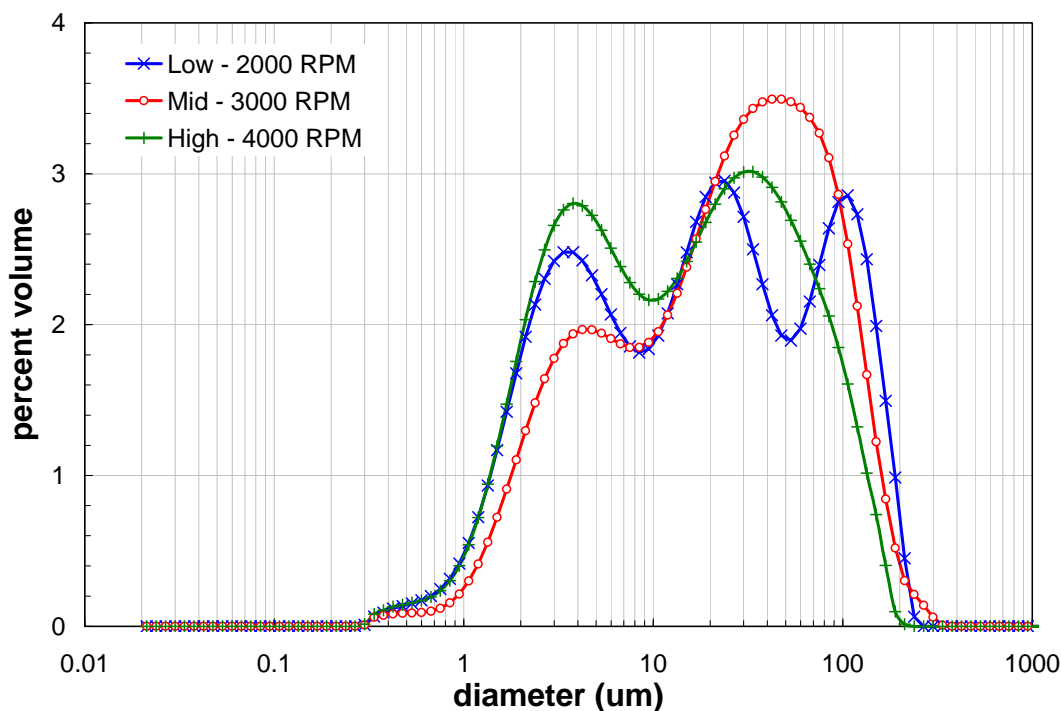
Figure 3.43. Pre-Sonication Volume Distribution Result for the Caustic-Leached and Washed Group 1 Solids (sample 555-G1-CL-PSD) as a Function of Pump Speed

Figure 3.44 shows changes that occur in the distribution of particles as a result of applying sonication. Relative to the PSD at measurement condition 1 (Table 3.17), the "during-sonication" PSD shows increases in the relative volume contribution of submicron and ~10- to 50-μm particles and a significant decrease in the contribution of 1- to 10-μm particles. Both the increase in the 10- to 50-μm particles and the decrease in the 1- to 10-μm particles suggest sonication-induced aggregation. Although the energy applied to particle systems by sonication typically disrupts agglomerates, there are cases where sonication can actually help particle systems overcome the particle-particle repulsion that prevents the formation of strong agglomerations (i.e., coagulation). An alternative explanation for the behavior observed in Figure 3.44 is that sonication eliminates (through dissolution or complete disruption) particles in the 1- to 10-μm particle range, effecting apparent increases in the contribution of submicron and 10- to 200-μm size ranges. Given that these solids have been thoroughly washed and allowed to equilibrate in the low-ionic-strength suspending phase, it is unlikely that any further dissolution occurred. After turning off the sonicator, there is little overall change in the PSD with the exception of an increased population of 30- to 100-μm agglomerates. This suggests that aggregate formation (or dissolution) continues after sonication is removed.
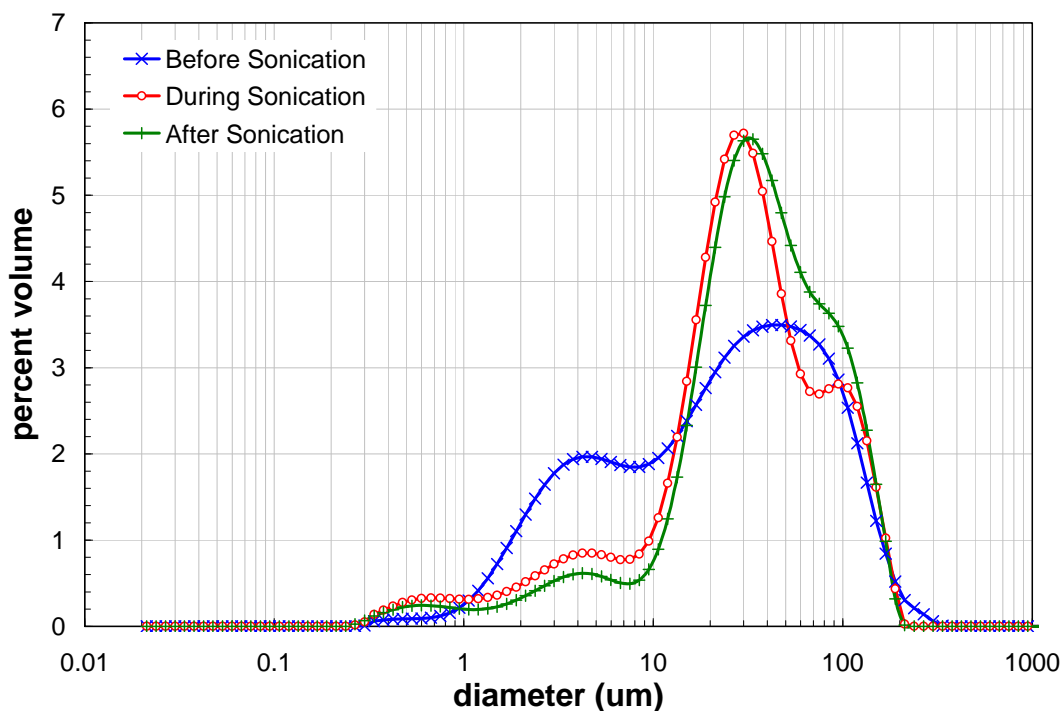
Figure 3.44. Volume Distribution Result for the Caustic-Leached and Washed Group 1 Solids Before, During, and After Sonication at 3000 RPM. Note: the during-sonication condition corresponds to measurement condition 6 (see Table 3.17).

Figure 3.45 shows the post-sonication PSD behavior of the caustic-leached and washed Group 1 solids sample as a function of analyzer pump speed. The trends are similar to those observed in the pre-sonication measurements. Increasing the pump speed (from 3000 to 4000 RPM) both increases the fraction of middle-sized (1- to 10-μm) particles and decreases the fraction of large (10- to 200-μm) particles, indicating shear disruption of flocculates. As before, low pump speeds (2000 RPM) show diminished particles in the 10- to 50-μm range, indicating loss of these particles to aggregate formation or poor suspension.
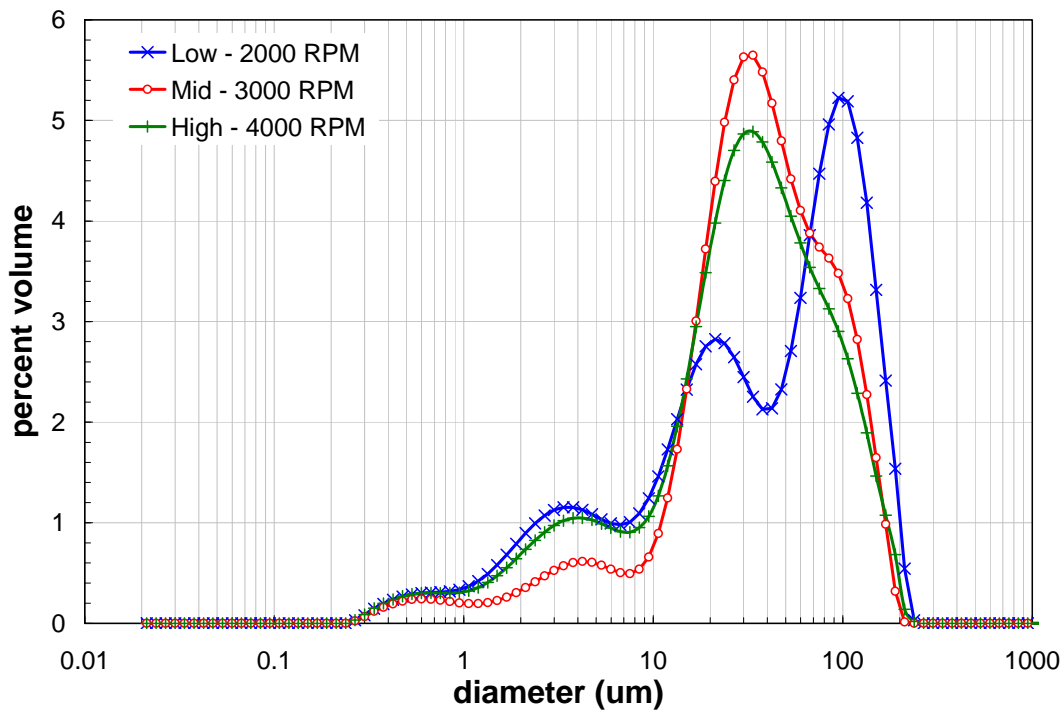
Figure 3.45. Post-Sonication Volume Distribution Result for the Caustic-Leached and Washed Group 1 Solids as a Function of Pump Speed

The influence of caustic-leaching and washing on the Group 1 particles can be evaluated by comparing the PSD for the source material (i.e., that for initial characterization sample TI483-G1-S-WL-PSD) to the caustic-leached and washed Group 1 Parametric PSD sample (555-G1-CL-PSD). The PSD measurement for the primary initial characterization samples is used for this comparison. Table 3.18 and Figure 3.46 indicate the changes that occur to the Group 1 solids PSD as a result of the caustic-leaching and washing operations. The caustic-leached solids show a significant contribution of large (~10- to 200-µm) particles not observed in the source Group 1 solids. It is speculated that this 10- to 200-µm fraction corresponds to particle flocs that form in the caustic-leached solids as a result of changed surface chemistry. The caustic-leached solids also show a small shoulder population spanning 0.3 to 10 µm. This lower range distribution shows maxima at 0.6 and 4 µm. It is possible that this population corresponds to remaining (i.e., those un-reactive to caustic) Group 1 solids as both distributions over this range are roughly bimodal.

Table 3.18. Cumulative Undersize Percentiles Showing the Influence of Caustic-Leaching and Washing on the PSD of Group 1 Solids at Measurement Condition 7—3000 RPM, Post-Sonication (see Table 3.17)

Sample	d(10) [µm]	d(50) [µm]	d(90) [µm]
Group 1 Initial Characterization (TI483-G1-S-WL-PSD-1)	1.0	5.0	23
Group 1 Caustic-Leached and Washed (555-G1-CL-PSD)	8.3	36	100
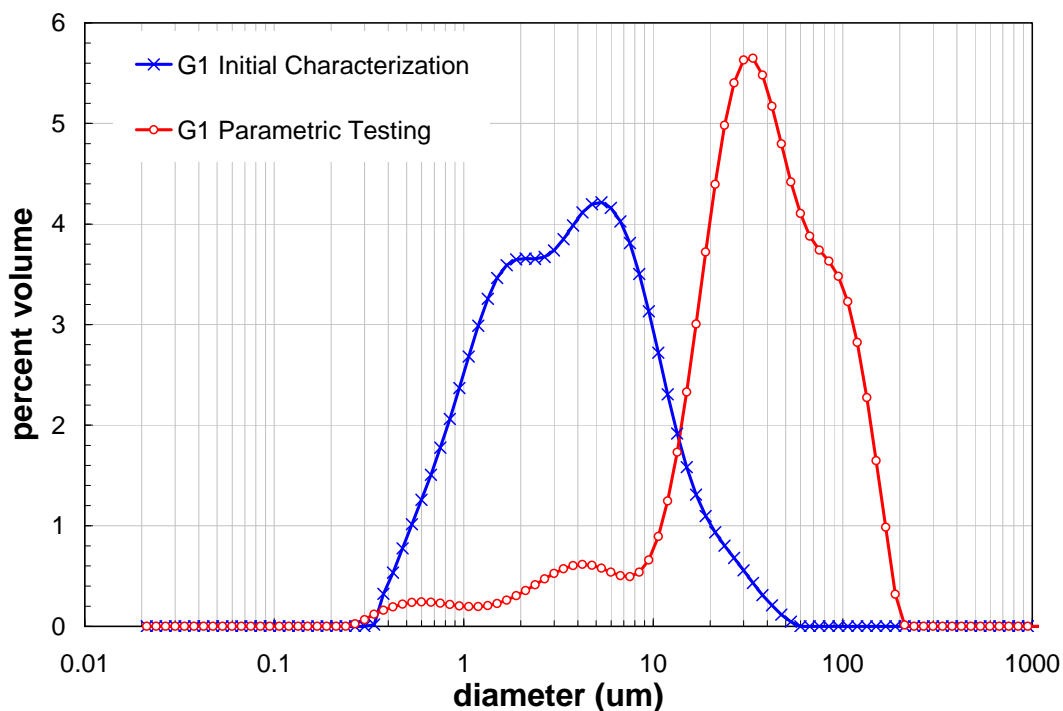
Figure 3.46. Influence of Caustic-Leaching and Washing on Group 1 (BiPO$_4$ sludge) Waste Solids PSD. All PSDs taken at measurement condition 7—3000 RPM, post-sonication (see Table 3.17)

3.4.6.4 Crystal Form and Habit

The following sections summarize the mineral-phase evaluation of the leached and washed solids.

3.4.6.4.1 XRD

The XRD pattern of the leached and washed solids (sample ID 555-G1-CL-XRD) is provided in Figure 3.47a; the background-subtracted XRD pattern with stick-figure phase identification is shown in Figure 3.47b.

Rutile, TiO$_2$, was used as an internal standard for 2-theta calibration. Identification was done on 2-theta calibrated data. This material is predominantly amorphous as indicated by the very broad peak system from about 12 to 37 degrees 2-theta. Another broad peak (centered at 14.60 degrees 2-theta with a FWHM of 1.68 degrees 2-theta) superimposed on that peak is indicative of boehmite (crystal density 3.01 g/cm^3, Wefers and Misra 1987) with a crystallite size on the order of 30 Å. One of the minor peaks present matches AlPO$_4$, berlinite (crystal density 2.62 g/cm^3, JADE, Version 8.0), but cannot be confirmed because the peak intensities are less than the background. Furthermore, the presence of AlPO$_4$ in the leached solids is unlikely because this compound has been shown to rapidly dissolve in NaOH solution (Lumetta 2008).

(a)

(b)
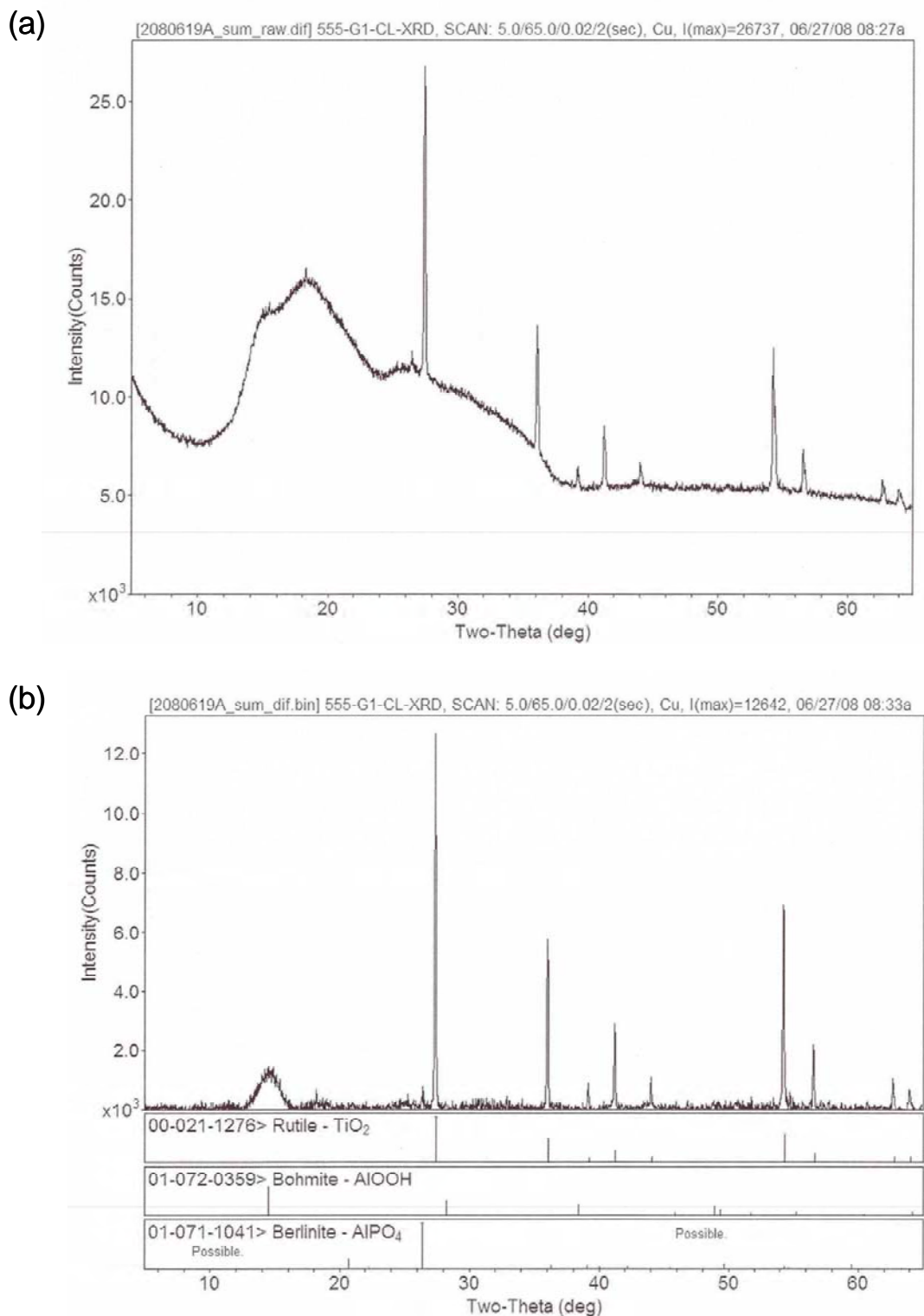
Figure 3.47. XRD Pattern of Caustic-Leached Group 1 Bi-Phosphate Sludge with Rutile (TiO$_2$) Internal Standard (a) Raw Data and (b) Background-Subtracted with Stick-Figure Peak Identification

3.4.6.4.2 SEM and TEM

Several SEM images are shown in Figure 3.48 as well as an elemental analysis of one area. The particles seen in these images are typically on the order of 5 to 50 µm. The elemental analysis shows a large amount of oxygen and carbon, which is an artifact of the sample preparation (carbon is sputtered onto the sample to eliminate problems with charging). If this is removed, and the other constituents normalized, the average weight percentages shown in Table 3.19 are obtained, which are in reasonable agreement with the values obtained by ICP-OES. These average values represent the average of thirteen individual particles that were examined. The Group 1 caustic leached solids were very homogeneous throughout the sample.
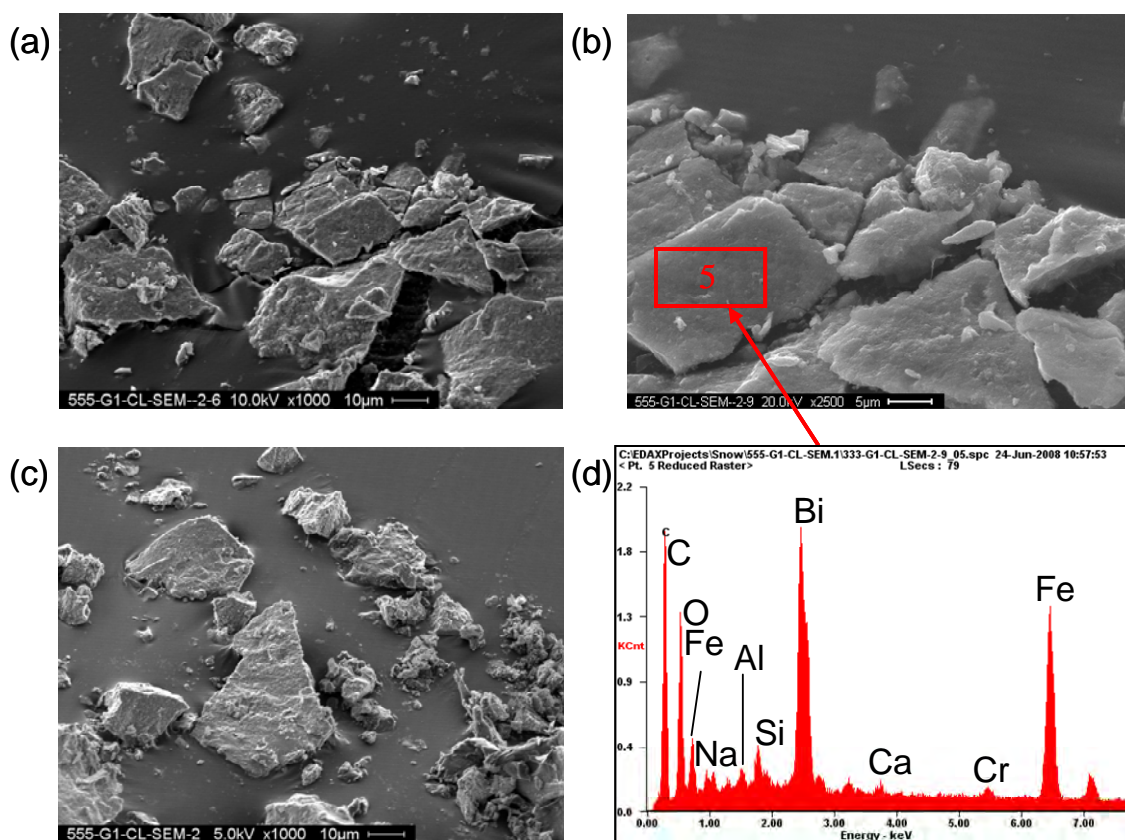
Figure 3.48. SEM Images of Group 1 Bi-Phosphate Sludge Caustic-Leached and Washed Solids (a) 10 kV, 1000×; (b) 20 kV, 2500×; (c) 5 kV, 1000×; (d) Elemental Map of Area 5 in (b)

Figure 3.49 shows STEM-HAADF images of particles in the Group 1 caustic-leached sample showing that the sample mostly consists of amorphous agglomerates. Figure 3.50 shows that on the larger scale, all that is seen is an amorphous solid. However, when a small area of this material is highly magnified, lattice fringes are seen, indicating the crystallinity of the agglomerated material. Although lattice fringes were observed, the material did not generate a clear selected area electron diffraction pattern. Because of the small crystallite size, the bulk material would be expected to appear amorphous to X-rays (which, as discussed above, is the case).

Table 3.19. Wt % of Various Elements by SEM and ICP-OES

Element	Avg Wt% by SEM	Wt% by ICP-OES
Na	2.1	1.4
Al	1.2	1.2
Si	2.3	2.0
Bi	48.2	31.5
Ca	0.9	0.6
Cr	1.8	1.3
Fe	43.6	30.5
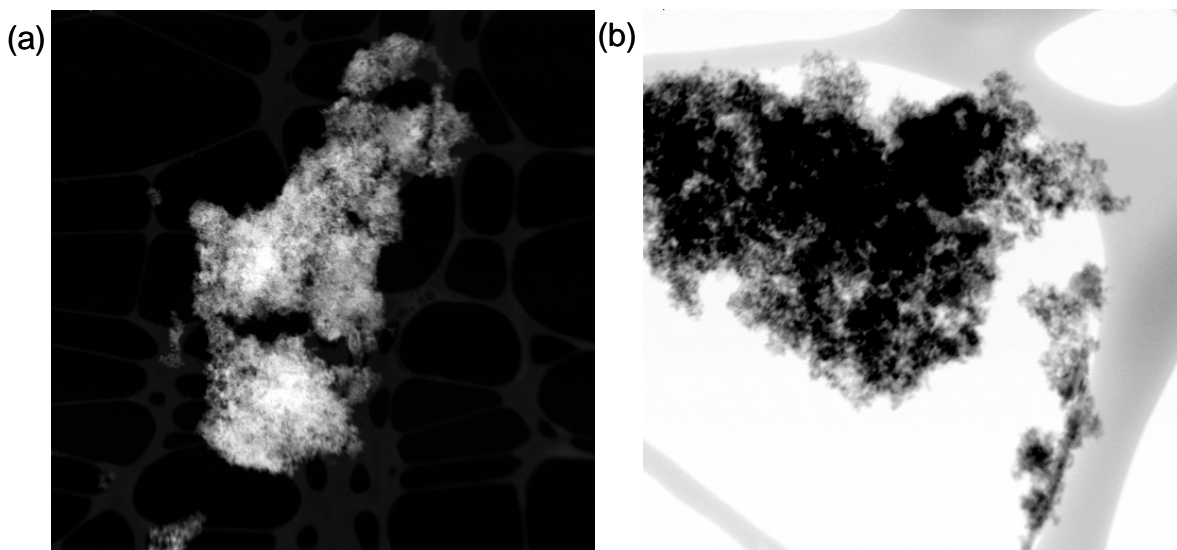
Figure 3.49. STEM-HAADF Images of Group 1 Bi-Phosphate Sludge Caustic-Leached and Washed Solids (a) Low Magnification; (b) Medium Magnification (inverted contrast)

Figure 3.51 shows EDS analysis of two areas of the sample. In several areas, bismuth and iron were seen by EDS. In one area, aluminum was seen. The major phase in the caustic-leached sludge, as indicated by the TEM examination, appears to be a nano-crystalline iron bismuth phase. Only a small amount of an aluminum oxide was detected, which might be boehmite as suggested by the XRD.
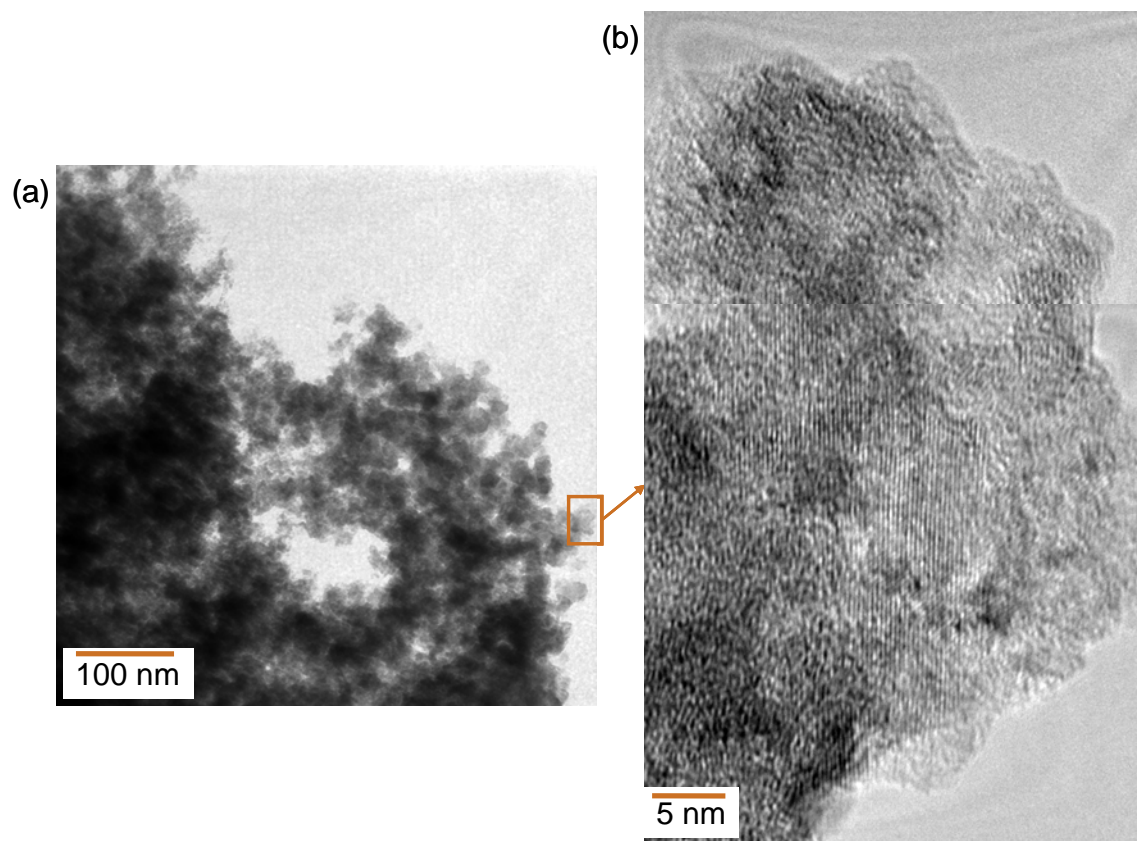
Figure 3.50. High Resolution TEM Images of Group 1 Bi-Phosphate Sludge Caustic-Leached and Washed Solids (a) Amorphous Solids; (b) Magnification Shows Lattice Fringes
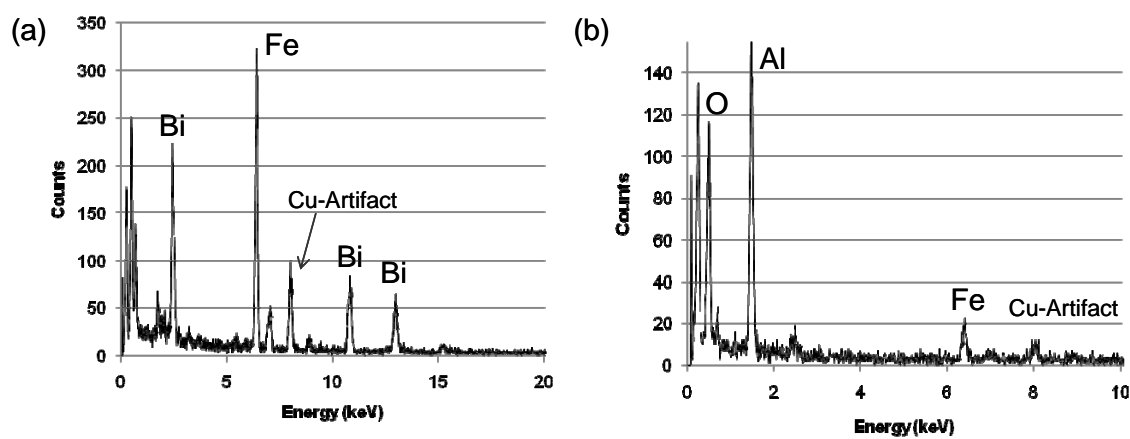
Figure 3.51. EDS Analysis of Group 1 Bi-Phosphate Sludge Caustic-Leached and Washed Solids (a) Fe and Bi; (b) Aluminum Oxide

3.4.6.4.3 Surface Area by BET

A BET measurement was conducted on the caustic-leached and washed solids, resulting in a surface area of 265.3 m^2/g. This shows an increase in relative surface area following caustic leaching from the average value of 94.5 m^2/g found in the initial, washed solids.

4.0   Group 2 Characterization of Bismuth Phosphate Saltcake

This section reports and discusses the analytical results for the bismuth phosphate saltcake (Group 2) slurry composite. The supernatant results represent the equilibrated aqueous phases in contact with the solids; the solids characterization results were obtained after three washes with 0.01 M NaOH.

4.1   Group 2 Characterization Experimental

Table 4.1 shows the samples obtained during homogenization and sample splitting. Sample processing supporting the Group 2 characterization activities were identical to those for Group 1 and are summarized in Figure 3.1.

Table 4.1. Group 2 Characterization Samples

Sample ID	Characterization Activity	Slurry Volume, mL	Slurry Mass, g
TI517-G2-AR-S1	Physical Properties	8.6	13.45
TI517-G2-AR-S2	Physical Properties	7.5	11.78
TI517-G2-AR-S3	Physical Properties	8.9	13.60
TI517-G2-AR-C1	Chemical characterization and crystal habit	9.2	14.24
TI517-G2-AR-C2	Chemical characterization and crystal habit	12	17.18
TI517-G2-AR-RH	Rheology	132	195.99

The specific washing scheme applied to the Group 2 saltcake is provided in Figure 4.1. After washing and centrifuging, the solids settled uniformly to the bottom of the cone with no observed stratification into layers (Figure 4.2).
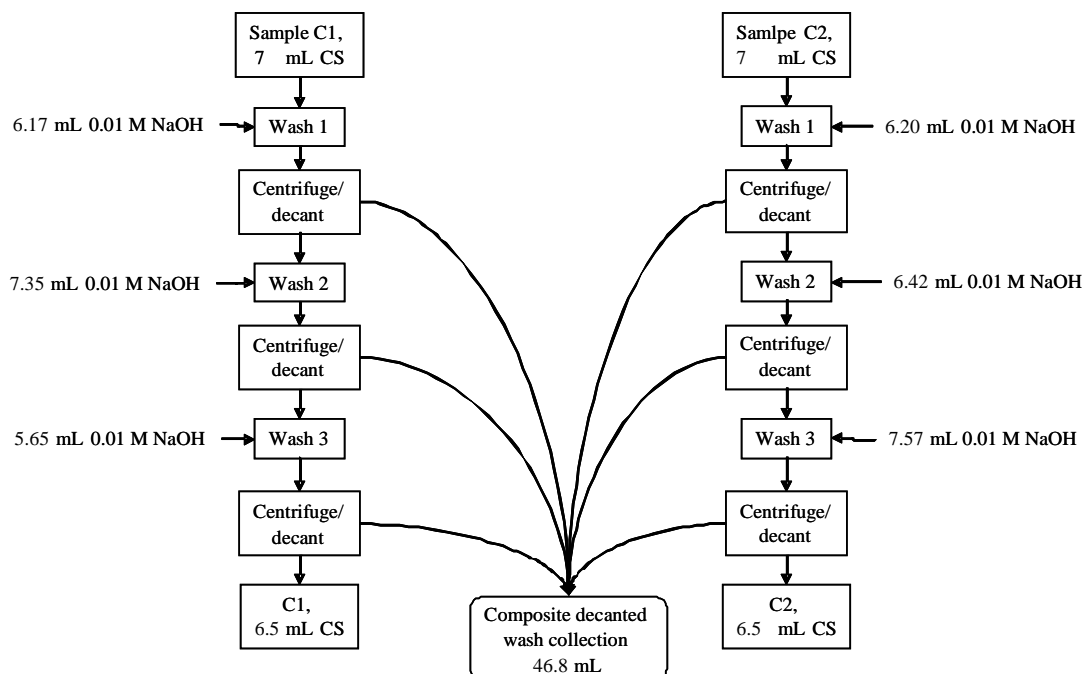
Figure 4.1. Wash Sequence of Group 2 Saltcake Supporting Initial Characterization

Figure 4.2. Chemical Characterization Sample of Group 2 Centrifuged Solids

4.2 Group 2 Characterization Results

4.2.1 Physical Properties of the Composite Slurry

The original Group 2 sample slurry was thick and difficult to stir and had a large percentage of solids in relation to supernatant liquid. These factors made it difficult to obtain reproducible representative samples. In the nine samples taken during the Group 2 characterization effort, the volume of settled solids varied from 75% to 90% (Figure 4.3), indicating considerable variability in the amount of solids

collected in each sample (error bars represent estimated errors at the time of measurement). For the three samples taken specifically for the settling test, good agreement in the settled-solids volume was observed between S1 (90%) and S2 (89%), but these were considerably higher than the value obtained for S3 (79%). The latter value is more consistent with the original sample, as can be seen from Figure 4.3).
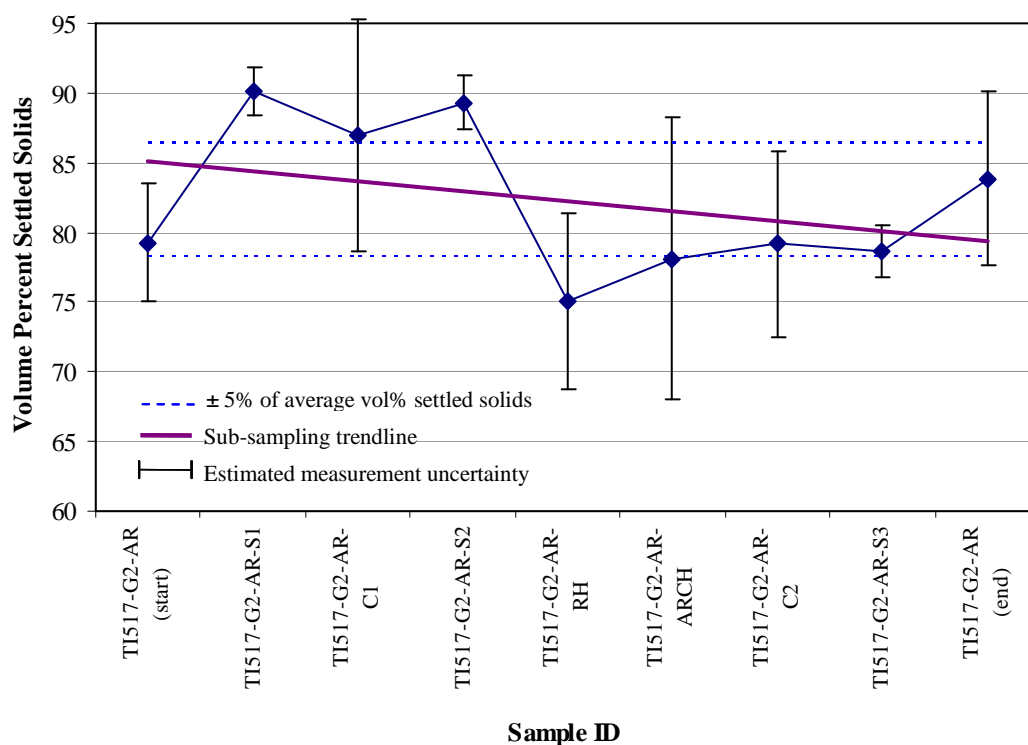
Figure 4.3. Group 2 Samples Vol% Settled Solids after 24-h

Figure 4.4 shows the settling data for the Group 2 samples in two different manners: the volume percent of the settled solids as a function of time and the solids height as function of time. The settling data indicate gradual settling of solid materials over the first 36 to 48 hours with complete settling by 72 hours. The observed settling behavior is consistent with slurries in which the initial solids loading is near the gel point (Rector and Bunker 1995). Only a short initial period of free settling of the solids would be expected in this regime. Once the gel point is reached, settling slows dramatically. The initial settling rate was ~0.9 cm/h.
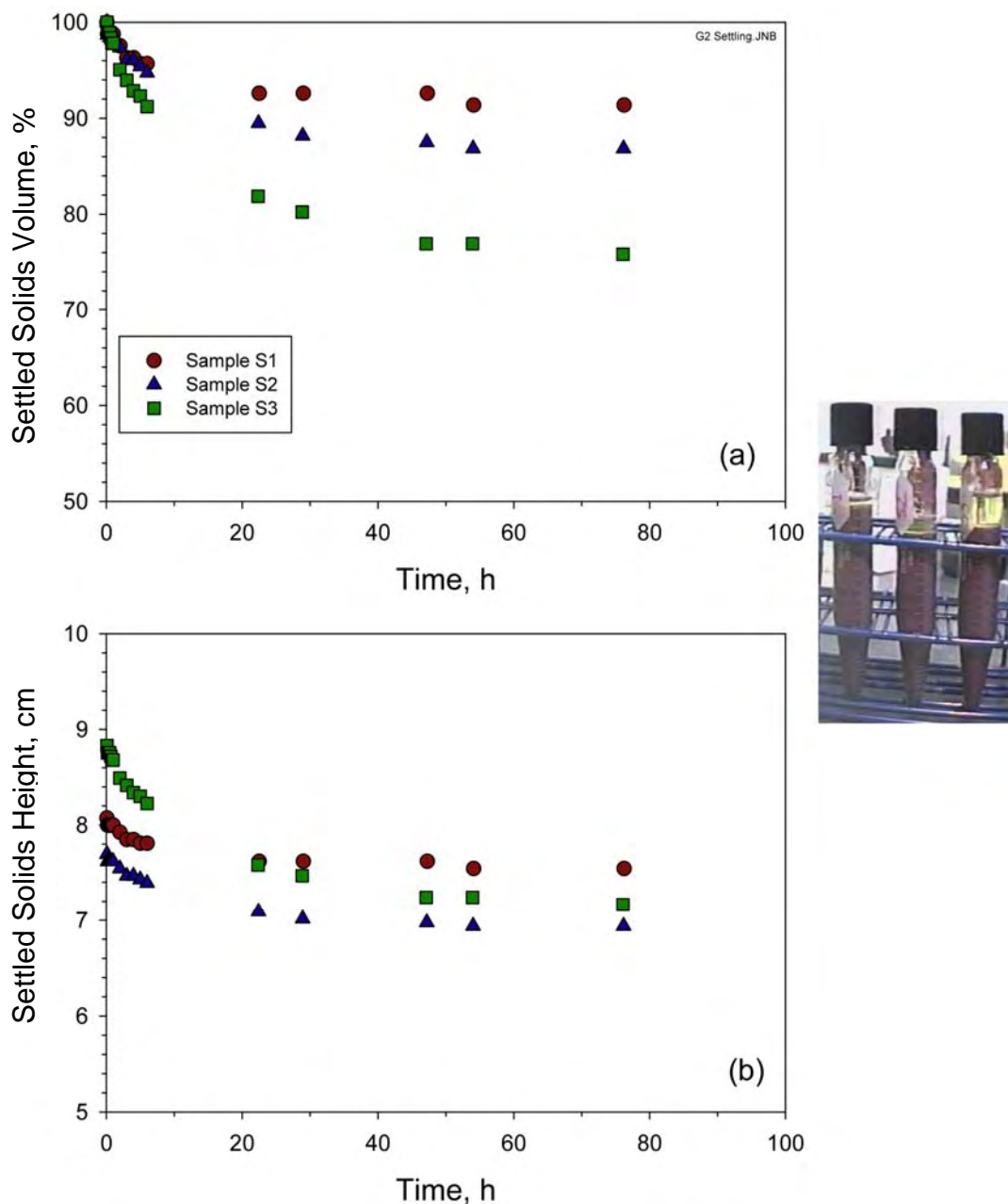
Figure 4.4. Group 2 Settling Data: a) Volume % Settled Solids Versus Time and b) Settled Solids Height Versus Time. Inset: photograph of the samples used in the settling experiments.

Table 4.2 presents the physical properties of the Group 2 samples, including the propagated 1-σ error, the average values of the triplicate measurements, and the relative standard deviation. Again, the variation in measurements can be attributed to the uneven sample distribution.

Table 4.2. Physical Properties of Homogenized Group 2 Saltcake

Description	AR-S1	AR-S2	AR-S3	Nominal 1σ error	Avg.	RSD[a] (%)
Bulk Sample						
Density (g/mL)	1.82	1.55	1.60	0.07	1.66	8.7
Total Solids (wt%)	62.9%	55.0%	51.9%	0.05%	56.6%	10.0
Total Undissolved Solids (wt%)	46.2%	36.2%	29.8%	0.1%	37.4%	22.1
Settled Solids						
Density (g/mL)	1.73	1.60	1.60	0.07	1.64	4.6
Vol% relative to the total sample volume	92.5%	85.7%	76.7%	6%	85.0%	9
Wt% relative to the total sample weight	94.6%	88.7%	80.8%	5%	88.0%	8
Total Undissolved Solids (wt%)	46.2%	40.3%	34.9%	2%	40.5%	14
Wet Centrifuged Solids						
Density (g/mL)	1.83	1.72	1.74	0.09	1.76	3.3
Vol% relative to the total sample volume	81.1%	67.1%	57.6%	5%	68.6%	17
Wt% relative to the total sample weight	85.6%	74.8%	65.6%	0.1%	75.3%	13
Total Undissolved Solids (wt%)	52.9%	48.7%	44.5%	3%	48.7%	9
Total Solids (wt%)	67.7%	63.2%	62.3%	0.1%	64.4%	4
Supernatant						
Density (g/mL)	1.211	1.213	1.245	0.106	1.223	1.6
Total Dissolved Solids (wt%)	29.8%	28.8%	30.9%	0.2%	29.8%	4
Water Content (g/g)	0.7019	0.7116	0.6914	0.0026	0.7016	1.4
(a) RSD = relative standard deviation						

4.2.2   Rheology of the Composite Slurry

4.2.2.1 Shear Strength

A single measurement of shear strength was made on settled solids in sample jar TI517-G2-AR-RH. As was the case with the Group 1 solids, the limited volume of settled solids (< 100 mL) made it impossible to satisfy the geometric constraints for vane immersion. As a result, the shear-strength result was not independent of container geometry and may not even be representative of the actual shear strength of the settled solids. For this reason, no duplicate measurements were taken. The single value reported herein should be taken as a rough estimate of settled-solids strength.

The settled solids in test jar TI517-G2-AR-RH had been fully dispersed 67 hours before testing and allowed to settle undisturbed for the entire 67-hour period between dispersion and testing. The shear-strength test was performed directly in the 250-mL Qorpak sample jars in which the slurry was provided. The shear strength of the Group 2 slurry was tested in a manner identical to that for the Group 1 slurry (see Section 3.2.2.1).

The single observation at 67 hours of settling time indicates a shear strength of 21 Pa. Because the geometric constraints required for shear strength testing could not be met given the current settled solids volume, this results is only an order-of-magnitude estimate. Some caution should be taken when applying it for engineering design. On the other hand, the shear strength attained by Group 2 settled solids over 2 to 3 days of settling is relatively low. For comparison, the shear strength is less than the 30 Pa design basis for slurry yield stress in the pretreatment facility. It should be noted that only the 2- to 3-day observation of the transient shear strength behavior was made in accordance with the test plan. The limited solids volume available after sampling of the material for the flow curve testing prevented the shear strength from being examined at longer settling periods.

4.2.2.2 Flow Curve

Flow curve testing for both slurry and supernatant samples employed an MV1 cup and rotor. Each flow curve measurement was accomplished according to the procedure outlined in Section 3.2.2.2. Visual inspection of the Group 2 slurry before testing found no observable solids settling during transfer from sample jar to rheometer measurement cup. In addition, when performing step 7 (Section 3.2.2.2), the rotor torques measured while mixing were constant. This indicates that for short periods of time, such as the 3-minute mixing step or the time required to transfer the sample to the measuring cup (~5 minutes), settling and shear history effects were minimal for the Group 2 slurry sample.

Figure 4.5 shows the results of flow curve testing for the Group 2 initial characterization slurry sample, TI517-G2-AR-RH.   This slurry showed non-Newtonian behavior at all temperatures studied, with all flow curves showing small but finite yield stresses (~1 Pa) and linear stress behavior over 0 to 1000 s^{-1}, with exception of the strong downward curvature observed near zero. The latter was almost certainly an artifact created by poor rotational sampling. Flow curve hysteresis was absent in all measurements, including 60°C (where hysteresis is typically observed for slurry samples). The latter indicated that evaporation did not significantly impact the rheological properties of the Group 2 slurry sample. Increasing the slurry temperature appeared to cause a decrease in slurry consistency (i.e., the slope of the flow curve data); the decrease in consistency between 25 and 40°C was similar in magnitude to that between 40 and 60°C. The yield stress did not appear to change significantly with temperature.
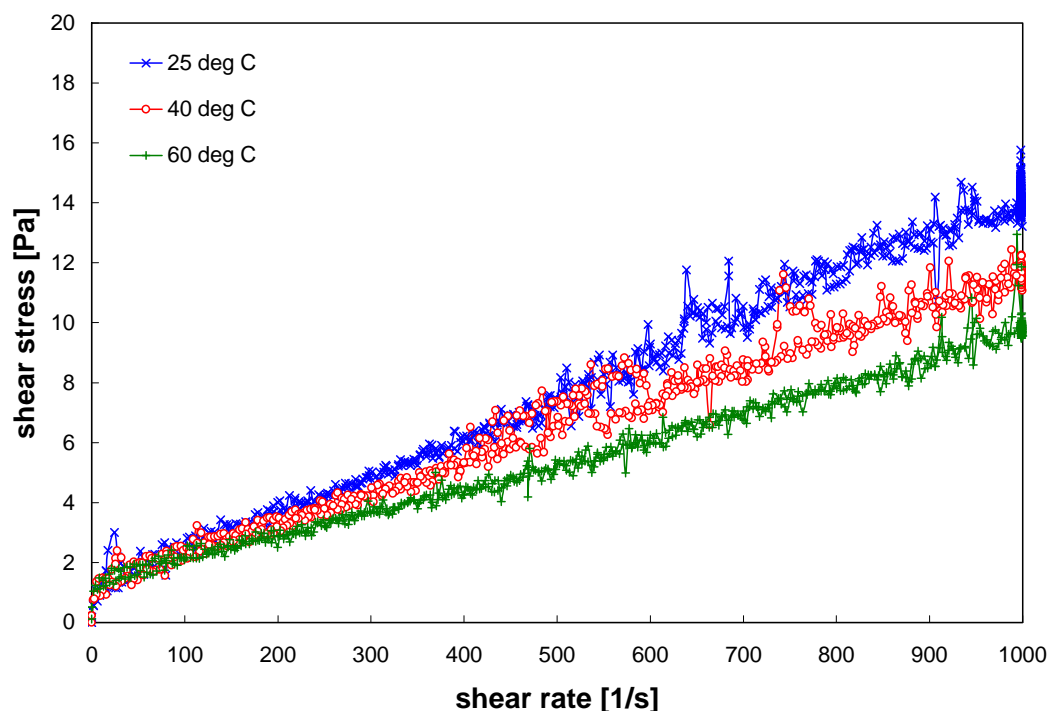
Figure 4.5. Flow Curve (shear stress versus shear rate) for the Group 2 Initial Characterization Slurry Sample TI517-G2-AR-RH at 25, 40, and 60°C. Note: the second repeat measurement for 25°C is shown here, as it is the closest to the 40 and 60°C measurements in time.

In previous studies of tank waste rheology, increases in yield stress with increasing slurry temperature have usually been observed. These increases were typically associated with increased solids concentration and were accompanied by flow curve hysteresis. As such, the absence of both increased slurry yield and flow curve hysteresis with increasing temperature are self-consistent. Regarding slurry consistency, the observed decrease at higher temperatures can be attributed to lower suspending phase viscosity (as pure liquid viscosity generally decreases with increasing temperature). Similar behavior has been observed in previous studies of dilute slurries and tank waste supernatants. With this in mind, it should be noted that the rheology of high ionic strength aqueous particle suspensions is complex. Attributing the changes observed to physical phenomena described above is tenuous when based on flow curve data alone as other mechanisms can yield similar bulk rheological behavior.

Table 4.3 summarizes the best-fit rheological parameters for flow curve data for sample TI517-G2-AR-RH. Only Bingham-Plastic and Herschel-Bulkley models were evaluated, and both fits employ the entire range of shear rate.[a] An example of the quality of the data fit these parameters provide is shown in Figure 4.6, which shows both Bingham-Plastic and Herschel-Bulkley flow curve fits at 40°C. In terms of capturing the range of magnitude, curvature, slope, and yield, both Herschel-Bulkley and Bingham-Plastic

---

(a) This typically includes 0 to 1000 s^{-1} for both up- and down-ramp measurements and the period of constant rotation at 1000 s^{-1}. However, the fitting analysis for the first measurement at 25°C (i.e., measurement 1 of 2) does not consider the period of constant rotation at 1000 s^{-1}, as the rotor appears to have over-spun during this phase of the measurement, causing a significant variation of stress during the constant-rotation period here.

equations provide roughly the same fit. Additionally, the fitting parameters confirm a number of the observations made in the preceding paragraphs. Specifically, they show that at 37 wt% UDS (Table 4.2):

- The Bingham-Plastic and Herschel-Bulkely yield stresses typically range from 1.0 to 1.7 Pa. Given the typically ±0.5 Pa measurement limit for the M5 system, differences between these yield stresses are minor and in most cases insignificant.

- Bingham-Plastic consistency ranges from 8.6 to 14 cP and decreases monotonically with increasing temperature.

- The Herschel-Bulkely flow indices fall between 0.9 and 1.2, indicating that the flow curve curvature is minor and that, overall, the behavior is consistent with the Bingham-Plastic model.

Regarding measurement repeatability, the two measurements at 25°C show similar consistencies (~13 cP) but slightly different yield stresses (1.7 Pa from the primary measurement versus 1.1 Pa for the replicate). As stated in the preceding paragraph, the difference between the regressed yield stresses for primary and replicate measurements is probably not significant given that the difference (0.6 Pa) is very near the instrument limit of accuracy (~0.5 Pa).

Table 4.3. Results of Fitting Analysis for Rheology Sample TI517-G2-AR-RH

Model	Temperature [°C]	Yield Stress [Pa]	Consistency [Pa·s^n]	Flow Index	R
Bingham-Plastic (0 to 1000 s^{-1})	25 (1 of 2)	1.7	0.014	n/a	0.976
	25 (2 of 2)	1.1	0.013	n/a	0.996
	40	1.3	0.010	n/a	0.993
	60	1.1	0.0086	n/a	0.995
Herschel-Bulkley (0 to 1000 s^{-1})	25 (1 of 2)	1.1	0.029	0.90	0.976
	25 (2 of 2)	1.1	0.013	1.01	0.996
	40	1.0	0.019	0.92	0.994
	60	1.5	0.0028	1.2	0.996

For ease of reference, apparent viscosities at 33, 100, 500, and 1000 s^{-1} were derived from each measurement. For each temperature, the 33, 100, and 500 s^{-1} reference viscosities were determined from the average of up-ramp and down-ramp flow curve data and from the fitting parameters provided in Table 4.3. The apparent viscosity at 1000 s^{-1} averages apparent viscosity measurements over the period of constant rotation at 1000 s^{-1}. As a point of comparison, apparent viscosities at 33 s^{-1}, 100 s^{-1}, 500 s^{-1}, and 1000 s^{-1} were also calculated using the Bingham-Plastic and Herschel-Bulkley fitting parameters in Table 4.3. The results of these analyses are provided in Table 4.4 and show that apparent viscosities typically range from 42 to 67 cP at 33 s^{-1}, 20 to 31 cP at 100 s^{-1}, 10 to 18cP at 500 s^{-1}, and 10 to 16 cP at 1000 s^{-1}.

In summary, the Group 2 initial characterization slurry sample, TI517-G2-AR-RH, shows rheological properties consistent with a Bingham Plastic model. This slurry exhibits a small but finite yield stress that remains unchanged with temperature and a near-linear flow curve slope over 0 to 1000 s^{-1} that decreases with increasing temperature, most likely as a result of decreased suspending-phase viscosity. Flow curve hysteresis effects were not observed, which indicates that evaporation of the suspending phase did not noticeably increase slurry viscosity. Based on the Bingham-Plastic fitting parameters, the yield stress of this slurry is approximately 1 Pa; the consistency ranges from ~13 cP at 25°C to 8.6 cP at 60°C.

Table 4.4. Apparent Viscosity of Sample TI517-G2-AR-RH

Source	Temperature [°C]	Apparent Viscosity [cP]			
		@ 33 s^{-1}	@ 100 s^{-1}	@ 500 s^{-1}	@ 1000 s^{-1}
Measured	25 (1 of 2)	144	31	17	16
	25 (2 of 2)	49	25	15	14
	40	53	23	14	12
	60	50	22	10	10
Bingham-Plastic	25 (1 of 2)	67	31	17	16
	25 (2 of 2)	45	24	15	14
	40	51	24	13	12
	60	42	20	11	10
Herschel-Bulkley	25 (1 of 2)	56	30	18	15
	25 (2 of 2)	46	24	15	14
	40	44	23	13	12
	60	51	21	10	10
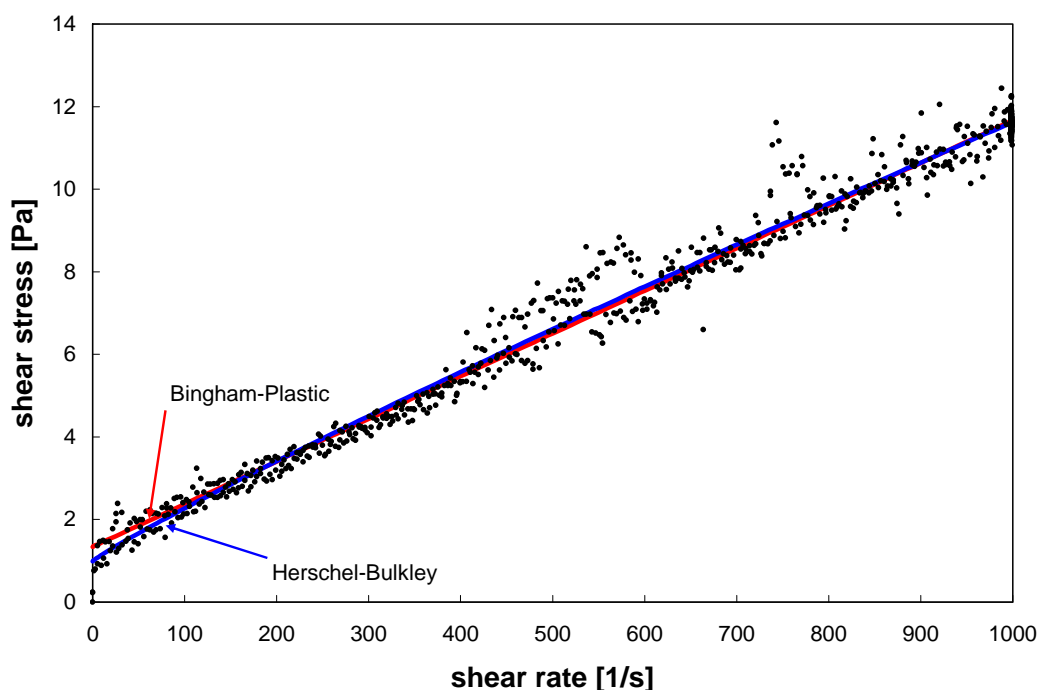
Figure 4.6. Model Fits of Flow Curve Data for Group 2 Initial Characterization Slurry Sample TI517-G2-AR-RH at 40°C. Both model fits consider the full shear rate range of 0 to 1000 s^{-1}.

4.2.3 Chemical and Radiochemical Composition

A density determination was done on the supernatant phases of the two samples taken for chemical characterization. The density was determined to be 1.251 ± 0.002 g/mL (T = 28°C) based on the average masses of five 1-mL volume deliveries. This result is comparable to that determined as part of the physical-property testing procedure (density = 1.223 g/mL). The density of the composite washing solution was 1.080 g/mL.

The average radioanalytical results for the supernatant, composited wash solution, and washed solids are provided in Table 4.5 along with the applicable RPDs, measure of precision between duplicates). The gross-beta results showed good agreement with the sum of beta emitters: ^{137}Cs and ^{90}Sr (in secular equilibrium with ^{90}Y) thus indicating that no other major source of beta-gamma activity was present. The gross alpha activity measured in the solids agreed with the summation of alpha emitters (^{238}Pu, $^{239+240}$Pu, and ^{241}Am).

Table 4.5. Radionuclide Characterization of the Group 2 Saltcake

Analyte	Supernatant		Wash Composite		Washed Solids	
	µCi/mL	RPD	µCi/mL	RPD[a]	µCi/g[b]	RPD
^{137}Cs	2.46E+1	na	4.36E+0	na	9.97E+1	11
^{60}Co	<3.E-4	na	<2.E-5	na	1.07E-2	34
^{241}Am	<2.E-2	na	<1.E-3	na	4.21E-1	30
^{238}Pu	4.96E-6	6.5			1.44E-2	40
$^{239+240}$Pu	8.24E-5	7.8			2.67E-1	17
^{90}Sr	3.28E-3	7.0			1.79E+2	10
Gross alpha	<5.E-4	na	na		5.05E-1	6
Sum of alpha	8.74E-5	7.0			7.02E-1	25
Gross beta	2.45E+1	0.4			4.63E+2	10
Sum of beta	2.46E+1	na			4.58E+2	10
Opportunistic						
^{154}Eu	<2.E-3	na	<7.E-5	na	4.84E-2	26
^{155}Eu	<1.E-2	na	<1.E-3	na	<0.1	na
ASR 7974; Reference date is July 15, 2007.						
(a) This sample was not required to be run in duplicate; therefore, an RPD was not calculated.						
(b) Analyte concentrations are calculated on a dry-mass basis.						
Notes: na = not applicable						

The chemical composition of the washed Group 2 solids is provided in Table 4.6. The supernatant liquid consisted primarily of sodium nitrate with minor contributions of other sodium salts. The free-hydroxide concentration in the supernatant liquid was 0.295 M. The anionic and cationic charge balance was evaluated for the supernatant, resulting in a relative 1.3% difference, and the total S and P values (determined by ICP-OES) and SO_4^{2-} and PO_4^{3-} (determined by IC) were compared, and all were determined to be well within analytical uncertainties.

Major constituents in the washed solids were sodium, aluminum, phosphorus, and silicon, while iron, uranium, calcium, and chromium provided minor contributions. Overall good agreement was obtained between the two different sample preparation methods as well as the uranium results between KPA and the ICP-OES analyses.

Table 4.6. Chemical Characterization of the Group 2 Test Material

Analyte	Supernatant Acid Digestion µg/mL	M	RPD	Wash Composite Acid Digestion µg/mL	M	RPD	Washed Solids[a] KOH fusion µg/g	RPD	Acid Digestion µg/g	RPD
Al	2,030	7.52E-2	0.0	322	1.19E-2		112,500	8	122,500	0.8
B	98.6	9.12E-3	1.0	19.8	1.83E-3		[105]	[10]		
Bi	<2.27	<1.E-5		[2.3]	[1.1E-5]		[895]	[12]	1,030	1.9
Cd	<0.24	<2.E-6		<0.24	<2.E-6		90.2	9	106	2.8
Cr	798	1.53E-2	0	161	3.10E-3		7,485	9	8,285	0.6
Fe	[7.45]	[1.3E-4]	[4]	[2.3]	[4.1E-5]		21,150	12	23,000	1.7
K	979	2.50E-2	1	186	4.76E-3				[240]	[33]
Mn	<0.20	<4.E-6		<0.20	<4.E-6		1,034	15	1,009	4.3
Na	112,000	4.87E+0	1.79	36,900	1.61E+0		177,000	10	192,000	0.0
Ni	[0.72]	[1.2E-5]	[35]	[0.61]	[1.0E-5]				4,750	0.4
S	3,845	1.20E-1	0.3	2,480	7.74E-2		[1,450]	[7]	[1,350]	[7]
Si	[8.25]	[2.9E-4]	[10.9]	11.7	4.17E-4		31,650	7		
Sr	<0.02	<2.E-7		<0.02	<2.E-7		4,005	12	4,540	0.0
U	<8.33	<3.E-5		<8.27	<3.E-5		14,650	6	16,250	0.6
Zn	[3.5]	[5.4E-5]	[5.7]	[0.85]	[1.3E-5]		[325]	[3]	399	2.0
Zr	<0.81	<9.E-6		<0.80	<9.E-6		<59		[110]	[0]
U KPA							15,250	7		
nitrite	11,600	2.52E-1	3.4	2,015	4.38E-2	9.43				
nitrate	177,000	2.85E+0	4.52	30,550	4.93E-1	9.5				
phosphate	2,805	2.95E-2	0.4	5,965	6.28E-2	9.9				
sulfate	11,550	1.20E-1	4.33	8,280	8.62E-2	9.7				
oxalate	1,305	1.48E-2	0.77	5,835	6.63E-2	9.4				
free OH		0.30	3.4							
TOC as C	765	0.064	1.3							
TIC as C	6,500	0.542	0							
Opportunistic										
fluoride	4200	2.21E-1	3.81	8480	4.39E-1	3				
chloride	776.5	2.19E-2	1.42	126	3.72E-3	9				
Ag	[0.55]	[5.1E-6]		<0.42	<3.9.E-6		<17		[8.5]	[11.8]
As	<6.93	<9.3.E-5		<6.88	<9.2.E-5		<269		<95	
Ba	<0.34	<2.4.E-6		<0.33	<2.4.E-6		[230]	[9]	257.0	0.0
Be	<0.01	<1.3.E-6		<0.01	<1.3.E-6		<1.0		[0.9]	[1.1]
Ca	[5.0]	[1.2E-4]	8	[3.6]	[9.0E-5]		[9,200]	[7]	9,795	0.3
Ce	<1.19	<8.5.E-6		<1.18	<8.4.E-6		<202		<16	
Co	[0.65]	[1.1E-5]		<0.38	<6.5.E-6		<22		[33.5]	[2.99]
Cu	<0.48	<7.6.E-6		<0.48	<7.5.E-6		[155]	[32]	80.3	0.9
Dy	<0.35	<2.1.E-6		[0.47]	[2.9E-6]		<52		<4.8	
Eu	<0.11	<7.1.E-7		<0.11	<7.1.E-7		<16		<1.5	

Table 4.6. Chemical Characterization of the Group 2 Test Material

| Analyte | Supernatant | | | Wash Composite | | | Washed Solids[a] | | | |
| | Acid Digestion | | | Acid Digestion | | | KOH fusion | | Acid Digestion | |
	µg/mL	M	RPD	µg/mL	M	RPD	µg/g	RPD	µg/g	RPD
La	<0.13	<9.5.E-7		<0.13	<9.4.E-7		<11		[18.8]	[8.0]
Li	<0.54	<7.8.E-5		[0.92]	[1.3E-4]		<32		[48.5]	[10.3]
Mg	<0.70	<2.9.E-5		<0.69	<2.8.E-5		[1,100]	[18]	1,255	0.8
Mo	8.01	8.35E-5	3	[4.6]	[4.8E-5]		<30		<9	
Nd	<1.71	<1.2.E-5		<1.69	<1.2.E-5		<311		[43.5]	[6.9]
P	859	2.77E-2	0.23	1,800	5.81E-2		45,800	10	49,900	0.8
Pb	<3.68	<1.8.E-5		<3.65	<1.8.E-5		[1,010]	[24]	1,385	0.7
Pd	<1.25	<1.2.E-5		<1.24	<1.2.E-5		<183		<17	
Rh	<2.51	<2.4.E-5		<2.49	<2.4.E-5		<120		<35	
Ru	<0.82	<8.1.E-6		<0.81	<8.0.E-6		<52		<11	
Sb	<3.12	<2.6.E-5		<3.10	<2.5.E-5		<171		<43	
Se	<4.87	<6.2.E-5		<4.83	<6.1.E-5		<291		<67	
Sn	22.4	1.88E-4		[5.9]	[5.0E-5]		<272		[80.5]	[16.1]
Ta	<1.32	<7.3.E-6		<1.31	<7.3.E-6		<59		<18.2	
Te	<3.14	<2.5.E-5		<3.11	<2.4.E-5		<231		<43.1	
Th	<1.18	<5.1.E-6		[1.2]	[5.2E-6]		<180		<16	
Ti	<0.10	<2.0.E-6		[0.11]	[2.3E-6]		[135]	[7]	178	11.8
Tl	<6.45	<3.2.E-5		<6.41	<3.1.E-5		<209		<89	
V	[0.64]	[1.3E-5]		[1.5]	[2.9E-5]		[34]	[12]	46.1	1.7
W	<1.49	<8.1.E-6	0	[8.7]	[4.7E-5]		<92		<20	
Y	<0.08	<9.5.E-7		<0.08	<9.4.E-7		<20		[4.1]	[17.3]

(a) Analyte concentrations are calculated on a dry-mass basis.

ASR 7974.

Analyte uncertainties were typically within ±15% (2-σ); results in brackets indicate that the analyte concentrations were less than the minimum detection limit (MDL) and greater than the estimated quantitation limit (EQL), and uncertainties were >15%. Opportunistic analytes are reported for information only; QC requirements did not apply to these analytes.

The fractional distribution of selected analytes between the supernatant, wash solution, and solids phases is shown in Table 4.7 and Figure 4.7. The bulk of the sodium (86%) and sulfur (as sulfate, 97%) partitioned to the aqueous phase as a result of the initial contact with water during homogenization and the continued water washing. The phosphorus (75%) and aluminum (86%) remained primarily in the solids phase while the chromium was split between the aqueous (49%) and solids (51%) phases.

The total P concentrations in the supernatant and wash solutions determined by ICP-OES were equivalent to the phosphate concentrations determined by IC. Likewise, the total S concentrations were equivalent to the sulfate concentrations. Therefore, the mobilized forms represented the water-soluble sulfate and phosphate salts. For most analytes, the concentration in the wash composite was ~20% of that in the supernatant. However, the phosphate (and total P) concentration in the wash composite was greater than that in the supernatant liquid, and the sulfur in the wash was ~60% of that in the supernatant, indicating that phosphate and sulfur were further dissolved as a result of water washing.

Table 4.7. Phase Distribution of Selected Analytes in Group 2

Analyte	Supernatant %	Wash Solution %	Solids %	Water-Wash Factor %
Cr	44.9	4.8	50.4	49.6
Al	13.1	1.1	85.8	14.2
Na	73.6	12.7	13.6	86.4
P	11.9	13.1	74.9	25.1
S	72.6	24.6	2.8	97.2
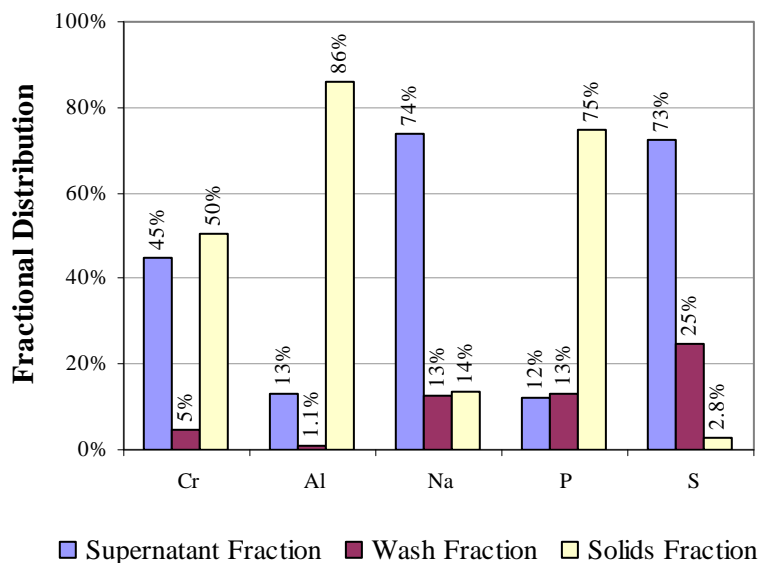
Figure 4.7. Selected Analyte Phase Distribution for Group 2

4.2.4 Particle Size

Figure 4.8 and Figure 4.9 present the results of Group 2 initial-characterization particle-size analysis as a function of test condition. Figure 4.8 through Figure 4.10 show the differential volume population distribution for the primary Group 2 initial characterization sample (see Appendix H for the duplicate sample results) and allow a qualitative examination of the PSD behavior with respect to pump speed and sonication. Table 4.8 is a summary of the measured oversize diameter percentiles (by volume/weight) for the primary, TI517-G2-S-WL-PSD-21. Table 4.9 presents the same results for the duplicate standard, TI517-G2-S-WL-PSD-2. Both tables present cumulative oversize diameters corresponding to the 10th, 50th, and 90th volume/weight percentiles, hereafter referred to as d(10), d(50), and d(90), respectively. More extensive percentile results are provided in Appendix I. These tables will be used to quantitatively examine reproducibility and changes in particle size.

Figure 4.8 shows the PSD for the primary Group 2 initial characterization sample as a function of pump speed before sonication. The distribution of particles ranges from 0.3 to 20 μm, and peaks between 3 and 5 μm, and has a low population peak around 200 μm at 4000 RPM. With exception of the appearance of the second peak around 200 μm at 4000 RPM, the distribution is continuous and uni-modal. That is, the

PSD is a single broad population of particles centered at 3 to 5 µm. It is possible that the 200-µm peak is an artifact of the measurement and analysis; however, the duplicate sample confirms the appearance of a large size population (20 to 200 µm) at high pump speeds. As such, the 200-µm peak is likely caused by a relatively large Group 2 particle species that is difficult to suspend and thus that is poorly sampled by the analyzer. Changes in the primary population peak (i.e., that over 0.3 to 20 µm) with respect to changes in flow rate are minor. The 3000 RPM PSD peaks at 2 to 3 µm, whereas the 2000 and 4000 RPM peak over 3 to 5 µm. The increase in the population peak diameter as flow rate is increased from 3000 RPM to 4000 RPM is expected, as higher pump speeds are capable of suspending any larger particle and particle aggregates. It is possible that this improved suspension is maintained through the subsequent PSD set-point, thus accounting for the higher population peak diameter of 2000 RPM measurement relative to the initial 3000 RPM measurement.
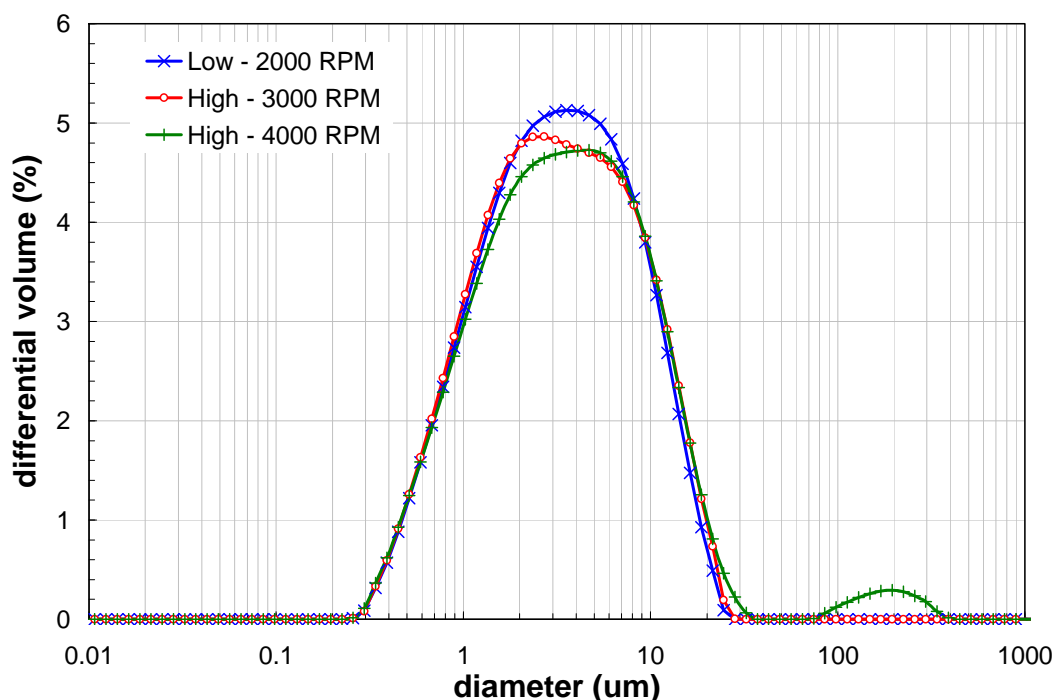
Figure 4.8. Pre-Sonication Volume Distribution Result for the Primary Group 2 Initial Characterization Sample as a Function of Pump Speed

Figure 4.9 shows the PSD as a function of sonication. This figure indicates that sonication shifts the entire particle population to smaller diameters and substantially increases the central (2 to 6 µm) population of particles, probably as a result of particle aggregate disruption. Disruption is evidenced by a slightly decreased fraction of 6 to 20 µm and a slightly increased fraction of sub-micrometer particles. The increased population over the 2 to 6 µm was observed to occur before the application of sonic energy (see Figure 4.7); however, sonication appears to further enhance the population of 2 to 6 µm over that observed at 2000 RPM before sonication. The cause of this observation could be 1) breakdown of the 6- to 20-µm into 2- to 6-µm particles and/or 2) increased suspension of particles as a result of input of sonic energy (similar to the improvements caused by increased flow in Figure 4.8).
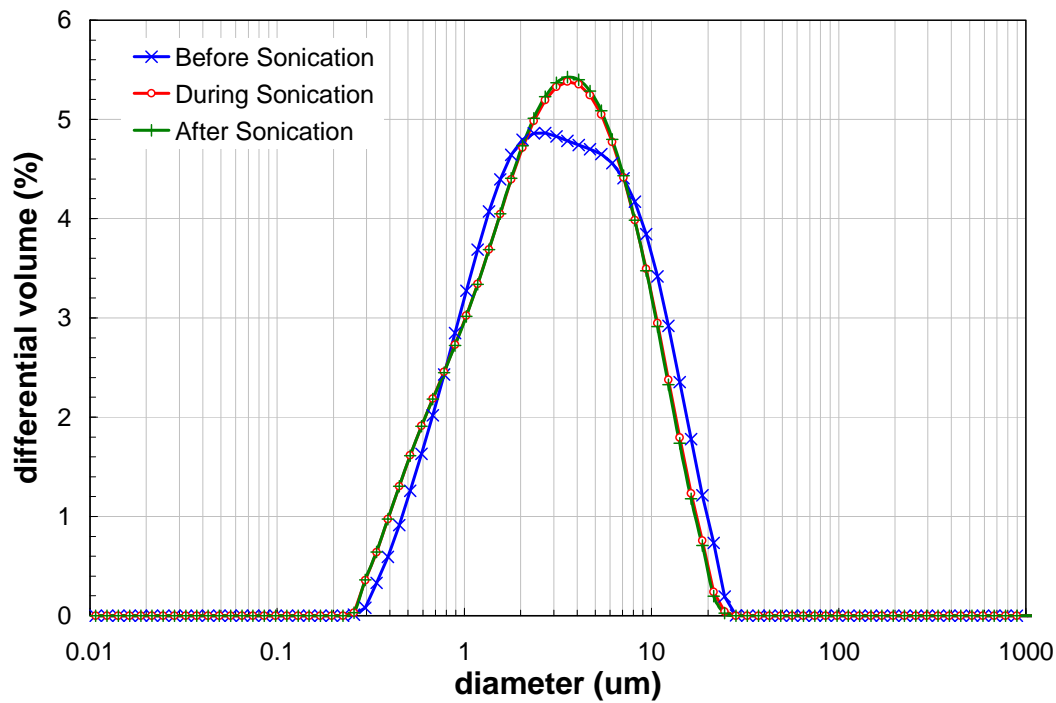
Figure 4.9. Volume Distribution Result for the Primary Group 2 Initial Characterization Sample as a Function of Sonication (75% power)
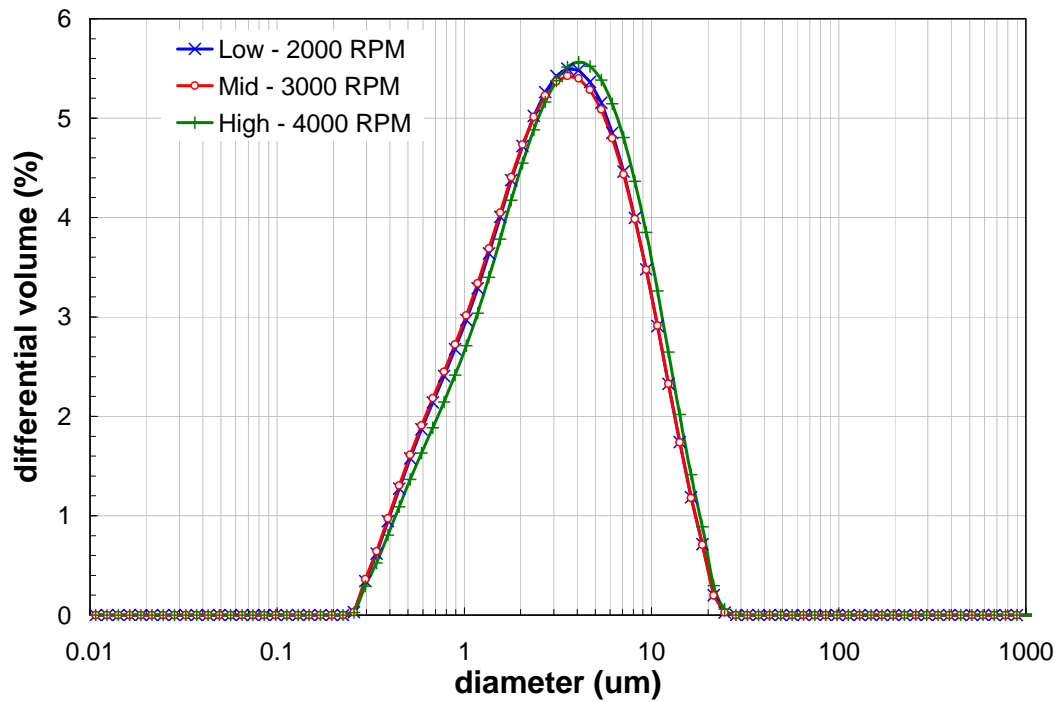
Figure 4.10. Post-Sonication Volume Distribution Result for the Primary Group 2 Initial Characterization Sample as a Function of Pump Speed

Figure 4.10 shows the primary Group 2 initial characterization PSD as a function of pump speed after the sample dispersion has been sonicated. Here, changes in pump speed do not appear to significantly change the distribution, with the exception of a slight increase in peak population diameter at 4000 RPM. This increase is likely a result of a small improvement in large particle suspension as a result of increased mechanical agitation. From the observation of PSD insensitivity to pump speed, we may conclude that sonicated Group 2 solids are stable with respect to transient effects such as shear-induced agglomeration and mechanical effects such as shear break-up of particle aggregates. In addition, the 200-μm peak is absent from the 4000 RPM post-sonication PSD. This supports the conclusion that sonication has disrupted particle aggregates and indicates that aggregate recovery does not occur over the duration of PSD measurement (~15 minutes).

Table 4.8 shows select cumulative oversize percentiles for the primary Group 2 particle dispersion (TI517-G2-S-WL-PSD-1). Using these results as a reference, the behavior of Group 2 initial characterization particle size as a function of pump speed and sonication can be quantitatively evaluated. Specifically, the following observations can be made:

- In general, the d(10) falls between 0.77 and 0.88 μm, the d(50) between 3.1 and 3.5 μm, and the d(90) between 9.6 and 13 μm.

- The listed diameter percentiles appear to be slightly sensitive to changes in pump speed, both before and after sonication. Increases in flow appear to affect increases in the mean diameter [i.e., the d(50)]; however, the change is near to the instrument limit of accuracy (10%). For example, an increase from 3000 to 4000 RPM before sonication increases the mean particle diameter from 3.2 to 3.5 μm. This is an increase of 9.4% and, as such, is close but still below the limit of significance.

- Sonication of the Group 2 solids dispersion slightly decreases the particle size, but the change for the mean diameter is well below the instrument's measurement sensitivity. The PSD results at 3000 RPM indicate that sonication lowers the mean particle size from 3.2 to 3.1 μm. This represents a decrease of ~3% in the mean particle size and is not significant relative to the measurement accuracy (10%).

Table 4.8. Particle Size Analysis Percentile Results of the Primary Group 2 Initial Characterization Sample, TI517-G2-S-WL-PSD-1

Measurement Condition	Pump Speed	Sonication	d(10) [μm]	d(50) [μm]	d(90) [μm]
1	3000	pre-sonic	0.86	3.2	11
2	4000	pre-sonic	0.87	3.5	13
3	2000	pre-sonic	0.88	3.2	10
4	3000	25%	0.79	3.1	10
5	3000	50%	0.77	3.1	10
6	3000	75%	0.77	3.1	9.7
7	3000	post-sonic	0.77	3.1	9.6
8	4000	post-sonic	0.84	3.4	10
9	2000	post-sonic	0.78	3.1	9.6

Table 4.9. Particle Size Analysis Percentile Results of the Duplicate Group 2 Initial Characterization Sample, TI517-G1-S-WL-PSD-2

Measurement Condition	Pump Speed	Sonication	d(10) [μm]	d(50) [μm]	d(90) [μm]
1	3000	pre-sonic	0.83	3.5	14
2	4000	pre-sonic	0.84	4.0	21
3	2000	pre-sonic	0.85	3.6	13
4	3000	25%	0.86	3.6	12
5	3000	50%	0.86	3.6	12
6	3000	75%	0.85	3.6	11
7	3000	post-sonic	0.84	3.5	11
8	4000	post-sonic	0.85	3.5	11
9	2000	post-sonic	0.87	3.7	13

Behavior of the duplicate sample PSD with respect to pump speed and sonication mirrors and confirms that of the primary sample. However, the PSD of the duplicate sample favors consistently larger diameters than that of the primary at equivalent measurement conditions. Table 4.10 shows the absolute relative percent difference between the d(10), d(50), and d(90) values determined for the primary and duplicate Group 2 initial characterization samples, as calculated by Eq. 3.1. The listed RPDs indicate that there is a slight difference between samples.

Table 4.10. Absolute Relative Percent Difference Between Primary and Duplicate Group 1 Initial Characterization Samples

Measurement Condition	Pump Speed	Sonication	Absolute RPD d(10)	d(50)	d(90)
1	3000	pre-sonic	4.4%	9.8%	28%
2	4000	pre-sonic	4.3%	15%	63%
3	2000	pre-sonic	3.4%	11%	24%
4	3000	25%	9.8%	17%	20%
5	3000	50%	11%	17%	19%
6	3000	75%	10%	16%	17%
7	3000	post-sonic	9.6%	14%	15%
8	4000	post-sonic	0.6%	4.7%	10%
9	2000	post-sonic	12%	20%	36%

For particle-size measurements on the Malvern Mastersizer 2000, RPDs of up to 10% are generally expected, given the accuracy of the instrument. The results for Group 2 initial characterization samples show RPDs that range from 1 to 63%, depending on the measurement condition and percentile examined. Based on the large number of RPDs greater than 10% in Table 4.10, it is likely that there is a significant size difference in the solids species in the primary and duplicate sample. The largest RPDs are observed in the before- and during-sonication measurement conditions; however, a significant number of the post-sonication RPDs still exceed 10%, indicating that sonication does not completely eliminate the size difference between the samples. The results indicate that duplicate sampling picked up a greater population of large particles, most likely in the form of particle aggregates. While sonication of the dispersions tends to eliminate some of the size disparity between primary and duplicate sample, it still

remains a significant effect after sonication. The most consistent measurement state after sonication is that at 4000 RPM. Here, the RPDs are at or below the limit of measurement accuracy (10%). This could suggest that the difference in primary and duplicate PSD is solely a result of particle aggregation and that high shear and sonication can eliminate this difference. However, this conclusion cannot be stated with confidence without additional PSD measurements to confirm it. Overall, there is a significant difference in the size of primary and duplicate Group 2 solids with respect to the limit of instrument accuracy.

Figure 4.11 and Figure 4.12 show how the differences in the primary and duplicate PSDs described in the preceding paragraphs manifest in the differential volume distributions. Figure 4.11 compares the primary and duplicate PSDs at 3000 RPM before sonication. With respect to the pre-sonication comparison, both distributions show the same trends in population with size, namely, a peak population at 2 to 3 µm and a broad particle volume plateau over 2 to 6 µm. The primary difference is that the duplicate sample has a significantly increased population of 10 to 20 µm. This causes the larger percentiles observed in Table 4.9 (relative to those in Table 4.8) and >10% RPDs in Table 4.10.

Figure 4.12 compares primary and duplicate distributions after sonication. It shows that the increased particle size observed in the duplicate sample before sonication is maintained after sonication. Overall, the primary and duplicate distributions show the same uni-modal peak centered around 3 to 5 µm and spanning 0.3 to ~25 µm. The main difference is that the duplicate distribution is shifted to larger particle diameters. From a qualitative aspect, the difference between the primary and duplicate distributions after sonication appears less than that before sonication (an observation confirmed by the results in Table 4.10). This supports the earlier assertion that the difference between samples may be in their state of particle aggregation.
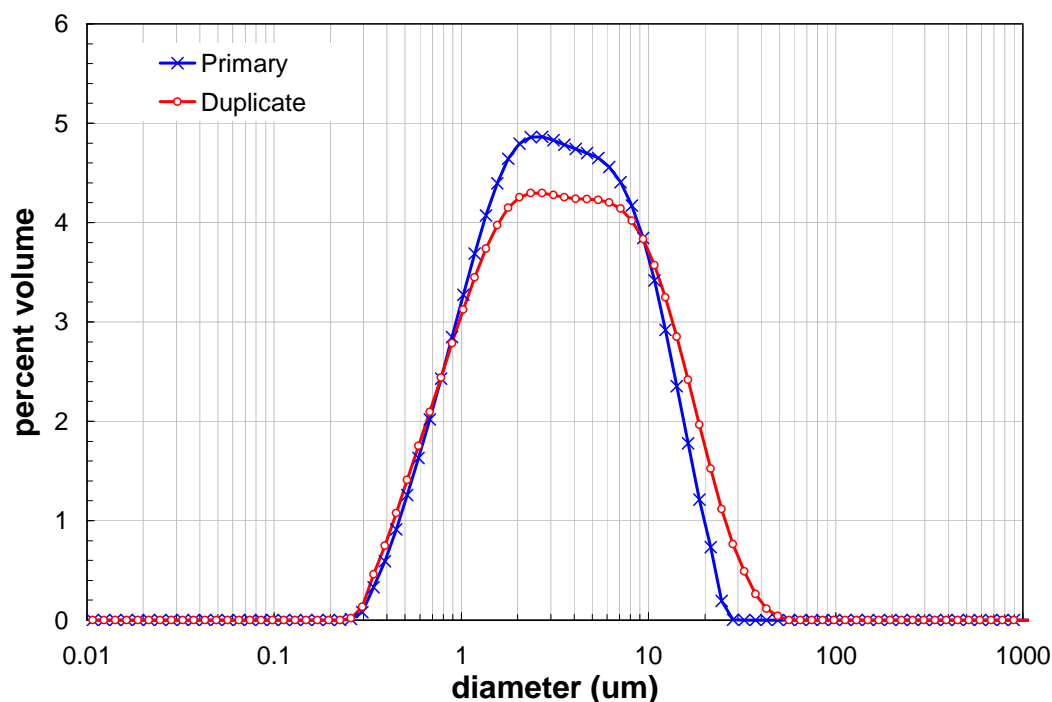
Figure 4.11. Comparison of Primary and Duplicate Sample Differential Volume PSD at 3000 RPM Before Sonication for the Group 2 Solids
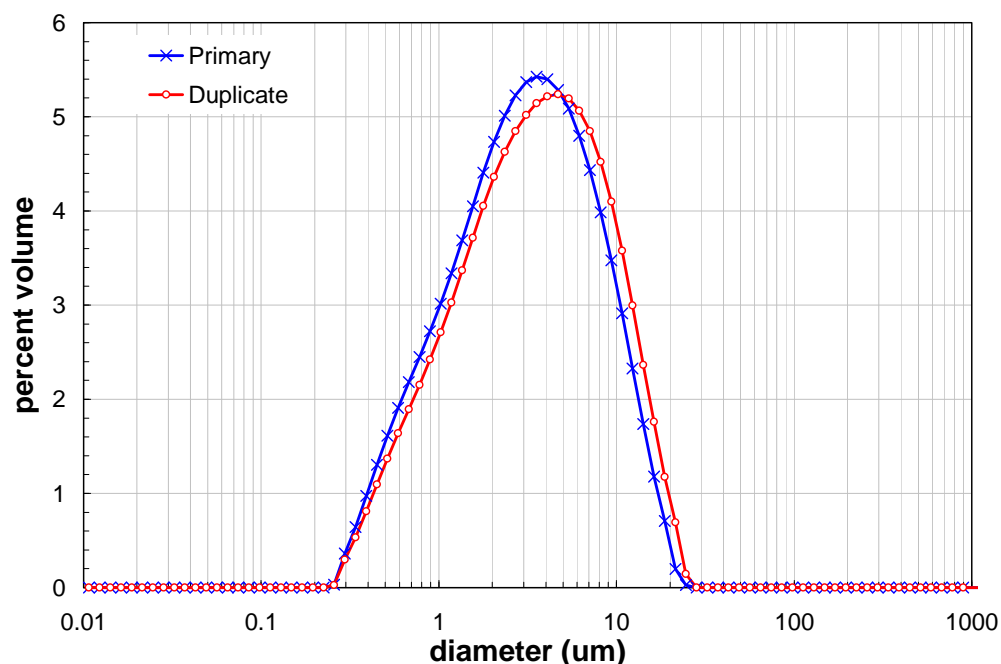
Figure 4.12. Comparison of Primary and Duplicate Sample Differential Volume PSD at 3000 RPM After Sonication for the Group 2 Solids

In summary, particle-size analysis of initial characterization Group 2 (bismuth phosphate saltcake) samples indicates a broad distribution of solids particle sizes ranging from 0.3 μm to ~30 μm and also suggests the presence of a coarse, difficult-to-suspend fraction of material around 100 μm in diameter. The initial distribution of solids is nearly uni-modal, with a peak population that ranges from 2 to 5 μm, depending on the pump speed used for measurement. Increases in pump speed appear to assist the suspension of large particles as evidenced by the increase in the mean particle diameter and the appearance of a small ~100-μm particle population peak as the pump speed was increased from 3000 to 4000 RPM. In-cell sonication of the Group 2 solids dispersion increases the central (2 to 6 μm) population of particles while also causing a slight increase in the population of sub-micrometer particles. Both changes are likely a result of particle aggregate disruption. This disruption is irreversible within the time-frame of analysis, as the PSD does not change measurably with time or pump speed after sonication is stopped.

4.2.5 Surface Area

A 57-mg sample was analyzed for surface area by BET with the following result: 46 m^2/g.

4.2.6 Crystal Form and Habit

The background-subtracted XRD pattern (rutile used as an internal standard) for Group 2 washed solids is provided in Figure 4.13. The crystalline phases identified were gibbsite [γ-Al(OH)$_3$, crystal density 2.42 g/cm^3, Wefers and Misra 1987], cancrinite [Na$_{7.92}$(AlSiO$_4$)$_6$(NO$_3$)$_{1.7}$(H$_2$O)$_{2.34}$, crystal density 2.414 g/cm^3, JADE Version 8.0, calculated value], and urancalcarite [Ca(UO$_2$)$_3$CO$_3$(OH)(H$_2$O)$_3$, crystal density 4.03 g/cm^3, JADE Version 8.0, calculated value]. Dorfmanite [Na$_2$HPO$_4$(H$_2$O)$_2$, crystal density 2.07 g/cm^3, CRC 1978] was also identified.
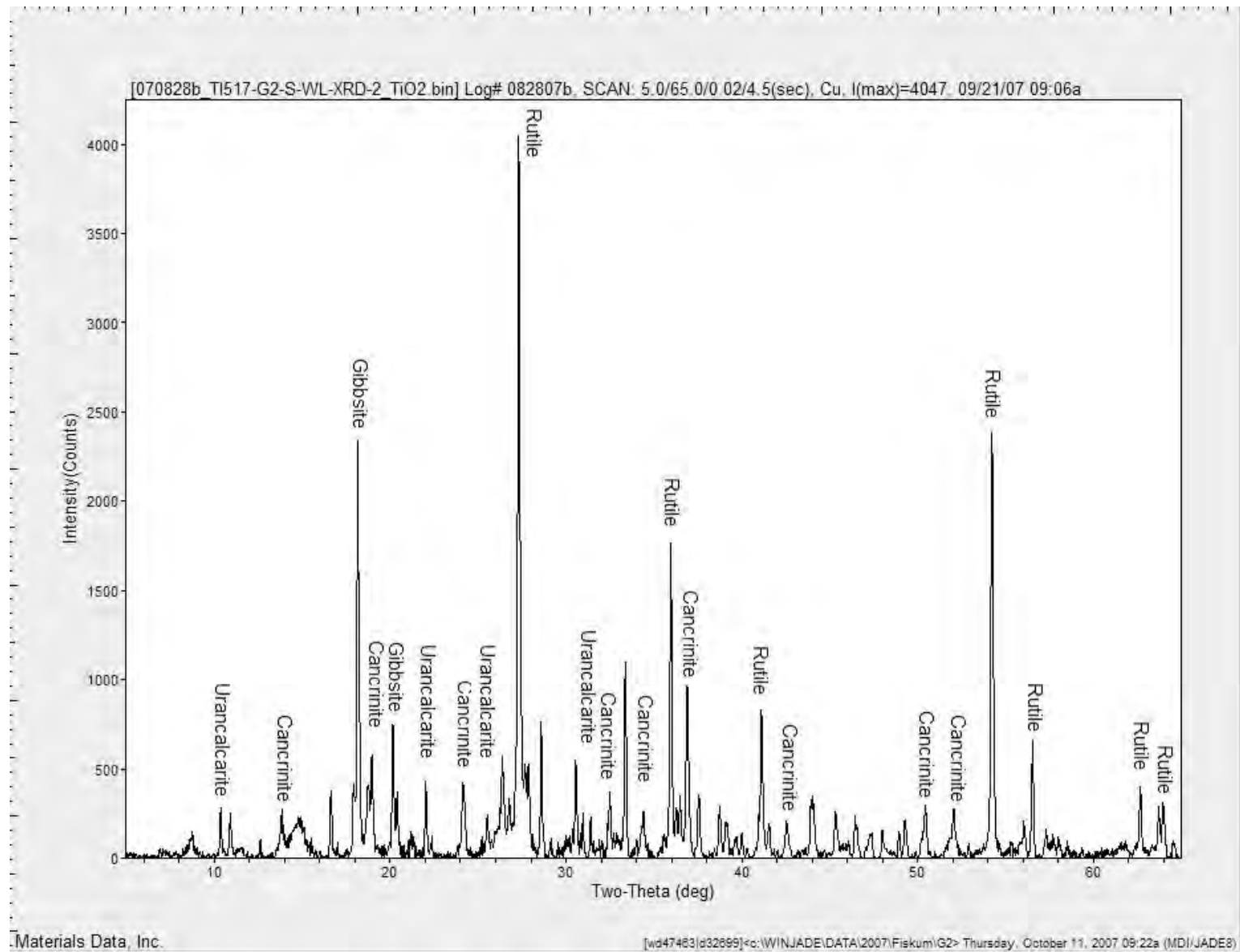
Figure 4.13. XRD Pattern of Washed Group 2 Solids, Background-Subtracted

SEM, coupled with EDS, was used to obtain information regarding the particle morphology and elemental distribution within the Group 2 solid phases. Several SEM images of the washed solids are shown in Figure 4.14. Small particles appear to be agglomerating together to form a larger mass of solids.
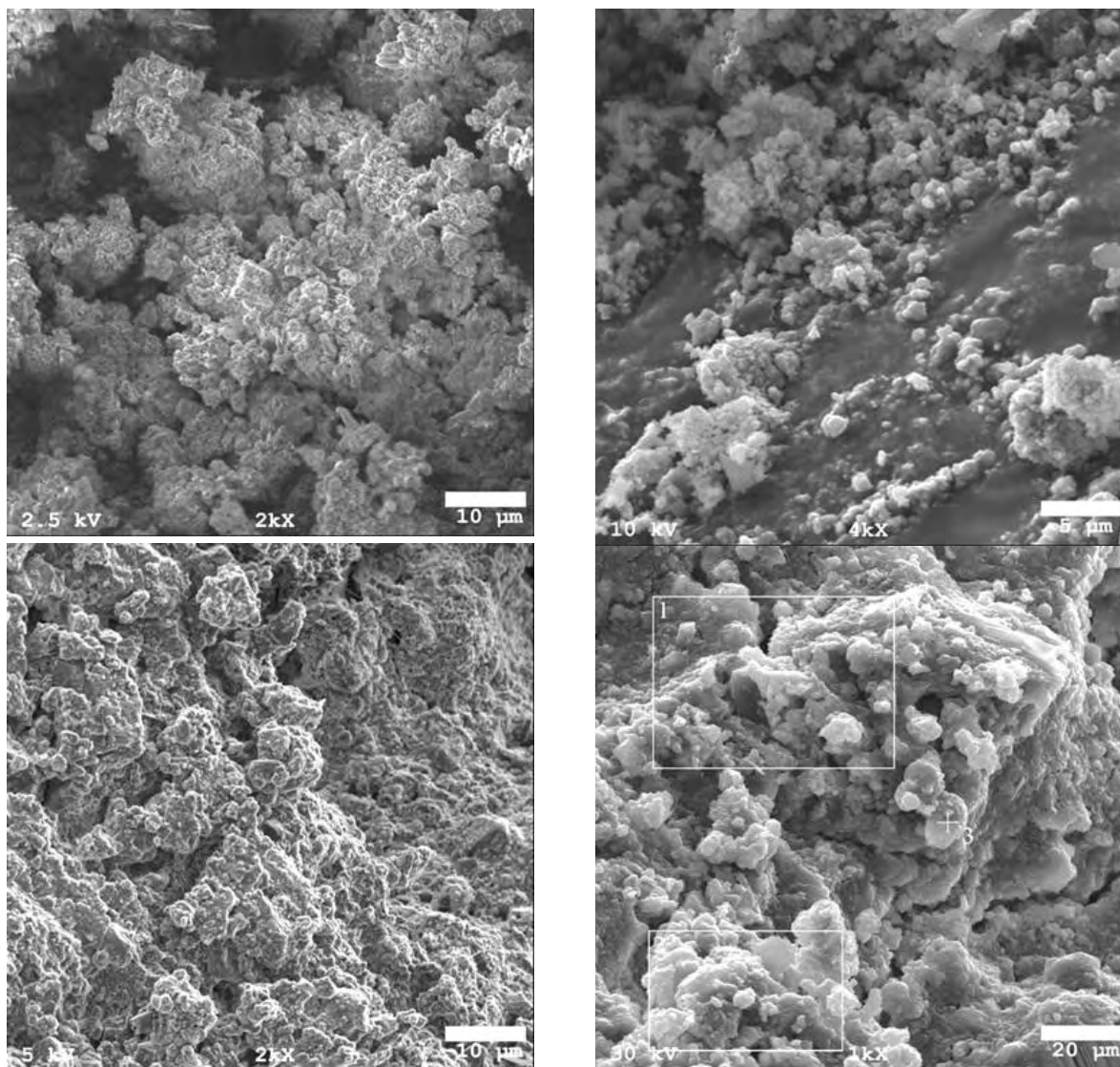
Figure 4.14. SEM Images of Group 2 Initial Characterization Solids

The EDS spectra of selected solids phases are shown in Figure 4.15. The spectrum indicates the presence of elements (Al, Na, Si, P, Cr, Ca, U and Fe) that were identified in significant quantities in the ICP-OES analysis of the bulk material. Figure 4.16 shows an elemental map for the washed Group 2 solids. An item of note on this map is the close association of the Na, Al, Si, and P. This is consistent with the XRD result indicating that the washed Group 2 solids contained cancrinite [$Na_{7.92}(AlSiO_4)_6(NO_3)_{1.7}(H_2O)_{2.34}$]. The phosphorus could be contributed by entrained dorfmanite [$Na_2HPO_4(H_2O)_2$]. The other major components appear to be evenly distributed across the image, suggesting that these are likely present as the individual oxides or hydroxides that are intermingled together.
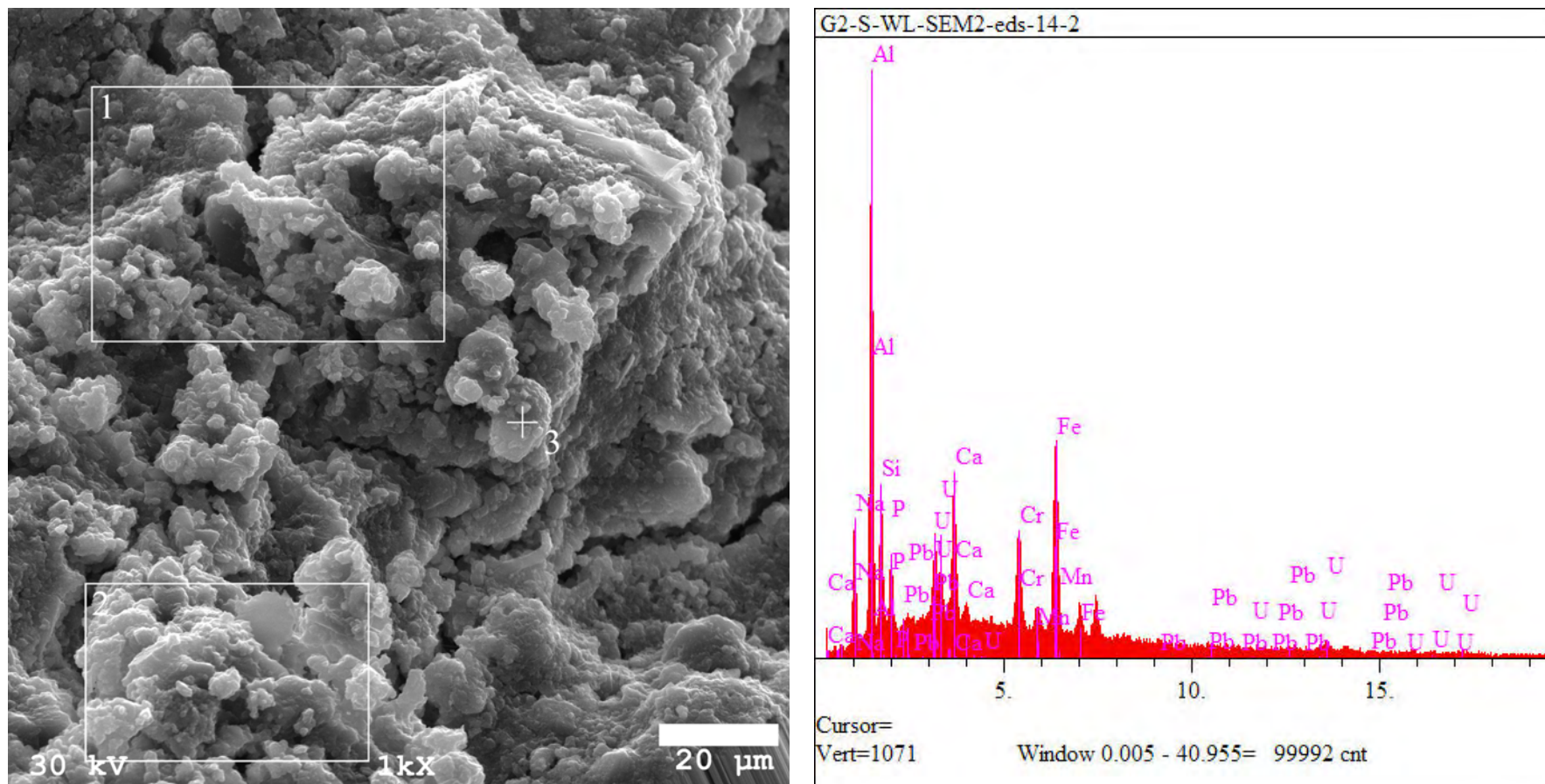
Figure 4.15. SEM-EDS Image Group 2 Initial Characterization Solids
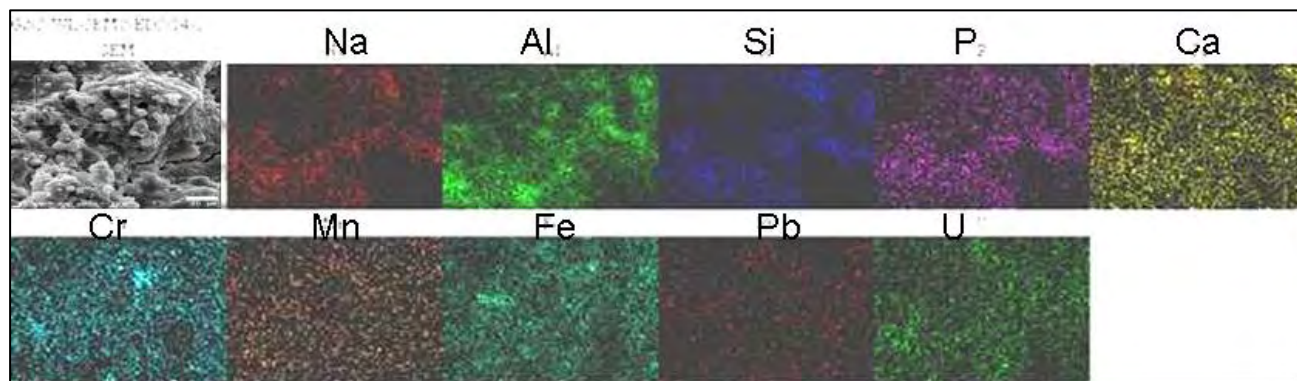
Figure 4.16. EDS Elemental Map of Group 2 Solids

TEM examination of the washed Group 2 solids revealed a number of different types of phases. A particle can be seen in the upper left-hand corner of Figure 4.17 that is a pure aluminum oxide or hydroxide material. Presumably, this particle is gibbsite, based on its shape and the XRD data discussed earlier. This gibbsite particle is on the order of 2 µm in size. The material in the lower half of Figure 4.17 is primarily iron oxide, with some associated Al, Si, and P. Whereas the iron oxide species in Figure 4.17 appears to consist of an agglomerate of submicron primary particles, the iron oxide particle shown in Figure 4.18 appears to be a single particle in excess of 5 µm in length. The image at the lower right hand corner of Figure 4.18 shows an agglomeration of submicron particles with a rather broad distribution of elements including Al, Ca, Cr, Fe, Si, and U. Figure 4.19 shows an expanded view of this agglomerate. The EDS spectra indicate that these agglomerated particles are mainly aluminosilicates, typically with incorporated transition metals, although the larger particle to the upper right in Figure 4.19 is relatively free of transition metals. Point 3 at the lower right hand portion of the figure is rich in Sr and Ca.
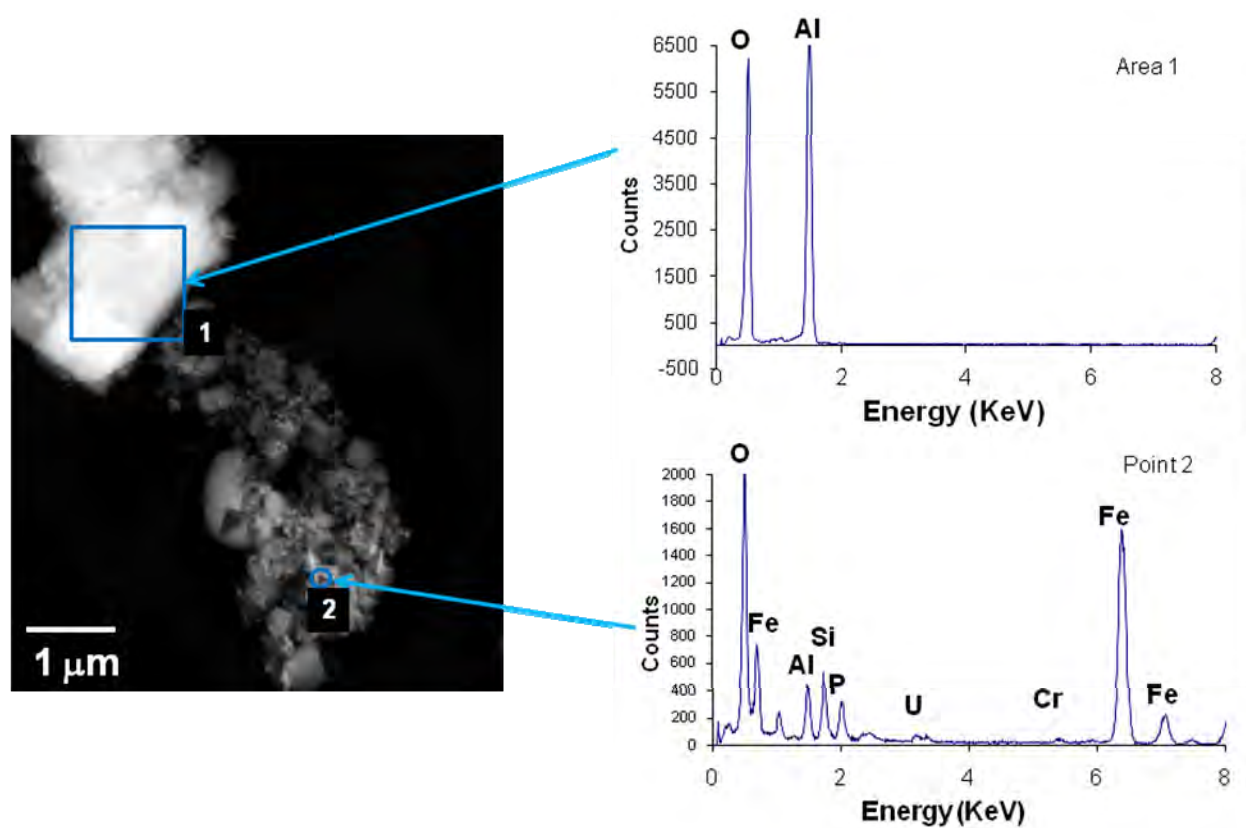
Figure 4.17. TEM Image of the Washed Group 2 Solids Indicating a Gibbsite Particle (upper left) and an Iron Oxide Particle (lower half)
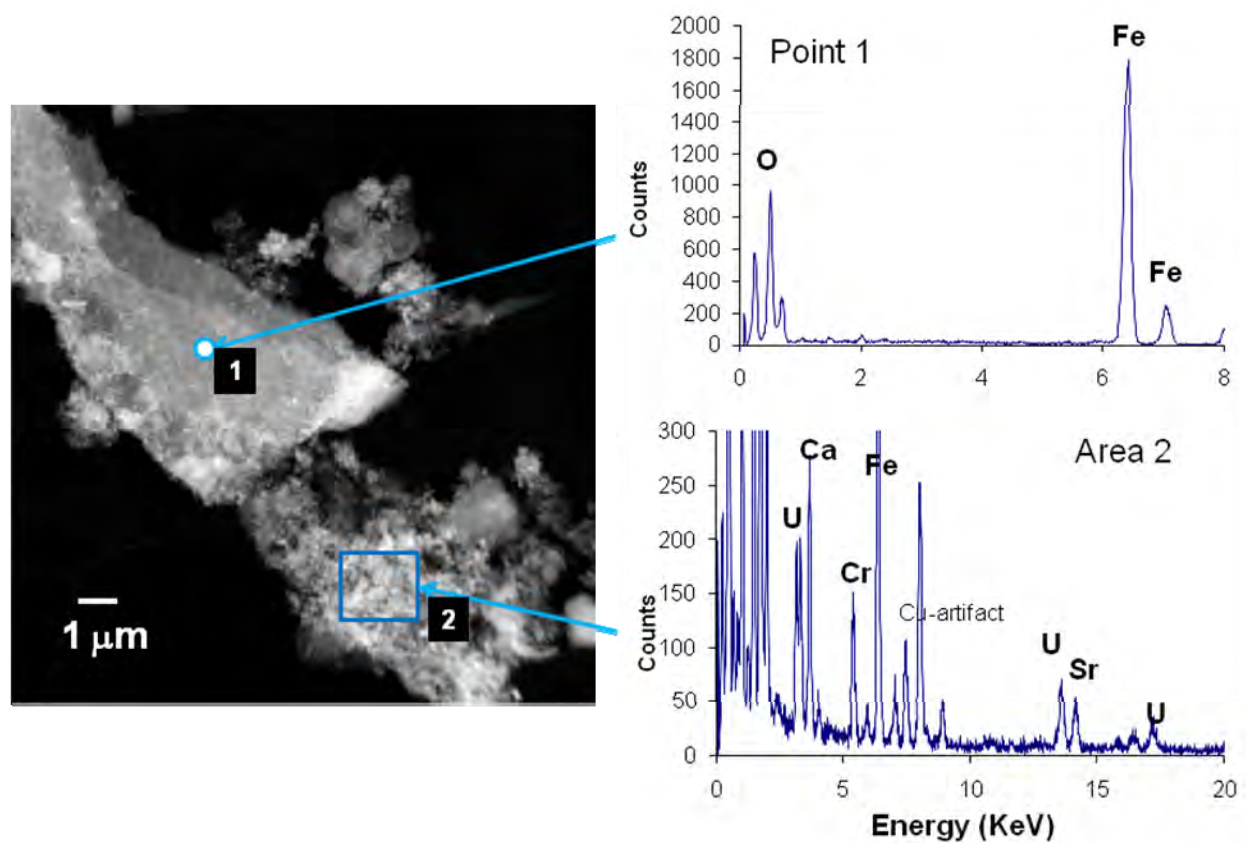
Figure 4.18. TEM Image of the Washed Group 2 Solids Indicating a Large Iron Oxide Particle (upper left) and an Agglomeration of Mixed Phases (lower right)
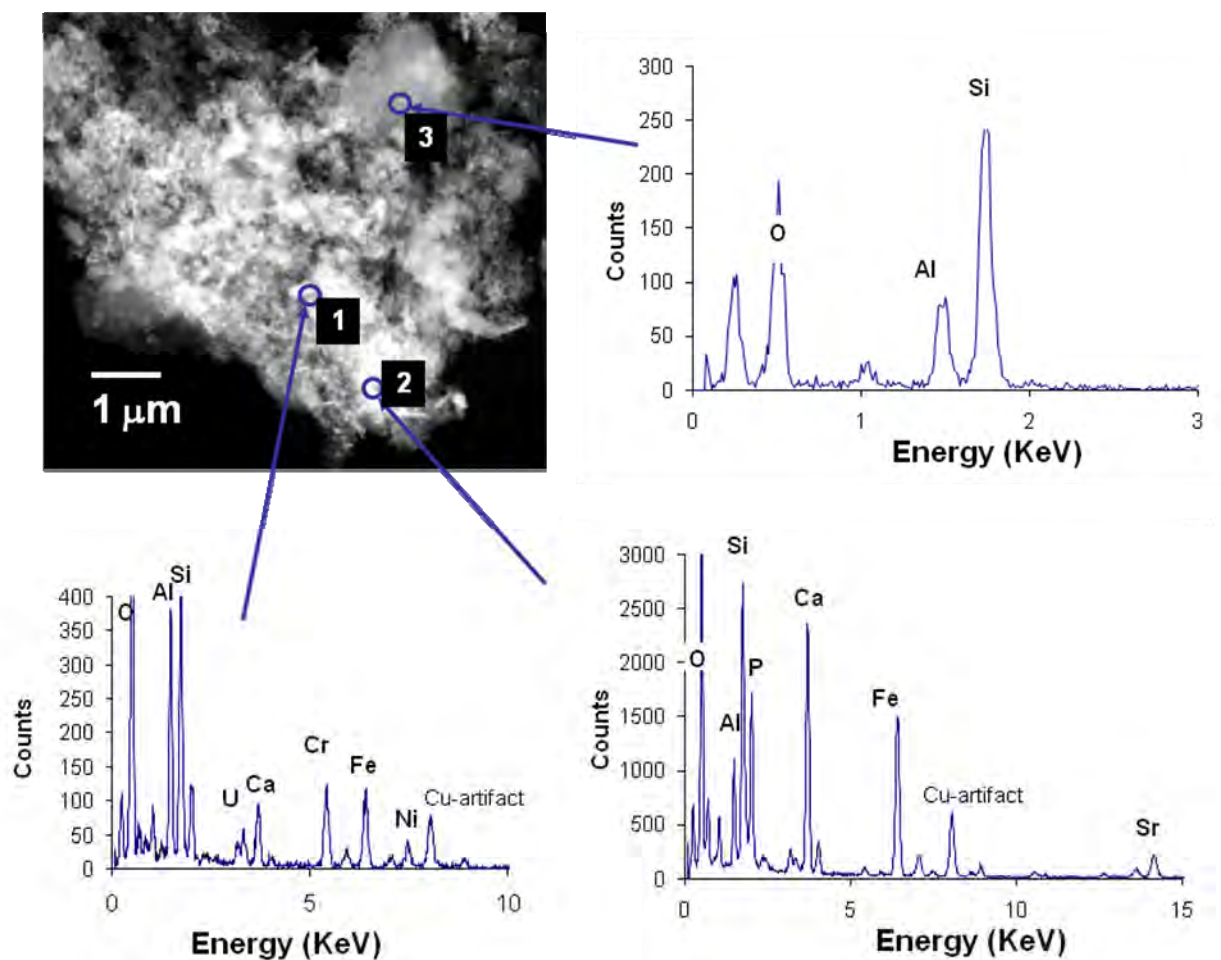
Figure 4.19. TEM Image of an Agglomeration of Mixed Phases in the Washed Group 2 Solids

Figure 4.20 shows a relatively pure phase containing oxygen, sodium, and phosphorus. This would be consistent with the mineral dorfmanite—$Na_2HPO_4 \cdot 2H_2O$—which was also identified in the XRD pattern. The bright particle in the lower part of Figure 4.21 is a uranium-rich phase, predominantly a uranium oxide of some sort. The remaining material in Figure 4.21 is an aluminosilicate, probably dominated by cancrinite as was suggested by the XRD analysis.
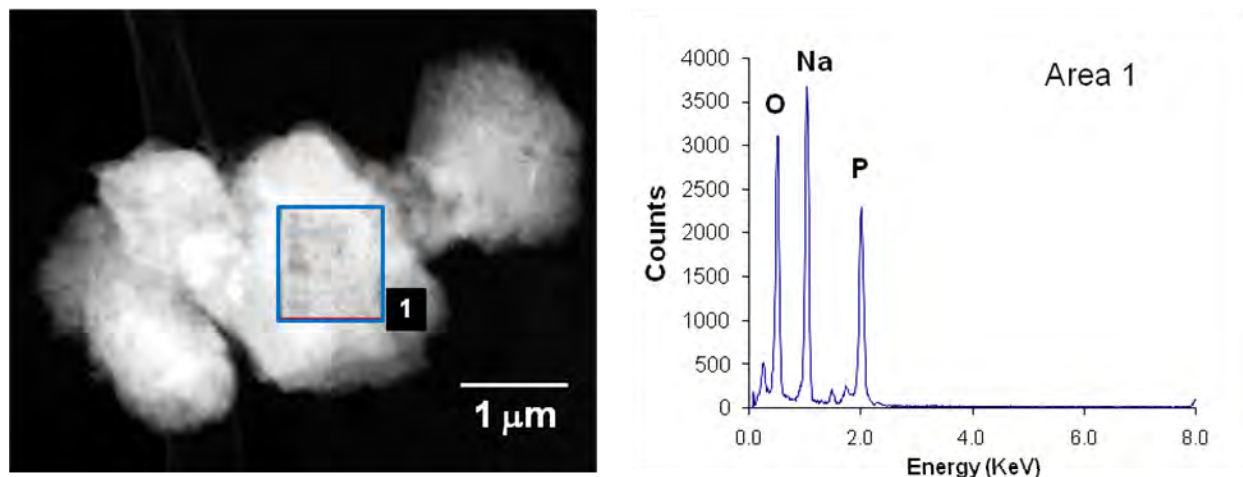
Figure 4.20. TEM Image of the Washed Group 2 Solids Indicating a Sodium Phosphate Phase, Presumably Dorfmanite
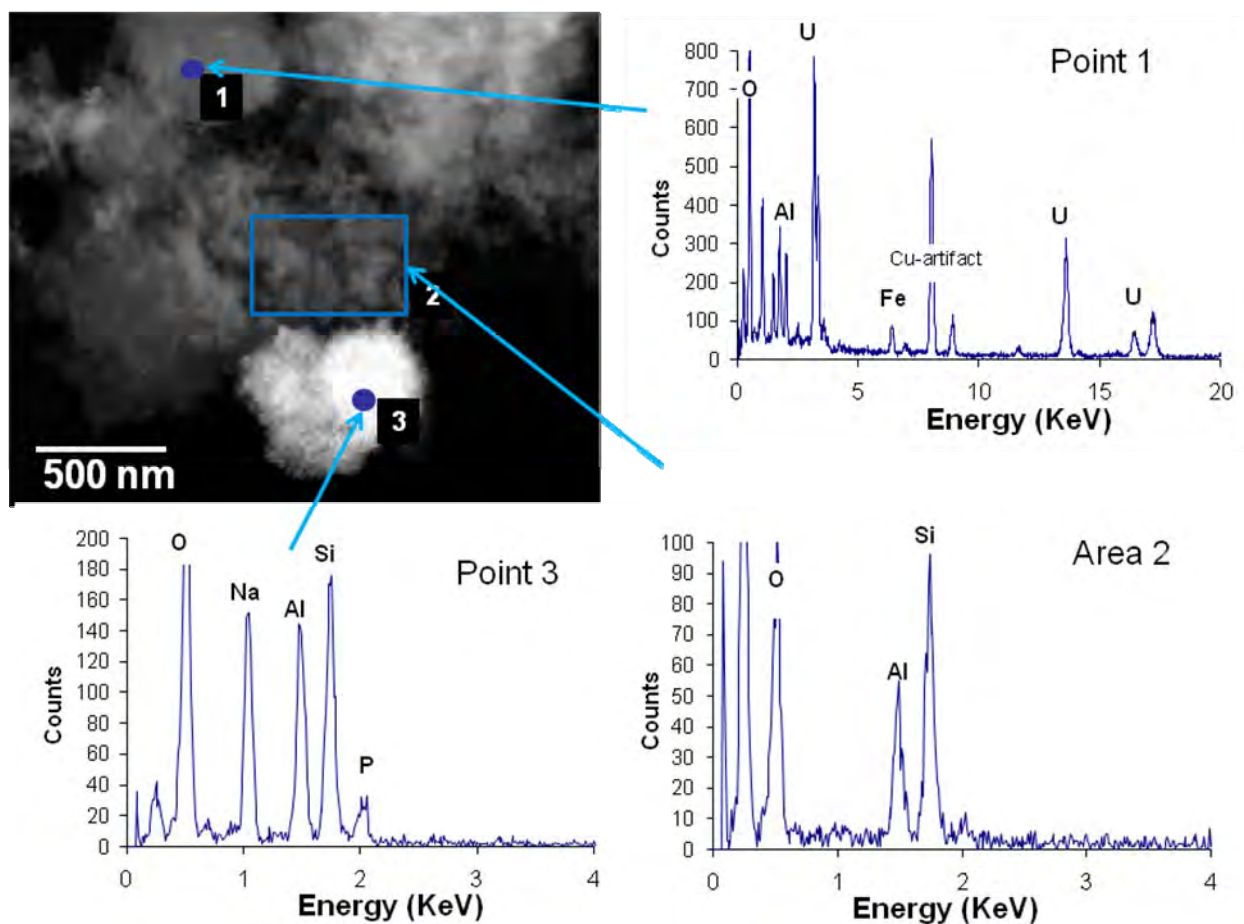
Figure 4.21. TEM Image of the Washed Group 2 Solids Indicating Aluminosilicate and Uranium-Rich Phases

4.2.7 Vibrational Spectroscopy[a]

In addition to the tools previously applied to characterize Hanford tank sludge solids, we are investigating the use of vibrational spectroscopic tools to further characterize the solids. Vibrational spectroscopy is complementary to the techniques described above and offers an advantage over diffraction techniques in that useful information can be obtained even if the sample is amorphous. The vibrational spectroscopic tools being used include FTIR and Raman spectroscopies. The sample of washed Group 2 solids that was used for the BET measurements (sample ID TI517-G2-S-WL-BET-1) was examined using FTIR spectroscopy, and the sample of Group 2 solids washed for the parametric leaching tests (sample ID TI517-G2-S-WL-B) was examined by Raman spectroscopy. In the case of the FTIR spectral measurement, a small portion of the Group 2 solids was placed directly on an attenuated total reflectance (ATR) cell equipped with a diamond ATR plate, and the spectrum was recorded with a Bruker ALPHA-P spectrometer (Bruker Optics, Billerica, Massachusetts). The Raman spectrum was recorded directly through a 2-Dram glass vial using an InPhotonics Model RS2000-3b-670 Raman spectrometer (Norwood, Massachusetts). The spectrometer was equipped with a fiber optic probe with a 670-nm excitation laser.

To assist in interpreting the vibrational spectra of the tank waste samples, spectra were recorded for a series of inorganic compounds that are likely to be present in the tank waste solids. Ultimately, we intend to create a searchable spectral library with the spectra of the known compounds that can be used to help determine the compounds present in the actual waste. However, for the Group 2 solids, we relied primarily on the above-described results (especially the XRD data) to help guide in interpreting the vibrational spectroscopic data.

The Raman spectrum of the washed Group 2 solids did not prove to be very informative, although there was clear evidence for the presence of gibbsite, based on the very distinctive pattern of four hydroxyl stretching bands at 3364, 3435, 3525, and 3619 cm^{-1}. Figure 4.22 compares the FTIR spectrum of the washed Group 2 solids with a spectrum calculated assuming the presence of selected phases. The calculated spectrum was obtained in the following way. The FTIR spectral data for the compounds assumed to be present were imported into Microsoft Excel™. The composite spectrum of these species (for n species present) was taken as:

$$A = \sum_{i=1}^{n} w_i A_i \qquad (4.1)$$

where A is the composite absorbance at a given wavelength, A_i is the measured absorbance for species i at that wavelength, and w_i is the weighting factor for species i. The Solver function of Excel™ was used to minimize the sum of the squares of the residuals between the calculated and measured spectra, with the w_i values being varied during the minimization process. The following compounds were included in the fitting procedure: gibbsite, nitrate cancrinite, $Na_2HPO_4 \cdot 2H_2O$, amorphous $FePO_4 \cdot xH_2O$, and $Na[UO_2PO_4] \cdot 3H_2O$. Gibbsite was obtained from a commercial supplier. The amorphous $FePO_4 \cdot xH_2O$ was prepared as described in Section 3.4.1. Nitrate cancrinite was prepared by a literature method (Liu et al. 2005), and its FTIR spectrum agreed very well with that reported in the literature. Dibasic sodium phosphate, $Na_2HPO_4 \cdot 2H_2O$, was prepared by slow evaporation of a solution of Na_2HPO_4 (dissolved as

---

(a) The vibrational spectroscopic results presented here are for indication only.

$Na_2HPO_4 \cdot 7H_2O$ obtained from Aldrich Chemical Co.) at 59°C (Templeton et al. 1990).[a] This species was included in the spectral fitting because of the evidence for dorfmanite in the XRD analysis. Sodium meta-autunite, $Na[UO_2PO_4] \cdot 3H_2O$, was previously prepared and characterized at PNNL (Wellman et al. 2005). During the fitting process, the Solver function indicated no significant contribution to the spectrum from $Na_2HPO_4 \cdot 2H_2O$ (i.e., the weighting factor for this compound was calculated to be zero), which calls into question the assignment of this phase in the XRD. So the calculated spectrum in Figure 4.22 contains contributions from gibbsite, cancrinite, amorphous $FePO_4 \cdot xH_2O$, and $Na[UO_2PO_4] \cdot 3H_2O$.

As can be seen from Figure 4.22, the calculated spectrum is in reasonable agreement with the measured spectrum, but the presence of gibbsite, cancrinite, amorphous $FePO_4 \cdot xH_2O$, and $Na[UO_2PO_4] \cdot 3H_2O$ does not represent a complete description of the Group 2 solids. In particular, the band at 991 cm^{-1} is not well reproduced in the calculated spectrum. This band is likely due to a phosphate species or a silicate-containing compound. It could also be due to a carbonate species such as urancalcarite, $Ca(UO_2)_3CO_3(OH)(H_2O)_3$, which was identified in the XRD analysis of the Group 2 solids. It would be useful to synthesize the latter compound and add this to the vibrational spectral library.
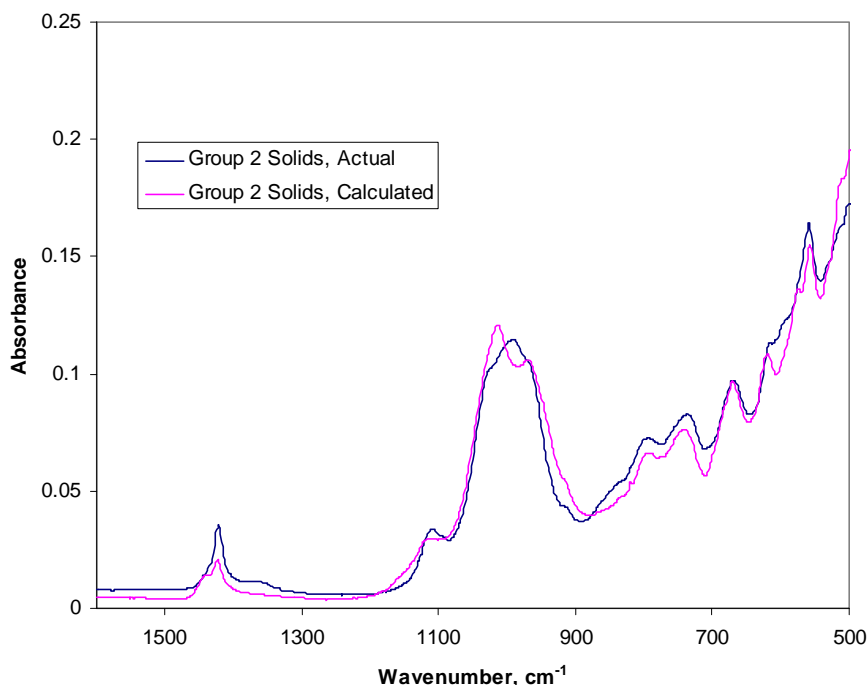
Figure 4.22. Measured and Calculated FTIR Spectrum of the Washed Group 2 Solids

---

(a) Although the literature indicated the material obtained in this manner should be the dorfmanite phase, $Na_2HPO_4 \cdot 2H_2O$, XRD analysis (for indication only) suggested the material was actually 87% anhydrous Na_2HPO_4 (nahpoite) and 13% dorfmanite.

4.3   Group 2 Batch Parametric Leaching: Experimental

This section describes the methods used to conduct the leach testing for the Group 2 bismuth phosphate saltcake composite samples. Testing on the Group 2 solids focused on evaluating gibbsite leaching chemistry in actual tank waste. The composite material was rinsed with 0.01 M NaOH, subdivided, and subjected to a parametric test matrix for caustic leach testing as discussed in the following sections.[a]

4.3.1   Initial Washing of the Group 2 Solids

The Group 2 composite solids sample was washed in the same manner as the Group 1 sample (Section 3.3.1). In this case, a 34.5-g aliquot of the homogenized slurry was removed with a large transfer pipet and transferred to a 200-mL centrifuge bottle. At a concentration of 0.29 g dry water-insoluble solids per gram of slurry, the 34.5-g slurry contained ~10 g of water-insoluble solids. After centrifuging at ~1200 G for 15 min, the supernatant liquid was removed, and the centrifuged solids volume was determined to be ~15 mL based on volume graduations on the sample bottle. Approximately 45 mL (3× the centrifuged solids volume) of 0.01 M NaOH was added to wash the solids, and the slurry was mixed for 15 min with an overhead mixer. The slurry was centrifuged at ~1200 G for 15 min, and then the supernatant was removed. The washing steps were repeated twice for a total of three washes.

4.3.2   Division of the Washed Group 2 Solids

To subdivide the washed Group 2 solids for the leaching tests, 100 mL of DI water was added to the solids. This resulted in a final volume of ~110 mL (or 10 g solids in 112 g of slurry, equivalent to 8.9 wt% UDS).

The thinned slurry was homogenized with an overhead mixer equipped with a 3-bladed stainless steel impeller. Seven ~14 g slurry samples were transferred to 125-mL HDPE bottles with a large disposable polyethylene pipet. Each sample contained ~1 g UDS. The samples were removed from the hot cell for follow-on processing at the fume hood workstation.

One additional sample (549-G2-WL-Solids) containing approximately 3.9 g of slurry (equivalent to 0.34 g dry solids) was transferred to a 60-mL HDPE bottle. A portion of this sample was submitted for a KOH fusion and the following subsequent analyses: ICP-OES metals, GEA, Pu, total alpha, total beta, ^{90}Sr, and U by KPA. These analyses were performed to establish the starting composition of the washed solids.

4.3.3   Caustic Leaching of the Washed Group 2 Solids

The leaching test matrix for the seven samples is summarized in Table 4.11. The test matrix evaluated the effects of free hydroxide concentration (1 to 5 M NaOH) and temperature (60 to 100°C) on gibbsite leaching kinetics.

(a) Testing was conducted according to TI-RPP-WTP-549, *Parametric Caustic Leach Test of Group 2 Hanford Bi-Phosphate Saltcake Waste*, L Snow, October 2007.

Table 4.11. Group 2 Caustic Leaching Conditions

| Bottle ID | Free OH, M | | Na, M | | Temperature, °C[b] |
	Target	Measured[a]	Target	Measured[a]	
G2-60-3	3	3.04	3	3.19	60
G2-80-1	1	0.96	1	1.09	80
G2-80-3a	3	2.99	3	3.16	80
G2-80-3b	3	3.05	3	3.10	80
G2-80-3c	3	3.01	3	3.03	80
G2-80-5	5	5.00	5	5.00	80
G2-100-3	3	3.09	3	3.29	100
(a) The measured analyte concentrations represent the equilibrium concentration obtained after a 24-h contact time. (b) The temperature uncertainty was ± 2.5°C Analytical Service Request (ASR): 8032					

The Group 2 leaching tests were conducted in the same manner as the Group 1 leaching tests (see Section 3.3.3). Sodium hydroxide (19 M) was added to each aliquot of washed solids slurry in the following amounts: 5.3 mL to yield 1 M NaOH, 15.8 mL to yield 3 M NaOH, and 26.3 mL to yield 5 M NaOH. The leaching mixtures were then diluted to a final volume of 100 mL (with an estimated uncertainty of 2 mL) with DI water. The contact time with the concentrated NaOH was brief (<5 min). The remainder of the procedure was identical to that for the Group 1 tests.

The equilibrium concentration values for free hydroxide and sodium are shown in Table 4.11 and were based on results from the samples taken at 24 hours.

4.3.4 Washing of Caustic-Leached Group 2 Solids for Analysis

The solids from the triplicate samples (G2-80-3a, -3b, -3c, leached at 80°C in 3 M NaOH) were prepared for characterization as shown in Figure 4.23. Again, the process followed was essentially the same as that for the leached Group 1 solids (Section 3.3.4).
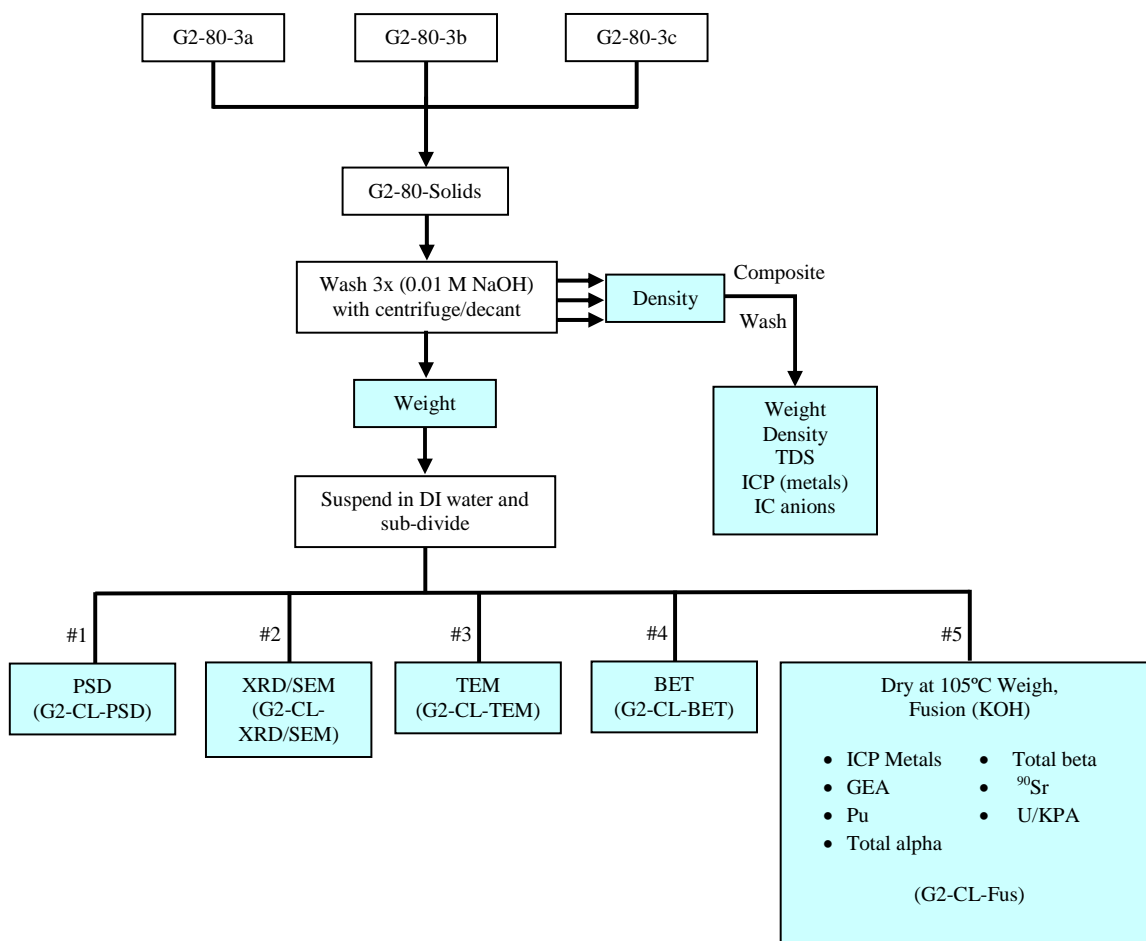
Figure 4.23. Washing, Subdivision, and Analysis Scheme for the Group 2 Caustic Leached Solids

4.4 Group 2 Bi-Phosphate Saltcake Waste Parametric Caustic Leaching Test Results

The water-insoluble component of the Group 2 waste sample contained 11.3 wt% Al (as gibbsite, cancrinite, and urancalcarite) as well as 4.6 wt% P. Accordingly, the parametric caustic leach testing of this sample was directed toward understanding the gibbsite and phosphorus dissolution behavior for the actual tank waste to understand and subsequently match the dissolution properties to a stimulant material. The parametric leaching results and residual solids composition are discussed in the following sections.

4.4.1 Time, Temperature, and Hydroxide Effects on Aluminum Dissolution from the Group 2 Solids

The aluminum dissolution behavior for the washed Group 2 solids was evaluated as a function of time, temperature, and free-hydroxide concentration. Based on the total Al concentration in the solids material (149.5 mg Al/g) and the wt% UDS of the starting slurry (5.76%), the complete dissolution of Al would result in a concentration of 1.21 mg Al/mL or 0.0447 M under the leaching conditions used in these experiments. This expected maximum concentration is about 20% less than the maximum Al concentration measured in the leachates (0.056 M Al). The reason for this discrepancy is not known. In

this discussion, the reported wt% of Al dissolved at each sampling point was calculated based on the final concentration in the triplicate solids samples, as discussed in Section 4.4.6.2.

The Al leaching data at a constant temperature of 80°C and the varying free-hydroxide concentrations are presented in Figure 4.24. The triplicate tests run at 3-M free hydroxide and 80°C provide a measure of experimental precision. The observed scatter in the data was within the analytical characterization uncertainty of ±15%.

There was only a slight dependence of Al dissolution on the hydroxide concentration. Dissolution had reached a steady-state in 4 to 8 hours. The rapid dissolution of the Al is consistent with the fast dissolution of gibbsite under these leaching conditions. The Al dissolution was similar in 3 and 5 M NaOH, and only somewhat slower in 1 M NaOH. However, the dissolution in all concentrations of NaOH reached a steady-state (~60% dissolved) within 8 h. Approximately 40% of the Al present in the washed Group 2 solids appears to be in the form of aluminosilicates, which is consistent with the high Si content found for the residual solids from leaching in 3 M NaOH at 80°C. The Al/Si molar ratio in 3 M NaOH/80°C leached-solids was 1.0 (*vide infra*)—consistent with a cancranite aluminosilicate phase. The Al present as aluminosilicate is not readily removed by caustic leaching at 80°C and up to 5 M NaOH.
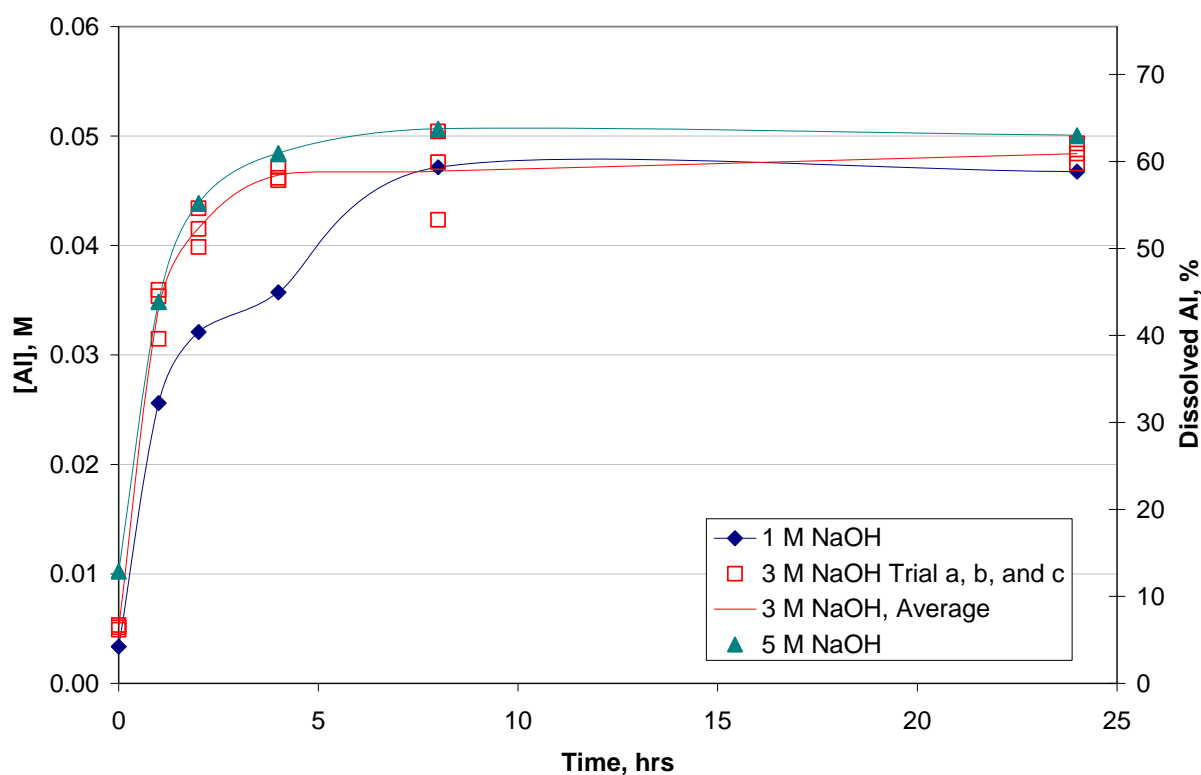
Figure 4.24. Aluminum Concentration Versus Time at 80°C Leach Temperature in 1, 3, and 5 M NaOH Solutions for Group 2, Bi-Phosphate Saltcake

The aluminum leaching data at a constant NaOH concentration of 3 M at varying temperatures is summarized in Figure 4.25. There was some variability in the initial (t = 0) Al concentrations; this might have been due to variability in the initial sub-sampling or from differences introduced when the NaOH

solution was first added to the sample (e.g., slight differences in the time interval between NaOH addition and dilution to 100 mL). The data indicate a clear dependence of the Al dissolution rate on the temperature. The times to reach a steady-state Al concentration were 2, 4, and >8 (but less than 24) h at 100, 80, and 60°C, respectively. Dissolution at 60 and 80°C reached approximately 60% dissolved after 24 h, while approximately 70% of the Al was dissolved after 24 h at 100°C. This suggests that ~10% of the Al is in a form not readily removed at 80°C, but can be dissolved by raising the temperature to 100°C. The remaining ~30% of the Al (presumably aluminosilicate) is resistant to removal by caustic leaching.
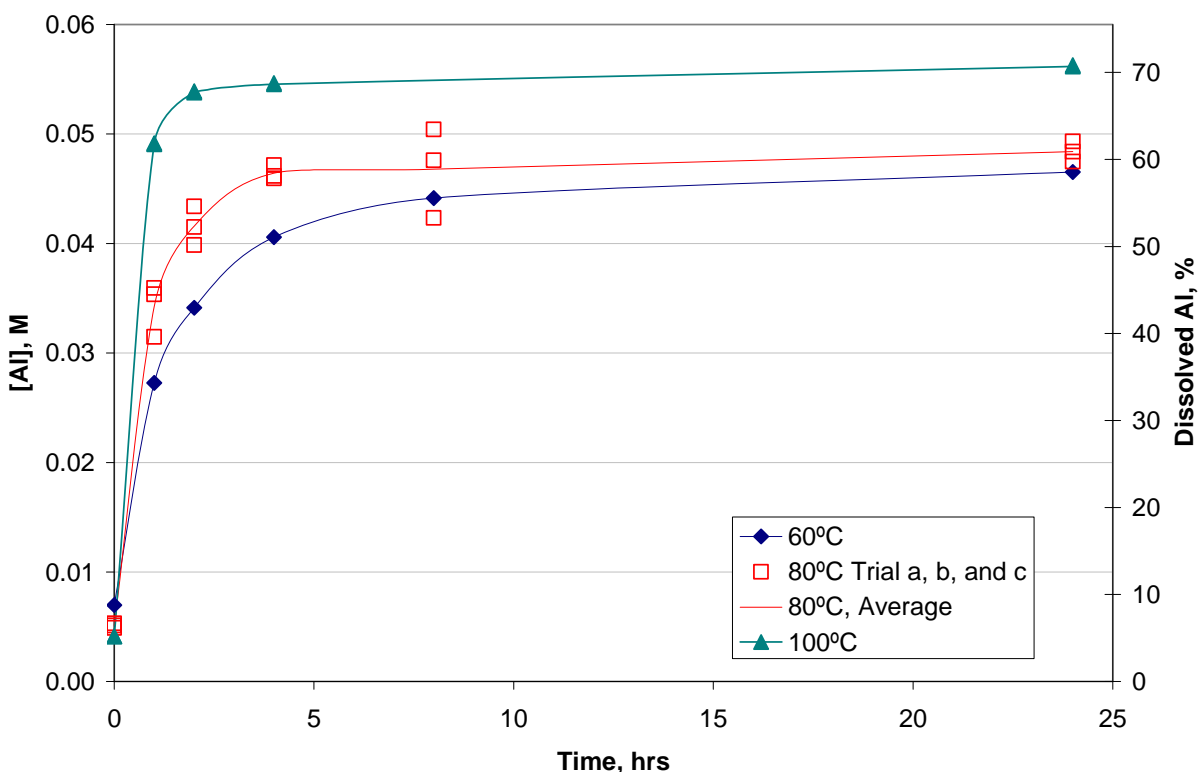
Figure 4.25.   Aluminum Concentration and Percent Dissolved in 3 M NaOH for Group 2, Bi-Phosphate Saltcake. Note: the 8 h/100°C data point is suspected to be inaccurate and so was not plotted here.

4.4.2   Time, Temperature, and Hydroxide Effects on Chromium Dissolution

The Cr dissolution behavior for the washed Group 2 solids was evaluated as a function of time, temperature, and free hydroxide concentration. The chromium leaching data at a constant temperature of 80°C and varying free-hydroxide concentrations is summarized in Figure 4.26. Again, the triplicate runs at 3 M free hydroxide and 80°C provided a measure of experimental precision. The scatter in the data was within the analytical uncertainty of ±15%.

There was only a slight dependence of Cr dissolution on the hydroxide concentration. Unlike with the dissolution of Al, Cr never reached a steady-state for leaching in 3 and 5 M NaOH, rather the Cr removal gradually increased up to a value of 70% removed after 24 hours of leaching. This observation is

consistent with oxidation of Cr(III) to Cr(VI) by adventitious oxygen present in the system. In the case of 1 M NaOH, the Cr removal did appear to stabilize at only ~45% after 8 h of leaching; continued leaching to 24 h under these conditions did not remove significantly more Cr.
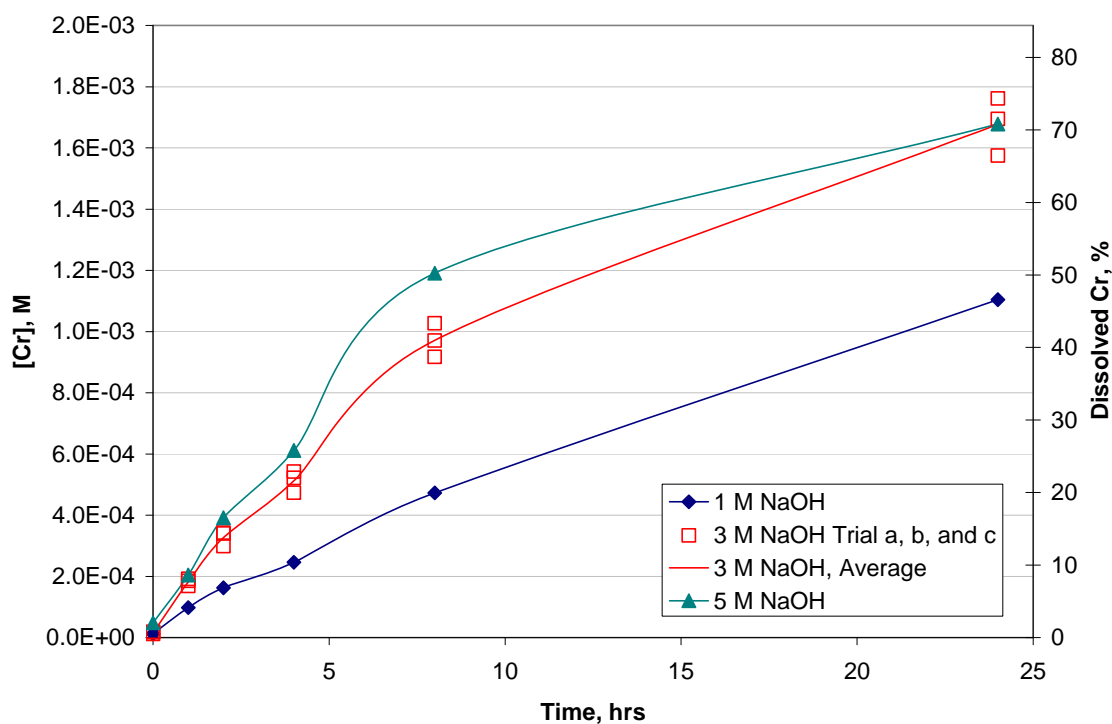
Figure 4.26. Chromium Concentration Versus Time at 80°C Leach Temperature in 1, 3, and 5 M NaOH Solutions for Group 2, Bi-Phosphate Saltcake

The chromium leaching data at a constant NaOH concentration of 3 M at varying temperatures is summarized in Figure 4.27. These data indicate that the Cr removal is strongly temperature dependent. Under the leaching conditions of 80°C in 3 M NaOH, Cr would be the limiting component for the formation of glass waste forms. For Al to be the limiting component, 85% of the Cr needs to be removed from the water-insoluble Group 2 solids under these leaching conditions. Dissolution at 80°C reached approximately 70% dissolved after 24 h, while only 30% of the Cr was dissolved after 24 h at 60°C. Unfortunately, the Cr removed at the baseline condition of leaching at 100°C for 8 h could not be confidently evaluated because the measured Cr value (2.3×10^{-3} M) is suspected to be inaccurate. This value is suspect because of the low aliquot mass recorded for the sample that was analyzed. If the measured value is correct, it would indicate ~90% Cr removal under these conditions. However, if it is assumed that the Al concentration at 8 h/100°C is the same as that at 4 h (which is reasonable based on Figure 4.25), the "correct" Cr concentration can be estimated to be 1.8×10^{-3} M.[a] The latter value corresponds to ~76% Cr removed.

(a) The measured Cr concentration at 8 h/100°C was 120 µg/mL. Since the Al concentration at 4 h was measured to be 1472 µg/mL, and that at 8 h was measured to be 1908 µg/mL, the corrected 8-h Cr concentration can be estimated as follows:

Cr corrected = (120 µg/mL)(1472/1908) = 92.6 µg/mL or 1.8×10^{-3} M

Assuming the mechanism of Cr removal in caustic leaching to be due to oxidation by adventitious oxygen, the rate of air oxidation of the Cr in the washed Group 2 solids was much faster than that observed for the air oxidation of Cr in the Group 6 sample (Fiskum et al. 2008), where the sample was 38% Cr, and the caustic leach factor was only 0.04. In comparison, the Group 2 sample is only 25% Cr, and the caustic leach factor is 0.7. Depending on what the sample is blended with during leaching, it could still require oxidative leaching. Either Al or Cr will be the limiting component for the formation of glass waste forms.
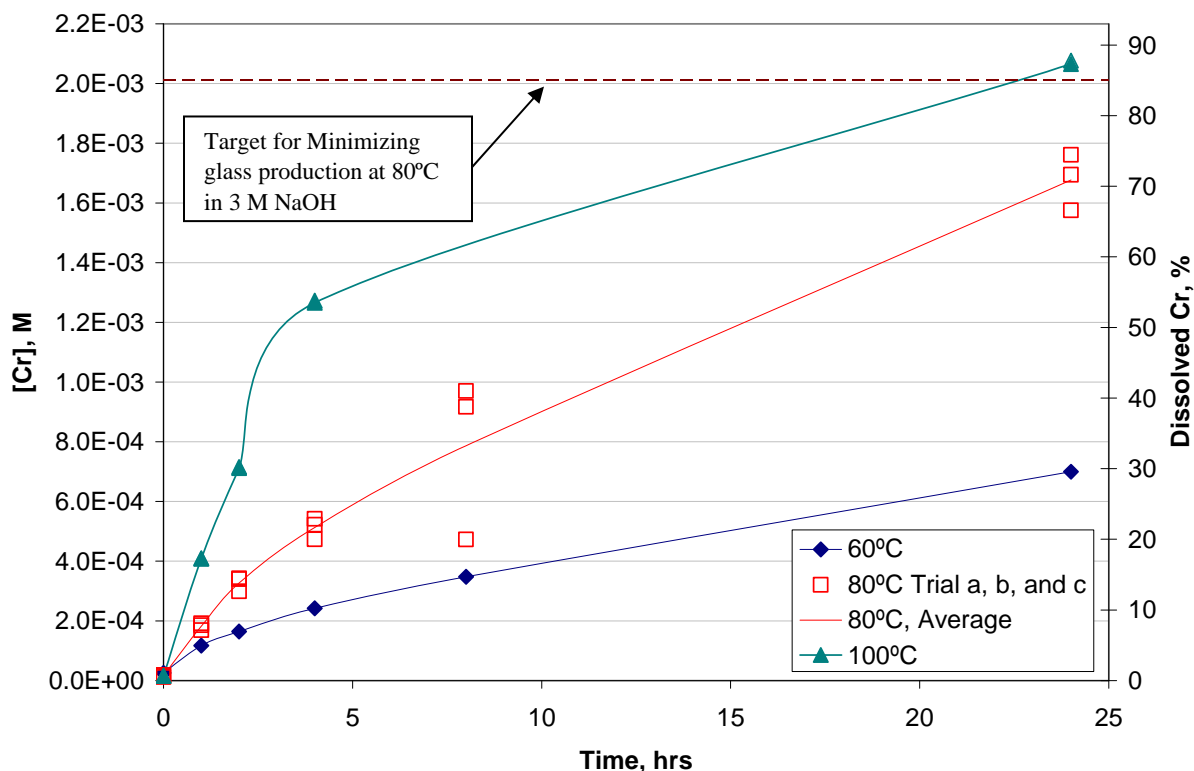
Figure 4.27. Chromium Concentration and Percent Dissolved in 3 M NaOH for Group 2, Bi-Phosphate Saltcake. Note: the 8 h/100°C data point is suspected to be inaccurate and so was not plotted here.

4.4.3   Time, Temperature, and Hydroxide Effects on Phosphorus Dissolution

The P dissolution behavior for the washed Group 2 solids was evaluated as a function of time, temperature, and free hydroxide concentration. The P leaching data at a constant temperature of 80°C and varying free-hydroxide concentrations is summarized in Figure 4.28. Again, the triplicate runs at 3 M free hydroxide and 80°C provided a measure of experimental precision.

There was only a slight dependence of P dissolution on the hydroxide concentration. Unlike with the dissolution of Al, P never reached a steady-state during the leaching process. The P data were rather scattered, above the analytical uncertainty of ±15% for the triplicate samples. All data showed some

scatter, with the amount of P in solution seeming to be nearly the same from the time = 0 point to the time = 24 h point.
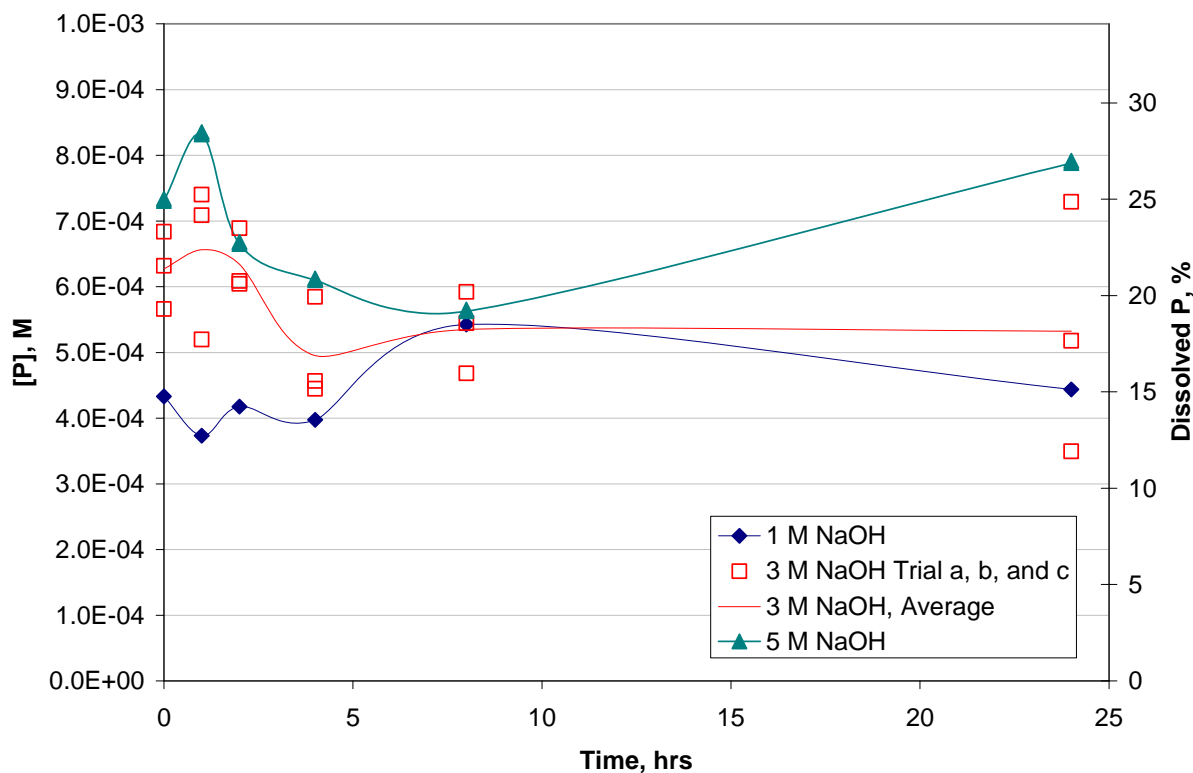
Figure 4.28. Phosphorus Concentration Versus Time at 80°C Leach Temperature in 1, 3, and 5 M NaOH Solutions for Group 2, Bi-Phosphate Saltcake

The P leaching data at a constant NaOH concentration of 3 M at varying temperatures is summarized in Figure 4.29. Because of the scatter in the data, it is somewhat difficult to draw any conclusions from these results. The apparent initial drop in the P concentration, followed by a subsequent rise, is particularly difficult to explain. Comparison of the final P concentrations at 60°C versus 100°C does suggest that the P removal is dependent on temperature. However, the maximum P removal was 23%; obtained by leaching in 3 M NaOH at 100°C. In this respect, the P behavior in the Group 2 solids is much different than that for the Group 1 solids. That is, the bulk of the P present in the Group 2 solids is resistant to removal by caustic leaching, whereas P was removed from the Group 1 solids under relatively mild conditions.
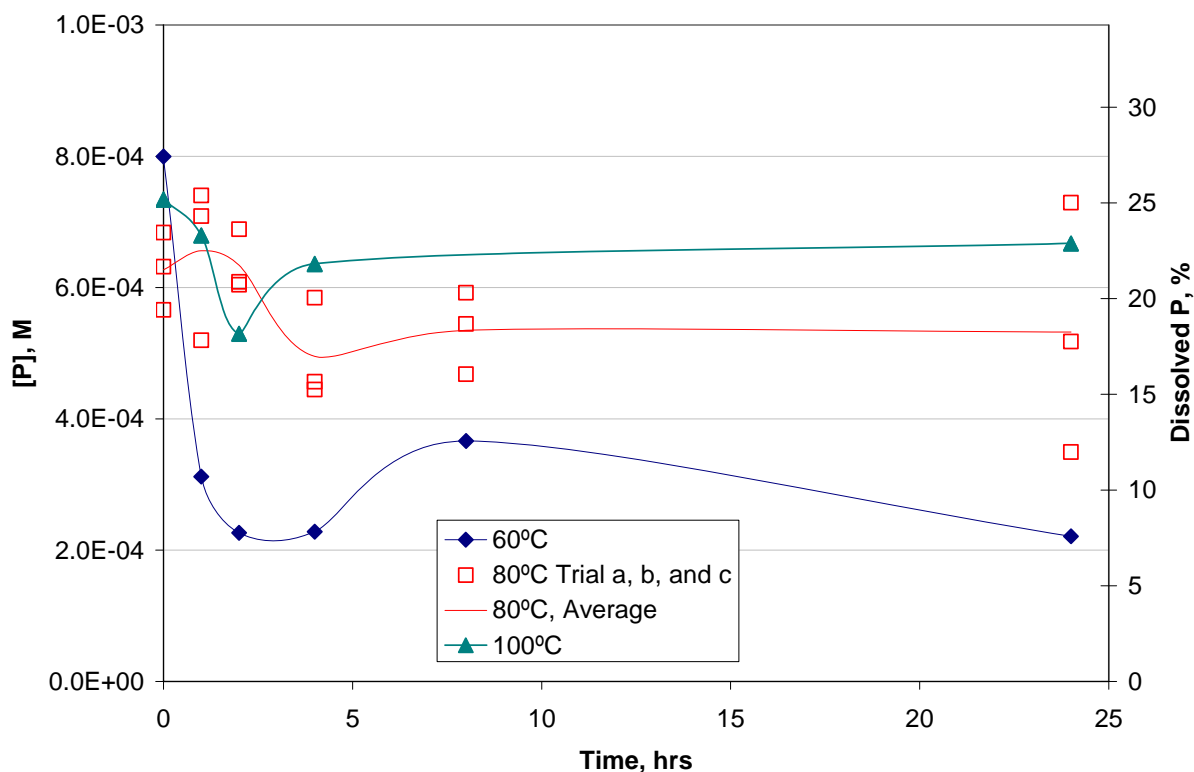
Figure 4.29. Phosphorus Concentration and Percent Dissolved in 3 M NaOH for Group 2, Bi-Phosphate Saltcake. Note: the 8 h/100°C data point is suspected to be inaccurate and so was not plotted here.

4.4.4 Anion, Silicon, and Iron Leach Behavior

The concentration of Si was measured opportunistically by ICP-OES. The anionic compositions were also assessed at each sampling period. Anion and Si concentrations in the leachate did not significantly change during the leach testing. The results are summarized in Appendix J.

Iron concentrations were also measured opportunistically by ICP-OES. The Fe concentrations in the leachates were variable. However, they appeared to generally increase relative to the first sampling period at 0 hr ($<5 \times 10^{-5}$ M Fe) to the 24-hr sampling period ($\sim 1 \times 10^{-4}$ M Fe).

4.4.5 Assessment of Final Leach Conditions

A summary of the final (24-h) leach-solution chemistry and physical parameters is shown in Table 4.12. The final free-hydroxide and sodium concentrations were at the targeted values within the uncertainty of the analytical methods (±15%). The calculated percentage of aluminum that was removed at each leaching condition is also shown. Appendix J summarizes the concentrations of Al, Cr, Fe, Na, P, Si, fluoride, nitrite, nitrtate, phosphate, and sulfate in the final leach solutions. The GEA results for ^{60}Co and [241]Am were <MDL; the GEA results are also provided in Appendix J.

Table 4.12. Group 2 Bismuth Phosphate Saltcake Leaching Final Aqueous Phase Conditions

Temp., °C	Density, g/mL	Free OH, M	Na, M	Al, M	Wt % Al Removed
60	1.13	3.04	3.19	4.56E-02	58
80	1.06	0.96	1.09	4.68E-02	58
80 trial a	1.13	2.99	3.16	4.93E-02	61
80 trial b	1.13	3.05	3.10	4.75E-02	59
80 trial c	1.12	3.01	3.03	4.90E-02	60
80	1.19	5.00	5.00	5.00E-02	62
100	1.18	3.09	3.29	5.62E-02	70

4.4.6 Comparison of Initial and Caustic Leached and Washed Solids Properties

The Group 2 solids that had been caustic leached at 80°C in 3 M NaOH for 24 h were combined and washed in preparation for analysis. The wash solution composition and the washed solids chemical, radiochemical, particle size, and crystal habit are discussed.

4.4.6.1 Leached Solids Wash Solution

The densities of the three sequential wash solutions were 1.019, 1.007, and 1.008 g/mL, respectively. The composite wash solution (82.16 mL volume) density, ICP metals, and anion composition are shown in Table 4.13.

Table 4.13. Solids Wash Solution Composition and Density

Analyte	µg/mL	Analyte	µg/mL	Density Measurement	Value
Al	103.5	Si	13.6	Density	1.004 g/mL
Cr	7.3	nitrate	469.7		
Na	5,399	phosphate	[4.5]		
P	[2.1]	sulfate	[0.81]		

4.4.6.2 Chemical and Radiochemical Composition

The initial composition of washed solids (before caustic leaching) is provided in Table 4.14 along with selected results from the initial characterization study (i.e., values taken from Table 4.5 and Table 4.6). The solids composition after leaching in 3 M NaOH at 80°C for 24 h and washing is also shown in Table 4.14. The solids from the initial characterization had been washed three times, resulting in an estimated 26-wt% salt entrainment from the supernatant phase, but the "before leaching" material had been more extensively washed, i.e., no salt entrainment (except for NaOH from the washing liquid) was expected. The composition of the material used for the parametric leaching tests was considerably different from that of the initial characterization sample. This can best be seen by comparing the ratios of the masses of the various components to that of iron in the sample (Table 4.15).[a] The amount of sodium

---

(a) This comparison assumes that Fe is not soluble in the washing medium.

Table 4.14. Group 2 Bi-Phosphate Saltcake Leached Solids Composition and Leach Factors (Dry Mass Basis)

Analyte	Avg. Initial Charac. µg/g[a] (ASR 7974)	Avg. Before Leaching, µg/g (ASR 8032)	Avg. After Leaching, µg/g (ASR 8032)	Observed Leach Factor[b]
Al	117,500	149,500	91,450	0.61
B	[105]	<161	<186	0.27
Bi	1030	2,675	3,650	0.13
Cd	98	275	329	0.24
Cr	7,885	22,850	10,300	0.71
Fe	22,075	47,100	84,500	--
Mn	1,020	2,140	4,110	--
Na	185,000	[78,500]	[100,000]	--
S	[1,400]	[1,322]	[3,250]	--
Si	31,650	42,800	92,250	--
Sr	4,270	9,110	17,450	--
U	15,450	46,100	59,850	0.18
Zn	399	975	1,725	--
Zr	[110]	<107	<124	0.27
U (KPA)	15,250	47,420	58,740	0.21
	µCi/g			
^{60}Co	1.07×10^{-2}	1.44×10^{-2}	2.53×10^{-2}	--
^{90}Sr	1.79×10^{2}	4.95×10^{2}	8.00×10^{2}	0
^{137}Cs	9.97×10^{1}	1.30×10^{2}	1.93×10^{2}	0.06
^{154}Eu	4.84×10^{-2}	1.53×10^{-1}	2.38×10^{-1}	0.01
^{155}Eu	<0.1	5.58×10^{-2}	8.57×10^{-2}	0.03
$^{239+240}$Pu	2.67×10^{-1}	3.85×10^{-1}	5.70×10^{-1}	0.06
^{241}Am	4.21×10^{-1}	1.05	1.64	0.01
total alpha	5.05×10^{-1}	1.32	1.86	0.11
total beta	4.63×10^{2}	1.84E+03	1.84×10^{3}	0.37
^{238}Pu	1.44×10^{-2}	1.56E-02	2.27×10^{-2}	0.08
Opportunistic				
Ag	[8.5]	<31	<35	0.27
As	<269	<493	<570	0.27
Ba	257	545	1,010	--
Be	<1.0	<3	<2	0.49
Ca	9,800	[25,000]	[40,000]	0
Ce	<202	<369	<427	0.27
Co	[33]	[105]	[155]	0.06
Cu	80.3	[310]	[1,095]	--
Dy	<52	<94	<109	0.27
Eu	<16	<30	<35	0.27
La	[19]	[115]	[170]	0.06
Li	[48]	100	--	1.00
Mg	1,255	2,450	4,690	--

Table 4.14 (Contd)

Analyte	Avg. Initial Charac. µg/g (ASR 7974)	Avg. Before Leaching, µg/g (ASR 8032)	Avg. After Leaching, µg/g (ASR 8032)	Observed Leach Factor
Mo	<30	<54	<63	0.27
Nd	[43]	<569	<657	0.27
P	47,850	14,800	19,000	0.19
Pb	1,385	3,280	2,925	0.43
Pd	<183	<335	<388	0.27
Rh	<120	<220	<254	0.27
Ru	<52	<94	<109	0.27
Sb	<171	<312	<361	0.27
Se	<291	<533	<616	0.27
Sn	[80]	<498	<576	0.27
Ta	<59	<107	<124	0.27
Te	<231	<423	<489	0.27
Th	<180	<330	<381	0.27
Ti	178	265	640	--
Tl	<209	<383	<443	0.27
V	46.1	<25	<29	0.27
W	<92	<168	<194	0.27
Y	[4.1]	<36	<42	0.27

(a) The values listed here are the average of the values obtained by the KOH fusion and acid digestion methods (see Table 4.5 and Table 4.6). In those cases, in which one method yielded high uncertainty, the most reliable value is presented in this table.

(b) Leach factors calculated by the "concentration factor" method, described in the text.

Table 4.15. Comparison of Fe-Normalized Compositions of the Initial Group 2 Characterization Sample and the Washed Group 2 Sample Used for Parametric Leaching for Selected Components

Component	g Component/g Fe	
	Initial Characterization	Before Leaching
Al	5.3	3.2
Cr	0.36	0.49
Na	8.4	1.7
P[a]	2.2	0.3
Si	1.4	0.9
Sr	0.19	0.19
U	0.7	1.0

(a) Determined opportunistically.

present in the leaching sample was approximately 5 times less than that in the initial characterization sample, confirming the supposition that soluble sodium salts were removed more extensively when washing the solids before leaching. This appears to be the result of washing sodium phosphate from the solids because there is an ~7-fold decrease in the phosphorus content relative to Fe (caveat: the phosphorus data were determined opportunistically). The Al concentration in the Group 2 solids also decreased 40% with more extensive washing of the solids (again, relative to Fe). The Cr concentration with respect to the Fe concentration was higher in the more extensively washed leaching sample; however, this might be due to experimental uncertainty.

Because the amount of Al projected to be in the initial solids was 20% less than that found in the final leachate solutions, the data from the Group 2 caustic leaching experiments were analyzed by the three methods described in Section 3.4.6.2 for determining the percent of each component removed during leaching. In the case of the Group 2 solids, the leached solids were dominated by Al (9.1 wt%), Cr (1.0 wt%), Fe (8.4 wt%), Na (10 wt%), Si (9.2 wt%), Sr (1.7 wt%), and U (6.0 wt%), and the analysis of the leachate solutions showed that Bi, Cd, Fe, Mn, Sr, and U had not dissolved after the initial water washing. The relative concentration factor (CF) of these analytes averaged 2.63 in the final washed solids, based on the concentration ratio after washing to the initial characterization washed sample. This term was used to determine the specific analyte wash factors according to Equation 4.2:

$$ WF = 1 - \left(\frac{C_w}{C_I \times 2.63} \right) \tag{4.2} $$

where WF is the water wash factor, C_W is the washed analyte concentration, and C_I is the initial analyte concentration.

Analysis of the caustic leachate solutions also indicated that the same metals (Bi, Cd, Fe, Mn, Sr, and U) did not dissolve after the caustic leach. The relative concentration factor of these analytes averaged 1.58 in the final leached solids, based on the ratio of the analyte concentrations after leaching to before leaching (after washing). This term was used to determine the specific analyte leach factors according to Equation 4.3

$$ LF_3 = 1 - \left(\frac{C_L}{C_W \times 1.58} \right) \tag{4.3} $$

where LF_3 is the caustic leach factor, C_L is the leached analyte concentration, and C_W is the washed analyte concentration.

Results from all three methods are given in Table 4.16. For Al, the results from all three methods are different, with method one giving the highest values and method three giving the lowest values. For P, all three methods had reasonably good agreement. For Cr, methods two and three gave nearly identical results, with Method 1 giving lower results. All values of percent leached plotted in this section and shown in Table 4.12 and Table 4.14 were calculated using method three, the "concentration factor" method.

Table 4.16. Group 2 Bi-Phosphate Slurry Leach Factors

Temp., °C	Free [OH], M	Na, M	Fraction Removed Based on initial solids/leachate solution			Fraction Removed Based on final solids/leachate solution			Fraction Removed Based on initial/final solids ("concentration factor" method)		
			Al	Cr	P	Al	Cr	P	Al	Cr	P
60	3.04	3.19	1.04	0.20	0.06	0.80	0.31	0.09	0.58	0.29	0.07
80	0.96	1.09	1.05	0.31	0.12	0.80	0.49	0.19	0.58	0.46	0.14
80 trial a	2.99	3.16	1.10	0.50	0.19	0.83	0.76	0.29	0.61	0.74	0.22
80 trial b	3.05	3.10	1.07	0.48	0.09	0.83	0.75	0.17	0.59	0.71	0.11
80 trial c	3.01	2.99	1.08	0.44	0.13	0.83	0.73	0.23	0.60	0.66	0.16
80	5.00	5.00	1.12	0.48	0.21	0.86	0.75	0.34	0.62	0.71	0.24
100	3.09	3.29	1.26	0.59	0.17	0.97	0.92	0.29	0.70	0.87	0.20

As shown in Figure 4.30, approximately 62% of the mass dissolved with washing 3 times in 0.01 M NaOH. An additional 9% of the mass dissolved after leaching for 24 h in 3 M NaOH at 80°C.
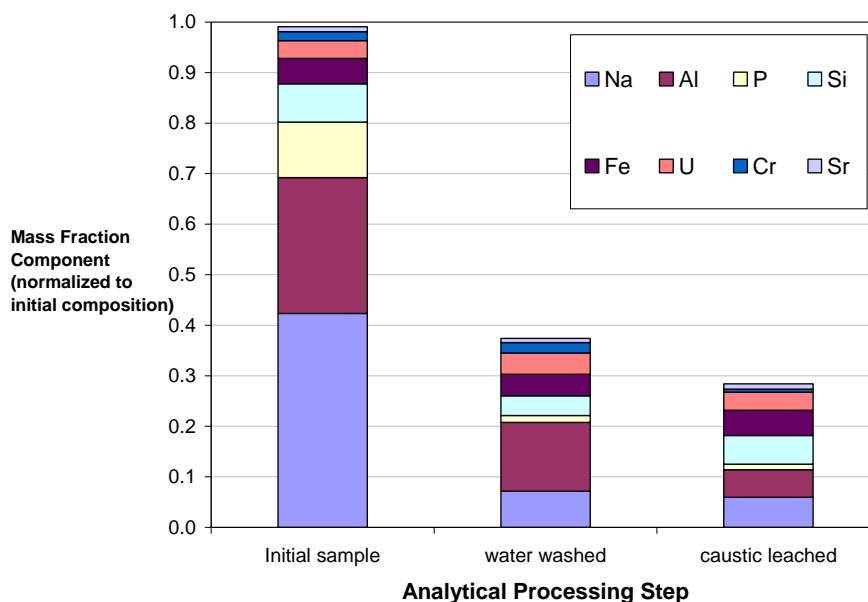
Figure 4.30. Group 2 Bi-Phosphate Saltcake Reduction in Solid Mass with Water Washing and Caustic Leaching

The FTIR spectra of the Group 2 solids before and after caustic leaching (3 M NaOH, 80°C, 24 h) were measured using a diamond ATR sample cell (Figure 4.31).[a] As discussed in Section 4.2.7, the FTIR spectrum of the washed solids before leaching can mostly be explained by the presence of gibbsite, nitrate cancrinite, amorphous $FePO_4 \cdot xH_2O$, and (perhaps) $Na[UO_2PO_4] \cdot 3H_2O$. The FTIR spectrum of the

---

(a) FTIR spectra presented for indication only.

leached Group 2 solids is distinctly different from that for the solids before leaching. The FTIR spectra clearly show the removal of gibbsite from the solids as evidenced by the disappearance of the characteristic hydroxyl bands in the range 3375 to 3650 cm^{-1}. The elimination of bands due to amorphous (or crystalline) $FePO_4 \cdot \times H_2O$ would also be expected upon caustic leaching because of metathesis to $Fe(OH)_3$ and sodium phosphate. The FTIR spectrum supports this by a large reduction in the relative intensity of the phosphate bands in the range 925 to 1150 cm^{-1}. Beyond that, interpreting the FTIR spectrum of the leached solids is somewhat difficult. One surprising observation is the apparent drastic reduction in the amount of nitrate cancrinite present, which is indicated by the nitrate band at 1422 cm^{-1} being very weak compared to the other bands observed in the spectrum of the leached solids. Thus, it appears that the nitrate cancrinite is converted to some other aluminosilicate form during the caustic leaching process. The nature of the resulting aluminosilicate species is not obvious from the FTIR spectrum, but the XRD analysis confirms the formation of a nitrate-free cancrinite phase (*vide infra*). A cancrinite phase is also supported by the Al:Si molar ratio of 1.0.
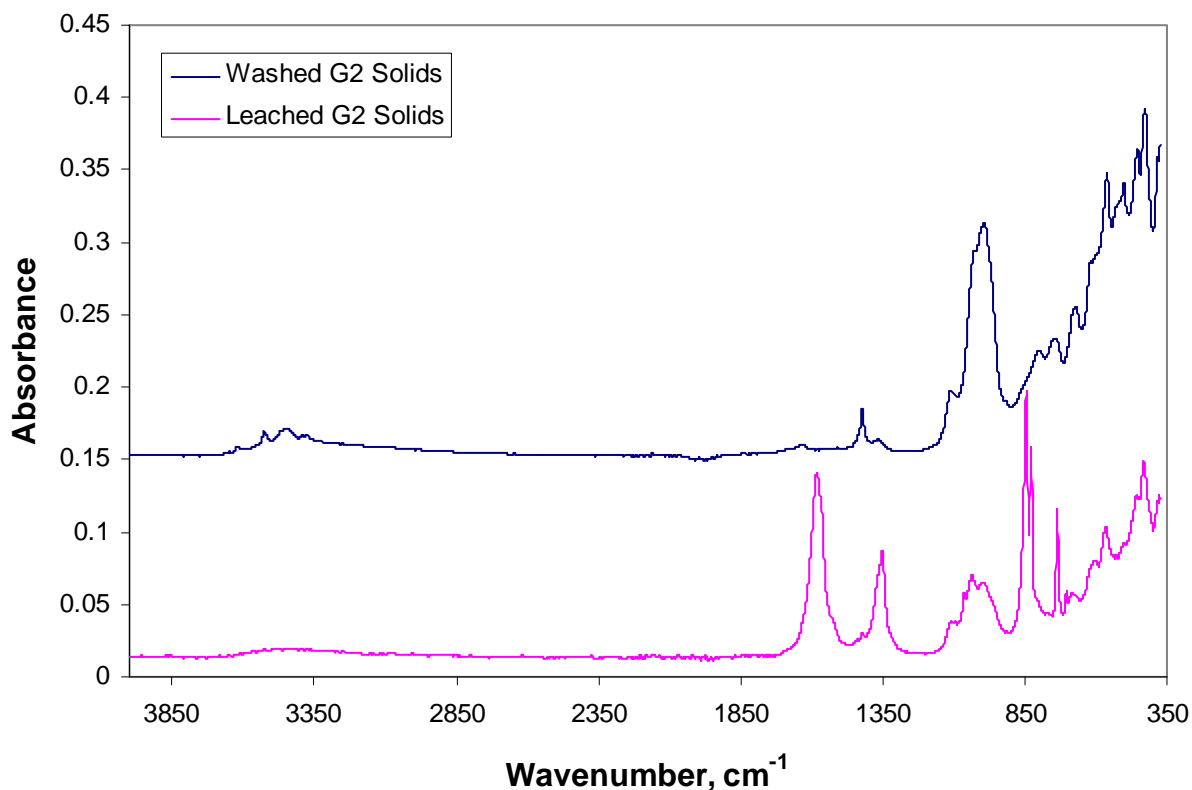
Figure 4.31. FTIR Spectra of the Group 2 Solids Before and After Leaching in 3 M NaOH at 80°C for 24 h

The FTIR examination of the leached Group 2 solids does provide insight into the reason for the low removal of P for this waste group compared to the Group 1 material. Careful examination of the FTIR spectrum indicates bands at 565, 602, and 1034 cm^{-1}, which can be attributed to hydroxyapatite. The corresponding bands measured for a pure sample of hydroxyapatite were at 564, 601, and 1030 cm^{-1}. Furthermore, an examination of the elemental composition of the leached Group 2 solids (Table 4.14) corroborates this conclusion. The measured P/Ca molar ratio was 0.61, which compares very well with the expected P/Ca molar ratio of 0.60 for $Ca_5(OH)(PO_4)_3$.

Heating of the Group 2 solids would not change their elemental composition but rather would alter their chemical speciation. Thermal gravimetric analysis (TGA) was performed for four Group 2 samples. The solids were washed three times with 0.01$\underline{M}$ NaOH and then three times in water; after each washing step the material was centrifuged and the wash liquid decanted. The sample would then be best represented by data in the middle column of Table 4.14 or Figure 4.30, wherein the aluminum and iron contents were about 15 and 5%, respectively.

Thermogravametric analysis of the washed Group 2 solids before caustic leaching also provides some insight into the leaching behavior for these solids. TGA data were acquired for four Group 2 tank waste samples, while scanning to a temperature of 830°C. In all cases, the major mass loss component/heat response in the TGA/DTA (DTA = differential thermal analysis) scans, respectively were directly consistent with gibbsite and a small quantity of goethite and magnetite. As determined by the TGA, the Group 2 tank waste solids contained 8.0 wt% Al as gibbsite. Because the known Al content in the Group 2 solids was about 15% by ICP analysis (Table 4.14), the TGA predicts that ~53% (i.e., 8 ÷ 15) of the Al should be readily removed during caustic leaching of the Group 2 solids. Leaching of the Group 2 tank waste indeed removed 61% of the aluminum as is indicated in Table 4.14.

TGA suggests that iron is in equilibrium with at least 3 phases in the Group 2 solids—goethite, magnetite, and ferric hydroxide. A conservative (i.e., maximum) estimate for the mass fraction contributed to the washed Group 2 solids from these three species is 7.6 wt %. This corresponds to 4.2 wt% Fe, which is in reasonable agreement with the value of 4.7 wt% measured by ICP-OES (Table 4.14). Iron present as hematite, iron silicate or aluminate phases could account for extra mass (an additional 0.5 wt% of Fe) present in the solids, but none of these phases would be expected to be leached from the tank-waste under caustic conditions, or identified by the thermal methods used here.

4.4.6.3 Particle-Size Distribution

PSD measurements were performed on the caustic-leached and washed Group 2 solids (sample ID 549-G2-CL-PSD). Because the in-cell sonicator on the Hydro µP was not functional at the time of measurement for this sample, only data for measurement conditions 1 to 3 are available (Table 4.17). Two separate measurements, an initial and replicate, were run for this sample to assess reproducibility.

Table 4.17 and Table 4.18 show select cumulative undersize percentiles derived from initial and replicate PSD measurements, respectively, for the caustic-leached and washed Group 2 solids. Reproducibility between the initial and replicate runs was generally reasonable, with the exception of the d(90) values at pump speeds of 2000 and 3000 RPM. Both the initial and the replicate results for cumulative percent undersize show similar trends with respect to pump speed. First, d(10) values appear relatively insensitive to changes in pump speed. The d(50) values at 3000 and 2000 RPM are similar, but show a significant (>10%) increase at 4000 RPM. The d(90) shows progressive increases with increasing pumping rate, with a dramatic jump as speed is increased from 3000 to 4000 RPM.

Table 4.17. Initial Particle-Size Analysis Percentile Results for the Caustic-Leached and Washed Group 2 Solids (sample 549-G2-CL-PSD)

Measurement Condition	Pump Speed	Sonication	d(10) [μm]	d(50) [μm]	d(90) [μm]
1	3000	n/a	0.59	1.9	8.4
2	4000	n/a	0.61	3.5	64
3	2000	n/a	0.62	1.8	7.0

Table 4.18. Replicate Particle-Size Analysis Percentile Results for the Caustic-Leached and Washed Group 2 Solids (sample 549-G2-CL-PSD)

Measurement Condition	Pump Speed	Sonication	d(10) [μm]	d(50) [μm]	d(90) [μm]
1	3000	n/a	0.60	2.6	30
2	4000	n/a	0.66	4.8	70
3	2000	n/a	0.56	2.4	16

Figure 4.32 and Figure 4.33 show the initial and replicate PSD measurements, respectively, for the leached Group 2 solids. The PSD observed in the initial measurement spans from ~0.2 to 20 μm (at 3000 RPM) and exhibits a maximum population between 1 and 2 μm and a large shoulder population in the range 3 to 20 μm. The initial measured PSD at 2000 RPM compares well to that at 3000 RPM. A decrease in the relative population contribution of 10 to 20 μm indicates that particles in this size range might be difficult-to-suspend. At 4000 RPM, a large secondary peak spanning 20 to 200 μm and with a peak population at 60 μm is observed. This peak is likely composed of difficult-to-suspend particles. It should be noted that similar 20- to 200-μm peaks are observed at 4000 RPM in Group 1/2 mixed waste solids derived from CUF testing (see Section 5.5.3).

The replicate measurement shows a much broader PSD relative to the initial measurement. The relative volume contribution of 20 to 200 μm particles is increased at all pump speeds even though it has a similar size distribution to that observed in the initial measurement over 0.2 to 20 μm. Figure 4.34 compares the initial and replicate PSD measurements for sample 549-G2-CL-PSD at 3000 RPM. As indicated above, the distributions are similar with the exception of the secondary peak spanning 30 to 200 μm in the replicate sample. This peak appears to correspond to the same species of particles yielding the secondary 20- to 200-μm peak observed at 4000 RPM during the initial measurement. The contribution for particles in this upper range decreases with decreasing flow (i.e., at 2000 RPM, Figure 4.33), supporting the supposition that the particles making up this peak are difficult to suspend. It is not known why the replicate measurement shows these 20- to 200-μm particles at all flows; however, it is possible that the second sampling of the sample vial containing 549-G2-CL-PSD solids yielded an increased volume of large particles relative to the first.
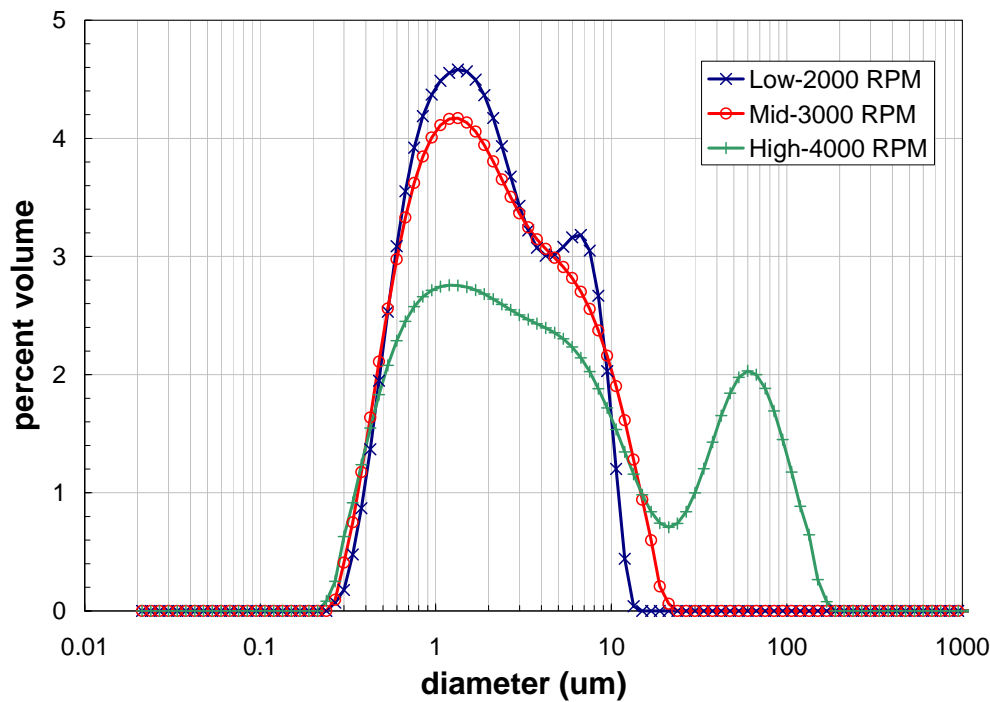
Figure 4.32. Volume Distribution Result for the Caustic-Leached and Washed Group 2 Solids (sample 549-G2-CL-PSD) as a Function of Pump Speed (initial measurement)
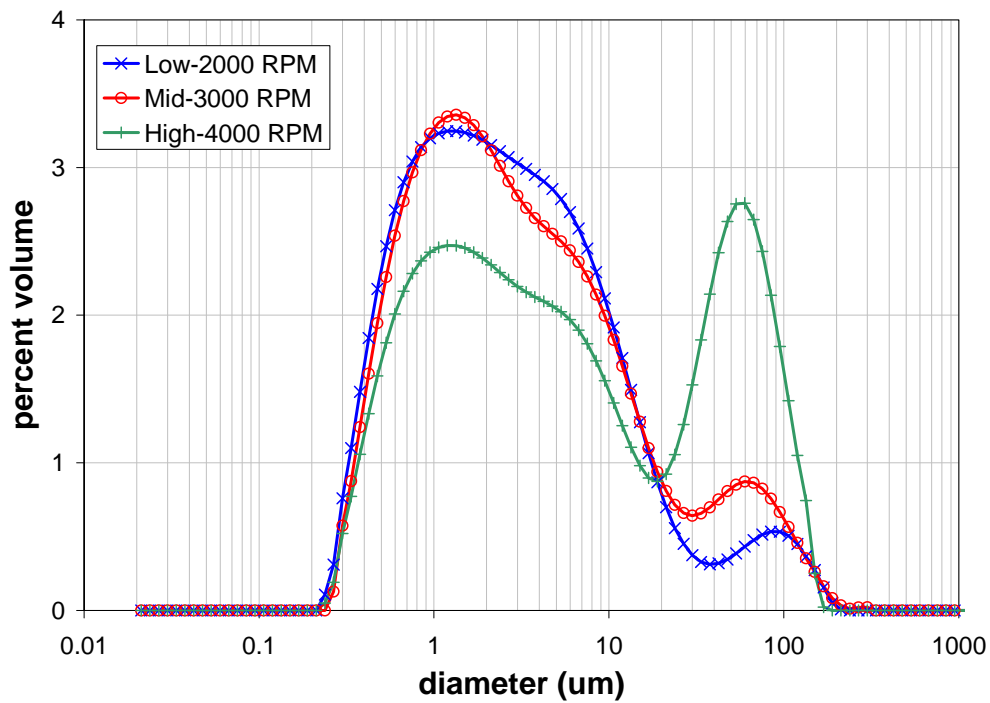
Figure 4.33. Volume Distribution Result for the Caustic-Leached and Washed Group 2 Solids (sample 549-G2-CL-PSD) as a Function of Pump Speed (replicate measurement)
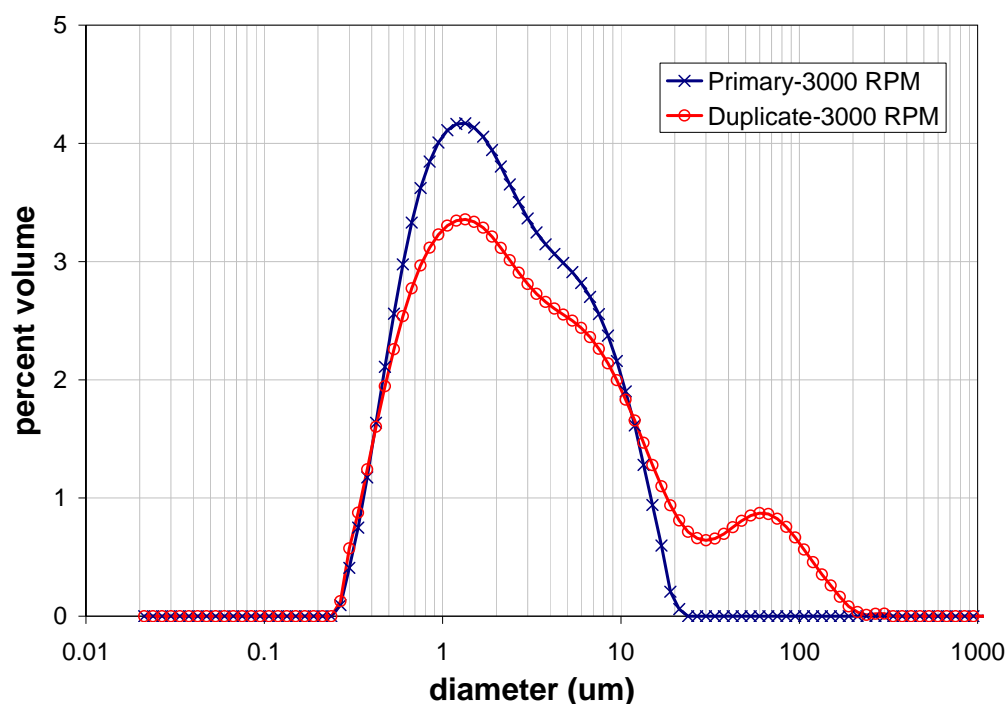
Figure 4.34. Comparison of Initial and Replicate PSD Measurements for the Caustic-Leached and Washed Group 2 Solids

Table 4.19 shows the relative percent difference (RPD) between initial and replicate cumulative undersize percentiles. The d(10) values compare well, typically being within 10%. Both d(50) and d(90) values show significant differences, with RPDs greater than 10%. It should be noted that the large RPDs for d(50) and d(90) result from the significantly higher fraction of 20- to 200-µm particles observed in the replicate measurement PSD. This is illustrated by the reasonable (~10%) comparison of initial and replicate d(90)s at 4000 RPM, where both samples exhibit a suspension of 20- to 200-µm particles. Overall, the initial and replicate RPD calculations indicate a difference in sub-sampling of the material for the PSD measurements.

Table 4.19. Relative Percent Difference Between the Initial and Replicate PSD Percentile Results for Sample 549-G2-CL-PSD

Measurement Condition	Pump Speed	Relative % Difference		
		d(10) [µm]	d(50) [µm]	d(90) [µm]
1	3000	1.3	34	260
2	4000	8.3	38	11
3	2000	10	34	130

The influence of caustic-leaching and washing of the Group 2 solids can be evaluated by comparing PSDs for the source material (i.e., that for initial characterization sample TI517-G2-S-WL-PSD) to the caustic-leached and washed Group 2 Parametric PSD sample (549-G2-CL-PSD). The PSD for the primary initial

characterization sample and initial parametric testing measurement are used for this comparison. Since only pre-sonic PSD measurements are available for sample 549-G2-CL-PSD, comparisons are made at measurement condition 1 (3000 RPM, before sonication). Table 4.20 and Figure 4.35 show the changes that occur to the Group 2 solids PSD as a result of caustic-leaching and washing. Based on Figure 4.35, the caustic-leaching and washing operations appear to reduce the fractional contribution of 2- to 20-μm particles while increasing the fractional contribution of 0.2- to 2-μm particles. The overall result is a reduction in particle size, likely as a result of either dissolution of material from the surface of particles or breakage of agglomerates. The reported cumulative percent undersize diameters in Table 4.20 confirm a decrease in particle size upon caustic leaching of the Group 2 solids.

Table 4.20. Cumulative Undersize Percentiles Showing the Influence of Caustic-Leaching and Washing on the PSD of Group 2 Solids at Measurement Condition 1: 3000 RPM, Before Sonication

Sample	d(10) [μm]	d(50) [μm]	d(90) [μm]
Group 2 Initial Characterization (TI517-G2-S-WL-PSD-1)	0.86	3.2	11
Group 2 Caustic-Leached and Washed (549-G2-CL-PSD)	0.59	1.9	8.4
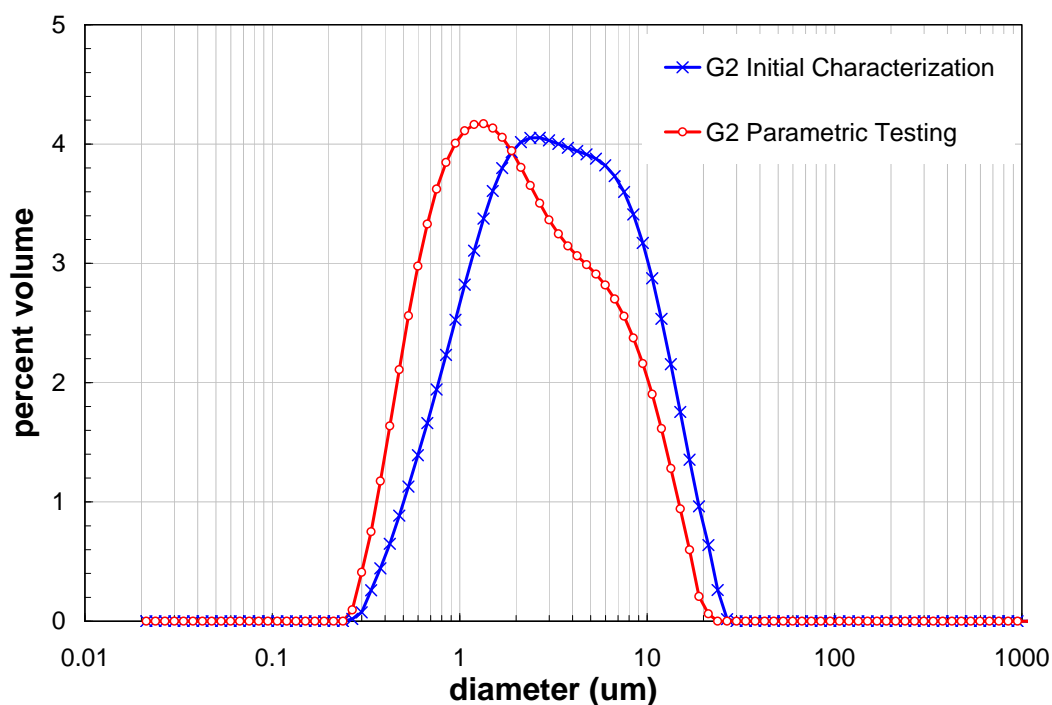
Figure 4.35. Influence of Caustic-Leaching and Washing on Group 2 Waste Solids PSD. All PSDs taken at measurement condition 1: 3000 RPM, before sonication.

4.4.6.4 Crystal Form and Habit

The following sections summarize the mineral-phase evaluation of the leached and washed solids.

4.4.6.5 XRD

The XRD pattern of the leached and washed solids is provided in Figure 4.36a; the background-subtracted XRD pattern with stick-figure phase identification is shown in Figure 4.36b.

Rutile, TiO_2, was used as an internal standard for 2-theta calibration. Identification was done on 2-theta calibrated data. Four crystalline phases were positively identified. These included Cancrinite [$Na_{7.14}Al_6Si_{7.08}O_{26.73}(H_2O)_{4.87}$, crystal density 2.375 g/cm^3, JADE Version 8.0, calculated value] and clarkeite [$Na(UO_2)O(OH)$, crystal density 6.792 g/cm^3, JADE Version 8.0, calculated value], which are both excellent matches to the observed data. Uranium dioxide (UO_2, crystal density 10.96 g/cm^3, CRC 1978) is a good match to the data; its strongest peak is overlapped by clarkeite, but two isolated confirming peaks in the observed data confirm the identification. Iron hydroxide oxide [$Fe_{1.833}(OH)_{0.5}O_{2.5}$, crystal density 4.981 g/cm^3, JADE Version 8.0, calculated value] is a fair match; its strongest peak is partially overlapped by clarkeite, and three other peaks occur on the shoulders of other observed peaks.

Amorphous material accounts for a significant amount of the leached Group 2 solids, as indicated by the broad amorphous peak from about 10 to 30 degrees 2-theta in the raw data displayed in Figure 4.36a. This amorphous material cannot be characterized by XRD.

(a)

[080401b_TI579-G2-CL_TiO2_sum_raw.dif] Log# 033108b-j, SCAN: 5.0/65.0/0.02/2(sec), Cu, I(max)=11394, 08/14/08 08:53a

(b)

[080401b_TI579-G2-CL_TiO2_sum_bin.bin] Log# 033108b-j, SCAN: 5.0/65.0/0.02/2(sec), Cu, I(max)=8690, 08/14/08 08:57a

00-021-1276> Rutile - TiO_2

01-087-1714> Clarkeite - $Na((UO_2)O(OH))$

01-073-6315> Cancrinite - $Na_{7.14}Al_6Si_{7.08}O_{26.73}(H_2O)_{4.87}$

01-071-6417> Uranium - UO_2

01-076-0182> $Fe_{1.833}(OH)_{0.5}O_{2.5}$ - Iron Hydroxide Oxide
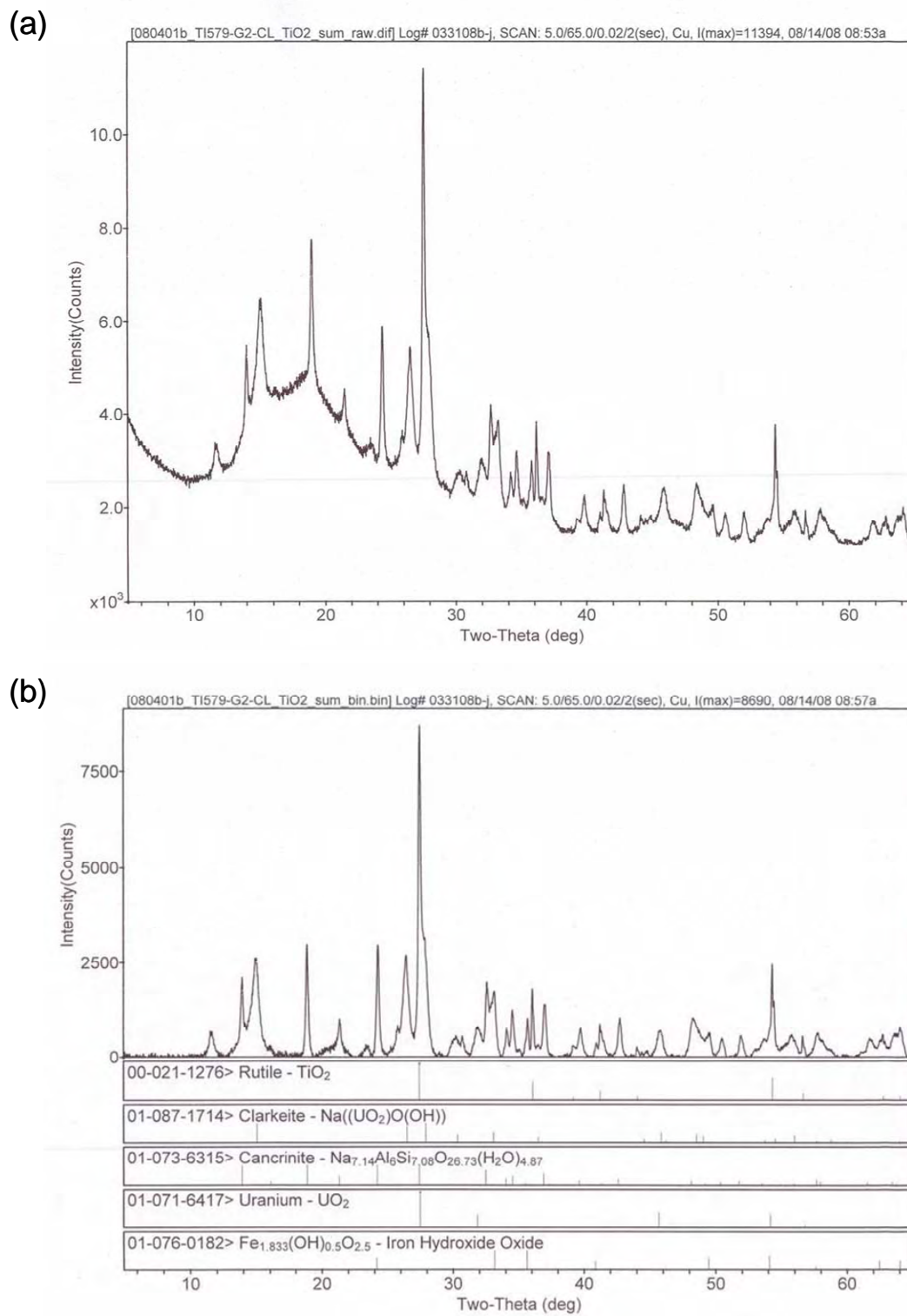
Figure 4.36. XRD Pattern of Caustic Leached Group 2 Bi-Phosphate Saltcake with Rutile (TiO_2) Internal Standard (a) Raw Data and (b) Background-Subtracted with Stick-Figure Peak Identification

4.51

4.4.6.5.1 SEM and TEM

Several SEM images are shown in Figure 4.37. The particles seen in these images are typically on the order of 5 to 60 µm, which is consistent with the PSD data reported above.
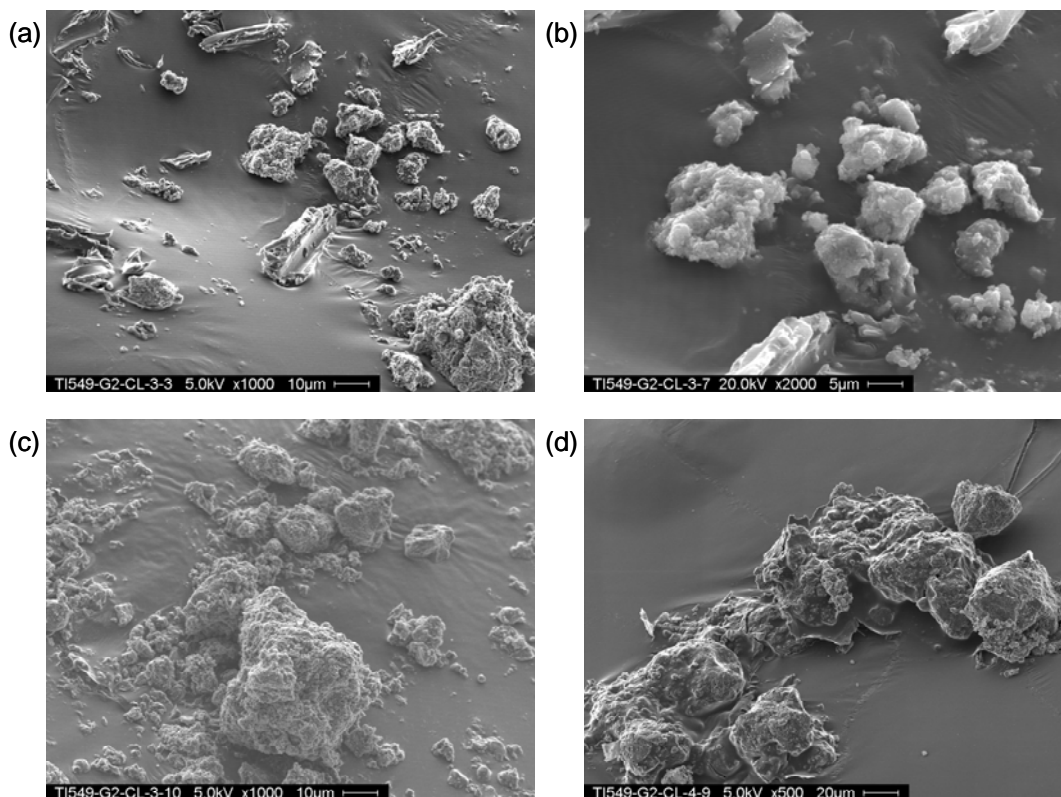
Figure 4.37. SEM Images of Group 2 Bi-Phosphate Saltcake Caustic Leached and Washed Solids
(a) 5 kV, 1000×; (b) 20 kV, 2000×; (c) 5 kV, 1000×; (d) 5 kV, 500×

Figure 4.38 and Figure 4.39 each show an SEM image along with EDS spectra of three different particles for each. The elemental analysis shows a large amount of oxygen and carbon, which is an artifact of the sample preparation (carbon is sputtered onto the sample to eliminate problems with charging). If this is removed, and the other constituents are normalized, the weight percentages shown in Table 4.21 for each analysis are obtained. It is interesting to note that there is a great deal of variability between particles. Whereas for the Group 1 leached sample, most of the particles had the same chemical makeup, the Group 2 leached solids consisted of particles with distinct compositions. The particle at spot 6 in Figure 4.38 and the particle at spot 3 in Figure 4.39 each consist of only Na, Al, and Si, which is consistent with the identification of cancrinite in the XRD analysis.

The remaining four particles that were examined by EDS and shown in these two figures were composed of several different elements. Two have very similar compositions to one another. The particle at spot 3 in Figure 4.38 and the particle at spot 2 in Figure 4.39 both have high concentrations of U (23.4%) and Fe (23.0%), along with about half as much Na (12.2%), Al (9.5%), and Ca (12.1%). Weight percents shown in parentheses are the averages of the two particles. The last two particles have high concentrations of Na, Al, Si (16 to 28%) as well as lower concentrations of U and Fe (7 to 14%).
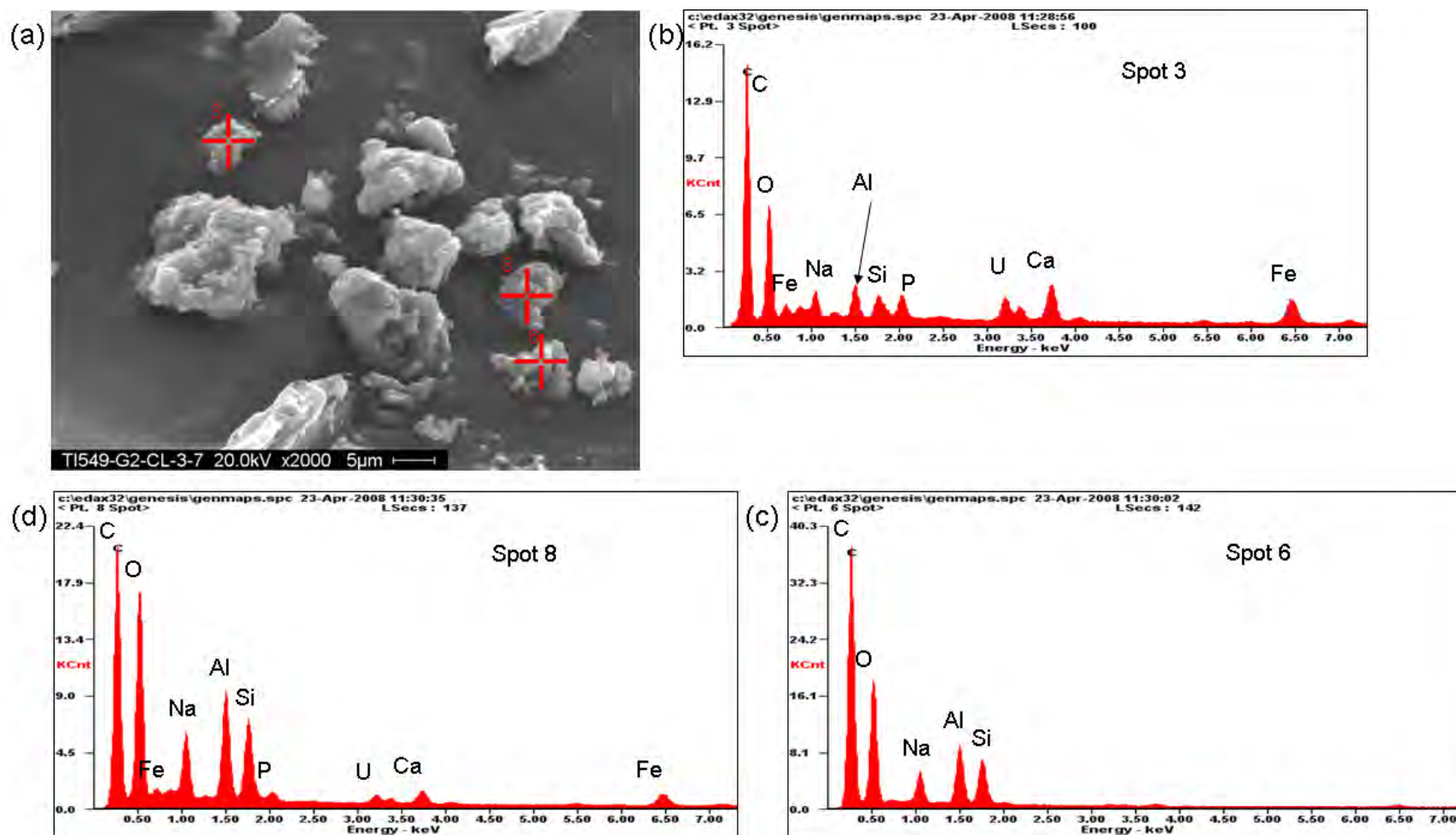
Figure 4.38. SEM Image of Group 2 Bi-Phosphate Saltcake Caustic Leached and Washed Solids with EDS Spectra (a) SEM Image; (b) EDS Spectra of Spot 3; (c) EDS Spectra of Spot 6; (d) EDS Spectra of Spot 8
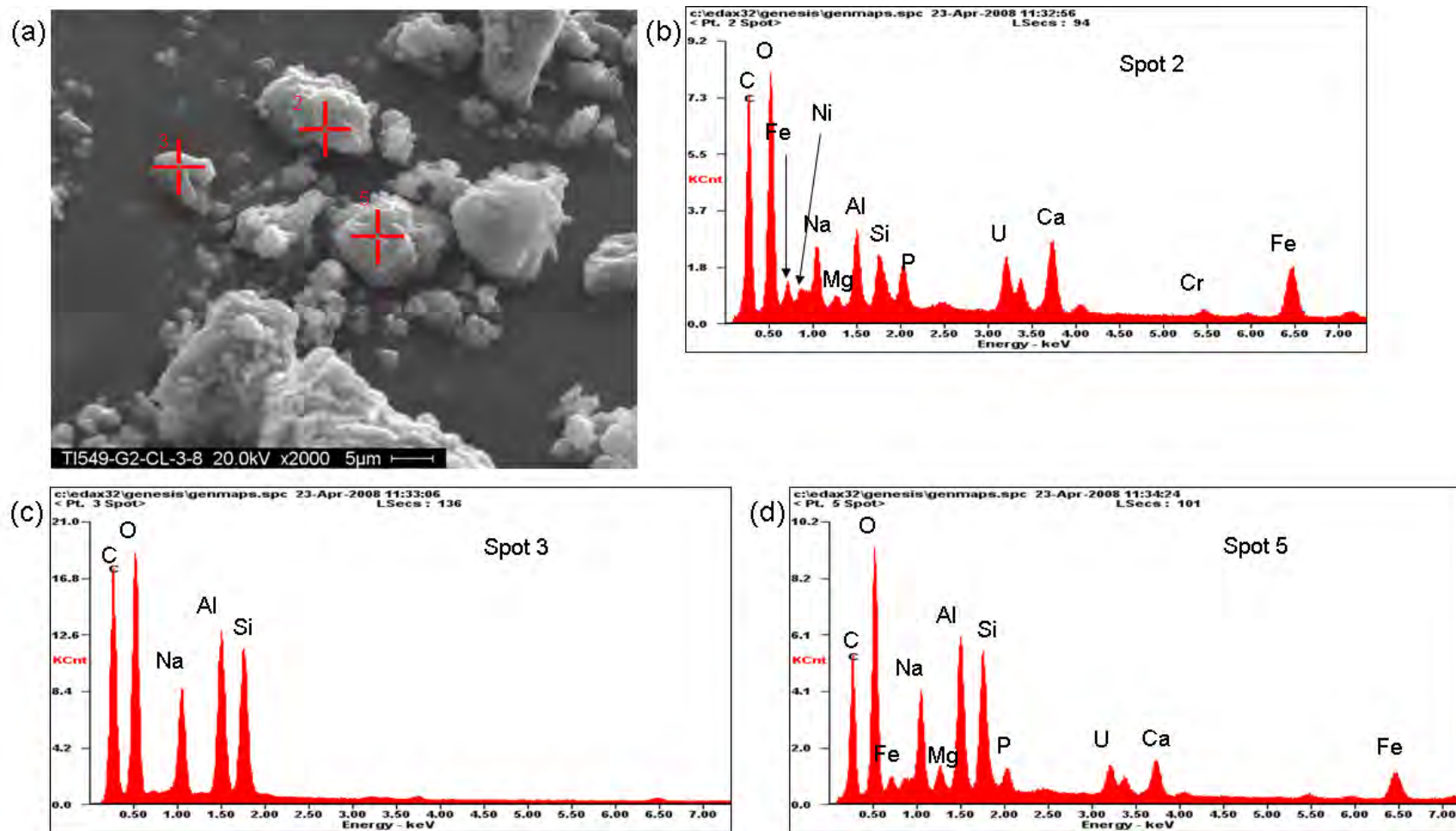
Figure 4.39. SEM Image of Group 2 Bi-Phosphate Saltcake Caustic Leached and Washed Solids with EDS Spectra (a) SEM Image; (b) EDS Spectra of Spot 2; (c) EDS Spectra of Spot 3; (d) EDS Spectra of Spot 5

Table 4.21. Normalized Weight Percents for Various Analytes Found by EDS of SEM Images for Figure 4.38 and Figure 4.39

| Element | Normalized Weight Percent | | | | | |
	Fig 4.38 Spot 3	Fig 4.38 Spot 6	Fig 4.38 Spot 8	Fig 4.39 Spot 2	Fig 4.39 Spot 3	Fig 4.39 Spot 5
Na	10.8	32.1	26.9	13.5	33.7	20.3
Mg	0	0	0	1.7	0	3.5
Al	9.0	38.4	27.6	10.0	34.5	20.8
Si	5.1	29.5	20.3	5.8	31.8	16.5
P	6.3	0	1.7	5.1	0	2.6
U	23.6	0	7.3	23.2	0	13.6
Ca	13.1	0	4.5	11.0	0	5.8
Cr	0	0	0	1.9	0	0
Fe	24.6	0	11.8	21.3	0	12.2
Ni	7.6	0	0	6.4	0	4.6

Figure 4.40 provides an SEM-EDS map of selected elements in the leached and washed solids. Al, Fe, and Si are present throughout most of the sample. However, there are several areas where these three elements are more concentrated, confirming the suspicion of the insoluble aluminum being an aluminosilicate. This would suggest that iron is also associated with the aluminosilicate phase. The largest particle containing these three elements can be seen in the upper-right-hand quadrant of the micrograph. It is also easy to see that in the corresponding area in the maps of Ca, U, P, and Na, these elements are either not present or present in very small quantities. A correlation can also be seen between calcium and uranium in several spots, where these two appear to be more highly concentrated. Phosphorus and sodium are fairly evenly distributed throughout the area.
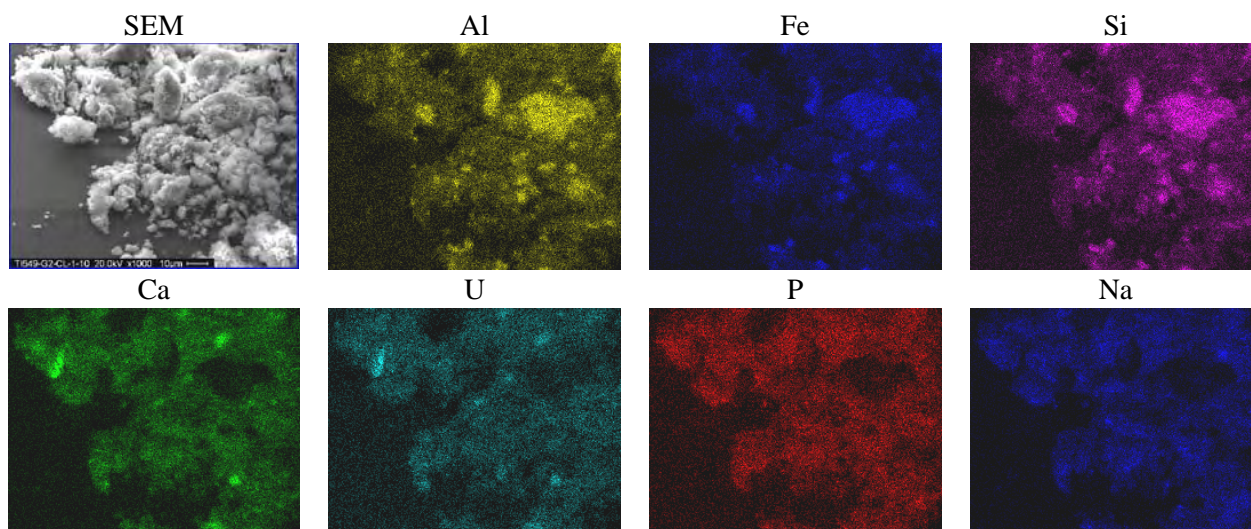
Figure 4.40. SEM-EDS Image of Caustic Leached Group 2 Bi-Phosphate Saltcake with Al, Fe, Si, Ca, U, P, and Na Maps

Figure 4.41 shows that the caustic leached solids consist of mixed phase agglomerates with a high surface area. Spherical and elongated particles are seen. The TEM images of the particles were used to estimate the size range of the particles. Using multiple images, measurements were made along the diagonals of the particles. These measurements were then listed and ordered. The data were fit to a $\log_e$–normal distribution. Figure 4.42 is a cumulative number distribution of agglomerates identified during STEM-HAADF imaging that describes the probability of particle sizes from the TEM images. The mathematical fit represents a $\log_e$-normal distribution. The average particle size was ~400 nm.
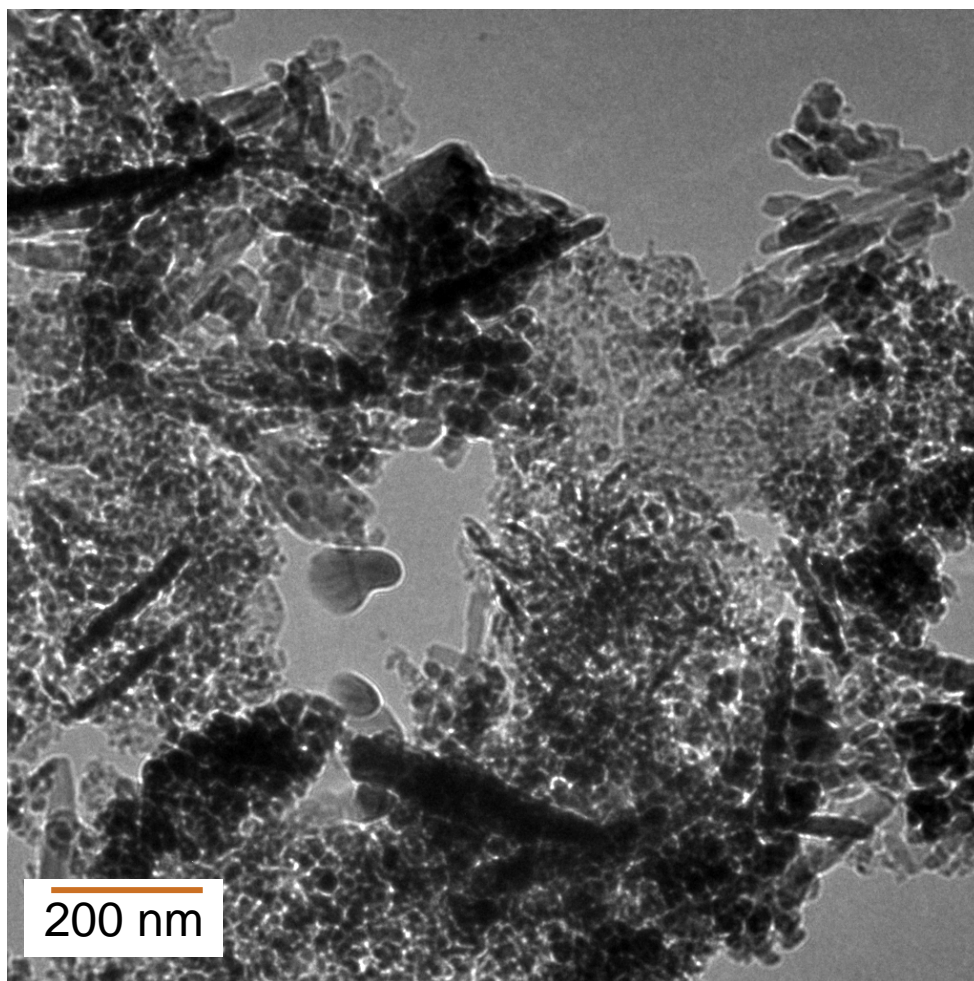
Figure 4.41. TEM Image of Caustic Leached Group 2 Bi-Phosphate Saltcake
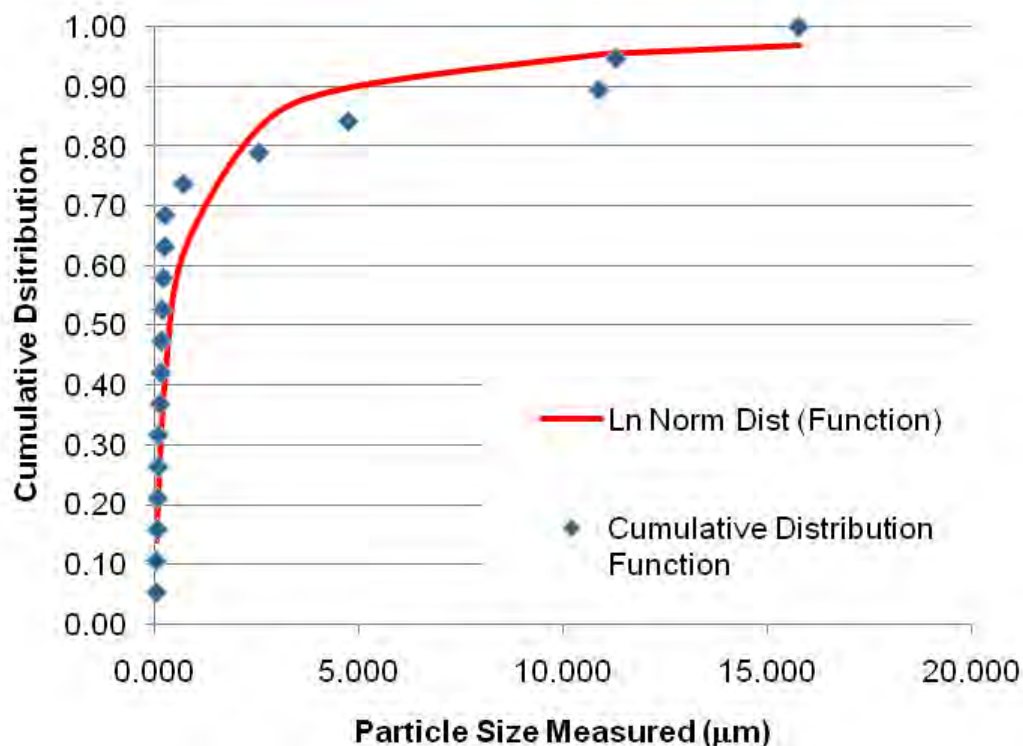
Figure 4.42. Cumulative Distribution Plot of Caustic Leached Group 2 Bi-Phosphate Saltcake and a Mathematical Fit to the Data

Figure 4.43 shows a typical TEM image with EDS analysis of several different regions in the sample. Area 3 is a uranium-rich area, also having several other elements, such as Mg, Na, Si, Al, P, Fe, Co, and Ni. In areas 1 and 2, uranium is not seen, but these other elements are. Point 1 consists of Si, Al, and Fe, which agrees with EDS data from SEM, showing that these three elements are associated in some way. The metals having the highest concentrations (as shown in Table 4.14) in the caustic leached solids are all seen with EDS analysis of the leached solids.

Figure 4.44 and the EDS analysis shows that there are particles in this agglomerate that consist only of iron, other particles that consist of uranium, and there is also an area that has calcium, strontium, and phosphorus. Figure 4.45 shows two different areas of the sample. In Figure 4.45 (a) and (b), an agglomerate that consists of uranium, iron, and manganese is shown. Although there is some overlap of the three elements, it appears that this is mostly three discrete phases. The darker spots in (a) correspond to Mn, which is surrounded in the top particle by iron. The lower half of the image shows an area of Mn surrounded by uranium. There are also solids in the middle and on the lower left of the image that appear to be a pure uranium phase. Figure 4.45(c) shows several needle-shaped crystals of a pure iron phase, surrounded by round areas of a pure uranium species.
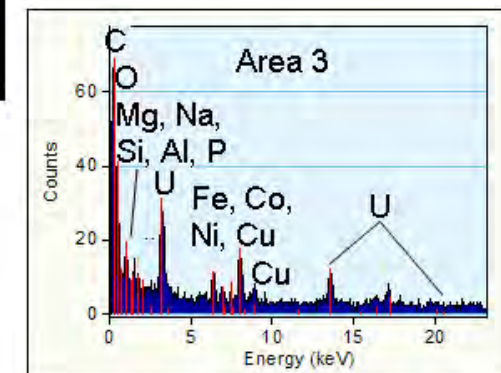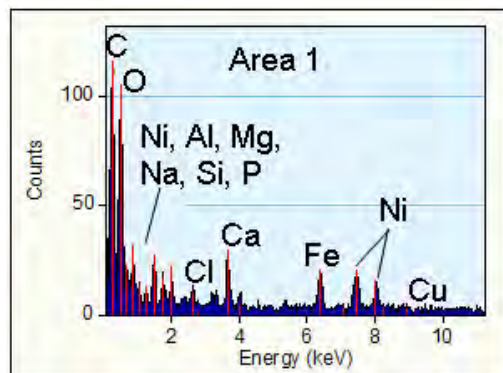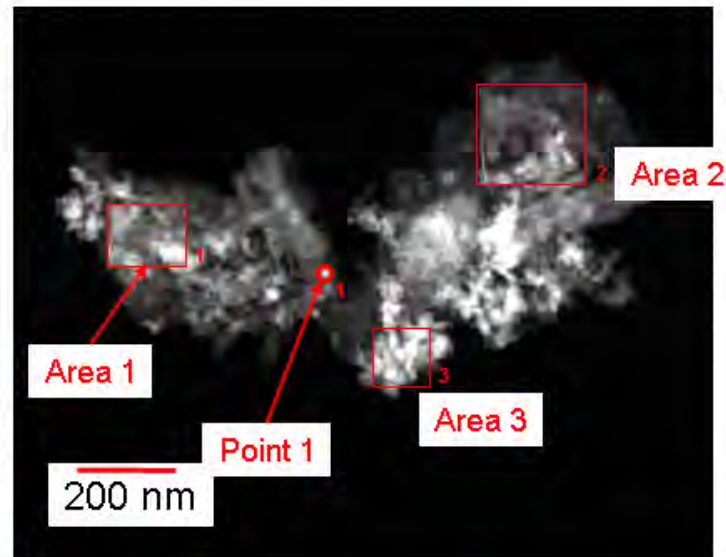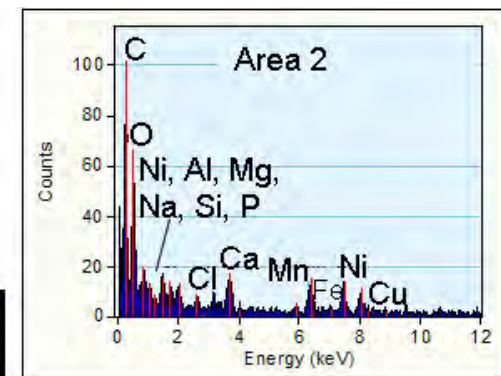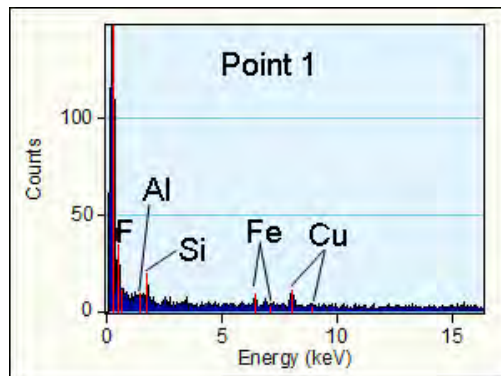
Figure 4.43. STEM-HAADF Image with EDS Analysis
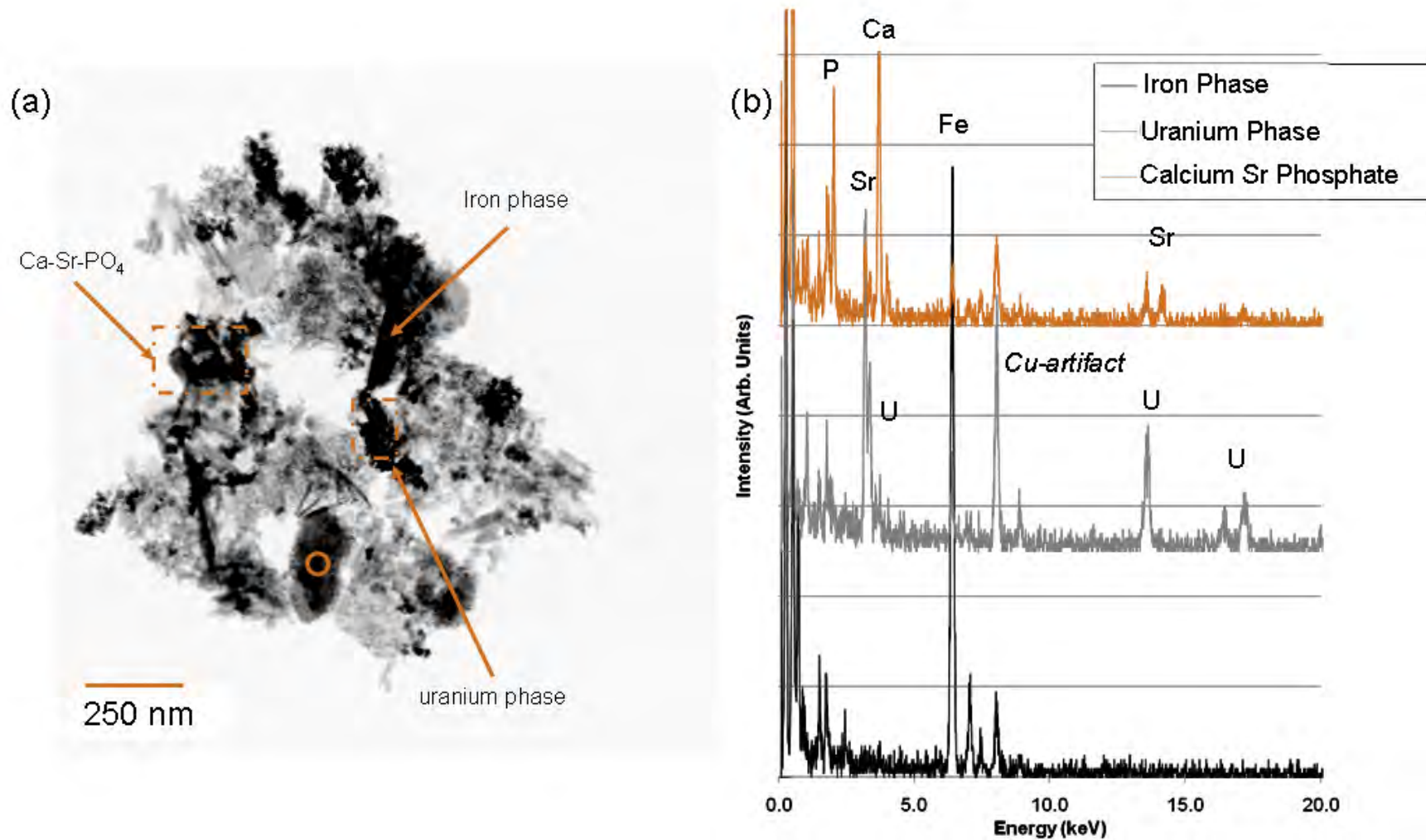
Figure 4.44. TEM Image with EDS Analysis Showing Uranium and Iron Rich Particles
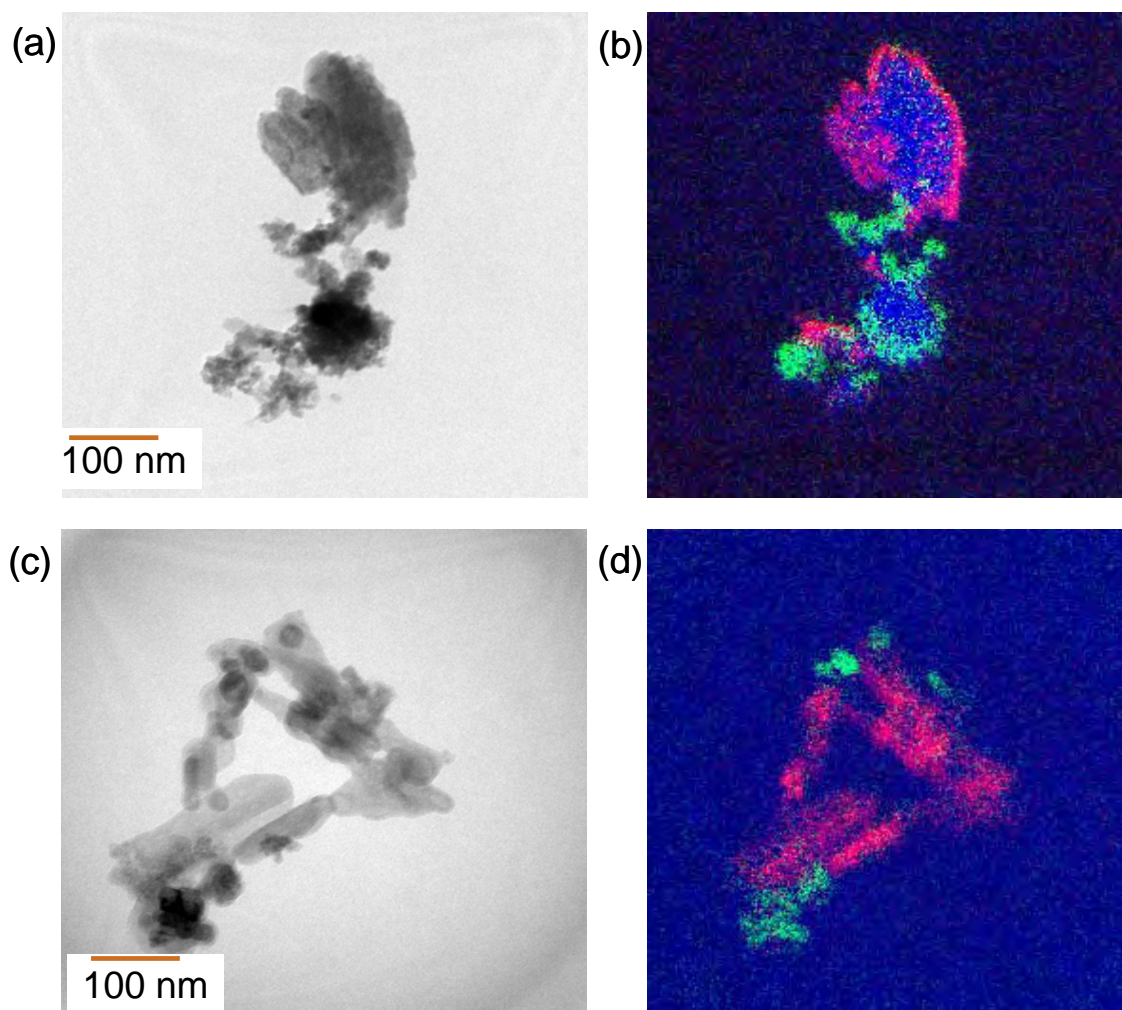
Figure 4.45. Energy Filtered TEM Images: (a) EFTEM Image Showing Particles Rich in U, Fe, and Mn; (b) EELS Elemental Mapping of (a); (c) EFTEM Image Showing Particles Rich in U and Fe; (d) EELS Elemental Mapping of (c). Color coding: U is green, Fe is red, and Mn is blue.

4.4.6.6 Surface Area by BET

A BET measurement was conducted on the caustic leached and washed solids, resulting in a surface area of 79.7 m^2/g. This shows an increase in relative surface area following caustic leaching from the value of 46.3 m^2/g found for the initial washed solids.

5.0 Group 1/2 CUF Filtration and Leach Testing and Results

This section describes the filtration/leaching tests[a] performed with a composite blend of the Group 1 bismuth phosphate sludge and the Group 2 bismuth phosphate saltcake (referred to here as the Group 1/2 sample). Descriptions of the experimental methods and analyses performed can be found in Appendix K.

5.1 Test Scheme

Figure 5.1 outlines the testing of the blended Group 1/2 sample.
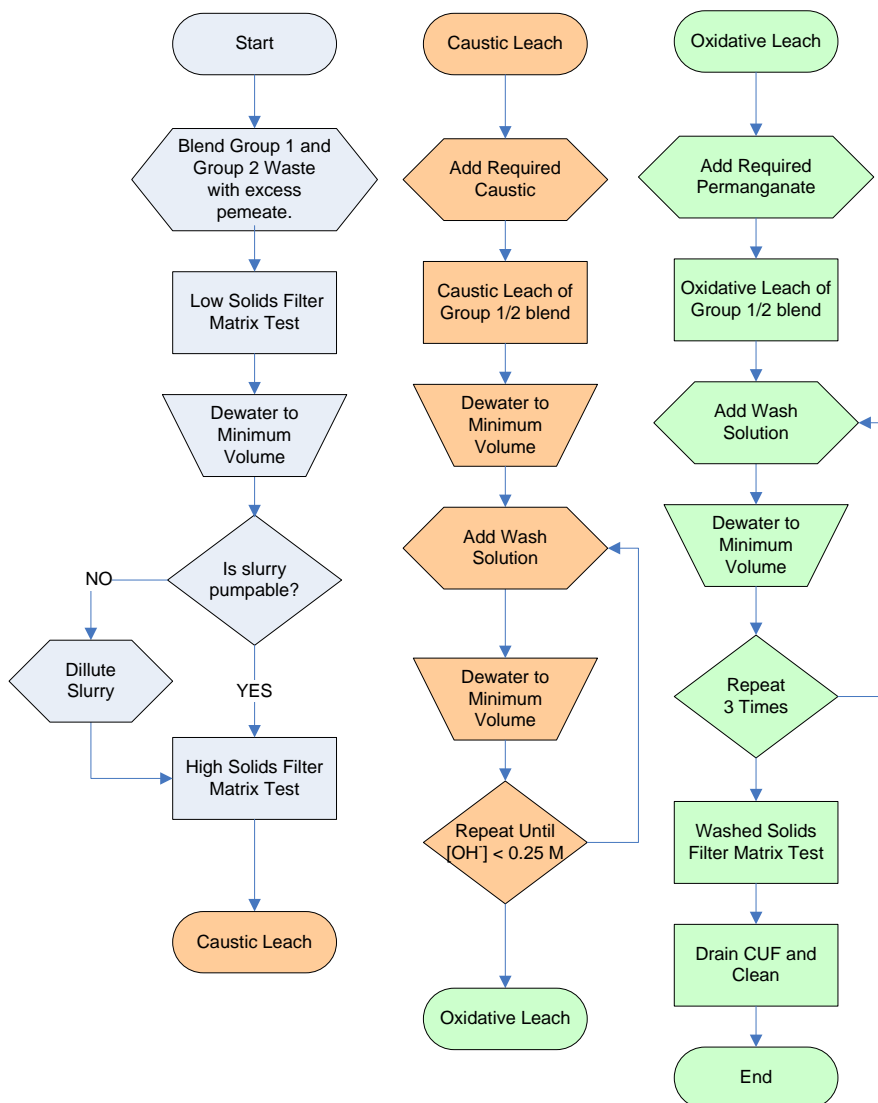
Figure 5.1. Group 1/2 Test Flowchart

(a) Conducted according to TI-RPP-WTP-572, *HLW Filtration and Caustic/Oxidative Leaching of Group 1/2 Composite Waste*, R Shimskey, January, 2008.

The goals of this test were to:

- Evaluate the filtration of the bismuth phosphate sludge and saltcake wastes blended together

- Evaluate the effectiveness of caustic leaching in removing aluminum, phosphorus, and chromium from the blended waste

- Evaluate the effectiveness of oxidative leaching (using sodium permanganate) in removing chromium from the blended waste

- Evaluate the filtration of the washed leached solids.

The initial slurry introduced to the CUF skid used the inventory of the Group 1 and 2 sludge samples diluted with excess Group 2 permeate to produce a composite slurry with a target UDS concentration of 9 wt%. The combined slurry was to contain 520 grams of UDS and an estimated volume of 4 L. A filter test matrix was performed on the diluted slurry waste as described in Appendix K, and then the material was to be dewatered to a target concentration of 20 wt% UDS, if possible. To achieve that, the slurry was to be dewatered to a target volume of 2 L. At this point, an abridged test matrix was performed to evaluate the change in the filtration behavior after concentrating the waste slurry.

Next, the waste slurry was removed from the CUF skid to be caustic leached. The slurry reservoir tank functioned as a batch reaction vessel, but first had to be drained and isolated from the skid's piping. Once the tank was isolated, the slurry was returned to the slurry reservoir tank and was blended with a caustic solution for the leaching. The amount of caustic added was based on a prediction[a] of 60% dissolution of aluminum in the Group 1 solids and 90% dissolution of aluminum in the Group 2 solids. Sufficient caustic was added to maintain aluminum solubility after cooling to ambient temperature. The amount of caustic added was determined using the gibbsite solubility data using an empirical model developed by C. Misra, as reported by Li et al. (2005). The empirical model used is shown in Equation 5.1 where concentrations of aluminum and sodium hydroxide are in moles/liter, and T is the absolute temperature of the solution in Kelvin.

$$\ln([Al]) = 5.71 - \frac{2486.70}{T} + \frac{33.71[NaOH]}{T} + \ln([NaOH])$$

(5.1)

The volume of the addition was established to include the volume of water representing the leaching solution and the volume increase predicted to occur from heating with steam injection in the UFP2 vessel. The leach solution was heated to 100°C over a 5.3-h interval and held at 100°C for 8 h. The slurry permeate was sampled during the heat ramp and temperature soak to evaluate the aluminum dissolution rate during these two periods. Afterwards, the solution was allowed to cool back to room temperature over a 12-h interval. At this point, the leached slurry solution in the slurry reservoir tank was allowed to enter the piping of the CUF skid, and it was dewatered to the minimum operating volume for the filtration skid.

(a) The dissolution factors were based on data assembled in report WTP-RPT-151 (GJ Lumetta and RT Hallen, Review *of Caustic Leaching Testing With Hanford Tank Sludges*). Results of parametric studies for the Group 1 and 2 composites were not available at this time.

Five equal volumes (1.2 L each) of caustic rinse solutions were then added to the leached solids slurry and dewatered each time. The NaOH concentration of each rinse solution was established to maintain sufficient free hydroxide in solution such that the aluminum concentration was always below saturation. The caustic concentration of each rinse solution was calculated by:

- Estimating the initial Al concentration of the caustic leachate using the assumptions of the Al leach factor stated above.

- Assuming perfect mixing, the addition of each rinse solution would decrease the aluminum concentration by 50%.

- The final free hydroxide concentration of the supernate needed to prevent Al precipitation at that concentration was calculated. This was done in the same manner that the targeted free hydroxide concentration was calculated for the caustic leachate solution—using reported Al/OH solubility data (Li et al. 2005) to ensure that sufficient hydroxide was present to prevent Al precipitation.

- The additional mass of hydroxide needed to be added to the supernate was then calculated and this amount of hydroxide was added to the rinse solution as NaOH.

As the Al concentration decreases, the free hydroxide concentration required to maintain solubility decreases as well, allowing more dilute rinse solutions to be used over time. After the fifth rinse, the free hydroxide level of the washed permeate was predicted to be below the 0.25 M level needed to perform oxidative leaching.

Once the slurry was rinsed after caustic leaching, it was removed from the CUF skid for oxidative leaching. As before, the waste solution was returned to the slurry reservoir tank once the tank was isolated from the filtration piping. At this point, a solution of 1 M sodium permanganate was added to the slurry. Sufficient sodium permanganate solution was added to achieve a 1:1 molar ratio of Mn to the predicted quantity of Cr in the waste solids. After the solution was added to the waste slurry, it was mixed for 6 hours at room temperature. Slurry permeate samples were periodically collected during this time to evaluate the chromium dissolution rate for the blended waste sample. After 6 hours, the oxidative leaching slurry was immediately rinsed with three equal-volume washes of 0.01 M NaOH solution. After dewatering the last rinse solution, a final test matrix was performed. The combined slurry was further dewatered to a minimum volume to increase the UDS concentration higher than that from the previous test and to obtain additional dewatering data for the leached waste. After dewatering the combined leached slurries from both tests, an abridged filter matrix test was performed on the dewatered slurry to compare how the filtration behavior changed after leaching.

Slurry and permeate samples were periodically collected to track the solid loading in the waste slurry and the chemical components of the slurry to perform mass balance calculations afterwards. This was done to evaluate the effectiveness of the process to separate LAW waste components from the HLW components in the waste sample. Chemical analyses were performed by the ASO, under the QA requirements discussed in Appendix D. All analyses performed by ASO were performed under Analytical Service Request (ASR) 8113; the analytical results are compiled in Appendix M.

5.2 *Initial Feed Characterization*

Figure 5.2 summarizes the preparation of the initial Group 1/2 feed composite. The low-solids slurry was composed of 2,161 grams of homogenized Group 1 slurry (TI508-G1-AR-J1 through -J7), 158 grams of Group 1 rinse solution (TI508-G1-Rinse), 881 grams of homogenized Group 2 slurry (TI517-G2-AR), 2,011 grams of Group 2 supernatant, and 33.2 grams of solid sodium hydroxide (98% NaOH). The mass of UDS present in the composite waste slurry was estimated to be 520 grams, based on the physical-property data reported in Table 3.2 for Group 1 and Table 4.2 for Group 2. After the slurry was blended in the slurry reservoir using the overhead mixer, the pump began circulating the slurry through the filter. Filtrate was then allowed to flow through the mass flow meter of CUF permeate piping. Once the measured density of the mass flow meter appeared stable, the back-pulse chamber was filled with permeate. After the back-pulse chamber and permeate piping were filled, an estimated 200 mL of slurry supernate was removed from the circulating slurry, which is referred to as the system permeate holdup volume.
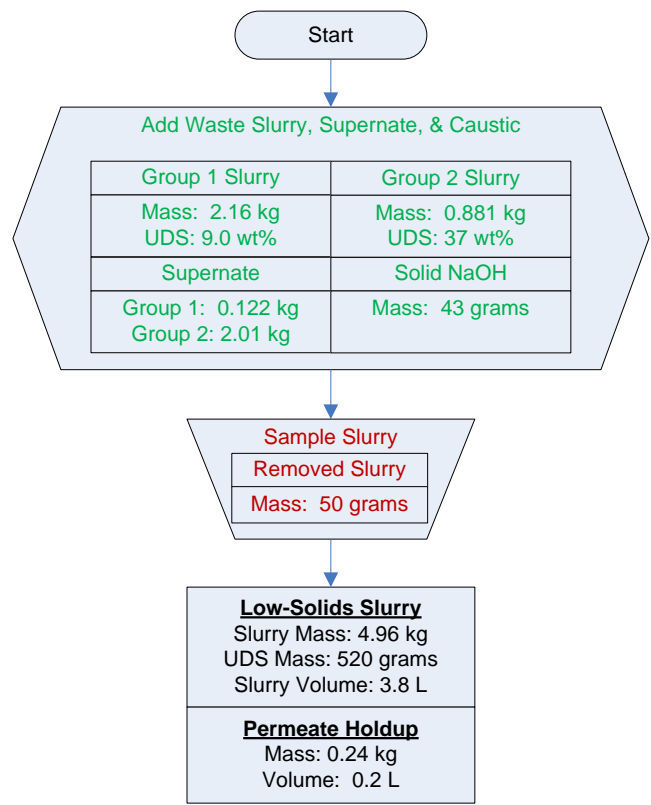
Figure 5.2. Flow Diagram of the Initial Feed Composite and Sampling
Note: Mass and volume values in figure are rounded to the nearest significant digit of accuracy.

After the slurry and permeate piping were filled, the circulating slurry was sampled for characterization. Physical-property measurements were performed on two samples collected in 10- to 15-mL glass centrifuge tubes that were allowed to settle for a minimum of 24 hours and then centrifuged for a minimum of 1 hour at 1000 G. The average results from the two samples are detailed in Table 5.1. The definition of each term in the table is:

- Slurry density: The measured density of the sampled circulating slurry using the net weight of the sample and the volume of the sample collected.

- Supernate density: The measured density of the decanted slurry supernate after centrifuging the sample at 1000 G for a minimum of 1 hour.

- Settled Solids: The solid volume fraction of the slurry after gravity settling for a minimum of 24 hours.

- Centrifuged UDS: The weight percent of UDS present in the centrifuged solids fraction of the slurry after decanting the supernatant liquid.

- Total Solids (TS): The TS fraction of the slurry.

- UDS: The UDS fraction of the slurry

- Dissolved Solids (DS): The DS fraction of the supernate. This is not the same as the DS of the slurry, which is equal to the difference between the TS and UDS measurements of the slurry.

Table 5.1. Low-Solids Slurry Physical-Properties Measurements

Slurry Density (g/mL)	1.30
Supernate Density (g/mL)	1.21
Settled Solids (Vol%)	58%
Centrifuged UDS (Wt%)	25%
Total Solids of the Slurry (Wt%)	33%
Dissolved Solids of the Supernate (Wt%)	28%
UDS of the Slurry (Wt%)	7.2%

The average measured UDS of the sampled slurry (7.2 wt%) was lower than the expected value of 10 to 11 wt% (0.52 kg ÷ 4.96 kg = 10.5 wt%). The difference between the two values was likely a result of grabbing a non-homogenous slurry sample from the slurry reservoir pot. After the test was completed, the mixer blade from the overhead mixer was found to have come off the mixing shaft. Erosive wear at the bottom of the blade caused failure of the crimp seal that attached the mixer blade to the shaft collar. Because of this, it cannot be assumed that the slurry was well mixed inside the slurry reservoir when the physical-property samples were collected.

An overall mass balance was performed on the composite slurry through the CUF testing. Using the composition of the Group 1 slurry in Section 3 and Group 2 slurry in Section 4, the initial composition of the blended slurry for the Group 1 and Group 2 slurry was calculated. Using a supernate sample analysis performed on the slurry to confirm that no dissolution of solids occurred during mixing, the composition of the slurry was calculated as shown in Table 5.2. Measurements of opportunistic analytes from the ICP-OES metals analysis of the slurry supernate is reported in
Table 5.3.

Table 5.2. Group 1/2 Low-Solids Slurry Total Inventory and Composition

	Slurry[a]	Liquid Fraction[b]		Solids Fraction[c]	
Mass (kg)	5.19	4.68		0.52	
Wt% of Slurry	100%	90.0%		10.0%	
Metal	**g**	**g**	**µg/mL**	**g**	**µg/g**
Al	5.0E+01	3.6E+00	9.4E+02	4.6E+01	8.9E+04
Bi	2.1E+01	< 1.E-2	< 4.E+0	2.1E+01	4.1E+04
Cr	5.6E+00	1.8E+00	4.8E+02	3.8E+00	7.2E+03
Fe	2.8E+01	2.0E-02	5.3E+00	2.8E+01	5.4E+04
Mn	4.2E-01	3.5E-04	9.0E-02	4.2E-01	8.1E+02
Na	5.2E+02	3.9E+02	1.0E+05	1.3E+02	2.5E+05
P	4.5E+01	4.0E+00	1.0E+03	4.1E+01	7.9E+04
S	1.9E+01	2.0E+01	5.3E+03	n/a[d]	n/a[d]
Si	1.9E+01	4.1E-02	1.1E+01	1.9E+01	3.6E+04
Sr	1.7E+00	8.8E-04	2.3E-01	1.7E+00	3.2E+03
U	7.2E+00	4.2E-01	1.1E+02	6.8E+00	1.3E+04
Radiochemical	**Slurry**	**Liquid Fraction**		**Solid Fraction**	
Isotopes	**mCi**	**mCi**	**mCi/mL**	**mCi**	**mCi/g**
Co-60	5.4E+00	< 2.E-1	< 4.E-5	5.4E+00	1.0E-02
Cs-137	9.5E+04	4.7E+04	1.2E+01	4.9E+04	9.4E+01
Eu-154	1.6E+01	< 8.E-1	< 2.E-4	1.6E+01	3.0E-02
Am-241	1.5E+02	< 8.E+0	< 2.E-3	1.5E+02	2.9E-01
Gross Alpha	2.9E+02	2.8E+00	7.3E-04	2.8E+02	5.5E-01
Gross Beta	2.3E+05	4.4E+04	1.1E+01	1.8E+05	3.5E+02
Sr-90	6.6E+04	3.7E+01	9.7E-03	6.6E+04	1.3E+02
Pu-239+240	2.0E+02	1.3E-01	3.2E-05	2.0E+02	3.8E-01
Pu-238	6.6E+00	7.3E-02	1.9E-05	6.6E+00	1.3E-02
Anions		**Liquid Fraction**		**Leached Solids Fraction**	
	µg/mL	**[M]**	**g**	**µg/g**	**g**
F	4.0E+03	2.1E-01	1.5E+01	2.6E+04	1.3E+01
C_2O_4	1.4E+03	1.6E-02	5.5E+00	< 4.E+1	< 2.E-2
NO_2	7.8E+03	1.7E-01	3.0E+01	1.2E+04	6.0E+00
NO_3	1.9E+05	3.1E+00	7.4E+02	2.9E+05	1.5E+02
SO_4	1.5E+04	1.5E-01	5.7E+01	2.4E+04	1.2E+01
PO_4	3.1E+03	3.3E-02	1.2E+01	9.2E+04	4.8E+01
OH	1.2E+03	6.9E-02	4.5E+00		

(a) Slurry mass components were calculated from characterization data (Sections 3 and 4) and the masses of materials that were added with simulant. Loss of mass from sampling was incorporated.
(b) Liquid fraction mass components were calculated using analytical results from supernate sample TI552-G6-A (ASO ID 08-01290) and the predicted mass of supernate in the system.
(c) Solids fraction mass components were calculated from the difference between the slurry component mass and liquid component mass fraction.
(d) Values for sulfur were calculated to be less than zero.

Table 5.3. Group 1/2 Low-Solids Supernate Opportunistic Composition

Opportunistic Analytes	Supernate Measured[a] μg/mL
Ag	<2.5E-1
As	<5.2E+0
Ba	[0.31]
Be	<6.3E-3
Ca	[2.8]
Ce	<1.2E+0
Co	<2.9E-1
Cu	<1.7E-1
Dy	<3.5E-1
Eu	<1.3E-1
La	<3.4E-1
Li	[1.0]
Mg	<2.8E-1
Mo	7.11
Nd	<6.5E-1
Pb	<3.9E+0
Pd	[1.2]
Rh	[2.1]
Ru	[1.1]
Sb	[4.35]
Se	[19]
Sn	[5.6]
Ta	<2.1E+0
Te	[5.15]
Th	[1.4]
Ti	[0.053]
Tl	<4.6E+0
V	[0.092]
W	[14]
Y	<5.3E-2

(a) Supernatant measured from, ASR 8113, sample TI552-G6-A (RPL ID 08-00218); reference date November 5, 2007.

Analyte uncertainties were typically within ±15%; results in brackets indicate that the analyte concentrations were greater than the method detection limit (MDL) and less than the estimated quantitation limit (EQL), and uncertainties were >15%.

Opportunistic analytes are reported for information only; quality control (QC) requirements did not apply to these analytes.

The influence of mixing Group 1 and Group 2 waste solids can be evaluated by comparing the PSDs for the source materials (i.e., those for initial characterization samples) to the initial PSD of the low-solids matrix slurry. Some caution must be used when interpreting these results as the initial characterization samples have not been subjected to the same level of shear that the CUF testing sample undergoes during circulation through the filtration loop.

Figure 5.3 shows the influence of mixing Group 1 and 2 solids in the CUF on the waste sample PSD; the PSD plots shown in the figure were determined after sonication. In overall behavior, the mixed waste PSD most resembles the Group 2 initial characterization sample PSD in that both samples are relatively unimodal. It is clear, however, that the mixed waste PSD is broader than that of the Group 2 source material. Specifically, the mixed Group 1/2 sample contains both particles larger than and smaller than those observed in the Group 2 initial characterization sample. Relative to the Group 1 source material, the mixed Group 1/2 CUF testing sample is composed of smaller sizes of particles/aggregates. Whereas Group 1 solids show particle contributions in the range of 20 to 50 µm, particles larger than 20 µm are absent from the CUF testing sample. It is possible that circulation of the Group 1/2 waste mixture in the CUF sheared apart the 20- to 50-µm particles characteristic of Group 1 waste solids. Likewise, this circulation-induced particle disruption could yield the increase in the relative contribution of submicron particles observed in the Group 1/2 CUF testing sample (relative to both Group 1 and Group 2 source material). Overall, the range of sizes observed in the Group 1/2 CUF testing sample is reasonable relative to the source material. However, the PSD for the mixed Group 1/2 solids indicates a shear breakage of particles as a result of circulation of the CUF slurry at a low-solids concentration.

Figure 5.4 shows the distribution of particle/aggregate sizes in the low solids slurry matrix before sonication. The graph indicates a broad distribution of particles ranging from ~0.3 to ~600 µm. The majority of particles fall between ~0.3 and ~200 µm, with a peak (maximum) population located between 1 and 2 µm and a secondary shoulder over the range of 4 to 20 µm. Distributions at 2000 and 3000 RPM are similar. At 4000 RPM, the appearance of a second population peak centered at ~60 µm confirms the presence of a larger, difficult-to-suspend, particle or agglomerate species.

Figure 5.5 shows changes that occur in the distribution of particles as a result of applied sonication. Sonication appears to reduce the relative population contribution of particles greater than 10 µm while increasing the relative contribution of particles from 3 to 10 µm. The likely mechanism for this change is sonic disruption of particle agglomerates greater than 10 µm. The similarity between the during- and after-sonication distributions suggests that the changes that occur during sonication are irreversible over the time frame of the post-sonication particle-size analyses (~15 minutes).
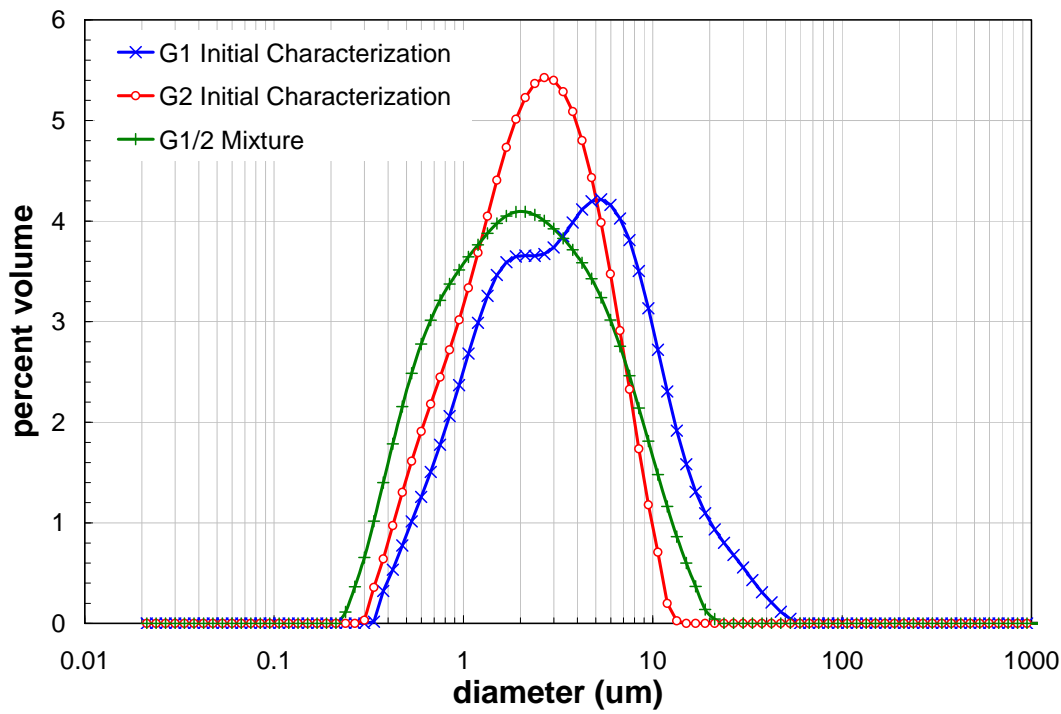
Figure 5.3. PSDs for the Individual Group 1 and 2 Composites and the Mixed Group 1/2 Composite (low solids slurry) After Sonication
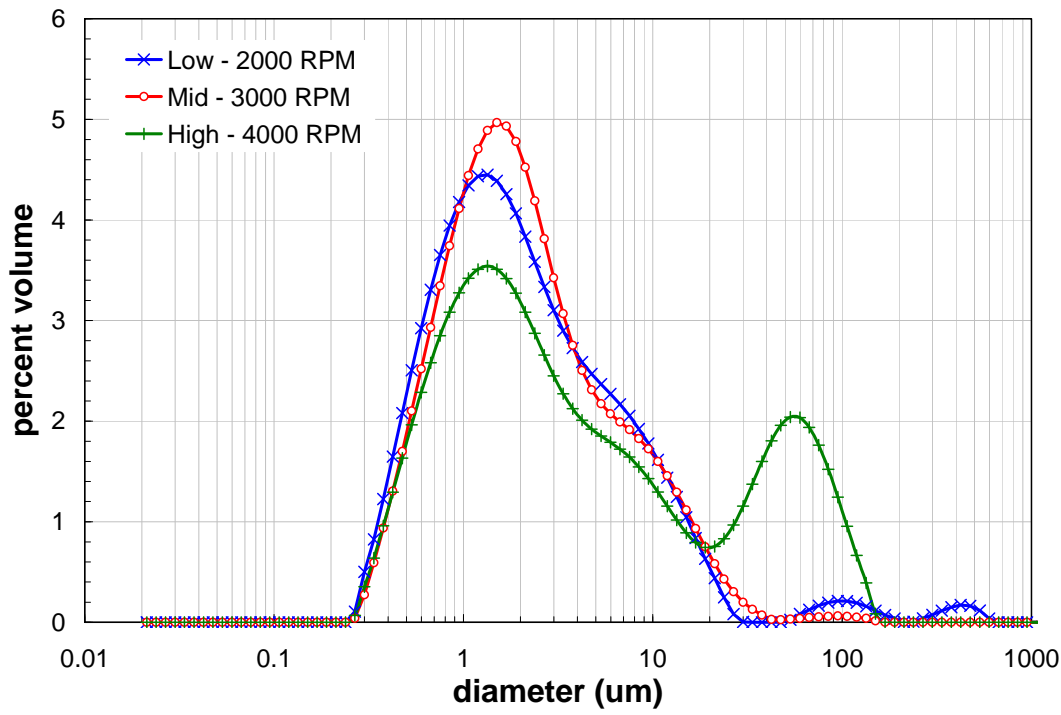
Figure 5.4. Low Solids Matrix Slurry PSD at Varying Pump Speeds Before Sonication
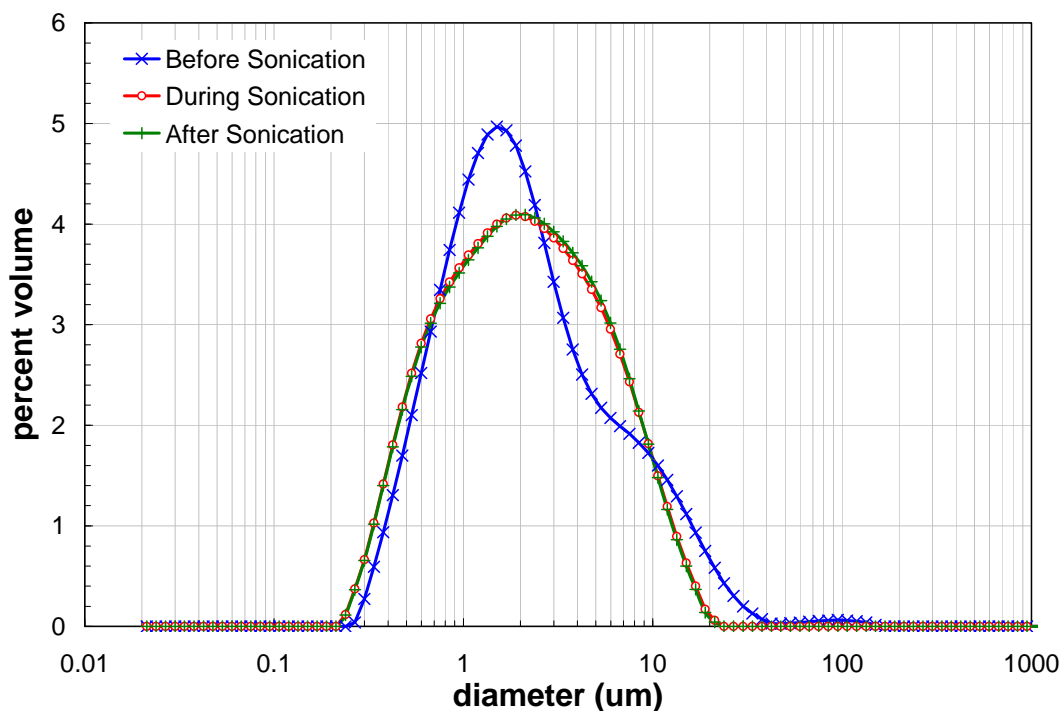
Figure 5.5. Low Solids Matrix Slurry PSD with Sonication

Figure 5.6 shows the results of flow curve testing for the low solids slurry. This slurry shows Newtonian behavior at all temperatures studied. There appears to be a slope transition near 500 s^{-1}, which could be indicative of alignment problems and/or Taylor vortex formation. The flow curves are free of hysteresis, which indicates that suspending phase evaporation is minor and/or does not affect the bulk rheological properties to a significant extent. Increased slurry temperature does not appear to change the rheological behavior between 25° and 40°C. A significant reduction in viscosity occurs between 40° and 60°C as evidenced by the decrease in the flow curve linear slope. The decrease in slurry viscosity with increasing temperature is consistent with decreased suspending phase viscosity.

Table 5.4 summarizes the best-fit and averaged Newtonian viscosities for the flow curve and constant-rotation data for the low-solids slurry. To avoid the inclusion of data influenced by Taylor Vortex formation, Newtonian model fits were restricted to 0 to 400 s^{-1}. All constant-rotation rate data correspond to 470 s^{-1}. Both constant-rotation and flow curve data measurements indicate a Newtonian viscosity for this slurry between 4.2 and 5.0 mPa·s at 25°C, 4.2 and 4.8 mPa·s at 40°C, and 3.0 and 3.1 mPa·s at 60°C. In general, the fitting results in Table 5.4 confirm the temperature trends discussed in the previous paragraph.
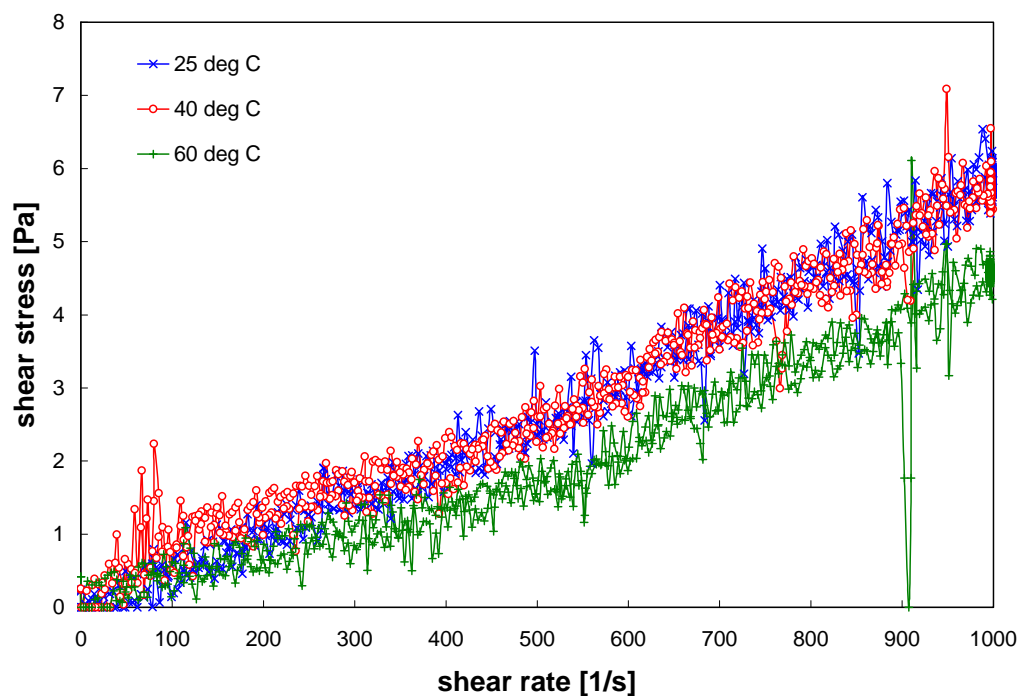
Figure 5.6. Flow Curve for the Group 1/2 CUF Low-Solids Slurry Sample at 25, 40, and 60°C

Table 5.4. Results of Fitting Analysis for Rheology of the Low-Solids Slurry

Model	Temperature [°C]	Newtonian Viscosity [mPa·s]	R
Flow Curve Fits (0 – 400 s⁻¹)	25 (1 of 2)	4.4	0.931
	25 (2 of 2)	5.0	0.945
	40	4.2	0.853
	60	3.0	0.817
Constant Rotation (470 s⁻¹)	25 (1 of 2)	4.2 ± 0.2	n/a
	25 (2 of 2)	4.8 ± 0.2	n/a
	40	4.8 ± 0.2	n/a
	60	3.1 ± 0.1	n/a

5.3 Filter Flux Testing and Dewatering of Waste Slurry

This section describes the filtration testing performed using the Group 1/2 composite before leaching, as shown in the left column of Figure 5.1. The following tests were performed.

- Initial clean water flux (CWF) testing to examine filter condition prior to testing.

- Filtration testing of the composite Group 1/2 waste slurry at a low-solids concentration as described in Section 5.2. Testing compares the effects of transmembrane pressure (TMP), axial velocity (AV), and operation time on filter flux.

- Dewatering of the waste slurry from 8 wt% UDS to 16% UDS at a constant TMP and AV to understand the impact of how solid concentration impacts filtration and compare to previous testing of other wastes.

- Filtration testing of the slurry at a high solid concentration. Like before, testing compares the effects of TMP, AV, and operation time on filter flux.

5.3.1 Initial Clean Water Flux Testing

Before loading waste into the CUF, a CWF test was performed with 0.01 M NaOH at three TMP conditions (10, 20, and 30 psid) and a constant AV of 11 ft/s. These tests were performed to establish the baseline condition of the filter before and after filtration of a composite waste group. In this case, the Group 1/2 initial CWF test followed the nitric acid cleaning of the filter after the Group 6/5 CUF testing according to TI-RPP-WTP-552, Rev. 0. The measured flux, shown in Figure 5.7, was somewhat less than the initial CWF test of the Group 6/5 waste (Table 5.5), but they were on the same order-of-magnitude. Two values were selected to characterize each TMP condition, one at the start and end of each condition, since a rapid decay of the flux was observed for these tests. The selected values were determined by using condition start and stop times recorded in TI-RPP-WTP-572, Rev. 0.
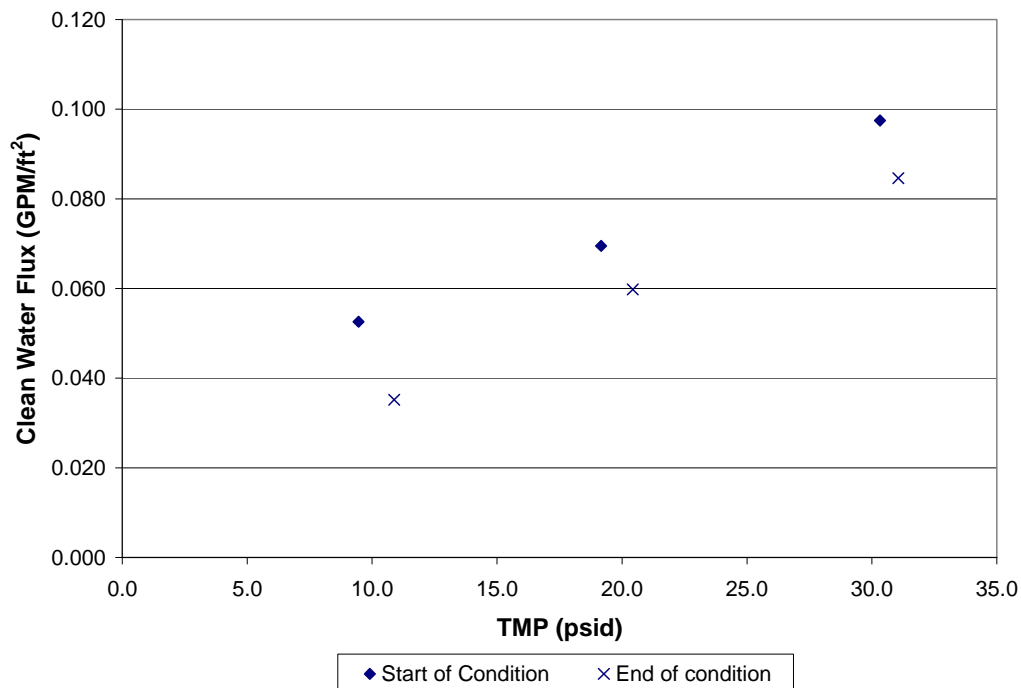
Figure 5.7. Initial CWF After Nitric Acid Cleaning from Group 6/5 Test

Table 5.5. Comparison of Initial CWF Between Group 1/2 and Group 6/5 Wastes

TMP	Group 1/2 Flux, Start of Condition (GPM/ft^2)	Group 1/2 Flux, End of Condition (GPM/ft^2)	Group 6/5 Flux, Start of Condition (GPM/ft^2)	Group 6/5 Flux, End of Condition (GPM/ft^2)
10	0.053	0.035	0.084	0.060
20	0.070	0.060	0.091	0.073
30	0.097	0.085	0.107	0.093
GPM = gallons per minute Performed at 25±2°C and using an AV of 11±0.2 ft/s. Filter flux data are temperature corrected, as described in Equation K.3 in Appendix K.				

5.3.2 Low-Solids Filter Matrix Testing (10 wt%)

Figure 5.8 shows that after sampling the slurry for physical characterization, the slurry mass inside the circulation loop was 4.96 kg, with 0.24 kg of supernate present inside the permeate piping and back pulse chamber. As discussed in the previous section, approximately 520 grams of UDS was to be present in the waste samples added. Using that for the UDS mass of the slurry, the UDS concentration of the slurry inside the circulation loop was estimated to be slightly above 10 wt%. This was the starting point for the low-solids filter matrix testing.
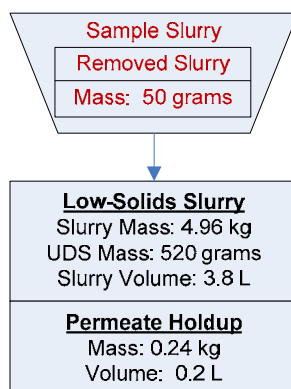
Figure 5.8. Flow Diagram of the Low-Solids Matrix Testing
Note: Mass and volume values in figure are rounded to the nearest significant digit of accuracy.

The low-solids filtration tests were performed according to the 11 test conditions described in Table K.1, Appendix K. The test conditions were performed sequentially with a minimum of 1 hour of constant recycle operation at each condition with back-pulsing between conditions. Table 5.6 provides a summary of the average operating conditions and flux for each condition, and Figure 5.10 compares the average AV and TMP for each test condition to the target value. These values were obtained by calculating the arithmetic mean of each value over the duration of the test condition. Flux data with respect to process time are given in Figure 5.9. As can be seen from the figure, the flux decayed rapidly within each test condition. Back-pulsing between conditions appears to temporarily reverse this effect. However, there appears to be a slight decrease trend in the filter flux over time even with back-pulsing.

To understand the individual impact of TMP and AV to filter flux, each average value from each test parameter was plotted against the average measured filter flux for each test (Figure 5.11 and Figure 5.12). To evaluate changes in the filter resistance during the test, the median operation time of each test (where t=0 hrs at the start of the test) was also plotted against the filter flux (Figure 5.13). The low-solids slurry exhibited a stronger dependence on TMP than AV over the range of conditions tested. The filter flux was found to be linearly proportional to TMP for the pressures tested (20 to 60 psid) while the AV was found to have no significant impact for the velocities tested (9 to 17 ft/s) at this slurry concentration. While the linear relationship to TMP implied that the slurry behaved according to the Darcy equation (Equation K-6, Appendix K), the R^2 correlation factor was only 0.68, implying that another parameter was impacting the filter flux. Examination of Figure 5.13 demonstrated a general decrease in the filter flux over the course of the test, and that filter resistance for the slurry was not at steady state. The linear correlation coefficient to process time was not very large (0.05).

Figure 5.14 and Figure 5.15 show data that have been further correlated and fitted to two empirical models combining the impact of each test parameter on the filter flux. From the fit equations, a strong dependence of filter flux on TMP was found with no significant impact from AV. As before, the filter flux was found to decrease with operation time, demonstrating that filter resistance was increasing over the course of the test. The linear model showed that 1 hour of operation the filter was equivalent to a decrease of ~1 psid of the TMP during this test. The exponential model predicted that doubling the operation time was equivalent to decreasing the TMP by ~10% during this test. While both modeling equations have high correlation factors, the use of this model should be limited to understanding how filter flux was influenced by TMP and operation time during this test. Because time was included in both models, offset parameters were developed, which limits the range that they could be applied. Both models do not predict a zero filter flux when the TMP is zero, which demonstrates that the input to these models must be bound by the range of TMP used in this filter test, shown in Table 5.6. The use of these models should also be limited to when the test matrix occurred because the filter resistance was not at steady state, and the parameters developed in these models would be expected to change past the 14-hour period that this model predicts.

Table 5.6. Average Operating Conditions and Filter Flux for the Low-Solids Matrix Test

Design Test Condition	Median Operation Time of Test[a] (hr)	Slurry Temp[b] (°C)	TMP[c] (psid)	Axial Velocity (ft/s)	Permeate Flowrate (mL/min)	Corrected Permeate Flux (GPM/ft^2)	Axial Pressure Drop[c] (psid/ft)
1	2.1	25.4	42.2	12.9	22.5	0.022	1.5
2	4.9	25.1	29.1	11.1	20.1	0.020	1.1
3	6.0	25.2	31.1	14.9	18.4	0.018	2.0
4	7.0	25.4	49.7	15.1	26.2	0.026	2.2
5	8.1	25.5	49.4	11.0	24.8	0.025	1.2
6	9.1	25.5	40.9	13.0	22.4	0.022	1.5
7	10.2	25.3	39.2	8.8	20.4	0.020	0.5
8	11.3	25.4	41.4	17.2	19.4	0.019	2.8
9	12.4	25.2	19.5	12.9	10.4	0.010	1.4
10	13.4	25.4	59.7	12.8	26.1	0.026	1.7
11	14.4	25.3	41.0	12.9	19.6	0.020	1.3

(a) Median operation time refers to the midpoint in processing time of the specific filtration test condition relative to the start time of the test (T = 0). Time periods between test conditions were excluded.
(b) Thermocouple accuracy ± 2°C.
(c) Pressure transducer accuracy ± 1 psig.
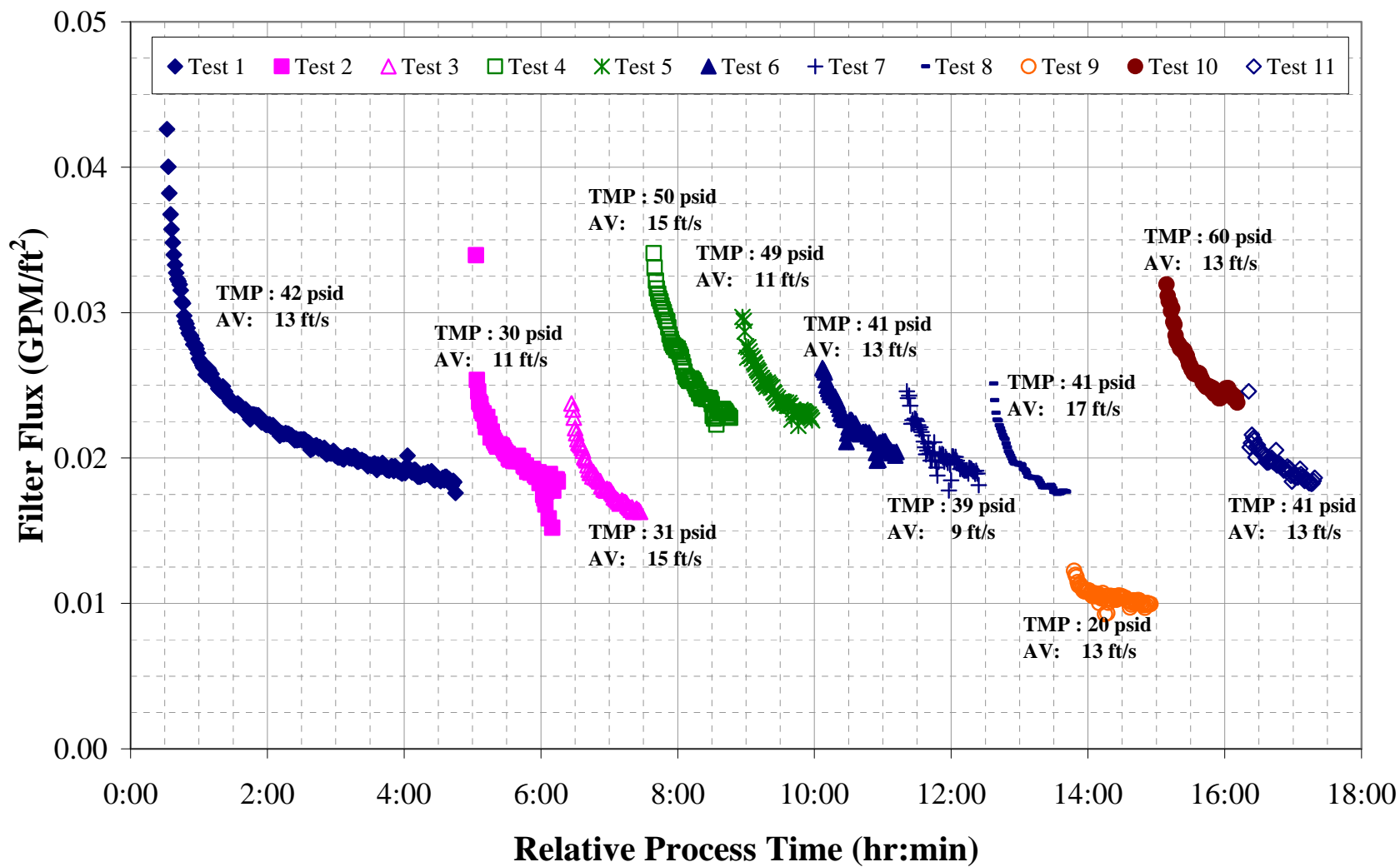
Figure 5.9. Filter Flux Data from Dilute Group 1/2 Matrix Test, 10 wt% UDS
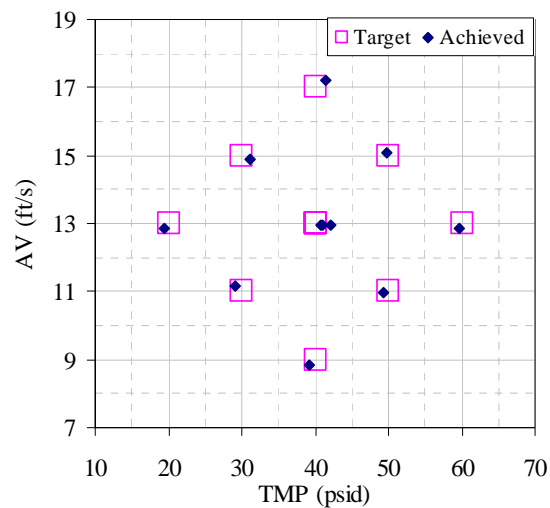
Figure 5.10. Group 1/2 Filter Test Matrix for Lows-Solids
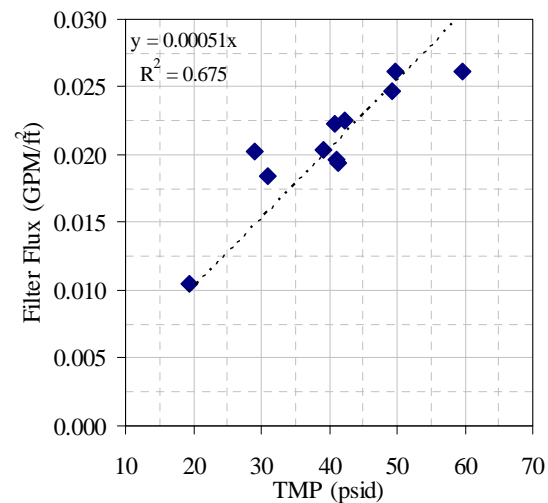
Figure 5.11. Group 1/2 Flux vs. TMP for Low-Solids
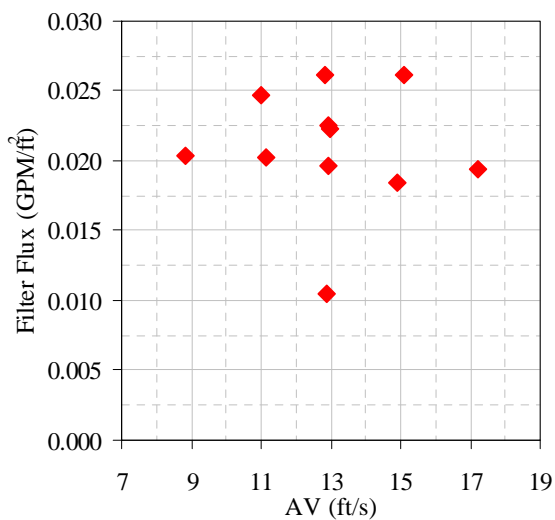
Figure 5.12. Group 1/2 Flux vs. AV for Low-Solids
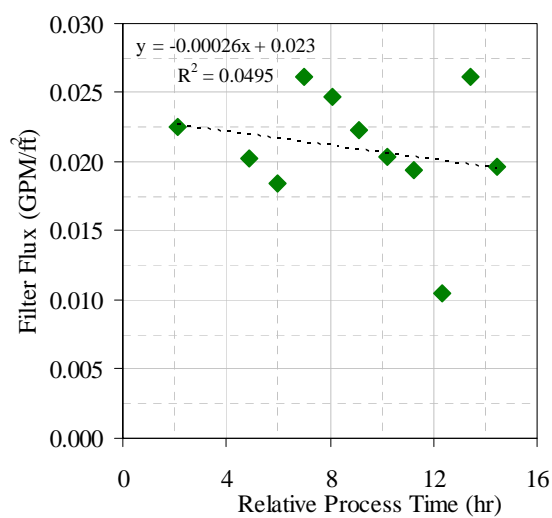
Figure 5.13. Group 1/2 Flux vs. Relative Time for Low-Solids
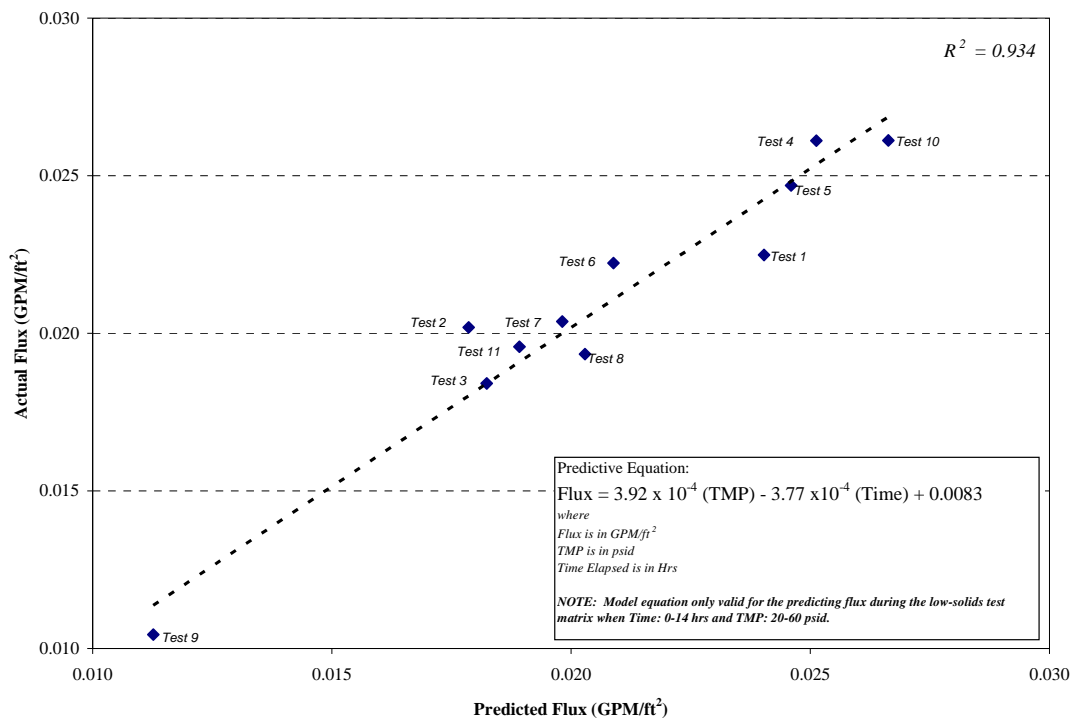
Figure 5.14. Linear Model of Filter Flux of Group 1/2 Slurry at Low-Solids Concentration
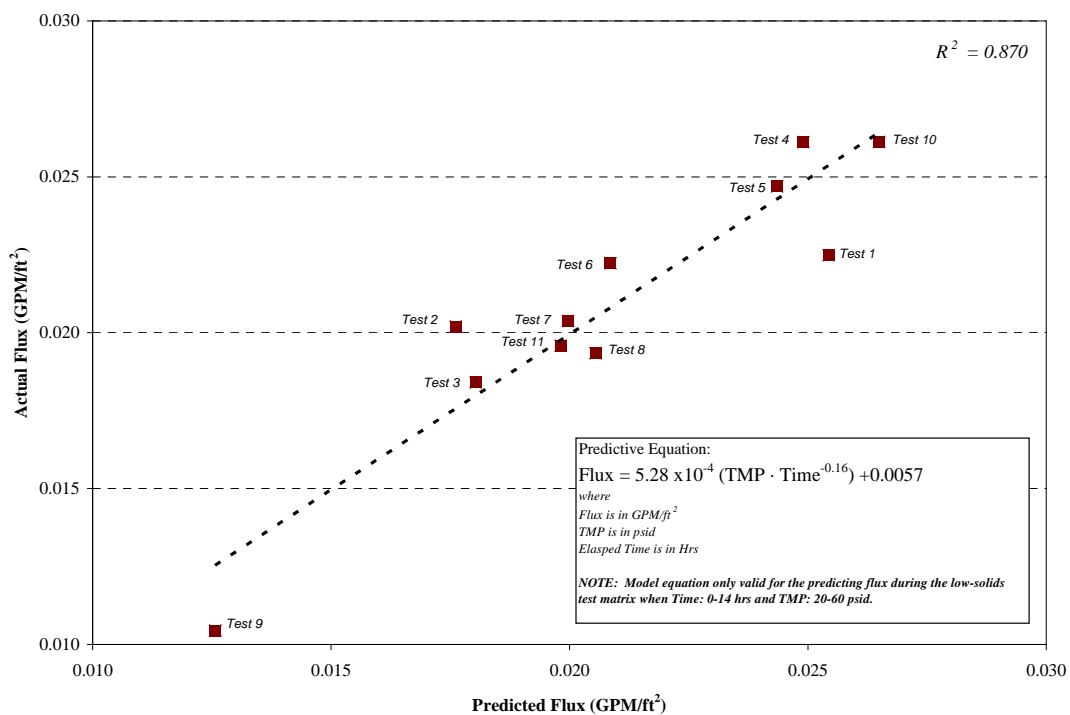
Figure 5.15. Exponential Model of Filter Flux of Group 1/2 Slurry at Low-Solids Concentration

5.3.3 Dewatering of Low-Solids Waste Slurry

Figure 5.16 illustrates the material flow for dewatering of the low-solids slurry. At the conclusion of the low-solids matrix, the tank level was measured by a conductivity level probe and correlated to a table of system volumes on Page 43 of 44 of TI-RPP-WTP-572, Rev. 0. A total of 2395 g of permeate were removed, corresponding to 1.98 L at the measured permeate density of 1.21 g/mL. An overview of the mass balance of the CUF system through the initial dewatering step is given in Table 5.7.   Based on the characterization data provided, the slurry UDS concentration was increased from 10 wt% to 20 wt%.

The measured filter flux for dewatering the slurry is plotted against relative process time in Figure 5.17. The filter flux during the dewatering of the low-solids slurry averaged around 0.017 GPM/ft^2. A slight decrease in the filter flux was observed over the course of ~2 hours that was similar in magnitude to the decrease observed during the low-solids matrix test. The change in the filter flux was believed to be from continued changes in the filter resistance and not due to changes in the slurry UDS concentration.
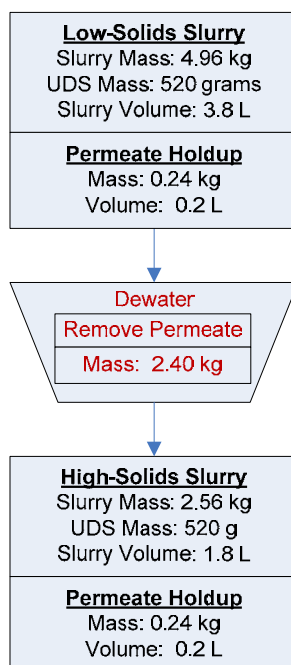
Figure 5.16. Flow Diagram of the Dewatering of the Low-Solids Slurry
Note: Mass and volume values in figure are rounded to the nearest significant digit of accuracy.

Table 5.7. Mass Balance Overview for Initial Slurry Dewatering to High-Solids Condition

Step	Mass Added or Removed (g)	Total System Mass (g)	Circulation Slurry Mass (g)[a]	Estimated UDS Mass (g)	Estimated UDS Conc. (wt%)	Measured UDS Concen. (wt%)
Load slurry into CUF, with added NaOH pellets	+5250	5250	5010	524	10.5 wt%	NA
Slurry sampling Low-Solids Slurry	-50	5200	4960	519	10.5 wt%	7.4 wt%
Dewater to High-Solids Slurry	-2400	2800	2560	519	20.3 wt%	14 wt%
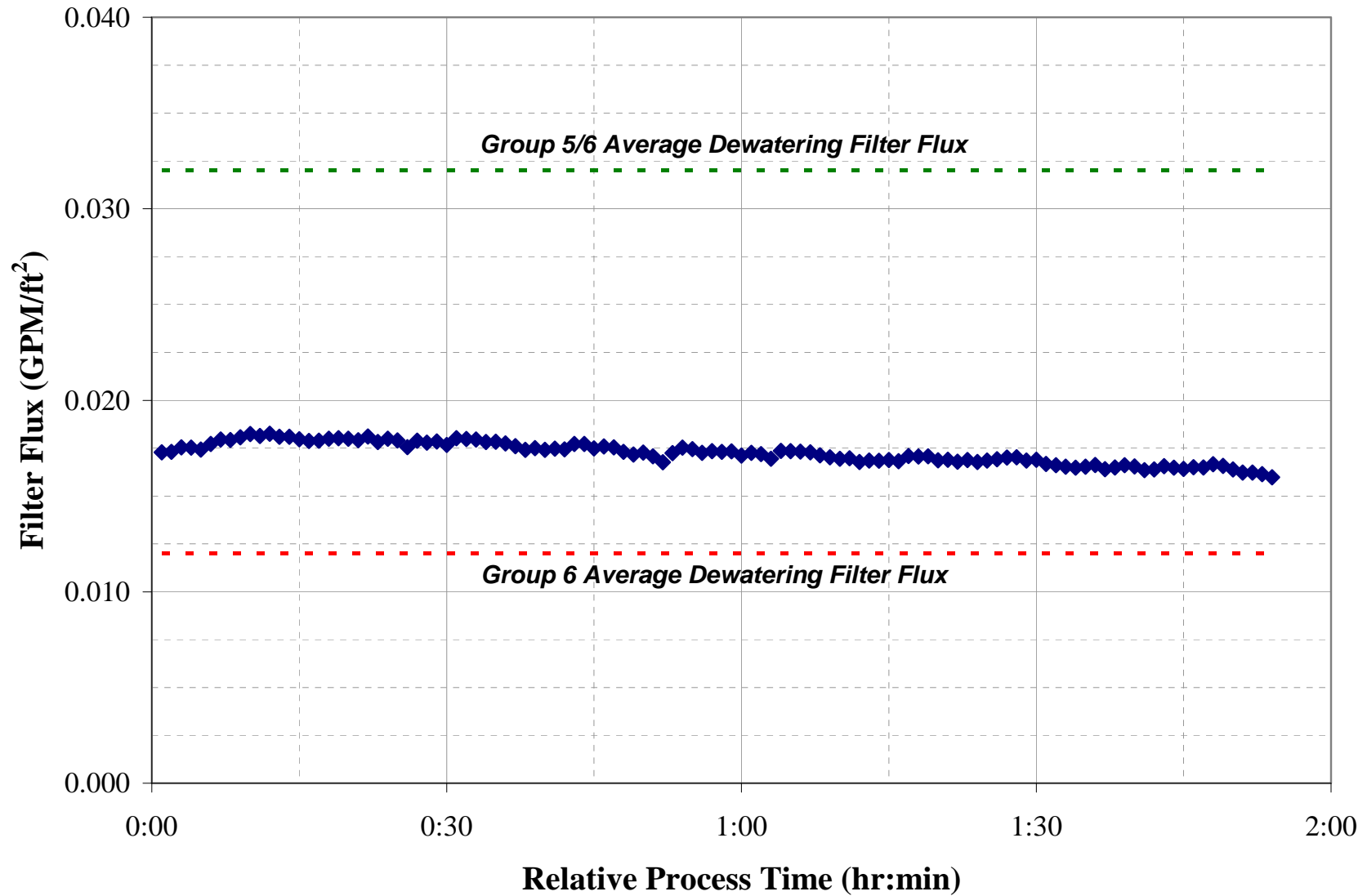
Figure 5.17. Filter Flux During Dewatering of Group 1/2 Blended Waste from 10 wt% to 20 wt% UDS

5.3.4 High-Solids Filter Matrix Testing

Figure 5.18 illustrates the material flow during the high-solids matrix testing. After dewatering, the slurry mass inside the circulation loop was estimated to be 2.56 kg while the permeate piping and back-pulse chamber contained 0.24 kg of filtered supernate. The wt% UDS for the matrix of the slurry inside the circulation loop used for the high-solids matrix test was estimated to be 20 wt%.

<div align="center">

Dewater
Remove Permeate
Mass: 2.40 kg

↓

High-Solids Slurry
Slurry Mass: 2.56 kg
UDS Mass: 520 g
Slurry Volume: 1.8 L

Permeate Holdup
Mass: 0.24 kg
Volume: 0.2 L

</div>
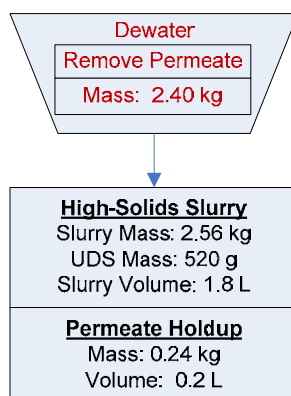
Figure 5.18. Flow Diagram of the High-Solids Matrix Testing
Note: Mass and volume values in figure are rounded to the nearest significant digit of accuracy.

The high-solids filtration tests were performed according to the eight test conditions described in Table K.2, Appendix K. The test conditions were performed sequentially with a minimum of 1 hour of constant recycle operation at each condition with back-pulsing between conditions. Table 5.8 provides a summary of the average operating conditions and flux for each condition. These values were obtained by calculating the arithmetic mean of each value over the duration of the test condition. The average TMP and AV of each test condition were plotted against the target values for each test in Figure 5.20.

Flux data with respect to process time are given in Figure 5.19. Compared to the low-solids test, the flux was significantly lower overall, and there was less flux decay within a given test condition. This might have been due the more rapid formation of a cake layer on the membrane at higher solids concentrations with a substantial amount of pore blockage present early at each test condition. The average filter flux measured at the standard conditions for the low-solids matrix tests (tests 1, 6, and 11) was 0.021 GPM/ft^2. The filter flux for tests at the standard condition (1, 5, and 8) was 0.016, 0.013, and 0.011 GPM/ft^2 in sequence, which is 35 to 50% lower than the initial filter flux measured. The decrease in the filter flux during the test also indicated a small, irreversible decline in flux with time, although this observation must be tempered by the fact that the average TMP for Test Condition 8 was 2.0 to 2.7 psid lower than Test Conditions 1 and 5. To the extent that flux is TMP dependent, this variation will affect comparisons of the average flux. The flux at test condition 4 at TMP=40 psid and AV=17 ft/s was surprising in that it was lower than the value for AV=9 ft/s at the same target TMP. Again, this might be attributed to relatively lower TMP (38.9 psid) at this condition compared to other conditions, or it may be further evidence of progressive membrane fouling, or some combination of both.

The average filter flux was plotted against TMP and AV for the eight conditions tested to make a qualitative judgment as to whether the slurry filtered more according to a membrane-resistance, pressure-dependent model or a cake-resistance, concentration polarization model. The comparisons are shown in

Figure 5.21 and Figure 5.22. From these charts, the TMP clearly has a stronger influence on flux, suggesting that the slurry behaves according to a membrane resistance model primarily and can be defined in terms of the Darcy equation. This supports the observation from the initial slurry dewatering that the slurry had not transitioned to cake-resistance-driven flux decay at the ending concentration of 20 wt% UDS. However, the correlation coefficient R^2 was only 0.77, implying that the filter resistance was changing. Filter flux was plotted against the median operation time of each test condition in Figure 5.23 to access changing in filter resistance over the course of the test. While the linear correlation of the plot was not very high (0.13), the filter flux was found to decrease gradually over the course of the test with time.

To compare these parameters to one another better, the filter matrix data were further correlated and fitted to two empirical models to verify these conclusions. The results of this analysis are shown in Figure 5.24 and Figure 5.25. From the fit equations, a strong dependence of filter flux on TMP was found with no significant impact from AV. Operation time also was found to have a small negative impact on filter flux, demonstrating fouling of the filter occurring that was not reversed by back-pulsing. The results were similar in magnitude to that seen in the low-solids test, where double the operation time was equivalent to ~10% decrease in the TMP. While both modeling equations have high correlation factors, the use of this model should be limited to understanding how filter flux was influenced by TMP and operation time during this test. Because time was included in both models, offset parameters were developed that limit the range to which they could be applied. Both models do not predict a zero filter flux when the TMP is zero, which demonstrates that the input to these models must be bound by the range of TMP used in this filter test, shown in Table 5.8. The use of these models should also be limited to when the test matrix occurred because the filter resistance was not at steady state, and the parameters developed in these models would be expected to change past the 8-hour period that this model predicts.

Table 5.8. Average Operating Conditions and Filter Flux for the High-Solids Matrix Test

Design Test Condition	Median Operation Time of Test[a] (hr)	Slurry Temp[b] (°C)	TMP[c] (psid)	Axial Velocity (ft/s)	Permeate Flowrate (mL/min)	Corrected Permeate Flux (GPM/ft^2)	Axial Pressure Drop[c] (psid/ft)
1	1.0	25.3	41.1	12.9	15.7	0.016	1.8
2	2.5	25.5	40.5	14.8	13.8	0.014	2.3
3	3.5	25.1	41.2	8.7	14.4	0.014	0.5
4	4.5	25.3	38.9	17.1	11.3	0.011	3.2
5	5.5	25.3	41.8	12.7	13.2	0.013	1.8
6	6.5	25.1	19.4	13.4	6.2	0.006	1.8
7	7.5	25.3	60.4	13.0	16.9	0.017	2.0
8	8.5	25.3	39.1	13.1	10.9	0.011	1.9

(a) Median operation time refers to the midpoint in processing time of the specific filtration test condition relative to the start time of the test (T = 0). Time period between test conditions were excluded
(b) Thermocouple accuracy ± 2°C.
(c) Pressure transducer accuracy ± 1 psig.
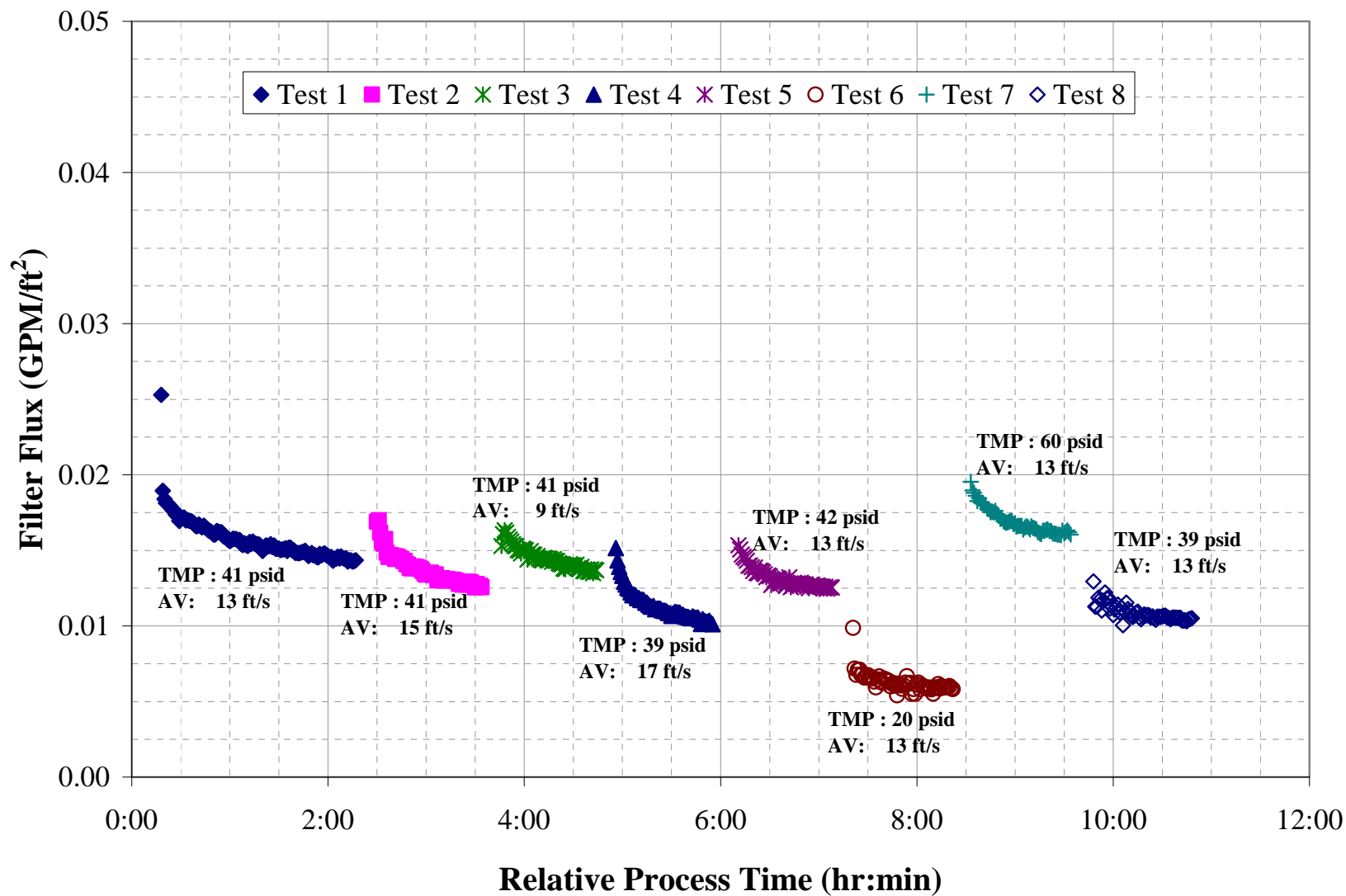
Figure 5.19. Filter Flux Data for Group 1/2 High-Solids Matrix, 20 wt% UDS
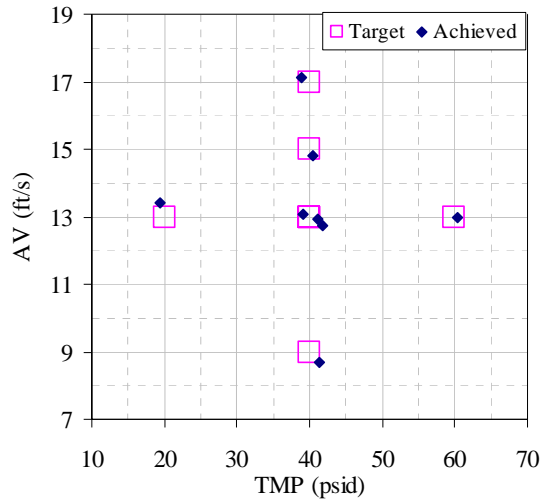
Figure 5.20. Group 1/2 Filter Test Matrix for High-Solid**s**
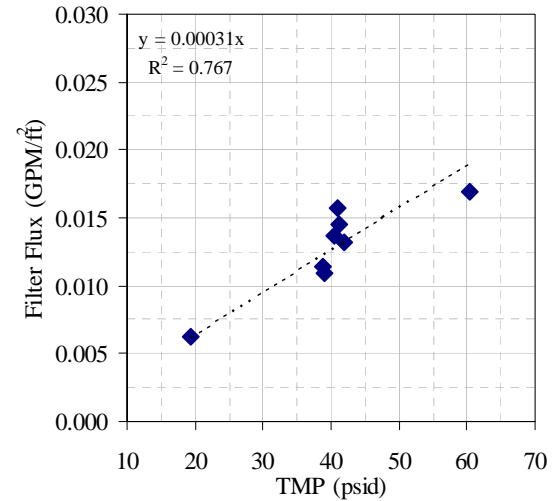
Figure 5.21. Group 1/2 Flux vs. TMP for High-Solids
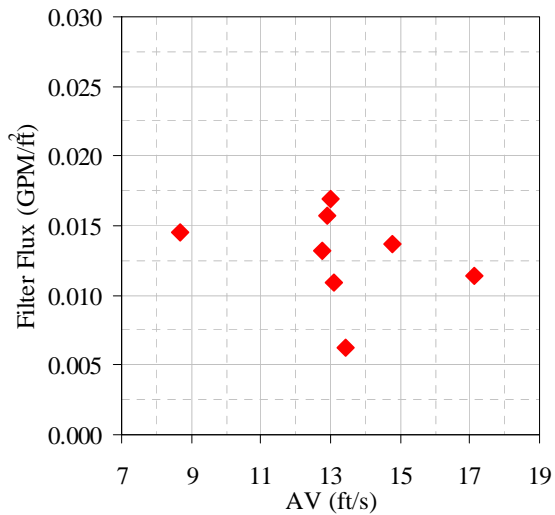
Figure 5.22. Group 1/2 Flux vs. AV for High-Solids
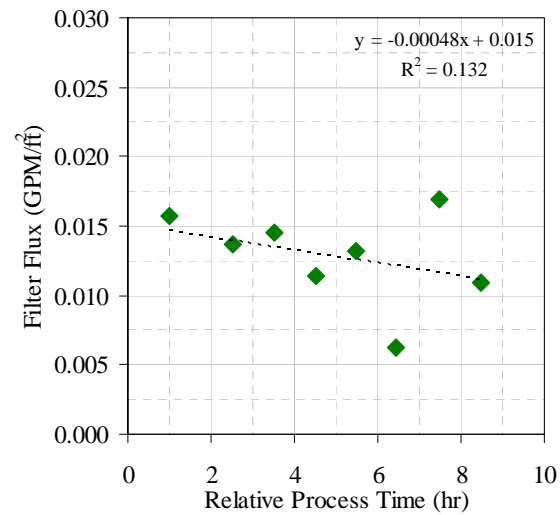
Figure 5.23. Group 1/2 Flux vs. Relative Time for High-Solids
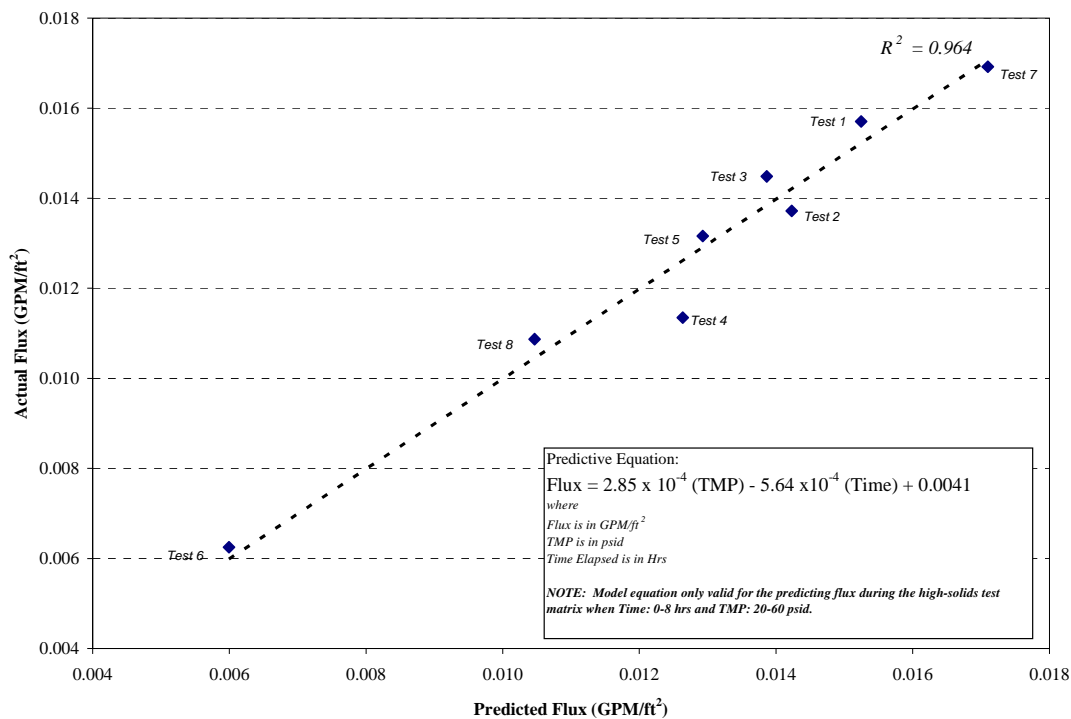
Figure 5.24. Linear Model of Filter Flux of Group 1/2 Slurry at High-Solids Concentration
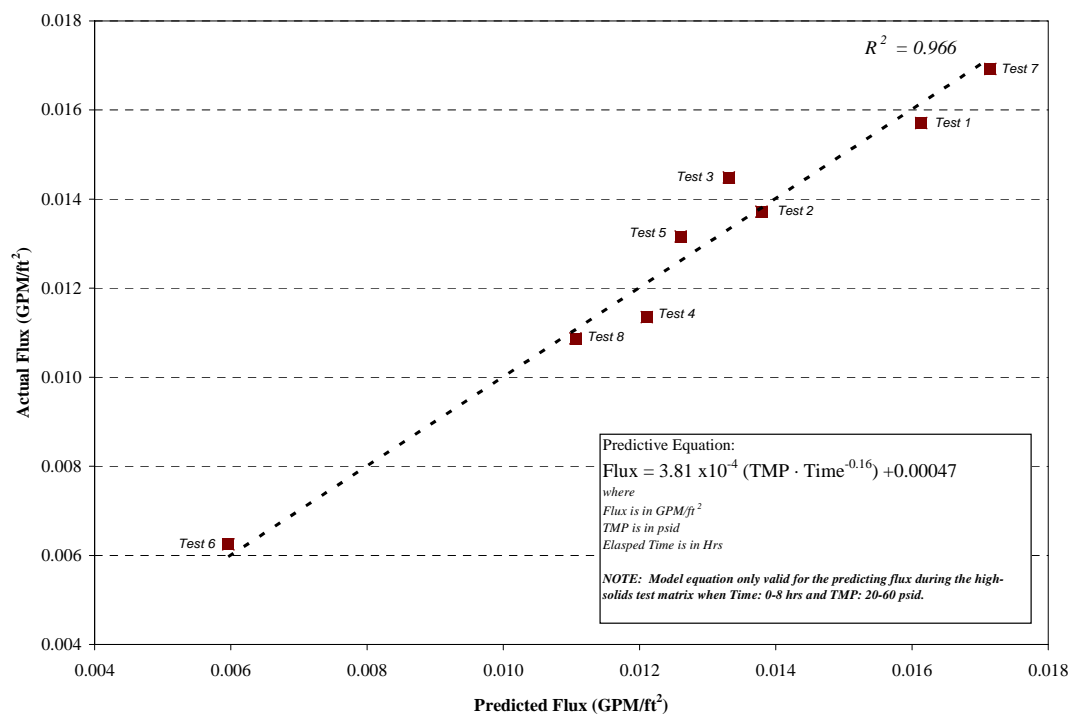
Figure 5.25. Exponential Model of Filter Flux of Group 1/2 Slurry at High-Solids Concentration

5.4 High-Solids Slurry Characterization

After completing the high-solids matrix test, the circulation slurry was sampled for physical and chemical analyses, as shown in Figure 5.26. Overall, 99 grams of the circulating slurry was removed containing an estimated 20 grams of UDS.

The physical properties and composition of this high-solids slurry are shown in Table 5.9 through Table 5.11. As discussed early, the predicted UDS concentration of the slurry (20 wt%) was significantly higher than the measured UDS concentration (14 wt%). While it was discussed earlier that problems with the overhead mixer were a likely reason that the slurry sample UDS was not representative of the circulating slurry, there are two other likely possibilities.

- The solids dissolved from mixing the Group 1 and Group 2 slurries.

- Measured UDS values of the Group 1 and Group 2 slurries were not as accurate as thought.

However, there was no evidence supporting either of these two theories. The composition of the Group 1/2 supernate shown in
Table 5.10 and
Table 5.11 correlates well with the supernate compositions reported in Sections 3 and 4, indicating that no significant dissolution of the solids occurred. Also, the solids composition calculated from mass balance data in
Table 5.10 (which assumed 500 grams of UDS was present) only differs by 10% with solids composition data reported in
Table 5.11, which was based on analytical measurements of the slurry. This difference was considered within the error range of the chemical analyses performed.

Based upon initial dewatering values, 8% of the aluminum and 30% of the chromium in the original slurry was present in the supernate in a soluble phase. This would explain the drop from low solids to high solids of the aluminum (8%) and chromium (20%) as the soluble portion exited upon dewatering. Sulfur in the slurry is accounted for completely by sulfate, which is highly soluble, its concentration decreasing significantly with each successive dewatering step. There is some soluble phosphate; however, the bulk of the phosphorus appeared to be tied up in insoluble forms. Based on work described elsewhere in this report, the water-insoluble phosphorus was likely in the form of iron(III) phosphate. Soluble anions in the supernatant as well as cesium all were reduced via the dewatering process.
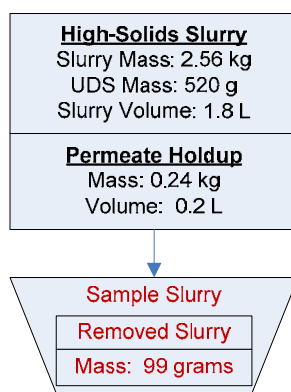
Figure 5.26. Sampling of the High-Solids Slurry

Note: Mass and volume values in figure are rounded to the nearest significant digit of accuracy.

Table 5.9. Physical Property Measurements of the High-Solids Slurry

Slurry Density (g/mL)	1.38
Supernate Density (g/mL)	1.20
Settled Solids (Vol%)	95%
Centrifuged UDS (Wt%)	26%
Total Solids of the Slurry (Wt%)	38%
Dissolved Solids of the Supernate (Wt%)	28%
UDS of the Slurry (Wt%)	14%

Table 5.10. Group 1/2 High-Solids Slurry Inventory and Composition

	Slurry[a]	Liquid Fraction[b]		Solids Fraction[c]	
Mass (kg)	2.70	2.20		0.50	
Wt% of Slurry	100%	81.5%		18.5%	
Metal	**g**	**g**	**µg/mL**	**g**	**µg/g**
Al	4.6E+01	1.7E+00	9.4E+02	4.5E+01	8.9E+04
Bi	2.0E+01	< 7.E-3	< 4.E+0	2.0E+01	4.1E+04
Cr	4.5E+00	8.8E-01	4.8E+02	3.6E+00	7.2E+03
Fe	2.7E+01	9.7E-03	5.3E+00	2.7E+01	5.4E+04
Mn	4.1E-01	1.6E-04	9.0E-02	4.1E-01	8.1E+02
Na	3.1E+02	1.8E+02	1.0E+05	1.2E+02	2.4E+05
P	4.1E+01	1.9E+00	1.0E+03	3.9E+01	7.9E+04
S	7.7E+00	9.7E+00	5.3E+03	N/A[d]	N/A[d]
Si	1.8E+01	1.9E-02	1.1E+01	1.8E+01	3.6E+04
Sr	1.6E+00	4.2E-04	2.3E-01	1.6E+00	3.2E+03
U	6.7E+00	2.0E-01	1.1E+02	6.5E+00	1.3E+04
Radiochemical Isotopes	**Slurry**	**Liquid Fraction**		**Solid Fraction**	
	mCi	**mCi**	**mCi/mL**	**mCi**	**mCi/g**
Co-60	5.2E+00	< 7.E-2	< 4.E-5	5.2E+00	1.0E-02
Cs-137	6.9E+04	2.2E+04	1.2E+01	4.7E+04	9.3E+01
Eu-154	1.6E+01	< 4.E-1	< 2.E-4	1.6E+01	3.2E-02
Am-241	1.4E+02	< 4.E+0	< 2.E-3	1.4E+02	2.9E-01
Gross Alpha	2.7E+02	1.3E+00	7.3E-04	2.7E+02	5.5E-01
Gross Beta	2.0E+05	2.1E+04	1.1E+01	1.8E+05	3.6E+02
Sr-90	6.4E+04	1.8E+01	9.7E-03	6.4E+04	1.3E+02
Pu-239+240	1.9E+02	6.0E-02	3.2E-05	1.9E+02	3.8E-01
Pu-238	6.5E+00	3.5E-02	1.9E-05	6.5E+00	1.3E-02
Anions	**Liquid Fraction**			**Leached Solids Fraction**	
	µg/mL	**[M]**	**g**	**µg/g**	**g**
F	4.0E+03	2.1E-01	7.3E+00	2.6E+04	1.3E+01
C$_2$O$_4$	1.4E+03	1.6E-02	2.6E+00	< 4.E+1	< 2.E-2
NO$_2$	7.8E+03	1.7E-01	1.4E+01	1.2E+04	5.8E+00
NO$_3$	1.9E+05	3.1E+00	3.5E+02	2.9E+05	1.4E+02
SO$_4$	1.5E+04	1.5E-01	2.7E+01	2.4E+04	1.2E+01
PO$_4$	3.1E+03	3.3E-02	5.6E+00	9.2E+04	4.6E+01
OH	1.2E+03	6.9E-02	2.1E+00		

(a) Slurry mass components were calculated from characterization data (Sections 3 and 4) and the masses of materials that were added with simulant. Loss of mass from sampling was incorporated.
(b) Liquid fraction mass components were calculated using analytical results from supernate sample TI572-G6-A (ASO ID 08-01290) and the predicted mass of supernate in the system.
(c) Solids fraction mass components were calculated from the difference between the slurry component mass and liquid component mass fraction.
(d) Values for sulfur in the solid inventory were calculated to be negative.

Table 5.11. Group 1/2 High-Solids Slurry Composition Based on ICP-OES/Radionuclide Characterization

Slurry Prep Method	ICP-OES Analytes	Dry Slurry[a] (µg/g)	Supernate[b] (µg/mL)	Dry Solids[c] (µg/g)
HF Assisted Acid Digestion, and KOH Fusion	Al	39,075	942	99,869
	Bi	19,900	<3.7E+0	53,232
	Cd	22.8	<4.2E-1	58.8
	Cr	3,915	480	8,087
	Fe	24,375	[5.3]	65,198
	K	952	552	-203
	Mn	354	[0.090]	946
	Na	263,000	100,000	205,543
	Ni	1,455	<3.0E-1	3,892
	P	38,825	1,025	98,785
	S	8,165	5,300	-4,557
	Si	18550.0	[10.6]	49584.8
	Sr	1,348	0.228	3,605
	U	6,058	108	15,671
	Zn	202	[0.54]	539
	Zr	76	<1.4E-1	202
	Ag	[4.63]	<2.6E-1	[11.1]
	Ba	89	[0.31]	235
	Be	0.455	<6.5E-3	1.184
	Ca	3,160	2.80	8,442
	Ce	71.9	<1.2E+0	186.1
	Co	[16]	<3.0E-1	[42]
	Cu	42.3	<1.7E-1	112.4
	La	[14]	<3.5E-1	[34]
	Li	27.6	[1.00]	68.9
	Mg	540	<2.9E-1	1,444
	Mo	[28]	7.11	[40]
	Nd	[18]	<6.7E-1	[44]
	Pb	513	<4.0E+0	1,352
	Ru	[12.53]	[2.1]	[23.08]
	Th	9.50	[5.15]	[0.24]
	Ti	59.0	1.40	150.9
	Tl	[74]	[0.053]	[197]
	V	15.0	<4.7E+0	16.6
	Y	[2.5]	<5.5E-2	[6.42]

Table 5.11 (Contd)

Slurry Prep Method	Radionuclides	Dry Slurry[a] (µCi/g)	Supernate[b] (µCi/mL)	Dry Solids[c] (µCi/g)
KOH Fusion	Co-60	4.42E-3	<4.E-5	1.16E-2
	Cs-137	6.28E+1	1.21E+1	1.08E+2
	Eu-154	<7.E-3	<2.E-4	<2.E-2
	Eu-155	<3.E-2	<2.E-3	<7.E-2
	Am-241	1.19E-1	<2.E-3	3.10E-1
	Total alpha	2.53E-1	7.32E-4	6.73E-1
	Total beta	1.45E+2	1.14E+1	3.30E+2
	Sr-90	5.61E+1	9.69E-3	1.50E+2
	Pu-239/240	1.34E-1	3.24E-5	3.60E-1
	Pu-238	3.74E-3	1.90E-5	9.91E-3

(a) Test sample TI572-G2-A, ASO ID 08-01290
(b) Test sample TI572-G2-6, ASO ID 08-01317
(c) Calculated using results from TI572-G2-A and TI572-G2-6
Note: Analytes in italics were measured opportunistically. Values in brackets [ ] are ≥ MDL but < EQL, with errors likely to exceed 15%.

Figure 5.27 shows the size distribution of particles in the high-solids slurry matrix before sonication. The distribution is broad, ranging from ~0.3 to 500 µm, and is characterized by a strong peak with a maximum population between 1 and 2 µm. At 2000 and 3000 RPM, the distribution shows a broad "shoulder" over the range 4 to 60 µm. In addition, the distributions at 2000 and 3000 RPM show a small population of large particles, ranging from 60 to ~600 µm with a peak population around 400 µm. This large particle population may represent flocculates that form under weak shear (resulting in the most significant 400 µm population at 2000 RPM). It could also result from poor interpretation of the light scattering signal. Regardless, the contribution of large (60 to 600 µm) particles is minor relative to that of particles making up the primary distribution (0.2 to 60 µm). At 4000 RPM, a secondary population peak centered at 50 µm appears. The latter is likely associated with difficult-to-suspend particles.

Figure 5.28 shows the effects of sonication on the high-solids slurry matrix at a pump speed of 3000 RPM. Sonication appears to reduce/eliminate the contribution of particles greater than 20 µm while increasing the contribution of particles between 2 and 20 µm. The original (pre-sonication) distribution appears to be preserved in a sub-micrometer shoulder population that spans 0.2 to 1 µm. The increase in relative contribution of 2- to 20-µm particles is likely a result of sonic disruption of particle agglomerates greater than 20 µm. The during- and after-sonication PSDs are relatively similar, indicating that the changes that occur during sonication are mostly irreversible over the time frame of these PSD measurements. On the other hand, a slight decrease in the peak population contribution of particles after sonic power is removed could indicate some reformation of agglomerates, but this decrease is not accompanied by significant changes in the span of the distribution.
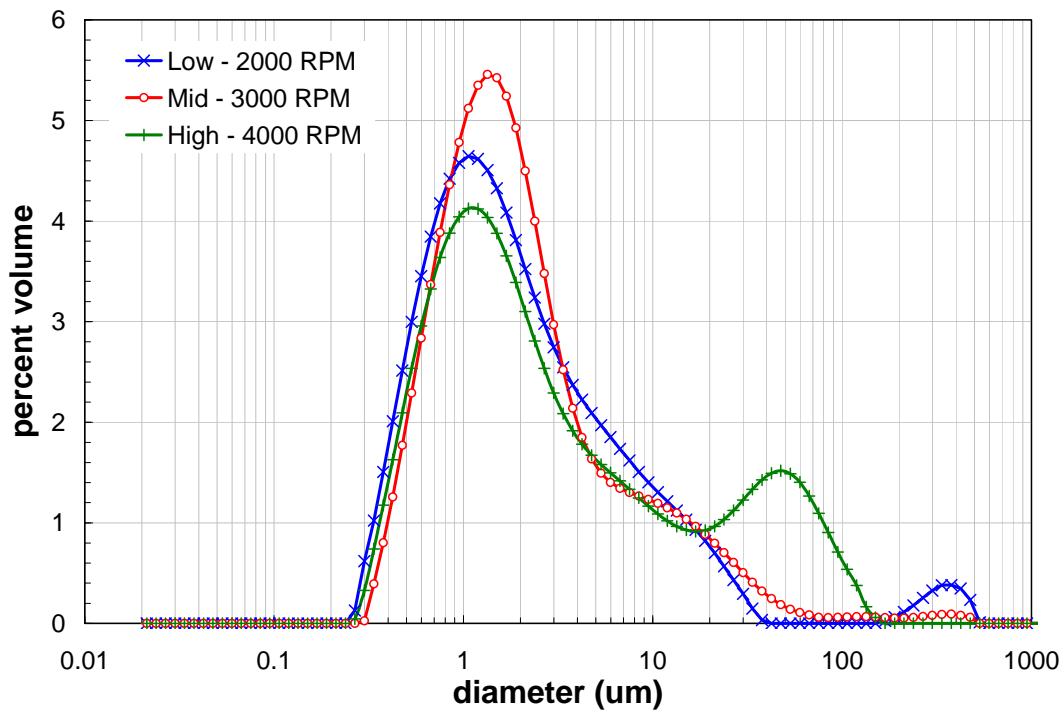
Figure 5.27. High-Solids Slurry Matrix PSD at Varying Pump Speeds
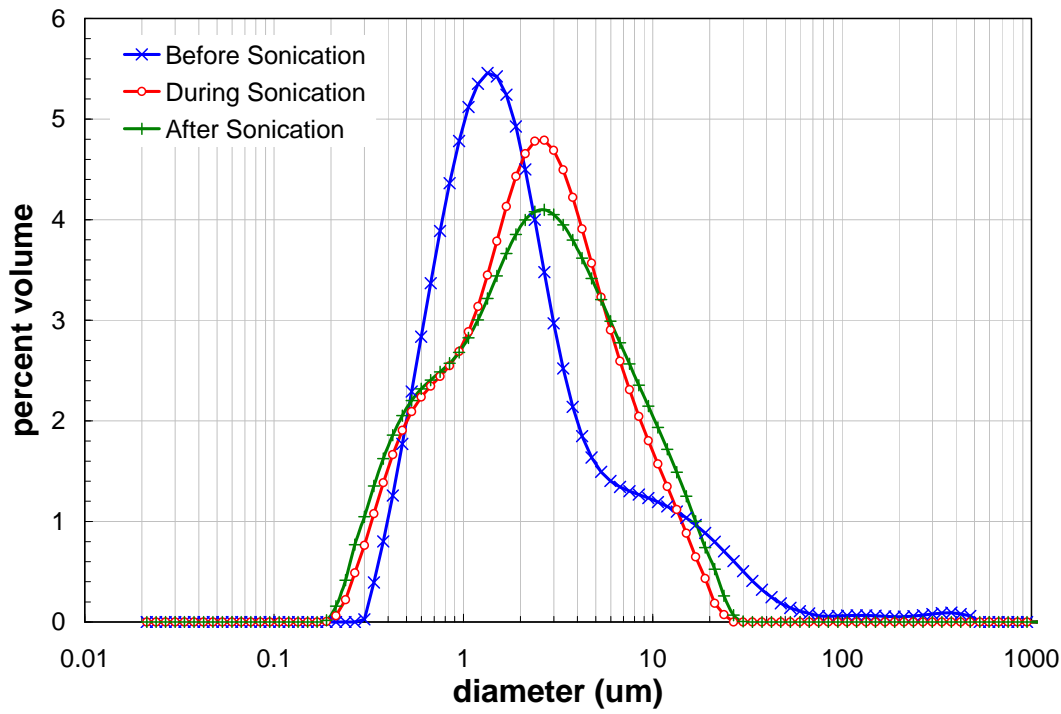
Figure 5.28. High-Solids Slurry Matrix PSD with Sonication at a Pump Speed of 3000 RPM

Figure 5.29 shows the results of flow curve testing for the high-solids slurry, which shows non-Newtonian behavior at all temperatures studied. All flow curves have a finite yield stress that falls between 2 and 4 Pa. The stress response over 0 to 1000 s^{-1} shows a slight downward curvature. The flow curves appear to be free of artifacts caused by poor sample rotation, such as significant downward curvature in the 0 to 100 s^{-1} range. Flow curve hysteresis is present in all flow curves, but appears to influence the 60°C measurement data to the greatest extent. Hysteresis at 25°C and 40°C results from a decrease in the stress required to shear the fluid over time. That is, at these temperatures, the down-ramp data always show a lower stress response than the up-ramp data. One potential cause for this type of hysteresis is continued shear alteration of the sample structure (such as shear breakup of aggregates). The nature of flow curve hysteresis changes at 60°C. Here, the down-ramp data show a higher stress response relative to the up-ramp data. This type of hysteresis is consistent with increased slurry concentration and rheology as a result of suspending phase evaporation.

Given the noise introduced into the measurement by flow curve hysteresis (~1 Pa), the increased slurry temperature does not appear to significantly change the observed yield stress. The slurry consistency appears to decrease as the temperature is increased from 25° to 60°C as evidenced by the decreasing flow curve slope over 0 to 1000 s^{-1}.

Table 5.12 summarizes the best-fit rheological parameters for flow curve data for the high-solids slurry. The fitting parameters show that:

- The Bingham-Plastic and Herschel-Bulkley yield stresses range from 2.7 to 3.2 Pa and 2.1 to 2.6 Pa (depending on temperature), respectively. Because the maximum difference between the yield stresses at different temperatures is only 0.5 Pa, it can be concluded that the yield stress does not change significantly with temperature.

- The Bingham-Plastic consistency decreases from 13 mPa·s at 25°C to 9.0 mPa·s at 60°C. This decrease is consistent with the temperature-dependence observations made in the preceding paragraph.

- The Herschel-Bulkley flow indices are all near 0.9, confirming that the flow curve data do have a slight downward curvature.

- The two replicate measurements at 25°C yield equivalent fitting parameters, given the limit of instrument accuracy (±0.5 Pa for yield stress and ±0.5 mPa·s for consistency).

For ease of reference, apparent viscosities at 33, 100, 500, and 1000 s^{-1} are derived from each measurement. For each temperature, the 33, 100, and 500 s^{-1} reference viscosities are determined from the average of up-ramp and down-ramp flow curve data. The apparent viscosity at 1000 s^{-1} averages apparent viscosity measurements over the period of constant rotation at 1000 s^{-1}. As a point of comparison, apparent viscosities at 33 s^{-1}, 100 s^{-1}, 500 s^{-1}, and 1000 s^{-1} were also calculated using the Bingham-Plastic and Herschel-Bulkley fitting parameters in Table 5.12. The results of these analyses are provided in Table 5.13 and show that apparent viscosities typically range from 76 to 110 mPa·s at 33 s^{-1}, 34 to 45 mPa·s at 100 s^{-1}, 14 to 20 mPa·s at 500 s^{-1}, and 12 to 16 mPa·s at 1000 s^{-1}.
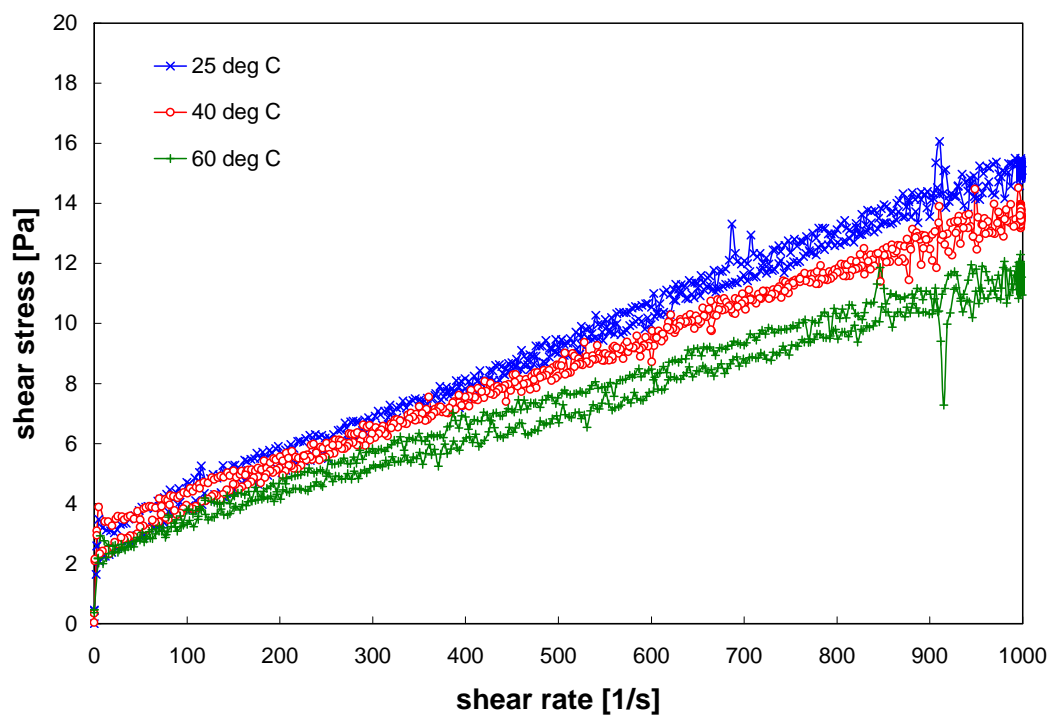
Figure 5.29. Flow Curve for the Group 1/2 CUF High Solids Slurry at 25, 40, and 60°C

Table 5.12. Results of Fitting Analysis for the High-Solids Slurry

Model	Temperature [°C]	Yield Stress [Pa]	Consistency [Pa·s^n]	Flow Index	R
Bingham-Plastic (0 – 1000 s^{-1})	25 (1 of 2)	3.2	0.013	n/a	0.995
	25 (2 of 2)	3.0	0.012	n/a	0.997
	40	3.1	0.011	n/a	0.997
	60	2.7	0.0090	n/a	0.992
Herschel-Bulkley (0 – 1000 s^{-1})	25 (1 of 2)	2.6	0.026	0.90	0.996
	25 (2 of 2)	2.5	0.024	0.91	0.997
	40	2.6	0.023	0.89	0.997
	60	2.1	0.023	0.87	0.993

Table 5.13. Apparent Viscosity of the High-Solids Slurry

Source	Temperature [°C]	Apparent Viscosity [mPa·s]			
		@ 33 s⁻¹	@ 100 s⁻¹	@ 500 s⁻¹	@ 1000 s⁻¹
Measured	25 (1 of 2)	96	44	19	16
	25 (2 of 2)	93	43	18	15
	40	96	41	17	14
	60	76	35	14	12
Bingham-Plastic	25 (1 of 2)	110	45	19	16
	25 (2 of 2)	100	42	18	15
	40	110	42	17	14
	60	89	36	14	12
Herschel-Bulkley	25 (1 of 2)	99	43	20	16
	25 (2 of 2)	92	41	19	15
	40	96	40	17	14
	60	79	34	15	12

Figure 5.30 and Table 5.14 compare the rheology of the source Group 1 and Group 2 slurries to the low-solids matrix (dilute) and high-solids matrix (concentrated) Group 1/2 CUF slurries. Both source materials for Group 1 and 2 show slightly non-Newtonian rheological characteristics with yield points near the instrument limit of detection. Of the two source materials, Group 2 shows "stronger" rheology, most likely a result of its much higher solids concentration (37.4-wt% USD) relative to Group 1 (9.0-wt% UDS). The dilute Group 1/2 mixture has an UDS concentration of 8.2-wt%, which is similar to that of Group 1. Based on the similar solids concentration, it is not surprising that the dilute slurry mixture has a consistency (5.0 mPa·s) that is similar to, but slightly less than, the consistency for source Group 1 (6.7 mPa·s). From this observation, it could be inferred that the Group 1 slurry rheology is dominant in the mixture; however, this inference is impossible to confirm without Group 2 slurry rheology at a UDS similar to that of the mixture.

Dewatering of the Group 1/2 slurry from the initial 8.2-wt% UDS to 16.0-wt% has the expected result of increasing the stress response of the fluid over all rates of shear examined. Concentrating the slurry changes the rheology from Newtonian, with a viscosity of 5.0 mPa·s to non-Newtonian, with a yield of 3.0 Pa and a consistency of 12 mPa·s. The concentrated slurry exhibits a higher stress response than either of the source materials. Given that the concentration of the high-solids matrix sample (16.0 wt%) is still significantly lower than the Group 2 source material (37.4 wt%), the increased stress response of the concentrated mixture relative to Group 2 suggests that Group 1 rheological properties are dominant. This is consistent with the observation made in the preceding paragraph.

Table 5.14. Effect of Waste Stream Mixing and Dewatering on Group 1/2 CUF Rheology (at 25°C)

Description	Solids Concentration	Rheology	Yield Stress [Pa]	Consistency [mPa·s]
Group 1 Source (TI508-G1-AR-RH1)	9.0-wt%	non-Newtonian*	0.3	6.7
Group 2 Source (TI517-G2-AR-RH)	37.4-wt%	non-Newtonian	1.1	13
Dilute Group 1/2 Mixture (TI572-G2-R1)	8.2-wt%	Newtonian	n/a	5.0
Concentrated Group 1/2 Mixture (TI572-G2-R2)	16.0-wt%	non-Newtonian	3.0	12
*Yield stress is not statistically different than zero. Flow curve is statistically Newtonian.				
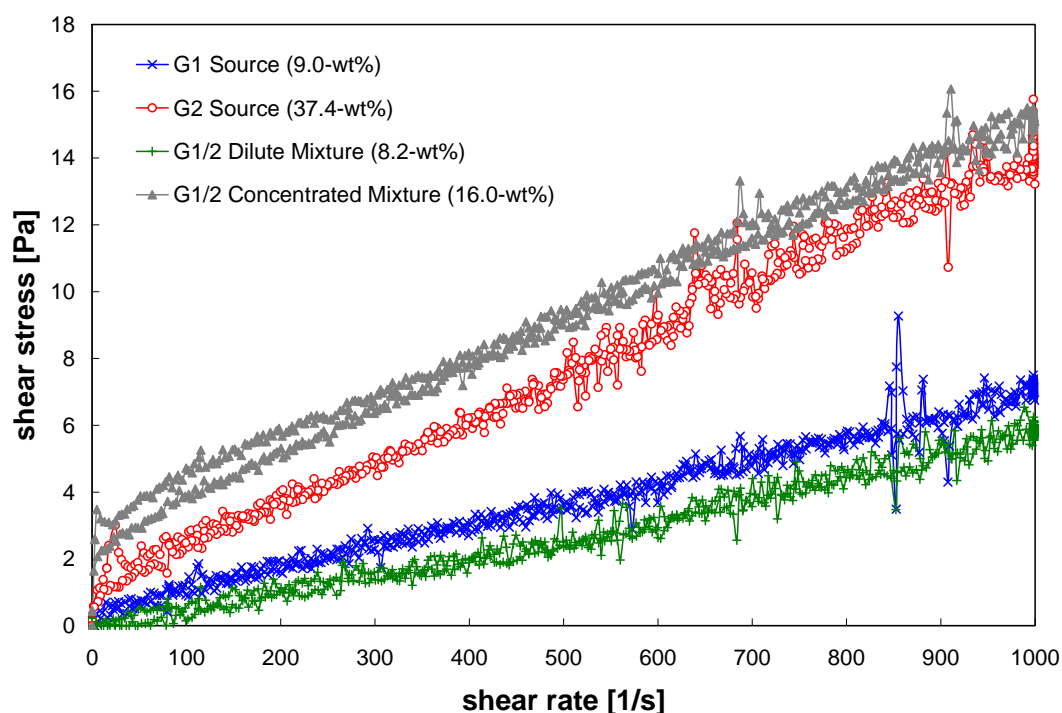
Figure 5.30. A Comparison of Feed Material (Group 1 and Group 2) and CUF 1/2 (high and low solids) Rheologies (measurements are at 25°C)

5.5 Caustic Leaching/Washing

After completing the filtration and rheological testing of the high-solids slurry, the slurry was drained from the system and prepared for caustic leaching (Figure 5.31). A total of 2,853 grams (approximately 2.3 L) of 7.6 M sodium hydroxide (NaOH) was to be added to the Group 1/2 slurry. The slurry loop was rinsed using part of the caustic addition for the leach and additional permeate that was remaining in the back-pulse chamber to flush solids out of the slurry piping. After the slurry and caustic additions were recovered from the system, the slurry reservoir was isolated from the slurry loop. During the transfer of the slurry and leach solution to the slurry reservoir, it was estimated that 5 wt% of the slurry and caustic solution was lost to hold-up in the containers used to store the slurry and leach solution after it was drained. The mass loss of the combined solution was 0.28 kg, which containing 25 grams of UDS.

At this point, the caustic leach of the recovered slurry proceeded as outlined in the middle column of Figure 5.1. This entailed:

- Batch caustic leaching of the slurry for removing aluminum and phosphorus

- Dewatering of leaching permeate from the slurry solids

- Batch washing of the caustic-leached slurry and dewatering of the solution afterwards. Five total wash solutions were added to the slurry to remove aluminum and phosphorus from the slurry and lower the free hydroxide level below 0.25 M for subsequent oxidative leaching.
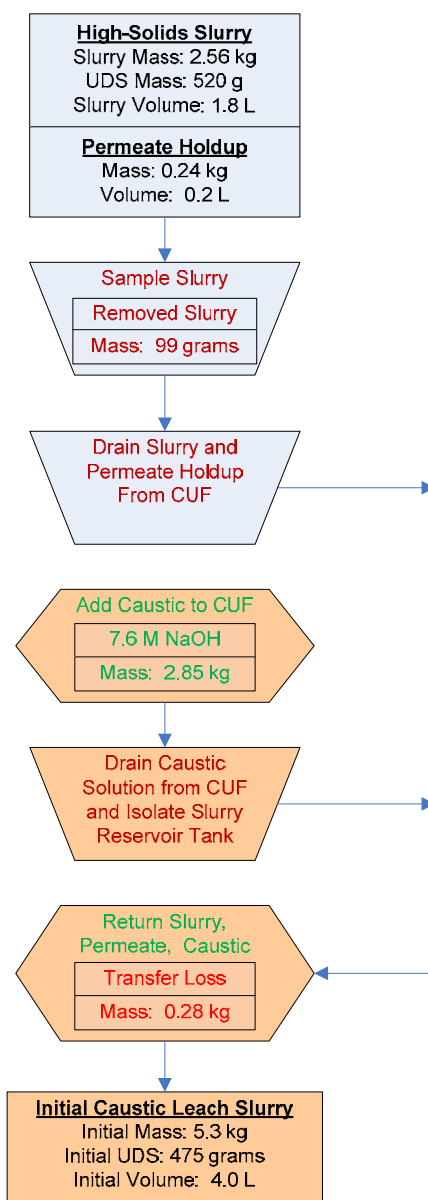
Figure 5.31. Flow Diagram for Batch Caustic Leaching

Note: Mass and volume values in figure are rounded to the nearest significant digit of accuracy.

5.5.1 Batch Caustic Leaching Results

The slurry was heated to 100°C over a 5.3-h period, held at 100°C (the control range was 90°C to 105°C) for an 8-hour leaching period, and then cooled for 8 hours. Level measurements were taken every half hour during the leaching step, and the slurry was adjusted as necessary with DI water to compensate for evaporation (Figure 5.32). Over the course of the test, 2.1 L were added to the vessel to maintain the leach volume at 4 L. After the leaching was completed, the volume of the slurry was 3.9 L, so approximately 2.2 L of water was estimated to have been lost to evaporation. Five slurry samples were collected—two during heat-up and three once the leach temperature was reached. Approximately 26 grams of slurry was sampled during the course of the leach with an estimated loss of 2 grams of UDS.
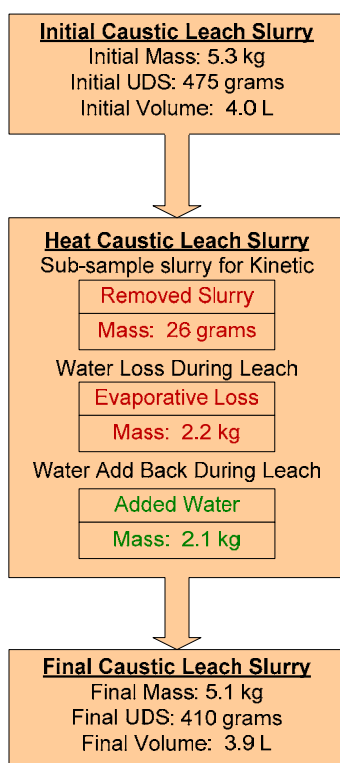
Figure 5.32. Group 1/2 Batch Leach Sampling/Evaporation Loss and Water Additions
Note: Mass and volume values in figure are rounded to the nearest significant digit of accuracy.

The slurry supernate was filtered from the samples and analyzed by ICP-OES (elemental analysis) and titration (for free hydroxide ion) to determine the kinetics of aluminum and phosphorus dissolution during the caustic leaching. The results of these analyses are provided in Table 5.15. The results reported are corrected for sample evaporation that occurred between the time the sample was collected and when it was sub-sampled by ASO. Aluminum, chromium, phosphorus, and potassium concentrations provided in Table 5.15 are plotted against each other in Figure 5.33. While the aluminum concentration in the supernate increases during the heat-up, there was little change in the chromium concentration. In the case of phosphorus, the measured concentration of the supernate at 40°C was almost 10 times lower than the predicted supernate concentration after the leach solution addition. The phosphorus concentration was observed to increase in the subsequent sample, collected at 76°C, but remained close to the initial concentration for the remainder of the leaching step.

The high-solids slurry inventory (
Table 5.10) predicted that 45 grams of insoluble aluminum was present. While preparing the slurry for caustic leaching, the inventory decreased by 5 wt% from transfer losses. Assuming that 43 grams of aluminum was present in the UDS of the slurry, the supernate concentrations of the slurry supernate samples were used to project the conversion of aluminum during the course of the leach, as shown in Figure 5.34. The one-hour heat-up sample indicated that 7 wt% of the solid aluminum had leached into solution. By 3 hours into the heat ramp-up, or approximately 75°C, the aluminum leach factor was 32 wt%, and by the beginning of the leach period (100°C), the Al leaching was essentially done, reaching a maximum leach factor of 45 wt%. It was estimated that 50 grams of the slurry solids was dissolved into the aqueous phase during the caustic leach.

Table 5.15. Concentration of Major Analyte Components of Filtered Caustic Leach Samples, Corrected for Sample Evaporation

	Start of Heatup[a] (25°C)	1-Hour Heatup[b] (40°C)	3-Hour Heatup[c] (76°C)	0-Hour Leach[d] (92°C)	4-Hour Leach[e] (97°C)	8-Hour Leach[f] (96°C)
	µg/mL	µg/mL	µg/mL	µg/mL	µg/mL	µg/mL
Al	4.1E+02	1.1E+03	4.0E+03	5.7E+03	5.5E+03	5.5E+03
Bi	< 2.E+0	< 1.E+1	1.7E+02	4.3E+02	1.9E+02	2.0E+02
Cr	2.1E+02	1.9E+02	1.9E+02	2.5E+02	2.2E+02	2.2E+02
Fe	2.3E+00	1.3E+00	1.9E+01	1.8E+01	1.2E+01	1.3E+01
K	2.4E+02	2.2E+02	2.2E+02	2.6E+02	3.2E+02	2.6E+02
Mn	3.9E-02	< 1.E-1	1.9E-01	< 9.E-2	2.6E-01	3.4E-01
Na	4.4E+04	1.5E+05	1.4E+05	1.6E+05	1.5E+05	1.6E+05
P	4.5E+02	7.0E+01	6.6E+02	6.0E+02	7.2E+02	7.0E+02
S	2.3E+03	4.8E+02	1.5E+03	5.2E+02	1.4E+03	1.6E+03
Si	4.6E+00	3.2E+02	4.6E+01	1.4E+02	2.2E+02	2.6E+02
Sr	9.9E-02	1.1E-01	3.2E-01	1.0E-01	2.3E-01	2.9E-01
U	4.7E+01	5.0E+01	6.3E+01	1.4E+01	4.4E+01	9.0E+00
	[M]	[M]	[M]	[M]	[M]	[M]
OH	4.6	4.8	4.6	4.7	4.7	4.3

Temperature in heading represents the sample temperature taken from the vessel. Accuracy of the thermocouple used was ±2°C. Samples were later allowed to cool to the hot cell temperature and were later sub-sampled for analyses to be performed outside the hot cell at room temperature.

(a) Predicted concentrations from mixing caustic addition (7.6 M) with slurry supernate. Composition of supernate based on sample TI572-G2-A, ASO ID 08-01290.

(b) Composition based on sample TI572-G2-C1, ASO ID 08-01304. Values divided by 1.41 to account for evaporative loss of sample.

(c) Composition based on sample TI572-G2-C2, ASO ID 08-01305. Values divided by 1.05 to account for evaporative loss of sample.

(d) Composition based on sample TI572-G2-C3, ASO ID 08-01306. Values divided by 1.53 to account for evaporative loss of sample.

(e) Composition based on sample TI572-G2-C4, ASO ID 08-01307. Values divided by 1.01 to account for evaporative loss of sample.

(f) Composition based on sample TI572-G2-C5, ASO ID 08-01308. Values divided by 1.03 to account for evaporative loss of sample.
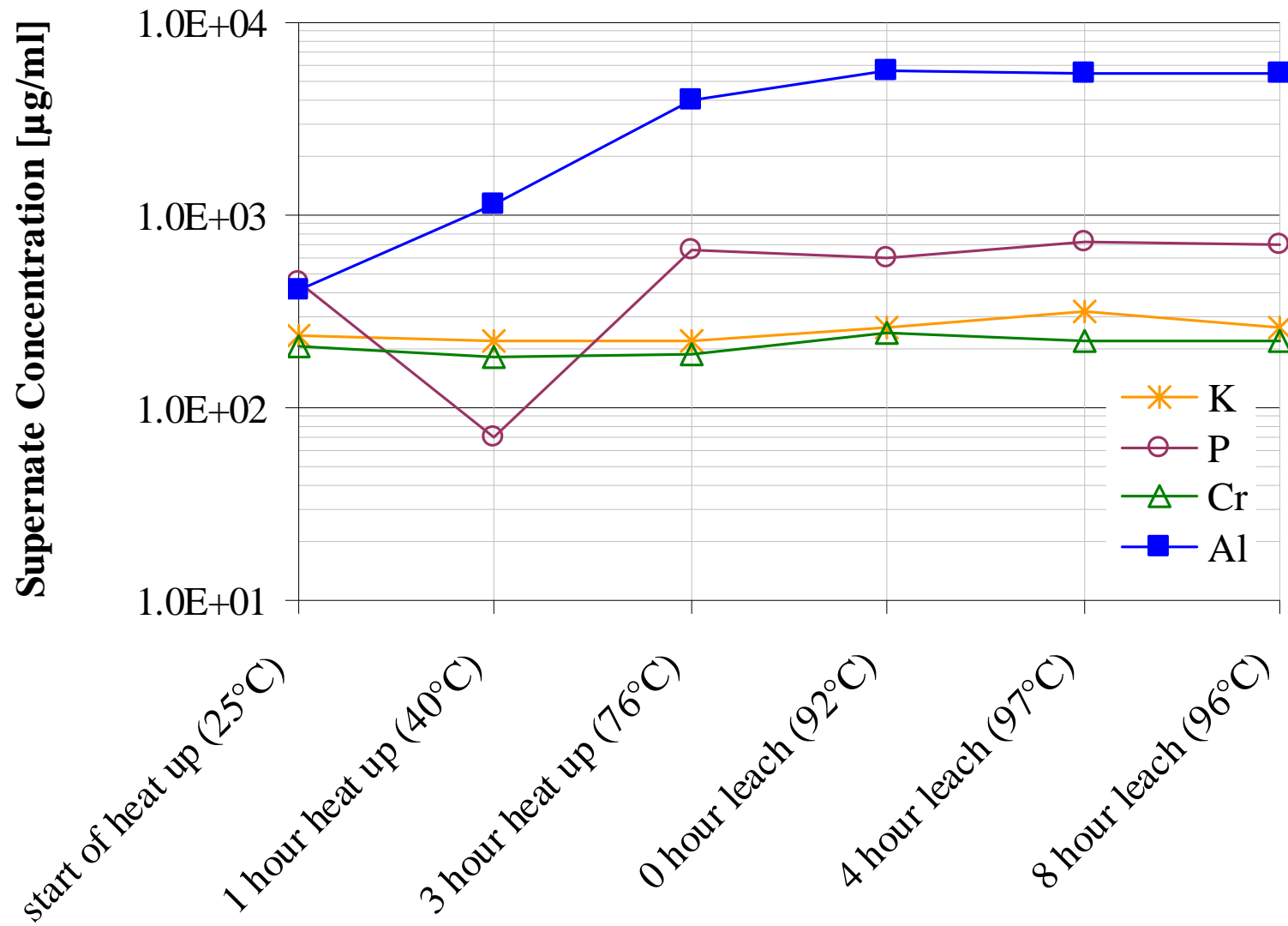
Figure 5.33. Concentration of Al, Cr, P, and K During Caustic Leach of Group 1/2 Slurry
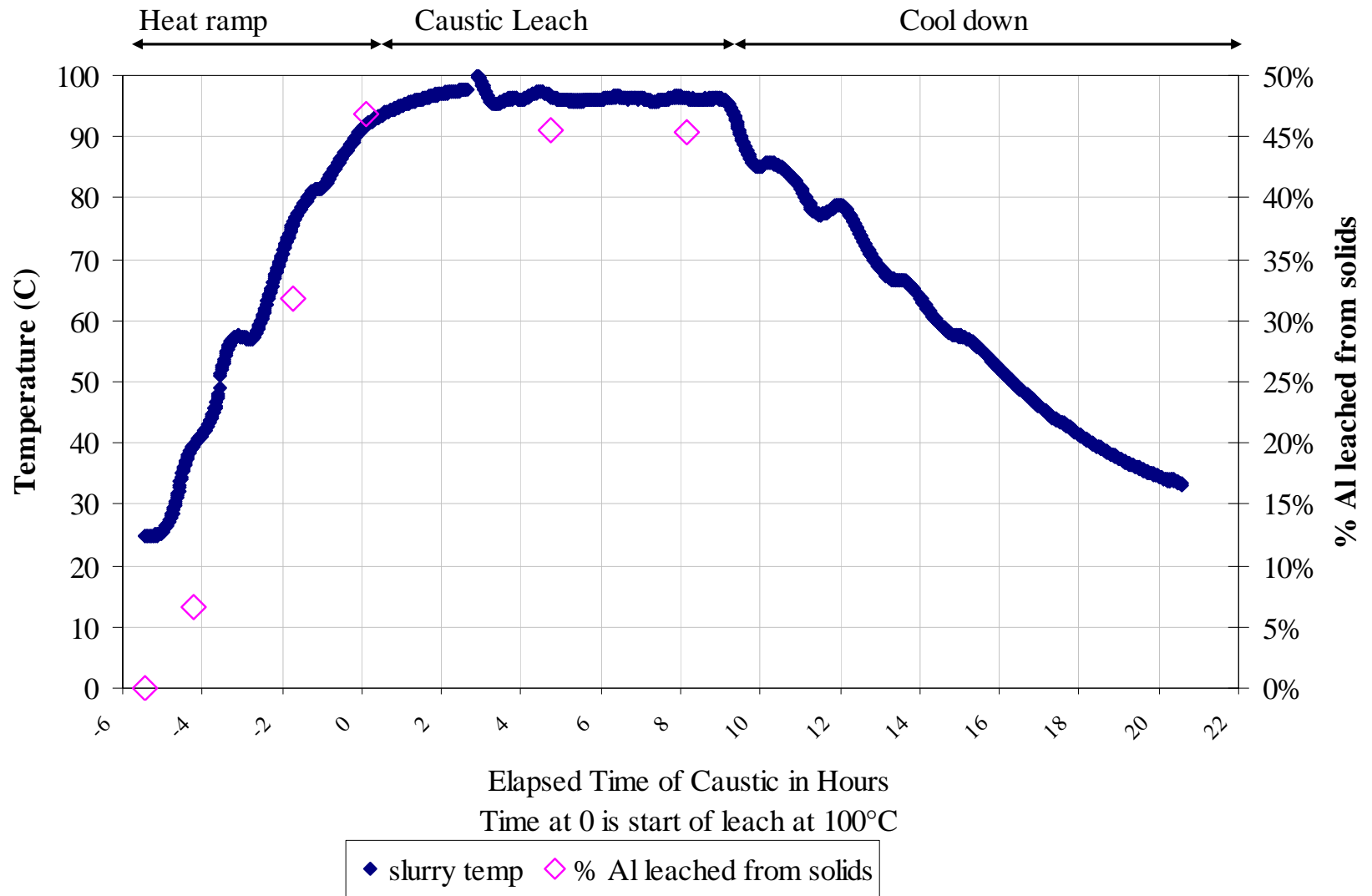
Figure 5.34. Temperature Profile/Aluminum Leach Factors During Caustic Leaching

5.5.2 Caustic Leaching Dewatering

After cooling the leached slurry over a twelve hour period, the valves isolating the tank from the pump and filter were opened in preparation for circulating the slurry and beginning the leach dewatering step when it was discovered that the pump head would not turn. It appeared to be frozen in place. The tank was isolated again, and any slurry that had drained into the flow lines was retrieved and added back to the tank. The sanitary fittings on the pump head were loosened, and a gel was discovered in the pump head that was described to be similar to tapioca pudding. The gel apparently formed in the slurry loop during the caustic leaching step. After several flushes of water, the gel was cleared, and the pump returned to normal operation for the dewatering step. It is hypothesized that this gel consisted of $Na_3PO_4 \cdot 12H_2O$ that precipitated from the reaction of residual slurry solids with the small amount of caustic solution that was used to flush the slurry loop before the leaching step.

Figure 5.35 summarizes the mass change in the slurry following the dewatering step of the caustic-leached Group 1/2 composite. The mass of the dewatered permeate collected was 3.28 kg (2.6 L). The remaining 1.3 L of slurry was split between the slurry and supernate circulation piping. It was estimated that 1.6 kg of the slurry was inside the slurry circulation loop while 0.25 kg of the slurry supernate were containing in the back pulse chamber and permeate piping.

Final Caustic Leach Slurry
Final Mass: 5.1 kg
Final UDS: 410 grams
Final Volume: 3.9 L

Dewater
Remove Permeate
Mass: 3.28 kg

Dewatered Leached Slurry
Slurry Mass: 1.6 kg
UDS Mass: 420 g
Slurry Volume: 1.1 L

Permeate Holdup
Mass: 0.25 kg
Volume: 0.2 L
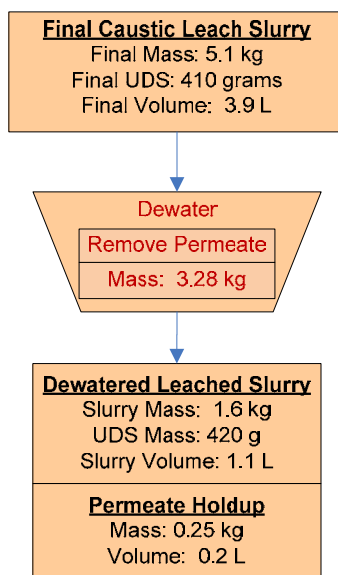
Figure 5.35. Flow Diagram for Caustic-Leach Dewatering Operations
Note: Mass and volume values in figure are rounded to the nearest significant digit of accuracy.

The leach dewatering step was conducted at the standard condition of TMP=40 psid and AV=13 ft/s. Dewatering proceeded slowly with an initial flux of ~0.010 GPM/ft^2 decreasing to ~0.008 GPM/ft^2 by the end of the run (Figure 5.36). The drop in flux relative to the initial dewatering step is due to changes in the suspending phase, namely increased permeate viscosity. It has been noted in previous sections that the filter flux was primarily driven by TMP for low- and high-solids loading, meaning that the flux can be modeled by the Darcy equation:

$$J = \frac{\Delta P_m}{\mu_{permeate} R_m}$$ (5.2)

where ΔP_m is the pressure drop across the filter membrane, $\mu_{permeate}$ is the viscosity of the permeate, and R_m is the overall resistance of the filter membrane. Assuming constant pressure drop and filter resistance, Equation 5.1 may be simplified to give the following relationship where flux at a given condition (J_1) may be calculated from the flux at a reference condition (J_0) by the ratio of the viscosities:

$$J_1 = J_0 \left(\frac{\mu_{permeate,0}}{\mu_{permeate,1}} \right)$$ (5.3)

Using the above relationship, the average flux for the leach dewatering step was estimated from the initial dewatering average flux. Viscosities and predicted values are summarized in Table 5.16. The predicted flux for the leach dewatering step is low using only viscosity. Since the TMP was the same for both steps, this may indicate a slight decrease in membrane resistance in the leach dewatering step attributable to the dissolution of deeply fouling particles by the caustic-leach solution. It may also indicate that the Darcy equation does not fully characterize the filtration of these slurries and may need to be supplemented by contributions from a gel polarization model for a better fit; however, the simple correlation of permeate viscosity substantially accounts for the difference in filter flux between the two dewatering steps.

Table 5.16. Prediction of Average Flux of Leach Dewatering Step from Initial Dewatering Flux Based on Viscosity Differences According to the Darcy Equation

Sample	Description	Viscosity at 25°C (mPa·s)	Predicted Average Flux (GPM/ft^2)	Actual Average Flux (GPM/ft^2)
G2-R2s	Permeate from initial dewatering	2.6	Reference value	0.017
G2-R3s	Permeate from leach dewatering	7.9	0.006	0.009
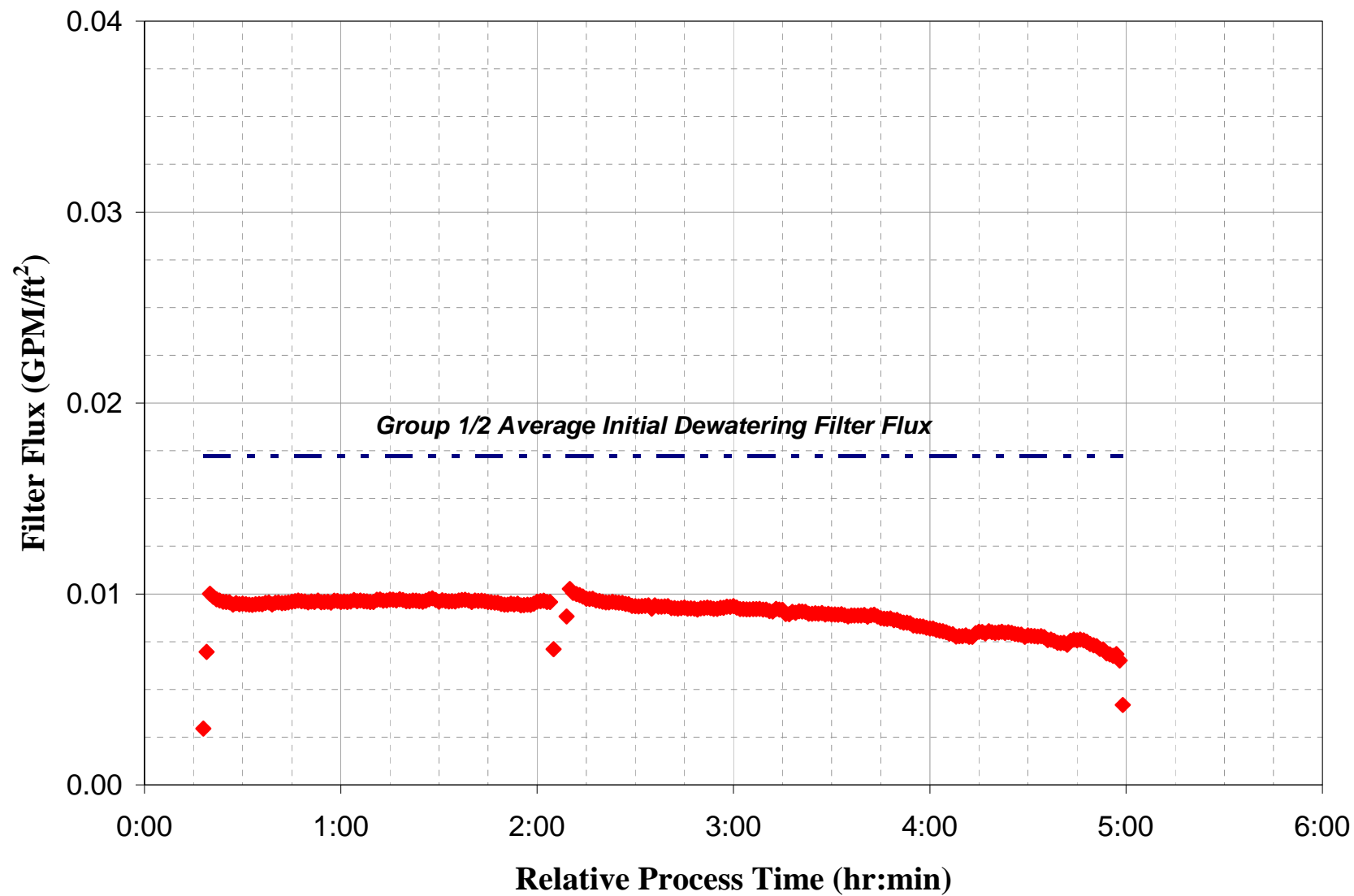
Figure 5.36. Permeate Flux During Leach Dewatering Step

5.5.3 Characterization of Dewatered Leached Slurry

After dewatering the leached slurry, the circulating slurry inside the slurry loop was sampled for physical and chemical characterization (Figure 5.37). The sampled slurry mass was 45 grams, and it was estimated that 10 grams of UDS was removed from the slurry, reducing the inventory to 410 grams.

The physical properties for the caustic-leached and dewatered slurry are shown in Table 5.17, and chemical properties are shown in Table 5.18 and Table 5.19. The measured UDS concentration of the slurry was 18 wt%, while the mass balance predicted the UDS concentration inside the slurry loop to be 26 wt% (0.42 kg ÷ 1.6 kg ≅ 26 wt%). The difference between the two results was likely due to the slurry not being homogenous inside the CUF because of problems with the overhead mixer. Comparing the predicted solid concentration based on mass-balance data (Table 5.18) to the calculated solid concentration using the measured composition of the slurry and supernate (Table 5.19) showed the results to be within 10% for aluminum and phosphorus. However, the slurry-based results were 20 to 25% higher for elements such as iron, chromium, and uranium.

Leach factors were calculated for analytes measured from the slurry analysis by comparing the composition of the leach slurry in Table 5.19 to the composition of the high-solids slurry in Table 5.11, using uranium and iron as a basis. Overall, only the aluminum fraction in the slurry solids significantly changed, with a calculated 0.58 leach factor. Phosphorus did not appear to have been removed from the solid phase at this point of the test. Because of the increase in the sodium concentration of the supernate from the caustic leach, insoluble phosphorus released as phosphate was believed to have re-precipitated as sodium phosphate. This theory was proven correct later, once the slurry was washed and the sodium concentration of the supernate decreased (Section 5.5.4).
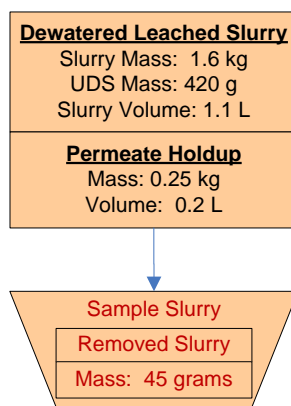
Figure 5.37. Sampling Losses for the Dewatered Leached Group 1/2 Slurry
Note: Mass and volume values in figure are rounded to the nearest significant digit of accuracy.

Table 5.17. Physical Property Measurements of the Dewatered Caustic Leached Slurry

Slurry Density (g/mL)	1.37
Supernate Density (g/mL)	1.18
Settled Solids (Vol%)	100%
Centrifuged UDS (Wt%)	26%
Total Solids of the Slurry (Wt%)	39%
Dissolved Solids of the Supernate (Wt%)	26%
UDS of the Slurry (Wt%)	18%

Table 5.18. Group 1/2 Caustic leached, Dewatered Slurry Inventory and Composition

	Slurry[a]	Liquid Fraction[b]		Solids Fraction[c]	
Mass (kg)	1.79	1.38		0.41	
Wt% of Slurry	100%	77.0%		23.0%	
Metal	g	g	µg/mL	g	µg/g
Al	2.9E+01	6.0E+00	5.1E+03	2.3E+01	5.6E+04
Bi	1.8E+01	1.8E-01	1.6E+02	1.8E+01	4.4E+04
Cr	3.6E+00	2.4E-01	2.1E+02	3.3E+00	8.1E+03
Fe	2.5E+01	9.7E-03	8.2E+00	2.5E+01	6.0E+04
Mn	3.7E-01	1.4E-03	1.2E+00	3.7E-01	9.0E+02
Na	2.7E+02	1.7E+02	1.4E+05	1.1E+02	2.6E+05
P	3.7E+01	3.6E-01	3.1E+02	3.7E+01	9.0E+04
S	2.2E+00	2.1E+00	1.8E+03	1.1E-01	2.7E+02
Si	1.6E+01	2.5E-01	2.2E+02	1.6E+01	3.8E+04
Sr	1.5E+00	1.1E-04	9.5E-02	1.5E+00	3.6E+03
U	6.2E+00	8.9E-03	7.6E+00	6.2E+00	1.5E+04
Radiochemical Isotopes	**Slurry**	**Liquid Fraction**		**Solid Fraction**	
	mCi	mCi	mCi/mL	mCi	mCi/g
Co-60	4.8E+00	< 4.E-2	< 3.E-5	4.8E+00	1.2E-02
Cs-137	4.1E+04	9.9E+03	8.5E+00	3.1E+04	7.4E+01
Eu-154	1.4E+01	< 1.E-1	< 1.E-4	1.4E+01	3.5E-02
Am-241	1.3E+02	< 2.E+0	< 2.E-3	1.3E+02	3.2E-01
Gross Alpha	2.5E+02	< 8.E-1	< 7.E-4	2.5E+02	6.1E-01
Gross Beta	1.6E+05	9.2E+03	7.8E+00	1.5E+05	3.7E+02
Sr-90	5.9E+04	4.7E+00	4.0E-03	5.9E+04	1.4E+02
Pu-239+240	1.8E+02	9.1E-03	7.7E-06	1.8E+02	4.3E-01
Pu-238	6.0E+00	< 1.E-3	< 1.E-6	6.0E+00	1.5E-02
Anions		**Liquid Fraction**		**Leached Solids Fraction**	
	µg/mL	[M]	g	µg/g	g
F	1.5E+03	8.0E-02	1.8E+00	2.9E+04	1.2E+01
C$_2$O$_4$	4.3E+02	4.9E-03	5.1E-01	1.2E+04	4.7E+00
NO$_2$	3.1E+03	6.8E-02	3.7E+00	3.7E+03	1.5E+00
NO$_3$	7.5E+04	1.2E+00	8.8E+01	9.1E+04	3.8E+01
SO$_4$	5.1E+03	5.3E-02	6.0E+00	1.1E+04	4.5E+00
PO$_4$	9.8E+02	1.0E-02	1.2E+00	1.3E+05	5.5E+01
OH	7.1E+04	4.2E+00	8.3E+01		

(a) Slurry mass components were calculated from characterization data (Sections 3 and 4) and the masses of materials that were added with simulant. Loss of mass from sampling was incorporated.
(b) Liquid fraction mass components were calculated using analytical results from supernate sample TI552-G6-D (ASO ID 08-01291) and the predicted mass of supernate in the system.
(c) Solids fraction mass components were calculated from the difference between the slurry component mass and liquid component mass fraction.

Table 5.19. Group 1/2 Dewatered Leached Slurry Composition and Calculated Solids Leach Factors

Slurry Prep Method	ICP-OES Analytes	Dry Slurry[a] (µg/g)	Supernate[b] (µg/mL)	Dry Solids[c] (µg/g)	Solids Leach Factor[d]
	Al	31,650	5,070	49,414	0.58
	Bi	27,200	157	59,149	0.06
	Cd	31.4	<4.2E-1	67.2	0.03
	Cr	5,025	206	10,224	-0.07
	Fe	34,200	8.24	75,123	NA
	K	[400]	286	-[257]	-0.07
	Mn	532	1.20	1,164	-0.04
	Na	320,500	142,000	140,289	0.42
	Ni	2,060	<2.9E-1	4,526	0.01
	P	43,950	309	95,354	0.18
	S	4,075	1,800	1,805	1.34
	Si	25000.0	215	54084.2	0.08
	Sr	1,900	[0.095]	4,175	0.02
	U	8,625	[7.6]	18,923	NA
HF Assisted Acid Digestion, and KOH Fusion, Concentration Factor of 1.18 based on U and Fe	**Zn**	249	17.5	478	0.25
	Zr	106	[0.49]	231	0.03
	Ag	[7.7]	<2.6E-1	[15.9]	-[.21]
	Ba	123	[0.23]	268	0.03
	Be	[0.25]	[0.062]	[0.30]	[.78]
	Ca	4,275	<7.5E-1	9,391	0.06
	Ce	103	<1.2E+0	220	0.00
	Co	19.8	<2.9E-1	42.3	0.15
	Cu	70.5	3.32	141.6	-0.07
	La	[21]	<3.4E-1	[44]	-[.08]
	Li	36.6	[0.61]	77.9	0.04
	Mg	737	<2.8E-1	1,618	0.05
	Mo	[41]	[3.6]	[75]	-[.6]
	Nd	[27]	<6.6E-1	[57]	-[.09]
	Pb	618	[22]	1,270	0.20
	Ru	<2.4E+1	[2.3]	<4.4E+1	NA
	Th	[12]	<3.2E+0	[14]	[49.96]
	Ti	83.4	<1.2E+0	178.4	0.00
	Tl	[110]	<5.3E-2	[242]	-[.04]
	V	16.1	<4.7E+0	16.9	0.14
	Y	3.40	<5.4E-2	7.26	0.04

Table 5.19 (Contd)

Slurry Prep Method	Radionuclides	Dry Slurry[a] (µCi/g)	Supernate[b] (µCi/mL)	Dry Solids[c] (µCi/g)	Solids Leach Factor[d]
KOH Fusion, Concentration Factor of 1.18 based on U and Fe	Co-60	5.71E-3	<3.E-5	1.24E-2	0.09
	Cs-137	4.79E+1	8.46E+0	7.16E+1	0.44
	Eu-154	2.52E-2	<1.E-4	5.48E-2	-1.73
	Eu-155	<4.E-2	<2.E-3	<8.E-2	NA
	Am-241	1.71E-1	<2.E-3	3.67E-1	-0.01
	Total alpha	5.07E-1	<7.E-4	1.11E+0	-0.40
	Total beta	2.18E+2	7.83E+0	4.47E+2	-0.15
	Sr-90	8.28E+1	4.03E-3	1.82E+2	-0.03
	Pu-239/240	2.01E-1	7.75E-6	4.43E-1	-0.04
	Pu-238	6.25E-3	9.82E-7	1.37E-2	-0.17

(a) Test sample TI572-G2-D, ASO ID 08-01291
(b) Test sample TI572-G2-9, ASO ID 08-01318
(c) Calculated using results from TI572-G2-D and TI572-G2-9.
(d) Calculated using dry solids concentration results listed in
(e) Table 5.11.
  Note: Analytes in italics were measured opportunistically. Values in brackets [ ] are
  ≥ MDL but < EQL, with errors likely to exceed 15%.

Figure 5.38 shows the size distribution of particles for the caustic-leached, dewatered slurry as a function of pump speed. All distributions show a primary particle population that ranges from 0.3 to 20 µm. This primary population is characterized by a strong peak population centered between 1 and 2 µm, which decays rapidly to a shoulder population spanning 5 to 20 µm. At 4000 RPM, a strong secondary peak spanning 20 to 200 µm is observed. This secondary population has a maximum at 60 µm and is similar to secondary populations observed in previous samples.

Figure 5.39 shows changes that occur in the PSD for the caustic-leached, dewatered slurry as a result of sonication. Applying sonic energy appears to reduce the relative contribution of ~0.6- to 3-µm particles while increasing both the relative contributions of submicron (0.2 to 0.6 µm) and 3- to 20-µm particles/agglomerates. The increase in submicron particles is likely a result of sonic disruption of larger particles and agglomerates. The origin for the increase in 3- to 20-µm particles is less certain. Potential sources include sonic disruption of agglomerates in the 20- to 200-µm range and/or sonication induced aggregation. Of these two possibilities, the former seems more likely. After sonication is removed, a recovery is observed in the 0.6- to 3-µm population at the expense of particles in both the submicron and the 3- to 20-µm range. This recovery indicates that changes that occur in the PSD are recoverable and correspond to a change in the state of particle aggregation.
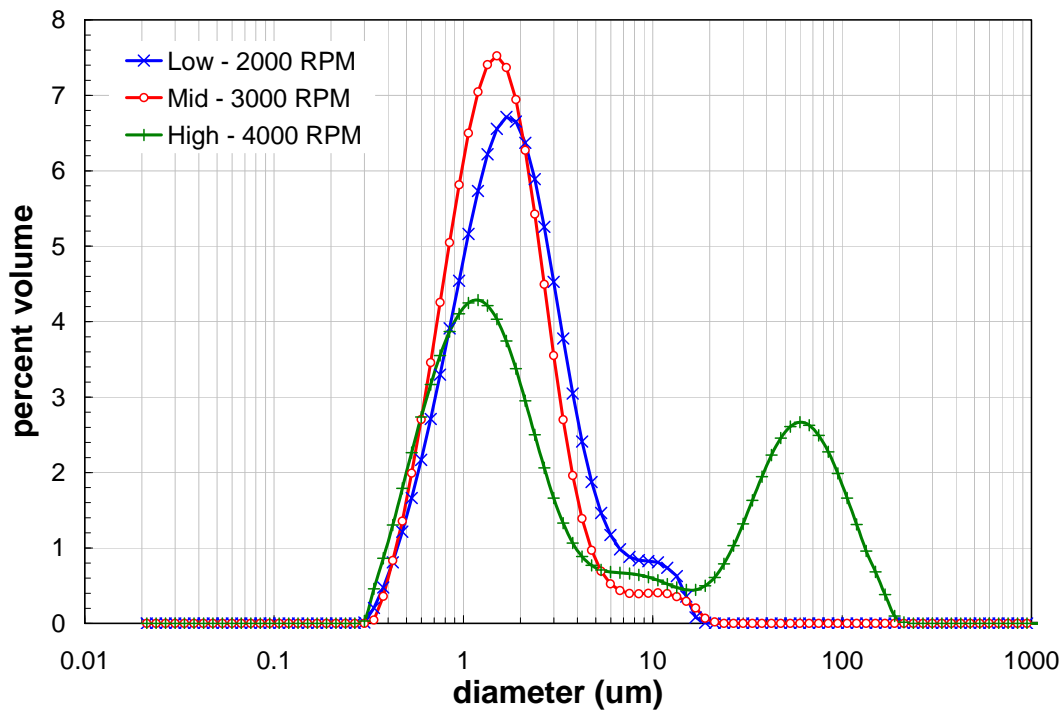
Figure 5.38. Caustic-Leached, Dewatered Slurry PSD as a Function of Pump Speed
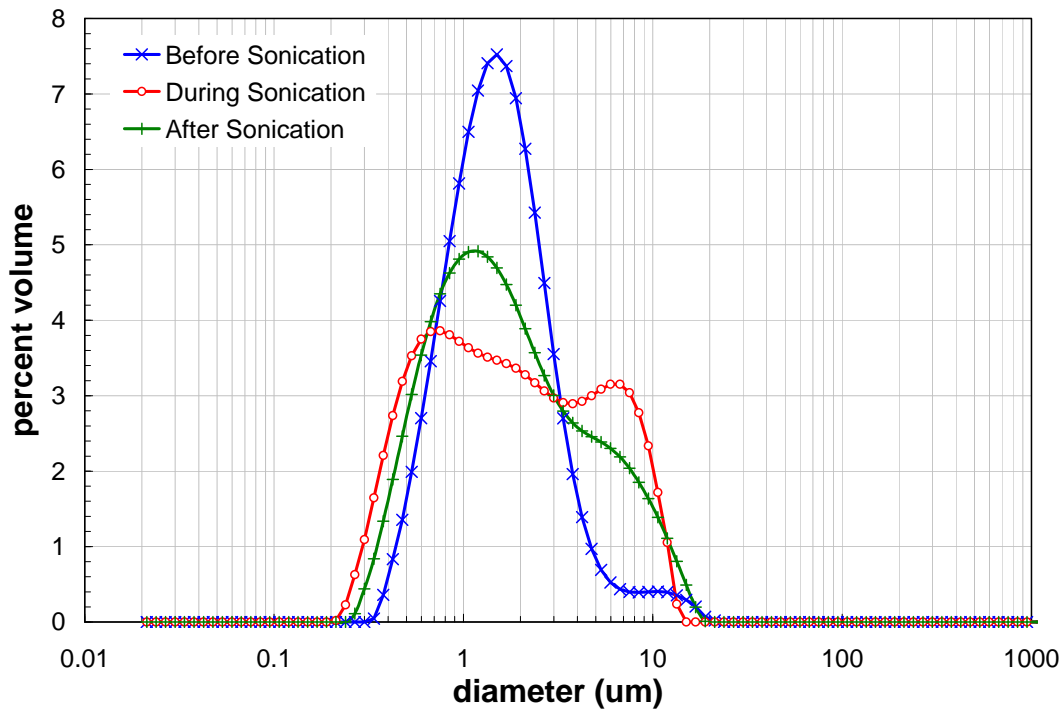
Figure 5.39. Caustic-Leached, Dewatered Slurry PSD as a Function of Sonication at 3000 RPM

Figure 5.40 shows the results of flow curve testing for the caustic-leached and dewatered slurry, which shows non-Newtonian behavior at all temperatures studied. The flow curves exhibited increasing yield stress with temperature. At 25°C, the yield stress was approximately 25 Pa, whereas at 60°C, it was approximately 50 Pa. Below 200 s^{-1}, all data showed strong downward curvature. Given the significant stress response for this sample (>20 Pa), the curvature at low shear is most likely a result of poor rotational sampling and sample elasticity. Beyond 200 s^{-1} the stress response was relatively linear, although the 60°C did show a slight downward curvature. Overall, the high-shear rate rheology is consistent with a Bingham-Plastic model.

Flow curve hysteresis is present in all flow-curve measurements. At 25° and 40°C, the hysteresis primarily occurs in the 100 to 200 s^{-1} range. Here, hysteresis likely resulted from excess material in the upper rotor recess being forced against the rotor wall by inertia and affecting an increase in the height of sheared material. For the 60°C measurement data, hysteresis is consistent with suspending phase evaporation effects.

As stated in the preceding paragraph, increased measurement temperatures observed higher yield stresses. At 25°, 40°, and 60°C, the yield stress for the caustic-leached and dewatered sample was approximately 25, 35, and 50 Pa. This increased yield stress could indicate an increase in the degree of solids structuring (i.e., aggregation) upon sample heating. However, given the significant hysteresis observed in the 60°C measurement, part (if not all) of the yield stress increase was likely a result of sample concentration through suspending phase evaporation. On the other hand, increased temperature resulted in a slight decrease in the flow curve slope. This is consistent with the pre-leach Group 1/2 slurry consistency behavior and is speculated to be a result of lowered suspending phase viscosity at higher temperatures.

Table 5.20 summarizes the best-fit rheological parameters for flow curve data for the leached dewatered slurry. The results in Table 5.20 confirm a number of the observations outlined in the preceding paragraphs. To be specific, they show that:

- The Bingham-Plastic and Herschel-Bulkley yield stresses ranged from 32 to 57 Pa and 13 to 37 Pa, respectively.

- Bingham-Plastic yield stress increased monotonically over the course of measurement. Similar behavior was observed in the Herschel-Bulkley yield stress. Given the current data, it is not possible to de-convolute the degree to which this change is driven by time, shear, and temperature.

- Bingham-Plastic consistency decreased from 29 mPa·s at 25°C to 23 mPa·s at 60°C.

Apparent viscosities at 33 s^{-1}, 100 s^{-1}, 500 s^{-1}, and 1000 s^{-1} were calculated using the Bingham-Plastic and Herschel-Bulkley fitting parameters in Table 5.20, as previously described. The results (Table 5.21) show that, depending on temperature, apparent viscosities typically range from 680 to 1800 mPa·s at 33 s^{-1}, 280 to 600 mPa·s at 100 s^{-1}, 89 to 140 mPa·s at 500 s^{-1}, and 57 to 81 mPa·s at 1000 s^{-1}. For the caustically leached, dewatered slurry, the apparent viscosity increased significantly (sometimes by a factor of nearly three) with increasing temperature.
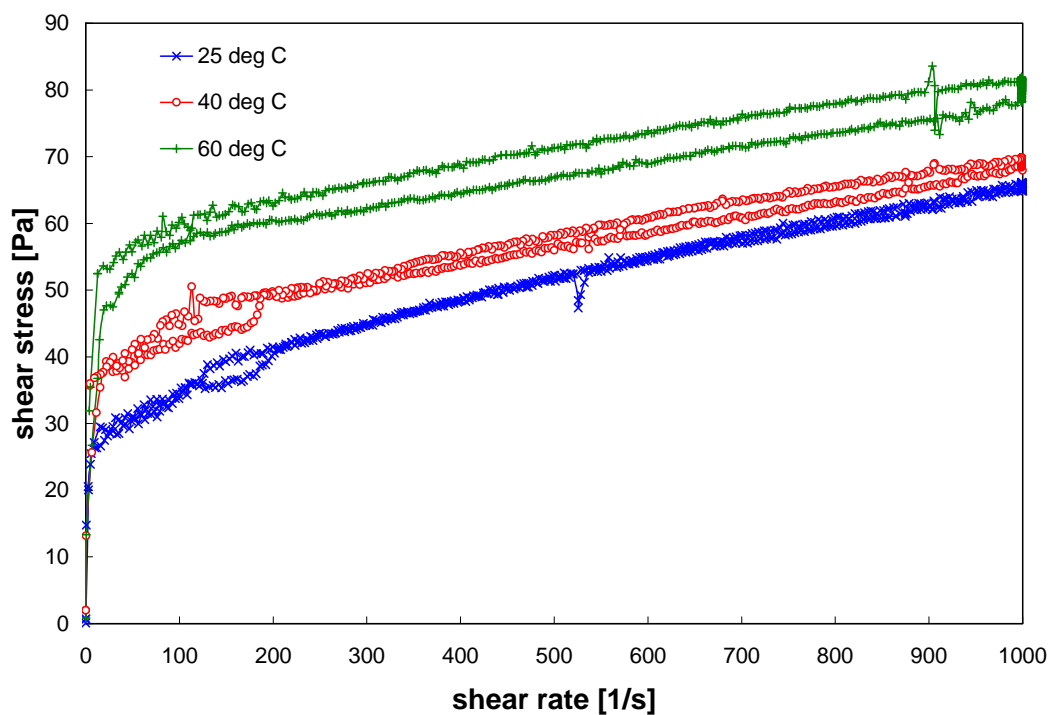
Figure 5.40. Flow Curve for the Group 1/2 CUF Caustic-Leached and Dewatered Slurry at 25, 40, and 60°C

Table 5.20. Results of Fitting Analysis for the Group 1/2 CUF Caustic-Leached and Dewatered Slurry

Model	Temperature [°C]	Yield Stress [Pa]	Consistency [Pa·s^n]	Flow Index	R
Bingham-Plastic (200 – 1000 s^{-1})	25 (1 of 2)	32	0.026	n/a	0.979
	25 (2 of 2)	37	0.029	n/a	0.997
	40	44	0.025	n/a	0.992
	60	57	0.023	n/a	0.961
Herschel-Bulkley (0 – 1000 s^{-1})	25 (1 of 2)	13	1.8	0.46	0.991
	25 (2 of 2)	19	1.6	0.49	0.996
	40	32	0.91	0.54	0.990
	60	37	3.5	0.36	0.963

Table 5.21. Apparent Viscosity of the Group 1/2 CUF Caustic-Leached and Dewatered Slurry

Source	Temperature [°C]	Apparent Viscosity [mPa·s]			
		@ 33 s^{-1}	@ 100 s^{-1}	@ 500 s^{-1}	@ 1000 s^{-1}
Measured	25 (1 of 2)	700	280	91	57
	25 (2 of 2)	900	340	100	66
	40	1200	430	110	70
	60	1600	590	140	81
Bingham-Plastic	25 (1 of 2)	980	340	89	57
	25 (2 of 2)	1100	400	100	66
	40	1400	470	110	70
	60	1800	600	140	81
Herschel-Bulkley	25 (1 of 2)	680	280	90	57
	25 (2 of 2)	850	340	100	65
	40	1200	430	120	69
	60	1500	560	140	80

5.5.4 Batch Caustic Washing

Figure 5.41 illustrates the material flow for the caustic washing steps. Following the caustic leach, the slurry was washed five times with decreasing concentrations of sodium hydroxide (0.56 M, 0.20 M, 0.06 M, 0.02 M, and 0.01 M). Over the course of the washing, 6.0 L were added to the CUF, while 5.6 L were removed. This increased the volume in the CUF by 0.4 L, while the circulating slurry mass stayed relatively the same due to changes in the supernate density. Grab samples of the filtered permeate were collected half-way between each dewatering step to assess the composition of the filtrate. The results were used to predict the slurry inventory and composition at each wash step, shown in Table 5.22 through Table 5.26
Table 5.26. The measured concentration of free hydroxide, radionuclides, and opportunistic ICP-OES analytes for each filtered wash solution is provided in Table 5.27.

Dewatered Leached Slurry
Slurry Mass: 1.6 kg
UDS Mass: 420 g
Slurry Volume: 1.1 L

Permeate Holdup
Mass: 0.25 kg
Volume: 0.2 L

Sample Slurry
Removed Slurry
Mass: 0.04 kg

Add 1st Wash
0.56 M NaOH
Mass: 1.21 kg

Add 2nd Wash
0.20 M NaOH
Mass: 1.19 kg

Add 3rd Wash
0.06 M NaOH
Mass: 1.19 kg

Dewater
Remove Permeate
Mass: 1.16 kg

Dewater
Remove Permeate
Mass: 1.26 kg

Dewater
Remove Permeate
Mass: 1.22 kg

Add 4th Wash
0.02 M NaOH
Mass: 1.19 kg

Add 5th Wash
0.01 M NaOH
Mass: 1.18 kg

Dewater
Remove Permeate
Mass: 1.21 kg

Dewater
Remove Permeate
Mass: 1.16 kg

Washed Leached Slurry
Slurry Mass: 1.6 kg
UDS Mass: 320 g
Slurry Volume: 1.5 L

Permeate Holdup
Mass: 0.21 kg
Volume: 0.2 L

Figure 5.41. Flow Diagram for Batch Caustic Washing
Note: Mass and volume values in figure are rounded to the nearest significant digit of accuracy.

Table 5.22. Group 1/2 Caustic leached Slurry Inventory and Composition after the First Wash

	Slurry[a]	Liquid Fraction[b]		Solids Fraction[c]	
Mass (kg)	1.84	1.43		0.41	
Wt% of Slurry	100%	77.7%		22.3%	
Metal	**g**	**g**	**µg/mL**	**g**	**µg/g**
Al	2.7E+01	2.8E+00	2.3E+03	2.4E+01	5.8E+04
Bi	1.8E+01	5.6E-02	4.5E+01	1.8E+01	4.4E+04
Cr	3.4E+00	1.5E-01	1.2E+02	3.3E+00	8.0E+03
Fe	2.5E+01	2.3E-03	1.9E+00	2.5E+01	6.0E+04
Mn	3.7E-01	5.3E-05	4.3E-02	3.7E-01	9.0E+02
Na	2.1E+02	9.3E+01	7.5E+04	1.2E+02	3.0E+05
P	3.7E+01	7.1E-01	5.8E+02	3.6E+01	8.8E+04
S	9.6E-01	1.6E+00	1.3E+03	-6.1E-01	-1.5E+03
Si	1.6E+01	1.1E-01	9.0E+01	1.6E+01	3.8E+04
Sr	1.5E+00	7.3E-05	5.9E-02	1.5E+00	3.6E+03
U	6.2E+00	1.3E-02	1.1E+01	6.2E+00	1.5E+04
Supernate Fraction					
Anion	**µg/mL**	**[M]**	**g**		
OH	3.8E+04	2.2E+00	4.7E+01		

(a) Slurry mass components were calculated from characterization data (Sections 3 and 4) and the masses of materials that were added with simulant. Loss of mass from sampling was incorporated.

(b) Liquid fraction mass components were calculated using analytical results from supernate sample TI552-G6-E (ASO ID 08-01309) and the predicted mass of supernate in the system.

(c) Solids fraction mass components were calculated from the difference between the slurry component mass and liquid component mass fraction.

Table 5.23. Group 1/2 Caustic Leached Slurry Inventory and Composition after the Second Wash

	Slurry[a]	Liquid Fraction[b]		Solids Fraction[c]	
Mass (kg)	1.77	1.38		0.39	
Wt% of Slurry	100%	77.9%		22.1%	
Metal	**g**	**g**	**µg/mL**	**g**	**µg/g**
Al	2.5E+01	1.6E+00	1.3E+03	2.4E+01	6.0E+04
Bi	1.8E+01	2.3E-02	1.8E+01	1.8E+01	4.6E+04
Cr	3.4E+00	9.2E-02	7.2E+01	3.3E+00	8.3E+03
Fe	2.5E+01	9.2E-02	7.2E+01	2.5E+01	6.3E+04
Mn	3.7E-01	1.5E-04	1.2E-01	3.7E-01	9.5E+02
Na	1.6E+02	1.4E+02	1.1E+05	2.1E+01	5.3E+04
P	3.5E+01	3.2E+00	2.5E+03	3.2E+01	8.1E+04
S	2.2E-01	3.0E+00	2.3E+03	-2.7E+00	-7.0E+03
Si	1.6E+01	6.4E-02	5.0E+01	1.6E+01	4.0E+04
Sr	1.5E+00	6.4E-02	5.0E+01	1.4E+00	3.6E+03
U	6.2E+00	6.4E-02	5.0E+01	6.1E+00	1.6E+04
Supernate Fraction					
Anion	**µg/mL**	**[M]**	**g**		
OH	2.2E+04	1.3E+00	2.8E+01		

(a) Slurry mass components were calculated from characterization data (Sections 3 and 4) and the masses of materials that were added with simulant. Loss of mass from sampling was incorporated.
(b) Liquid fraction mass components were calculated using analytical results from supernate sample TI552-G6-F (ASO ID 08-01310) and the predicted mass of supernate in the system.
(c) Solids fraction mass components were calculated from the difference between the slurry component mass and liquid component mass fraction.

Table 5.24. Group 1/2 Caustic Leached Slurry Inventory and Composition after the Third Wash

	Slurry[a]	Liquid Fraction[b]		Solids Fraction[c]	
Mass (kg)	1.75	1.41		0.34	
Wt% of Slurry	100%	80.5%		19.5%	
Metal	**g**	**g**	**µg/mL**	**g**	**µg/g**
Al	2.5E+01	5.8E-01	4.4E+02	2.4E+01	7.1E+04
Bi	1.8E+01	1.2E-02	8.9E+00	1.8E+01	5.3E+04
Cr	3.3E+00	3.8E-02	2.9E+01	3.3E+00	9.6E+03
Fe	2.5E+01	< 4.E-4	< 3.E-1	2.5E+01	7.2E+04
Mn	3.7E-01	< 4.E-5	< 3.E-2	3.7E-01	1.1E+03
Na	1.3E+02	3.8E+01	2.9E+04	9.5E+01	2.8E+05
P	2.9E+01	6.4E+00	4.9E+03	2.3E+01	6.8E+04
S	2.2E-01	3.8E-01	2.9E+02	-1.6E-01	-4.5E+02
Si	1.6E+01	3.0E-02	2.3E+01	1.6E+01	4.6E+04
Sr	1.5E+00	5.4E-05	4.1E-02	1.5E+00	4.4E+03
U	6.2E+00	< 5.E-3	< 4.E+0	6.2E+00	1.8E+04
Supernate Fraction					
Anion	**µg/mL**	**[M]**	**g**		
OH	1.0E+04	6.0E-01	4.7E+01		

(a) Slurry mass components were calculated from characterization data (Sections 3 and 4) and the masses of materials that were added with simulant. Loss of mass from sampling was incorporated.

(b) Liquid fraction mass components were calculated using analytical results from supernate sample TI552-G6-G (ASO ID 08-01311) and the predicted mass of supernate in the system.

(c) Solids fraction mass components were calculated from the difference between the slurry component mass and liquid component mass fraction.

Table 5.25. Group 1/2 Caustic leached Slurry Inventory and Composition after the Fourth Wash

	Slurry[a]	Liquid Fraction[b]		Solids Fraction[c]	
Mass (kg)	1.73	1.41		0.32	
Wt% of Slurry	100%	81.4%		18.6%	
Metal	**g**	**g**	**µg/mL**	**g**	**µg/g**
Al	2.5E+01	2.9E-01	2.2E+02	2.4E+01	7.6E+04
Bi	1.8E+01	5.3E-03	4.0E+00	1.8E+01	5.7E+04
Cr	3.3E+00	1.9E-02	1.4E+01	3.3E+00	1.0E+04
Fe	2.5E+01	1.2E-04	8.7E-02	2.5E+01	7.7E+04
Mn	3.7E-01	4.3E-05	3.2E-02	3.7E-01	1.2E+03
Na	1.1E+02	2.5E+01	1.9E+04	8.7E+01	2.7E+05
P	2.5E+01	5.7E+00	4.2E+03	1.9E+01	5.9E+04
S	2.2E-01	1.6E-01	1.2E+02	5.8E-02	1.8E+02
Si	1.6E+01	6.1E-02	4.6E+01	1.5E+01	4.8E+04
Sr	1.5E+00	3.1E-05	2.3E-02	1.5E+00	4.6E+03
U	6.2E+00	2.4E-03	1.8E+00	6.2E+00	1.9E+04
Supernate Fraction					
Anion	**µg/mL**	**[M]**	**g**		
OH	6.3E+03	3.7E-01	8.5E+00		

(a) Slurry mass components were calculated from characterization data (Sections 3 and 4) and the masses of materials that were added with simulant. Loss of mass from sampling was incorporated.
(b) Liquid fraction mass components were calculated using analytical results from supernate sample TI552-G6-H (ASO ID 08-01312) and the predicted mass of supernate in the system.
(c) Solids fraction mass components were calculated from the difference between the slurry component mass and liquid component mass fraction.

Table 5.26. Group 1/2 Caustic leached Slurry Inventory and Composition after the Fifth Wash

	Slurry[a]	Liquid Fraction[b]		Solids Fraction[c]	
Mass (kg)	1.75	1.43		0.32	
Wt% of Slurry	100%	81.7%		18.3%	
Metal	**g**	**g**	**µg/mL**	**g**	**µg/g**
Al	2.4E+01	1.7E-01	1.2E+02	2.4E+01	7.6E+04
Bi	1.8E+01	< 1.E-3	< 7.E-1	1.8E+01	5.7E+04
Cr	3.3E+00	1.1E-02	7.7E+00	3.3E+00	1.0E+04
Fe	2.5E+01	2.3E-04	1.6E-01	2.5E+01	7.7E+04
Mn	3.7E-01	1.7E-05	1.2E-02	3.7E-01	1.2E+03
Na	1.0E+02	1.4E+01	9.5E+03	8.7E+01	2.7E+05
P	2.2E+01	3.1E+00	2.1E+03	1.9E+01	5.9E+04
S	1.5E-01	9.2E-02	6.3E+01	5.7E-02	1.8E+02
Si	1.6E+01	2.4E-02	1.7E+01	1.5E+01	4.8E+04
Sr	1.5E+00	1.6E-05	1.1E-02	1.5E+00	4.6E+03
U	6.2E+00	< 3.E-6	< 2.E-3	6.2E+00	1.9E+04
Radiochemical Isotopes	**Slurry**	**Liquid Fraction**		**Solid Fraction**	
	mCi	**mCi**	**mCi/mL**	**mCi**	**mCi/g**
Co-60	4.8E+00	< 3.E-2	< 2.E-5	4.8E+00	1.5E-02
Cs-137	3.3E+04	3.2E+02	2.2E-01	3.2E+04	1.0E+02
Eu-154	1.4E+01	< 6.E-2	< 4.E-5	1.4E+01	4.5E-02
Am-241	1.3E+02	< 6.E-1	< 4.E-4	1.3E+02	4.1E-01
Gross Alpha	2.5E+02	< 9.E-1	< 6.E-4	2.5E+02	7.8E-01
Gross Beta	1.5E+05	3.1E+02	2.1E-01	1.5E+05	4.8E+02
Sr-90	5.9E+04	3.8E-01	2.6E-04	5.9E+04	1.8E+02
Pu-239+240	1.8E+02	< 2.E-3	< 1.E-6	1.8E+02	5.5E-01
Pu-238	6.0E+00	< 1.E-3	< 8.E-7	6.0E+00	1.9E-02
Anions	**Liquid Fraction**			**Leached Solids Fraction**	
	µg/mL	**[M]**	**g**	**µg/g**	**g**
F	8.6E+02	4.5E-02	1.2E+00	6.0E+03	1.9E+00
C₂O₄	2.0E+02	2.2E-03	2.9E-01	1.9E+03	5.9E-01
NO₂	5.8E+01	1.3E-03	8.4E-02	5.3E+02	1.7E-01
NO₃	1.5E+03	2.4E-02	2.2E+00	1.6E+04	5.3E+00
SO₄	1.6E+02	1.6E-03	2.3E-01	1.3E+03	4.2E-01
PO₄	6.7E+03	7.1E-02	9.7E+00	3.3E+04	1.1E+01
OH	3.3E+03	1.9E-01	4.8E+00		

(a) Slurry mass components were calculated from characterization data (Sections 3 and 4) and the masses of materials that were added with simulant. Loss of mass from sampling was incorporated.
(b) Liquid fraction mass components were calculated using analytical results from supernate sample TI552-G6-I (ASO ID 08-01292) and the predicted mass of supernate in the system.
(c) Solids fraction mass components were calculated from the difference between the slurry component mass and liquid component mass fraction.

Table 5.27. Caustic Wash Solutions Radionuclide and Opportunistic Compositions

	Wash 1	Wash 2	Wash 3	Wash 4	Wash 5	Composite Wash
ASO Sample ID	08-01309	08-01310	08-01311	08-01312	08-01292	08-01293
Density[a], g/mL>	1.15	1.09	1.07	1.05	1.03	NA
Analyte						
free OH, M	2.21 M	1.29 M	0.60 M	0.37 M	0.19 M	0.92 M
Analyte	μCi/mL	μCi/mL	μCi/mL	μCi/mL	μCi/mL	μCi/mL
^{137}Cs					2.17E-1	1.42E+0
^{60}Co					< 2.E-5	< 2.E-5
^{241}Am					< 4.E-4	< 1.E-3
^{90}Sr					2.62E-4	1.11E-3
^{238}Pu					< 8.E-7	< 1.E-6
$^{239+240}$Pu					< 1.E-6	6.07E-6
Gross alpha					< 6.E-4	< 7.E-4
Gross beta					2.10E-1	1.27E+0
^{154}Eu					< 4.E-5	< 8.E-5
Opportunistic Analytes						
Analyte	μg/mL	μg/mL	μg/mL	μg/mL	μg/mL	μg/mL
Ag	<2.6E-1	<2.6E-1	<2.6E-1	<5.1E-2	<5.1E-2	<5.1E-2
As	<5.2E+0	<5.3E+0	<5.4E+0	<1.1E+0	<1.1E+0	<1.0E+0
Ba	[0.22]	[0.22]	[0.21]	0.143	[0.12]	0.175
Be	[0.035]	[0.022]	[0.0074]	[0.0018]	[0.0018]	[0.0071]
Ca	[1.4]	12.0	[0.85]	[0.24]	[0.60]	<1.5E-1
Ce	<1.2E+0	<1.2E+0	<1.2E+0	<2.5E-1	<2.4E-1	<2.4E-1
Co	[1.20]	[0.53]	<3.0E-1	<5.9E-2	<5.9E-2	<5.8E-2
Cu	[0.66]	[0.45]	[0.27]	<3.4E-2	<3.4E-2	[0.098]
Dy	<3.5E-1	<3.6E-1	<3.6E-1	<7.1E-2	<7.1E-2	<7.0E-2
Eu	<1.3E-1	<1.4E-1	<1.4E-1	<2.7E-2	<2.7E-2	<2.7E-2
La	<3.4E-1	<3.4E-1	<3.5E-1	<6.9E-2	<6.9E-2	<6.8E-2
Li	[0.77]	[0.99]	[0.70]	[0.25]	[0.21]	0.347
Mg	<2.8E-1	<2.8E-1	<2.9E-1	<5.6E-2	<5.6E-2	<5.6E-2
Mo	[1.2]	<6.4E-1	<6.5E-1	<1.3E-1	[0.18]	[0.72]
Nd	<6.6E-1	<6.6E-1	<6.7E-1	<1.3E-1	<1.3E-1	[0.18]
Pb	[6.5]	<3.9E+0	<4.0E+0	<7.8E-1	<7.8E-1	[2.0]
Pd	[1.3]	<7.7E-1	[1.5]	[0.38]	<1.5E-1	[0.16]
Rh	[2.2]	<1.5E+0	<1.5E+0	<2.9E-1	[0.32]	[0.31]
Ru	<1.0E+0	<1.0E+0	<1.1E+0	<2.1E-1	<2.1E-1	<2.1E-1

Table 5.27 (Contd)

	Wash 1	Wash 2	Wash 3	Wash 4	Wash 5	Composite Wash
ASO Sample ID	08-01309	08-01310	08-01311	08-01312	08-01292	08-01293
Opportunistic Analytes						
Analyte	µg/mL	µg/mL	µg/mL	µg/mL	µg/mL	µg/mL
Sb	[6.3]	<2.5E+0	<2.5E+0	<4.9E-1	[0.92]	<4.8E-1
Se	[34.5]	[34]	[40]	[5.9]	[2.7]	<1.7E+0
Sn	[11.2]	[8.5]	[5.6]	<6.6E-1	<6.6E-1	[2.1]
Ta	<2.1E+0	<2.1E+0	<2.1E+0	<4.2E-1	<4.2E-1	<4.1E-1
Te	<3.2E+0	<3.2E+0	<3.2E+0	<6.4E-1	[0.90]	[0.75]
Th	[1.50]	[1.9]	[1.4]	<2.4E-1	<2.4E-1	<2.4E-1
Ti	<5.2E-2	[0.073]	<5.4E-2	<1.1E-2	<1.1E-2	[0.017]
Tl	<4.6E+0	<4.7E+0	<4.7E+0	<9.3E-1	<9.3E-1	<9.2E-1
V	[0.40]	[0.30]	[0.55]	0.185	[0.058]	[0.091]
W	[3.10]	<2.3E+0	<2.4E+0	<4.7E-1	[0.54]	[1.5]
Y	<5.3E-2	<5.4E-2	<5.5E-2	<1.1E-2	<1.1E-2	<1.1E-2

(a) Density values were obtained from the mass flow meter, which had not been calibrated to NQA-1 standards; they are reported for information only.
ASR 8113 Reference date: November 5, 2007.
Analyte uncertainties were typically within ±15%; results in brackets indicate that the analyte concentrations were greater than the method detection limit (MDL) and less than the estimated quantitation limit (EQL), and uncertainties were >15%.
Opportunistic analytes are reported for information only; QC requirements did not apply to these analytes.

The leached slurry consisted of 43 grams of insoluble aluminum, which was reduced to 23 to 24 grams of solid aluminum following the caustic leach, or a 45-wt% leach. After dewatering the caustic-leached slurry and performing five volumetric washes afterwards, the total aluminum in the slurry was reduced from an initial (low solids) value of 50 grams to a pre oxidative leach value of 23 total slurry grams (54%). No aluminum dissolved during oxidative leaching and washing as the total aluminum remained constant throughout the balance of the CUF testing. Over the course of the test, it was estimated that 4.6 grams of aluminum present in the slurry was lost from sampling, which was about 9 wt% of the original inventory present in the low-solids slurry. Figure 5.42 charts the mass change of the aluminum inventory normalized to the original slurry inventory to project the predicted inventory if no sampling occurred. Without sampling, the projected change in aluminum inventory after the fifth wash would be 45 wt%.

Unlike aluminum, the phosphorus inventory did not change significantly during the caustic leach and dewatering step. After dewatering the slurry, approximately 37 grams of insoluble phosphorus was present with almost none in the liquid phase. As the sodium concentration decreased in the slurry supernate, the mass of isolable phosphorus decreases as the solubility of sodium phosphate increases in the supernate. After the fifth wash, the quantity of insoluble phosphorus in the slurry decreased to 19 grams, which provided an estimated leach/wash factor of 49 wt%. It was estimated that the total mass of insoluble solids in the slurry decreased by 90 grams because the sodium phosphate dissolved. However, this term could be higher if the salt precipitated as a hydrated version of the salt. By this point of the test, 9 wt% of the original slurry was lost to sampling, decreasing the inventory by 5 grams.

Figure 5.43 plots the mass change of phosphorus inventory normalized to the original slurry inventory to project the predicted inventory if no sampling occurred. Without sampling, the projected change in phosphorus inventory after the fifth wash was 39 wt%.

The total chromium in the slurry decreased during caustic leaching and washing from 4.3 grams to 3.3 grams (23%). This is likely due to the oxidation of some Cr^{3+} to Cr^{6+} by adventitious oxygen and dewatering it with the existing water-soluble chromium in the slurry (WTP-RPT-173, Lumetta 2008). Taking slurry sampling into account, comparing the caustic-leached and washed-slurry composition (Table 5.26) to that of the high-solids slurry inventory just before caustic leaching (
Table 5.10) revealed no appreciable decrease in any radionuclide aside from an ~40% drop in cesium and a 9-wt% loss from the slurry transfer.
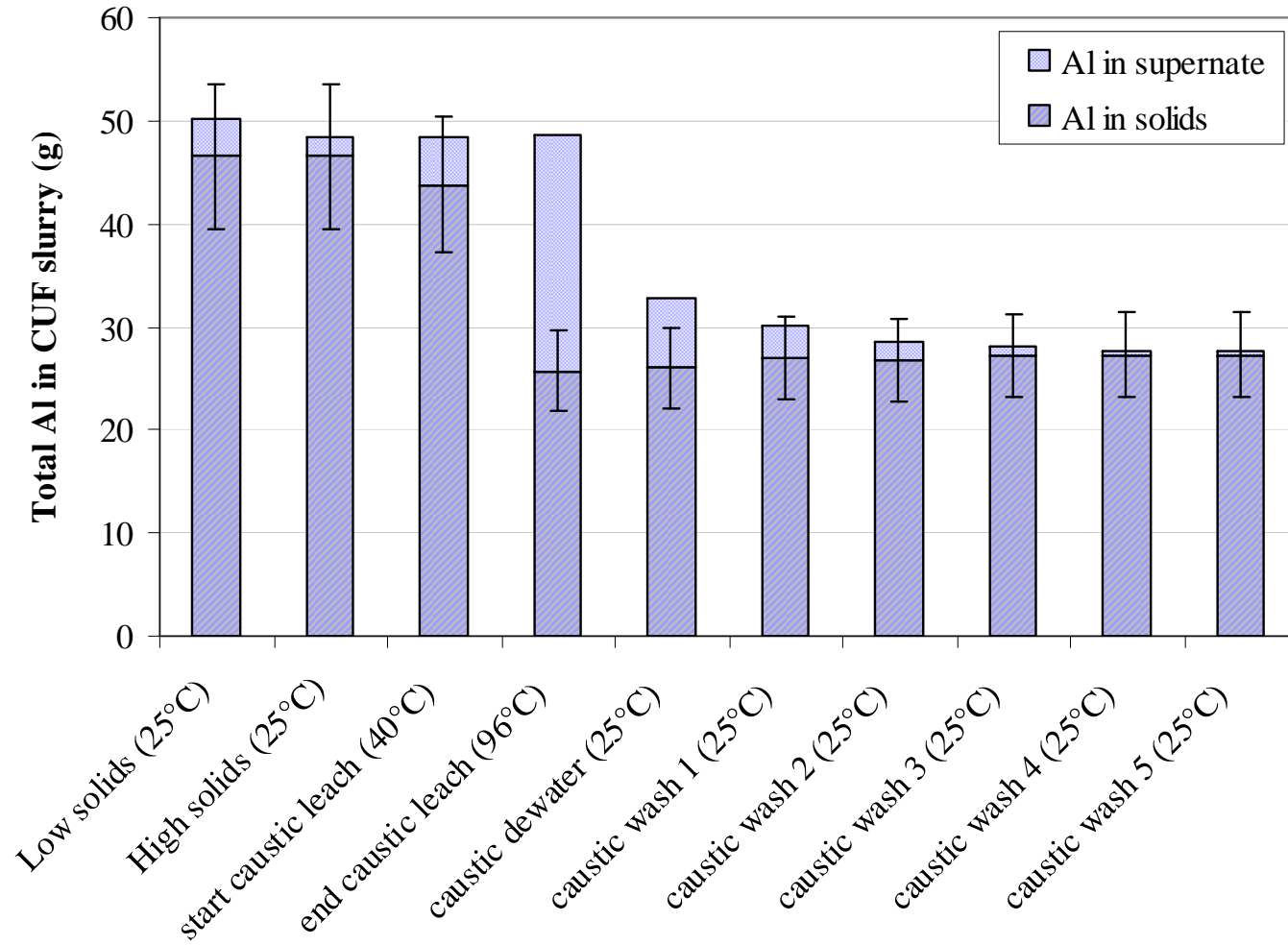
*Temperatures on X-axis represent the slurry temperature when sampled

Figure 5.42. Normalized Aluminum Inventory in Group 1/2 Slurry through Caustic Leach and Washing
(Inventory in Figure Normalized to Eliminate Sample Loss Impacts)
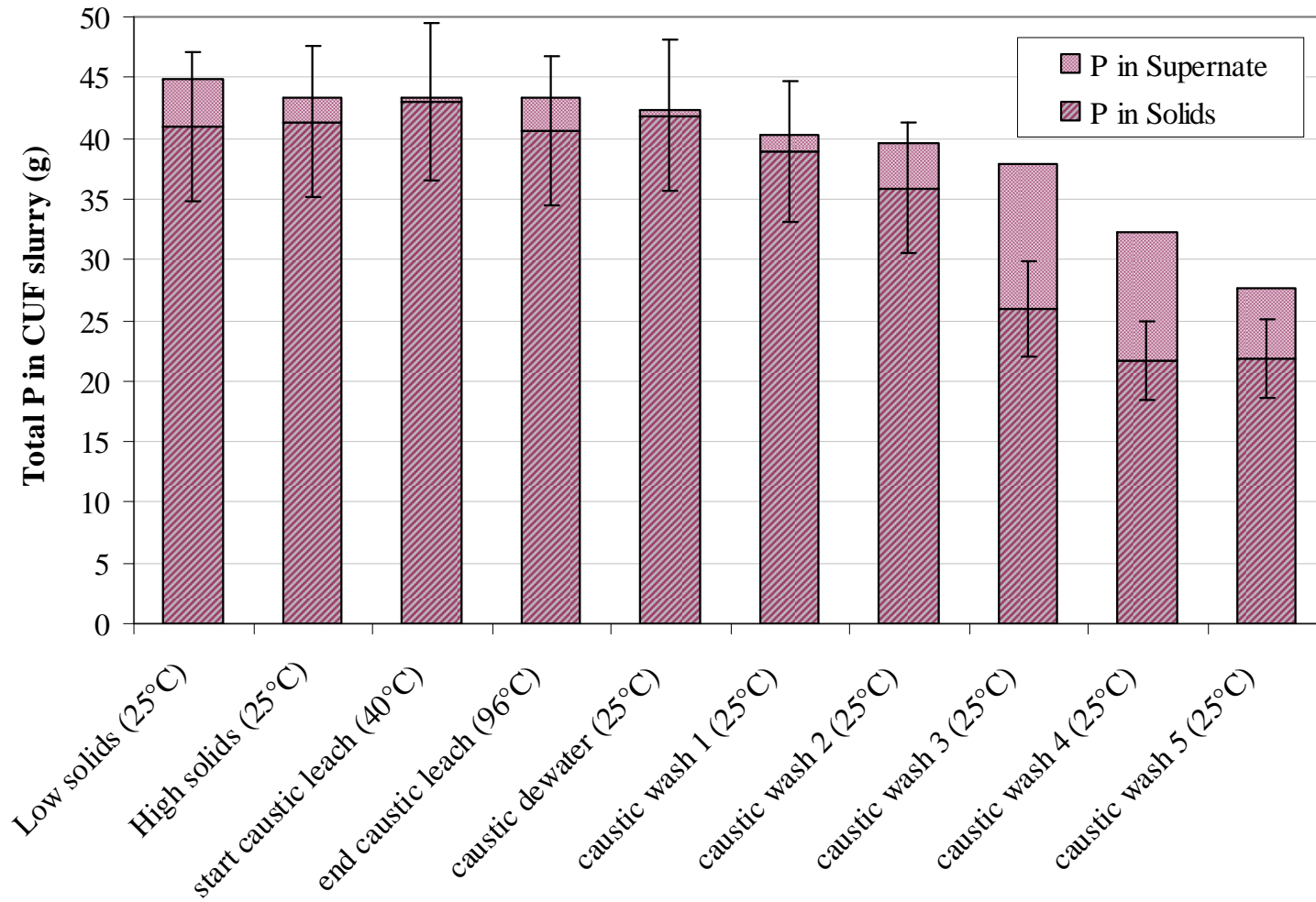
*Temperatures on X-axis represent the slurry sample temperature

Figure 5.43. Normalized Phosphorus Inventory in Group 1/2 Slurry through Caustic Leach and Washing
(Inventory in Figure Normalized to Eliminate Sample Loss Impacts)

5.5.5 Characterization of the Washed Caustic-Leached Slurry

After completing the fifth wash, the circulation slurry was sampled for physical and chemical analyses, as shown in Figure 5.44. Overall, 110 grams of the circulating slurry was removed containing an estimated 20 grams of UDS.

The physical properties of the washed slurry are detailed in Table 5.28. It should be noted that the solids in the slurry appeared flocculent and did not settle within 24 hours (as can be seen by the 96% settled solids value). The measured UDS of the slurry was again lower than the predicted UDS of the slurry (0.32 kg ÷ 1.6 kg ≅ 20 wt%). The analytical results for the composition of the washed caustic-leached slurry are provided in Table 5.29. Comparing the solid composition to that developed from mass balance calculations in Table 5.26 shows significant differences. Overall, the slurry analysis predicts the concentration to be higher for almost all the elements, indicating that more of the insoluble solids dissolved during washing. The exception to this was for phosphorus, which was almost six times lower than the mass balance calculation indicated. The leach-factor calculation for phosphorus was 0.94. The calculated leach factor for phosphorus is almost two times greater than the leach factor calculated from the mass balance results in the previous section, which was only 0.49. Besides phosphorus, the leach factor for ^{238}Pu was calculated to be 0.28. However, the leach factor is not significantly different from the analytical error for the analyte, which was 24% for the high solids composition.
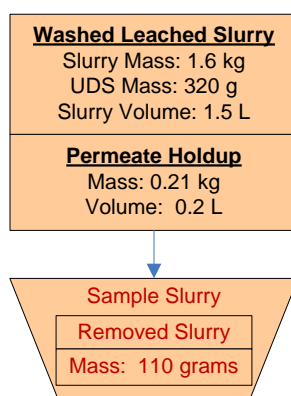
Figure 5.44. Sampling of the Washed Leached Slurry
Note: Mass and volume values in figure are rounded to the nearest significant digit of accuracy.

Table 5.28. Physical-Property Measurements of the Group 1/2 Caustic-Leached and Washed Slurry

Slurry Density (g/mL)	1.07
Supernate Density (g/mL)	0.98
Settled Solids (Vol%)	96%
Centrifuged UDS (Wt%)	32%
Total Solids of the Slurry (Wt%)	14%
Dissolved Solids of the Supernate (Wt%)	2.7%
UDS of the Slurry (Wt%)	11%

Table 5.29. Group 1/2 Washed Leach Slurry Composition and Caustic Leach Factor Calculations Based on ICP-OES/Radiochemical Characterization

Slurry Prep Method	ICP-OES Analytes	Dry Slurry[a] (µg/g)	Supernate[b] (µg/mL)	Dry Solids[c] (µg/g)	Solids Leach Factor[d]
	Al	80,250	115	96,136	0.52
	Bi	80,200	<7.3E-1	96,970	0.09
	Cd	125	<8.3E-2	150	-0.27
	Cr	13,300	7.65	16,022	0.02
	Fe	105,350	[0.16]	127,386	NA
	K	[140]	[5.4]	[127]	1.31
	Mn	1,625	[0.012]	1,965	-0.03
	Na	165,000	9,540	124,813	0.70
	Ni	5,690	<5.9E-2	6,880	0.12
	P	22,950	2,130	11,072	0.94
	S	[1,650]	63.1	[1,501]	1.16
	Si	84,700	16.5	102,288	-0.02
	Sr	6,030	[0.011]	7,291	-0.01
	U	26,850	<7.8E-1	32,460	NA
HF Assisted Acid Digestion, and KOH Fusion, Concentration Factor of 2.01 based on U and Fe	**Zn**	507	[0.50]	609	0.44
	Zr	580	<2.7E-2	701	-0.72
	Ag	20.1	<5.1E-2	23.9	-0.07
	Ba	357	[0.12]	431	0.09
	Be	0.839	[0.0018]	1.000	0.58
	Ca	12,800	[0.60]	15,473	0.09
	Ce	333	<2.4E-1	401	-0.07
	Co	55.9	<5.9E-2	67.1	0.21
	Cu	113	<3.4E-2	136	0.40
	La	56.0	<6.9E-2	67.2	0.03
	Li	91.4	[0.21]	108.8	0.22
	Mg	2,250	<5.6E-2	2,720	0.06
	Mo	[45]	[0.18]	[52]	[0.34]
	Nd	73.5	<1.3E-1	87.8	0.01
	Pb	1,970	<7.8E-1	2,376	0.13
	Ru	[25]	[0.32]	[28]	[0.40]
	Th	[45]	[0.90]	[47]	[98.97]
	Ti	249	<2.4E-1	299	0.01
	Tl	<9.4E+1	<1.1E-2	<1.1E+2	NA
	V	39.3	<9.3E-1	40.2	-0.21
	Y	10.9	<1.1E-2	13.1	-0.01

Table 5.29 (Contd)

Slurry Prep Method	Radionuclides	Dry Slurry[a] (µCi/g)	Supernate[b] (µCi/mL)	Dry Solids[c] (µCi/g)	Solids Leach Factor[d]
KOH Fusion, Concentration Factor of 2.01 based on U and Fe	Co-60	1.19E-1	<2.E-5	1.4E-1	-5.16
	Cs-137	1.30E+2	2.17E-1	1.6E+2	0.28
	Eu-154	9.07E-2	<4.E-5	1.1E-1	-2.19
	Eu-155	<6.E-2	<2.E-4	<7.E-2	NA
	Am-241	5.40E-1	<4.E-4	6.5E-1	-0.04
	Total alpha	1.38E+0	<6.E-4	1.7E+0	-0.23
	Total beta	7.23E+2	2.10E-1	8.7E+2	-0.31
	Sr-90	2.89E+2	2.62E-4	3.5E+2	-0.16
	Pu-239/240	6.96E-1	<1.E-6	8.4E-1	-0.16
	Pu-238	1.17E-2	<8.E-7	1.4E-2	0.29

(a) Test sample TI572-G2-I, ASO ID 08-01292
(b) Test sample TI572-G2-12, ASO ID 08-01319
(c) Calculated using results from TI572-G2-I and TI572-G2-12
(d) Calculated using results listed in
(e) Table 5.11
Note: Analytes in italics were measured opportunistically. Values in brackets [ ] are ≥ MDL but < EQL, with errors likely to exceed 15%.

Figure 5.45 shows the pre-sonication PSD for the caustic-leached, washed slurry as a function of pump speed. The distribution was characterized at all pump speeds by a strong primary peak centered at ~1 µm and spanning 0.3 to 3 µm. In all cases, small population peaks were observed over 5 to 200 µm. These secondary peaks may correspond to loose particle flocs.

Figure 5.46 shows the effect of sonication on the size distribution of the caustic-leached, washed slurry. A significant drop in the relative contribution of 0.6- to 2-µm particles was observed after applying sonic energy. This drop was accompanied by a dramatic increase in the relative volume contribution of 0.1- to 0.6-µm particles and 2- to 10-µm particles. Although the original 1-µm particle population peak appeared to be preserved in a small peak over the range 1 to 2 µm, a new dominant population formed at ~0.3 µm. The increased submicron fraction was likely formed by sonic disruption of particles. The origin for the increased 2 to 10 µm fractions was likely sonic disruption of the 5- to 200-µm floc populations. The increase in the population of 2 to 10 µm particles continued after sonication was removed and may indicate the partial recovery of some flocs.
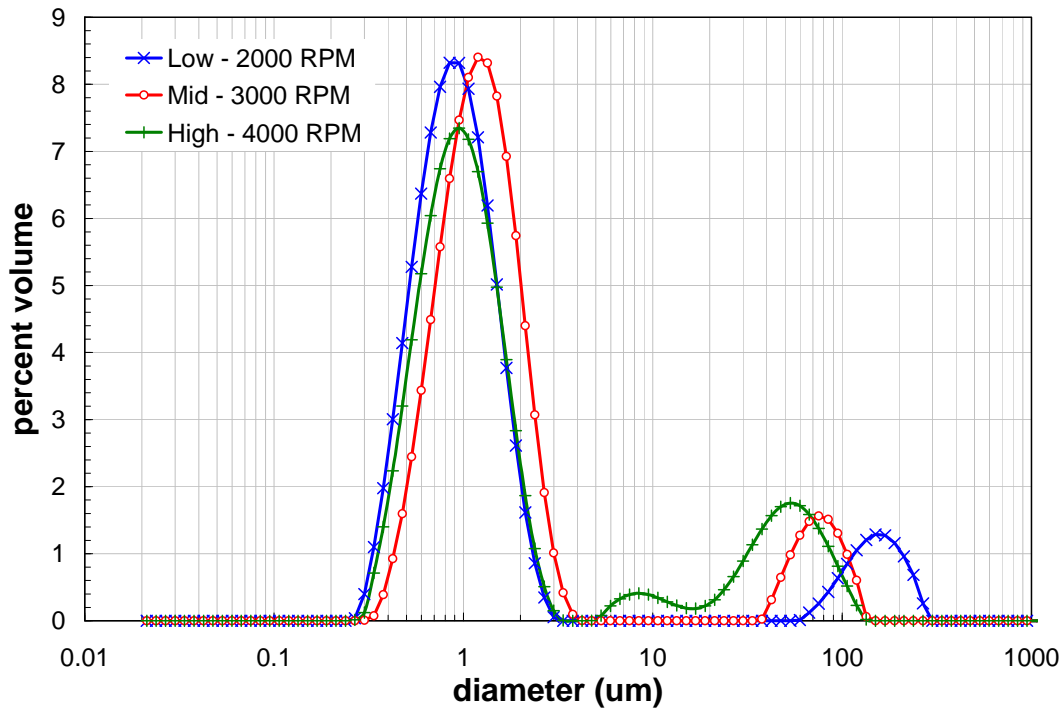
Figure 5.45. Caustic-Leached, Washed Slurry PSD as a Function of Pump Speed
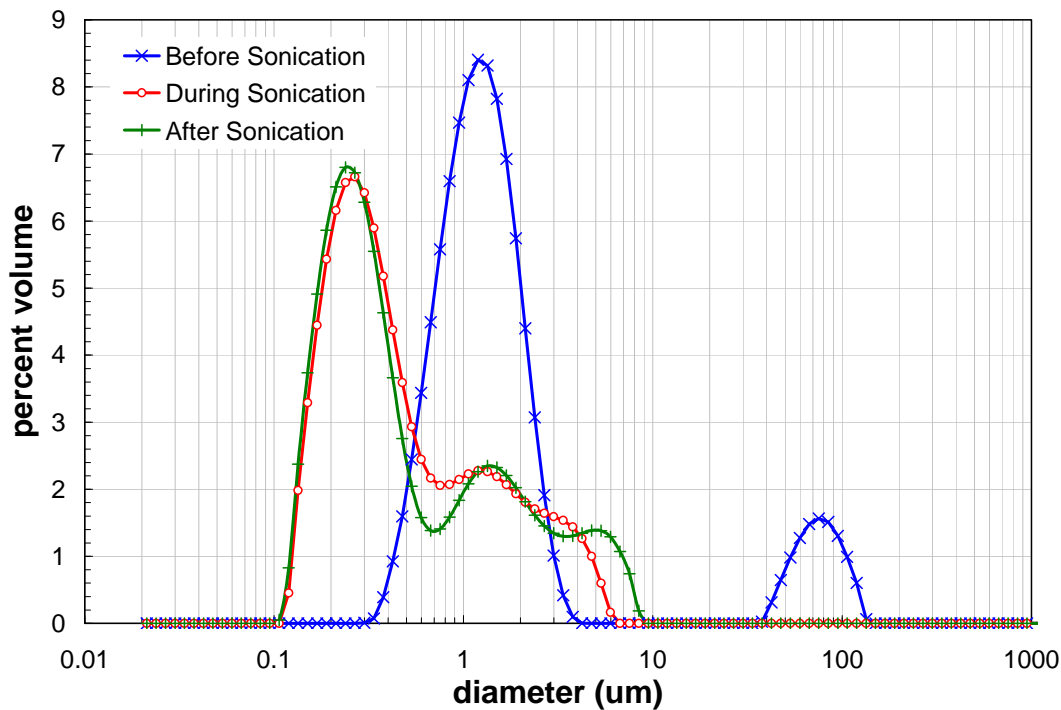
Figure 5.46. Caustic-Leached, Washed Slurry PSD as a Function of Sonication at 3000 RPM

Figure 5.47 shows the results of flow curve testing for the caustic-leached, dewatered, and washed slurry, which shows non-Newtonian behavior at all temperatures studied. The three flow curves showed finite yield stresses that fall around 4 to 6 Pa. The stress response over 0 to 1000 s^{-1} is mostly linear; however, the 25°C may have a slight downward curvature. The flow curves appear to be relatively free of artifacts caused by poor rotational sampling; strong curvature in the low-shear region is limited to shear rates below ~30 s^{-1}.

Flow curve hysteresis is present in the 25° and 40°C measurement data but is absent in the 60°C measurement data. This type of hysteresis is consistent with long-term shear breakup of particle agglomerates within the sample. The absence of shear hysteresis at 60°C, where evaporation of the suspending phase is usually significant, suggests that evaporation does not effect significant changes in the bulk rheology of this sample.

Flow curve yield stress and slope both decrease monotonically with increasing temperature. Given the noise and hysteresis in the low-shear data, it is difficult to determine if the change in yield stress is significant from qualitative examination of the flow curve data alone. Based on the fact that the data appear to overlap below 100 s^{-1}, the change is likely not significant (although quantitative evaluation may indicate otherwise). There appears to be a statistically significant drop in slurry consistency (i.e., flow curve slope) between 25° and 40°C. The decrease in slope continues from 40 and 60°C but is much less than observed over the first temperature jump.

Table 5.30 summarizes the best-fit rheological parameters for flow curve data for the leached and washed slurry. The fitting parameters confirm a number of the observations made above. In particular, they show that:

- The Bingham-Plastic and Herschel-Bulkley yield stresses range from 5.0 to 7.9 Pa and 4.6 to 6.1 Pa (depending on temperature), respectively. Because the maximum difference between the yield stresses at different temperatures is greater than 0.5 Pa, the variance is most likely significant. On the other hand, the final three regressed values of the Herschel-Bulkley yield stress (i.e., those at 25 [2 of 2], 40, and 60°C) all agree within the experimental limit of accuracy. Given the large degree of flow curve hysteresis, basing the significance solely off of the instrument limit of ±0.5 Pa may not be appropriate in this case.

- In terms of temperature dependence, the yield stress shows a monotonic decrease in magnitude as the temperature is increased from 25° to 60°C.

- The Bingham-Plastic consistency decreases from 11 mPa·s at 25°C to 5.4 mPa·s at 60°C. This decrease is consistent with the temperature-dependence observations made in the preceding paragraph and is likely a result of the suspending phase viscosity decrease.

- The Herschel-Bulkley flow indices are all near 0.7 to 0.9. This indicates some degree of non-linearity in the flow curve fit. However, based on the fit shown in Table 5.30, the Herschel-Bulkley fit favors the down-ramp and does not appear to be an appropriate average of both up- and down-ramp data. The cause of this fitting deficiency may be the strong downward curvature in the low-shear region (i.e., below 30 s^{-1}), resulting from poor rotational sampling. The overall result is that the Herschel-Bulkley fits show more curvature than appears appropriate, such that the 0.7 to 0.9 flow indexes are overstated and would be closer to unity if the poor rotational-sampling-data artifacts were eliminated.

Apparent viscosities at 33 s^{-1}, 100 s^{-1}, 500 s^{-1}, and 1000 s^{-1} were calculated using the Bingham-Plastic and Herschel-Bulkley fitting parameters in Table 5.30, as previously described. The results (Table 5.31) show

that apparent viscosities typically range from 150 to 300 mPa·s at 33 s⁻¹, 54 to 97 mPa·s at 100 s⁻¹, 15 to 28 mPa·s at 500 s⁻¹, and 10 to 19 mPa·s at 1000 s⁻¹. Both measured apparent viscosities and those calculated from fitting parameters decrease with increasing temperature and shear rate.
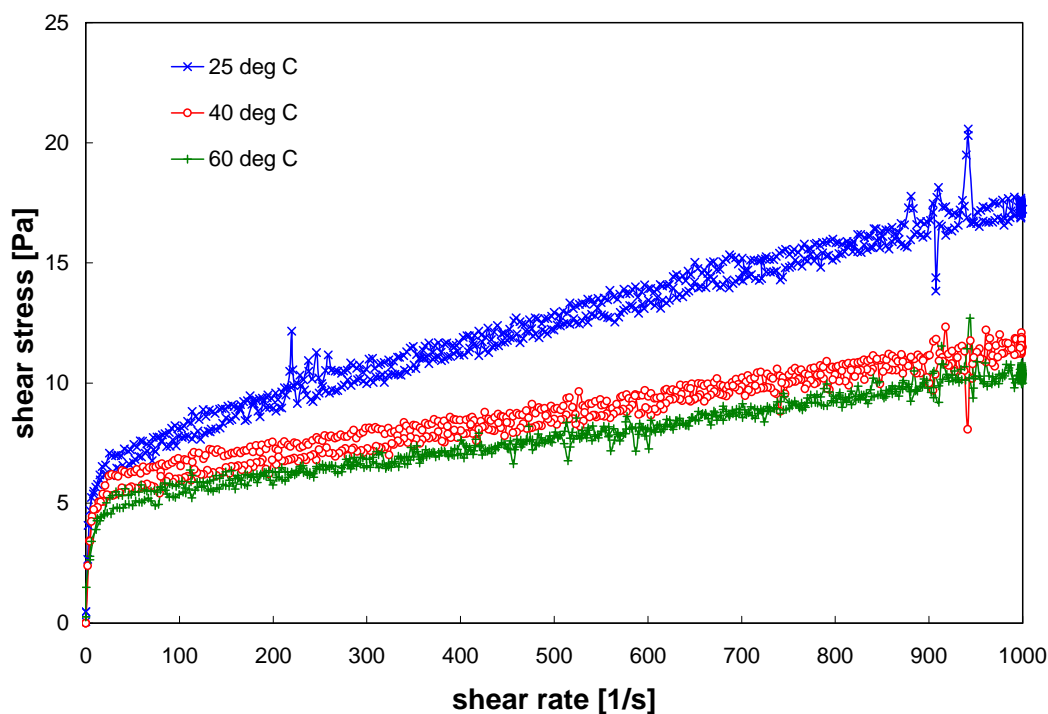
Figure 5.47. Flow Curve for the Group 1/2 CUF Caustic-Leached, Dewatered, and Washed Slurry at 25, 40, and 60°C

Table 5.30. Results of Fitting Analysis for Group 1/2 CUF Caustic-Leached, Dewatered, and Washed Slurry

Model	Temperature [°C]	Yield Stress [Pa]	Consistency [Pa·s^n]	Flow Index	R
Bingham-Plastic (0 – 1000 s⁻¹)	25 (1 of 2)	7.9	0.011	n/a	0.996
	25 (2 of 2)	7.7	0.0097	n/a	0.987
	40	5.9	0.0057	n/a	0.980
	60	5.0	0.0054	n/a	0.985
Herschel-Bulkley (0 – 1000 s⁻¹)	25 (1 of 2)	6.1	0.066	0.77	0.992
	25 (2 of 2)	5.2	0.11	0.68	0.992
	40	5.0	0.031	0.77	0.980
	60	4.6	0.014	0.87	0.987

Table 5.31. Apparent Viscosity of Group 1/2 CUF Caustic-Leached, Dewatered, and Washed Slurry

Source	Temperature [°C]	Apparent Viscosity [mPa·s]			
		@ 33 s⁻¹	@ 100 s⁻¹	@ 500 s⁻¹	@ 1000 s⁻¹
Measured	25 (1 of 2)	300	97	26	19
	25 (2 of 2)	200	79	25	17
	40	170	64	17	12
	60	160	56	16	10
Bingham-Plastic	25 (1 of 2)	250	90	27	19
	25 (2 of 2)	240	87	25	17
	40	180	64	17	12
	60	160	56	15	10
Herschel-Bulkley	25 (1 of 2)	210	83	28	19
	25 (2 of 2)	190	77	25	17
	40	170	61	18	12
	60	150	54	16	10

Table 5.32 and Figure 5.48 show the influence of caustic leaching and washing on the Group 1/2 waste rheology. The post-caustic-leach rheology corresponds to the dewatered (but not washed) slurry. Before leaching, the 16-wt% UDS initial slurry is non-Newtonian with a yield of 3.0 Pa and a consistency of 12 mPa·s. After caustic leaching and dewatering to 17.8-wt% UDS, the slurry is highly non-Newtonian (relative to the initial slurry) and has a yield stress of 37 Pa and a consistency of 29 mPa·s. Thus, for Group 1/2 wastes, caustic leaching is observed to dramatically increase slurry rheology. Specifically, the yield stress is increased by nearly a factor of 10 while consistency more than doubles. The mechanism by which this increase occurs is likely the metathesis of iron(III) phosphate, resulting in the formation of a sodium phosphate ($Na_3PO_4 \cdot 12H_2O$) gel. Increased dissolved solids and Na_3PO_4 gelation both serve to increase the viscosity of the slurry suspending phase.

Both fitting results and flow curve data indicate that, although washing does not eliminate non-Newtonian behavior, it does appear to reduce the slurry yield stress and consistency. The caustic-leached and dewatered slurry has a yield stress and consistency of 37 Pa and 29 mPa·s, respectively. In comparison, the caustic-leached, dewatered, and washed slurry has a yield stress and consistency of 7.7 Pa and 9.7 mPa·s, respectively. This constitutes a decrease of yield stress by a factor of 4 and consistency by a factor of 3. A decrease in slurry rheology as a result of washing is expected, given that washing reduces the concentration of dissolved species in the suspending phase (sodium phosphate in particular). However, not all of the decrease in rheology can be attributed to the washing process alone. The post-wash samples have a significantly lower UDS relative to the pre-wash sample. Reduced solids concentration will also effect a reduction in both yield stress and consistency. Without the benefit of additional rheology tests after each wash removal, it is impossible to quantify the individual contributions of washing and solids dilution to the overall reduction in rheology during the washing process.

Table 5.32. Effect of Caustic Leaching/Washing on Group 1/2 CUF Slurry Rheology

Description	Solids Concentration	Rheology	Yield Stress [Pa]	Consistency [mPa·s]
Initial Slurry (TI572-G2-R2)	16.0-wt%	Non-Newtonian	3.0	12
Caustic-Leached and Dewatered (TI572-G2-R3)	17.8-wt%	Non-Newtonian	37	29
Caustic-Leached and Washed (TI572-G2-R4)	12.0-wt%	non-Newtonian	7.7	9.7

A comparison of Group 1/2 CUF slurries showing the effect of caustic leaching on rheology at 25°C.
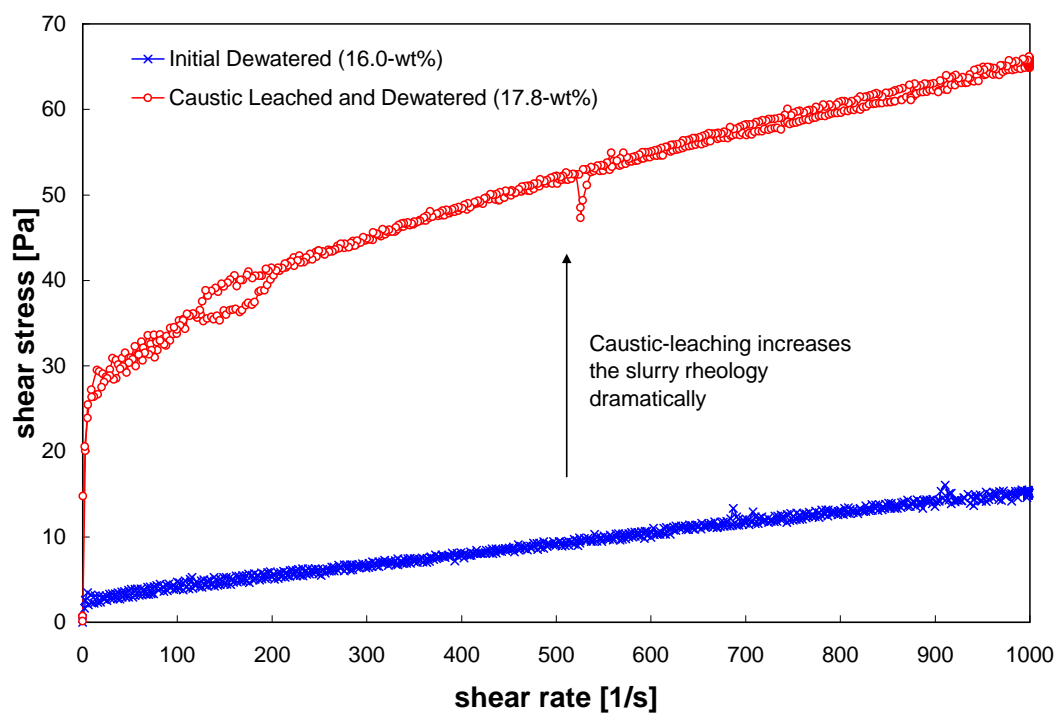
A comparison of Group 1/2 CUF slurries showing the effect of solids washing on rheology at 25°C.
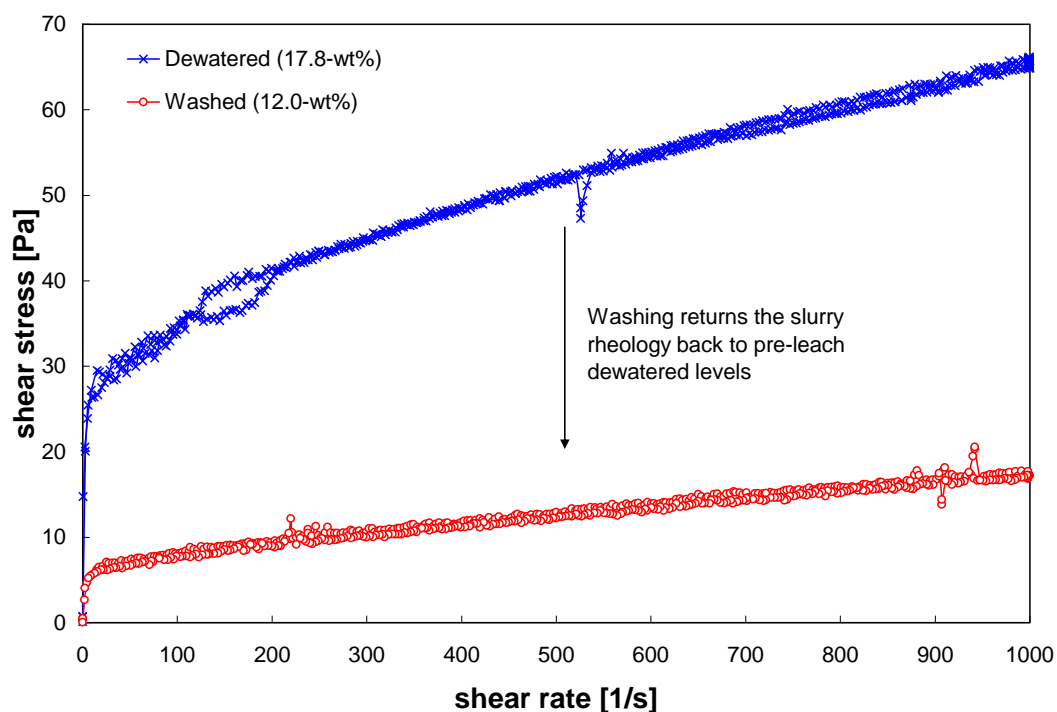
Figure 5.48. A Comparison of Group 1/2 CUF Slurries Showing the Effect of Caustic Leaching/Washing on Rheology at 25°C

5.5.6 Dewatering of Caustic Washes

The caustic-leached slurry was washed five successive times with NaOH solutions (1.2 L each) with decreasing sodium concentration to reduce the sodium concentration of the slurry to <0.25 M. The filter flux increased steadily during washing and reached a maximum average flux near 0.070 GPM/ft^2. The results are given in Table 5.33 and Figure 5.49.

The filter-flux data from the second, fourth, and fifth wash demonstrated a significant decrease in the filter flux within ten minutes of the dewatering. The observed decreases appeared similar to that predicted by the gel concentration model. However, without physical property measurements to confirm the UDS and centrifuged solids of the slurry at each step, this is conjecture. This decrease was not observed during dewatering of the third wash. However, the slurry was initially dewatering at a lower TMP. It is not clear how this may have impacted the filter results.

Table 5.33. Average Flux of Caustic Washes

	Wash Volume (L)	[NaOH] of wash (M)	[Na] of Slurry Supernate (M)	Average Filter Flux (GPM/ft^2)
Wash 1	1.2	0.56	2.21	0.026
Wash 2	1.2	0.20	1.29	0.051
Wash 3	1.2	0.06	0.60	0.049
Wash 4	1.2	0.02	0.37	0.067
Wash 5	1.2	0.01	0.19	0.069

First 10 minutes of dewatering of wash 3 is not shown because filtration was not performed at standard condition
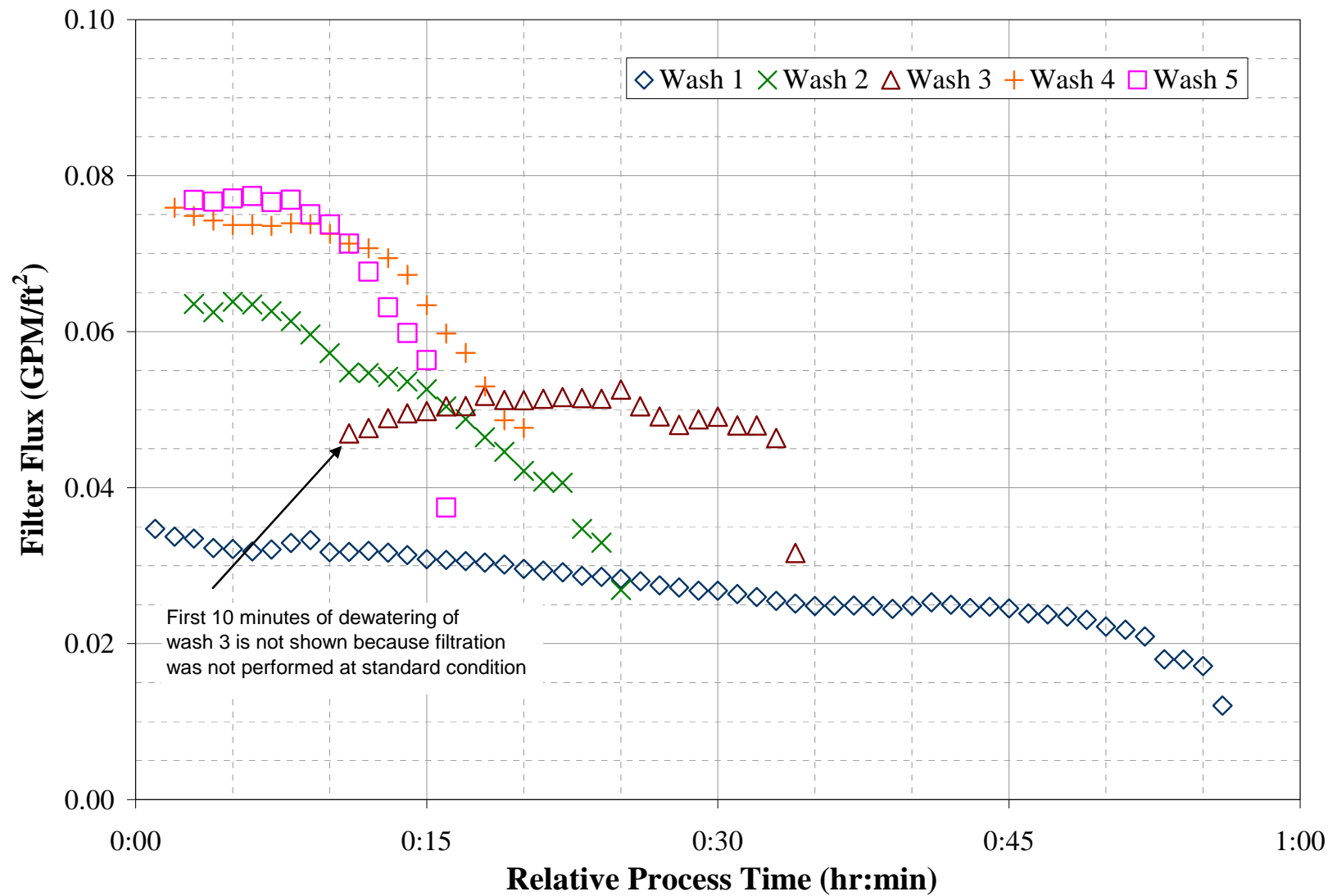
Figure 5.49. Flux Data from Dewatering Caustic Rinses at Standard Conditions (TMP = 40±5 psid, AV= 13±1 ft/s)

5.6 Oxidative Leaching/Washing

After completing the filtration and rheological testing of the washed caustic-leached slurry, the slurry was drained from the system and prepared for oxidative leaching (Figure 5.50). The system was rinsed using the additional permeate that was remaining in the back-pulse chamber and some dewatered permeate from the last rinse. After the slurry and permeate additions were recovered from the system, the slurry reservoir was isolated from the CUF. The recovered slurry and permeate were placed into the reservoir for oxidative leaching, as outlined in the right column of Figure 5.1. It was estimated that 5% of the slurry was lost during transfer operations, decreasing the inventory of the UDS by 15 grams.

The activities involved in this process were:

- Batch oxidative leaching of slurry for removing chromium

- Batch washing of the oxidative leached slurry and dewatering the solution afterwards.

- Three equal volumetric wash solutions (1.2 L each) were added to the slurry to remove dissolved chromium from the slurry.
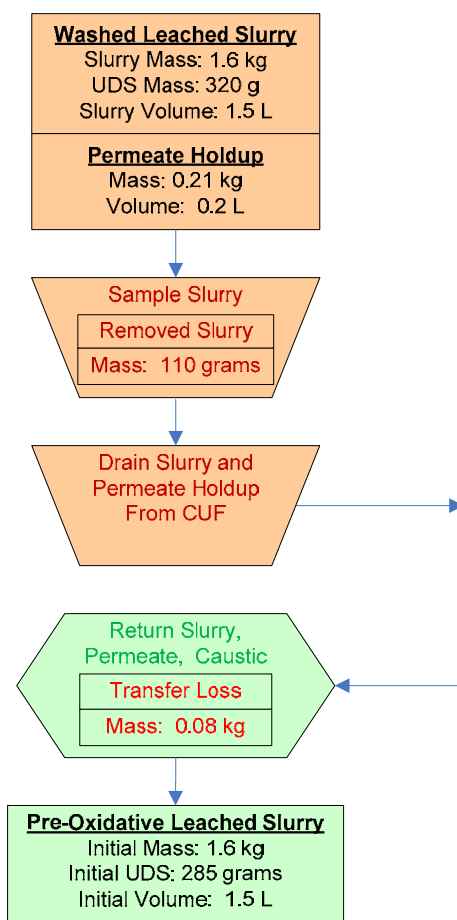
Figure 5.50. Process Flow for Batch Oxidative Leaching and Washing
Note: Mass and volume values in figure are rounded to the nearest significant digit of accuracy.

5.6.1 Batch Oxidative Leaching Results and Characterization

Figure 5.51 illustrates the material flow during the oxidative leaching and washing. Twenty three milliliters of 1 M sodium permanganate ($NaMnO_4$) was added to the dewatered, caustic-leached and washed slurry and allowed to react at room temperature (25°C) for 6 hours. The free hydroxide concentration during the oxidative leaching step was ~0.2 M. The amount of sodium permanganate added was based on a targeted Mn/Cr molar ratio of 1 and the assumption that 70% of the total Cr would have been removed during caustic leaching and washing. This assumption was conservative, but was based on combined wash/leach factors for Tanks B-104, BY-108, BY-110, BY-104, and BX-110 taken from TWIN data and reported by G. J. Lumetta and R.T. Hallen in *Review of Caustic Leaching Testing With Hanford Tank Waste Sludges* (WPT-RPT-151). However, only 30% of the total Cr was actually removed from the slurry during caustic leaching and washing. As a result, the Mn/Cr ratio during oxidative leaching was actually only 0.4, or 60% less than the targeted value.
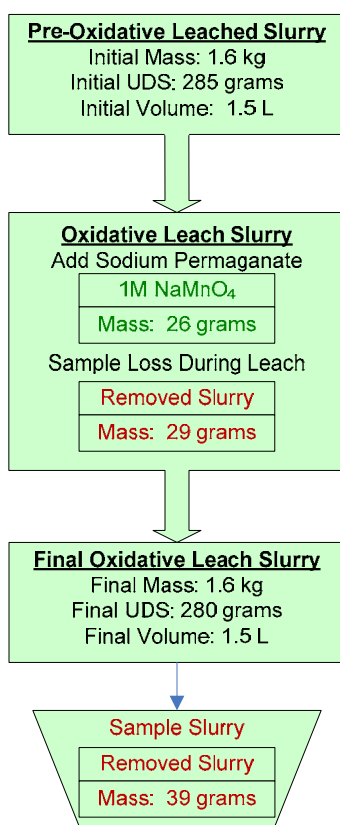
Figure 5.51. Process Flow for Oxidative Leach
Note: Mass and volume values in figure are rounded to the nearest significant digit of accuracy.

Based on samples taken during the oxidative leaching step, 27% of the water-insoluble chromium was removed by treatment with the sodium permanganate (Figure 5.52). The length of the oxidative leaching seemed to have no bearing on the amount of Cr removed. Analysis of the filtered supernate during oxidative leach dewatering did not show the presence of manganese at the end of the leach, indicating that all of the permanganate reacted, and Mn was precipitated in solid form. The reason for the low conversion of Cr—27% rather than 40% based on the reaction stoichiometry—is currently unknown. However, it was likely that the low conversion rate of insoluble Cr was partially due to the overhead

mixer not functioning properly during the leach and not suspending the insoluble solids off of the bottom of the slurry reservoir.
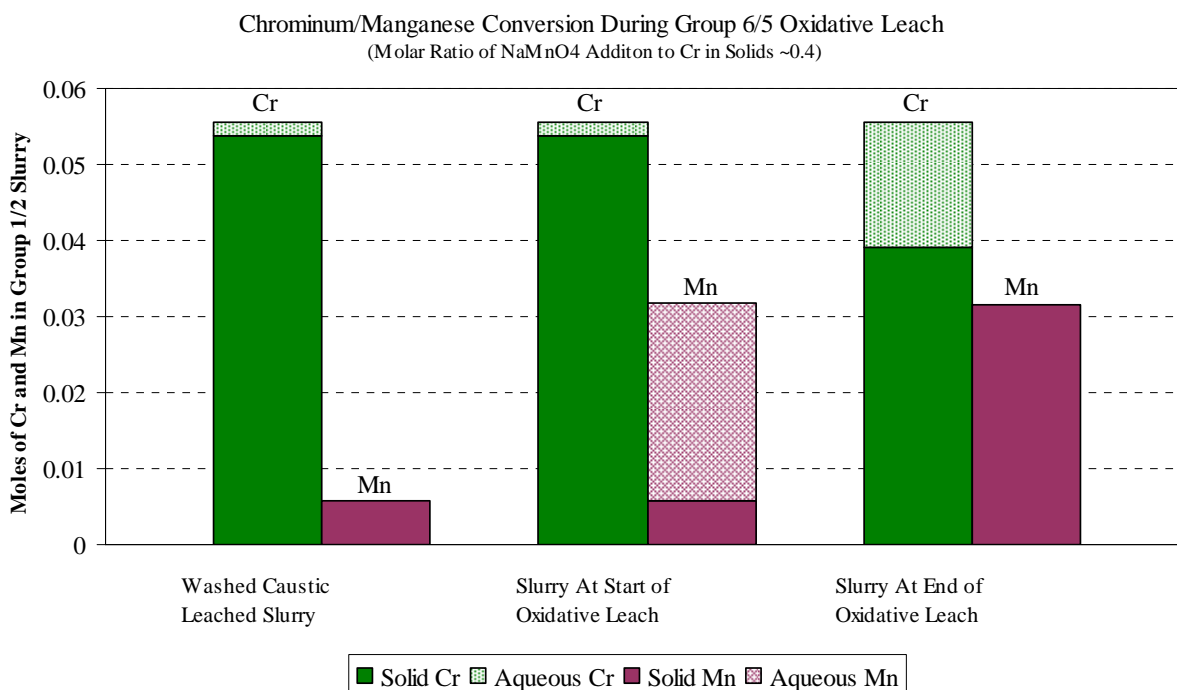
Figure 5.52. Moles of Chromium and Manganese in the Slurry Before and After Oxidative Leaching

After the 6-hour leach was completed, the oxidative leached slurry was sub-sampled inside the slurry reservoir before washing (Figure 5.51). Overall, 29 grams of the slurry was removed from the vessel containing an estimated 6 grams of solids. The physical properties of the oxidative leached, dewatered slurry are shown in Table 5.34 and chemical properties and leach factors in Table 5.35. Because the overhead mixer was not functional, the samples removed from the slurry were likely not representative of the slurry. The measured UDS of the sample was only 4.5 wt%, indicating very little solids were present. Also, the calculated leach factor for Cr was over 1.0, which is unlikely considered that the supernate concentration did not support this change in mass. It is likely that a majority of dense UDS remained at the bottom of the vessel while it was sub-sampled, skewing the results.

Table 5.34. Physical Property Measurements of the Group 1/2 Oxidative Leached Slurry

Slurry Density (g/mL)	1.05
Supernate Density (g/mL)	0.99
Settled Solids (Vol%)	61%
Centrifuged UDS (Wt%)	26%
Total Solids of the Slurry(Wt%)	6.9%
Dissolved Solids of the Supernate (Wt%)	2.5%
UDS of the Slurry (Wt%)	4.5%

Table 5.35. Group 1/2 Oxidative Leached Slurry Composition and Leach Factor Calculations Based on ICP-OES/Radiochemical Characterization

Slurry Prep Method	ICP-OES Analytes	Dry Slurry[a] (µg/g)	Supernate[b] (µg/mL)	Dry Solids[c] (µg/g)	Solids Leach Factor[d]
	Al	59,150	243	84,658	0.54
	Bi	59,900	[0.82]	90,964	0.07
	Cd	90.6	<8.5E-2	135.8	-0.25
	Cr	12,050	1,050	-4,101	1.27
	Fe	74,250	1.32	112,749	NA
	K	[330]	27.5	-[86]	0.77
	Mn	12,000	[0.098]	18,225	-9.44
	Na	197,500	15,300	-26,466	1.07
	Ni	4,650	<6.0E-2	7,062	0.02
	P	31,850	3,180	-19,473	1.11
	S	[2,200]	115	[888]	1.11
	Si	56200	28.4	84756	0.07
	Sr	4455	0.0596	6765	-0.02
	U	20,250	<8.0E-1	30,740	NA
HF Assisted Acid Digestion, and KOH Fusion, Concentration Factor of 1.85 based on U and Fe	**Zn**	394	<7.0E-2	596	0.40
	Zr	404	[0.076]	611	-0.64
	Ag	[17]	[0.063]	[24]	-[0.16]
	Ba	278	[0.13]	419	0.04
	Be	0.593	[0.0080]	0.729	0.67
	Ca	9,750	[0.77]	14,793	0.05
	Ce	247	<2.5E-1	370	-0.08
	Co	42.8	<6.0E-2	63.6	0.18
	Cu	87.9	<3.5E-2	132.8	0.36
	La	40.5	<7.0E-2	59.9	0.06
	Li	71.2	0.408	99.4	0.22
	Mg	1,700	<5.8E-2	2,581	0.03
	Mo	[40]	[0.84]	[42]	[0.42]
	Nd	55.0	<1.4E-1	80.6	0.01
	Pb	1,490	[2.2]	2,216	0.11
	Ru	[30]	<3.0E-1	[39]	[0.08]
	Th	[43]	[0.67]	[51]	[117.56]
	Ti	172	[1.5]	228	0
	Tl	[69]	[0.035]	[104]	[0.71]
	V	24.8	<9.5E-1	17.3	0.43
	Y	7.71	<1.1E-2	11.47	0.03

Table 5.35 (Contd)

Slurry Prep Method	Radionuclides	Dry Slurry[a] (µCi/g)	Supernate[b] (µCi/mL)	Dry Solids[c] (µCi/g)	Solids Leach Factor[d]
KOH Fusion, Concentration Factor of 1.85 based on U and Fe	**Co-60**	9.06E-3	<2.E-5	1.3E-2	0.38
	Cs-137	8.78E+1	5.61E-1	1.2E+2	0.39
	Eu-154	5.69E-2	<5.E-5	8.5E-2	-1.72
	Eu-155	<5.E-2	<4.E-4	<6.E-2	NA
	Am-241	4.14E-1	<7.E-4	6.1E-1	-0.07
	Total alpha	9.57E-1	<7.E-4	1.4E+0	-0.16
	Total beta	5.06E+2	5.05E-1	7.6E+2	-0.24
	Sr-90	2.00E+2	2.38E-3	3.0E+2	-0.10
	Pu-239/240	4.83E-1	1.46E-4	7.3E-1	-0.10
	Pu-238	9.75E-3	5.97E-6	1.5E-2	0.20

(a) Test sample TI572-G2-L5, ASO ID 08-01292
(b) Test sample TI572-G2-15, ASO ID 08-01301
(c) Calculated using results from TI572-G2-L5 and TI572-G2-15
(d) Calculated using results listed in
(e) Table 5.11
   Note: Analytes in italics were measured opportunistically. Values in brackets [ ] are ≥ MDL but < EQL, with errors likely to exceed 15%.

PSD measurements were also performed on the oxidative leached slurry. Figure 5.53 shows the pre-sonic size distribution of solids in the caustic-leached, dewatered slurry as a function of pump speed. All distributions show similar particle populations. A primary peak spanning 0.3 to 6 µm with a maximum population from 1 to 2 µm dominates the distribution. This peak shifts to smaller diameters at both 2000 and 4000 RPM, which may suggest particle-size reduction because of the lower ionic strength of the suspending phase, and/or shear forces were increased during analysis. Smaller secondary peaks occur from 6 to 200 µm and likely correspond to particle flocs. The relative contribution of these secondary peaks is highest at 4000 RPM, indicating the presence of difficult-to-suspend particles.

Figure 5.54 shows how sonication affects the PSD for the oxidative leached, dewatered slurry. Sonication causes a significant increase in the contribution of 0.2- to 1-µm particles and a significant decrease in the contribution of 1- to 5-µm particles. Accompanying these changes is an increase in the fraction of 5- to 20-µm particles and a complete elimination of particles larger than 20 µm. These changes are likely a result of sonic disruption of particles and flocs. After sonication is removed, an immediate recovery of 20- to 200-µm particles is observed, which suggests a rapid reformation of flocs.
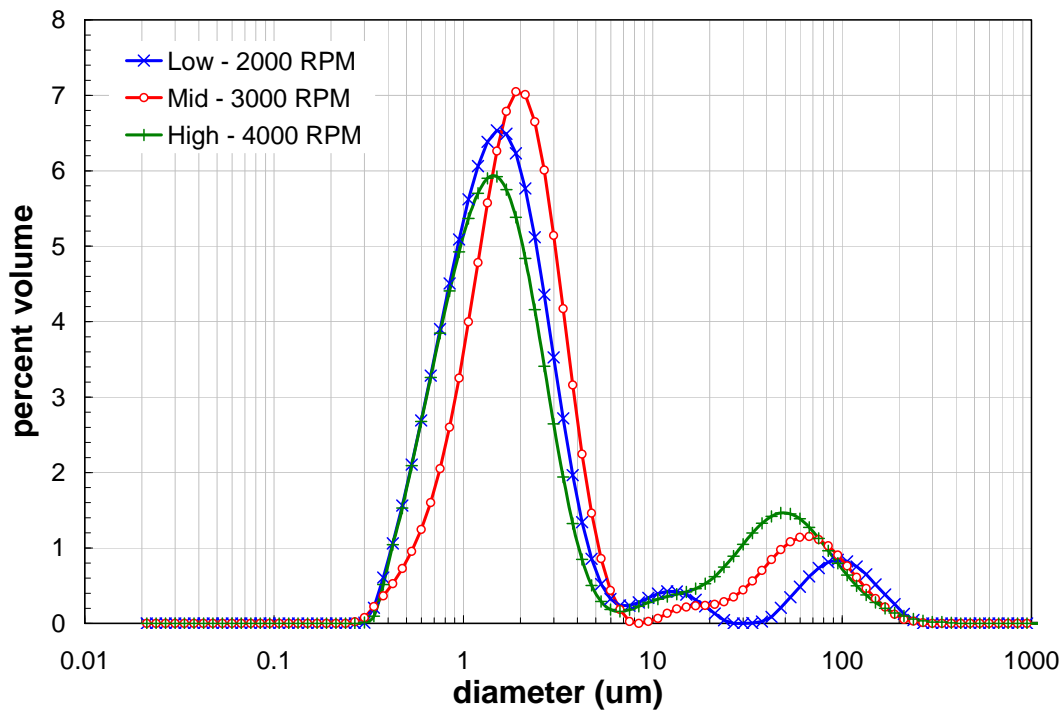
Figure 5.53. Oxidative Leached, Dewatered PSD as a Function of Pump Speed
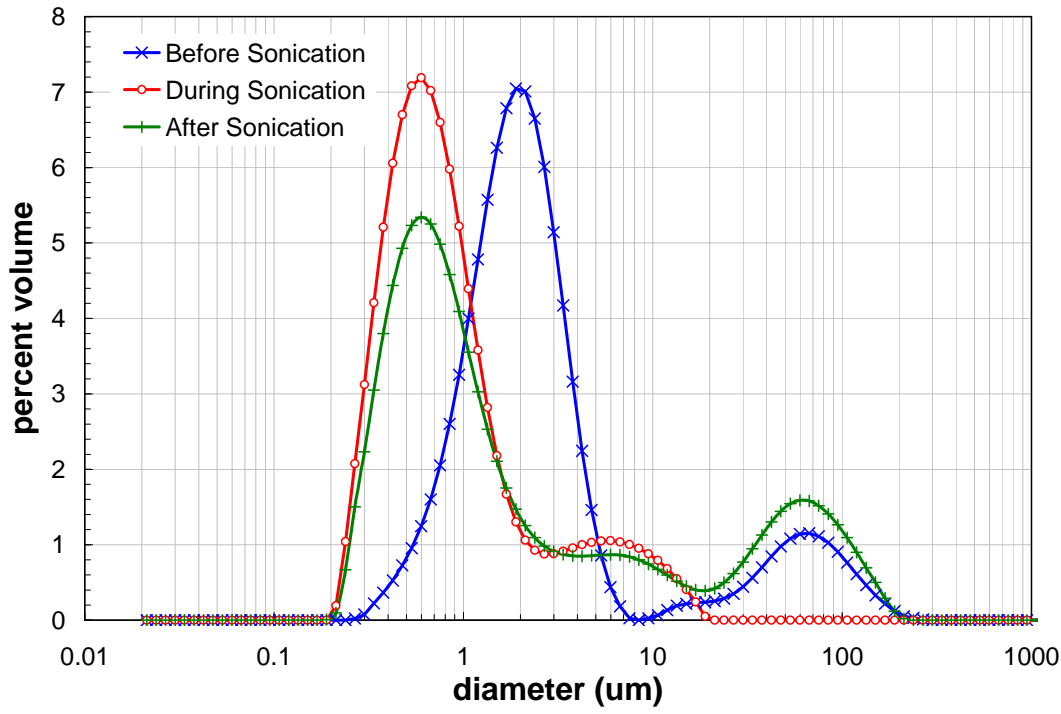
Figure 5.54. Oxidative Leached, Dewatered Slurry PSD as a Function of Sonication at 3000 RPM

5.6.2 Batch Oxidative Washing Results

The leached material was washed three times with 0.01 M NaOH (Figure 5.55), during which time the leached chromium was largely washed out of the slurry. The metals composition of the oxidative leached slurry following each of the washes is shown in Table 5.36 through Table 5.39.

The total Cr in the system before the caustic and oxidative leaching (low solids slurry) was 5.66 g. By the start of the oxidative leach test, the actual inventory of Cr had decreased to 2.9 grams. Leaching and washing afterwards decrease the total inventory to 2.0 grams. However, sampling and transfer losses accounted for 1 gram of lost Cr before the start of the leach. Figure 5.56 plots the corrected inventory of Cr throughout the test. The inventory at each step was normalized to the original slurry inventory and corrected for sample loss. It was projected that the total amount of Cr removed was 45% (Figure 5.57), if sampling did not occur. The solid leach factor of the Cr was 23% where 2.89 of the original 3.77 grams of Cr solids remained after the leach. Similarly, it was projected that half (50%) of the P was removed during leaching and dewatering operations if sampling was excluded.
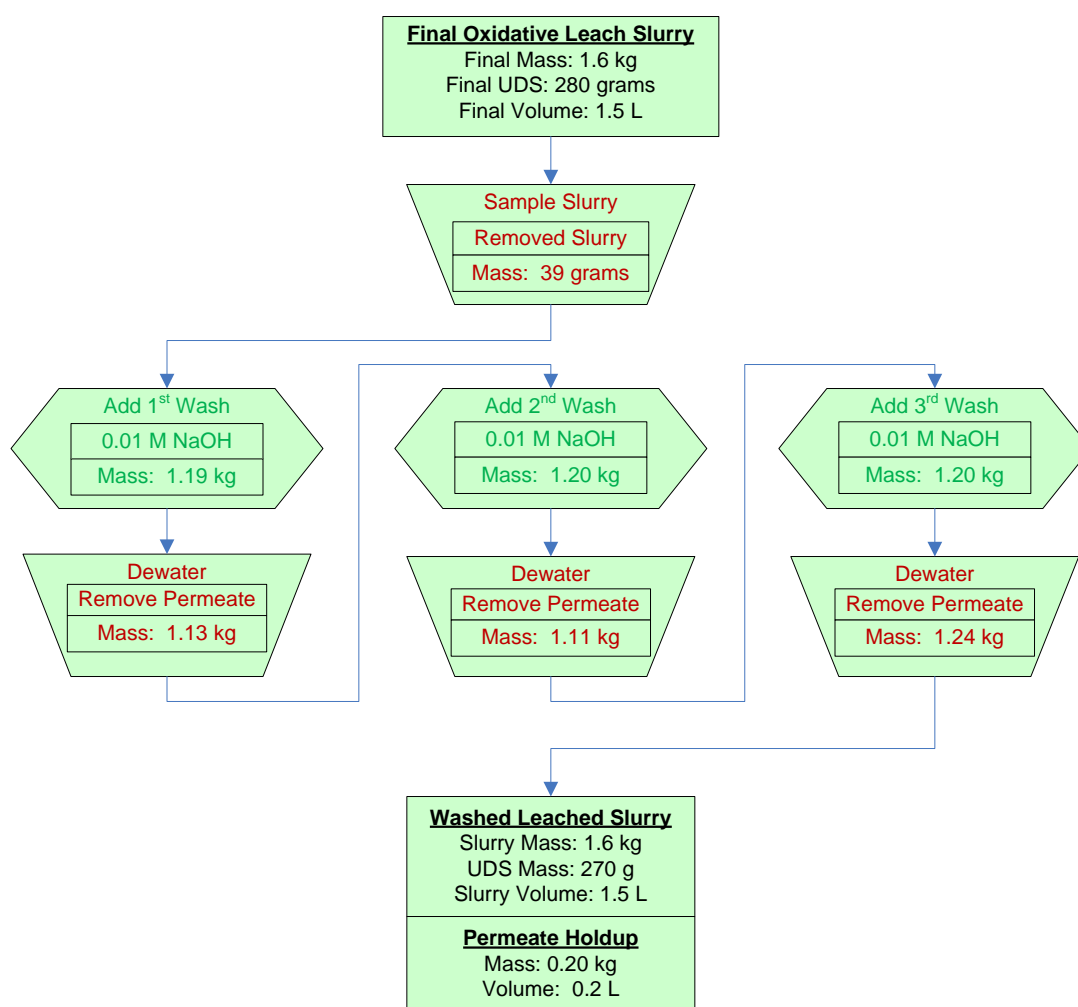
Figure 5.55. Process Flow for Washing after Oxidative Leaching
Note: Mass and volume values in figure are rounded to the nearest significant digit of accuracy.

Table 5.36. Slurry composition after the first wash of the Group 1/2 Oxidative leached Slurry (Including Permeate Hold-up)

	Slurry[a]	Liquid Fraction[b]		Solids Fraction[c]	
Mass (kg)	1.55	1.28		0.27	
Wt% of Slurry	100%	82.5%		17.5%	
Metal	g	g	µg/mL	g	µg/g
Al	2.1E+01	1.7E-01	1.4E+02	2.1E+01	7.7E+04
Bi	1.5E+01	3.0E-03	2.4E+00	1.5E+01	5.7E+04
Cr	2.5E+00	4.1E-01	3.4E+02	2.0E+00	7.5E+03
Fe	2.1E+01	5.3E-04	4.3E-01	2.1E+01	7.7E+04
Mn	1.7E+00	1.1E-05	8.8E-03	1.7E+00	6.1E+03
Na	8.6E+01	7.8E+00	6.4E+03	7.8E+01	2.9E+05
P	1.9E+01	1.4E+00	1.1E+03	1.8E+01	6.5E+04
S	9.8E-02	6.3E-02	5.1E+01	3.5E-02	1.3E+02
Si	1.3E+01	3.4E-02	2.8E+01	1.3E+01	4.7E+04
Sr	1.3E+00	1.5E-05	1.2E-02	1.3E+00	4.7E+03
U	5.2E+00	1.0E-03	8.1E-01	5.2E+00	1.9E+04
Supernate Fraction					
Anion	µg/mL	[M]	g		
OH	2.4E+03	1.4E-01	2.9E+00		

(a) Slurry mass components were calculated from characterization data (Sections 3 and 4) and the masses of materials that were added with simulant. Loss of mass from sampling was incorporated.
(b) Liquid fraction mass components were calculated using analytical results from supernate sample TI552-G6-M (ASO ID 08-01313) and the predicted mass of supernate in the system.
(c) Solids fraction mass components were calculated from the difference between the slurry component mass and liquid component mass fraction.

Table 5.37. Slurry Composition After the Second Wash of the Group 1/2 Oxidative Leached Slurry (Including Permeate Hold-up)

	Slurry[a]	Liquid Fraction[b]		Solids Fraction[c]	
Mass (kg)	1.62	1.35		0.27	
Wt% of Slurry	100%	83.2%		16.8%	
Metal	**g**	**g**	**µg/mL**	**g**	**µg/g**
Al	2.1E+01	2.3E-01	1.7E+02	2.1E+01	7.6E+04
Bi	1.5E+01	1.4E-03	1.1E+00	1.5E+01	5.7E+04
Cr	2.2E+00	3.6E-01	2.7E+02	1.8E+00	6.6E+03
Fe	2.1E+01	1.4E-03	1.1E+00	2.1E+01	7.7E+04
Mn	1.7E+00	8.1E-06	6.2E-03	1.7E+00	6.1E+03
Na	7.9E+01	7.7E+00	5.9E+03	7.2E+01	2.6E+05
P	1.8E+01	1.3E+00	9.7E+02	1.7E+01	6.2E+04
S	9.8E-02	7.7E-02	5.9E+01	2.1E-02	7.7E+01
Si	1.3E+01	4.4E-02	3.4E+01	1.3E+01	4.7E+04
Sr	1.3E+00	2.1E-05	1.6E-02	1.3E+00	4.7E+03
U	5.2E+00	2.4E-03	1.8E+00	5.2E+00	1.9E+04
Supernate Fraction					
Anion	**µg/mL**	**[M]**	**g**		
OH	7.8E+02	4.6E-02	1.0E+00		

(a) Slurry mass components were calculated from characterization data (Sections 3 and 4) and the masses of materials that were added with simulant. Loss of mass from sampling was incorporated.
(b) Liquid fraction mass components were calculated using analytical results from supernate sample TI552-G6-N (ASO ID 08-01314) and the predicted mass of supernate in the system.
(c) Solids fraction mass components were calculated from the difference between the slurry component mass and liquid component mass fraction.

Table 5.38. Slurry Inventory and Composition After the Third Wash of the Group 1/2 Oxidative Leached Slurry (including permeate hold-up)

	Slurry[a]	Liquid Fraction[b]		Solids Fraction[c]	
Mass (kg)	1.55	1.28		0.27	
Wt% of Slurry	100%	82.5%		17.5%	
Metal	**g**	**g**	**µg/mL**	**g**	**µg/g**
Al	2.1E+01	1.2E-01	9.0E+01	2.1E+01	7.6E+04
Bi	1.5E+01	3.8E-03	2.9E+00	1.5E+01	5.7E+04
Cr	2.0E+00	1.6E-01	1.2E+02	1.8E+00	6.7E+03
Fe	2.1E+01	1.2E-03	9.5E-01	2.1E+01	7.7E+04
Mn	1.7E+00	2.0E-05	1.5E-02	1.7E+00	6.1E+03
Na	7.6E+01	3.8E+00	2.9E+03	7.2E+01	2.6E+05
P	1.7E+01	5.9E-01	4.5E+02	1.7E+01	6.2E+04
S	6.0E-02	3.5E-02	2.7E+01	2.5E-02	9.0E+01
Si	1.3E+01	1.5E-02	1.2E+01	1.3E+01	4.7E+04
Sr	1.3E+00	1.1E-05	8.6E-03	1.3E+00	4.7E+03
U	5.2E+00	< 5.E-3	< 4.E+0	5.2E+00	1.9E+04
Radiochemical Isotopes	**Slurry**	**Liquid Fraction**		**Solid Fraction**	
	mCi	**mCi**	**mCi/mL**	**mCi**	**mCi/g**
Co-60	2.3E+00	< 3.E-2	< 2.E-5	2.3E+00	8.4E-03
Cs-137	2.7E+04	2.8E+02	2.1E-01	2.6E+04	9.7E+01
Eu-154	1.2E+01	< 8.E-2	< 6.E-5	1.2E+01	4.3E-02
Am-241	1.1E+02	< 1.E-1	< 1.E-4	1.1E+02	4.2E-01
Gross Alpha	2.1E+02	< 9.E-1	< 7.E-4	2.1E+02	7.6E-01
Gross Beta	1.3E+05	2.4E+02	1.8E-01	1.3E+05	4.8E+02
Sr-90	4.9E+04	2.5E-01	1.9E-04	4.9E+04	1.8E+02
Pu-239+240	1.5E+02	< 3.E-3	< 3.E-6	1.5E+02	5.6E-01
Pu-238	5.4E+00	< 3.E-3	< 3.E-6	5.4E+00	2.0E-02
Anions		**Liquid Fraction**		**Leached Solids Fraction**	
	µg/mL	**[M]**	**g**	**µg/g**	**g**
F	2.2E+02	1.2E-02	2.9E-01	2.2E+03	6.0E-01
C$_2$O$_4$	7.4E+01	8.4E-04	9.7E-02	1.2E+03	3.3E-01
NO$_2$	2.5E+01	5.5E-04	3.3E-02	3.3E+02	8.9E-02
NO$_3$	7.1E+02	1.1E-02	9.3E-01	1.2E+04	3.3E+00
SO$_4$	8.3E+01	8.7E-04	1.1E-01	1.3E+03	3.6E-01
PO$_4$	1.5E+03	1.6E-02	2.0E+00	1.2E+04	3.3E+00
OH	5.4E+02	3.2E-02	7.1E-01		

(a) Slurry mass components were calculated from characterization data (Sections 3 and 4) and the masses of materials that were added with simulant. Loss of mass from sampling was incorporated.

(b) Liquid fraction mass components were calculated using analytical results from supernate sample TI552-G6-O (ASO ID 08-01294) and the predicted mass of supernate in the system.

(c) Solids fraction mass components were calculated from the difference between the slurry component mass and liquid component mass fraction.

Table 5.39. Oxidative Wash Solutions Radionuclide and Opportunistic Compositions

	Wash 1	Wash 2	Wash 3	Composite Wash
ASO Sample ID	08-01313	08-01314	08-01294	08-01295
Density$^{(a)}$, g/mL>	1.04	1.03	1.01	NA
Analyte				
free OH, M	0.14 M	0.05 M	0.03 M	0.07 M
Analyte	µCi/mL	µCi/mL	µCi/mL	µCi/mL
^{137}Cs			2.10E-1	3.56E-1
^{60}Co			< 2.E-5	< 1.E-5
^{241}Am			< 1.E-4	< 5.E-4
^{90}Sr			1.90E-4	2.32E-4
^{238}Pu			< 3.E-6	< 2.E-6
$^{239+240}$Pu			< 3.E-6	< 3.E-6
Gross alpha			< 7.E-4	< 5.E-4
Gross beta			1.81E-1	2.94E-1
^{154}Eu			< 6.E-5	< 4.E-5
Opportunistic Analytes				
Analyte	µg/mL	µg/mL	µg/mL	µg/mL
Ag	<5.1E-2	<5.1E-2	<2.6E-1	[0.059]
As	<1.0E+0	<1.1E+0	<5.3E+0	<8.5E-1
Ba	[0.088]	0.166	0.308	0.247
Be	[0.0033]	[0.0017]	<6.4E-3	[0.0012]
Ca	[0.80]	3.31	[0.64]	[0.52]
Ce	<2.4E-1	<2.5E-1	<1.2E+0	<2.0E-1
Co	[0.14]	<5.9E-2	<3.0E-1	<4.7E-2
Cu	[0.047]	[0.060]	<1.7E-1	<2.8E-2
Dy	<7.1E-2	<7.1E-2	<3.6E-1	<5.7E-2
Eu	<2.7E-2	<2.7E-2	<1.4E-1	<2.2E-2
La	<6.8E-2	<6.9E-2	<3.4E-1	<5.5E-2
Li	[0.29]	0.318	[0.15]	0.239
Mg	<5.6E-2	<5.6E-2	<2.8E-1	<4.5E-2
Mo	<1.3E-1	<1.3E-1	<6.4E-1	[0.23]
Nd	<1.3E-1	<1.3E-1	<6.6E-1	<1.1E-1
Pb	<7.8E-1	<7.8E-1	[1.5]	<6.3E-1
Pd	[0.20]	<1.5E-1	<7.7E-1	<1.2E-1
Rh	<2.9E-1	<2.9E-1	<1.5E+0	[0.24]
Ru	<2.1E-1	<2.1E-1	<1.0E+0	<1.7E-1

Table 5.39 (Contd)

	Wash 1	Wash 2	Wash 3	Composite Wash
ASO Sample ID	08-01313	08-01314	08-01294	08-01295
Opportunistic Analytes				
Analyte	µg/mL	µg/mL	µg/mL	µg/mL
Sb	<4.9E-1	<4.9E-1	<2.5E+0	<3.9E-1
Se	[4.0]	[8.8]	[2.0]	<1.4E+0
Sn	[2.4]	[1.4]	<3.3E+0	<5.3E-1
Ta	<4.1E-1	<4.2E-1	<2.1E+0	<3.4E-1
Te	<6.3E-1	<6.4E-1	<3.2E+0	[0.59]
Th	[0.43]	[0.43]	<1.2E+0	[0.31]
Ti	<1.0E-2	[0.015]	<5.3E-2	[0.012]
Tl	<9.3E-1	<9.3E-1	<4.7E+0	<7.5E-1
V	0.244	0.208	[0.099]	[0.14]
W	[0.47]	<4.7E-1	<2.3E+0	<3.7E-1
Y	<1.1E-2	<1.1E-2	<5.4E-2	<8.7E-3
(a) Density values were obtained from the mass flow meter, which had not been calibrated to NQA-1 standards; they are reported for information only. ASR 8113 Reference date: November 5, 2007. Analyte uncertainties were typically within ±15%; results in brackets indicate that the analyte concentrations were greater than the method detection limit (MDL) and less than the estimated quantitation limit (EQL), and uncertainties were >15%. Opportunistic analytes are reported for information only; QC requirements did not apply to these analytes.				
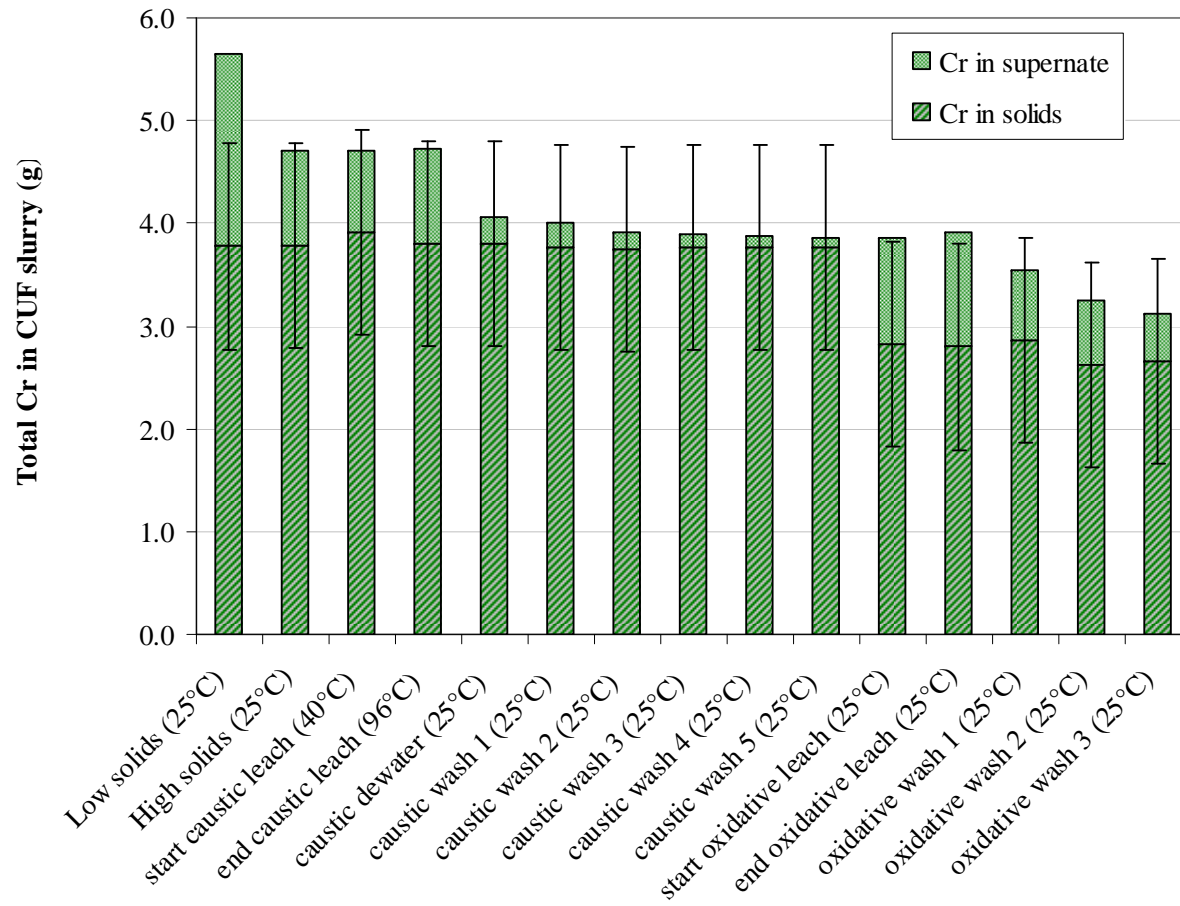
Temperatures on X-axis represent the slurry temperature when sampled

Figure 5.56. Normalized Chromium Inventory in Group 1/2 Slurry through Oxidative Leach and Washing
(Inventory in Figure Normalized to Eliminate Sample Loss Impacts.)
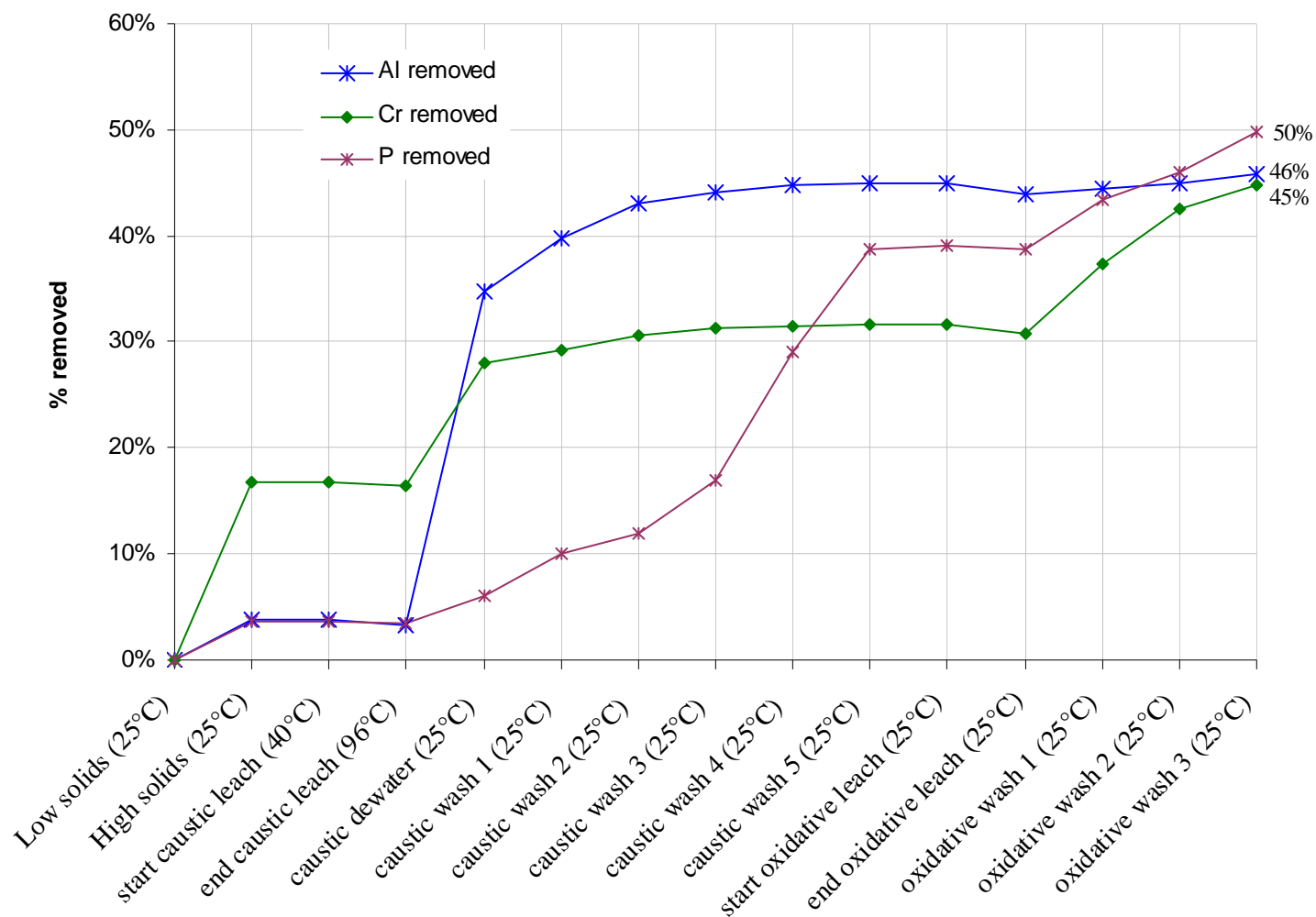
Temperatures on X-axis represent the slurry temperature when sampled.

Figure 5.57. Chromium, Phosphorus, and Aluminum Behavior in the Group 1/2 CUF Slurry
(Changes in Inventory in Figure Normalized to Eliminate Sample Loss Impacts.)

5.6.3 Dewatering Oxidative Washes Results

The oxidative leach slurry was washed three times with 1.2-L portions of 0.01 M NaOH. The full volume of each wash solution was mixed and dewatered from the slurry before adding the next wash solution. The filter flux during the oxidative leach washing steps is given in Figure 5.58. The chart contains a second axis for process temperature because the first two washes were conducted above the specified ambient process temperature.

This situation occurred because the chiller was not turned on again after the oxidative leach step. It is typical to put the chiller into stand-by mode during leaching steps and to start it again when filtration starts. In this case, the situation was realized near the beginning of the second wash, and the flux data corresponded to the decrease in temperature in that wash. Both corrected and uncorrected flux data (Equation K.3, Appendix K) are presented in the chart. If the temperature correction can be rightly extended to the range of temperatures in the wash steps, it may be asserted that the flux was essentially constant for the three wash steps (~0.040 GPM/ft^2). This is reasonable based on the fact that the permeate would be expected to change little between subsequent washings as only a relatively small amount of dissolved material is being washed away from the slurry.
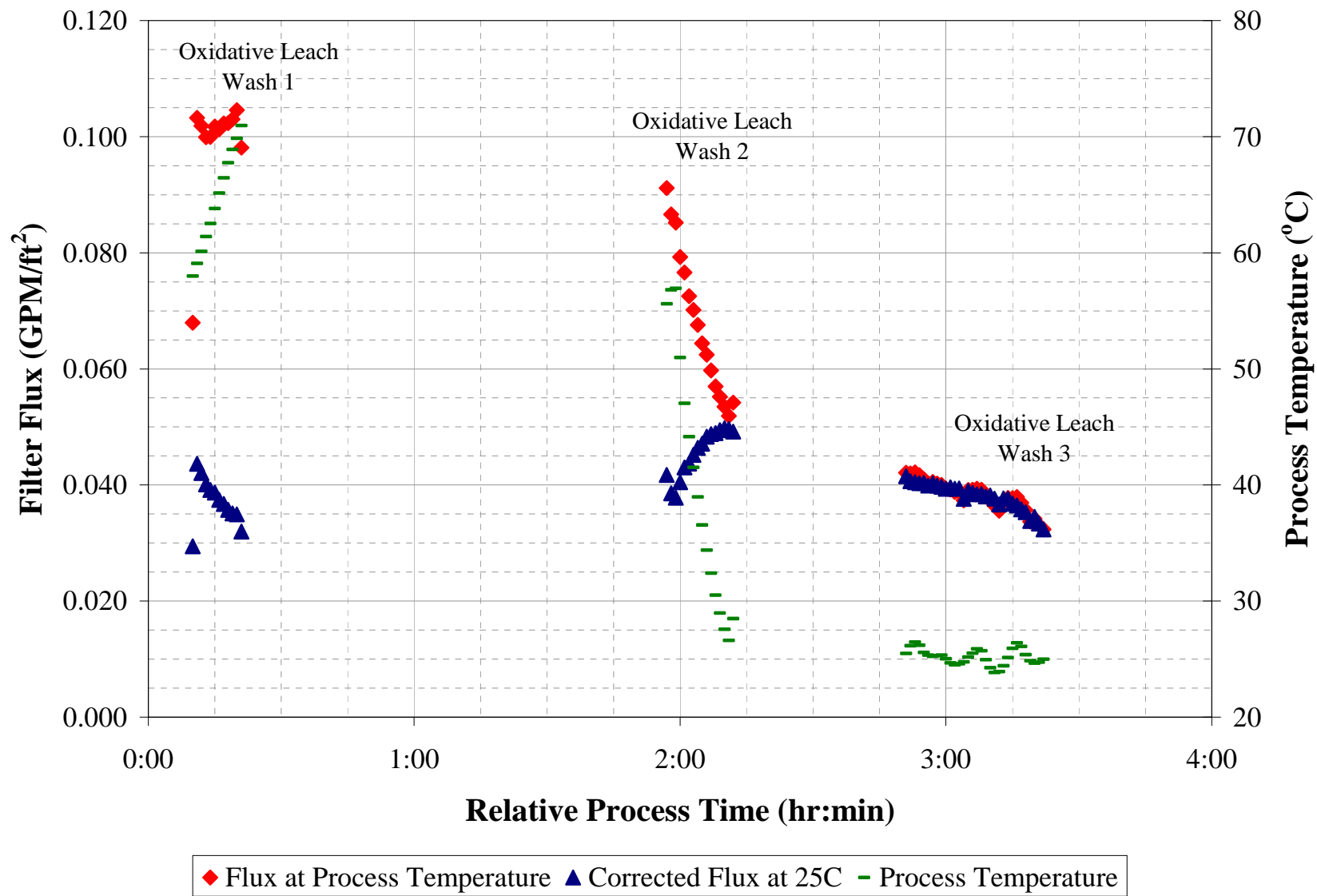
Figure 5.58. Flux Data from Dewatering Oxidative Washes

5.7 Final Dewater and Filter Flux Test Matrix

Figure 5.59 illustrates the material flow during the final filter flux testing matrix. Following the dewatering of the third wash of the oxidative leach slurry, approximately 300 mL of G2-OxWash3 permeate was added back to the slurry reservoir to aid pumping for the leached-solids filtration test matrix. Tests were performed according to the conditions described in Table K.2, Appendix K, sequentially with a minimum of 1 hour of constant recycle operation at each condition and back-pulsing between test conditions. The AV could not be increased beyond 15 ft/s at TMP=40 psid without exceeding the maximum operating speed of the pump. The measured UDS concentration of the slurry was 7.0% according to physical-properties measurements, while mass balance calculations project it to be over 2 times greater. Table 5.40 provides a summary of the average operating conditions and flux for each condition, and Figure 5.61 plots the average TMP and AV measured from each test condition against the target TMP and AV planned for the test. These values were obtained by calculating the arithmetic mean of each value over the duration of the test condition.

Washed Leached Slurry
Slurry Mass: 1.6 kg
UDS Mass: 270 g
Slurry Volume: 1.5 L

Permeate Holdup
Mass: 0.20 kg
Volume: 0.2 L

Dilute Slurry for Matrix Test
Returned Permeate
Mass: 0.28 kg

Leached Slurry Matrix
Slurry Mass: 1.9 kg
UDS Mass: 270 g
Slurry Volume: 1.5 L

Permeate Holdup
Mass: 0.20 kg
Volume: 0.2 L
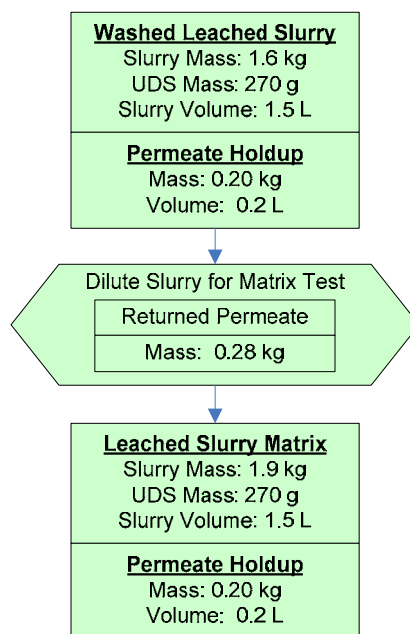
Figure 5.59. Flow Diagram for the Final Filter Flux Test Matrix
Note: Mass and volume values in figure are rounded to the nearest significant digit of accuracy.

The average filter flux ranged from 0.015 GPM/ft^2 for Test Condition 5 to 0.038 GPM/ft^2 for Test Condition 6. The filter flux was approximately 50% higher for this test matrix compared to the initial low-solids matrix for similar conditions. There was an observed decrease of permeate flux at the standard condition with time. The three tests at the standard condition (Test Conditions 1, 4, and 7) had average fluxes of 0.034, 0.032, and 0.028 GPM/ft^2, respectively, a relative percent decrease of 18%. The flux for Test Condition 4 might be on a slightly higher basis when compared to the other two as the TMP was slightly higher than the TMP for Test Conditions 1 and 7. Filter flux data are shown in Figure 5.60 with blue symbols for TMP=40 psid, pink for TMP=20 psid, and green for TMP=60 psid.

As can be seen by inspecting Figure 5.62 and Figure 5.63, the flux is dependent on both TMP and AV, defying a simple classification of the slurry into a membrane-resistance or cake-resistance model.

Figure 5.64 also demonstrated a negative trend in the filter flux over the course of the test, which was similar in magnitude to that seen in the previous filter tests, indicating that the filter resistance was still changing after days of testing. The data were further correlated and fitted to validate these conclusions. The results of this analysis are shown in Figure 5.65 and Figure 5.66. From the fit equations, TMP and AV were shown to have equal impact on filter flux. The operation time was also shown to have the same negative impact on filter flux seen from the previous filter testing. This implies that the agents in the slurry causing the irreversible fouling on the filter were not removed from caustic or oxidative leaching, such as iron. While both modeling equations have high correlation factors, the use of this model should be limited to understanding how filter flux was influenced by TMP, AV, and operation time during this test. Because all three parameters were included in both models, offset parameters were developed, which limits the range that they could be applied. Both models do not predict a zero filter flux when the TMP and AV is zero, which demonstrates that the input to these models must be bound by the range of TMP and AV used in this filter test, shown in Table 5.8. The use of these models should also be limited to when the test matrix occurred because the filter resistance was not at steady state, and the parameters developed in these models would be expected to change past the 8-hour period that this model predicts.

Table 5.40. Average Operating Conditions and Filter Flux for the High-Solids Matrix Test

Design Test Condition	Median Operation Time of Test[a] (hr)	Slurry Temp[b] (°C)	TMP[c] (psid)	Axial Velocity (ft/s)	Permeate Flowrate (mL/min)	Corrected Permeate Flux (GPM/ft^2)	Axial Pressure Drop[c] (psid/ft)
1	1.0	24.9	37.8	13.3	33.6	0.034	0.5
2	2.5	25.1	38.9	15.1	34.0	0.034	0.2
3	3.6	25.0	38.9	8.7	23.6	0.024	1.1
4	4.6	25.0	41.2	13.1	31.9	0.032	0.4
5	5.6	25.0	19.4	12.9	15.1	0.015	0.7
6	6.5	25.2	59.1	12.8	37.5	0.038	0.3
7	7.8	25.1	39.1	13.2	27.7	0.028	0.5
(a) Median operation time refers to the midpoint in processing time of the specific filtration test condition relative to the start time of the test (T = 0). Time periods between test conditions were excluded.							
(b) Thermocouple accuracy ± 2°C.							
(c) Pressure transducer accuracy ± 1 psig.							

5.95
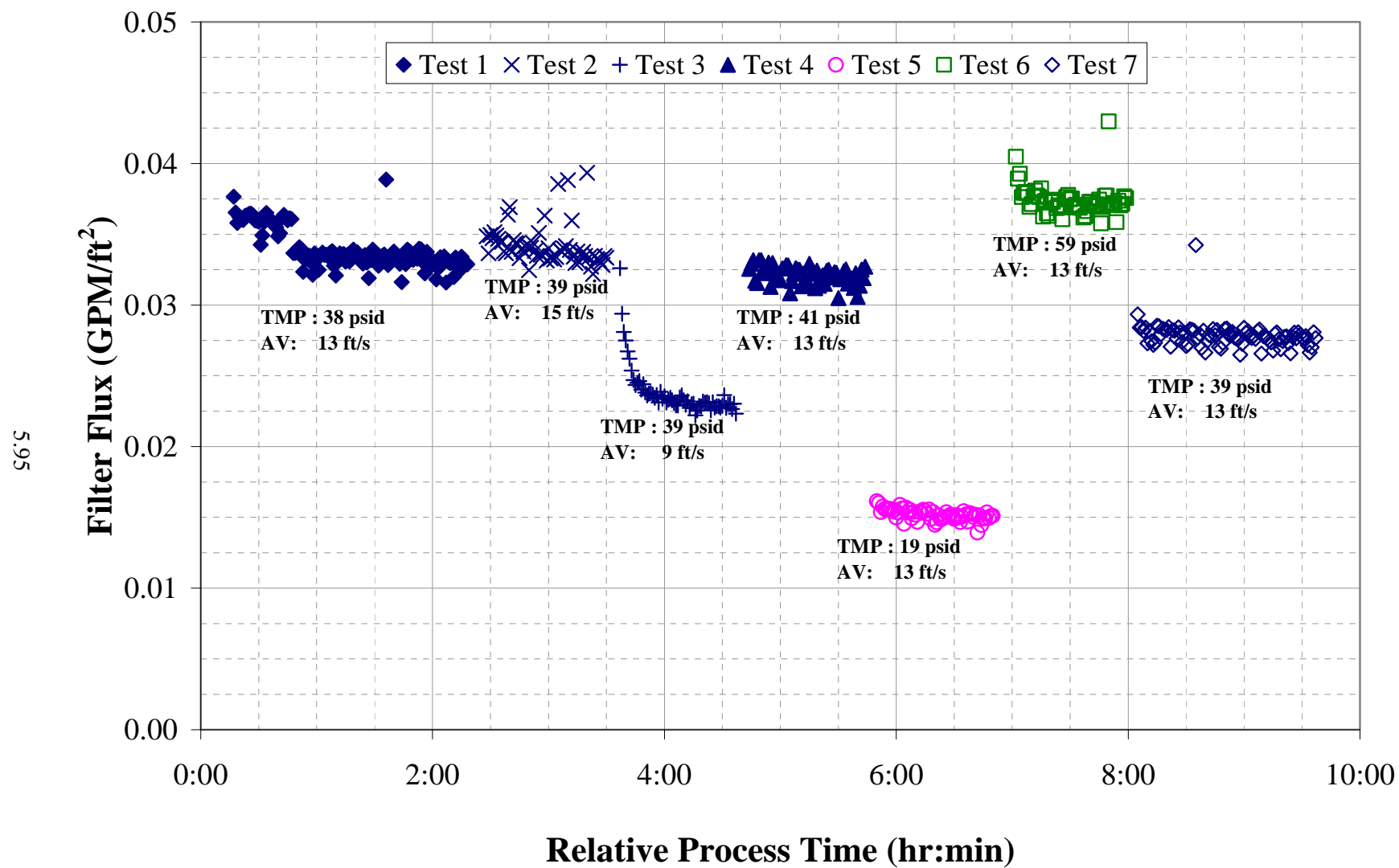
Figure 5.60. Final Filter Flux Testing of Washed Leached Group 1/2 Solids, 7-wt% UDS
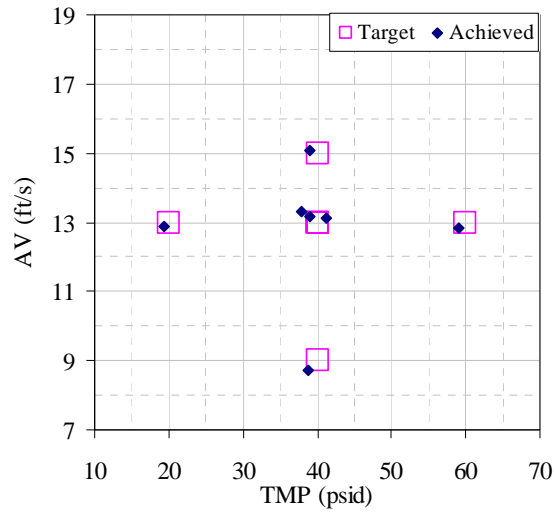
Figure 5.61. Group 1/2 Filter Test Matrix for Leached-Solids
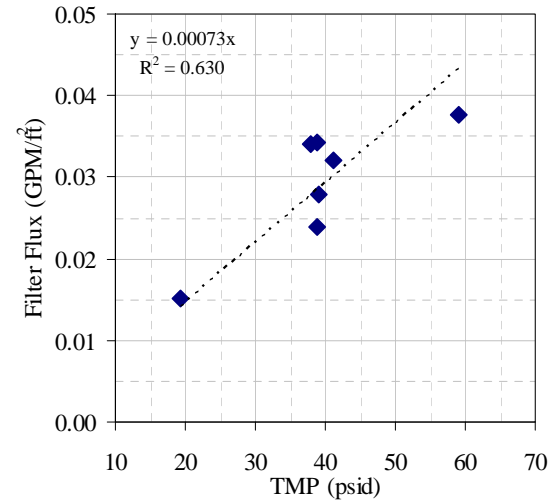
Figure 5.62. Group 1/2 Flux vs. TMP for Leached-Solids
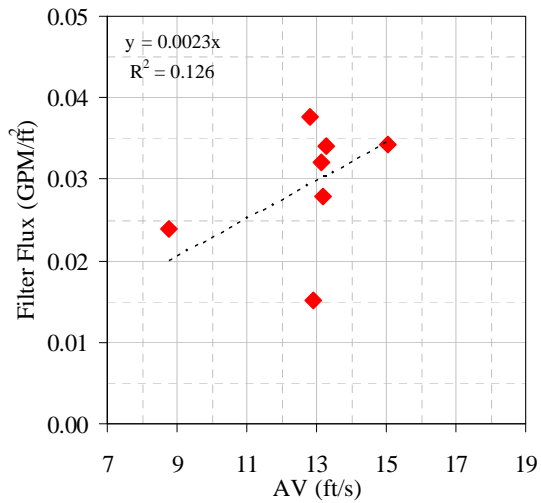
Figure 5.63. Group 1/2 Flux vs. AV for Leached-Solids
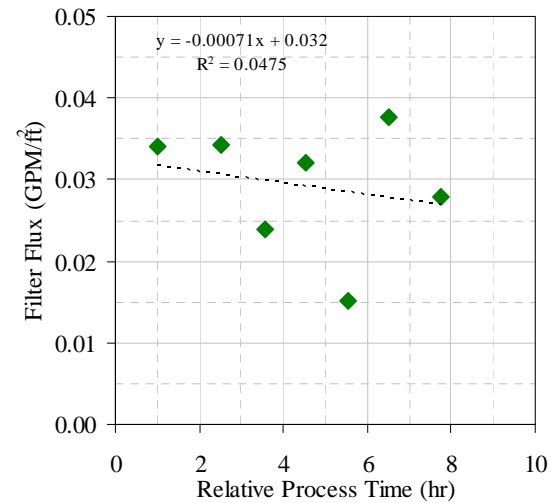
Figure 5.64. Group 1/2 Flux vs. Relative Time for Leached-Solids
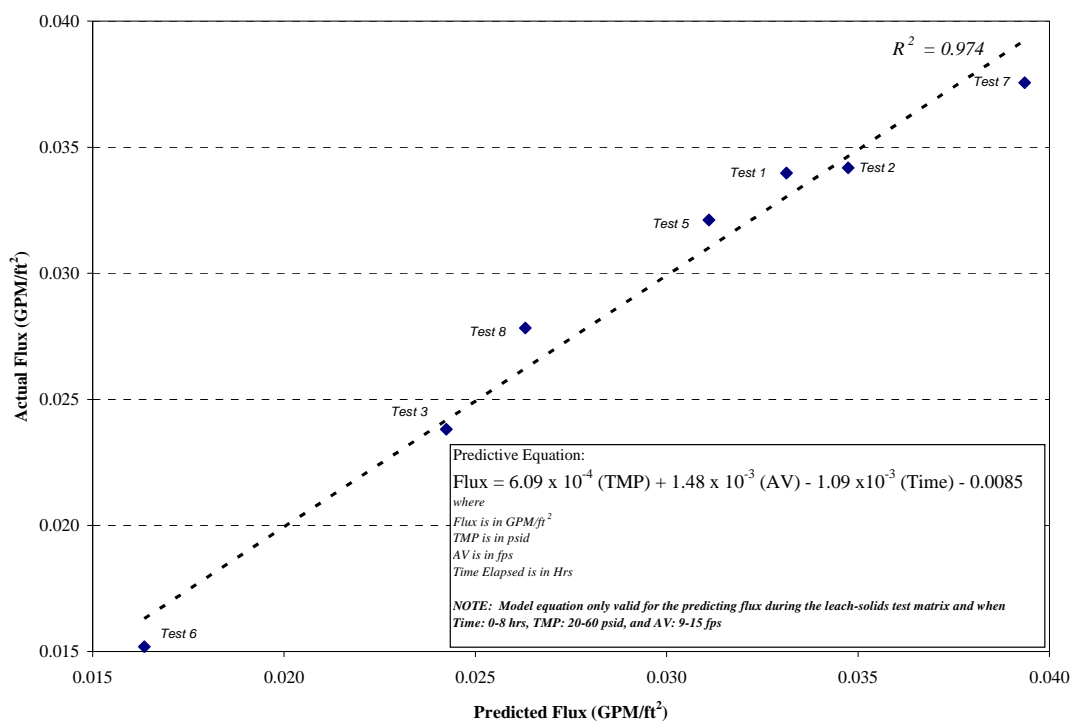
Figure 5.65. Linear Model of Filter Flux for Leached Group 1/2 Slurry
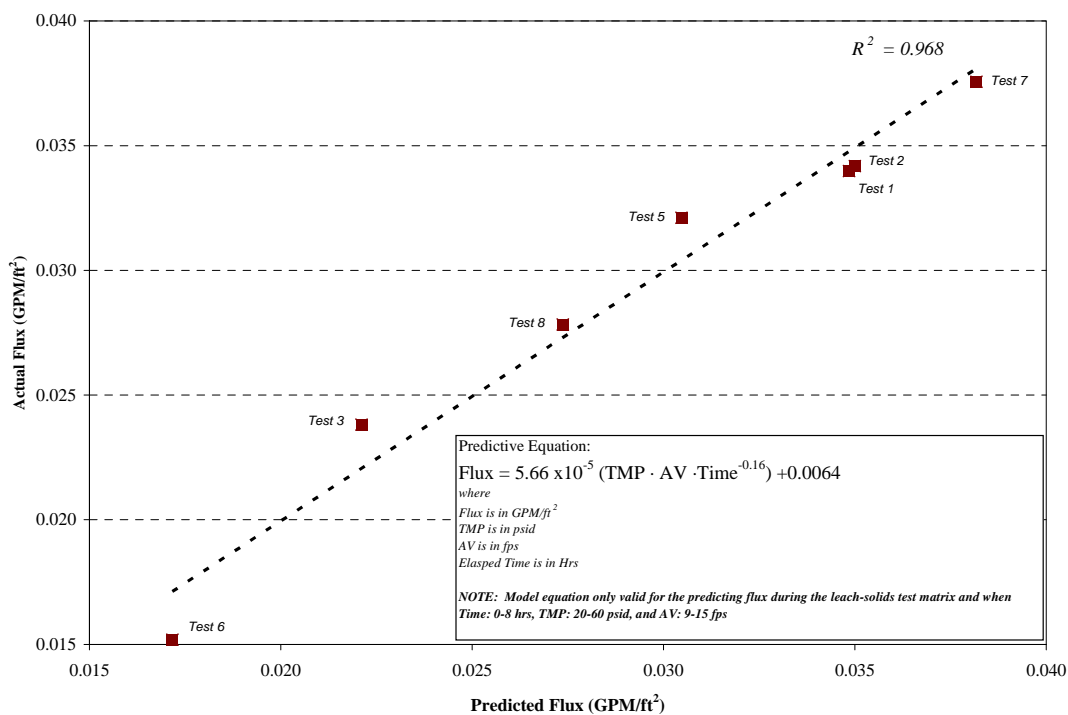
Figure 5.66. Exponential Model of Filter Flux for Leached Group 1/2 Slurry

After the conclusion of the leached solids matrix, the slurry was sampled and recovered from the system. The CUF was rinsed with 0.01 M NaOH to flush out residual solids from the tank and circulation loop. After several such rinses were complete, a CWF test was performed at TMP=10, 20, and 30 psid and AV=11 ft/s. This test captured the condition of the filter before acid cleaning. The system was then drained and cleaned by adding and circulating 1.5 L of 2 M HNO_3. Following this acid cleaning step, the system was rinsed with several liters of 0.01 M NaOH to dilute and flush the acid from the system, and another CWF test was performed. The results from these two CWF tests are presented in Figure 5.67.

Each TMP condition of a CWF test is characterized by a starting and final value on account of the rapid flux decay observed for these tests. There are several observations to make relative to these CWF tests:

- Overall, the CWF is an order of magnitude less than that recorded for the clean filter (see Figure K.9, Appendix K). This indicates that significant irreversible membrane fouling has occurred since loading the CUF into the hot cell and running two leaching and filtration tests.

- The flux is lower after Group 1/2 waste leaching and filtration compared to measured pre-run values. This supports observations of time-dependent flux decrease in matrix tests.

- The flux actually decreases on average as a result of nitric acid cleaning, suggesting that the nitric acid cleaning accomplishes nothing in terms of membrane resistance and may cause an apparent decrease in CWF by loosening solids on the tank walls and other exposed surfaces that are able to surface-foul the filter during CWF tests. This assertion rests on the observation that the flux can be repeatedly restored to a high initial value during CWF tests by back-pulsing.

There was clearly significant irreversible membrane fouling present at this point in the actual waste CUF testing that seems not to be affected by rinsing with inhibited water or by nitric acid cleaning. Because the iron content of the waste was higher than the previous materials tested (Group 5 and 6), it was suspected that iron particles, which would not be affected by leaching operations or a 2-M nitric clean, were the likely fouling agents. After the test was completed, the system was cleaned using 0.5 M oxalic acid before the next test. This cleaning solution was used because it had been proven to be effective in cleaning the filter system used for simulant development when dealing with iron rich simulants. The CWF testing of the filter before and after cleaning are shown in Figure 5.68. After cleaning, the filter flux improved from 0.036 GPM/ft^2 to 0.76 GPM/ft^2 at a TMP of 20 psid and an AV of 11 ft/s after running at steady state for 15 minutes. The dramatic improvement to the CWF supported the assumption that iron in the waste was likely fouling the filter over the course of the test.
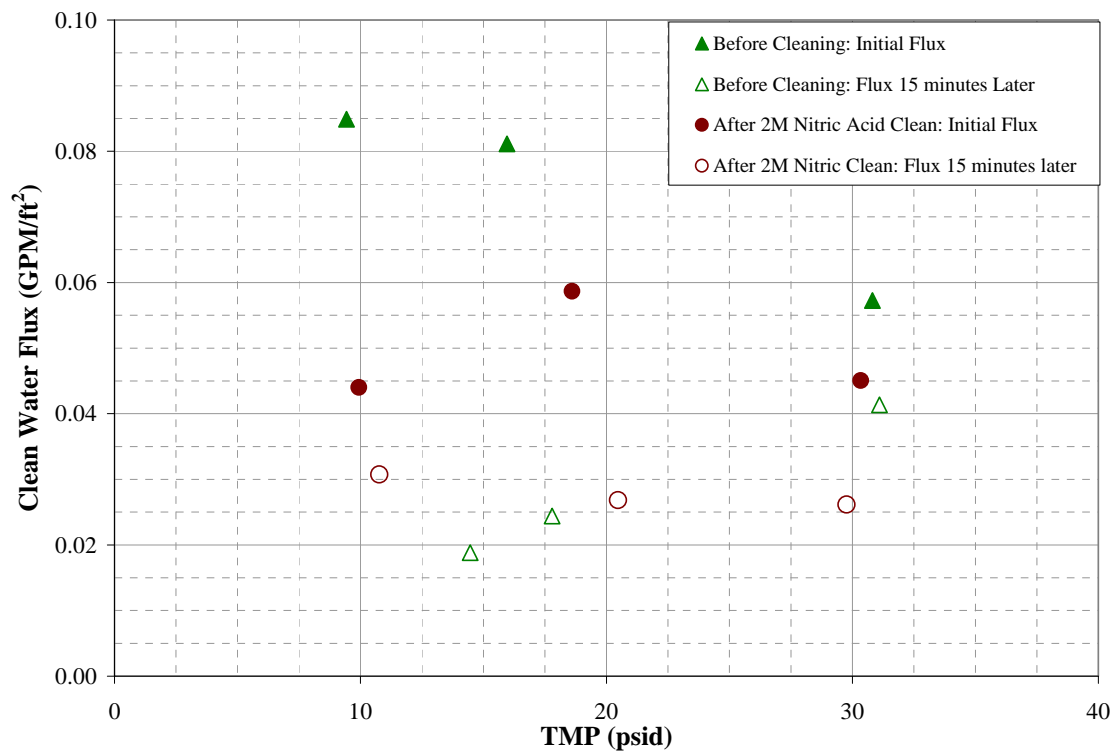
Figure 5.67. CWF Tests Before and After 2-M Nitric Cleaning
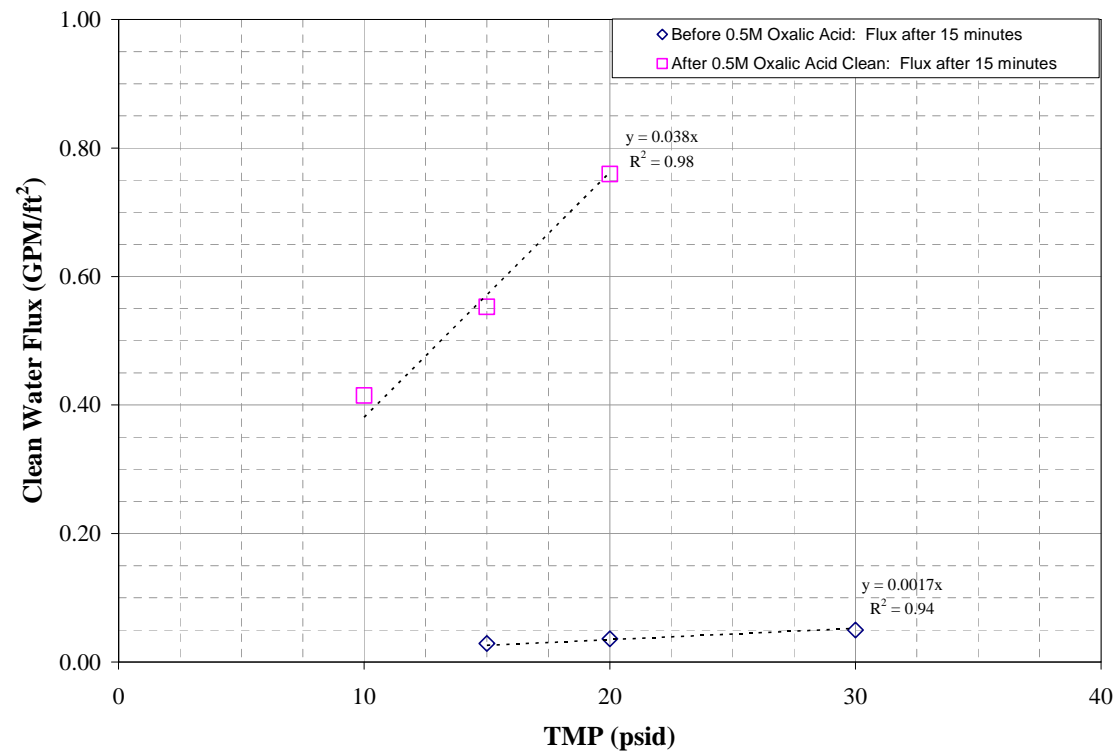
Figure 5.68. CWF Testing Before and After Cleaning with 0.5-M Oxalic Acid
Note: Filter flux measurements after oxalic acid cleaning were performed with a user calibrated flow device.

5.99

5.8 Characterization of the Washed Oxidative Slurry

To achieve a slurry composition that could meet test conditions for the leached high-solids matrix test, 288 grams of the third oxidative wash was added back to the CUF slurry. After completing the filter test matrix, the slurry was sub-sampled for physical and chemical characterization (Figure 5.69). Physical-property measurements of the final slurry are shown in Table 5.41 and the overall composition in Table 5.42 and Table 5.43. However, the results from Table 5.41 and Table 5.43 are likely skewed because the overhead mixer did not work. There are large differences in the reported composition of the UDS when comparing the results of Table 5.42 (based on mass balance calculations) and Table 5.43 (based on the slurry composition sample). With the mixer not operating, the sampled slurry was likely not representative of the slurry in its entirety.

Leached Slurry Matrix
Slurry Mass: 1.9 kg
UDS Mass: 270 g
Slurry Volume: 1.5 L

Permeate Holdup
Mass: 0.20 kg
Volume: 0.2 L

Sample Slurry
Removed Slurry
Mass: 64 grams
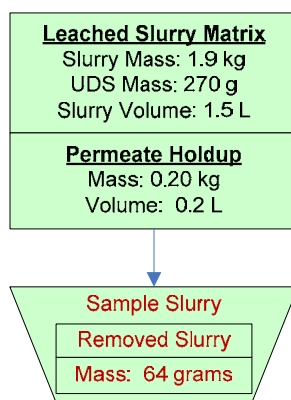
Figure 5.69. Sampling of the Leached Matrix Test Slurry
Note: Mass and volume values in figure are rounded to the nearest significant digit of accuracy.

Table 5.41. Physical Property Measurements of the CUF 1/2 Washed Oxidative Leached Slurry

Slurry Density (g/mL)	1.05
Supernate Density (g/mL)	0.98
Settled Solids (Vol%)	52%
Centrifuged UDS (Wt%)	33%
Total Solids of the Slurry (Wt%)	7.0%
Dissolved Solids of the Supernate (Wt%)	0.56%
UDS of the Slurry (Wt%)	6.5%

Table 5.42. CUF 1/2 Caustic and Oxidative Leached Material (final slurry including permeate hold-up)

	Slurry[a]	Liquid Fraction[b]		Solids Fraction[c]	
Mass (kg)	1.78	1.51		0.26	
Wt% of Slurry	100%	85.2%		14.8%	
Metal	g	g	µg/mL	g	µg/g
Al	2.1E+01	1.3E-01	8.7E+01	2.0E+01	7.8E+04
Bi	1.5E+01	4.3E-03	2.8E+00	1.5E+01	5.7E+04
Cr	2.0E+00	2.0E-01	1.3E+02	1.8E+00	6.8E+03
Fe	2.1E+01	1.2E-03	7.7E-01	2.1E+01	7.8E+04
Mn	1.6E+00	1.9E-05	1.3E-02	1.6E+00	6.1E+03
Na	7.6E+01	4.6E+00	3.0E+03	7.1E+01	2.7E+05
P	1.8E+01	7.3E-01	4.7E+02	1.7E+01	6.4E+04
S	6.4E-02	4.5E-02	2.9E+01	1.9E-02	7.2E+01
Si	1.2E+01	1.8E-02	1.2E+01	1.2E+01	4.7E+04
Sr	1.2E+00	1.1E-05	6.9E-03	1.2E+00	4.7E+03
U	5.1E+00	< 6.E-3	< 4.E+0	5.1E+00	1.9E+04
Radiochemical Isotopes	Slurry	Liquid Fraction		Solid Fraction	
	mCi	mCi	mCi/mL	mCi	mCi/g
Co-60	2.2E+00	< 3.E-2	< 2.E-5	2.2E+00	8.5E-03
Cs-137	2.6E+04	3.3E+02	2.1E-01	2.6E+04	9.9E+01
Eu-154	1.1E+01	< 9.E-2	< 6.E-5	1.1E+01	4.3E-02
Am-241	1.1E+02	< 2.E-1	< 1.E-4	1.1E+02	4.2E-01
Gross Alpha	2.0E+02	< 1.E+0	< 7.E-4	2.0E+02	7.6E-01
Gross Beta	1.3E+05	2.8E+02	1.8E-01	1.3E+05	4.8E+02
Sr-90	4.8E+04	2.9E-01	1.9E-04	4.8E+04	1.8E+02
Pu-239+240	1.5E+02	< 4.E-3	< 3.E-6	1.5E+02	5.6E-01
Pu-238	5.4E+00	< 4.E-3	< 3.E-6	5.4E+00	2.0E-02
Anions	Liquid Fraction			Leached Solids Fraction	
	µg/mL	[M]	g	µg/g	g
F	2.2E+02	1.2E-02	3.5E-01	2.2E+03	5.8E-01
C_2O_4	7.4E+01	8.4E-04	1.1E-01	1.2E+03	3.2E-01
NO_2	2.5E+01	5.5E-04	3.9E-02	3.3E+02	8.6E-02
NO_3	7.1E+02	1.1E-02	1.1E+00	1.2E+04	3.2E+00
SO_4	8.3E+01	8.7E-04	1.3E-01	1.3E+03	3.5E-01
PO_4	1.5E+03	1.6E-02	2.3E+00	1.2E+04	3.2E+00
OH	5.4E+02	3.2E-02	8.4E-01		

(a) Slurry mass components were calculated from characterization data (Sections 3 and 4) and the masses of materials that were added with simulant. Loss of mass from sampling was incorporated.
(b) Liquid fraction mass components were calculated using analytical results from supernate sample TI552-G6-O (ASO ID 08-01294) and the predicted mass of supernate in the system.
(c) Solids fraction mass components were calculated from the difference between the slurry component mass and liquid component mass fraction.

Table 5.43. Group 1/2 Washed Oxidative and Caustic Leach Slurry Composition and Overall Leach
Factor Calculations Based on ICP-OES/Radiochemical Characterization

Slurry Prep Method	ICP-OES Analytes	Dry Slurry[a] (μg/g)	Supernate[b] (μg/mL)	Dry Solids[c] (μg/g)	Solids Leach Factor[d]
HF Assisted Acid Digestion, and KOH Fusion, Concentration Factor of 1.80 based on U and Fe	**Al**	77,950	86.6	82,966	0.54
	Bi	81,450	[2.75]	87,983	0.08
	Cd	120	[0.22]	126	-0.20
	Cr	7,635	127	6,388	0.56
	Fe	104,000	[0.77]	112,382	NA
	K	[170]	[10.3]	[32]	[1.09]
	Mn	10,950	[0.013]	11,834	-5.95
	Na	123,000	2,985	88,971	0.76
	Ni	6,420	<3.0E-1	6,934	0.01
	P	14,400	470	8,641	0.95
	S	[945]	[29]	[594]	1.07
	Si	78600	11.7	84772	0.05
	Sr	5740	[0.0069]	6203	0.04
	U	27,250	<3.9E+0	29,391	NA
	Zn	495	[0.56]	527	0.46
	Zr	517	<1.4E-1	557	-0.53
	Ag	[16]	<2.6E-1	[13]	[0.32]
	Ba	361	[0.160]	388	0.08
	Be	0.675	<6.4E-3	0.635	0.70
	Ca	13,500	[0.79]	14,578	0.04
	Ce	343	<1.2E+0	353	-0.05
	Co	57.9	<3.0E-1	58.2	0.23
	Cu	114	<1.7E-1	120	0.41
	La	50.7	<3.4E-1	49.7	0.20
	Li	86.2	[0.15]	90.9	0.27
	Mg	2,280	<2.8E-1	2,460	0.05
	Mo	[41]	<6.4E-1	[34]	[0.52]
	Nd	78.4	<6.6E-1	74.9	0.05
	Pb	1,945	[1.5]	2,080	0.15
	Ru	[16.8]	<1.5E+0	-[3.58]	[1.09]
	Th	[27]	<3.2E+0	-[18]	-[42.23]
	Ti	248	<1.2E+0	250	0.08
	Tl	[110]	<5.3E-2	[118]	[0.67]
	V	34.7	<4.7E+0	-31.3	2.05
	Y	10.9	<5.4E-2	11.0	0.05

Table 5.43. (Contd)

Slurry Prep Method	Radionuclides	Dry Slurry[a] (µCi/g)	Supernate[b] (µCi/mL)	Dry Solids[c] (µCi/g)	Solids Leach Factor[d]
KOH Fusion, Concentration Factor of 1.80 based on U and Fe	Co-60	8.71E-3	<2.E-5	9.1E-3	0.56
	Cs-137	1.14E+2	2.10E-1	1.2E+2	0.38
	Eu-154	8.61E-2	<6.E-5	9.2E-2	-2.01
	Eu-155	<7.E-2	<2.E-4	<7.E-2	NA
	Am-241	4.92E-1	<1.E-4	5.3E-1	0.05
	Total alpha	1.00E+0	<7.E-4	1.1E+0	0.11
	Total beta	6.27E+2	1.81E-1	6.8E+2	-0.14
	Sr-90	2.66E+2	1.90E-4	2.9E+2	-0.07
	Pu-239/240	6.59E-1	<3.E-6	7.1E-1	-0.10
	Pu-238	1.10E-2	<3.E-6	1.2E-2	0.33
(a) Test sample TI572-G2-O, ASO ID 08-01294					
(b) Test sample TI572-G2-18, ASO ID 08-01321					
(c) Calculated using results from TI572-G2-O and TI572-G2-18.					
(d) Calculated using results listed in					
(e) Table 5.11.					
Note: Analytes in italics were measured opportunistically. Values in brackets [ ] are ≥ MDL but < EQL, with errors likely to exceed 15%.					

At the beginning of the test, it was estimated that 524 grams of solid material was present in the slurry; by the end, there was 263 grams, or 51 wt% of the original solids. Adjusting this value for the sampling that was done gives a total solids value of 70% of the original. Cesium was the only radionuclide that decreased by a significant factor during the leaches and the washes. As detailed in Figure 5.70, the cesium decreased by 49% to a value 51% of the initial feed. By contrast, the rest of the radionuclides decreased by only ±2%, based on mass-balance calculations that use the concentration of removed filtered supernate to projected mass changes. While Table 5.43 projects significant leach factors for ^{238}Pu and ^{60}Co, the composition of the supernate throughout the test does not support this sizeable decrease in the inventory.
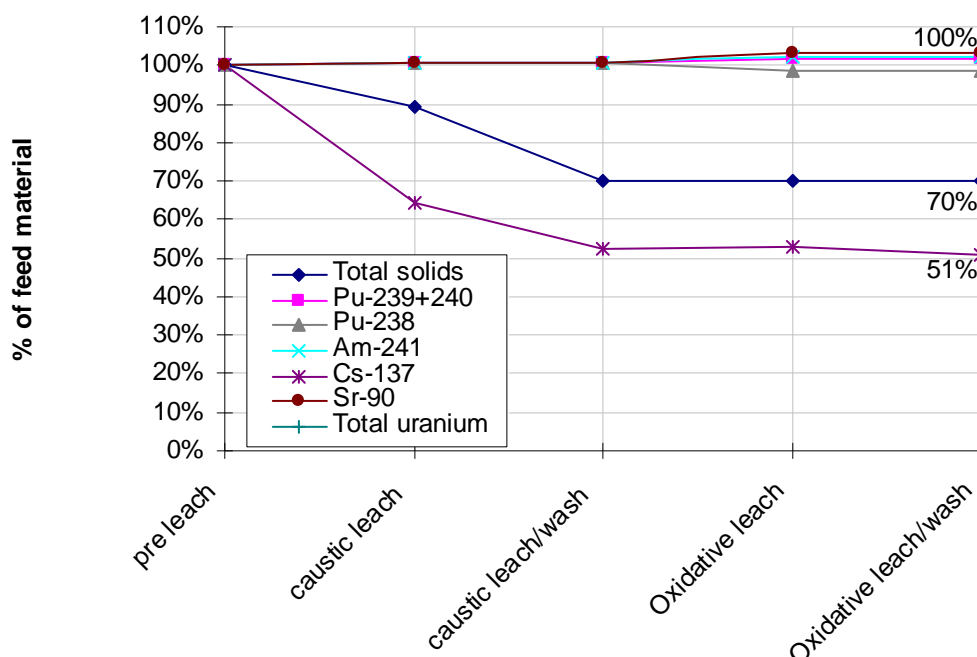
Figure 5.70. Radionuclides/Total Solids in CUF 1/2 Slurry, Adjusted for Sampling

The anions, specifically phosphate, in the permeate exhibit interesting behavior. While the nitrite, nitrate, sulfate, and oxalate follow an expected decrease (nitrite, nitrate, and sulfate decreasing consistently with each other, oxalate at a slower rate due to its relatively low solubility), phosphate increases in concentration after the caustic washes (Figure 5.71). During the same time period, the overall slurry phosphorus decreases (Figure 5.72). This can be explained by the precipitation of phosphate in higher concentrations of sodium (WTP-RPT-173, Lumetta 2008). Immediately after the caustic leach, the sodium concentration in the slurry supernate was 6 M. This caused insoluble phosphorus released as a phosphate ion from metathesis to re-precipitate as a sodium salt and still appear insoluble under these specific conditions. As the slurry was washed, the sodium concentration decreased, increasing the solubility of phosphate into the slurry's liquid phase. Repeated rinsing of the slurry afterwards allowed phosphates formed from the caustic leach to become soluble and be washed out of the slurry. This is further demonstrated in Figure 5.72. The caustic leached slurry has almost no phosphorus in the supernate and does not show a significant change in the insoluble fraction of the slurry. However, the fraction of phosphorus in the soluble liquid phase dramatically increases after the third wash, demonstrating that phosphorus was dissolving out of the insoluble phase. This indicates that the insoluble phosphorus was artificially elevated because of a large amount of "gelled" phosphate. All of these observations are consistent with the formation of sodium phosphate through metathesis of other metal phosphate (primarily $FePO_4$).
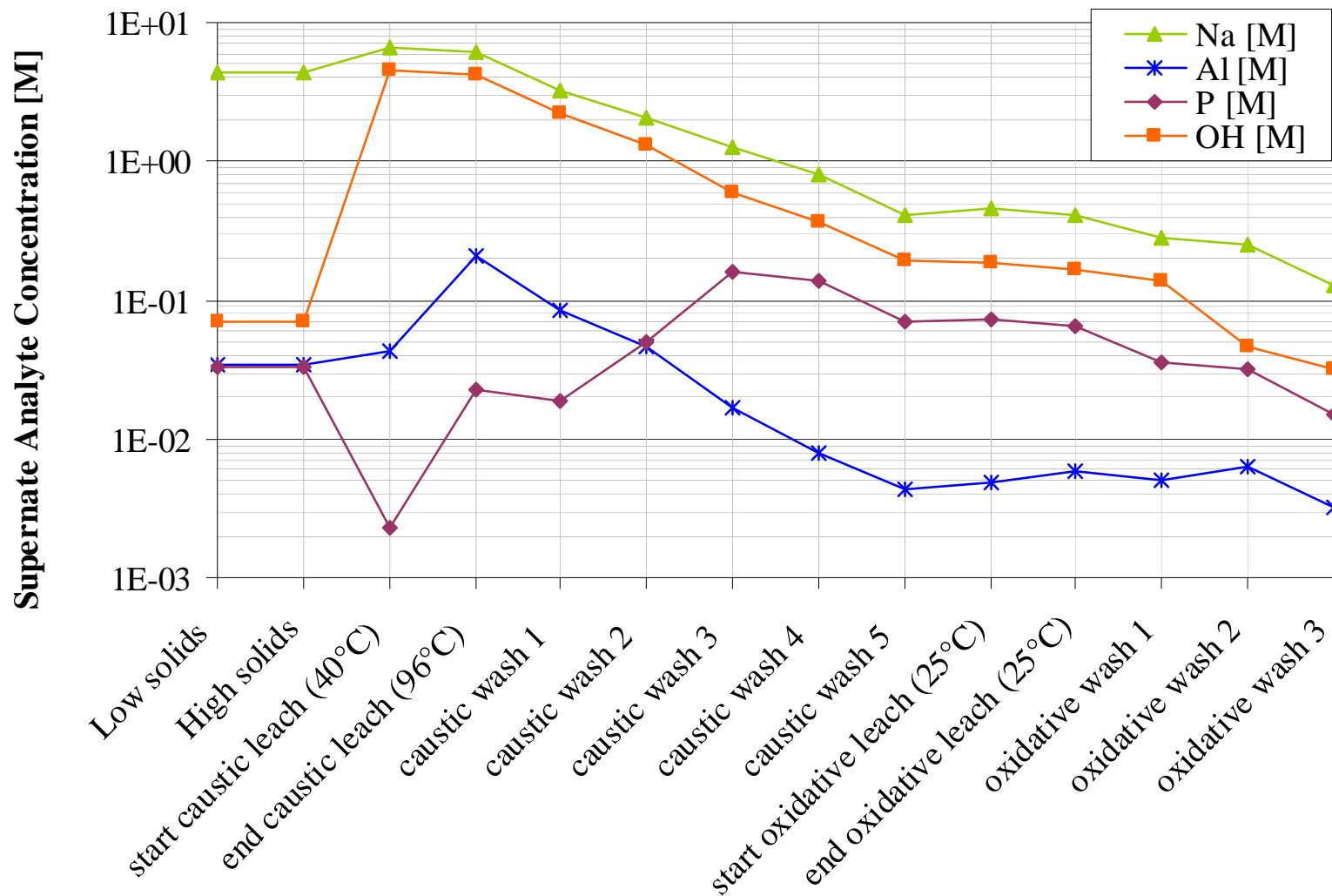
Figure 5.71. Sodium, Free Hydroxide, Al, and P Molarities During CUF Run
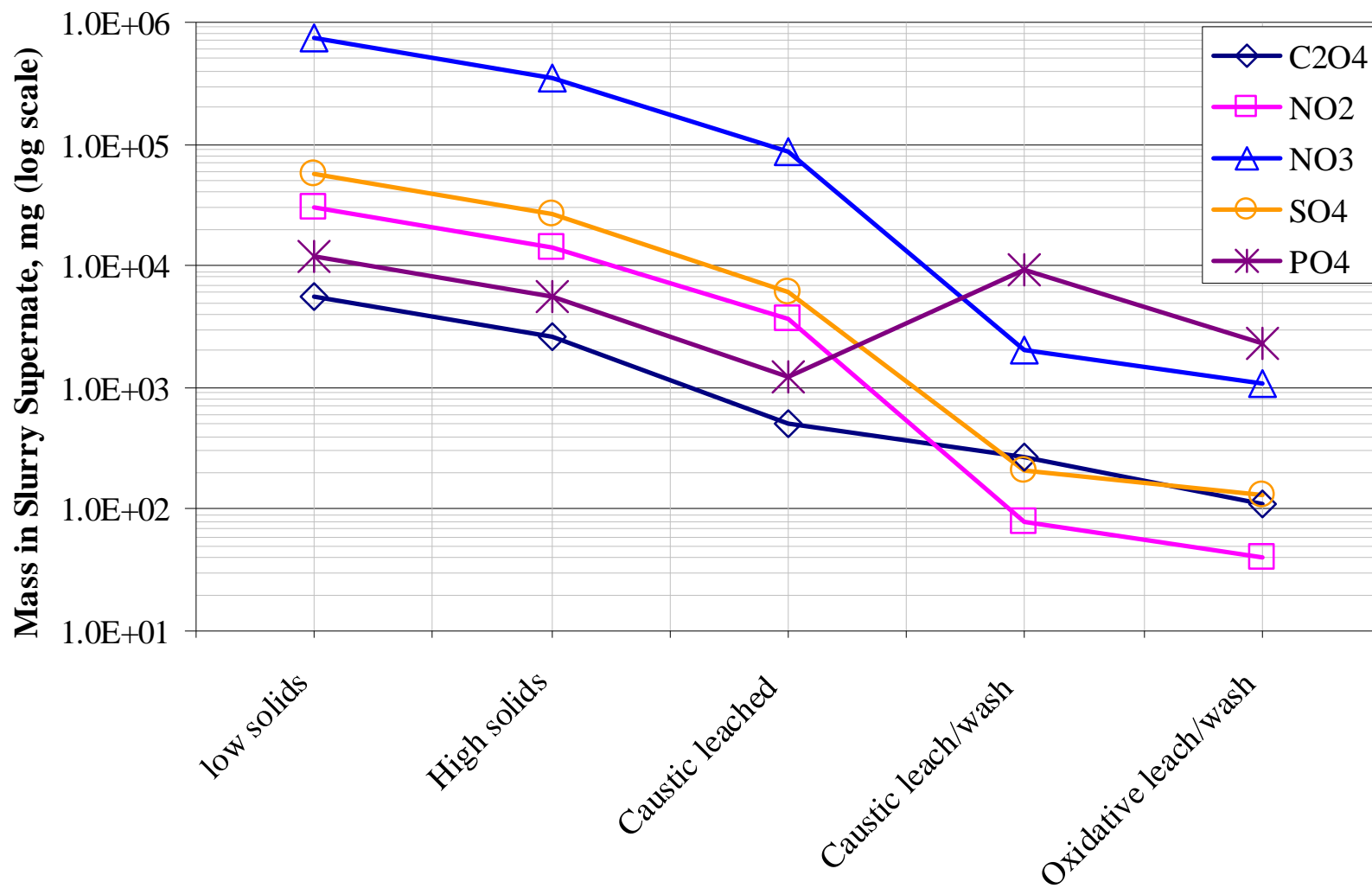
Figure 5.72. Inventory of Selected Anions in the Liquid Phase of the CUF 1/2 Slurry During Test

The surface area of the leached solids was determined by BET analysis and found to be 96.3 m^2/g. Sodium aluminum silicate nitrate hydrate [Na$_{7.92}$(AlSiO$_4$)$_6$(NO$_3$)$_{1.74}$(H$_2$O)$_{2.34}$] was the predominant phase found by XRD analysis (Figure 5.73). Other mineral phases found were clarkeite {Na[(UO$_2$)O(OH)]}, sodium aluminum carbonate silicate [3NaAlSiO$_4$·Na$_2$CO$_3$] and sodium uranium oxide [Na$_6$U$_7$O$_{24}$]. Phases that are possibly present, but not confirmed, are boehmite [AlOOH] and iron hydrogen phosphate hydrate [FeH$_2$PO$_3$O$_{10}$.H$_2$O].
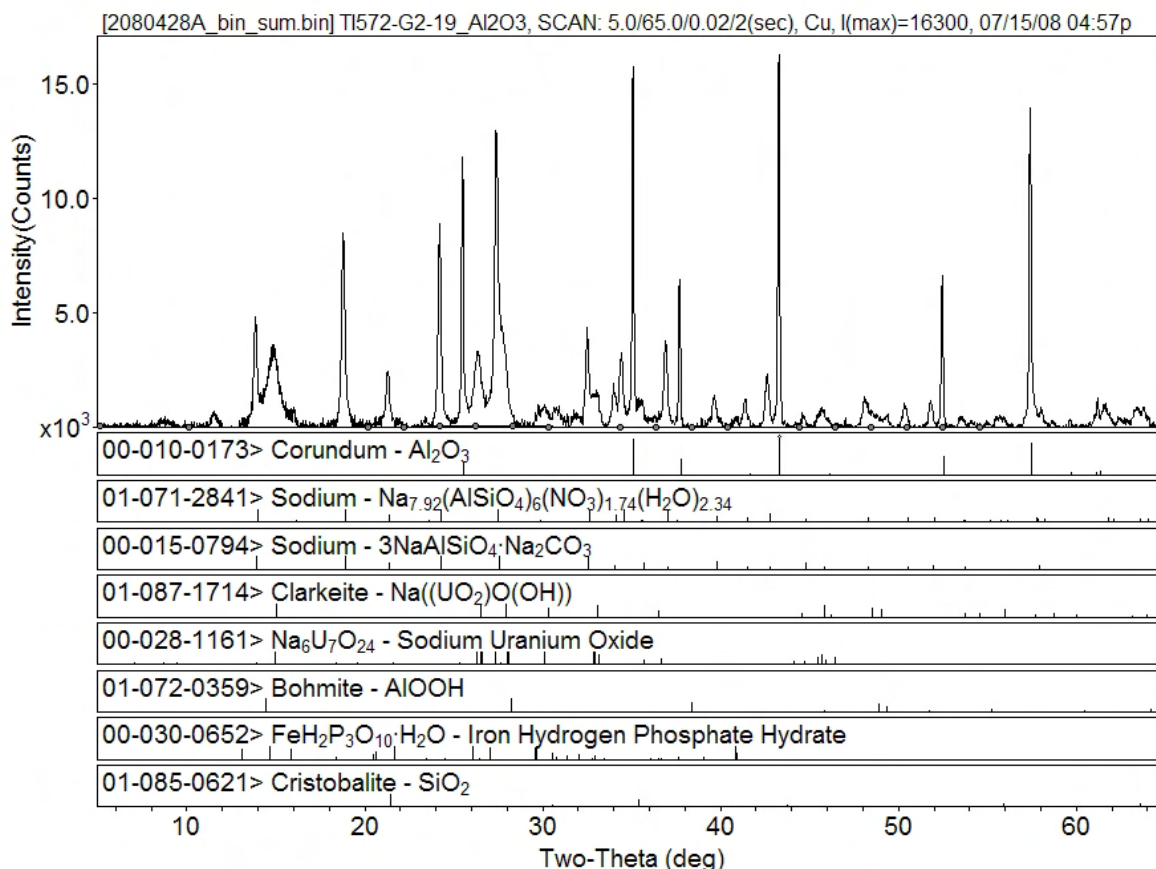
Figure 1.2. Phases identified, sample TI572-G2-19_Al2O3. Background subtracted data.

Figure 5.73. XRD Scan of CUF 1/2 Final Leached and Washed Solids

SEM (Figure 5.74 and Figure 5.75) and TEM (Figure 5.76) imaging as well as EDS analysis add validity to the XRD analysis and the suspected crystal forms present. Furthermore, a bismuth iron phase agglomerated with large particles of cancrinite was identified that would tend to make dissolution more difficult. XRD data suggested the presence of a uranyl oxide hydrate; however, TEM-EDS proves that the phase contains Si and a small amount of Al. Bismuth is present possibly as a mixed Al-P and Fe-Bi phase. EDS compositional analysis of this phase suggests that it is iron rich with aluminum incorporated into it. The uranium phase appears to be a uranium(VI) silicate with a high Si:U ratio.
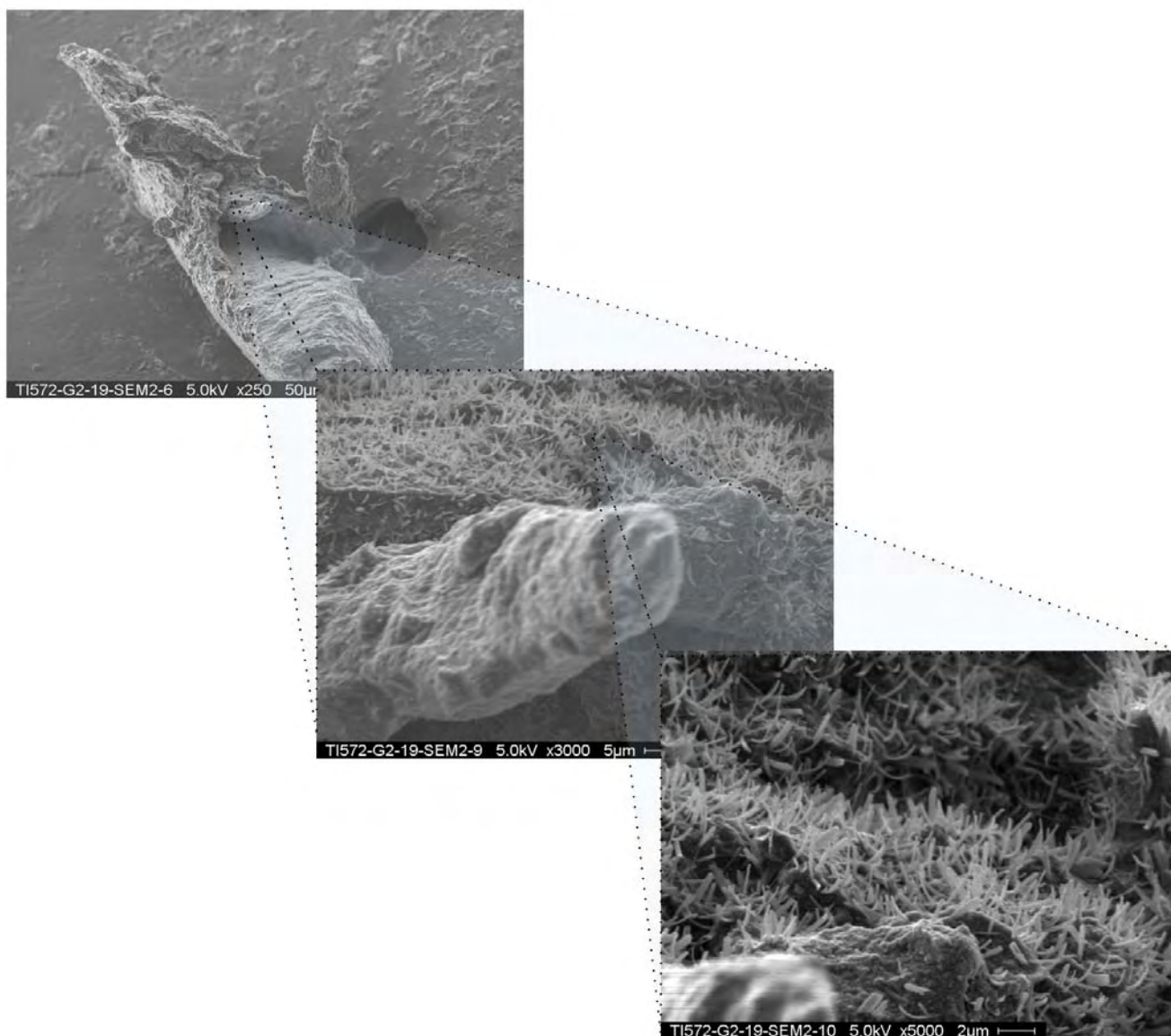
Figure 5.74. SEM Image of Leached/Washed CUF 1/2 Solids

Element	Wt%	At%
CK	31.68	54.39
OK	18.38	23.69
FeL	2.75	1.02
NaK	6.31	5.66
AlK	2.92	2.23
SiK	2.27	1.66
PK	0.49	0.32
BiM	4.98	0.49
UM	2.77	0.24
CaK	1.56	0.8
CrK	1.46	0.58
MnK	2.09	0.78
FeK	19.04	7.03
NiK	1.12	0.39
CuK	2.18	0.71
Matrix	Correction	ZAF

Element	Wt%	At%
CK	30.88	45.02
OK	33.68	36.86
NaK	11.26	8.58
AlK	5.18	3.36
SiK	4.27	2.66
PK	0.93	0.53
BiM	4.66	0.39
UM	1.57	0.12
CaK	0.74	0.32
CrK	0.44	0.15
MnK	0.62	0.2
FeK	5.77	1.81
Matrix	Correction	ZAF

Element	Wt%	At%
CK	39.48	62.77
OK	15.77	18.82
NaK	4.95	4.11
AlK	1.98	1.4
SiK	1.05	0.72
PK	0.2	0.12
BiM	1.42	0.13
CaK	0.35	0.17
MnK	3.02	1.05
FeK	27.1	9.27
NiK	1.37	0.45
CuK	3.32	1
Matrix	Correction	ZAF

Figure 5.75. SEM and EDS of Leached Washed CUF 1/2 Solids
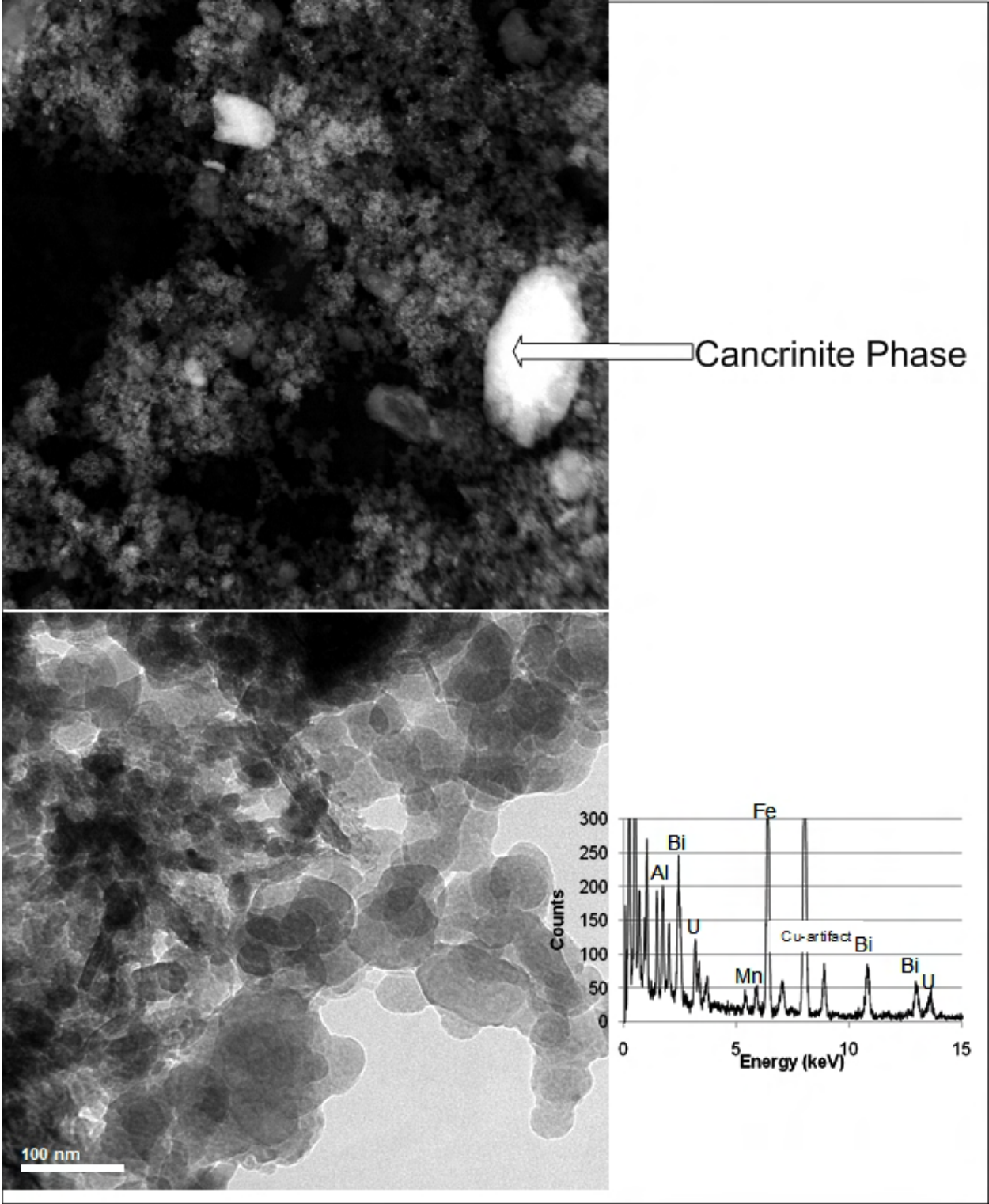
Figure 5.76. TEM Image of Leached Washed CUF Solids

Figure 5.77 shows the pre-sonication size distribution of solids for the oxidative leached, washed slurry as a function of pump speed. Regardless of pump speed, all distributions show a strong single peak spanning ~0.2 to 3 µm with a maximum population ranging from 0.7 to 0.8 µm. Secondary peaks appear at sizes larger than 3 µm. The initial measurement at 3000 RPM exhibits a secondary peak spanning 40 to 200 µm. At 4000 RPM, two adjacent secondary peaks form a continuous distribution of particles from 3 to just below 200 µm. A portion of the observed particle population at 4000 RPM may correspond to difficult-to-suspend particles observable only at 4000 RPM. Finally, the measurement at 2000 RPM indicates a single secondary peak spanning 3 to 10 µm. Although this peak is not observed at 3000 RPM, it is observed at the 4000 RPM measurement preceding the 2000 RPM set point. As such, it is likely that this peak corresponds to particles either suspended at 4000 RPM (that have yet to settle out) or particles formed by shearing apart particle flocs making up the secondary peaks observed at 3000 and 4000 RPM.

Figure 5.78 shows changes in the PSD for the oxidative leached, washed slurry that occur as a result of applied sonication. Similar to the oxidative leached sample, sonication reduces the relative contribution of intermediate particles (0.5 to 2 µm) while increasing the contributions of both submicron (0.1 to 0.5 µm) and 3- to ~10-µm particles. Secondary peaks greater than 10 µm in size were not observed either during or after sonication. This suggests full disruption of flocs at the end of sonication, either through sonic action or shear. It can be speculated that the submicron particles are the result of breakage (de-agglomeration) of particles in the 0.5- to 2-µm range and that 3- to 10-µm particles result from the breakage of flocs in the 10- to 200-µm range. Both during and after sonication measurements show similar distributions, indicating that agglomerate reformation does not occur over the time frame of the measurement.
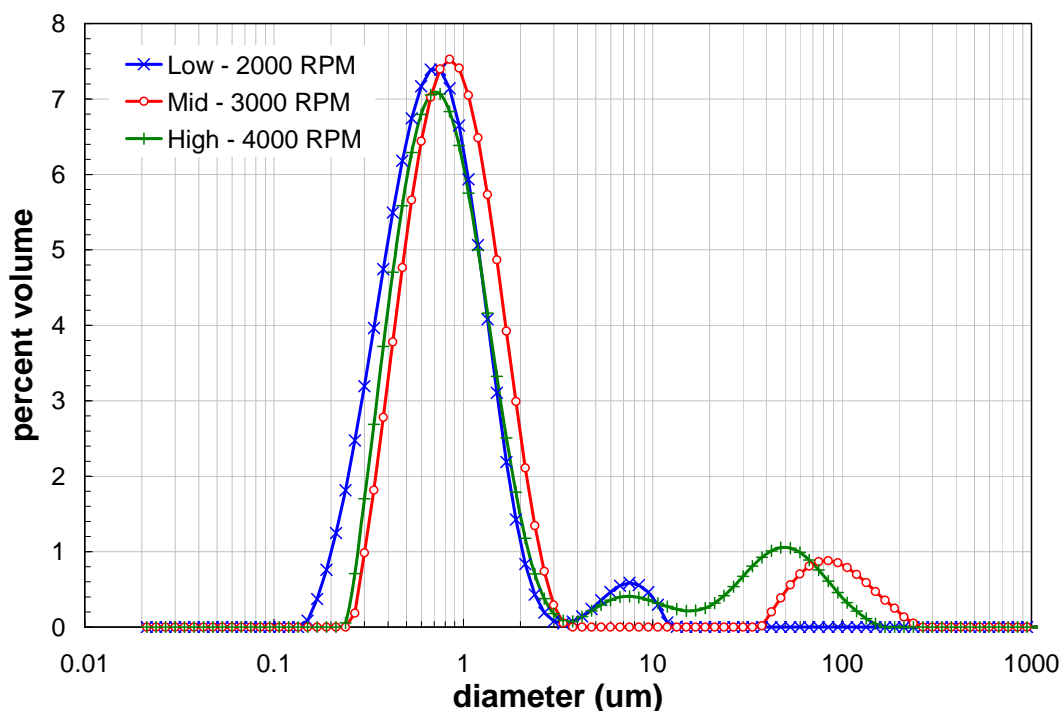
Figure 5.77. Oxidative Leached, Washed Slurry PSD as a Function of Pump Speed
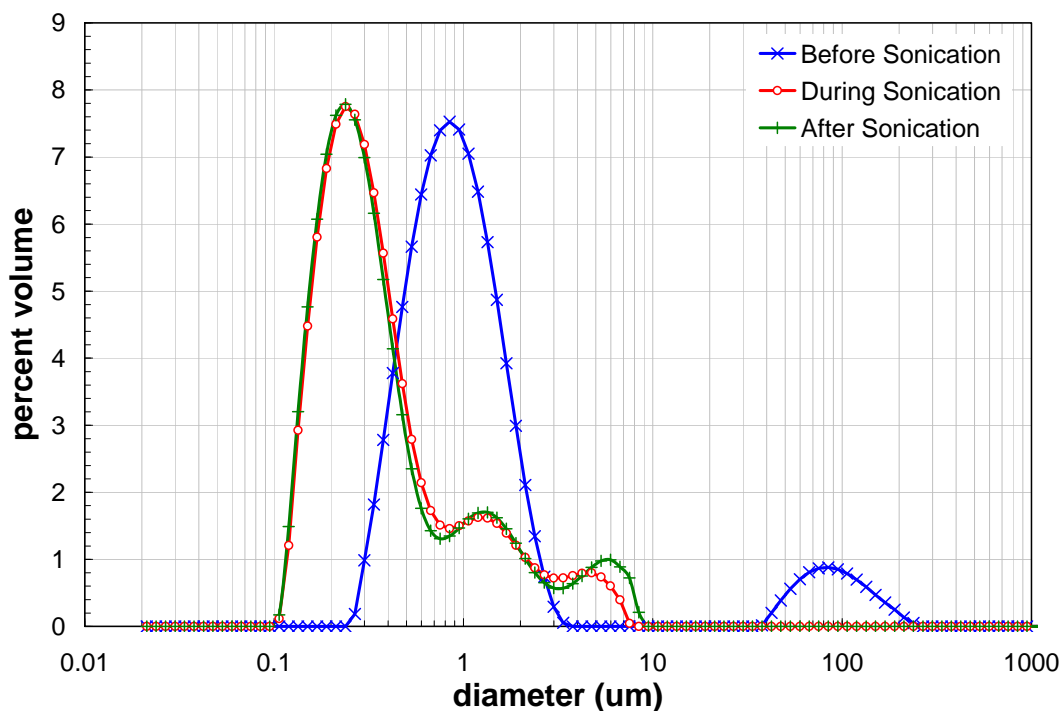
Figure 5.78. Oxidative Leached, Washed Slurry PSD as a Function of Sonication at 3000 RPM

Figure 5.79 shows the results of flow curve testing for the oxidative-leached and washed slurry, which shows Newtonian behavior. The flow curves for 40 and 60°C have a stress axis intercept greater than zero but less than the limit of instrument accuracy (±0.5 Pa). This may indicate weak non-Newtonian behavior; however, given the measurement noise of the M5 system, it is impossible to statistically distinguish any finite yield stress for this slurry based on the magnitude of its stress response. For this reason, the slurry shall be defined as Newtonian.

The flow curves are free of artifacts caused by poor sample rotation. Over shear rates from 0 to 400 s^{-1}, the stress response is linear. A slope transition is observed at ~500 s^{-1}, indicating the formation of Taylor Vortices. When fitting these flow curves, data for shear rates above 400 s^{-1} will be avoided to prevent the inclusion of data affected by vortex formation. Although it is difficult to observe because of significant data overlap and noise, flow curve hysteresis occurs in all measurements. Hysteresis manifests as a lower stress response on the down-ramp relative to the up-ramp. Given the relatively weak stress response of the material (~1 Pa at 500 s^{-1}), this type of hysteresis is consistent with rotor inertial effects. That is, the additional torque required to accelerate on the up-ramp increases its stress response, whereas the resisting torque of the fluid will help slow the rotor down during the down-ramp portion of testing, which reduces the apparent stress response of the fluid. As such, hysteresis is not associated with any changes to bulk sample rheology.

The noise-to-signal ratio is so significantly large that it is impossible to qualitatively evaluate whether temperature influences the oxidative-leached and washed slurry stress response. Based on Figure 5.79, the flow curves appear to be statistically similar. Table 5.44 summarizes the best-fit "Newtonian" viscosities for the oxidative leached and washed slurry flow-curve data as well as the viscosities

determined by constant rotation at 470 s^{-1} (i.e., the shearing step run before every measurement). The analysis results in Table 5.44 show that:

- The Newtonian viscosity appears to decrease slightly with increasing temperature (as expected based on suspending phase viscosity lowering).

- Given the best expected accuracy limit of ±0.5 mPa·s, the viscosities are similar to each other. Statistically, the viscosities determined from the flow curves at 25 (2 of 2), 40, and 60°C are the same.

- The repeat measurements at 25°C appear to show reasonable agreement. Although the flow curve fits show a larger-than-expected difference (0.7 mPa·s), the constant rotation analysis shows a difference that falls on the limit of instrument accuracy (0.5 mPa·s).

- The constant rotation and flow curve generally agree within ±0.5 mPa·s, with exception of the 40°C, which shows a 0.7- mPa·s difference.

Because the oxidative leached and washed slurry shows Newtonian behavior, the apparent viscosities should be nominally independent of shear and should be equal to the Newtonian viscosities reported in Table 5.44.
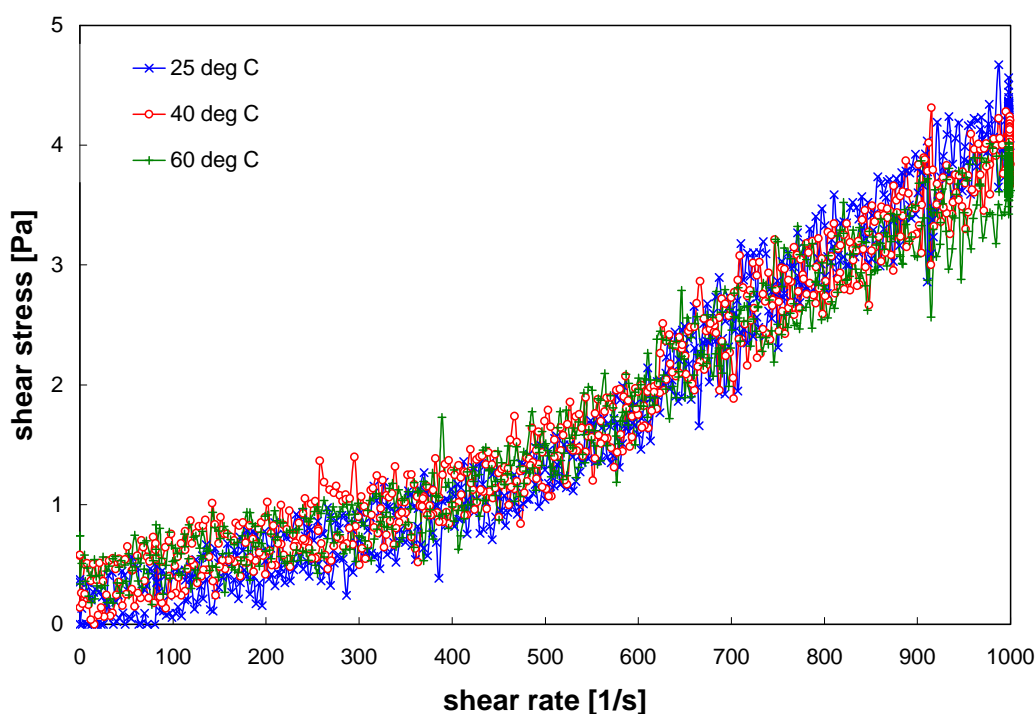
Figure 5.79. Flow Curve for the Group 1/2 CUF Oxidative Leached and Washed Slurry at 25, 40, and 60°C

Table 5.44. Results of Fitting Analysis for the Group 1/2 CUF Oxidative Leached and Washed Slurry

Model	Temperature [°C]	Newtonian Viscosity [mPa·s]	R
Flow Curve Fits (0 – 400 s^{-1})	25 (1 of 2)	2.8	0.862
	25 (2 of 2)	2.1	0.799
	40	2.0	0.757
	60	1.6	0.737
Constant Rotation (470 s^{-1})	25 (1 of 2)	2.8 ± 0.2	n/a
	25 (2 of 2)	2.3 ± 0.1	n/a
	40	2.7 ± 0.2	n/a
	60	1.2 ± 0.2	n/a

Table 5.45 and Figure 5.80 show the influence of oxidative-leaching and washing on the rheology of the caustic-leached, dewatered, and washed Group 1/2 waste slurry. Before oxidative leaching, the 12.0-wt% slurry showed a 7.7-Pa yield stress and a 9.7- mPa·s consistency. After oxidative leaching and washing, the slurry concentration was reduced to 6.8 wt%, and the slurry behavior was Newtonian with a viscosity of 2.1 mPa·s. The reduction in rheology appears to be a continuation of the reduction observed during washing of the caustic-leached and dewatered slurry. For the current process step, reduction is likely a result of both changes in the suspending phase chemistry and solids concentration. It is speculated that oxidative leaching and washing further reduces the concentration of both dissolved Na_3PO_4 and the UDS. A reduction in both would be consistent with a reduction in rheology, as 1) Na_3PO_4 lends strength to the suspending phase through gel formation and 2) increased UDS concentrations yield increased particle colloidal and frictional interactions.

Table 5.45. Effect of Oxidative-Leaching and Washing on Group 1/2 CUF Slurry Rheology (at 25°C)

Description	Solids Concentration	Rheology	Yield Stress [Pa]	Consistency [mPa·s]
Caustic-Leached, Dewatered, Washed (TI572-G2-R4)	12.0-wt%	non-Newtonian	7.7	9.7
Oxidative-Leached and Washed (TI572-G2-R5)	6.8-wt%	Newtonian	n/a	2.1
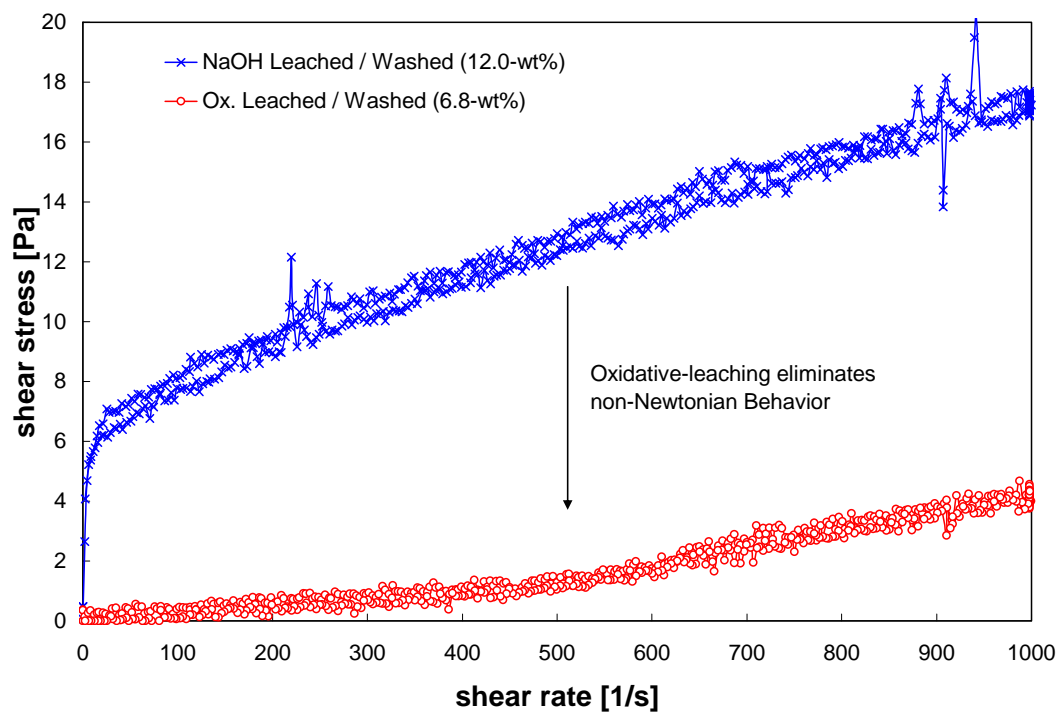
Figure 5.80. A Comparison of Group 1/2 CUF Slurries Showing the Effect of Oxidative-Leaching and Post-Oxidative-Leach Solids Washing on Rheology at 25°C

5.9 Summary and Lessons Learned from the Group 1/2 CUF Run

Filtration, chemical leaching, and physical characterization results are summarized in
Table 5.46,
Table 5.47, and Figure 5.81. During the course of the test, several problems occurred that impacted the performance of test and have created some uncertainty about the results. However, conducting the test created additional understanding about the process that had added benefits.

Failure of the Mixer Blade Due to Erosion
During the course of this test, the propeller mixing blade came off the shaft of the overhead mixer used to homogenize the slurry inside the slurry reservoir tank. Examination of the blade showed that erosive wear destroyed a crimp seal that attached the blade to the shaft collar. This was surprising, considering that this was only the third test performed with this mixer. However, the crimp seal holding the mixer blade to the shaft collar was at the base of the blade where agitation was the greatest. While the type of mixing used in this system was not prototypic, it demonstrated the highly erosive nature of the tank waste samples used for this test.

The lack of mixing inside the slurry reservoir likely caused several discrepancies during this test. The biggest issue was that physical properties results did not correlate well with predicted estimates. Typically, measured UDS results of the slurry were significantly lower than that predicted from characterization data. While the circulation of the slurry created some mixing inside the reservoir, it likely acted like a wide spot in the pipe, allowing a fraction of the solids to settle out. This would explain the difference between the measured and predicted UDS concentrations. Leaching and washing results from this test were also questionable. Conversions were not as high as that expected from the parametric studies, and comparison of phosphorus conversion using a mass-balance method (50%) to that based on slurry samples (100%) shows a big difference. Because phosphorus was found to be released during washing, it may be that the concentration of phosphorus was changing during dewatering as the slurry volume decreased and agitation improved inside the vessel. Samples of the wash were pulled halfway between the dewatering because it was assumed that the slurry was well mixed and would not change. However, the issues that made sampling for UDS a problem likely impacted sampling of the slurry solids for chemical and radiochemical analysis. Heavier particles likely were held up at the bottom of the slurry reservoir, making assumptions of homogeneity of the slurry not valid.

After this test was completed, a new mixing blade and shaft were installed. The blade was installed onto the shaft in a configuration where the crimp seal was protected from slurry erosion. In future tests, the quality of mixing was to be examined throughout the test. In future testing, using a mixer that measures the torque of the mixer blade is recommended as a method to monitor how mixing is occurring without looking into the tank itself.

Pump Plugging with Leached Slurry
Another issue that occurred during the test was that the circulation pump was not operational after the caustic leach. While preparing the slurry for leaching, the slurry was drained from the CUF. To flush additional solids out of the circulation lines, a small fraction of the caustic addition for the leach was used to rinse out the system piping and pump. After the leach was completed, it was discovered that the pump was stalled and that the drive shaft could not be rotated. The sanitary fittings connecting the circulation piping to the pump were loosened to examine the inside of the pump chamber. A gel was discovered in

the pump head that apparently formed in the slurry loop during the caustic leaching step. The pump was located close enough to the slurry reservoir that material inside the pump was heated up from thermal conduction of the attached piping and reacted. The main purpose of the leach was to cause metathesis of isolable phosphorus into a soluble phosphate salt. Because of the high concentration of caustic present in the line, it was hypothesized that this gel consisted of $Na_3PO_4 \cdot 12H_2O$ that precipitated from the reaction of residual slurry solids with the small amount of caustic solution that was used to flush the slurry loop before the leaching step. This gel was removed from the pump head by back pulsing water into the slurry piping and forcing it into the pump cavity. Eventually, the positive displacement blades of the pump broke free and the test was resumed.

Rheology testing of the dewatered caustic-leached slurry found that the final leached slurry possessed a very high shear strength (38 Pa). Analysis of the slurry composition afterwards showed that very little phosphate was in the aqueous phase of the slurry, indicating that phosphate released from metathesis had re-precipitated as sodium phosphate (likely hydrated) due to the high sodium concentration of the slurry. After the slurry was washed and the sodium concentration of the slurry supernate decreased, the phosphate became soluble and was released into the wash solutions. The shear strength of the slurry afterwards decreased to 8 Pa after washing and later became Newtonian after oxidative leaching and washing.

How the leached slurry behaved during the test helped explain what occurred in the pump:

- Caustic leaching releases insoluble phosphorus into the slurry supernate as phosphate.

- However, high sodium concentrations present from the addition of sodium hydroxide caused the phosphate to precipitate as sodium phosphate.

- This caused a change in the shear strength of the fluid. Because of the concentration of waste and caustic inside the pump, this effect was amplified and caused a plug to form that stalled the pump.

- Diluting the slurry with water by back pulsing water into the chamber allowed the sodium phosphate to re-dissolve.

- Once the phosphate became soluble, the yield stress of the slurry decreased. In the case of the pump, the back pulsing of water into the pump chamber lowered the shear strength of the "gel" inside the pump enough to allow the pump displacement blades to rotate freely.

To prevent this from occurring in future tests, the slurry lines and pump chamber will be flushed afterwards with water after flushing the lines using caustic. This will wash any waste material that is in contact with a reactant (such as caustic) from the piping to prevent problems with plugging and stalling of the pump. Future designs should incorporate better methods of flushing lines and the pump to recover solids in the lines as well as to dislodge highly concentrated slurries/packed solids that plug lines or the pump.

Predicting Sodium Permanganate Addition for Chromium Dissolution
The goal of the oxidative leach was to operate the leach when the free-hydroxide concentration was equal to or less than 0.25 M, and the molar ratio of Mn to Cr = 1:1. However, this proved difficult to do. This required that:

- The initial slurry mass be known and the slurry chemically characterized
- Losses of UDS be accounted for throughout the test
- The caustic leach factor of chromium due to caustic leaching be accurately accounted for.

In the previous test (Group 6/5 CUF), the initial slurry mass and composition, as well as the caustic leach factor for chromium, was well understood. However, in that test, the loss of UDS during the test was underestimated. The quantity of insoluble chromium was projected to be too high, and additional sodium permanganate was added. For this test, slurry sampling was considered to be more significant, and characterization data for the Group 1 and Group 2 slurry were known. However, leaching studies of the Group 1 and Group 2 wastes were just completed, and analytical results from this testing were not available in time for guiding the Group 1/2 CUF experiment. Because of this, the predicted caustic-leaching factors for chromium were derived from previous studies of the tanks present in the two groups. The highest value found for chromium dissolution was used, which was 70%. However, parametric studies found that chromium dissolution would be much lower (closer to 20 to 30%). This caused projections of insoluble chromium present in the slurry to be too low, making the sodium permanganate addition too conservative.

For this test, the Mn:Cr ratio during the oxidative leach test was only 0.4 rather than the target of 1.1. On the other hand, the Mn:Cr ratio for the Group 6/5 test was 1.7 (WPT-PRT-172, Shimskey 2009). Assumptions and compounding errors during both tests (e.g., mistakes with the permanganate additions for the Group 6/5 test and mixing issues with this test) caused significant deviation from the planned Mn:Cr molar ratio. These problems demonstrate the need for accurate mass balance, characterization, and leaching data of the waste to achieve a more precise Mn:Cr ratio for oxidative leaching.

Cleaning with 2 M Nitric Acid and 0.5 M Oxalic Acid

The test plan dictated that the filter was to be cleaned with 2 M nitric acid. And while that was done for the Group 5, Group 6/5, and Group 1/2 tests, cleaning did not return the filter to the original condition. Over the course of the three tests, the CWF measured decreased each time with nitric cleaning having little impact. Because the final CWF of the filter was only 0.07 GPM/ft^2 at a project TMP of 40 psid after nitric cleaning, it was felt another cleaning method needed to be tried.

Because 0.5 M oxalic acid successfully cleaned the filter being used for simulant development, this solution was used after nitric acid cleaning. The results of cleaning were dramatic, with the final CWF measured of the filter to be 0.7 GPM/ft^2 at 20 psid—or 1.4 GPM/ft^2 at 40 TMP.

Although 2 M nitric acid was proving not to be an effective cleaning agent for the waste tests so far, it was planned to continue to use it for the remaining testing planned. However, it was also planned to use oxalic acid to understand when it was an effective cleaning agent and when it was not.

Table 5.46. Group 1/2 CUF Filtration, PSD, and Rheology Test Result Summary

Filtration Step	Property	Results
Low Solids Filtration Testing (Section 5.2, 5.3.2)	Material Description	Group 1-2 diluted with excess supernatant from homogenization and circulated in CUF
	Measured UDS	7 wt%
	Predicted UDS	*10 wt%*
	Slurry Rheology @ 25°C-60°C *(Sample ID: TI572-G2-R1)*	Newtonian Viscosity: 5-3 mPa·s
	Particle Size	d(10): 0.56 μm d(50): 2.0 μm d(90): 7.4 μm
	Permeate Composition	[Na]: 4.4 M [Al]: 0.035 M [OH]: 0.07 M
	Permeate Viscosity (TI572-G2-R2s)	2.6 mPa-s @ 25°C
Dewatering of Waste Before Leaching (Section 5.3.3) *Target Filtration Conditions* *TMP: 40 psid* *AV: 13 ft/s*	Material Description	Dewatered Group 1-2 slurry
	Final Measured UDS	14 wt%
	Final Predicted UDS	*20 wt%*
	Permeate Composition	[Na]: 4.4 M [Al]: 0.035 M [OH]: 0.07 M
	Permeate Viscosity (*TI572-G2-R2s*)	2.6 mPa-s @ 25°C
High-Solids Filtration Testing (Section 5.3.4)	Material Description	Dewatered Group 1-2 slurry
	Measured UDS	14 wt%
	Slurry Rheology @ 25°C-60°C *(Sample ID: TI572-G2-R2)*	Non-Newtonian Yield Stress: 3.2-2.1 Pa Consistency: 10-23 mPa·s
	Particle Size	d(10): 0.52 μm d(50): 2.4 μm d(90): 9.5 μm
	Permeate Composition	[Na]: 4.4 M [Al]: 0.035 M [OH]: 0.07 M
	Permeate Viscosity (*TI572-G2-R3s*)	2.6 mPa-s @ 25°C

Table 5.46 (Contd)

Filtration Step	Property	Results
Caustic Leach Dewater (Section 5.5.2-5.5.3) *Target Filtration Conditions* *TMP: 40 psid* *AV: 13 ft/s*	Measured UDS	18 wt%
	Slurry Rheology @ 25°C-60°C *(Sample ID: TI572-G2-R3)*	Non-Newtonian Yield Stress: 32-57 Pa Consistency: 26-23 mPa·s
	Particle Size	d(10): 0.56 μm d(50): 1.6 μm d(90): 6.9 μm
	Permeate Composition	[Na]: 6.2 M [Al]: 0.20 M [OH]: 4.2 M
	Permeate Viscosity (*TI572-G2-R3s*)	7.9 mPa-s @ 25°C
Caustic Wash 1 (Section 5.5.4-5.5.5) *Target Filtration Conditions* *TMP: 40 psid* *AV: 13 ft/s*	Wash Solution	0.56 M NaOH
	Permeate Composition	[Na]: 3.3 M [Al]: 0.085 M [OH]: 2.2 M
Caustic Wash 2 (Section 5.5.4-5.5.5) *Target Filtration Conditions* *TMP: 40 psid* *AV: 13 ft/s*	Wash Solution	0.20 M NaOH
	Permeate Composition	[Na]: 2.1 M [Al]: 0.047 M [OH]: 1.3 M
Caustic Wash 3 (Section 5.5.4-5.5.5) *Target Filtration Conditions* *TMP: 40 psid* *AV: 13 ft/s*	Wash Solution	0.06 M NaOH
	Permeate Composition	[Na]: 1.3 M [Al]: 0.016 M [OH]:0.60 M
Caustic Wash 4 (Section 5.5.4-5.5.5) *Target Filtration Conditions* *TMP: 40 psid* *AV: 13 ft/s*	Wash Solution	0.02 M NaOH
	Permeate Composition	[Na]: 0.81 M [Al]: 0.008 M [OH]: 0.37 M

Table 5.46 (Contd)

Filtration Step	Property	Results
Caustic Wash 5 & Slurry Condition **(Section 5.5.4-5.5.5)** *Target Filtration Conditions* *TMP: 40 psid* *AV: 13 ft/s*	Wash Solution	0.01 M NaOH
	Permeate Composition	[Na]: 0.41 M [Al]: 0.004 M [OH]: 0.19 M
	Measured UDS	11 wt%
	Particle Size	d(10): 0.17 μm d(50): 0.36 μm d(90): 3.2 μm
	Rheology @ 25°C-60°C *(Sample ID: TI572-G2-R4)*	Non-Newtonian Yield Stress: 2.8-1.6 Pa Consistency: 11-5 mPa·s
Oxidative Leach Slurry **(Section 5.6)**	Measured UDS	5 wt%
	Particle Size	d(10): 0.38 μm d(50): 1.0 μm d(90): 61 μm
Oxidative Wash 1 (Section 5.6) *Filtration Conditions* *TMP: 40 psid* *AV: 13 fps*	Wash Solution	0.01 M NaOH
	Permeate Composition	[Na] : 0.28 M [OH]: 0.14 M
Oxidative Wash 2 *Filtration Conditions* *TMP: 40 psid* *AV: 13 fps*	Wash Solution	0.01 M NaOH
	Permeate Composition	[Na] : 0.26 M [OH]: 0.05 M
Oxidative Wash 3 & Final Slurry **(Section 5.6)** *Filtration Conditions* *TMP: 40 psid* *AV: 13 fps* **Final Filter Testing (Section 5.7)**	Wash Solution	0.01 NaOH
	Permeate Composition	[Na] : 0.13 M [OH]: 0.03 M
	Measured UDS	7 wt%
	Particle Size	d(10): 0.16 μm d(50): 0.30 μm d(90): 1.9 μm
	Rheology @ 25°C-60°C *(Sample ID: TI572-G2-R5)*	Newtonian Viscosity: 0.7-1.4 Pa Consistency: 5-3 mPa·s

Table 5.47. Summary of Overall Solid Leach Factors and Removal from Slurry

Element	Solid Leach Factors		Total Removal from Slurry[a] wt%
	Applying Total Mass Balance, wt%	Using Slurry and Supernate Analysis wt%	
Al	45 wt%	52-58 wt%	46 wt%
P	56 wt%	< 90 wt%	50 wt%
Cr	26 wt%	< 50 wt%	45 wt%
(a) Analyte mass percent removal includes the components in the initial supernate phase. Results were corrected to exclude sampling losses from this value.			
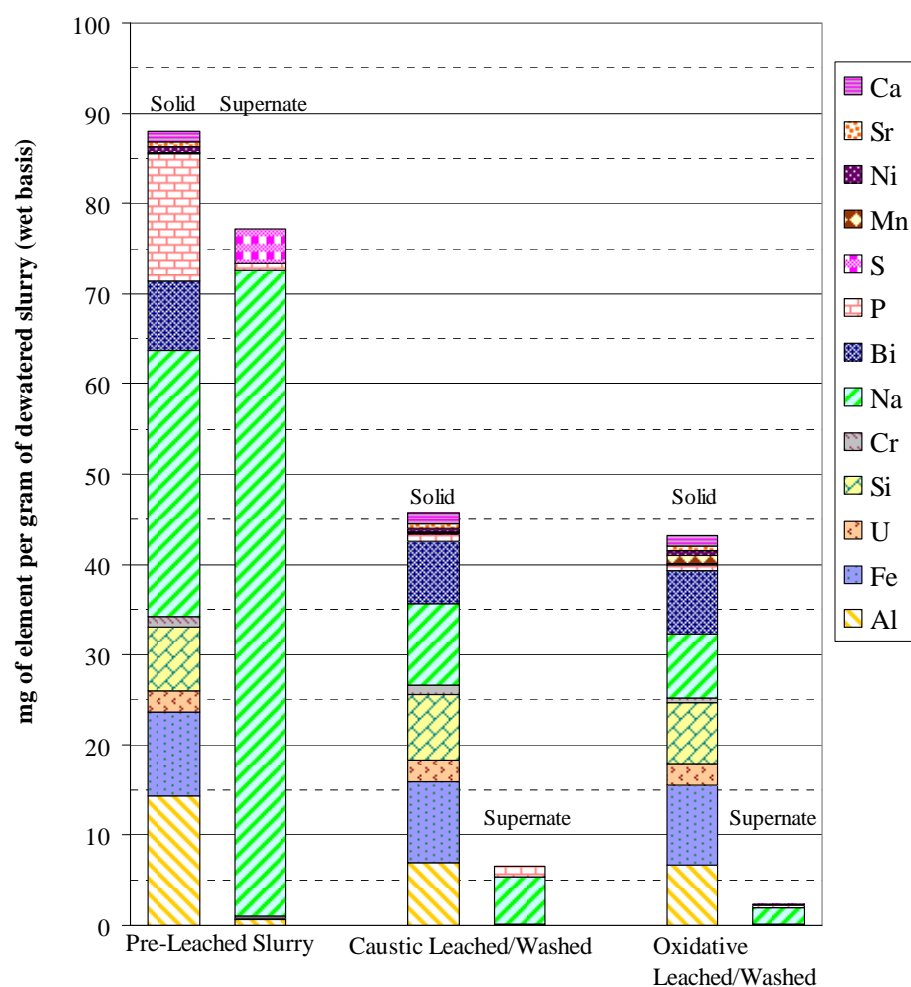
Figure 5.81. Comparison of Slurry Composition Before and After Leaching and Washing
(*Basis 1 gram of dewatered slurry: results taken from slurry ICP-OES Analysis.*)

6.0 Group 1/2 Post-CUF Batch Parametric Oxidative Leaching

A portion of the composite Group 1/2 sample that was subjected to caustic leaching and washing in the CUF apparatus was also subjected to a parametric oxidative leaching experiment. This experiment examined the influence of free-hydroxide concentration and the permanganate-to-chromium ratio on the efficacy of Cr removal and on the behavior of Pu and other criticality-safety-related components. This section reports and discusses the results of the parametric Group 1/2 post-CUF parametric leaching experiment.

6.1 Group 1/2 Post-CUF Batch Parametric Leaching: Experimental

Parametric oxidative leaching tests were performed on the blended Group 1 bismuth phosphate sludge sample and Group 2 bismuth phosphate saltcake sample to determine the behavior of chromium during leaching at different conditions. The composite Group 1/2 sample material as received after caustic leaching and washing with NaOH in the CUF was subdivided and subjected to a parametric test matrix for oxidative leach testing as discussed in the following sections.[a]

6.1.1 Preparation for Oxidative Leaching Tests

To successfully subdivide the sample, it was necessary to first determine the weight percent water-insoluble solids. One ~ 9.5-g slurry sample (584-G1/2-CL-Slurry) was removed from the hot cell, and two aliquots from this sample were dried to constant weight. Since the material had been previously washed in the CUF, the dried solids obtained in this way were assumed to represent the UDS. Based on this, it was determined that the slurry contained 14.7 wt% UDS. To determine the amount of leachable Cr in the slurry, an initial estimate was made of the Cr content in one 3.6-g portion of the slurry, and an oxidative leach was performed with an excess of $NaMnO_4$. After 6 hours, a sample was removed and submitted for analysis by UV/Vis spectroscopy; the amount of Cr oxidized under these conditions was taken to be the amount of leachable Cr in the slurry (5,040 µg leachable Cr in 0.5 g of solids).

6.1.2 Division of the Caustic Leached and Washed Group 1/2 Solids

Seven ~ 3.6-g slurry samples were transferred to 125-mL HDPE bottles with a large disposable polyethylene pipet. Each sample contained ~ 0.5 g UDS. The samples were removed from the hot cell for follow-on processing at the fume hood workstation.

6.1.3 Oxidative Leaching of the Caustic Leached Group 1/2 Solids

The leaching conditions for each of the seven samples are summarized in Table 6.1. The test matrix was designed to evaluate the effects of the Mn/Cr molar ratio (0.75, 1.0, 1.25, and 1.5) at a constant hydroxide concentration (0.25 M) and the effect of hydroxide concentration (0.25 and 1.25 M) at a high Mn/Cr molar ratio (1.25) on the chromium leaching kinetics and efficacy. Sodium hydroxide (19 M) was added to each aliquot of washed solids in the following amounts: 0.66 mL to yield 0.25 M NaOH, and 3.3 mL to yield 1.25 M NaOH. The slurry mixtures were then diluted to 50 mL (with an estimated uncertainty of 2

(a) Testing was conducted according to TI-RPP-WTP-456, *Parametric Oxidative Leach Test of Group 1/2 Hanford Tank Waste, Post-CUF Test*, L Snow, January, 2008.

mL) with DI water. Contact time with the concentrated NaOH was brief (<5 min). The sample bottles were mixed by swirling by hand, the solids were allowed to settle until sufficient clear liquid was available to sample, and then approximately 2.0 mL of the clarified leachate solution was withdrawn with a transfer pipette and filtered through a 0.45-μm pore size nylon syringe filter; the syringe filter and the syringe had been pre-heated in an oven to the sample temperature before filtering in an effort to minimize temperature changes impacting the sample. One 0.5-mL sample of filtered solution was acidified with 15 mL of 0.3 M HNO_3 for analysis by ICP-OES; another 0.5-mL sample of filtered solution was added to 2.5 mL of 2 M HNO_3 for analysis of plutonium, and one 0.5-mL sample of filtered leachate was analyzed directly (or following dilution in 0.096 M NaOH) using UV/vis for chromate concentration. The remaining filtered solution was returned to the leaching vessel. This was the time = 0 sample.

Aliquots of 1 M $NaMnO_4$ (freshly prepared and filtered) were then added to each sample, resulting in the following amounts: 0.073 mL to yield 0.75 Mn/Cr mole ratio, 0.097 mL to yield 1.0 Mn/Cr mole ratio, 0.121 mL to yield 1.25 Mn/Cr mole ratio, and 0.146 mL to yield a 1.5 Mn/Cr mole ratio. The sample bottles were weighed after each addition of reagents (NaOH, water, and $NaMnO_4$). The time of addition of $NaMnO_4$ was defined as T_0. Each leaching vessel was closed with a cap equipped with a tube condenser. The condenser was used to eliminate pressurization and minimize water loss while at the same time minimizing the spread of contamination. The leaching mixtures were shaken for 24 hours at 200 RPM resulting in good suspension of the solids. Samples were withdrawn in the same manner as the time = 0 sample at 0.5, 1, 2, 4, 6, and 24 hours. At 24 hours, additional samples of the leachate were filtered for analysis to determine the free-hydroxide ion concentration and U by KPA.

After the final samples were taken at temperature, the slurries were removed from the mixing/heating block and cooled to ambient temperature. The slurries were centrifuged, and the leachates were decanted.[a]

The equilibrium concentration values for free hydroxide and sodium are shown in Table 6.1 and were based on results from the samples taken at 24 hours.

(a) The contact dose rates of the leached solids were too high to safely conduct transfer to volume-graduated centrifuge tubes to assess the volume of centrifuged solids.

Table 6.1. Oxidative Leaching Conditions for Group 1/2 Caustic-Leached Solids

Bottle ID	Free OH, M		Na, M		Mn/Cr Mole Ratio		Temperature, °C[c]
	Target	Measured[a]	Target	Measured[a]	Target	Actual[b]	
584-G1/2-OL-0.75	0.25	0.29	0.25	0.33	0.75	0.59	45
584-G1/2-OL-1a	0.25	0.29	0.25	0.33	1.0	0.79	45
584-G1/2-OL-1b	0.25	0.28	0.25	0.33	1.0	0.79	45
584-G1/2-OL-1c	0.25	0.27	0.25	0.31	1.0	0.79	45
584-G1/2-OL-1.25	0.25	0.29	0.25	0.33	1.25	0.98	45
584-G1/2-OL-1.5	0.25	0.28	0.25	0.32	1.5	1.19	45
584-G1/2-OL-1.25-1.25	1.25	1.38	1.25	1.44	1.25	0.98	45

(a) The measured analyte concentrations represent the equilibrium concentration obtained after a 24-h contact time.

(b) As mentioned in Section 6.1.1, the amount of $NaMnO_4$ added to achieve the desired Mn/Cr mole ratio was calculated based on the amount of Cr leached during a preliminary 6-h contact of a portion of the slurry with excess $MnMnO_4$. However, this method underestimated the amount of Cr in the slurry because that portion that is unreactive towards permanganate was not accounted for. ICP-OES analysis of the solids indicated the total Cr concentration was 6,425 μg per 0.5 g of solids (versus 5,040 μg leachable Cr in 0.5 g of solids). The Actual Mn/Cr mole ratios listed here were calculated using the total Cr concentration determined by ICP-OES and the amount of $NaMnO_4$ that was added to each sample.

(c) The temperature uncertainty was ± 2.5°C.

Analytical Service Request (ASR): 8111

6.1.4 Washing of Oxidative-Leached Group 1/2 Solids for Analysis

The solids from the triplicate samples (G1/2-OL-1a, -1b, -1c, leached at 40°C in 0.25 M NaOH at a Mn/Cr of 1) were prepared for characterization as shown in Figure 6.1. The process followed was essentially the same as that for the leached Group 1 solids (Section 3.3.4).
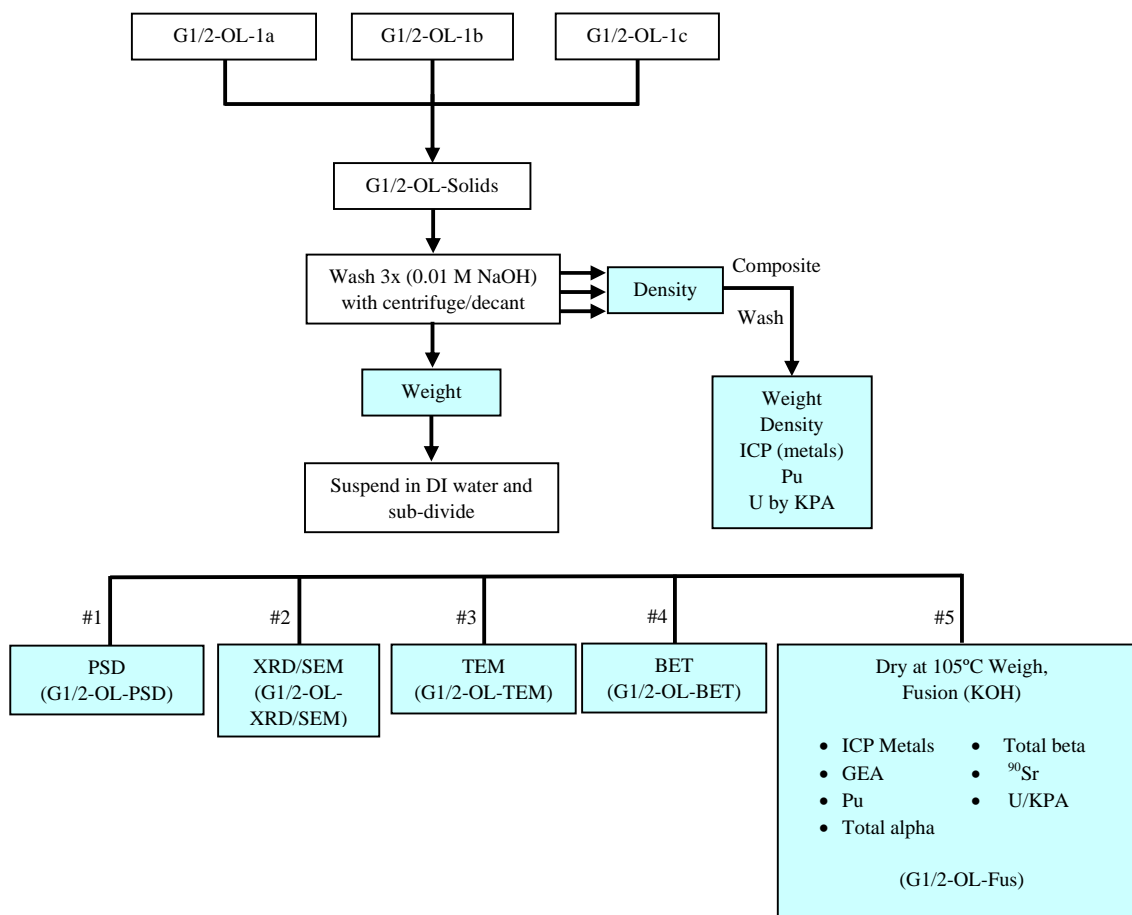
Figure 6.1. Washing, Subdivision, and Analysis Scheme for the Group 1/2 Oxidatively Leached Solids

6.2 Group 1/2 Bi-Phosphate Sludge/Saltcake Waste Parametric Oxidative Leaching Test Results

As discussed in Section 4.4, the Cr concentration in the caustic-leached Group 2 solids is sufficiently high that Cr would be expected to be the component limiting HLW glass waste loading for this material. Thus, oxidative leaching of the caustic-leached Group 2 solids to remove Cr is of interest. To investigate the oxidative leaching behavior of the caustic-insoluble Cr component, the combined Group 1/2 sample that was caustic leached in the CUF was subjected to parametric oxidative leaching tests. The objective of this testing was to gain an understanding of the Cr dissolution behavior for the actual tank waste to help guide development of suitable Cr-containing simulants. Another objective was to determine the extent of Pu mobilization during oxidative leaching. The latter issue is of concern for criticality safety within the WTP. The results from the parametric oxidative leach testing and the composition of the residual solids are discussed in the following sections.

6.2.1 Chromium Behavior During Oxidative Leaching of the Caustic-Leached Group 1/2 Solids

The oxidation of Cr as a function of time, free-hydroxide concentration, and Mn/Cr molar ratios was evaluated. Based on the total Cr concentration in the initial (caustic-leached) solids material (12.85 mg Cr/g), and the wt% UDS of the starting slurry (14.66%), the complete dissolution of Cr would result in a concentration of 0.138 mg Cr/mL or 0.003 M. The Cr did not completely dissolve under any of the conditions examined in this experiment. In this discussion, the reported wt% of Cr dissolved at each sampling point was calculated based on the final Cr concentration in the triplicate samples, as discussed in Section 6.2.6.2.

The oxidative leaching data at constant temperature and varying free-hydroxide concentrations and Mn/Cr molar ratios are shown in Figure 6.2. A measure of experimental precision is shown by the triplicate tests conducted at 0.25 M free hydroxide at 45°C with a Mn/Cr mole ratio of 0.79. The scatter was within the analytical uncertainty of ± 15%.

Under all testing conditions, >50% of the Cr was removed from the solid phase within the first 30 min of contact time. Most of the Cr oxidation occurred within the first 30 minutes, and equilibrium was achieved within 6 h for samples having Mn/Cr molar ratios of 0.59 and 0.79. Samples with higher amounts of Mn dissolved an additional 2 to 4% of Cr between 6 and 24 h. Increasing the Mn/Cr mole ratio from 0.59 to 0.79 directly increased the amount of Cr in solution (initially and at equilibrium conditions). The test conditions at the sub-stoichiometric Mn/Cr molar ratios of 0.59 and 0.79 mobilized ~ 56% and 66% of the Cr, respectively. The stoichiometric and super-stoichiometric amounts of 0.98 and 1.19 Mn/Cr mole ratio resulted in ~ 72% Cr dissolution. The amount of NaOH (0.25 or 1.25 M) at the Mn/Cr molar ratio of 0.98 had no effect on the amount of Cr dissolved.

Figure 6.3 shows the average of the 2-, 4-, 6-, and 24-hr data points taken under all conditions of NaOH concentration as a function of the Mn/Cr molar ratio. The y-axis error bars define the standard deviation of all results at the given Mn/Cr mole ratios. From the 0.59 to 0.79 Mn/Cr mole ratio, there was a slight impact of time on the dissolution of chromium up to 6 h. There was no significant impact of time on the dissolution of Cr beyond 6 h. At the high Mn/Cr mole ratios of 0.98 and 1.19, there was a slight time dependence from 6 to 24 h. The main factor controlling dissolution was the amount of added permanganate up to an excess of permanganate. There was no added value in adding greater excesses of permanganate (from a Mn/Cr mole ratio of 0.98 to 1.19).
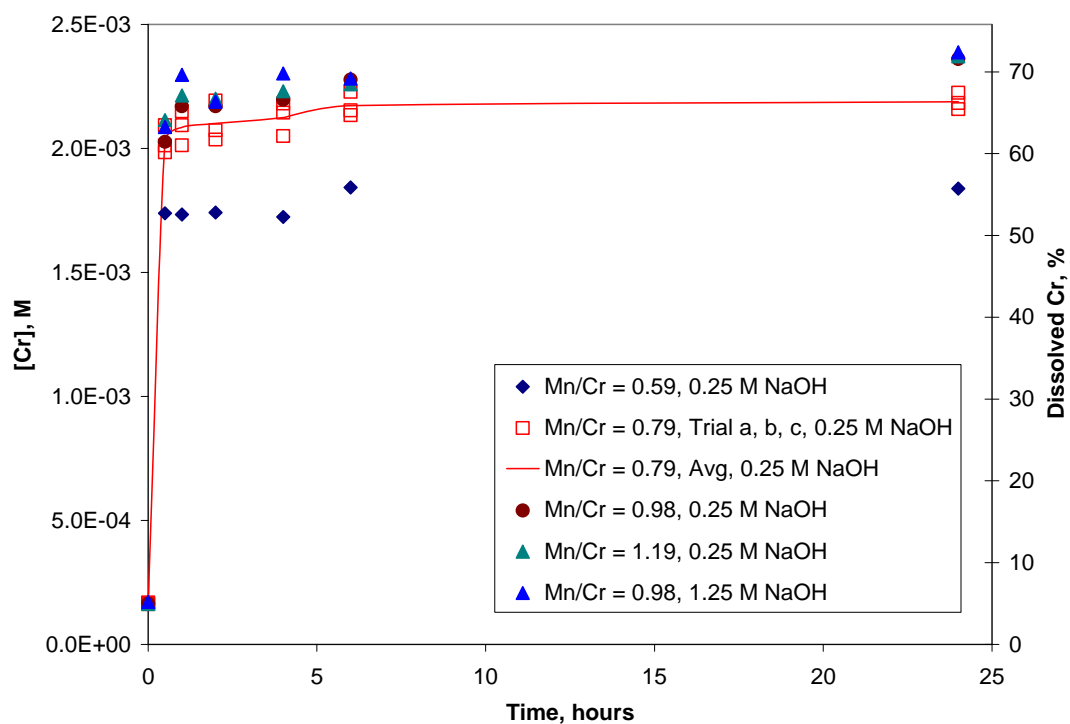
Figure 6.2. Chromium Concentration Versus Time at 45°C with Mn/Cr Mole Ratios of 0.59, 0.79, 0.98, and 1.19 in 0.25 M NaOH, and at a Mn/Cr Mole Ratio of 0.98 in 1.25 M NaOH for Group 1/2 Bi-Phosphate Sludge/Saltcake (During Oxidative Leaching)
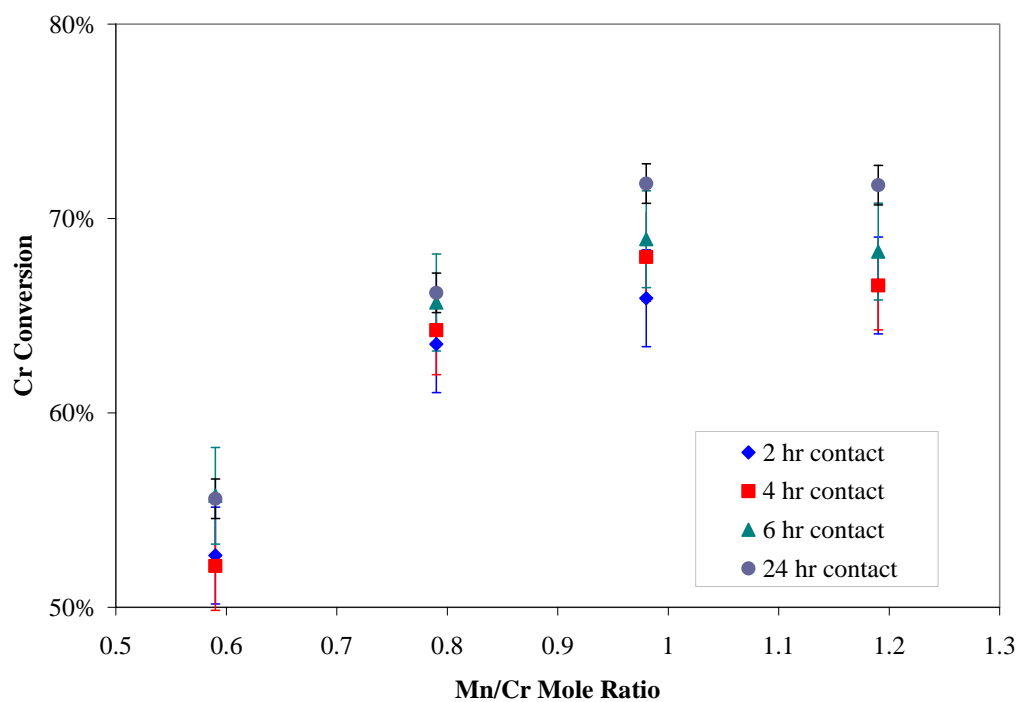
Figure 6.3. Amount of Chromium Removed as a Function of Mn/Cr Mole Ratio and Time for Group 1/2 Bi-Phosphate Sludge/Saltcake (During Oxidative Leaching)

For each sample, the total Cr concentration was measured by ICP-OES, and the Cr(VI) (as chromate) concentration was measured by UV/Vis spectrophotometry. Results from the two measurement techniques for three test conditions are shown in Figure 6.4. Results for all tests are tabulated in Appendix L along with the percent difference between the two techniques. The agreement between the two techniques was excellent; all were within 14%, and in most cases were well within 10%. The differences in the Cr concentrations determined by ICP-OES and by spectrophotometry were well within the analytical uncertainty.
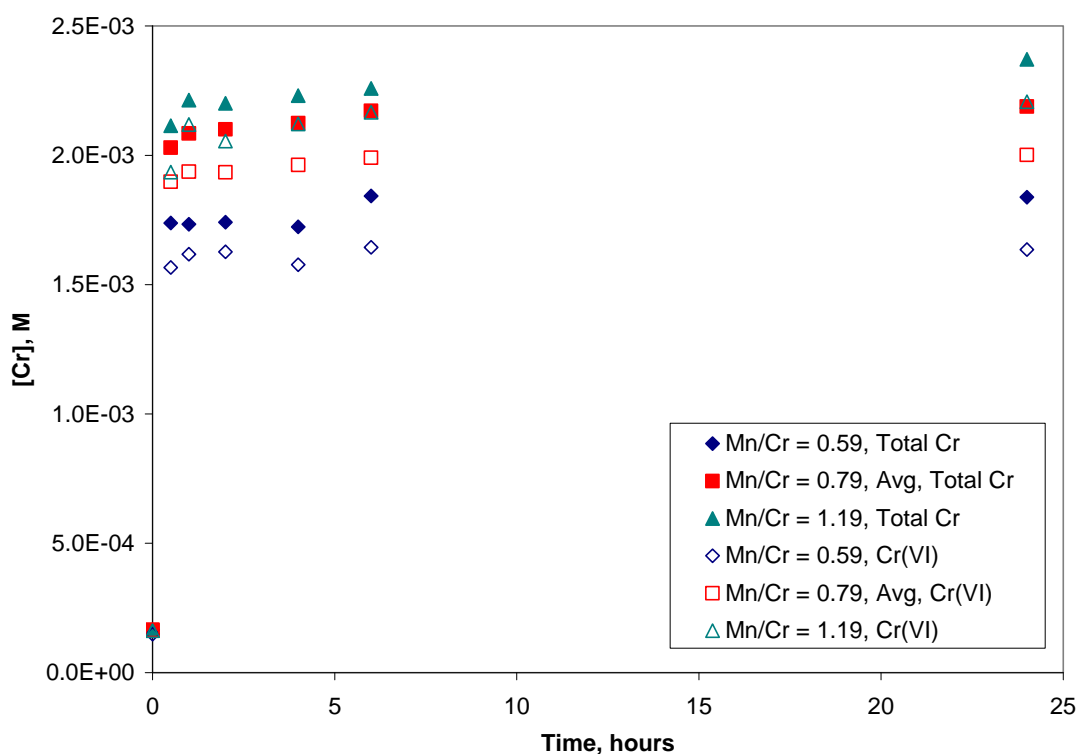
Figure 6.4. Total Chromium and Cr(VI) Concentrations Versus Time for Group 1/2 Bi-Phosphate Sludge/Saltcake (during oxidative leaching). Conditions: 45°C leaching temperature in 0.25 M NaOH at Mn/Cr molar ratios of 0.59, 0.79, and 1.19.

6.2.2 Aluminum Behavior During Oxidative Leaching of the Caustic-Leached Group 1/2 Solids

The Al dissolution behavior during the oxidative leaching tests was evaluated as a function of time, free-hydroxide concentration, and the Mn/Cr molar ratio. Based on the total Al concentration in the initial (caustic leached) solids material (77.85 mg Al/g) and the wt% UDS of the starting slurry (14.66%), the complete dissolution of Al would result in a concentration of 0.838 mg Al/mL or 0.03 M. Complete Al dissolution was not reached in this experiment. In this discussion, the reported wt% of Al dissolved at each sampling point was calculated based on the final Al concentration in the triplicate samples, as discussed in Section 6.2.6.2.

The leaching data at constant temperature and varying free-hydroxide concentrations and Mn/Cr molar ratios are shown in Figure 6.5. A measure of experimental precision is shown by the triplicate tests conducted at 0.25 M free hydroxide at 45°C with a Mn/Cr mole ratio of 0.79. The scatter was within the analytical uncertainty of ±15%.

Under all six test conditions in 0.25 M NaOH, ~ 21% of the Al dissolved within 24 h of contact time. Equilibrium conditions were achieved within 6 h. Increasing the Mn/Cr mole ratio from 0.59 to 1.19 had no impact on the amount of Al in solution (initially and at equilibrium conditions). The amount of NaOH (0.25 or 1.25 M) at the Mn/Cr molar ratio of 0.98 had an effect on the amount of Al dissolution, increasing it from 21% to 38%. The latter result suggests that the Al did not completely dissolve during caustic leaching of the Group 1/2 solids in the CUF apparatus. This might be explained by the relatively low liquid-to-solids ratio (8 mL leachate/g solids per Figure 5.26) during leaching in the CUF compared to that used in the parametric leaching experiments (100 mL/g solids).
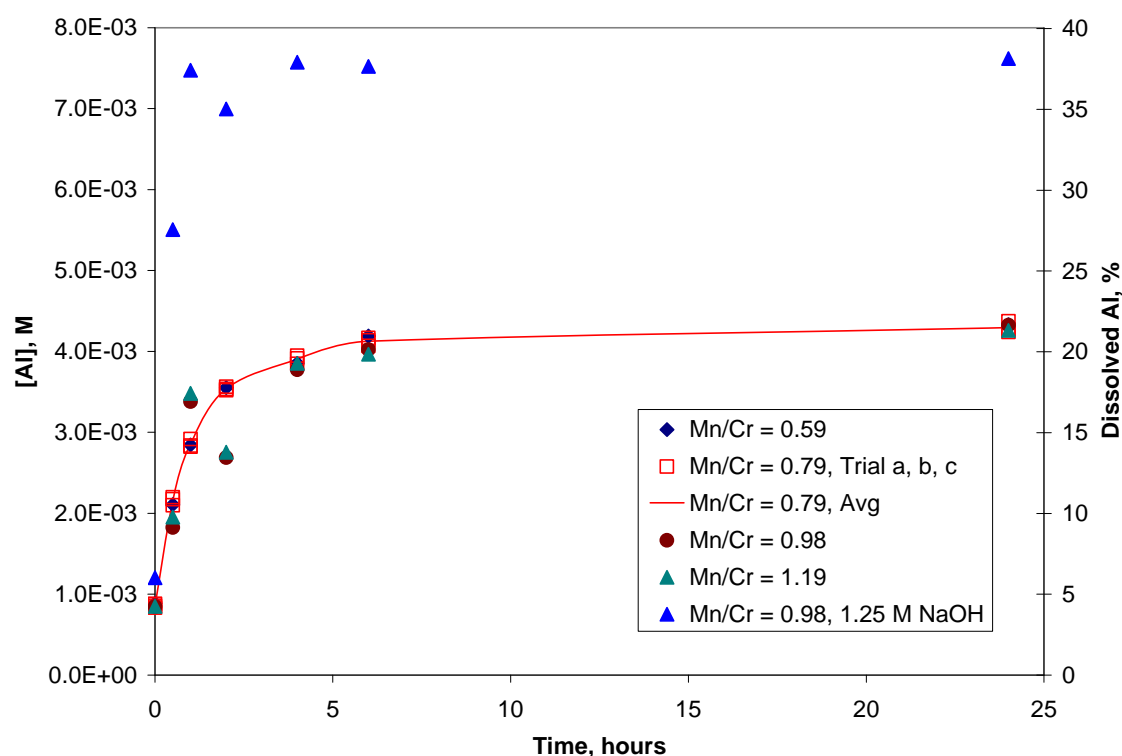
Figure 6.5. Aluminum Concentration Versus Time at 45°C Leach Temperature at Mn/Cr Mole Ratios of 0.59, 0.79, 0.98, and 1.19 in 0.25 M NaOH, and at a Mn/Cr Mole Ratio of 0.98 in 1.25 M NaOH for Group 1/2 Bi-Phosphate Sludge/Saltcake (During Oxidative Leaching)

6.2.3 Phosphorus Behavior During Oxidative Leaching of the Caustic-Leached Group 1/2 Solids

The P dissolution during oxidative leaching was determined as a function of time, temperature, free-hydroxide concentration, and the Mn/Cr molar ratio. Based on the total P concentration in the initial (caustic leached) solids material (14.75 mg P/g) and the wt% UDS of the starting slurry (14.66%), the complete dissolution of P would result in a concentration of 0.159 mg P/mL or 0.005 M. The P did not

completely dissolve in this experiment. In this discussion, the reported wt% of P dissolved at each sampling point was calculated based on the final solids concentration in the triplicate samples, as discussed in Section 6.2.6.2.

The leaching data at constant temperature and varying free-hydroxide concentrations and Mn/Cr molar ratios are shown in Figure 6.6. A measure of experimental precision is shown by the triplicate tests conducted at 0.25 M free hydroxide at 45°C with a Mn/Cr mole ratio of 0.79. The scatter was within the analytical uncertainty of ± 15%.

Under all six test conditions in 0.25 M NaOH, 58 to 62% of the residual P following caustic leaching was dissolved within 24 h, and equilibrium was achieved within 6 h. Increasing the Mn/Cr mole ratio from 0.59 to 1.19 had no impact on the amount of P in solution (initially and at equilibrium conditions). The amount of NaOH (0.25 or 1.25 M) at the Mn/Cr molar ratio of 0.98 also had no effect on the amount of P dissolution.
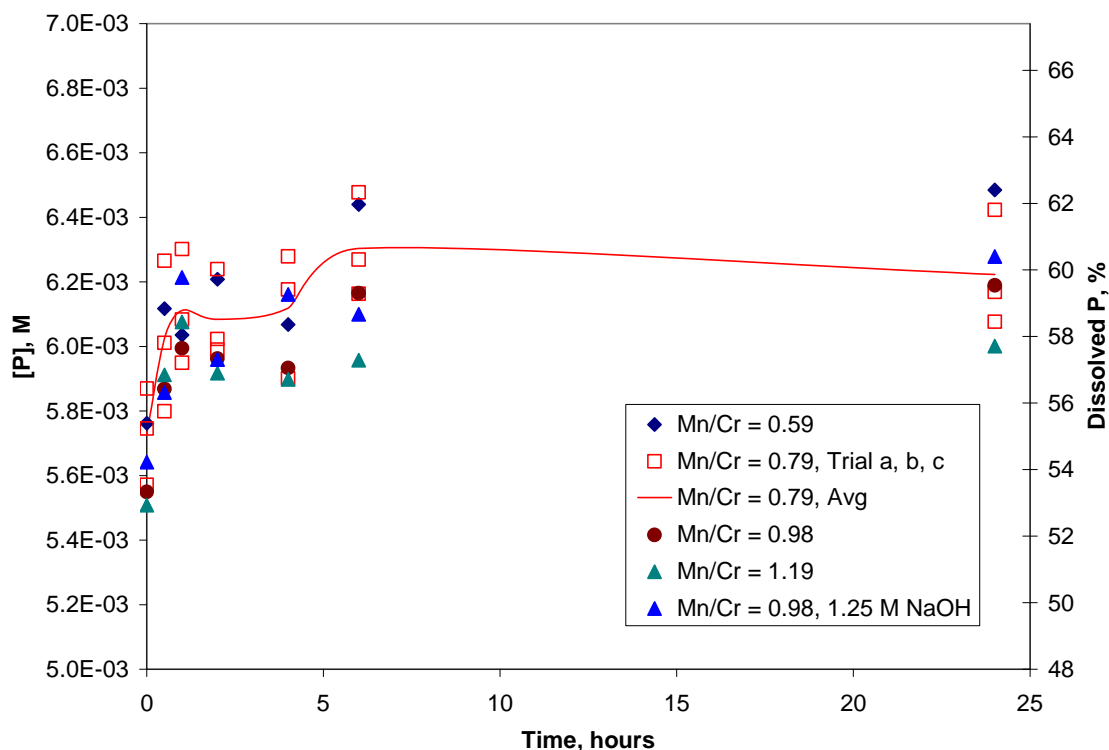
Figure 6.6. Phosphorus Concentration Versus Time at 45°C Leach Temperature at Mn/Cr Mole Ratios of 0.59, 0.79, 0.98, and 1.19 in 0.25 M NaOH, and at a Mn/Cr Mole Ratio of 0.98 in 1.25 M NaOH for Group 1/2 Bi-Phosphate Sludge/Saltcake (during oxidative leaching)

6.2.4 Behavior of Plutonium and Other Safety-Related Components During Oxidative Leaching of the Caustic-Leached Group 1/2 Solids

The $^{239+240}$Pu and ^{238}Pu concentrations were measured for each leaching condition and at each sampling time. The amount of $^{239+240}$Pu dissolved, expressed in terms of the percent dissolved,[a] is shown in Figure 6.7; numeric values are provided in Appendix L. The results obtained from the ^{238}Pu measurement were similar to that for $^{239+240}$Pu. Also shown on in Figure 6.7 as a point of reference are the Pu concentrations (assuming all the $^{239+240}$Pu activity is attributed only to the isotope ^{239}Pu) in terms of grams Pu/L at 10 and 40% dissolution of the Pu. As previously observed (Fiskum et al. 2008), the Pu dissolution was strongly dependent on the free-hydroxide concentration. There was a large (~6×) increase in the Pu concentration when the NaOH concentration was increased from 0.25 M to 1.25 M. For example, after leaching for 6 h at a Mn/Cr ratio of 0.98, the $^{239+240}$Pu concentration was 1.54×10^{-3} µCi/mL at 1.25 M NaOH and 2.54×10^{-4} µCi/mL at 0.25 M NaOH. Clearly, low free-hydroxide concentrations will need to be maintained to minimize Pu mobilization during oxidative leaching of Cr. It is unclear why there is such a large drop in Pu concentration for the 24-h sampling point in 1.25 M NaOH with a Mn/Cr mole ratio of 0.98. The difference in values for ^{238}Pu is greater than the 15% uncertainty in the analytical results.

The U concentrations in the oxidative leaching solutions remained low (see Appendix L) under all conditions examined. Typically, the U concentration was ~3 µg/mL after leaching for 24 h. The exception was during leaching in 1.25 M NaOH at a Mn/Cr ratio of 0.98; in that case, the U concentration in solution reached a level of ~8 µg/mL. The Fe content of the leachates was also very low, generally < 1 µg/mL. In some samples (e.g., the 1-h sample for the 0.25 M NaOH, Mn/Cr = 0.98 case), elevated concentrations of Fe were observed. But this was likely because of Fe-contamination of the sample since the time points before and after displayed much less Fe. At 0.25 M NaOH and Mn/Cr ≤ 0.79, Mn was below the detection limit. Manganese was observed to be in the leachate solutions at Mn/Cr = 0.98 or higher, but the amount in solution decreased with time and was below the detection limit at 24 h. The concentrations of Ni and Cd were below the detection limits in nearly all solutions analyzed. The B concentrations were near the detection limit and always < 1 µg/mL.

(a) To obtain the percent Pu removed values plotted in Figure 6.7, the total amount of Pu in the solution was divided by the amount of Pu in the caustic-leached solids used for each leaching experiment (~0.38 µCi $^{239+240}$Pu) and then multiplied by 100 to get the percent removed value.
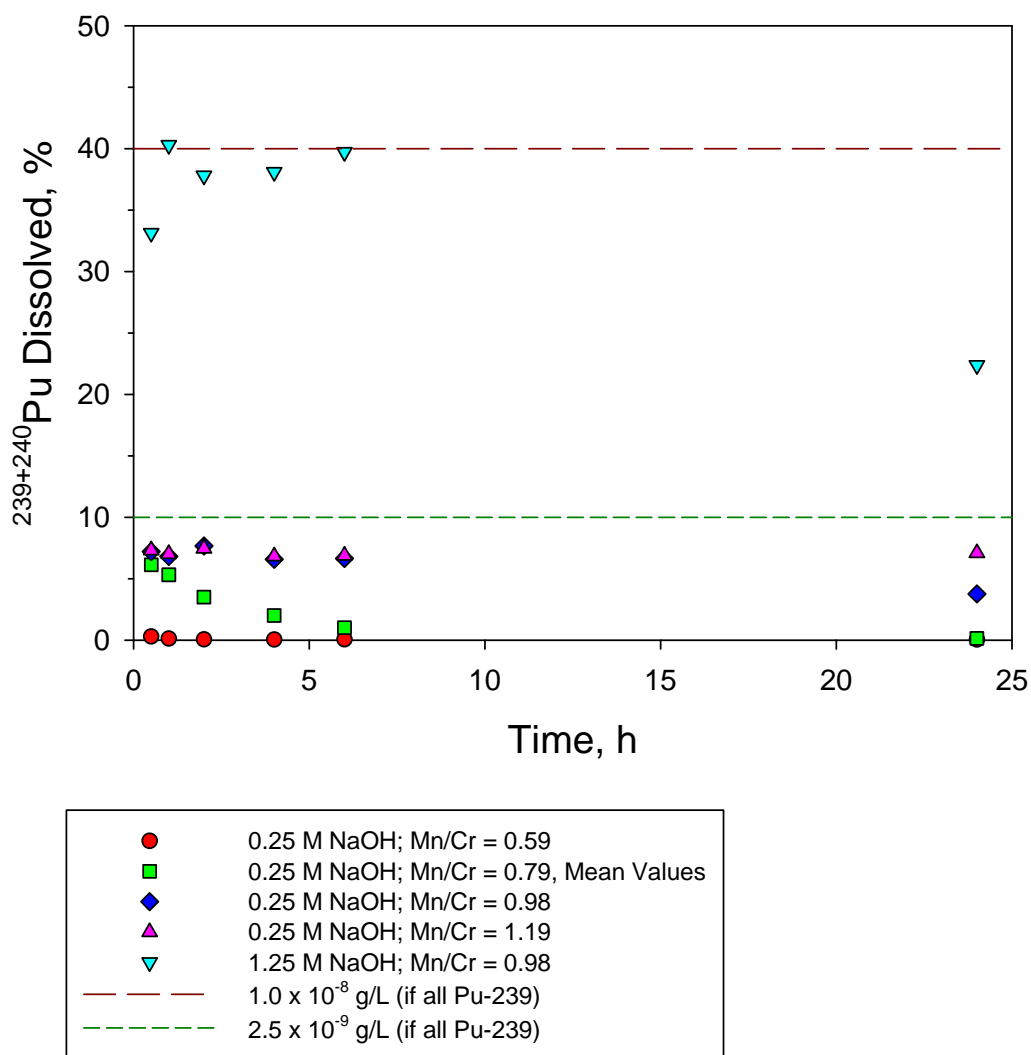
Figure 6.7. Effect of Free-Hydroxide Concentration on Pu Mobilization During Oxidative Leaching for Group 1/2 Bi-Phosphate Sludge/Saltcake

6.2.5 Assessment of Final Leach Conditions

A summary of the final (24-hr) leach solution chemistry and physical parameters is shown in Table 6.2. The final free-hydroxide and sodium concentrations were at the targeted values, within the uncertainty of the analytical method (±15%). The calculated amount of Cr removed at each leaching condition is also shown in the table. Appendix L summarizes the concentrations of total Cr, Cr(VI), Al, B, Cd, Fe, Mn, Na, Ni, P, Si, U, U by KPA, $^{239+240}$Pu, and ^{238}Pu in the leaching solutions.

Table 6.2. Group 1/2 Bi-Phosphate Sludge/Saltcake Oxidative Leaching Final Aqueous Phase Conditions

Temp, °C	Free OH, M	Na, M	Mn/Cr Mole Ratio	Density, g/mL	Cr, M	% Cr Removed
45	0.29	0.33	0.59	1.03	1.83E-03	56
45 (trial a)	0.28	0.33	0.79	1.02	2.22E-03	67
45 (trial b)	0.28	0.33	0.79	1.01	2.16E-03	65
45 (trial c)	0.27	0.31	0.79	1.02	2.18E-03	66
45	0.29	0.33	0.98	1.02	2.36E-03	71
45	0.28	0.32	1.19	1.02	2.37E-03	72
45	1.38	1.44	0.98	1.07	2.39E-03	72
Analytical Service Request: ASR 8111						

6.2.6 Composition of Group 1/2 Caustic and Oxidatively Leached and Washed Solids

The Group 1/2 solids that had been oxidatively-leached at 45°C in 0.25 M NaOH with a Mn/Cr mole ratio of 0.79 for 24 h were combined and washed in preparation for analysis. The wash solution composition and the washed solids chemical, radiochemical, particle size, and crystal habit are discussed.

6.2.6.1 Leached Solids Washing Solution

The densities of the three sequential washing solutions were 1.006, 1.000, and 1.005 g/mL, respectively. The composite washing solution (126.05 mL volume) density, ICP metals, U measured by KPA, and Pu concentration are shown in Table 6.3.

Table 6.3. Solids Wash Solution Composition

Analyte	M	Density[a]	g/mL
Al	2.30E-03	Composite wash	1.00
Bi	4.45E-06	**Radionuclides**	**µCi/mL**
Cr	1.19E-04	$^{239+240}$Pu	2.52E-06
Fe	[2.50E-05]	^{238}Pu	< 1.3E-7
Mn	[6.21E-07]		
Na	3.25E-02		
P	[5.12E-04]		
Si	1.98E-03		
U (ICP)	[1.11E-05]		
U (KPA)	1.07E-06		
(a) Temperature was 21.8°C. ASR 8111 Analyte uncertainties were typically within ±15% (2-s); results in brackets indicate that the analyte concentrations were greater than the minimum detection limit (MDL) and less than the estimated quantitation limit (EQL), and uncertainties were >15%.			

WTP-RPT-166, Rev. 0

6.2.6.2 Chemical and Radiochemical Composition of the Oxidatively Leached Group 1/2 Solids

Table 6.4 presents the composition of the Group 1/2 solids after oxidative leaching at 45°C for 24 h in 0.25 M NaOH at a Mn/Cr molar ratio of 0.79, and subsequent washing. For comparison, the composition of the starting caustic-leached and washed solids is also provided in the table. The largest mass fraction of the solids was composed of Fe followed by Na, Si, Bi, Al, U, Mn, P, Ni, and Cr. The fraction of each component removed (as determined by the concentration factor method) as a result of oxidative leaching is also given in Table 6.4. A large amount (66%) of the Cr was removed from the solids, as well as 60% of the P. Approximately 20% of the Al and Si were also mobilized to the aqueous phase. Uranium and iron remained in the solids phase.

As was done for the Group 1 and Group 2 solids, the data from the Group 1/2 oxidative leaching experiments were analyzed by the three methods described in Section 3.4.6.2 for determining the percent of each component removed during leaching. In the case of the Group 1/2 solids, the caustic-leached solids were dominated by Fe (10.4 wt%), Si (8.1 wt%), Al (7.8 wt%), Bi (7.3 wt%), U (2.6 wt%), P (1.5 wt%), and Cr (1.3 wt%), and the analysis of the leachate solutions showed that Fe, Ni, Sr, U, and Zn had not dissolved. The relative CF of these analytes averaged 1.31 in the final oxidatively leached and washed solids, based on the ratio of analyte concentration after oxidative leaching and washing to analyte concentration after caustic leaching and washing. This term was used to determine the specific analyte leach factors according to Equation 6.1.

$$ LF_3 = 1 - \left(\frac{C_{OL}}{C_{CL} \times 1.31} \right) \tag{6.1} $$

where LF_3 is the caustic-leach factor, C_{OL} is the oxidatively leached analyte concentration, and C_{CL} is the caustic-leached analyte concentration.

Results from all three methods are given in Table 6.5. For Al, the results from all three methods are slightly different, with method one giving the lowest values and method three giving the highest values. For P, there was a greater difference between results from each method, with method one giving the highest values and method three giving the lowest values. For Cr, the results from all methods are slightly different, with method one giving the highest values and method three giving the lowest values. All values of percent leached plotted in this section and shown in Tables 6.2 and 6.4 were calculated using method three, the "concentration factor" method.

Table 6.4. Leached Solids Composition and Leach Factors of Group 1/2 Bi-Phosphate Sludge/Saltcake (Water-Insoluble Solids)

Analyte	After Caustic Leaching, μg/g[a] (ASR 8111)	After Oxidative Leaching, μg/g[a] (ASR 8111)	Observed Leach Factor
Al	77,850	79,833	0.21
B	[48]	[43]	--
Bi	73,050	82,967	0.13
Cd	[131]	160	--
Cr	12,850	5,677	0.66
Fe	103,500	135,667	--
Mn	1,610	14,733	--
Na	na	87,550	--
Ni	5,995	7,630	0.03
P	14,750	7,740	0.60
S	<666.729	<640.608	--
Si	81,350	86,467	0.19
Sr	5,800	7,453	0.02
Zn	502	685	--
Zr	na	[211]	--
U (ICP)	25,800	33,500	--
U (KPA)	23,152	33,870	--
Radionuclides	**μCi/g[a]**	**μCi/g[a]**	**Observed Leach Factor**
[239-240]Pu	7.12E-01	8.73E-01	0.06
[238]Pu	1.29E-02	1.45E-02	0.14
[90]Sr	2.86E+02	3.47E+02	0.07
Total alpha	1.41E+00	1.68E+00	0.09
Total beta	7.12E+02	8.33E+02	0.10
Opportunistic	**After Caustic Leaching, μg/g[a] (ASR 8111)**	**After Oxidative Leaching, μg/g[a] (ASR 8111)**	**Observed Leach Factor**
Ag	<6.251	[17]	--
As	<162.515	<156.148	--
Ba	349	450	0.01
Be	<0.200	[.7]	--
Ca	[17,000]	[17,667]	--
Ce	[344]	420	--
Co	[45]	[60]	--
Cu	99.3	161	-0.24
Dy	<12.084	<11.611	--
Eu	<1.542	[1.7]	--
K	<16668.215	16194.33	--
La	[49]	[71]	--
Li	103	113	0.16

Table 6.4 (contd)

Opportunistic	After Caustic Leaching, μg/g[(a)] (ASR 8111)	After Oxidative Leaching, μg/g[(a)] (ASR 8111)	Observed Leach Factor
Mg	2,195	2,817	
Mo	<30.003	[33]	--
Nd	[42]	[88]	--
Pb	1,865	2,437	--
Pd	<26.669	<25.624	--
Rh	<54.172	<52.049	--
Ru	[30]	[30]	--
Sb	<129.179	<138.949	--
Se	<458.376	[595]	--
Sn	[160]	<144.407	--
Ta	<83.341	<80.076	--
Te	<108.343	<104.099	--
Th	[255]	[118]	--
Ti	245	321	0.00
Tl	<125.012	<120.114	--
V	[39]	[35]	--
W	<107.945	<84.080	--
Y	[9.75]	13.9	--
(a) Dry mass basis. ASR 8111, radioisotope reference date: January 31, 2008. Analyte uncertainties were typically within ±15% (2-s); results in brackets indicate that the analyte concentrations were greater than the minimum detection limit (MDL) and less than the estimated quantitation limit (EQL), and uncertainties were >15%.			

Table 6.5. Group 1/2 Bi-Phosphate Sludge/Saltcake Leach Factors

Temp., °C	Free [OH], M	Mn/ Cr	Fraction Removed Based on Initial Solids/Leachate Solution			Fraction Removed Based on Final Solids/Leachate Solution			Fraction Removed Based on Initial/Final Solids ("concentration factor" method)		
			Al	Cr	P	Al	Cr	P	Al	Cr	P
45	0.29	0.75	0.14	0.68	1.25	0.17	0.62	0.81	0.22	0.56	0.62
45 Trial a	0.28	1	0.14	0.83	1.24	0.17	0.74	0.78	0.21	0.67	0.62
45 Trial b	0.28	1	0.14	0.81	1.19	0.17	0.73	0.77	0.21	0.65	0.58
45 Trial c	0.27	1	0.14	0.82	1.20	0.17	0.73	0.77	0.22	0.66	0.59
45	0.29	1.25	0.14	0.90	1.23	0.17	0.79	0.77	0.22	0.71	0.60
45	0.28	1.5	0.14	0.90	1.19	0.17	0.80	0.75	0.21	0.72	0.58
45	1.38	1.25	0.24	0.89	1.21	0.30	0.80	0.78	0.38	0.72	0.60

As shown in Figure 6.8, approximately 12 wt% of the metal solids (represented primarily by Al, P, Si, and Cr) dissolved in the oxidative-leach process. Based on the composition of the residual solids, Cr would still be expected to be the component limiting the HLW glass loading; although if 70% rather than 66% of the Cr had been dissolved (based on the "concentration factor" method), Fe would become the limiting component.
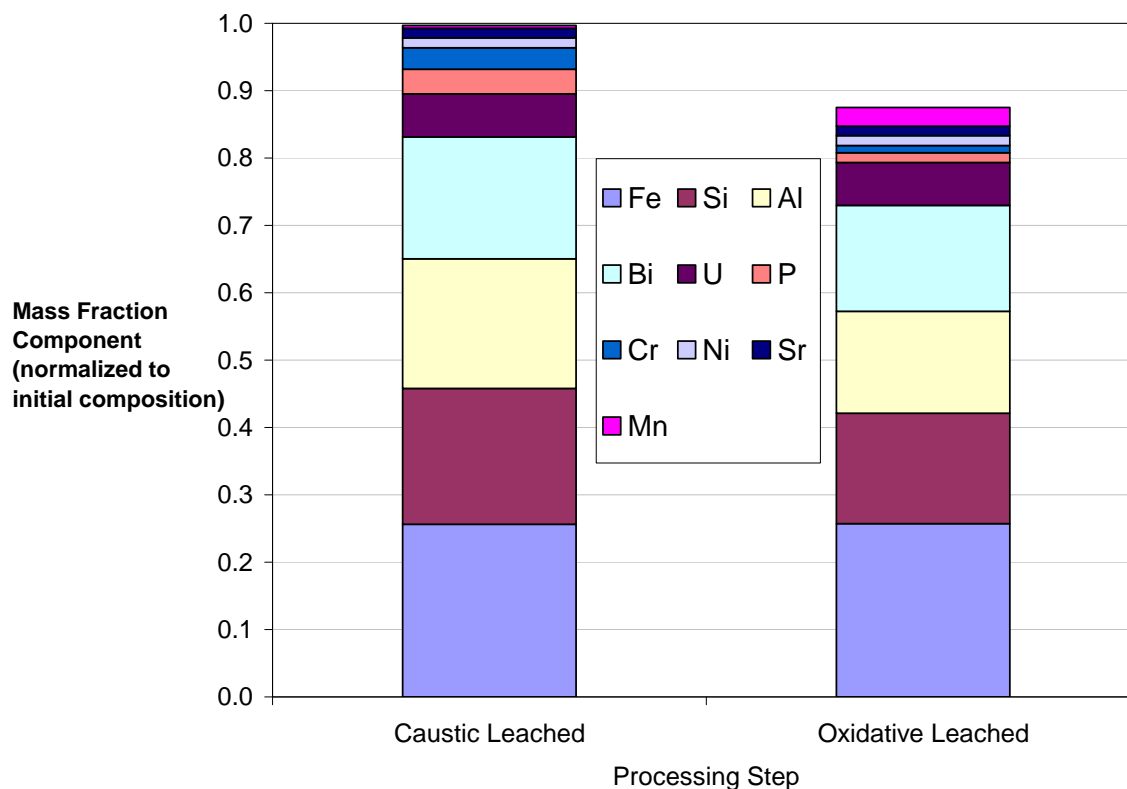
Figure 6.8. Group 1/2 Bi-Phosphate Sludge/Saltcake Reduction in Solid Mass with Oxidative Leaching

Notes: Caustic-leaching conditions: Caustic leached in CUF, ~ 7 M NaOH, slurry was heated to 100°C over a 5.3-h period, held at 100°C for an 8-h leach, and then cooled for 8 h. Oxidative-leaching conditions: Mn:Cr mole ratio = 0.79, 45°C, 1.25 M NaOH for 24 h.

6.2.6.3 Particle-Size Distribution

The waste solids comprising Sample 584-G1/2-OL-PSD are a mixture of Group 1 ($BiPO_4$ sludge) and Group 2 ($BiPO_4$ saltcake) solids that have been both caustic- and oxidatively-leached as part of a series of parametric testing studies. Table 6.6 shows select cumulative undersize percentiles derived from particle-size analysis. Here, the d(10) ranges from 0.24 to 0.69 μm, the d(50) ranges from 0.55 to 1.4 μm, and the d(90) ranges from 1.2 to 2.5 μm.

Pre-sonication percentile results suggest a relatively stable size distribution with respect to pump speed. Both d(10) and d(50) appear to decrease over the course of measurements 1 to 3, suggesting possible size reduction as a result of shear (or dilution of the suspending phase). Applying sonic energy effects substantial (greater than 10%) reductions in all reported percentiles. This is suggestive of sonic disruption

of particle agglomerates. A slight recovery in the d(90) value is observed after the immediate removal of sonic energy, indicating that agglomerate reformation may occur during measurement condition 7. Post-sonication percentiles at 3000 and 2000 RPM are statistically similar (i.e., within 10% of each other), suggesting similar states of particle suspension and agglomeration in both. An increase in the d(50) and d(90) values at 4000 RPM may indicate improved suspension and suggests the presence of difficult-to-suspend particles. On the other hand, the 4000 RPM measurement corresponds to the final test condition and could also suggest continued particle agglomeration over longer periods of time.

Table 6.6. Particle Size Analysis Percentile Results for Sample 584-G1/2-OL-PSD

Measurement Condition	Pump Speed	Sonication	d(10) [μm]	d(50) [μm]	d(90) [μm]
1	3000	pre-sonic	0.69	1.4	2.5
2	2000	pre-sonic	0.69	1.3	2.4
3	4000	pre-sonic	0.59	1.2	2.4
4	3000	25%	0.49	0.93	1.8
5	3000	50%	0.34	0.69	1.3
6	3000	75%	0.27	0.59	1.2
7	3000	post-sonic	0.24	0.55	1.4
8	2000	post-sonic	0.25	0.56	1.3
9	4000	post-sonic	0.24	0.61	2.0

Figure 6.9 shows the PSD for Sample 584-G1/2-OL-PSD before sonication as a function of pump speed. All distributions show a strong peak spanning 0.3 to 5 μm and having a maximum between 1 and 2 μm. Distributions at 2000 and 3000 RPM are uni-modal. At 4000 RPM, a small secondary peak spanning 5 to 10 μm appears and is probably representative of difficult-to-suspend (i.e., dense) particles or agglomerates.

Figure 6.10 shows the changes that occur in the distribution of particles as a result of applied sonication. Sonication effects a significant reduction in particle size, with the primary population shifting to smaller particle sizes. During sonication, the primary population of particles spans 0.1 to 2 μm, has a population maximum at 0.7 μm, and exhibits a small shoulder population over 2 to 5 μm. Size reduction is likely a result of sonic disruption of particle agglomerates. After sonication is removed, a decrease in the relative contribution of 0.4- to 1-μm particles and a corresponding increase in the relative contribution of 2- to 5-μm particles are observed. This is suggestive of agglomerate reformation and could indicate that changes in the particle size as a result of sonication are reversible. It also confirms the observation of agglomeration in measurement condition 7 based on the percentiles in Table 6.6.
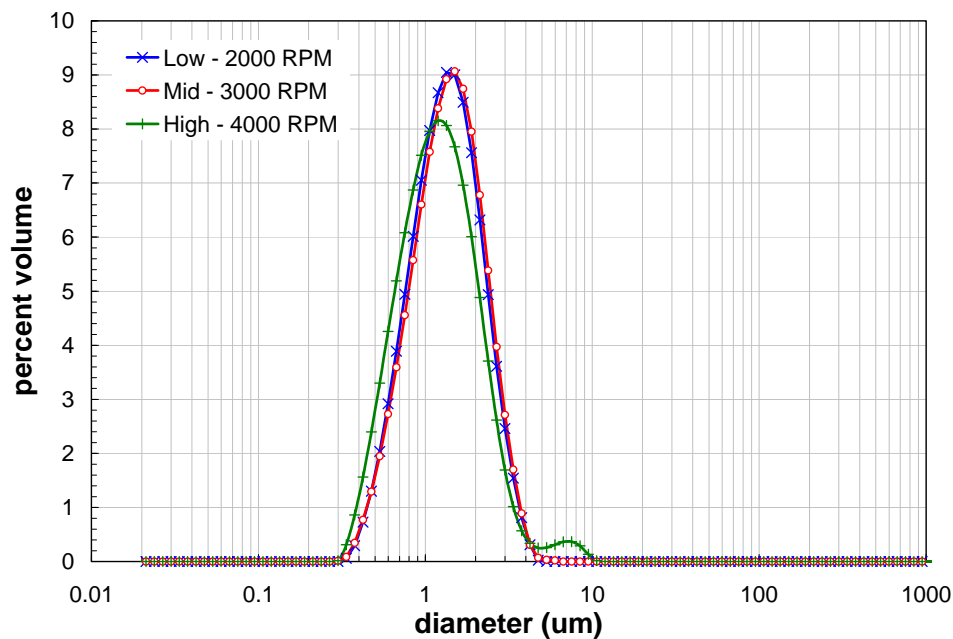
Figure 6.9. Pre-Sonication Volume Distribution Result for Sample 584-G1/2-OL-PSD as a Function of Pump Speed
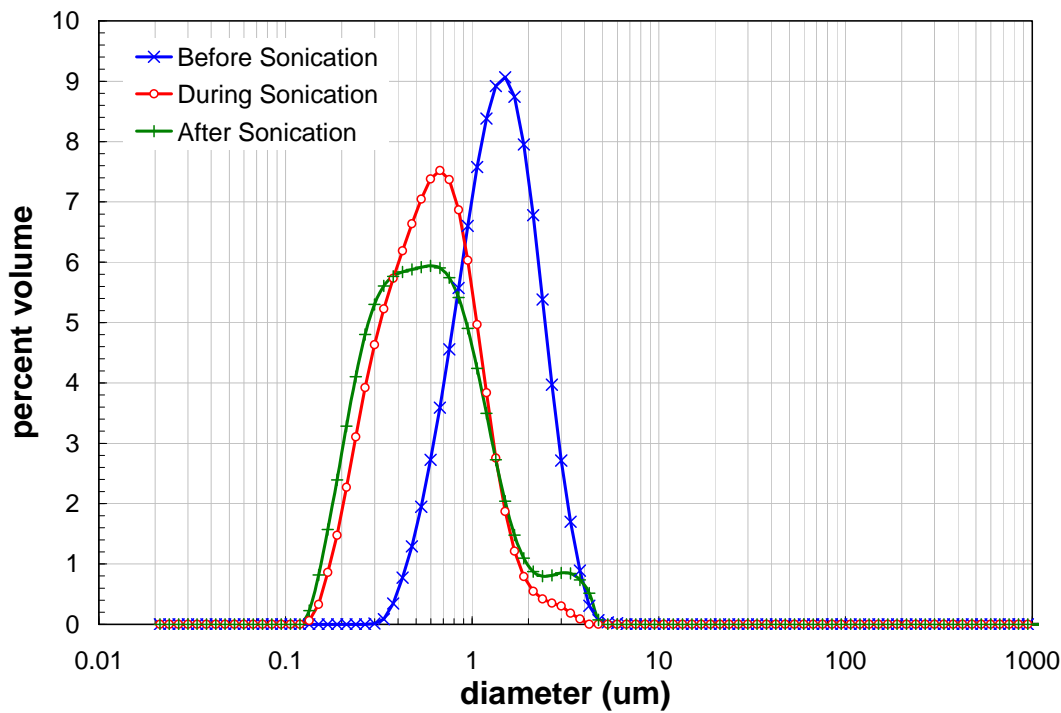
Figure 6.10. Volume Distribution Result for Sample 584-G1/2-OL-PSD Before, During, and After Sonication at 3000 RPM. Note: the during-sonication condition corresponds to measurement condition 6 (see Table 6.6).

Figure 6.11 shows the post-sonication PSD behavior of Sample 584-G1/2-OL-PSD as a function of analyzer to pump speed. With exception of changes in the secondary population of particles (likely agglomerates) over 2 to 5 µm, the distributions are relatively insensitive to changes in analyzer pump speed. With regard to the 2- to 5-µm population, the relative volume contribution of particles in this range appears to scale with analyzer pump speed. Specifically, 2000 RPM shows the lowest volume contribution of 2- to 5-µm particles, whereas 4000 RPM shows the highest. This suggests that the 2- to 5-µm particles are likely "difficult-to-suspend" particles and that the differences in the post-sonication PSDs are likely a result of differences in the state of particle suspension.
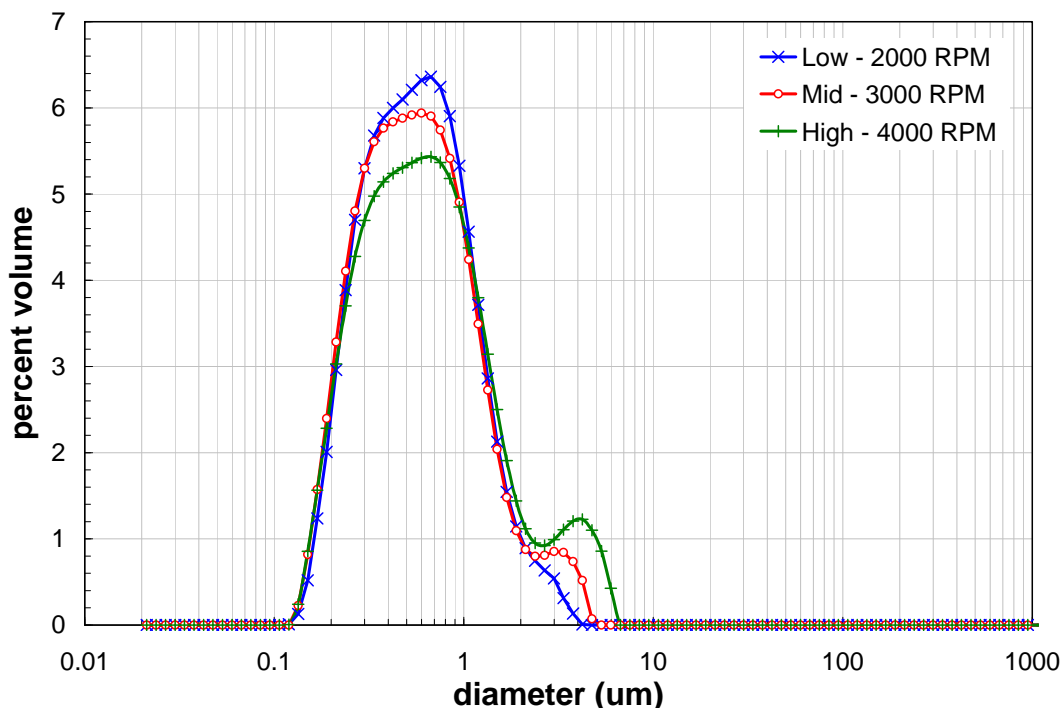
Figure 6.11. Post-Sonication Volume Distribution Result for Sample 584-G1/2-OL-PSD Sample as a Function of Pump Speed

The effect of both caustic and oxidative leaching on Group 1/2 mixed waste solids PSD can be evaluated by comparing to the PSD for the untreated Group 1/2 CUF slurry. Here, the parametric testing sample (584-G1/2-OL-PSD) is compared to the untreated high-solids CUF slurry sample (TI572-G2-6-PSD). In addition, a comparison of the oxidative-leached and washed sample from the CUF studies (Sample TI572-G2-18-PSD) and the parametric testing oxidative-leached sample (584-G1/2-OL-PSD) will be made to highlight any differences or similarities between the leached solids from different studies.

Table 6.7 and Figures 6.12 and 6.13 show changes that occur to the Group 1/2 mixed solids PSD as a result of caustic- and oxidative-leaching and washing. Relative to the unleached material, the size distribution of particles in the caustic- and oxidative- leached and washed waste solids favors smaller particle sizes. Relative to the CUF testing sample, the leached solids derived from parametric testing favor larger particle sizes. However, both samples contain significant fractions of submicron particles and relatively small contributions of 1- to 10-µm particles. As discussed in Section 5, the small particle

sizes observed the oxidative-leached samples are likely a result of weakening of particle aggregates during the washing (rather than the leaching) operations.

Table 6.7. Cumulative Undersize Percentiles Showing the Influence of Caustic and Oxidative Leaching and Washing on the PSD of Group 1/2 Mixed Waste Solids at Measurement Condition 7— 3000 RPM, post-sonication (see Table 6.6).

Sample	d(10) [μm]	d(50) [μm]	d(90) [μm]
Untreated Group 1/2 CUF Slurry (TI572-G2-6-PSD)	0.52	2.4	9.5
CL/OL Washed CUF Slurry (TI572-G2-18-PSD)	0.16	0.30	1.9
CL/OL Washed Parametric Slurry (584-G1/2-OL-PSD)	0.24	0.55	1.4
CL = caustic leaching; OL = oxidative leaching			
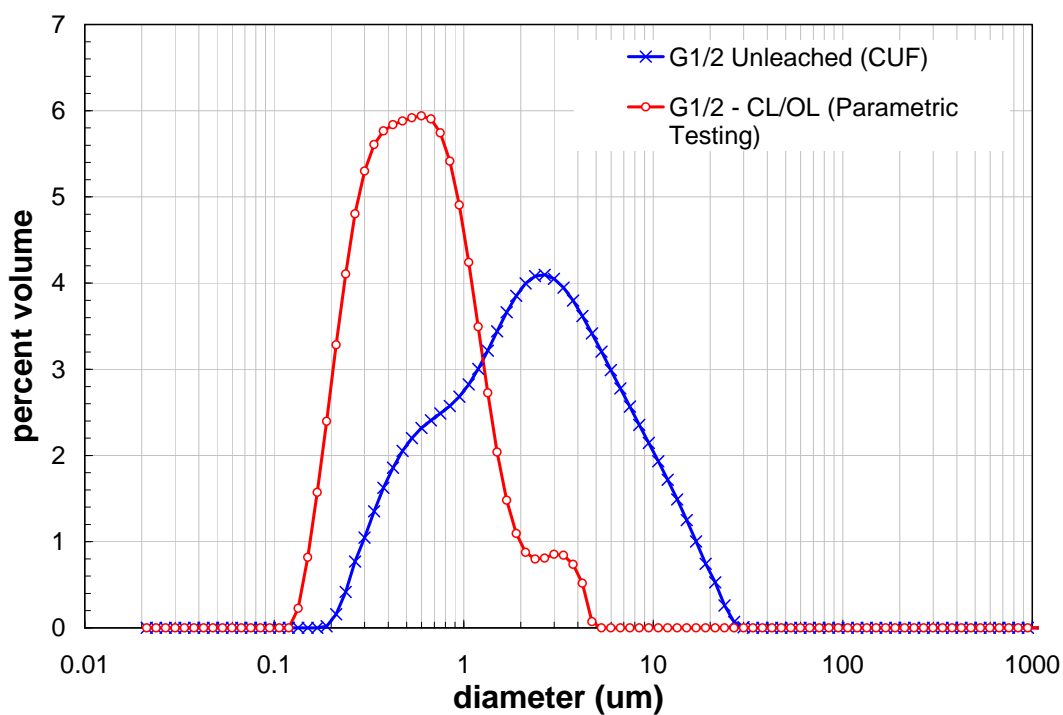
Figure 6.12. Influence of Caustic and Oxidative Leaching and Washing on Group 1/2 Mixed Waste Solids PSD. All PSDs taken at measurement condition 7—3000 RPM, post-sonication (see Table 6.6).
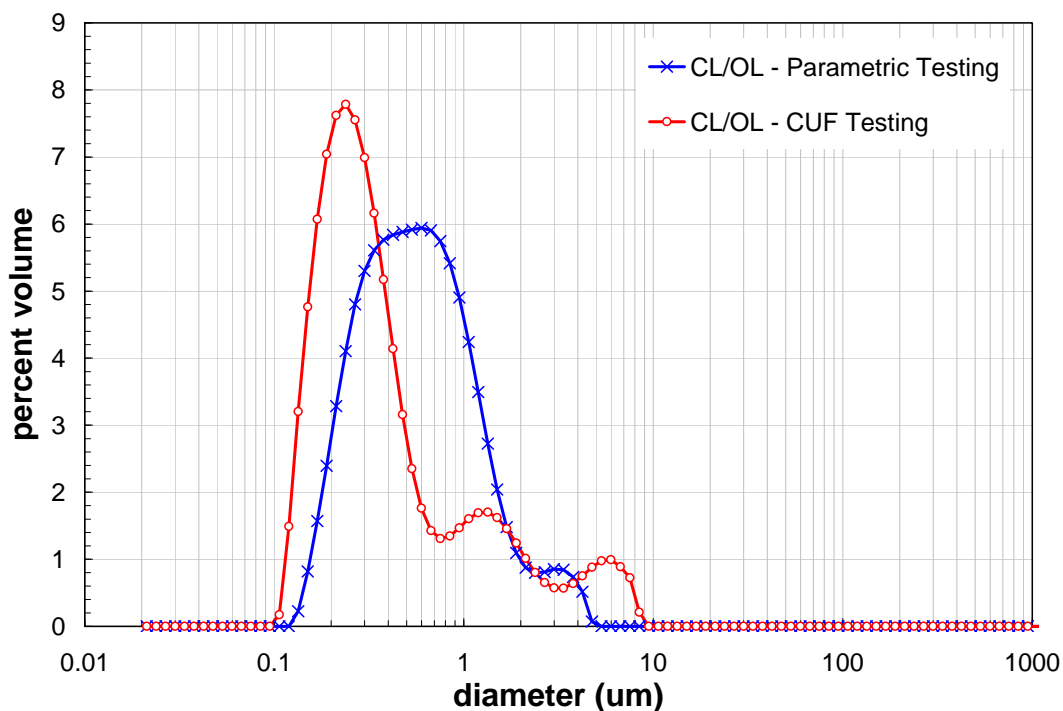
Figure 6.13. Comparison of Caustic- and Oxidatively-Leached and Washed Group 1/2 Mixed Waste Solids PSD from Parametric and CUF Testing. All PSDs taken at measurement condition 7—3000 RPM, post-sonication (see Table 6.6).

To summarize, the PSDs of the leached solids for Group 1/2 were measured and the effects of chemical leaching on the particle size determined. The sample generally showed complex particle-size behavior with respect to both flow rate and sonication. The sample showed a uni-modal distribution of particles spanning 0.3 to 5 μm and having a maximum between 1 and 2 μm. High pump speeds indicate a relatively small-volume contribution of difficult-to-suspend 4- to 10-μm particles. Applying sonic energy effects a significant reduction in particle size, with the majority of particles after sonication having a size smaller than 1 μm. Post sonication PSD measurements suggest partial recovery of particle structures greater than 1 μm, which is suggestive of aggregate reformation.

In terms of the effects of chemical leaching, the PSD results indicate that caustic and oxidative leaching decreases the apparent particle size of mixed Group 1/2 solids. The resulting size distribution is populated by a majority of submicron particles. The size distribution derived from parametric testing is similar to that of caustic/oxidative leached 1/2 solids derived from CUF testing. It is speculated that the combination of leaching and washing operations renders the Group 1/2 particle aggregates susceptible to size disruption.

6.2.6.4 Crystal Form and Habit

The following sections summarize the mineral-phase evaluation of the leached and washed solids.

6.2.6.4.1 XRD

The XRD pattern of the leached and washed solids is provided in Figure 6.14a; the background-subtracted XRD pattern with stick-figure phase identification is shown in Figure 6.14b.

Rutile, TiO_2, was used as an internal standard for 2-theta calibration. Identification was done on 2-theta calibrated data. Two crystalline phases were positively identified. These included hydroxycancrinite ($1.06Na_2O \cdot Al_2O_3 \cdot 1.60SiO_2 \cdot 1.6H_2O$) and clarkeite [$Na(UO_2)O(OH)$]. The broad clarkeite peak at 14.95 indicates a crystallite size of about 196 Å.

Amorphous material accounts for a significant amount of the leached Group 1/2 solids, as indicated by the broad amorphous peak from about 10 to 30 degrees 2-theta in the raw data displayed in Figure 6.14a. This amorphous material cannot be characterized by XRD.

(a)

(b)
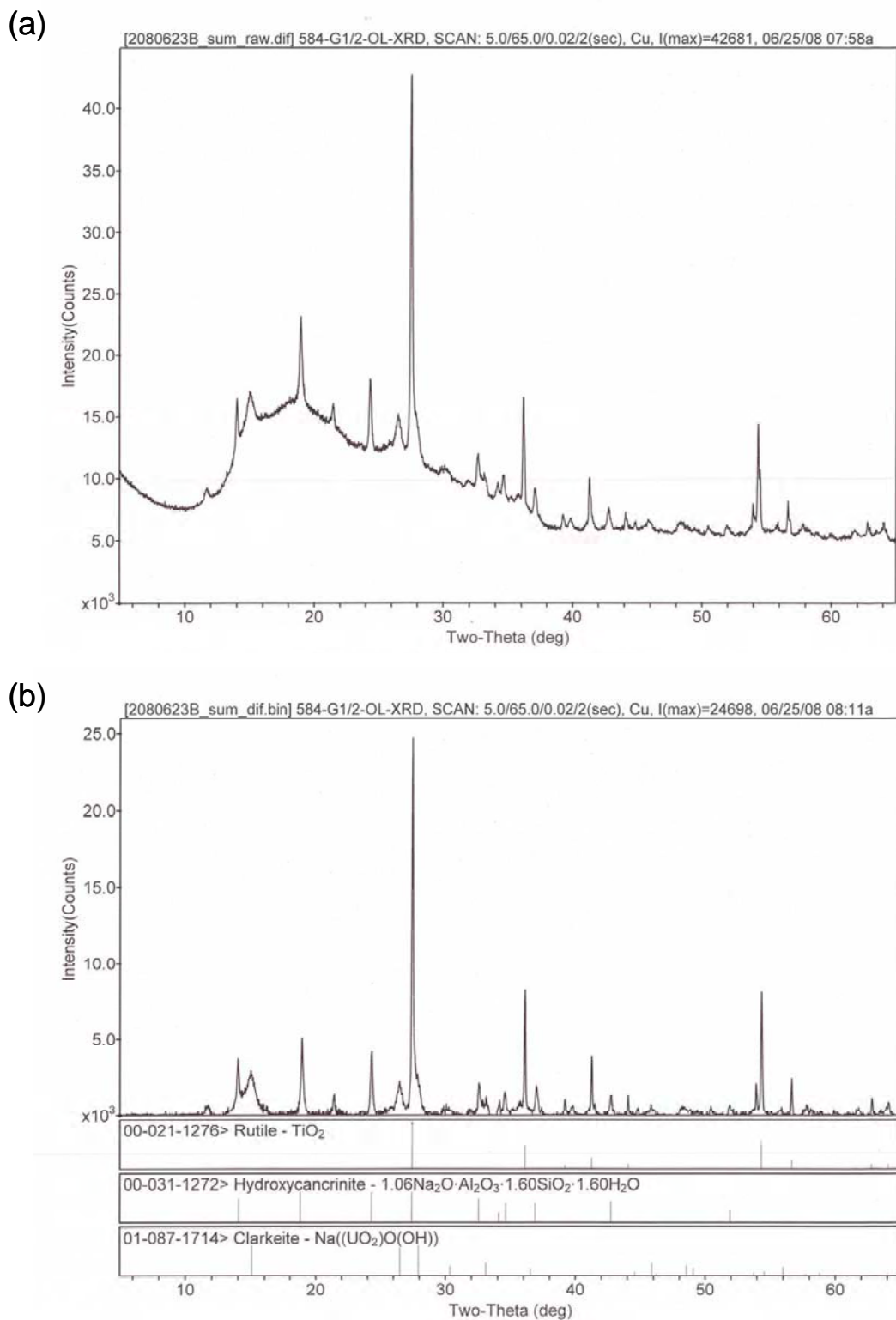
Figure 6.14. XRD Pattern of Oxidatively Leached Group 1/2 Bi-Phosphate Sludge/Saltcake with Rutile (TiO$_2$) Internal Standard (a) Raw Data and (b) Background-Subtracted with Stick-Figure Peak Identification

6.2.6.4.2 SEM and TEM

Several SEM images of the oxidatively leached Group 1/2 solids are shown in Figure 6.15. The particles seen in these images are typically on the order of 5 to 40 μm, with one particle in Figure 6.13c being ~ 140 μm. The smaller particles are consistent with the PSD data reported above. However, no particles larger than ~ 20 μm were seen by PSD.

(a)

584-G12-OL-SEM-7 20.0kV x2500 5μm

(b)

584-G12-OL-SEM-2-2 5.0kV x1000 10μm

(c)

584-G12-OL-SEM-1 5.0kV x500 20μm

(d)

584-G12-OL-SEM-3 5.0kV x250 50μm
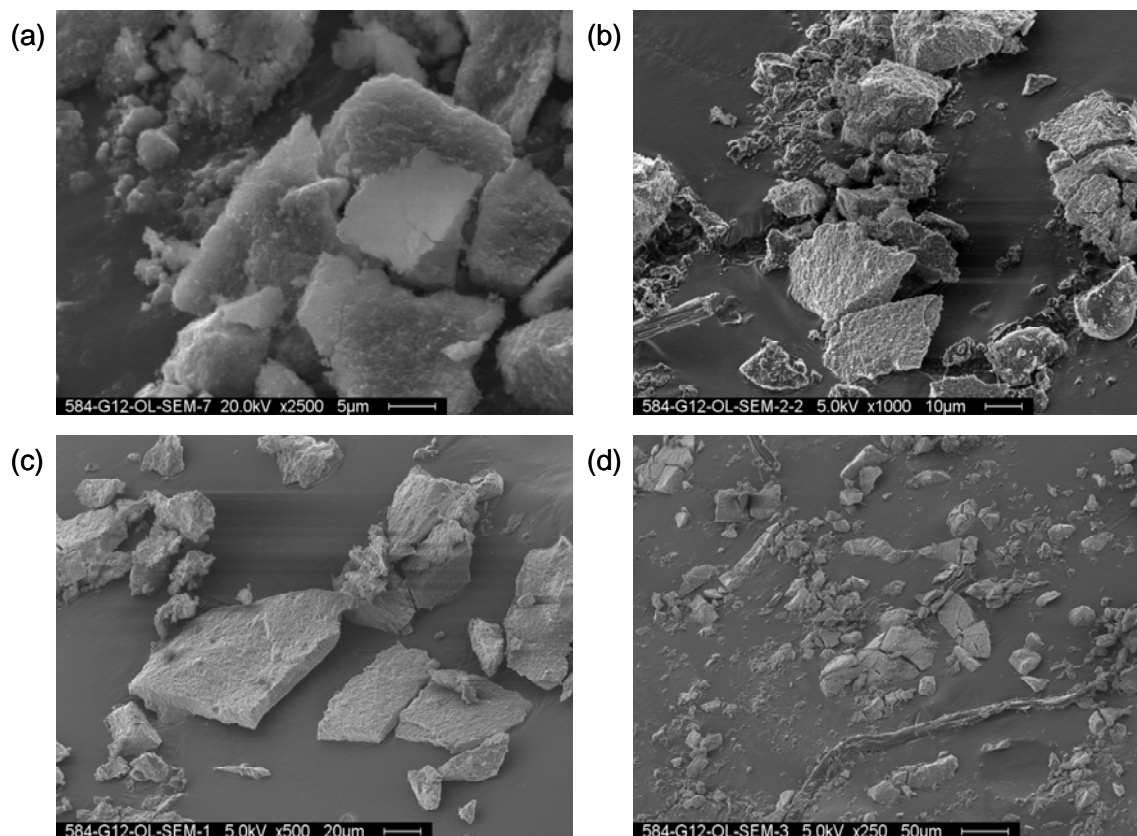
Figure 6.15. SEM images of Group 1/2 Bi-Phosphate Sludge/Saltcake Oxidatively Leached and Washed Solids (a) 20 kV, 2500×; (b) 5 kV, 1000×; (c) 5 kV, 500×; (d) 5 kV, 250×.

Figures 6.16 through 6.18 each show an SEM image along with EDS spectra of two different particles for each. The elemental analysis shows a large amount of oxygen and carbon, which is an artifact of the sample preparation (carbon is sputtered onto the sample to eliminate problems with charging). If this is removed, and the other constituents normalized, the weight percentages shown in Table 6.8 for each analysis are obtained. As was found for the Group 1 caustic-leached solids, the SEM EDS examination indicated that most of the particles had similar elemental composition. A total of 23 particles were analyzed by SEM EDS. Unlike the Group 2 solids where several particles were found to contain only Na, Al, and Si, in this case, only one particle having only these constituents (as well as a small amount of iron, 2.73 wt% Fe) was found (Figure 6.18 spot 7). The three particles shown in Figure 6.16 spot 5, Figure 6.15 spot 1, and Figure 6.18 spot 3 each consist of the nine elements that were found in the majority of the particles, at concentrations that were within 2% of the average of all 23 analyses.

The remaining two particles that were examined by EDS and shown in these three figures were composed of the same elements, just in higher or lower concentrations. The particle in Figure 6.16 spot 1 had much less Na than the other particles (7.9 wt% compared to an average of 17.2%) as well as slightly higher concentrations of U (8.0 wt% compared to an average of 6.1%) and Ca (3.9 wt% compared to an average of 2.8%). The particle in Figure 6.17 spot 4 had less Al and P than the other particles (8.4 and 0.7 wt%, respectively, compared to an average of 14.0 and 1.2%) and much more Fe (39.5 wt% compared to an average of 25.0%).
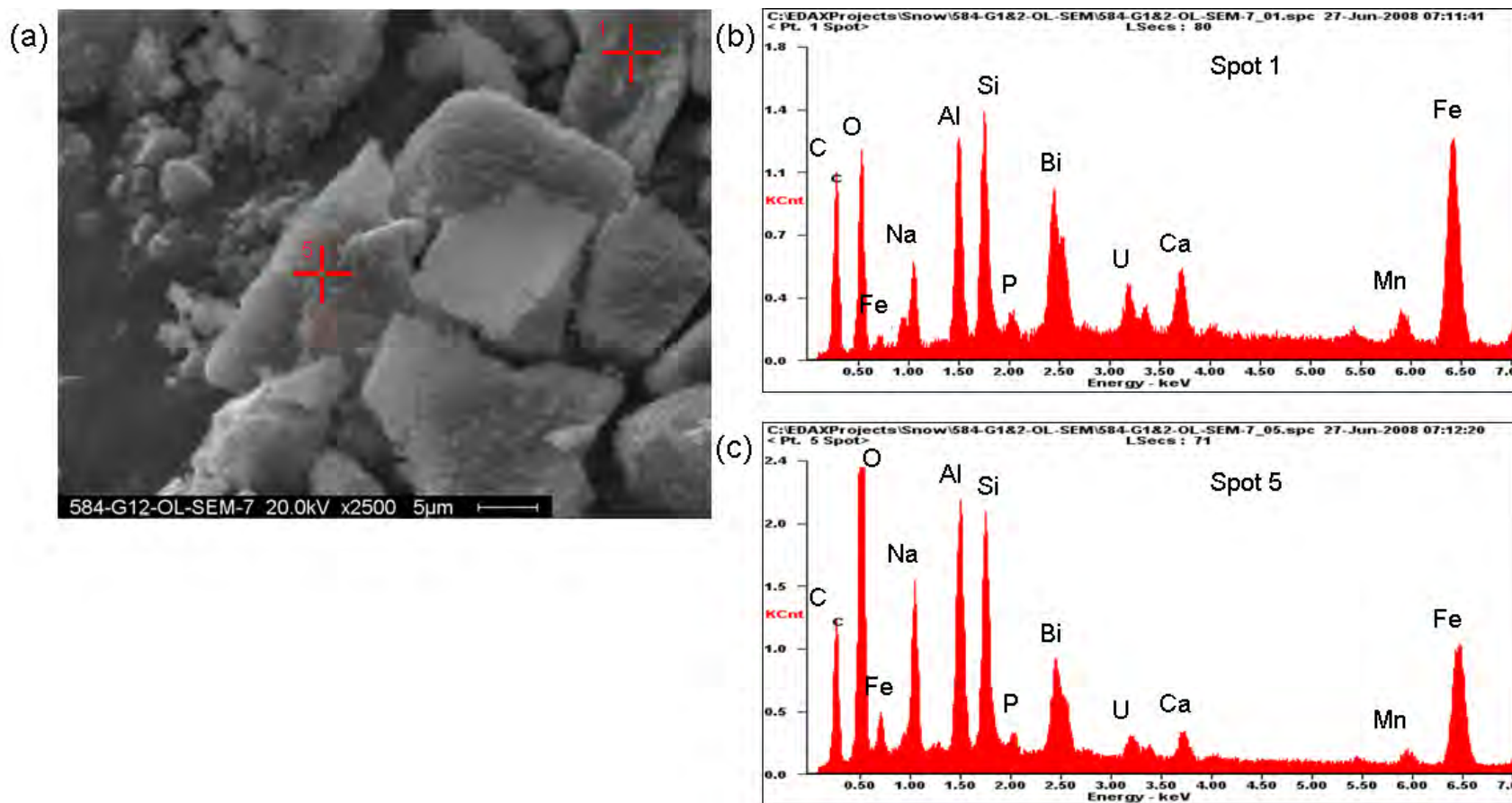
Figure 6.16. SEM Image of Group 1/2 Bi-Phosphate Sludge/Saltcake Oxidatively Leached and Washed Solids with EDS Spectra (a) SEM Image; (b) EDS Spectra of Spot 1; (c) EDS Spectra of Spot 5
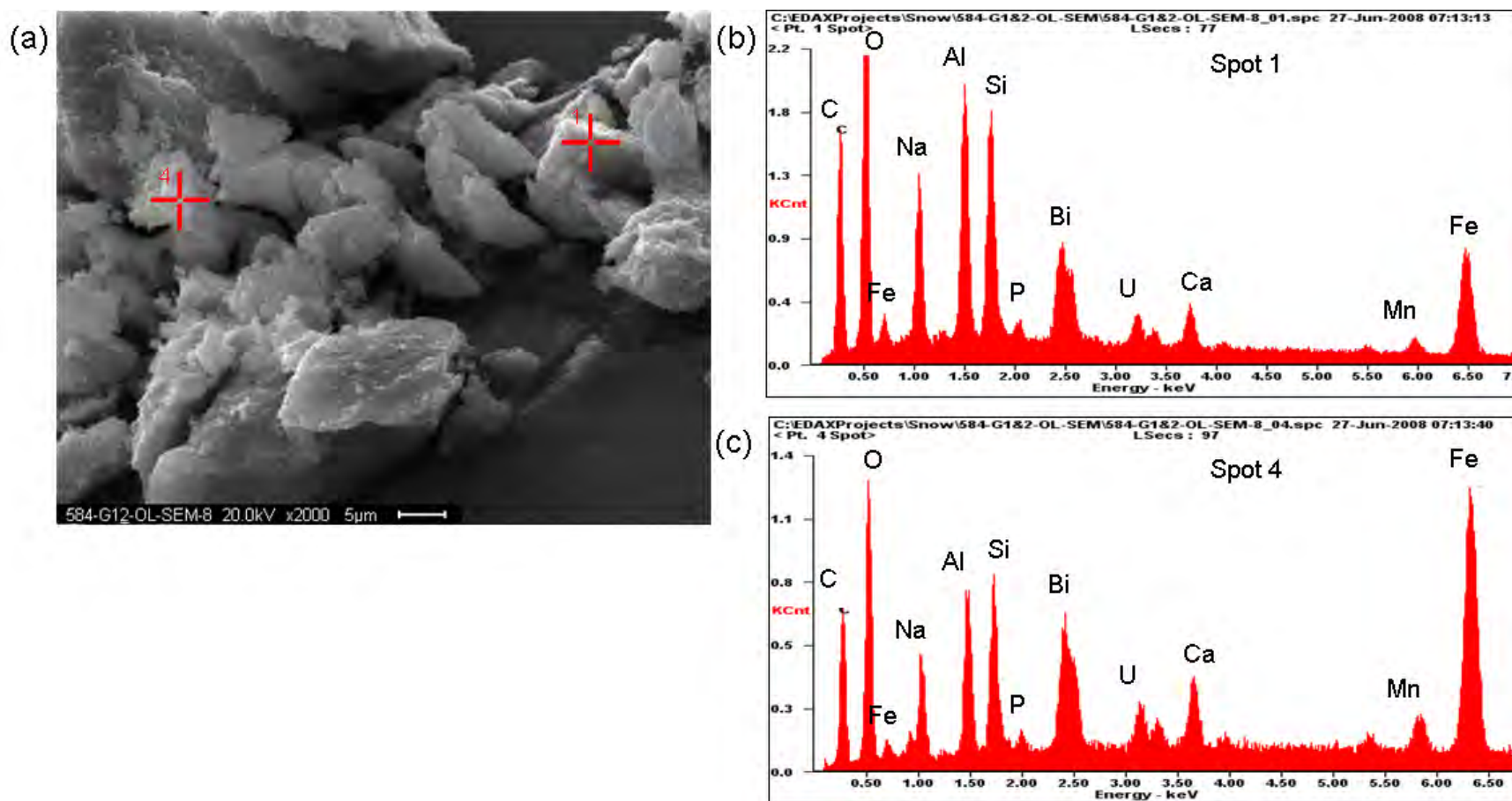
Figure 6.17. SEM Image of Group 1/2 Bi-Phosphate Sludge/Saltcake Oxidatively Leached and Washed Solids with EDS Spectra (a) SEM Image; (b) EDS Spectra of Spot 1; (c) EDS Spectra of Spot 4
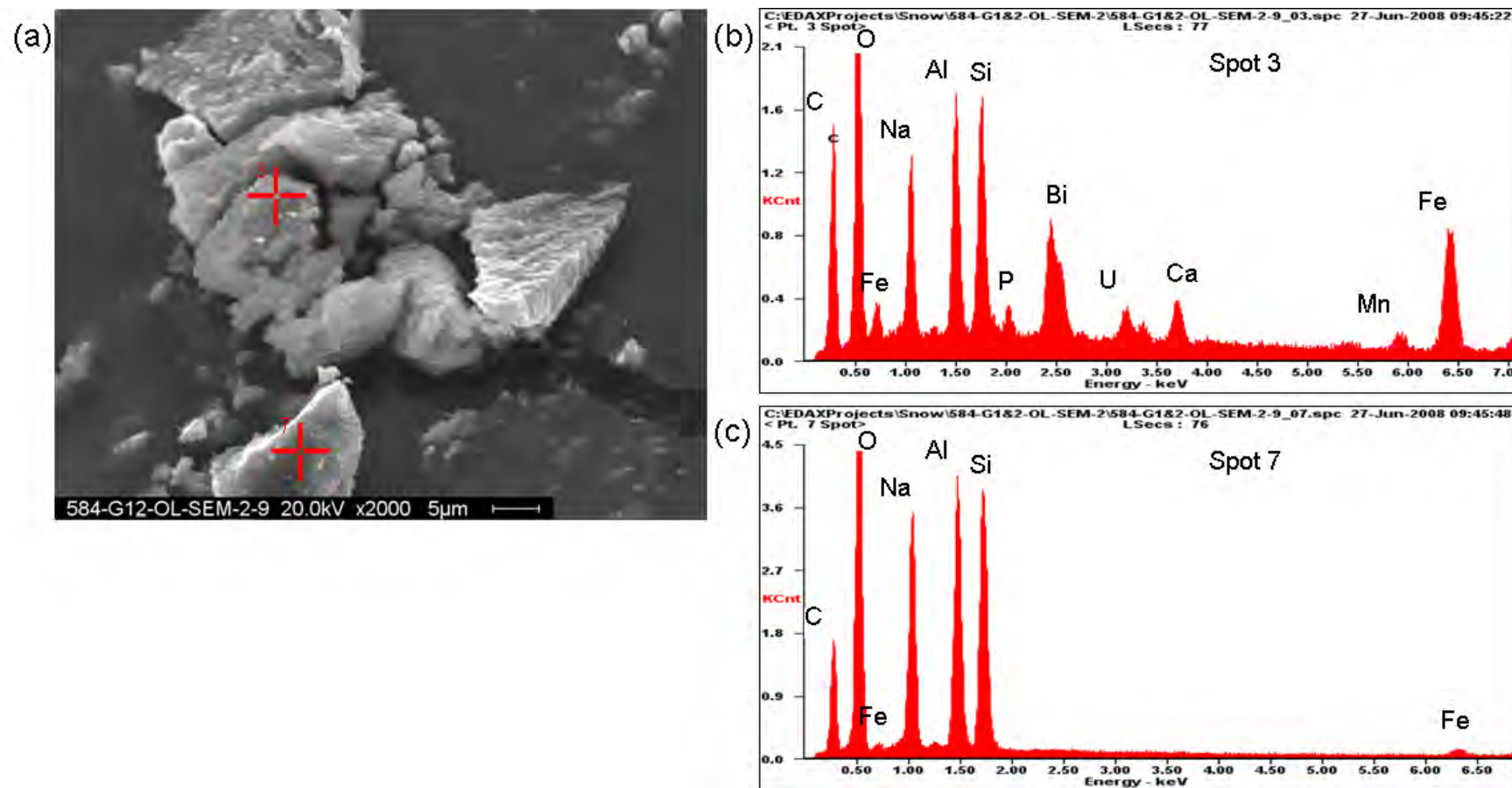
Figure 6.18. SEM Image of Group 1/2 Bi-Phosphate Sludge/Saltcake Oxidatively Leached and Washed Solids with EDS Spectra (a) SEM Image; (b) EDS Spectra of Spot 3; (c) EDS Spectra of Spot 7

Table 6.8. Normalized Weight Percents for Various Analytes Found by EDS of SEM Images for Figures 6.6, 6.17, and 6.18

Element	Normalized Weight Percent						
	Fig 6.14 Spot 1	Fig 6.14 Spot 5	Fig 6.15 Spot 1	Fig 6.15 Spot 4	Fig 6.16 Spot 3	Fig 6.16 Spot 7	Avg of all 23 Analyses
Na	7.9	17.3	16.9	9.5	17.3	38.7	17.2
Al	10.2	15.5	15.2	8.4	13.6	29.8	14.0
Si	9.7	13.3	13.0	7.6	12.3	28.8	11.8
P	0.9	1.2	1.1	0.7	1.4	0	1.2
Bi	19.9	17.3	19.0	17.5	19.6	0	18.5
U	8.0	5.1	6.8	7.8	6.3	0	6.1
Ca	4.0	2.3	3.00	3.8	3.1	0	2.8
Mn	4.0	2.3	2.7	5.2	2.8	0	3.3
Fe	31.5	25.7	22.4	39.5	23.7	2.7	24.9

Figure 6.19 provides an SEM-EDS map of selected elements in the leached and washed solids. Iron, bismuth, silica, and sodium are concentrated within the same area, suggesting a complex consisting of these elements. Further evidence of this is seen with TEM, as discussed below, where a likely match to a compound containing Fe, Bi, and Si is found. Calcium, manganese, and uranium are fairly evenly distributed throughout the area.
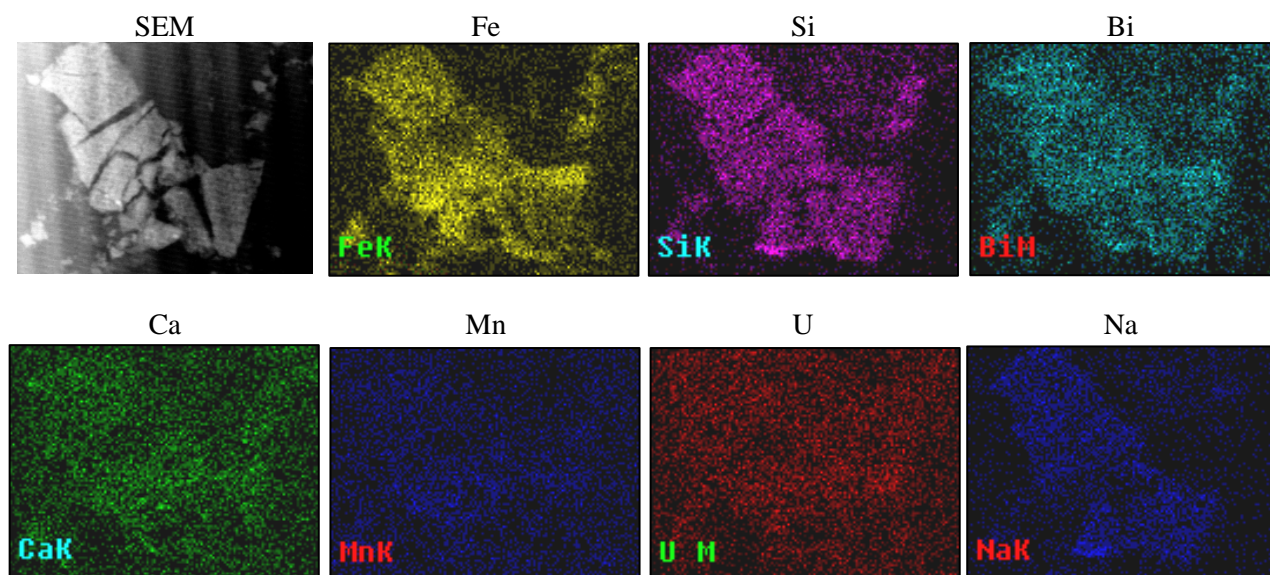
Figure 6.19. SEM-EDS Image of Oxidatively Leached Group 1/2 Bi-Phosphate Sludge/Saltcake with Fe, Si, Bi, Ca, Mn, U, and Na Maps

Figure 6.20 shows four different TEM images of the oxidatively leached solids. The solids are agglomerates of small round particles that consist mainly of iron and bismuth, as well as larger particles of cancrinite. Cancrinite was identified with EDS and electron diffraction as large euhedral particles surrounded by a bismuth phase. Hydroxycancrinite was identified by XRD. Cancrinite and hydroxycancrinite have very similar patterns in XRD and are difficult to distinguish.
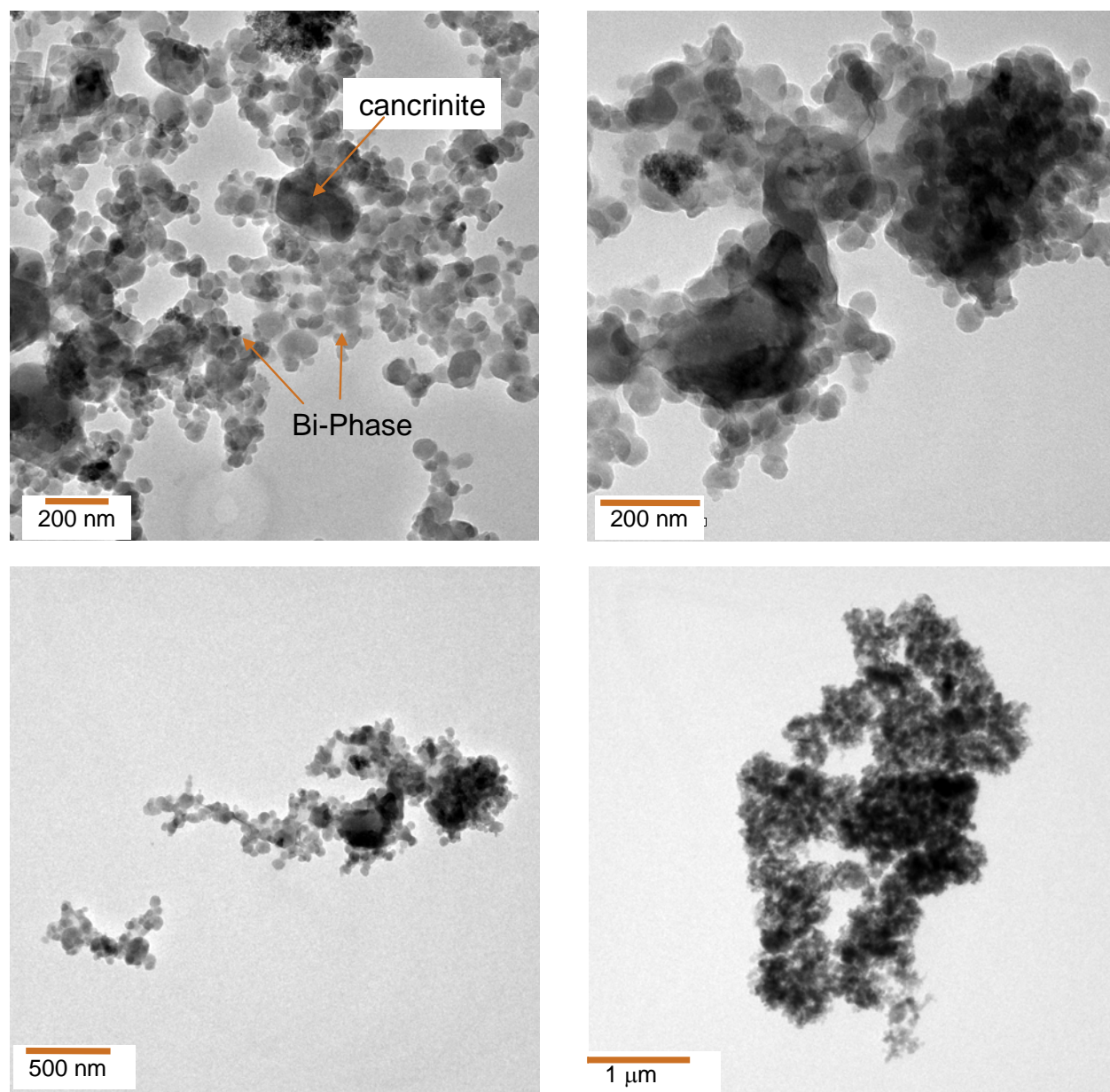
Figure 6.20. TEM Images of Oxidatively-Leached Group 1/2 Bi-Phosphate Sludge/Saltcake

Figure 6.21 shows a typical TEM image with EDS analysis of two regions in the sample. Figure 6.21a shows the STEM-HAADF image and the two areas where EDS spectra were taken. Figure 6.21b is a TEM image of the same agglomerate shown in 6.21a. The smaller particles are Bi-Fe phases, as shown by the EDS spectrum in Figure 6.21c and 6.21d. The larger particle in the upper right of Figure 6.21b is a cancrinite particle. Using various sized nano-probes in TEM mode and STEM, the dominant phase in the sample was determined to be a bismuth iron oxide. The phase composition is consistent with bismuthoferrite. It is present as agglomerates that are variable in size. Based on EDS analysis, the iron content appears to be variable.
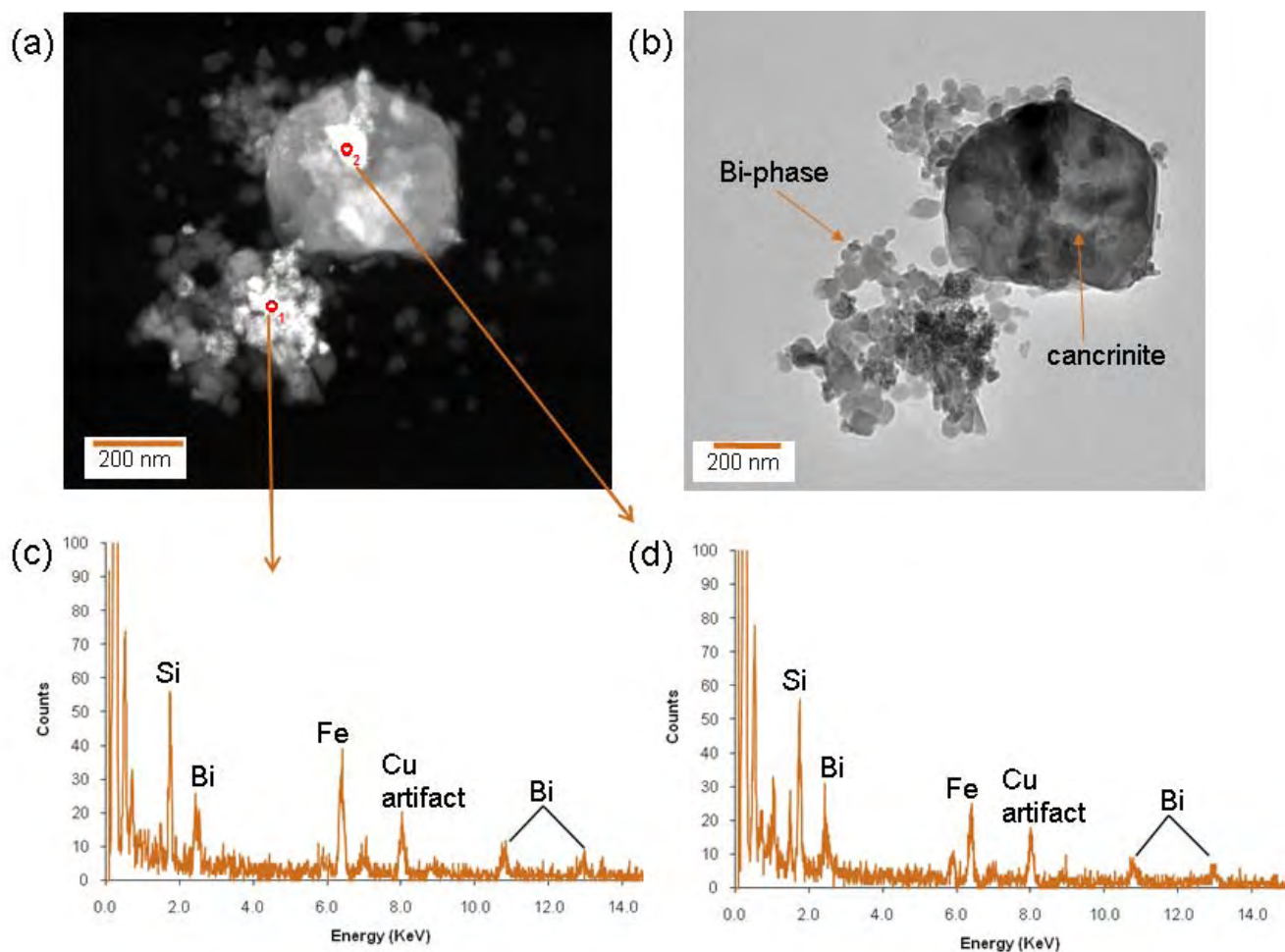
Figure 6.21. TEM Images with EDS Analysis: (a) STEM-HAADF Image; (b) TEM Image Showing Cancrinite Particle and Bi-Fe Phases; (c) EDS Spectrum of Bi-Fe Phase; (d) EDS Spectrum of a Bi-Fe Particle that is Under the Cancrinite Particle

Results from electron diffraction analysis of the iron bismuth particles in this sample are compared to literature values for a bismuth iron phase, bismuthoferrite [$Fe_2Bi(SiO_4)_2(OH)$] in Table 6.9 (Zhukhlistov and Zvyagin 1977) The measured D-spacings on these particles are very good matches to those reported in the literature. This is also in agreement with the SEM EDS map shown in Figure 6.19, where Bi, Fe, and Si seem to be at high concentrations in the same area. The bismuthoferrite phase was not identified in the bulk XRD analysis, perhaps because of the very small (~50 nm) size of the primary crystals.

Table 6.9. Electron Diffraction Analysis Data for Group 1/2 Bi-Phosphate Sludge/Saltcake Oxidatively Leached Solids

Measured D-Spacing (Å)	Literature D-Spacing (Å)	hkl
3.13, 3.10	3.1534	-1 1 2
1.90	1.90	-1 3 3
1.605	1.607	-1 3 4
1.59	1.5900	-1 5 2
1.42	1.4291	-2 0 5
1.205	1.207	-2 4 5
1.131	1.12	
1.117	1.11	

Not all of the iron was associated with bismuth. Figure 6.22 shows an EDS spectrum of a particle that is high in iron, but has a low concentration of bismuth. Based on the ICP analysis of the oxidatively leached and washed solids, the molar ratio of iron to bismuth is 6, suggesting that although a portion of the iron is bound to bismuth, there is still an excess of iron that most likely exists as an iron oxide.
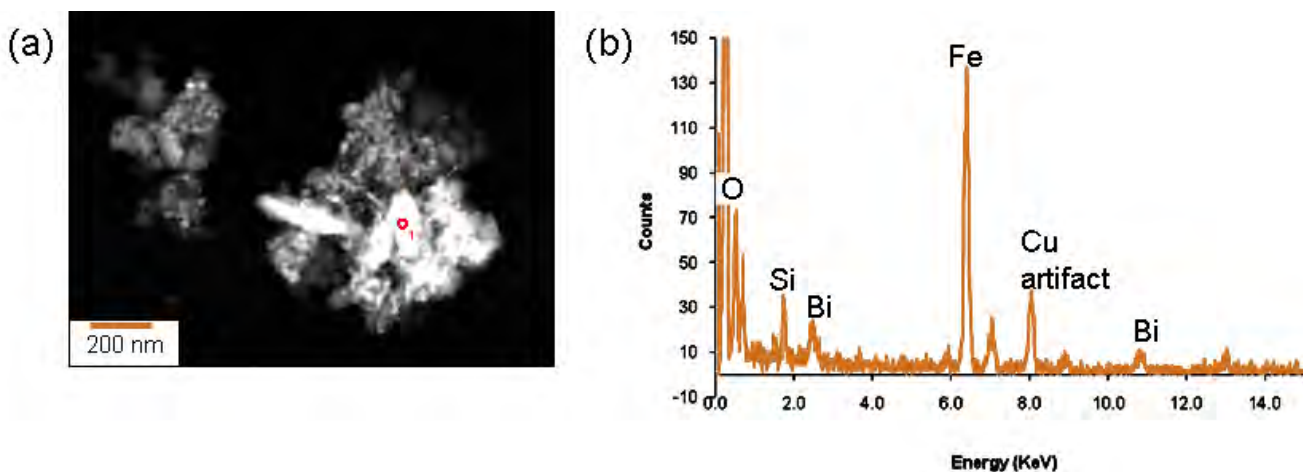
Figure 6.22. Particle High in Iron (a) TEM Image; (b) EDS Analysis Showing High Iron Content as Well as Very Little Bismuth

Figure 6.23 shows the analysis of a cancrinite phase; the EDS spectrum is shown in Figure 6.23b. The [100] direction of the crystal is shown. Figure 6.24 shows the identification of a uranium phase. Three EDS spectra are shown in Figure 6.24b. The top spectrum shows the U phase. The particle that was examined is circled in Figure 6.24a. The middle spectrum shows another analysis of a phase high in Bi and Fe, and the bottom spectrum could possibly be another cancrinite particle.
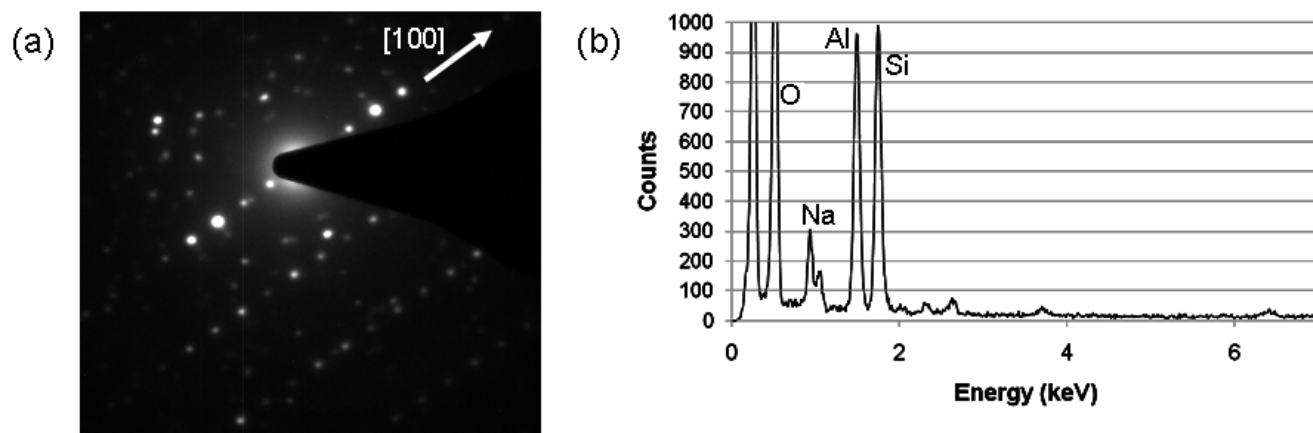
Figure 6.23. TEM Analysis of Cancrinite Phase: (a) SAED Image; (b) EDS Spectrum
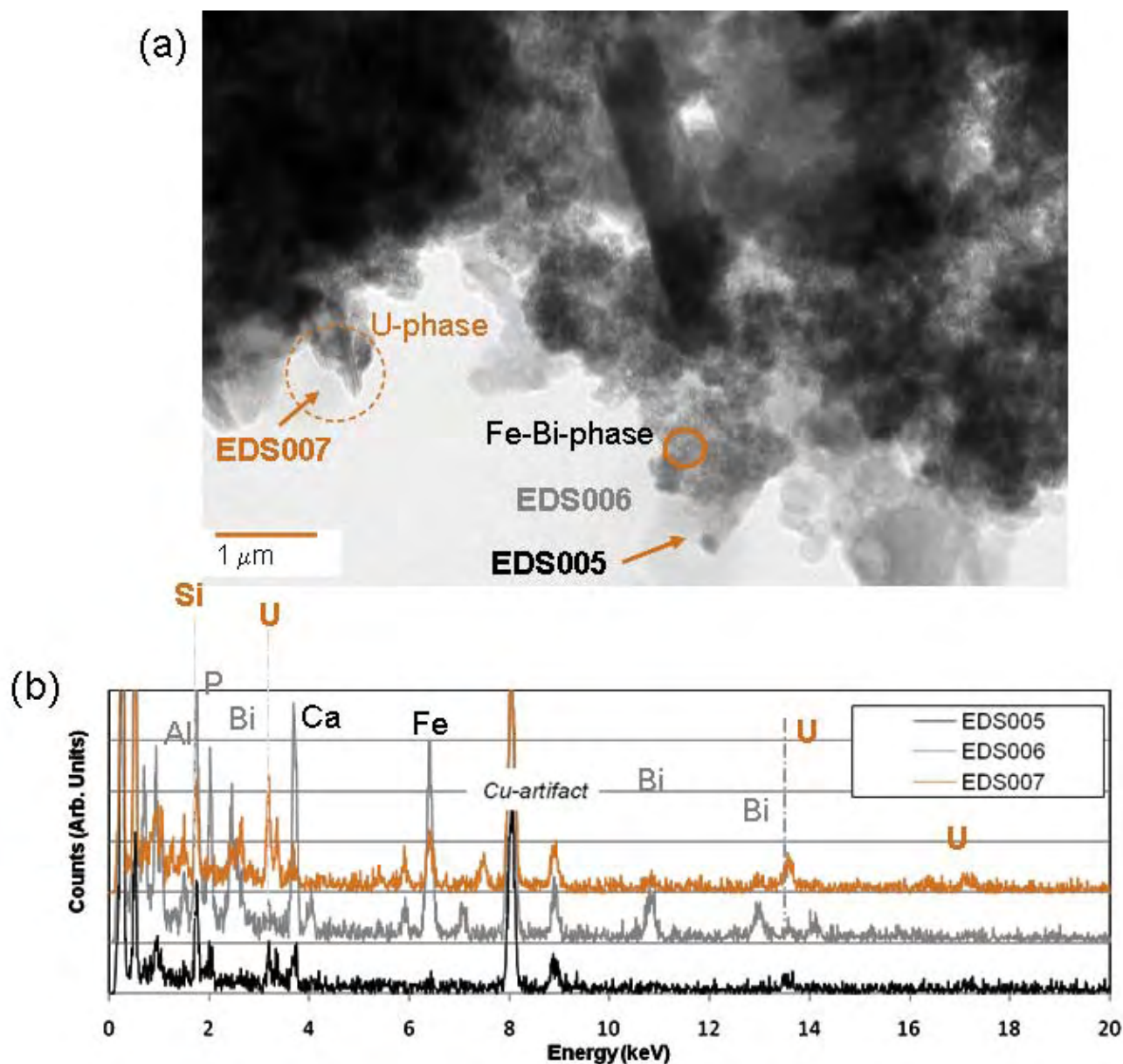
Figure 6.24. (a) TEM Image; (b) EDS Analysis Showing Uranium Phase, Iron Bismuth Phase, and Cancrinite

Figure 6.25 shows a TEM with an EDS spectrum of a metal particle that is high in nickel. The particle is composed of nickel, chromium, iron, and molybdenum. This composition is similar to a corrosion-resistant metal such as Hastalloy X (47Ni-22Cr-18Fe-9Mo-0.6W-1.5Co) that was used as cladding material at the Hanford site in the 1960s. Corrosion in the tank sludge might have removed iron preferentially over time from the metallic particles.
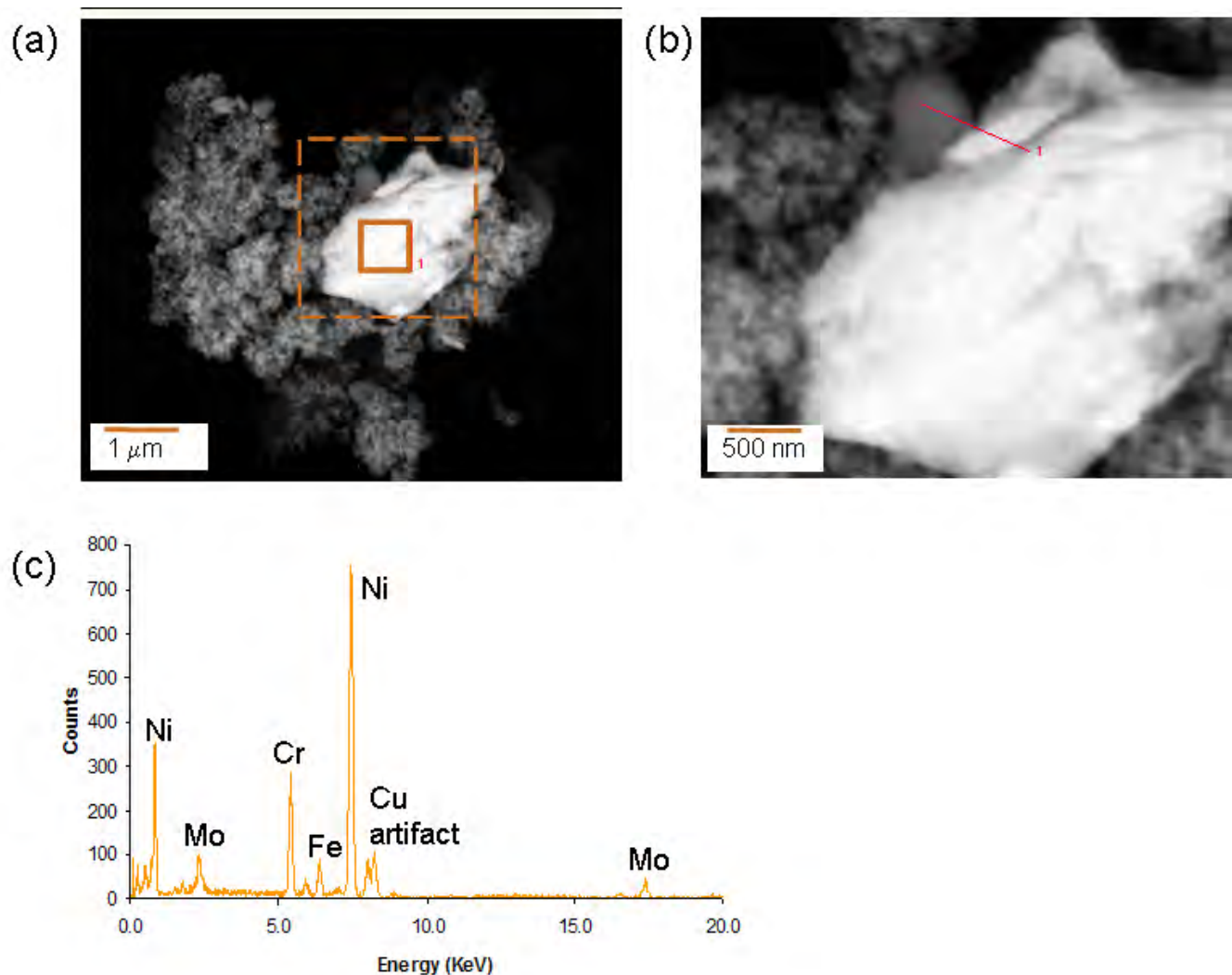
Figure 6.25. TEM image of a Nickel Particle: (a) TEM Image; (b) Close-up of Area in the Dotted Square in (a); (c) EDS Spectrum Taken of the Area 1 Shown in (a)

6.2.6.5 Surface Area by BET

A BET measurement was conducted on the oxidatively leached and washed solids, resulting in a surface area of 125.9 m^2/g. This is higher than the value of 96.3 m^2/g found for the solids that were oxidatively leached in the CUF. However, this could be due to the difference in amount of Cr that was leached from the two experiments. In the CUF, only 26% of the Cr was leached from the solids, while in the parametric tests, 66% of the Cr was leached.

7.0 Summary

Tank waste sludge and saltcake at the Hanford Site have been categorized into eight general groupings representing ~75 wt% of the total high-level waste mass expected to be processed through the WTP. Two of the eight groups, Group 1 and Group 2, are the subject of this report. Group 1 represents bismuth phosphate sludge waste containing a high fraction of phosphate; Group 2 represents bismuth phosphate saltcake, which contains a large fraction of the tank waste aluminum, chromium, phosphate, and sulfate.

Multiple samples representative of these two waste groups, all of which had been stored for ~10 years or more, were identified in the 222S sample archive. Materials representative of Group 1 (and containing high P) were obtained from archived samples from tanks B-104, T104, BX-112, and S-107, although the sample composite used was dominated by the B-104 waste. Materials representative of Group 2 were selected from archived samples from tanks BX-110, BX-111, BY-104, BY-105, BY-107, BY-108, BY-109, BY-110, BY-112, T-108, T-109, TX-104, and TX-113. These materials were combined into their respective composite group using water to suspend solids during mixing and dissolve the water-soluble species.

The tank waste composites were extensively characterized for physical properties, rheological properties, and chemical composition of the solids and liquid phases as well as the crystal habit of the insoluble solids. Table 7.1 summarizes the physical properties for the Group 1 and Group 2 samples, and Table 7.2 summarizes selected elemental analysis information.

Group 1 Parametric Testing

The Group 1 bismuth phosphate sludge waste was subjected to parametric caustic leach testing to understand phosphorus dissolution characteristics and to support the development of a suitable simulant material for this type of waste (although simulant development was outside the scope of the work reported here). Leaching was conducted in a 1:100 solids-mass to solution-volume ratio under varying hydroxide concentrations (1, 3, and 5 M) and varying temperature (40, 60, and 80°C). Periodic sampling (1 to 24 h) and analysis was conducted to determine the reaction behavior at each reaction condition. Table 7.3 provides the composition of the residual solids from leaching the Group 1 solids in 3 M NaOH at 40°C for 24 h, along with the leach factors for selected waste components. The following are the key conclusions from this work.

- Under all caustic leaching conditions examined, phosphate removal from the Group 1 solids was rapid with essentially complete removal typically being achieved after 2 h.

- Even before heating, adding 1 M NaOH resulted in ~60% P removal from the Group 1 solids; this was accompanied by a dramatic color change from beige to rusty-red.

- Identifying specific phases present in the Group 1 solids was difficult because of the amorphous nature of the solids. It is hypothesized that the phosphorus in the washed Group 1 solids was primarily in the form of an iron(III) phosphate phase, which rapidly metathesizes to ferric hydroxide (yielding the rusty-red color) and sodium phosphate. FTIR spectroscopy, SEM-EDS examination, and chemical observations support this hypothesis.

- Seventy-five to 85% of the Al present in the washed Group 1 solids readily dissolved in caustic media (1 to 3 M NaOH).

- Chromium was not readily removed from the Group 1 solids. Even under the most rigorous caustic leaching conditions examined (3 M NaOH at 80°C), only 22% of the Cr was removed after 24 h of leaching.

- Chromium would likely be the component constraining waste loading in the HLW glass for the Group 1 solids remaining after leaching in 3 M NaOH at 40°C.

- The PSD for the leached Group 1 solids shifted to larger particle sizes compared to the un-leached material. This could be attributed to either dissolution of the smaller particles originally present (with the larger particles being insoluble in caustic) or to the formation of agglomerates in the leached material (or a combination of both). The PSD for the leached Group 1 solids is broad, spanning 0.3 to 300 μm, and multimodal. At a pump speed of 3000 RPM, the distribution is dominated by a peak with a maximum population at 30 to 40 μm. There is a secondary population of particles spanning from 0.3 to 8 μm, which decreases when the pump speed is increased. This observation suggests breakage of agglomerates through the shear action of the pump.

Table 7.1. Summary of Major Physical Properties and Mineral Phases of Group 1 Bismuth Phosphate Sludge and Group 2 Bismuth Phosphate Saltcake

Physical Properties	Group 1 Bismuth Phosphate Sludge Slurry	Group 2 Bismuth Phosphate Saltcake Slurry
Total slurry volume	2,163 mL	814 mL
Total UDS	9.0 wt%	37.4 wt%
Bulk density	1.31 g/mL	1.66 g/mL
Centrifuged solids	36.7 vol%	68.6 vol%
Shear strength[a]	15 Pa	21 Pa
Apparent viscosity[b]	6 to 26 cP	49 to 144 cP
Behavior	Newtonian (mostly)	Non-Newtonian
Bingham Yield Stress	< 0.5 Pa	1.4 Pa
PSD	Peak: 10 μm Range: 0.3–100 μm	Peak: 4 μm Range: 0.3–30 μm
Surface Area	95 m²/g	46 m²/g
(a) Strength of settled solids 67 hours after mixing. (b) Apparent viscosity taken at a shear rate of 33 s⁻¹.		

Table 7.2. Summary of Elemental Composition of Group 1 Bismuth Phosphate Sludge and Group 2 Bismuth Phosphate Saltcake Slurries

Major Analytes	Group 1 Bismuth Phosphate Sludge		Group 2 Bismuth Phosphate Saltcake	
	Solids, μg/g[(a)]	Aqueous, μg/mL	Solids, μg/g[(a)]	Aqueous, μg/mL
Al	27,400	< 4	117,500	2,030
Bi	103,100	< 3	1,030	<3
Cr	5,082	26	7,885	798
Fe	95,525	<2	22,100	[7.5]
Mn	427	<0.2	1,020	<0.2
Na	148,750	89,300	184,500	112,000
P[(b)]	81,300	4,720	47,850	859
S	[3,100]	5,360	[1,400]	3,845
Si	42,850	12.6	31,650	[8]
U	11,400	Not Measured	15,250	Not Measured
(a) Dry mass basis of washed solids.				
(b) Determined opportunistically.				

Table 7.3. Composition of Caustic-Leached Group 1 Solids with Leach Factors of Selected Analytes (3 M NaOH, 40°C, 24 h)

Analyte	Leached Solids, μg/g[(a)]	Fraction Leached	Analyte	Leached Solids, μCi/g[(a)]	Fraction Leached
Al	[11,500]	0.84	^{60}Co	7.15×10^{-3}	--
B	[240]	0.44	^{90}Sr	1.35×10^{2}	--
Bi	314,500	0.03	^{137}Cs	1.25×10^{0}	0.98
Cd	<12.1	0.96	$^{239+240}$Pu	1.86×10^{0}	--
Cr	13,300	0.08	^{241}Am	1.74×10^{-1}	0.05
Fe	304,500	--			
Mn	1,290	--			
Na	[14,000]	0.96			
P	[795]	1.00			
S	[840]	0.82		No data	
Si	19,850	0.88			
Sr	3,160	0.03			
Zn	193	0.86			
U (KPA)	7,900	0.72			
(a) Dry mass basis of washed solids.					

Group 2 Parametric Testing

The Group 2 bismuth phosphate saltcake solids contained significant concentrations of Al, Cr, P, and S after washing with dilute hydroxide. Removing these components is desired to increase waste loading in the HLW glass. Gibbsite and nitrate cancrinite were determined to be in the Group 2 solids through both XRD and FTIR analysis. Other phases suggested by the XRD analysis included urancalcarite $Ca(UO_2)_3CO_3(OH)(H_2O)_3$ and dorfmanite ($Na_2HPO_4(H_2O)_2$), although there was no evidence for the latter

in the FTIR spectrum, and this species would not be expected to survive the initial washing process. The precise mineralogical forms of phosphorus, chromium, and sulfur are not yet well characterized for the Group 2 solids.

The Group 2 waste was subjected to parametric caustic leaching tests to determine the Al, Cr, and P dissolution characteristics; the P results were determined opportunistically. Leaching was conducted in a 1:100 solids-mass to solution-volume ratio under varying hydroxide concentrations (1, 3, and 5 M) and varying temperature (60, 80, and 100°C). Periodic sampling (1 to 24 h) and analysis was conducted to determine changes in component dissolution at each reaction condition. Table 7.4 provides the composition of the residual solids from leaching the Group 2 solids in 3 M NaOH at 80°C for 24 h, along with the leach factors for selected waste components. The following are the key conclusions from this work.

- Aluminum dissolution from the Group 2 solids was similar under all conditions examined, indicating only a slight dependence on hydroxide concentration and temperature. Steady-state Al concentrations were reached within 4 to 8 h. The steady-state concentrations corresponded to ~60% Al dissolved, indicating that ~40% of the Al in the Group 2 solids was resistant to caustic leaching. This behavior would reasonably be explained by ~60% of the Al present as gibbsite and the remainder as aluminosilicates, such as cancrinite.

- Chromium removal from the Group 2 solids displayed only a slight dependence on the hydroxide concentration. For leaching in 3 and 5 M NaOH (at 80°C), the Cr removal gradually increased up to a value of 70% removed after 24 h of leaching. In the case of 1 M NaOH, the Cr removal did appear to stabilize at only ~45% after 8 h of leaching.

- Chromium removal from the Group 2 solids was strongly temperature dependent when measured at a constant hydroxide concentration of 3 M. In order to not exceed the glass loading limits of Cr in the HLW form, approximately 85% of the Cr needs to be removed from the water-insoluble Group 2 solids. This condition was just met at 24 hours in 3 M NaOH at 100°C. Dissolution at 80°C reached approximately 70% dissolved after 24 hours, while only 30% of the Cr was dissolved after 24 hours at 60°C. Oxidative leaching might be required to sufficiently remove Cr from the Group 2 solids.

- Phosphorus removal from the Group 2 solids was not strongly influenced by NaOH concentration, but did display some temperature dependence. Nevertheless, P removal from the Group 2 solids was much lower than that observed for Group 1. Only about 25% of the P was removed from the Group 2 solids under the most aggressive conditions examined (i.e., 24 h leaching with 5 M NaOH at 80°C or 3 M NaOH at 100°C). This can be attributed to P being present in the form of hydroxyapatite, $Ca_5(OH)(PO_4)_3$, which is a very stable phase under caustic leaching conditions (Lumetta 2008).

- The PSD (at a pump speed of 3000 RPM) for the leached Group 2 solids displayed particles in the range of ~0.2 to 20 μm with a maximum population between 1 and 2 μm and a large shoulder population in the range of 3 to 20 μm. At a pump speed of 4000 RPM, a large secondary peak spanning 20 to 200 μm and with a peak population at 60 μm was observed, indicating the presence of particles that are difficult to suspend. Caustic leaching resulted in a decrease in the PSD for the Group 2 solids, which is likely a result of either material dissolving from the particle surfaces or agglomerates breaking.

Table 7.4. Composition of Caustic-Leached Group 2 Solids with Leach Factors of Selected Analytes (3 M NaOH, 80°C, 24 h)

Analyte	Leached Solids, µg/g[a]	Percent Leached	Analyte	Leached Solids, µCi/g[a]	Percent Leached
Al	91,450	0.61	^{60}Co	2.53×10^{-2}	--
B	<186	0.27	^{90}Sr	8.00×10^{2}	0
Bi	3,650	0.13	^{137}Cs	1.93×10^{2}	0.06
Cd	329	0.24	$^{239+240}$Pu	5.70×10^{-1}	.06
Cr	10,300	0.71	^{241}Am	1.64×10^{0}	0.01
Fe	84,500	--			
Mn	4,110	--			
Na	[100,000]	--			
P	19,000	0.19			
S	[3,250]	--		No data	
Si	92,250	--			
Sr	17,450	--			
Zn	1,725	0.27			
U	59,850	0.19			
(a) Dry mass basis of washed solids.					
Analyte uncertainties were typically within ±15% (2-σ); results in brackets indicate that the analyte concentrations were less than the minimum detection limit (MDL) and greater than the estimated quantitation limit (EQL), and uncertainties were >15%.					
Radionuclide reference date: June 7, 2007.					
"--" calculation could not be made from one or more "less-than" values.					

Group 1/2 CUF Testing

A blend of the Group 1 and Group 2 solids was made at a UDS concentration of 8 wt% (low-solids slurry) for CUF testing. The filter flux for the low-solids slurry was dependent upon the TMP in the range of TMPs examined (20 to 60 psid), but the axial velocity had no significant influence of the filter flux in the range of 8 to 18 ft/s. Fouling of the membrane was observed while the low-solids slurry was being filtered. Although the flux could be mostly restored by back-pulsing, some irreversible fouling of the membrane occurred during the course of the low-solids slurry tests. The filter fluxes decreased rapidly during filtration of the low-solids slurry. The filter flux was stable at ~0.017 GPM/ft^2 during dewatering of the low-solids Group 1/2 slurry to an UDS concentration of 16 wt% (resulting in the high-solids slurry).

Although the decline in the filter flux over time was less pronounced for the high-solids slurry compared to the low-solids slurry, the overall filter flux was significantly lower for the high-solids slurry. The average fluxes measured at the standard conditions for the high-solids slurry were sequentially 0.016, 0.013, and 0.011 GPM/ft^2, indicating a small, but apparently irreversible, decline in flux with time. For the high-solids Group 1/2 slurry, the filter flux was dependent upon the TMP, but not the AV.

Caustic leaching of the Group 1/2 slurry in NaOH (with the free hydroxide concentration = 4.6 M initially and 3.9 M at the conclusion of leaching) at 100°C led to 41% removal of Al from the solids. Less Al was removed than during the individual parametric leaching tests for Group 1 and Group 2, which is likely because of the lower caustic-to-solids ratio used during leaching in the CUF apparatus. Approximately

41% of the P was removed from the Group 1/2 slurry by caustic leaching, but most of this removal actually occurred during the third and fourth washing steps following the caustic leaching. The amount of P removed suggests dominance of the Group 2 solids in the composite because the parametric tests indicated most the P in the Group 2 solids was resistant to caustic leaching, whereas P was easily removed from the Group 1 solids. Another contributor to the low P removal might have been the relatively low liquid-to-solids ratio used during washing in the CUF, leading to incomplete dissolution of $Na_3PO_4 \cdot 12H_2O$. Approximately 23% of the Cr was removed during the caustic leaching and subsequent water washing.

At the initiation of the dewatering step following caustic leaching, it was discovered that the pump head was clogged with a gel. This gel is hypothesized to be caused by precipitation of $Na_3PO_4 \cdot 12H_2O$ from the caustic-leaching solution. Similar gels have been observed in experiments examining phosphate solubility in simulated caustic-leaching solutions. The phosphate concentration in the process solutions will need to be carefully managed with respect to the solubility of $Na_3PO_4 \cdot 12H_2O$ to avoid gel formation in the WTP. In the case of the clogged pump, the gel could be cleared by flushing with water. The filter flux during dewatering of the caustic leachate was low (<0.01 GPM/ft^2) and declined approximately 2% during the course of the 5-h filtration test. The filter flux increased with successive washing of the caustic-leached slurry.

The caustic leached slurry was washed five times using solutions with progressively decreasing NaOH concentrations. Dewatering steps were conducted in the CUF after each washing step. The average permeate flux increased steadily with decreasing NaOH concentration in the washing medium, reaching a maximum average flux of 0.07 GPM/ft^2 during the final washing step.

Oxidative leaching of the caustic leached solids with sodium permanganate resulted in only an additional ~25% removal of Cr from the solids (for a total of 48% of the Cr removed). Based on the reaction stoichiometry, and the amount of permanganate used, 40% removal of the Cr was expected to be leached. The reason for the low Cr conversion is currently unknown. During the first two washings of the oxidative-leached slurry, the temperature was above ambient because the chiller was inadvertently not turned on. When corrected for the effects of higher temperature, the data indicated that filter flux was essentially constant at ~0.04 GPM/ft^2 during the three washes of the oxidatively-leached solids.

The filter flux was dependent upon the TMP during the final dewatering of the Group 1/2 slurry, but also showed an apparent dependence on the AV. So, simple classification of the final slurry into a membrane-resistance or cake-resistance model is not obvious. Comparison with the initial clean water flux measurements suggests an irreversible fouling of the membrane following the leaching and filtration tests.

Group 1/2 Post-CUF Parametric Testing

A portion of the caustic-leached and washed Group 1/2 sample was subjected to parametric leaching with permanganate. The parameters examined included NaOH concentration (0.25 and 1.25 M) and the Mn/Cr molar ratio (0.59, 0.79, 0.98, and 1.19). In all cases, Cr reaction with the MnO_4^- was rapid, with near-steady state Cr concentration reached within 1 h of leaching. As would be expected, the amount of Cr removed from the Group 1/2 solids was dependent upon the Mn/Cr ratio, with the most impact observed in going from Mn/Cr = 0.59 to Mn/Cr = 0.79. Above a Mn/Cr ratio of 0.79, there was only a minor improvement in the amount of Cr removed, and there was virtually no difference between the results with

Mn/Cr = 0.98 and Mn/Cr = 1.19. About 65% of the Cr from the caustic-leached Group 1/2 solids was removed by treatment with 0.79 molar equivalent of Mn(VII) in 0.25 M NaOH at 45°C.

The reaction of Cr(III) with permanganate can be represented by the following equation::

$$Cr(III)(s) + MnO_4^-(aq) + OH^-(aq) \rightarrow CrO_4^{2-}(aq) + MnO_2(s) + 2H_2O \qquad (7.1)$$
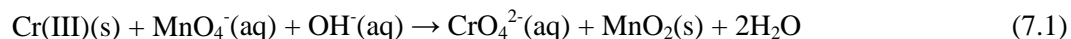
Although this reaction would suggest a dependence of Cr leaching on the hydroxide concentration, virtually no improvement in Cr removal was observed when the NaOH concentration was raised from 0.25 to 1.25 M. This suggests that under the conditions examined, there is sufficient excess hydroxide ion at 0.25 M NaOH so that the reaction is not constrained by this component. On the other hand, the Al dissolution was ~70% higher at 1.25 M NaOH compared to 0.25 M during the oxidative leaching at 45°C. This result was somewhat surprising in that the solids had been previously leached with caustic. It is possible that the caustic-to-aluminum ratio during the CUF caustic leaching was not sufficiently high to dissolve all the leachable Al.

Under all six test conditions in 0.25 M NaOH, 58 to 62% of the P was dissolved within 24 h, and equilibrium was achieved within 6 h. Increasing the Mn/Cr mole ratio from 0.75 to 1.5 had no impact on the amount of P in solution (initially and at equilibrium conditions). The amount of NaOH (0.25 or 1.25 M) at the Mn/Cr molar ratio of 1.25 also had no effect on the amount of P dissolution.

The Pu dissolution during oxidative leaching of the Group 1/2 solids was strongly dependent on the free-hydroxide concentration, with the Pu concentration increasing by approximately 6-fold when the NaOH concentration was increased from 0.25 M to 1.25 M. For example, after leaching for 6 h at a Mn/Cr ratio of 0.98, the $^{239+240}$Pu concentration was 1.54×10^{-3} µCi/mL at 1.25 M NaOH and 2.54×10^{-4} µCi/mL at 0.25 M NaOH. Clearly, low free-hydroxide concentrations will need to be maintained to minimize Pu mobilization during oxidative leaching of Cr.

Under all conditions examined, the U concentrations in the oxidative leaching solutions remained low, with the U concentration typically ~3 µg/mL after leaching for 24 h. The exception was during leaching in 1.25 M NaOH at a Mn/Cr ratio of 1.25; in that case, the U concentration in solution reached a level of ~8 µg/mL. The Fe, Ni, Cd, and B concentrations in the oxidative leaching solutions were also very low, generally below the detection limit or < 1 µg/mL. Manganese was observed to be in the leachate solutions at Mn/Cr = 1.25 or higher, but the amount in solution decreased with time and was below the detection limit at 24 h. The mechanism by which the excess Mn precipitates is not yet understood.

Appendix A

Analytical Methods

Appendix A

Analytical Methods

This section describes the analytical methods used to determine the chemical and radiochemical composition of the Group 1 and Group 2 samples.

A.1 Sample Preparation for Chemical Characterization

The samples taken for chemical characterization were centrifuged at 1000 G for 1 hr, and then the supernatant liquids were decanted. The solids were washed with three successive additions of 0.01 M NaOH.[a] After adding each washing solution, the sample was agitated for 15 min and centrifuged 30 min at 1000 G, and the liquid phase was removed. The three wash solutions were combined into a composite and passed through a 0.45-micron pore size nylon filter. The supernatant and wash-solution densities were determined by measuring the masses of 1-mL volume deliveries four times per sample.

More 0.01 M NaOH was added to the washed solids so that the slurry could be easily mixed with a Teflon-coated stirbar, and the solids were suspended. Aliquots of the suspended-solids slurries were taken for chemical and radiochemical analysis, PSD, BET, SEM, TEM, and XRD analyses. The washed solid slurry sample aliquots taken for chemical analysis were dried to constant mass at 105°C; the solids chemical analysis was based on the dry sample mass. The supernatant liquid and the filtered solids washing solution were provided directly to the Analytical Services Operation (ASO) for chemical characterization.

A.2 Chemical and Radioisotope Characterization

The following sections describe the procedures used to support the chemical and radiochemical characterization of the solids and aqueous samples. Aqueous samples were distributed directly to the free hydroxide, ion chromatrography (IC), and total inorganic carbon/total organic carbon (TIC/TOC) analytical workstations. The solids and liquids required a digestion step before distribution to the ICP-OES and radiochemistry workstations.

A.2.1 Free Hydroxide

The free hydroxide concentration was determined by potentiometric titration with standardized HCl according to procedure RPG-CMC-228, *Determination of Hydroxyl (OH⁻) and Alkalinity of Aqueous Solutions, Leachates, and Supernates and Operation of Brinkman 636 Auto-Titrator*. The free hydroxide was defined as the first inflection point on the titration curve. Quality control (QC) samples were generated at the analytical workstation and included a sample replicate determination, process blank, blank spike (BS), and matrix spike (MS).

(a) Specific wash volumes are provided in the context of the results discussion.

A.2.2 Anions

Anions were determined by ion chromatography using a Dionix ICS-2500 IC system equipped with a conductivity detector according to procedure RPG-CMC-212, *Determination of Common Anions by Ion Chromatography*. Additional sample dilutions from 100× to 25,000× were required to accurately measure the analytes. QC samples were generated at the analytical workstation and included a sample replicate determination, process blank, BS, and MS.

A.2.3 TIC/TOC

The TIC was determined by using silver-catalyzed hot persulfate (HP) oxidation according to procedure RPG-CMC-385, *Carbon Measured in Solids, Sludge, and Liquid Matrices*. The hot persulfate wet oxidation method was used. This method takes advantage of acid decomposition of the carbonate (TIC measure) followed by oxidation of organic carbon (TOC measure) using acidic potassium persulfate at 92 to 95°C. QC samples were generated at the analytical workstation and included a sample replicate determination, process blank, BS, and MS.

A.2.4 Acid Digestion

Aqueous samples were digested with acid according to procedure PNL-ALO-128, *HNO₃-HCl Acid Extraction of Liquids for Metals Analysis Using a Dry-Block Heater*. The acid-digested solutions were brought to a nominal 25-mL volume (resulting in a nominal 25× dilution where the initial sample size was 1-mL); absolute volumes were determined based on final solution weights and densities. As part of the analytical preparation batch, the ASO processed a digestion preparation blank (PB), a BS, and an MS. The spike solution contained a broad suite of stable elements; radionuclides were not included in the digestion preparation. Aliquots of the BS, MS, and PB, along with the sample aliquots, were delivered to the ICP-OES workstation for analysis; sample and PB aliquots were delivered to the radiochemical workstations for separations supporting specific radioisotope analysis.

A.2.5 KOH Fusion

The potassium hydroxide (KOH) fusion was conducted in the shielded analytical facility (hot cells) according to PNL-ALO-115, *Solubilization of Metals from Solids using KOH-KNO₃ Fusion*. A nominal sample size of 0.1 to 0.2 g dry solids was combined with a KOH/KNO₃ flux mixture and fused at 550°C for 1 hour in a nickel crucible. The fused material was acidified with HNO₃, taken to a 100-mL volume with DI water, and then split for metals and radionuclide analysis. Samples were typically prepared in duplicate along with a fusion blank and a laboratory control sample (LCS) (SRM-2710, Montana Soil, purchased from the National Institute for Science and Technology [NIST]).

A.2.6 NaOH/Na₂O₂ Fusion

The NaOH/Na₂O₂ fusion was conducted in the shielded analytical facility (hot cells) according to PNL-ALO-114, *Solubilization of Metals from Solids using a Na₂O₂-NaOH Fusion*. A nominal sample size of 0.1 to 0.2 g dry solids was combined with a NaOH/Na₂O₂ flux mixture and fused at 550°C for 1 hour in a zirconium crucible. The fused material was acidified with HNO₃, taken to a 100-mL volume with DI water, and then split for metals analysis. The sample was prepared in duplicate along with a fusion blank and an LCS (SRM-2710, Montana Soil).

A.2.7 HF-Assisted Acid Digestion

The HF-assisted acid digestion was conducted in the Sample Receiving and Preparation Laboratory according to PNL-ALO-138, *HNO₃-HF-HCl Acid Digestion of Solids for Metals Analyses Using a Dry Block Heater*. A nominal sample size of 0.1 to 0.2 g dry solids was contacted with a mixture of concentrated HF and HNO_3 and evaporated to dryness in a Teflon® reaction tube. Concentrated HCl was then added, and the sample was evaporated to dryness a second time. Additional concentrated HNO_3 and HCl were added, the reaction tube was capped tightly, and the mixture was heated in a dry-block heater at 95°C for 6.5 h. The digestate was cooled, brought to a 50-mL volume, and then split for metals analysis. The sample was prepared in duplicate along with a fusion blank and an LCS (SRM-2710, Montana Soil).

A.2.8 Metals Analysis by ICP-OES

Metals were measured by ICP-OES according to procedure RPG-CMC-211, *Determination of Elemental Composition by Inductively Coupled Argon Plasma Optical Emission Spectrometry (ICPOES)*. The preparative QC samples (duplicate, PB, BS, MS) were processed along with analytical workstation QC (post digestion spike and serial dilution).

A.2.9 U (KPA)

Uranium was determined directly from samples prepared by KOH fusion using a Chem Chek Instruments KPA according to procedure RPG-CMC-4014, Rev. 1, *Uranium by Kinetic Phosphorescence Analysis*. The LCS did not contain U, so preparative QC was limited to the duplicate and PB. A post-digestion spike was conducted at the analytical workstation.

A.2.10 Gamma Energy Analysis

Gamma energy analysis was performed with direct or diluted samples that were prepared from acid digestion, fusion, or neat (see Figure 4.1). Sample counting was conducted according to procedure RPG-CMC-450, *Gamma Energy Analysis (GEA) and Low-Energy Photon Spectroscopy (LEPS),* using high-purity germanium detectors. Extended count times (up to 20 h) were employed as needed to achieve low detection limits. In many cases, the Compton background from the high ^{137}Cs activity (661 keV) limited the achievable detection limit of lower-energy gamma emitters (e.g., [241]Am at 59 keV). The QC associated with the GEA analysis was composed of the sample duplicate and PB; because this is a direct analysis, no additional QC samples were required.

A.2.11 Gross Alpha and Gross Beta

Aqueous samples were prepared for gross alpha and beta determinations by acid-digestion, and the washed-solids samples were prepared by KOH/KNO_3 fusion. Prepared sample aliquots were plated directly onto stainless steel planchets according to procedure RPG-CMC-4001, *Source Preparation for Gross Alpha and Gross Beta Analysis*. The mounts prepared for gross alpha analysis were counted with Ludlum alpha scintillation counters. The gross alpha analysis tends to be confounded by the dissolved solids in the sample matrix. The solids can absorb the alpha particles, decreasing the intensity relative to the detector, which biases the results low. The sources prepared for gross beta analysis were counted with an LB4100 gas-proportional counter. In both cases, counting operations were conducted according to procedure RPG-CMC-408, Rev.1, *Total Alpha and Total Beta Analysis*. The preparative QC included the sample duplicates and the preparation blank. The BS and MS were prepared at the analytical workstation on sample dilutions.

A.2.12 Pu Isotopes: ^{238}Pu and $^{239+240}$Pu

The ^{238}Pu and $^{239+240}$Pu activities were measured from aqueous samples prepared by acid-digestion and washed solids samples prepared by KOH/KNO$_3$ fusion. Radiochemical separations were conducted according to procedure RPG-CMC-4017, *Analysis of Environmental Water Samples for Actinides and Strontium-90* (analyte purification using ion exchange); source preparation was conducted according to RPG-CMC-496, *Coprecipitation Mounting of Actinides for Alpha Spectroscopy* (co-precipitation of PuF$_3$ with LaF$_3$); and alpha counting was conducted according to RPG-CMC-422, Rev.1, *Solutions Analysis: Alpha Spectrometry*. The preparative QC included the sample duplicates and the preparation blank. The BS and MS were prepared at the analytical workstation on sample dilutions.

A.2.13 Strontium-90

The ^{90}Sr activities were measured from aqueous samples prepared by acid-digestion, and washed-solids samples were prepared by KOH/KNO$_3$ fusion. Radiochemical separation was conducted according to procedure RPG-CMC-476, *Strontium-90 Separation Using Eichrom Strontium Resin*; source preparation and beta counting were conducted according RPG-CMC-474, *Measurement of Alpha and Beta Activity by Liquid Scintillation Spectrometry*.

A.2.14 Chromate

The Cr(VI) concentration was determined from the major optical absorbance band of chromate (CrO$_4^{2-}$) with a maximum at 372 nm in selected leachate samples. The determination of chromate concentration in diluted leachates was based on the linear relationship between optical absorbance of the sample at the peak maximum (A$_{372}$) and concentration of Cr(VI) in the analyzed solution (C$_{chromate}$) as illustrated below:

$$A_{372} = \varepsilon_{372} \cdot C_{chromate} \cdot l \tag{A.1}$$

where ε_{372} is the molar absorptivity of the chromate peak at 372 nm (expressed in M^{-1}cm^{-1}), and l is the optical path length of a spectrophotometric cell (expressed in cm) used to contain the analyzed sample.

The linearity of Equation A.1 was verified in a calibration experiment using a series of solutions with a known concentration of chromate in a 0.24-M NaOH matrix. The calibration curve showed good linearity (R^2 =0.9994) with a slope equal to 5312 $\pm$ 43 M^{-1} in the dynamic range of 0.0069 mM to 0.42 mM of chromate.

The same spectrophotometric cell was used in all subsequent experiments in the determination of sample chromate concentrations. For this reason, it was not necessary to determine the actual optical pathlength of the cell. Therefore, the chromate concentration was calculated simply as the ratio of A$_{372}$ and the slope of the calibration curve

$$C_{chromate} = A_{372}/slope \tag{A.2}$$

Most of the samples submitted for chromate analysis were too concentrated in chromate to be measured directly. In these cases, the samples were diluted with 0.24 M NaOH to lower the chromate concentration to less than 0.2 mM so as to have optical readings within the linearity range of the calibration plot. Applying 0.24 M NaOH instead of water verified that the Cr(VI) in the diluted solutions was present exclusively as the chromate species.

The UV-visible measurements were made on a 400 Series charge-coupled device array spectrophotometer (Spectral Instruments Inc, Tucson, AZ) with a 200- to 950-nm scanning range. The solutions were held in PLASTIBRAND$^{®}$ 1-cm cuvettes. The 0.24 M NaOH solution (diluent) was used to obtain the baseline

reading before measuring the chromate-containing samples. Because NIST-traceable standards were not used, the calculated chromate concentrations are reported for information only.

Appendix B

Physical Properties Determination and Rheology Methods

Appendix B

Physical Properties Determination and Rheology Methods

This appendix describes the experimental methods used to determine rheological properties and physical properties, including particle size distribution and surface area measurements.

B.1 Physical Properties

The physical-property characterization was conducted according to procedure RPL-COLLOID-02, Rev. 1, *Measurement of Physical and Rheological Properties of Solutions, Slurries and Sludges*, which is consistent with the WTP guidelines document.[a] Samples for physical-properties characterization were taken in triplicate near the beginning (S1), middle (S2), and end (S3) of the aliquoting activity following slurry homogenization. Samples sizes were generally between 10 and 15 mL. The samples were collected in volume-graduated, glass centrifuge tubes.

Settling studies were conducted by thoroughly agitating the samples and then allowing the solids to settle by gravity with periodic measurement of the settled-solids volume. The sample tubes were undisturbed over the 3-day settling period. Following the settling measurements, the samples were centrifuged at ~1000 G for 1 hour. The total sample volume and solids volume were recorded to assess the vol% wet centrifuged solids (WCS). The centrifuged supernatants were decanted and transferred to tared graduated cylinders; the net solution masses and volumes were determined. The remaining wet centrifuged solids were weighed in the centrifuge tubes to assess gross densities. The supernatant samples were transferred to tared glass vials. Both the supernatant fractions and the residual solids fractions (containing interstitial supernatant) were air-dried and then transferred to a 105°C oven for continued drying until constant mass was attained. The data collected were processed as described by Smith and Prindiville[a] to determine the volume and weight percent of wet solids (total, settled, and centrifuged), densities, total undissolved solids, and dissolved solids content.

B.2 Rheology

Rheological testing was conducted on the solids in contact with the supernatant generated as part of the homogenization process. Testing was conducted according to RPL-COLLOID-02, *Measurement of Physical and Rheological Properties of Solutions, Slurries and Sludges*. For the current study, two regions of tank waste flow behavior are considered: 1) incipient motion in settled tank waste solids (shear strength) and 2) non-elastic flow of tank waste slurries and supernates (flow curve).

B.2.1 Shear-Strength Testing

For tank waste slurries, a finite stress must be applied before the material will begin to flow. The stress required to transition the material from elastic deformation to viscous flow is referred to as the shear

---

[a] 24590-WTP-GPG-RTD-001, Rev 0, "Guidelines for Performing Chemical, Physical, and Rheological Properties Measurements," G. L. Smith and K. Prindiville, May 2002.

strength, and its origin can be attributed to static and kinetic friction between individual particles and/or aggregates, the strength of the matrix supporting the coarse fraction (i.e., the interstitial fluid), and sludge cohesion arising from interparticle adhesive forces such as van der Waals forces.

The shear strength was measured using the vane method. For the vane technique, the stress required to begin motion is determined by slowly rotating a vane immersed in the test sample's settled solids while continuously monitoring the resisting torque as a function of time. A material's static shear strength is then associated with the maximum torque measured during the transition from initial to steady-state vane rotation.

The maximum torque required for incipient motion is dependent on vane geometry. To account for vane geometry affects, shear strength is expressed in terms of the uniform and isotropic stress acting over the surface area of the cylinder of rotation swept out by the vane. The shear strength is related to the maximal torque during incipient motion according to Equation B.1 (Barnes and Dzuy 2001):

$$\tau_{SS} = \frac{M_{max}}{4\pi R^3 \left(\dfrac{H}{2R} + \dfrac{1}{3}\right)} \qquad (B.1)$$

Here, τ_{ss} is the shear strength [N/m^2], M_{max} is the maximum torque [N·m], and R and H are the radius and height of the cylinder of rotation swept out by the vane [m]. Because the shear band observed upon slow rotation of the vane does not extend appreciably beyond the vane paddles, R and H are taken to be the dimensions of the vane itself.

B.2.2 Flow Curve Testing

Non-elastic flow of tank waste slurries and supernates is characterized with rotational viscometry. The typical result of such testing is a set of flow curve data, which shows the stress response of a material to a range of applied rates-of-deformation. Specifically, flow-curve testing allows characterization of a material's shear stress, τ, and response as a function of applied shear rate, $\dot{\gamma}$. Once measured, flow curve data can be interpreted with several constitutive equations for the viscous stress/rate-of-strain relationship. Such analysis allows the flow behavior over a broad range of conditions to be described with just a few rheological descriptors such as viscosity, yield stress, consistency, and flow index.

A concentric cylinder rotational viscometer operated in controlled-rate mode was used for flow-curve testing of tank waste slurries and supernates. Rotational viscometers operate by placing a given volume of test sample into a measurement cup of known geometry. A cylindrical rotor attached to a torque sensor is then lowered into the sample until the slurry is even with, but does not cover, the top of the rotor. A single-point determination of a fluid's flow properties is made by spinning a rotor at a known rotational speed, Ω, and measuring the resisting torque, M, acting on the rotor. The torque acting on the rotor can be directly related to the shear stress (τ) at the rotor using the equation,

$$\tau = \frac{M}{2\pi H R_I^2} \qquad (B.2)$$

where R_I and H are the radius and height of the rotor, respectively (see Figure B.1). Shear stress has units of force per area (N/m²). The rotational rate is related to the shear rate. However, calculating the fluid shear rate at the rotor is complicated by the fact that the shear rate depends on both the measurement system geometry and the fluid rheological properties. For the simplest fluids (i.e., Newtonian fluids), the shear rate ($\dot{\gamma}$) of the fluid at the rotor can be calculated given the geometry of the cup rotor shear by using the equation,

$$\dot{\gamma} = \left(\frac{2R_O^2}{R_O^2 - R_I^2} \right) \Omega \tag{B.3}$$

Here, R_I is the inner radius of the cup, such that the gap width between cup and rotor is (R_O to R_I). The shear rate has units of inverse seconds [s^{-1}]. Calculating shear rate for materials showing more complex shear-stress versus shear-rate behavior (i.e., non-Newtonian fluids) requires estimates of yield stress and degree of shear-thinning or shear-thickening. As the goal of rheological testing is to determine and quantify such behavior, these values are typically not known. This requirement can be circumvented by using a cup and rotor system with a small gap (~1 mm) for fluid shear. For fluid flow in small gap cup and rotor systems, shear-rate effects introduced by fluid properties are minimized such that Equation B.3 provides an accurate determination of shear rate for non-Newtonian materials. Shear rates examined in this study spanned the range from 1 to 1000 s^{-1}.
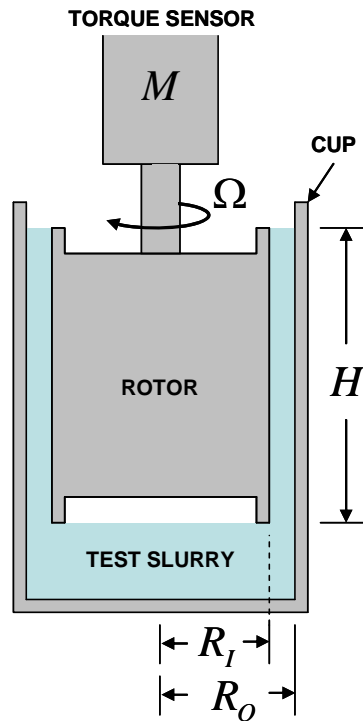
Figure B.1. Rotor and Cup Geometry Used in Rotational Viscometry Testing

The resistance of a fluid to flow is often described in terms of the fluid's apparent viscosity, η_{app}, which is defined as the ratio of the shear stress to shear rate:

$$\eta_{app} = \frac{\tau}{\dot{\gamma}} \tag{B.4}$$

For Newtonian fluids, the apparent viscosity is independent of shear rate. For non-Newtonian fluids, the apparent viscosity will vary as a function of shear rate. The units of apparent viscosity are Pa·s, although it is typically reported in units of centipoise (cP; where 1 cP = 1 mPa·s).

Flow-curve data are usually combined plots of τ and η_{app} as a function of $\dot{\gamma}$. As stated above, flow-curve data can be interpreted with several constitutive equations (i.e., flow curves), allowing the data to be characterized with just a few rheological descriptors. The behavior of tank waste sludges, slurries, and supernates can be described by four common flow-curve equations:

- **Newtonian**—Newtonian fluids flow as a result of any applied stress and show constant viscosity over all shear conditions. The flow curve for Newtonian fluids is,

$$\tau = \eta\dot{\gamma} \tag{B.5}$$

  where η is the Newtonian viscosity.

- **Ostwald (Power Law)**—Power-law fluids flow as a result of any applied stress and have viscosities that either increase or decrease with increasing shear rate. They are described by,

$$\tau = m\dot{\gamma}^{n} \tag{B.6}$$

  where *m* is the power-law consistency index, and *n* is the power-law index. Power-law fluids with *n < 1* are referred to as psuedoplastic (shear-thinning), whereas power-law fluids with *n > 1* are referred to as dilatant (shear-thickening).

- **Bingham Plastic**—Bingham plastics are fluids that show finite yield points. A finite stress (i.e., the yield stress), must be exceeded before these types of materials flow. Once flow is initiated, the stress response of the material is Newtonian over the rest of the shear-rate range. Bingham plastics are described by,

$$\tau = \tau_{O}^{B} + k_{B}\dot{\gamma} \tag{B.7}$$

  where τ_{O}^{B} is the Bingham yield index, and k_{B} is the Bingham consistency index.

- **Herschel-Bulkley**—Fluids that behave in accordance with a Herschel-Bulkley model show a finite yield followed by power-law behavior over the rest of the shear-rate range. They are described by,

$$\tau = \tau_{O}^{H} + k_{H}\dot{\gamma}^{b} \tag{B.8}$$

where τ_O^H is the Herschel-Bulkley yield index, k_H is the Herschel-Bulkley consistency index, and b is the Herschel-Bulkley power-law index.

Power-law fluids, Bingham plastics, and Herschel-Bulkley fluids are examples of non-Newtonian fluids. In general, liquids without internal and/or interconnected structures (such as tank waste supernates) are Newtonian. Sludges and slurries are typically non-Newtonian, but their exact behavior depends on the concentration of solids and suspending phase chemistry. Sufficiently dilute slurries may show Newtonian behavior.

B.2.3 Rheology Instrumentation

Rheological characterization was accomplished using a Rotovisco® RV20 Measuring System M equipped with an M5 measuring head sold by HAAKE Mess-Technik GmbH u. Co. (now the Thermo Electron Corporation, Madison, WI). The M5 measuring head is a "Searle" type viscometer capable of producing rotational speeds up to 500 revolutions per minute (RPM) and measuring torques up to 0.049 N·m. The minimum rotational speed and torque resolution achievable by this measuring head are 0.05 RPM and 0.49 mN·m, respectively.

Specific measurement tools, such as cup and rotor assemblies and shear vanes, are attached to measure selected rheological properties. Shear-strength measurements employed an 8-mm × 16-mm (radius × height) shear vane tool. Flow-curve measurements employed an MV1 stainless steel measuring cup and rotor. The dimensions of the MV1 and vane measuring systems are listed in Table B.1.

Table B.1. Vane and Cup and Rotor Measuring System Dimensions

Measuring System	Vane/Rotor Radius, mm	Vane/Rotor Height, mm	Cup Radius, mm	Gap Width, mm
Vane Tool	8	16	> 16	> 8
MV1	20.04	60	21	0.96

The temperature was controlled with a combination of the standard measuring system M temperature jacket and a Cole-Parmer® Polystat® Temperature-Controlled Recirculator, Model Number C-12920-00. The temperature jacket provided a heat-transfer area between the cup and the recirculating fluid. The jacket temperature was monitored using a Type-K thermocouple (Omega Model TJ36-CASS-116-G-6-CC). Temperature control was employed only for flow-curve measurements. The shear strengths (τ_{ss}) were measured at ambient temperature (~30°C in the hot cells).

The rheometer was controlled and data were acquired with a remote computer connection using the RheoWin Pro Job Manager Software, Version 2.96 (Thermo Electron Corporation, Copyright© 1997). During measurement, the software automatically collects and converts rotor torque readings into shear stresses based on Equation B.1 (for vane testing) or Equation B.2 (for flow-curve testing). Likewise, the software also automatically converts the rotational rate readings into shear rates based on Equation B.3.

Rheology Materials and Methods

No sample treatment was performed before analysis with the exception of the mechanical agitation required to mix and sub-sample selected waste jars.

B.2.4 Shear-Strength Testing

Before testing, the tank waste slurry samples were mixed thoroughly and subsequently allowed to settle for 48 to 72 h. When possible, the shear strength was measured by immersing the 8- × 16-mm vane tool to a depth of 15 mm into the settled solids.   The vane was slowly rotated at 0.3 RPM for 180 s. For the entire duration of rotation, the time, rotational rate, and vane torque were continuously monitored and recorded. At the end of the measurement, shear stress-versus-time data were parsed, and the maximum measured shear stress (i.e., the material's shear strength) was determined.

B.2.4.1 Flow Curve Testing

Each flow curve was measured over a 15-min period and split into three 5-min intervals. Over the first 5 min, the shear rate was smoothly increased from zero to 1000 s^{-1}. For the second 5 min, the shear rate was held constant at 1000 s^{-1}. For the final 5 min, the shear rate was smoothly reduced back to zero. During this time, the resisting torque and rotational rate were continuously monitored and recorded.

Before each test, the sample was left undisturbed in the measuring system for 5 min to allow temperature equilibration. The sample was then mixed for 3 min using the measuring system rotor to re-disperse any settled solids and to pre-shear slurries before measurement.

Flow-curve tests were run at 25, 40, and 60°C. Because of limited sample volume, all three temperature tests were performed on the same sample. To combat the effects of sample evaporation, a moisture barrier was installed over the opening at the top of the temperature jacket during testing, and after each test, the cup was raised so that fresh sludge/slurry filled the measurement gap.

B.3 Particle-Size Attributes

Determination of particle physical attributes, including size distribution and surface area, are discussed in the following sections.

B.3.1 Particle-Size Distribution

Particle size distributions were characterized according to procedure RPL-COLLOID-01, Rev. 1, *Particle Size Analysis Using Malvern MS2000*. This procedure uses a Mastersizer 2000 (Malvern Instruments, Inc., Southborough, MA 01772 USA) with a Hydro µP wet dispersion accessory. Malvern lists the Mastersizer particle-size measurement range as nominally 0.02 to 2000 µm. The actual PSD measurement range is dependent on the accessory used as well as the properties of the solids being analyzed. When coupled with the Hydro µP wet dispersion accessory, the nominal listed measuring range is reduced to 0.02 to 150 µm. The Malvern 2000 uses laser diffraction technology to define PSD.

The Hydro µP wet-dispersion accessory consisted of a 20-mL sample flow cell with a continuous variable and independent pump and ultrasound. Both flow and sonication can be controlled and altered during measurement. PSD measurements were made before, during, and after sonication, allowing determination of the influence of each on the sample PSD. The primary measurement functions of the Malvern analyzer were controlled through Mastersizer 2000 software, Version 5.1 (Malvern Instruments, Ltd. Copyright$^{©}$ 1998-2002).

The optical properties applied to the test samples are summarized in Table B.2. For initial characterization and parametric testing samples, bismuth oxide (Bi_2O_3) optical properties were assumed. With regard to CUF testing samples, the optical properties for boehmite were employed for both pre- and post-caustic leach samples. After oxidative-leaching, the optical properties of Bi_2O_3 were used. It should be noted that using boehmite and Bi_2O_3 properties (as well as a single species refractive index) to represent the optical properties of the mixture of solid species and mineral phases in the tank waste is not exact. However, given the species diversity in the sample and tendency for tank waste particles to aggregate, the measurement analysis still provides an adequate representation of the apparent particle size of the wastes. Correction of assumed refractive indexes to a more accurate value typically does not significantly alter the particle size distribution determined by the original analysis.

The solids were dispersed in 0.01 M NaOH for the PSD measurements. The sample dispersion was added drop-wise to the instrument (while the pump was active) until an ~10% obscuration was reached. For all samples, less than 10 mg of solids was required to reach the desired obscuration in the 20-mL flow cell.

Table B.2. Optical Properties Applied To Test Materials

Test	Material Selected for Optical Properties[a]	Refractive Index (RI)	Absorption
Initial Characterization			
Group 1	Bismuth Oxide	1.91	1.0
Group 2	Bismuth Oxide	1.91	1.0
Parametric Testing			
Group 1	Bismuth Oxide	1.91	1.0
Group 2	Bismuth Oxide	1.91	1.0
Group 1/2 Mixture	Bismuth Oxide	1.91	1.0
CUF Testing			
All Samples	Bismuth Oxide	1.91	1.0
Pre-Leach Low-Solids	Boehmite	1.66	1.0
Pre-Leach High-Solids	Boehmite	1.66	1.0
Caustic-Leached	Boehmite	1.66	1.0
Caustic-Leached / Washed	Boehmite	1.66	1.0
Oxidative-Leached	Bismuth Oxide	1.91	1.0
Oxidative-Leached / Washed	Bismuth Oxide	1.91	1.0
All/Suspending Phase	Water[a]	1.33	n/a
(a) See Ref Malvern Instruments Ltd., April 1997.			

The size distributions of particles were measured under varying flow conditions before, during, and after sonication. The test matrix employed for analysis is shown in Table B.3. For each condition, three successive 20-second measurements of PSD were taken. An average of these measurements was then generated by the analyzer software. Both individual measurement and average were saved to the analyzer data file. Once measurements were complete, the sonic power for the next condition was set, the sample was given 30 to 60 seconds to equilibrate, and the next set of measurements was taken.

Table B.3. Prototypic Particle-Size Analysis Test Matrix

Condition No.	Pump Speed (RPM)	Sonic Power	Comment
1	3000	0%	pre-sonic measurement
2	2000	0%	pre-sonic measurement
3	4000	0%	pre-sonic measurement
4	3000	25%	sonicated measurement
5	3000	50%	sonicated measurement
6	3000	75%	sonicated measurement
7	3000	0%	post-sonic measurement
8	2000	0%	post-sonic measurement
9	4000	0%	post-sonic measurement

B.3.2 Surface Area (BET)

Samples were prepared for surface-area measurements in an effort to minimize solidification into a monolith upon drying. To this end, the solids were rinsed twice with ethanol and twice again with diethyl ether according to procedure TPR-RPP-WTP-486, *Procedure for BET Sample Preparation Using Ethanol and Ethyl Ether as Drying Agents.* Each rinse was conducted in a centrifuge tube. The solids were well suspended in the rinse solution, and then the phases were separated by centrifuging and decanting. The final ethyl ether rinse was used to transfer the solids slurry to the sample cell. The diethyl ether was then evaporated at room temperature directly from the sample cell.

The sample was further dried and out-gassed using the Quantachrome Instruments Monosorb Model MS-21 (Boynton Beach, FL) outgassing station. This entailed pre-flushing nitrogen through the sample cell for ~10 min and then heating and flushing for overnight (>10 h) at 110°C.

The surface-area measurements were conducted according to OCRWM-BET-01, *Surface Area Measurement with a Monosorb Gas Analyzer,* which is consistent with ASTM method D5604-96, Test Method B (Single-Point Surface Area by Flowing Gas Apparatus). The flow gas used in the measurement mode was composed of 30% nitrogen in helium. The system was calibrated per manufacturer instructions. The system performance was assessed using a 29.9 ± 0.75 m^2/g carbon surface area standard Lot D-6 obtained from Micromeritics (Norcross, GA).

Appendix C

Crystal Form and Habit

Appendix C

Crystal Form and Habit

This section describes the methods used to determine the crystal forms and habits of the tank solids samples. The solids crystal characteristics were determined on small aliquots of the solids. In all cases, the solids sample fractions were allowed to air dry at room temperature in preparation for analysis. This effort was intended to minimize morphological changes that might occur upon heating. The methods applied for XRD, SEM, and TEM evaluations are discussed in the following sections.

C.1 X-Ray Diffraction

The sample mounts for XRD examination were prepared from the dried solids according to procedure RPL-PIP-4, *Preparing Sealed Radioactive Samples for XRD and Other Purposes*. Specimens were pulverized to a powder with a boron carbide mortar and pestle, mixed with an internal standard (rutile, TiO_2, or alumina, Al_2O_3), and mounted on a glass slide. In some cases, the internal standard was omitted to provide better clarity of the sample diffraction pattern free from potential interference from the internal standard diffraction pattern. The XRD examination was conducted according to procedure PNNL-RPG-268, *Solids Analysis, X-Ray Diffraction Using RGD #34*. Process parameters included examining the X-ray 2-theta range from 5 to 65 degrees with a step size of 0.02 degrees and a dwell time of 20 seconds.

Phase identification was performed with JADE, Version 8.0 (Materials Data Inc., Livermore, CA) software search and peak match routines with comparison to the International Centre for Diffraction Data (ICDD) database PDF-2, Version 2.0602 (2006). The ICDD database included the Inorganic Crystal Structure Database (ICSD) maintained by Fachinformationszentrum, Karlsuhe, Germany. Phase identification incorporated chemistry restrictions based on the elements determined from chemical analysis.

C.2 Scanning Electron Microscopy

A small sample was transferred with a wooden Q-tip stem onto carbon tape supported by an aluminum pedestal mount. The sample was analyzed using the radiation-shielded Amray Model 1610T SEM according to RPL-611A-SEM, *Scanning Electron Microscope Examinations*. In selected cases, the mount was carbon-coated. Selected sample areas were evaluated by energy dispersive X-ray spectroscopy (EDS) for qualitative elemental composition.

C.3 Transmission Electron Microscopy

The TEM samples were prepared in a two-step methanol rinsing process. A small amount of the sludge slurry was mixed and transferred into methanol; a drop of the methanol slurry was transferred into a second vial containing methanol; then a drop of this second solution was deposited onto a lacey carbon TEM grid. The particles were air-dried on the lacey grid. Note that the sample drying process may induce changes in the morphology of the particle agglomerates. However, the objective of the TEM

investigation was to look at the fundamental characteristics and sizes of individual particle crystallites that are not dependent on drying effects.

The TEM examinations were performed on an FEI Tecnai G2-30 (FEI Inc., Hillsboro, OR) with a field emission filament operating at 300 keV equipped with a Scanning Transmission Unit and High Angle Annular Dark-Field Detector (HAADF), energy dispersive X-ray detector, and a Gatan Imaging Filter (GIF), model GIF2000 (Gatan Inc., Pleasanton, CA). Particle or area analysis was performed by identifying the composition with EDS and electron energy-loss spectroscopy (EELS). Images were obtained with either the scanning transmission electron microscopy (STEM) system or normal bright-field imaging. Energy-filtered images were also obtained with the image filter to produce element-specific area maps.

C.4 Electron Energy-Loss Spectroscopy

The EELS spectra were obtained using a 0.6-mm entrance aperture and an energy dispersion of 0.1 eV/channel. Low-loss spectra (including the zero loss peak) were acquired with an integration time of <0.2 s and core-loss spectra between 2 and 5 s. To reduce potential beam reduction, the acquisition time was kept as small as possible. The spectra were collected in the imaging mode of the transmission electron microscope and were corrected for dark current and channel-to-channel gain variation of the charge coupled device (CCD) detector.

The core-loss regime was energy calibrated, and the energy drift was measured while data were being acquired by collecting zero-loss spectra before or after core-loss spectra were collected. The position of the C-K ($1s$) peak at 284 eV (arising from transitions to the π^* molecular orbital) from the TEM lacy carbon support film was used to evaluate the energy calibration and as a means of roughly checking that the energy resolution was sufficient for collecting data.

Two methods were adopted for determining the chemical state of chromium in the sludge samples. In the first method, we obtained the following ratio defined as:

$$I-ratio = \frac{I(L_3)}{I(L_2)} \tag{C.1}$$

L_2 and L_3 are the intensities of background-corrected Cr-absorption edges. The second method was to look at the O:Cr ratio as an indication of oxygen content. Oxygen detection with EELS is more accurate that with x-rays because the loss in energy of the primary beam is measured instead of an emitted x-ray, as in the case of EDS analyses, which can be subjected to significant attenuation.

Appendix D

Quality Assurance and Quality Control

Appendix D

Quality Assurance and Quality Control

This appendix describes the quality assurance (QA) program and QC measures applied to the conduct of work.

D.1 Application of WTPSP Quality Assurance Requirements

PNNL's QA program is based on requirements defined in DOE Order 414.1C, Quality Assurance, and 10 CFR 830, Energy/Nuclear Safety Management, Subpart A–Quality Assurance Requirements (a.k.a., the Quality Rule). PNNL has chosen to implement the requirements of DOE Order 414.1C and 10 CFR 830, Subpart A by integrating them into the laboratory's management systems and daily operating processes. The procedures necessary to implement the requirements are documented through PNNL's Standards-Based Management System.

PNNL implemented the RPP-WTP quality requirements by performing work in accordance with the *River Protection Project – Waste Treatment Plant Support Program (RPP-WTP) Quality Assurance Plan* (RPP-WTP-QA-001, QAP). Work was performed to the quality requirements of NQA-1-1989 Part I, Basic and Supplementary Requirements, NQA-2a-1990, Part 2.7, and DOE/RW-0333P, Rev 13, *Quality Assurance Requirements and Descriptions (QARD)*. These quality requirements are implemented through the *River Protection Project – Waste Treatment Plant Support Program (RPP-WTP) Quality Assurance Manual* (RPP-WTP-QA-003, QAM).

A matrix that cross-references the NQA-1, NQA-2a, and quality assurance requirements and descriptions (QARD) requirements with PNNL's procedures for this work was given in the test plan, TP-RPP-WTP-467.[a] It included justification for those requirements not implemented. The QA requirements of DOE/RW-0333P, Rev 13, QARD and DOE Order 414.1C were not identified as a requirement for this work in the test specification.

D.2 Conduct of Experimental and Analytical Work

Experiments that were not method-specific were performed in accordance with PNNL's procedures QA-RPP-WTP-1101 "Scientific Investigations" and QA-RPP-WTP-1201 "Calibration and Control of Measuring and Testing Equipment," verifying that sufficient data were taken with properly calibrated measuring and test equipment (M&TE) to obtain quality results.

As specified in the supporting Test Specification, 24590-PTF-TSP-RT-06-0001, Rev. 0, BNI's Quality Assurance Project Plan (QAPjP), PL-24590-QA00001, was not applicable because the work was not performed in support of environmental/regulatory testing, and the data will not be used as such.

(a) SK Fiskum, TP-RPP-WTP-467, Rev. 0, 2/2/07 and Rev. 1 7/31/07, *Characterization and Small Scale Testing of Hanford Wastes to Support the Development and Demonstration of Leaching and Ultrafiltration Pretreatment Processes,* Pacific Northwest National Laboratory, Richland, WA.

Balances are calibrated annually by a certified contractor, QC Services, Portland, Oregon. A balance performance check was conducted each day the balance was used.

ASO conducted analytical testing according to the Statement of Work RPP-WTP-QA-005, Rev. 2, *Analytical Support by the PNNL RPL Analytical Support Operation.* The analytical results and raw data are traceable through the project files according to the Analytical Services Request (ASR) number and RPL number.

D.3 Internal Data Verification and Validation

PNNL addressed internal verification and validation activities by conducting an independent technical review of the final data report in accordance with PNNL's procedure QA-RPP-WTP-604. This review verified that the reported results were traceable, that inferences and conclusions were soundly based, and the reported work satisfied the Test Plan objectives. This review procedure is part of PNNL's RPP-WTP Quality Assurance Manual.

Appendix E

Duplicate Sample Differential Particle Size
Plots for the Initial Group 1 Sample

Appendix E

Duplicate Sample Differential Particle Size Plots for the Initial Group 1 Sample

Figures E.1, E.2, and E.3 show the differential volume distribution as a function of particle diameter for the duplicate Group 1 initial characterization sample, TI483-G1-S-WL-PSD-2. Specifically, Figure E.1 shows the pre-sonication PSDs as a function of pump speed, Figure E.2 shows the PSDs as a function of sonication, and Figure E.3 shows the post-sonication PSDs as a function of pump speed.
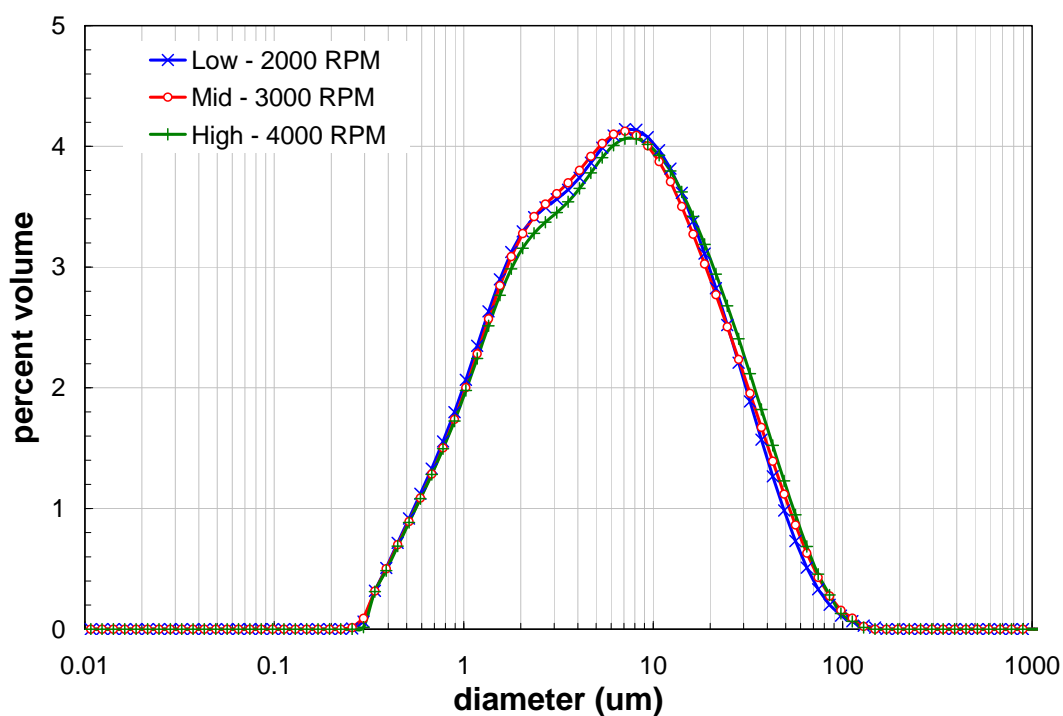
Figure E.1. Pre-Sonication Volume Distribution Result for the Duplicate Group 1 Initial Characterization Sample as a Function of Pump Speed
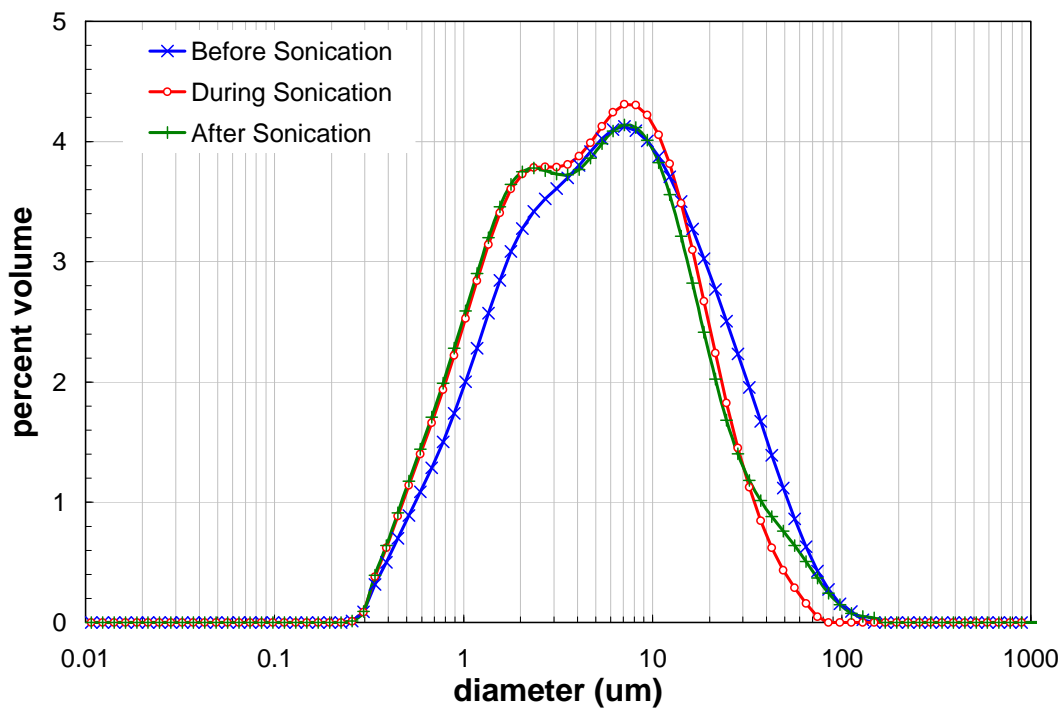
Figure E.2. Volume Distribution Result for the Duplicate Group 1 Initial Characterization Sample as a Function of Sonication (75% power)
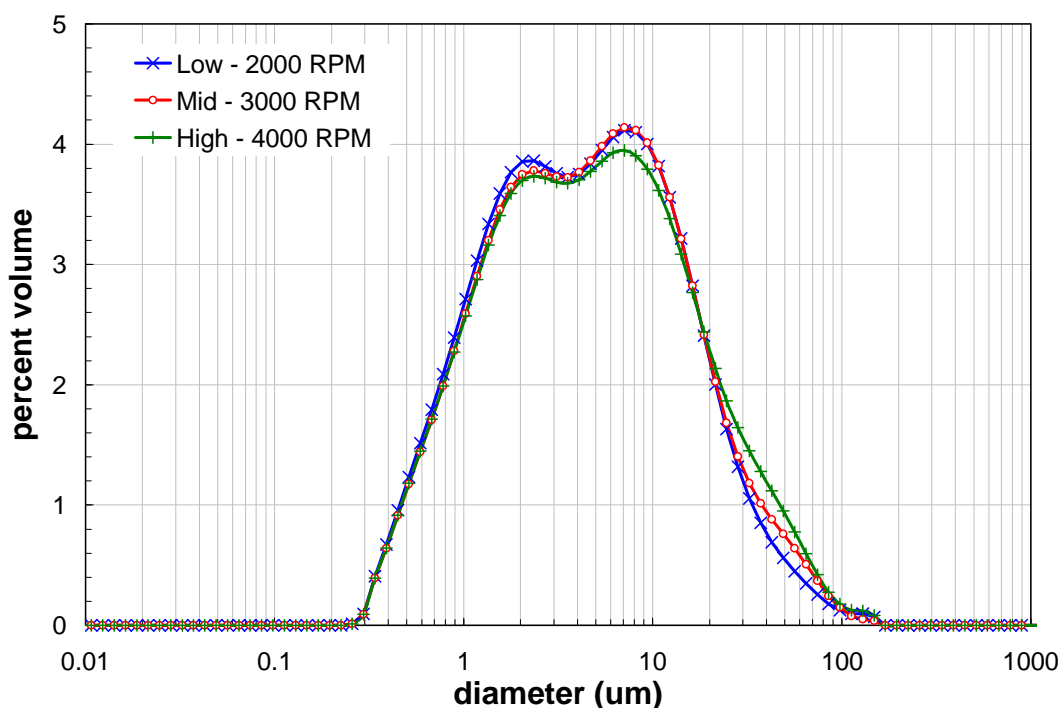
Figure E.3. Post-Sonication Volume Distribution Result for the Duplicate Group 1 Initial Characterization Sample as a Function of Pump Speed

Appendix F

Detailed Cumulative PSD for the Initial Group 1 Sample

Appendix F

Detailed Cumulative PSD for the Initial Group 1 Sample

Tables F.1 and F.2 present detailed cumulative oversize distributions (by volume/weight) for Group 1 Initial Characterization samples TI483-G1-S-WL-PSD-1 and -2, respectively. The results are reported as a function of test condition. This appendix does not provide a discussion of the detailed distributions; however, a portion of these results (specifically, the 10th, 50th, and 90th diameter percentiles) are presented and discussed in the main body of the report.

Table F.1. Cumulative Oversize Diameter Distributions for the Primary Group 1 Initial Characterization Sample, TI483-G1-S-WL-PSD-1

Test Condition	Volume / Weight Cumulative Oversize Diameter (µm)														
	1%	5%	10%	20%	25%	30%	40%	50%	60%	70%	75%	80%	90%	95%	99%
1 - 3000/pre-sonic	0.44	0.80	1.2	2.2	2.7	3.4	4.9	6.9	9.6	14	16	20	31	43	67
2 - 2000/pre-sonic	0.45	0.81	1.2	2.1	2.7	3.3	4.9	6.9	9.6	13	16	19	30	41	64
3 - 4000/pre-sonic	0.45	0.81	1.2	2.1	2.7	3.3	5.0	7.0	9.7	14	16	19	30	41	64
4 - 3000/25%	0.45	0.78	1.2	2.0	2.4	3.0	4.5	6.4	8.8	12	14	17	26	35	55
5 - 3000/50%	0.44	0.74	1.1	1.8	2.2	2.7	4.1	5.8	8.0	11	13	15	24	33	55
6 - 3000/75%	0.43	0.71	1.0	1.7	2.0	2.5	3.6	5.2	7.2	9.9	12	14	22	31	61
7 - 3000/post-sonic	0.43	0.70	1.0	1.6	2.0	2.4	3.5	5.0	7.1	9.8	12	14	23	35	71
8 - 2000/post-sonic	0.43	0.69	0.97	1.6	1.9	2.3	3.3	4.8	6.8	9.5	11	13	21	31	66
9 - 4000/post-sonic	0.43	0.69	0.99	1.6	2.0	2.4	3.5	5.0	7.1	10	12	14	24	37	77

Table F.2. Cumulative Oversize Diameter Distributions for the Duplicate Group 1 Initial Characterization Sample, TI483-G1-S-WL-PSD-2

Test Condition	Volume / Weight Cumulative Oversize Diameter (µm)														
	1%	5%	10%	20%	25%	30%	40%	50%	60%	70%	75%	80%	90%	95%	99%
1 - 3000/pre-sonic	0.42	0.73	1.1	1.8	2.3	2.8	4.0	5.7	8.0	11	14	17	28	40	69
2 - 2000/pre-sonic	0.43	0.73	1.1	1.8	2.2	2.7	4.0	5.7	7.9	11	13	16	26	37	64
3 - 4000/pre-sonic	0.44	0.74	1.1	1.9	2.3	2.9	4.2	6.0	8.5	12	15	18	29	41	68
4 - 3000/25%	0.43	0.71	1.0	1.7	2.1	2.5	3.7	5.3	7.4	10	12	14	22	30	50
5 - 3000/50%	0.42	0.69	0.99	1.6	2.0	2.4	3.5	5.0	7.0	9.6	11	14	21	29	48
6 - 3000/75%	0.41	0.66	0.94	1.5	1.8	2.2	3.2	4.6	6.4	8.8	10	12	19	26	45
7 - 3000/post-sonic	0.41	0.65	0.92	1.5	1.8	2.2	3.1	4.5	6.4	9.0	11	13	21	34	68
8 - 2000/post-sonic	0.40	0.64	0.90	1.4	1.7	2.1	3.0	4.3	6.1	8.6	10	12	20	29	64
9 - 4000/post-sonic	0.41	0.65	0.92	1.5	1.8	2.2	3.2	4.6	6.6	9.4	11	14	24	38	73

Table F.3 shows the absolute relative percent difference (RPD) between primary and duplicate results, which is calculated as:

$$RPD = \left| \frac{d_d(n) - d_p(n)}{d_p(n)} \right| \tag{F.1}$$

where $d_p(n)$ and $d_d(n)$ are the primary and duplicate cumulative oversize diameters corresponding to the nth percentile. As before, this appendix does not provide a discussion of the RPD results; however, the RPD for the 10th, 50th, and 90th diameter percentiles are presented and discussed in the main body of this interim report.

Table F.3. Relative Percent Difference Between Primary and Duplicate Group 1 Initial Characterization Samples (TI483-G1-S-WL-PSD-1 and -2, respectively) as a Function of Test Condition

Test Condition	Absolute RPD (%)														
	1%	5%	10%	20%	25%	30%	40%	50%	60%	70%	75%	80%	90%	95%	99%
1 - 3000/pre-sonic	3.2	8.7	12	15	17	18	18	17	17	16	16	15	12	7.9	2.3
2 - 2000/pre-sonic	4.5	9.8	12	15	17	18	19	18	17	17	16	16	13	8.9	0.9
3 - 4000/pre-sonic	4.0	8.5	10	13	14	15	15	14	13	11	9.7	8.2	4.1	0.6	6.7
4 - 3000/25%	4.5	8.8	11	13	14	15	17	16	15	15	14	14	13	13	10
5 - 3000/50%	4.1	7.7	9.4	11	12	13	14	14	13	13	12	12	12	13	13
6 - 3000/75%	5.1	7.3	8.4	9.3	9.8	10	12	12	11	11	11	11	13	16	26
7 - 3000/post-sonic	4.9	6.9	7.9	8.4	8.7	9.3	10	10	9.3	8.7	8.4	8.1	6.8	5.3	5.2
8 - 2000/post-sonic	5.2	7.0	8.0	8.7	9.1	9.7	11	11	10	9.6	9.3	9.0	7.9	6.4	2.0
9 - 4000/post-sonic	4.9	6.6	7.5	7.9	8.1	8.4	8.8	8.3	7.2	5.8	4.7	3.2	2.3	2.8	5.0

Appendix G

**Group 1 Analytical Results
from Parametric Leaching**

Appendix G: Group 1 Analytical Results from Parametric Leaching

Table G.1 provides information about analyte concentrations during leaching at various time increments at 40ºC, Table G.2 at 60ºC, and Table G3 at 80ºC.

Table G.1. Analyte Concentrations as a Function of Time for Leaching at 40ºC

Analyte	Analyte Concentration and Density at Given Time After Cooling to Ambient (~21°C) Temperature; g/mL for Density; µg/mL for Metals and Anions; µCi/mL for Radionuclides					
	0 hr	1 hr	2 hr	4 hr	8 hr	24 hr
1 M NaOH						
Density	1.05	1.06	1.06	1.06	1.05	1.05
Al	123	265	278	284	275	292
B	[1.3]	[1.7]	[1.7]	[1.6]	[1.6]	[1.6]
Bi	[4.1]	8.5	7.8	8.3	7.2	7.075
Cd	<0.06	<0.06	<0.06	<0.06	0.06	<0.06
Cr	[0.59]	0.98	1.2	1.6	1.9	3.7
Fe	[5.0]	[4.1]	[3.4]	[3.1]	2.9	[2.9]
Mn	<0.05	<0.05	<0.05	<0.05	0.05	<0.05
Na	24,771	26,652	26,498	26,646	25,266	26,220
Ni	<0.15	<0.15	<0.15	<0.15	0.15	<0.15
P	687	1,140	1,157	1,157	1,112	1,173
S	<8.4	[15.1]	[11.5]	[13.3]	12.0	[10.9]
Si	90.0	282	405	461	450	465
Sr	[0.03]	[0.03]	[0.02]	[0.02]	0.02	[0.02]
U	72.2	76.6	74.8	73.3	69.3	72.0
Zn	3.0	3.5	3.7	3.4	3.4	3.4
Zr	<0.21	<0.21	<0.21	<0.21	0.21	<0.21
Fluoride	289	663	659	656	631	682
Nitrite	<1.5	[1.8]	[1.8]	[1.8]	<1.8	[1.8]
Nitrate	181	184	183	181	179	191
Phosphate	2,197	3,644	3,663	3,660	3,522	3,836
Sulfate	33.7	56.0	53.4	51.9	51.9	53.9
^{60}Co						<3.E-6
^{137}Cs						0.28
^{154}Eu			Not Measured			<1.E-5
^{155}Eu						<9.E-5
^{241}Am						<2.E-4
Opportunistic Analytes						
Ag	<0.11	<0.11	<0.11	<0.11	<0.11	<0.11
As	[2.8]	<1.8	<1.8	<1.8	<1.8	<1.8
Ba	[0.11]	<0.09	[0.09]	[0.20]	<0.086	[0.16]
Be	<0.00	<0.00	<0.00	<0.00	<0.00	<0.00

Table G.1 (Contd)

Analyte	Analyte Concentration and Density at Given Time After Cooling to Ambient (~21°C) Temperature; g/mL for Density; µg/mL for Metals and Anions; µCi/mL for Radionuclides					
	0 hr	1 hr	2 hr	4 hr	8 hr	24 hr
Ca	<0.54	<0.55	<0.54	<0.54	<0.54	<0.54
Ce	<0.31	<0.31	<0.31	<0.31	<0.30	<0.31
Co	<0.10	<0.10	<0.10	<0.10	<0.10	<0.10
Cu	[0.41]	[0.35]	[0.34]	[0.34]	[0.35]	[0.34]
Dy	<0.09	<0.09	<0.09	<0.09	<0.09	<0.09
Eu	<0.03	<0.03	<0.03	<0.03	<0.03	<0.03
K	[6.6]	[6.3]	[11.8]	[13.9]	[8.5]	[14.0]
La	<0.03	<0.03	<0.03	<0.03	<0.03	<0.03
Li	[0.20]	[0.44]	[0.44]	[0.40]	[0.43]	[0.43]
Mg	<0.18	<0.18	<0.18	<0.18	<0.18	<0.18
Mo	<0.17	[0.20]	<0.17	<0.24	[0.24]	<0.17
Nd	<0.44	<0.45	<0.44	<0.44	<0.44	<0.44
Pb	<0.96	<0.96	<0.95	<0.95	<0.94	<0.95
Pd	<0.32	<0.33	<0.32	<0.32	<0.32	<0.32
Rh	<0.65	<0.66	<0.65	<0.65	<0.64	<0.65
Ru	<0.21	<0.21	<0.21	<0.21	<0.21	<0.21
Sb	<0.81	<0.82	<0.81	<0.80	<0.80	<0.81
Se	[2.6]	<1.3	[4.4]	[1.3]	[2.6]	[2.8]
Sn	<0.52	<0.52	[0.94]	[0.51]	<0.51	<0.52
Ta	<0.34	<0.35	<0.34	<0.34	<0.34	<0.34
Te	<0.82	<0.82	<0.81	<0.81	<0.80	<0.81
Th	<0.31	<0.31	<0.31	<0.30	<0.30	<0.30
Ti	<0.02	<0.03	<0.02	<0.02	<0.02	<0.02
Tl	<1.68	<1.69	<1.67	<1.66	<1.65	<1.67
V	<0.08	<0.08	<0.08	<0.08	<0.08	<0.08
W	<0.39	<0.39	<0.39	<0.38	<0.38	<0.38
Y	<0.02	<0.02	<0.02	<0.02	<0.02	<0.02
3 M NaOH, Trial a						
Density	1.13	1.14	1.14	1.14	1.14	1.14
Al	222	302	312	313	320	337
B	<2.3	<2.4	<2.4	<2.3	<2.3	<2.3
Bi	42	53	57	64	60	67
Cd	<0.31	<0.31	<0.31	<0.31	<0.31	<0.31
Cr	[2.3]	[2.2]	[2.6]	[3.7]	5.8	12.5
Fe	27.0	[19.1]	[17.2]	[16.1]	[16.5]	[11.9]
Mn	[0.27]	<0.27	<0.27	<0.26	<0.26	<0.26
Na	73,322	73,817	75,191	75,397	74,306	74,988
Ni	<0.75	<0.75	<0.75	<0.74	<0.75	<0.73
P	851	1,057	1,117	1,170	1,169	1,188
S	<42.0	<42.3	<42.2	<41.9	<42.0	[55.1]
Si	288	513	530	527	529	536
Sr	[0.06]	[0.08]	[0.07]	[0.06]	[0.06]	[0.06]

Table G.1 (Contd)

Analyte	Analyte Concentration and Density at Given Time After Cooling to Ambient (~21°C) Temperature; g/mL for Density; µg/mL for Metals and Anions; µCi/mL for Radionuclides					
	0 hr	1 hr	2 hr	4 hr	8 hr	24 hr
U	[90.1]	[100]	[99.8]	[99.3]	[99.5]	[101]
Zn	[5.3]	[5.9]	[5.9]	[5.9]	[5.6]	[5.5]
Zr	<1.0	<1.0	<1.0	<1.0	<1.0	<1.0
Fluoride	453	654	700	694	693	697
Nitrite	<1.8	[1.7]	[1.8]	[1.8]	[1.7]	[1.8]
Nitrate	213	187	196	194	202	198
Phosphate	2,905	3,477	3,781	3,830	3,871	3,881
Sulfate	33.6	60.2	64.1	70.0	64.0	59.7
^{60}Co						<2.E-6
^{137}Cs						0.28
^{154}Eu			Not Measured			<6.E-6
^{155}Eu						<9.E-5
^{241}Am						<3.E-4
Opportunistic Analytes						
Ag	<0.54	<0.55	<0.55	<0.54	<0.54	<0.54
As	<9.0	<9.0	<9.0	<9.0	<9.0	<8.8
Ba	<0.43	<0.44	<0.44	<0.43	<0.44	<0.43
Be	<0.02	<0.02	<0.02	<0.02	<0.02	<0.02
Ca	[3.7]	[5.9]	[7.8]	<2.699	<2.705	[4.0]
Ce	[1.8]	<1.548	[1.6]	<1.536	[1.9]	<1.515
Co	<0.50	<0.50	<0.50	<0.50	<0.50	<0.49
Cu	[0.93]	[1.1]	[1.0]	[0.99]	[0.90]	[0.92]
Dy	<0.45	<0.45	<0.45	<0.45	<0.45	<0.44
Eu	<0.14	<0.14	<0.14	<0.14	<0.14	<0.14
K	[34.2]	[26.9]	[40.6]	[34.1]	[43.5]	[45.9]
La	<0.17	<0.17	<0.17	<0.17	<0.17	<0.17
Li	<0.70	<0.70	<0.70	<0.70	<0.70	<0.69
Mg	<0.90	<0.91	<0.90	<0.90	<0.90	<0.89
Mo	[1.8]	[0.91]	[1.0]	<0.838	[1.9]	[0.89]
Nd	<2.2	<2.2	<2.2	<2.2	<2.2	<2.2
Pb	<4.8	<4.8	<4.8	<4.7	<4.8	<4.7
Pd	<1.6	<1.6	<1.6	<1.6	<1.6	<1.6
Rh	<3.2	<3.3	<3.3	<3.2	<3.2	<3.2
Ru	<1.1	<1.1	<1.1	<1.1	<1.1	<1.0
Sb	<4.0	<4.1	<4.1	<4.0	<4.0	<4.0
Se	[7.5]	<6.3	[9.0]	[13.3]	<6.3	[15.3]
Sn	<2.6	<2.6	<2.6	[3.4]	<2.6	<2.5
Ta	<1.7	<1.7	<1.7	<1.707	<1.7	<1.7
Te	<4.1	<4.1	<4.1	[5.0]	<4.1	<4.0
Th	<1.5	<1.5	<1.5	<1.5	<1.5	<1.5
Ti	<0.12	<0.13	<0.12	<0.12	<0.12	<0.12
Tl	<8.3	<8.4	<8.4	<8.3	<8.3	<8.2
V	<0.40	<0.41	<0.41	<0.40	<0.40	<0.40

Table G.1 (Contd)

Analyte	Analyte Concentration and Density at Given Time After Cooling to Ambient (~21°C) Temperature; g/mL for Density; μg/mL for Metals and Anions; μCi/mL for Radionuclides					
	0 hr	1 hr	2 hr	4 hr	8 hr	24 hr
W	<1.9	<1.9	<1.9	<1.9	<1.9	<1.9
Y	<0.11	<0.11	<0.11	<0.11	<0.11	<0.11
3 M NaOH, Trial b						
Density	1.13	1.14	1.14	1.14	1.13	1.14
Al	151	288	295	308	300	321
B	<2.4	<2.4	<2.4	<2.3	<2.3	<2.3
Bi	37.5	47.4	54.4	68.4	67.7	71.1
Cd	<0.31	<0.31	<0.31	<0.31	<0.31	<0.31
Cr	[2.7]	[1.9]	[2.7]	[4.0]	5.1	11.5
Fe	27.2	[18.8]	[17.8]	[18.6]	[15.5]	[13.0]
Na	75,857	76,245	76,845	77,031	73,334	76,034
Ni	<0.75	<0.75	<0.75	<0.74	<0.75	<0.74
P	727	875	962	1,182	1,159	1,175
S	<42.2	<42.4	<42.2	<41.8	<42.0	[49.5]
Si	328	505	519	535	528	532
Sr	[0.06]	[0.06]	[0.07]	[0.06]	[0.06]	[0.06]
U	[81.2]	[91.0]	[96.8]	[99.0]	[109]	[95.8]
Zn	[4.7]	[5.6]	[5.3]	[5.9]	[5.9]	[6.2]
Zr	<1.05	<1.05	<1.05	<1.04	<1.04	<1.04
Fluoride	279	570	602	682	697	678
Nitrite	[1.7]	[1.8]	[1.8]	[1.8]	[2.4]	<1.8
Nitrate	187	192	192	191	198	198
Phosphate	2,321	2,889	3,131	3,796	3,919	3,830
Sulfate	35.0	64.1	54.3	56.2	62.5	57.3
[60]Co						<3.E-6
[137]Cs						0.30
[154]Eu			Not Measured			<1.E-5
[155]Eu						<8.E-5
[241]Am						<4.E-5
Opportunistic Analytes						
Ag	<0.55	<0.55	<0.55	<0.54	<0.54	<0.54
As	<9.006	<9.052	<9.012	<8.925	<8.965	<8.917
Ba	<0.44	<0.44	<0.44	<0.43	<0.44	<0.43
Be	<0.02	<0.02	<0.02	<0.02	<0.02	<0.02
Ca	[5.6]	[3.5]	<2.718	[3.1]	[3.0]	<2.7
Ce	<1.5	<1.6	<1.5	<1.5	[1.6]	<1.5
Co	<0.50	<0.50	<0.50	<0.49	<0.50	<0.49
Cu	[0.91]	[0.72]	[0.66]	[0.77]	[0.78]	[0.87]
Dy	<0.45	<0.45	<0.45	<0.45	<0.45	<0.45
Eu	<0.14	<0.14	<0.14	<0.14	<0.14	<0.14
K	[40.6]	[20.1]	[26.6]	[25.7]	[30.1]	[37.1]
La	<0.17	<0.17	<0.17	<0.17	<0.17	<0.17

Table G.1 (Contd)

Analyte	Analyte Concentration and Density at Given Time After Cooling to Ambient (~21°C) Temperature; g/mL for Density; µg/mL for Metals and Anions; µCi/mL for Radionuclides					
	0 hr	1 hr	2 hr	4 hr	8 hr	24 hr
Li	<0.70	<0.71	<0.70	<0.70	<0.70	<0.70
Mg	<0.91	<0.91	<0.91	<0.90	<0.90	<0.90
Mo	<0.84	[1.8]	[1.3]	[1.1]	[0.87]	[1.1]
Nd	<2.2	<2.2	<2.2	<2.2	<2.2	<2.2
Pb	<4.8	<4.8	<4.8	<4.7	<4.8	<4.7
Pd	<1.6	<1.6	<1.6	<1.6	<1.6	<1.6
Rh	<3.3	<3.3	<3.3	<3.2	<3.2	<3.2
Ru	<1.1	<1.1	<1.1	<1.1	<1.1	<1.1
Sb	<4.1	<4.1	<4.1	<4.0	<4.0	<4.0
Se	[15.0]	[20.7]	[15.3]	<6.3	[16.5]	<6.3
Sn	<2.6	<2.6	<2.6	<2.6	<4.0	<2.6
Ta	<1.7	<1.7	<1.7	<1.7	<1.7	<1.7
Te	<4.1	<4.1	<4.1	<4.0	<4.1	<4.0
Th	<1.5	<1.5	<1.5	<1.5	<1.5	<1.5
Ti	<0.12	<0.13	<0.12	<0.12	<0.12	<0.12
Tl	<8.4	<8.4	<8.4	<8.3	<8.3	<8.3
V	<0.41	<0.41	<0.41	<0.40	<0.40	<0.40
W	<1.9	<1.9	<1.9	<1.9	<1.9	<1.9
Y	<0.11	<0.11	<0.11	<0.11	<0.11	<0.11
3 M NaOH, Trial c						
Density	1.13	1.14	1.14	1.14	1.14	1.13
Al	132	252	284	300	306	308
B	<2.4	<2.3	<2.3	<2.3	<2.3	<2.3
Bi	36.3	42.5	52.9	66.9	67.0	65.5
Cd	<0.31	<0.31	<0.31	<0.31	<0.31	<0.30
Cr	[2.1]	[2.0]	[2.6]	[3.4]	5.2	9.9
Fe	27.2	[17.7]	[18.0]	[18.1]	[15.4]	[12.4]
Mn	<0.27	<0.26	<0.26	<0.26	<0.26	<0.26
Na	73,591	73,602	73,974	75,936	74,356	73,085
Ni	<0.75	<0.75	<0.74	<0.75	<0.74	<0.72
P	733	826	994	1,161	1,140	1,145
S	<42.3	<42.0	<41.8	<42.1	<41.5	<40.8
Si	265	491	517	538	516	525
Sr	[0.06]	[0.07]	[0.06]	[0.07]	[0.06]	[0.05]
U	[87.7]	[96.3]	[102]	[103]	[95.2]	[96.6]
Zn	[4.7]	[5.3]	[5.3]	[5.9]	[5.8]	[5.1]
Zr	<1.0	<1.0	<1.0	<1.0	<1.0	<1.0
Fluoride	256	495	589	666	670	681
Nitrite	<1.8	[1.8]	[1.7]	[1.8]	[1.8]	[2.4]
Nitrate	169	188	186	190	188	194

Table G.1 (Contd)

Analyte	Analyte Concentration and Density at Given Time After Cooling to Ambient (~21°C) Temperature; g/mL for Density; µg/mL for Metals and Anions; µCi/mL for Radionuclides					
Analyte	0 hr	1 hr	2 hr	4 hr	8 hr	24 hr
Phosphate	2,367	2,639	3,188	3,731	3,744	3,812
Sulfate	44.4	54.3	59.5	61.3	52.2	66.9
^{60}Co						<3.E-6
^{137}Cs						0.24
^{154}Eu			Not Measured			<1.E-5
^{155}Eu						<8.E-5
^{241}Am						<2.E-4
Opportunistic Analytes						
Ag	<0.55	<0.54	<0.54	<0.54	<0.54	<0.53
As	<9.0	<9.0	<8.9	<9.0	<8.9	<8.7
Ba	<0.44	<0.43	<0.43	<0.44	<0.43	<0.42
Be	<0.02	<0.02	<0.02	<0.02	<0.02	<0.02
Ca	[3.1]	[4.0]	<2.693	[3.4]	[3.0]	<2.6
Ce	<1.6	<1.5	[1.6]	<1.5	<1.5	<1.5
Co	<0.50	<0.50	<0.50	<0.50	<0.49	<0.48
Cu	[0.94]	[0.93]	[0.84]	[1.3]	[0.89]	[0.85]
Dy	<0.45	<0.45	<0.45	<0.45	<0.45	<0.44
Eu	<0.14	<0.14	<0.14	<0.14	<0.14	<0.14
K	[34.4]	[31.1]	[34.0]	[40.5]	[43.0]	<15.206
La	<0.17	<0.17	<0.17	<0.17	<0.17	<0.17
Li	<0.70	<0.70	<0.70	[0.78]	<0.69	<0.68
Mg	<0.91	<0.90	<0.90	<0.90	<0.89	<0.88
Mo	[1.628]	<0.84	<0.84	<0.84	<0.83	<0.82
Nd	[2.2]	<2.2	<2.2	<2.2	<2.2	<2.1
Pb	<4.8	<4.8	<4.7	<4.8	<4.7	<4.6
Pd	<1.6	<1.6	<1.6	<1.6	<1.6	<1.6
Rh	<3.3	<3.2	<3.2	<3.3	<3.2	<3.2
Ru	<1.1	<1.1	<1.1	<1.1	<1.0	<1.0
Sb	<4.1	<4.0	<4.0	<4.0	<4.0	<3.9
Se	[8.77]	[10.9]	[11.8]	[10.6]	[20.6]	[7.6]
Sn	<2.6	<2.6	<2.6	<2.6	<2.6	[2.7]
Ta	<1.7	<1.7	<1.7	<1.7	<1.7	<1.7
Te	<4.1	<4.1	<4.0	<4.1	<4.0	<3.9
Th	<1.5	<1.5	<1.5	<1.5	<1.5	<1.5
Ti	<0.13	<0.12	<0.12	<0.12	<0.12	<0.12
Tl	<8.4	<8.3	<8.3	<8.4	<8.2	<8.1
V	<0.41	<0.40	<0.40	<0.40	<0.40	<0.39
W	<1.9	<1.9	<1.9	<1.9	<1.9	<1.9
Y	<0.11	<0.11	<0.11	<0.11	<0.11	<0.11

Table G.2. Analyte Concentrations as a Function of Time for Leaching at 60ºC

Analyte	Analyte Concentration and Density at Given Time After Cooling to Ambient (~21°C) Temperature; g/mL for Density; µg/mL for Metals and Anions; µCi/mL for Radionuclides					
	0 hr	1 hr	2 hr	4 hr	8 hr	24 hr
1 M NaOH						
Density	1.05	1.08	1.08	1.06	1.06	1.05
Al	83.8	275	292	289	296	300
B	[1.2]	[1.7]	[1.6]	[1.5]	[1.6]	[1.6]
Bi	[4.0]	12.8	16.4	16.6	17.2	17.1
Cd	<0.06	<0.06	<0.06	<0.06	<0.06	<0.06
Cr	[0.59]	1.6	2.4	3.2	4.5	7.8
Fe	[4.7]	6.4	5.8	5.8	[5.0]	[5.0]
Mn	<0.05	<0.05	<0.05	<0.05	<0.05	<0.05
Na	24,455	26,903	27,029	26,440	26,603	26,835
Ni	<0.15	<0.15	<0.15	<0.15	<0.15	<0.15
P	589	1,130	1,183	1,162	1,167	1,172
S	[11.8]	[15.3]	[15.9]	[14.9]	[13.0]	[12.7]
Si	69.5	455	459	444	447	438
Sr	[0.03]	[0.03]	[0.03]	[0.03]	[0.03]	[0.03]
U	66.7	77.8	80.5	78.3	77.9	78.0
Zn	2.8	3.7	3.7	3.7	3.8	3.6
Zr	<0.21	<0.21	<0.21	<0.21	<0.21	<0.21
Fluoride	189	634	671	699	661	661
Nitrite	<1.8	[1.8]	[1.8]	[1.8]	[1.8]	<1.8
Nitrate	172	192	187	192	183	185
Phosphate	1,850	3,482	3,666	3,801	3,624	3,622
Sulfate	25.1	50.7	50.9	56.2	54.8	54.1
^{60}Co	Not Measured					<2.E-6
^{137}Cs						0.27
^{154}Eu						<7.E-6
^{155}Eu						<9.E-5
^{241}Am						<1.E-4
Opportunistic Analytes						
Ag	<0.11	<0.11	<0.11	<0.11	<0.11	<0.11
As	<1.8	<1.8	<1.8	<1.8	[2.0]	<1.8
Ba	[0.12]	[0.23]	<0.09	[0.13]	[0.10]	[0.12]
Be	<0.00	<0.00	<0.00	<0.00	<0.00	<0.00
Ca	<0.54	<0.54	<0.54	<0.54	<0.54	[0.56]
Ce	[0.37]	[0.31]	<0.31	<0.31	<0.31	<0.31
Co	<0.10	<0.10	<0.10	<0.10	<0.10	<0.10
Cu	[0.37]	[0.40]	[0.37]	[0.34]	[0.37]	[0.37]
Dy	<0.09	<0.09	<0.09	<0.09	<0.09	<0.09
Eu	<0.03	<0.03	<0.03	<0.03	<0.03	<0.03
K	[10.0]	[13.4]	[15.6]	[16.2]	[18.0]	[19.3]
La	<0.03	<0.03	<0.03	<0.03	<0.03	<0.03
Li	[0.15]	[0.40]	[0.44]	[0.43]	[0.47]	[0.40]
Mg	<0.18	<0.18	<0.18	<0.18	<0.18	<0.18

Table G.2 (Contd)

Analyte	Analyte Concentration and Density at Given Time After Cooling to Ambient (~21°C) Temperature; g/mL for Density; µg/mL for Metals and Anions; µCi/mL for Radionuclides					
	0 hr	1 hr	2 hr	4 hr	8 hr	24 hr
Mo	[0.22]	[0.30]	[0.23]	<0.17	[0.29]	[0.17]
Nd	<0.44	<0.44	<0.44	<0.44	<0.44	<0.44
Pb	<0.95	<0.95	<0.96	<0.95	<0.95	<0.95
Pd	<0.32	<0.32	<0.32	<0.32	<0.32	<0.32
Rh	<0.65	<0.65	<0.65	<0.65	<0.65	<0.65
Ru	<0.21	<0.21	<0.21	<0.21	<0.21	<0.21
Sb	<0.81	<0.81	<0.81	<0.81	<0.81	[0.84]
Se	[4.4]	[1.4]	[3.0]	[3.1]	[4.7]	[1.8]
Sn	<0.52	[0.87]	[0.91]	<0.52	<0.52	<0.52
Ta	<0.34	<0.34	<0.34	<0.34	<0.34	<0.34
Te	<0.81	<0.81	<0.81	<0.81	<0.81	<0.81
Th	<0.31	<0.31	<0.31	<0.30	<0.30	<0.30
Ti	<0.02	<0.02	<0.02	<0.02	<0.02	<0.02
Tl	<1.7	<1.7	<1.7	<1.7	<1.7	[1.9]
V	<0.08	<0.08	<0.08	<0.08	<0.08	<0.08
W	<0.39	<0.39	<0.39	<0.39	<0.38	<0.39
Y	<0.02	<0.02	<0.02	<0.02	<0.02	<0.02
3 M NaOH						
Density	1.14	1.15	1.15	1.13	1.14	1.14
Al	131	292	328	331	338	331
B	<2.3	<2.3	<2.4	[2.4]	<2.3	<2.3
Bi	34.6	98.7	123	124	129	125
Cd	<0.31	<0.31	<0.31	<0.31	<0.31	<0.31
Cr	[3.4]	[4.0]	6.9	9.8	13.5	21.1
Fe	30.4	[22.9]	[23.1]	[20.0]	[18.0]	[15.1]
Mn	[0.34]	<0.26	<0.27	<0.27	<0.26	<0.26
Na	74,194	72,111	79,096	76,185	76,206	75,131
Ni	<0.74	<0.74	<0.75	<0.75	<0.74	<0.74
P	686	1,074	1,194	1,186	1,183	1,163
S	<41.8	[43.33]	<42.3	<42.2	<41.9	<41.8
Si	162	504	541	540	536	532
Sr	[0.07]	[0.08]	[0.09]	[0.08]	[0.09]	[0.08]
U	[83.5]	[99.0]	109.73	109.28	[105]	[105]
Zn	[5.6]	[5.9]	[5.6]	[5.9]	[6.8]	[5.9]
Zr	<1.0	<1.0	<1.0	<1.0	<1.0	<1.0
Fluoride	267	696	701	768	235	731
Nitrite	[1.8]	[1.8]	[1.8]	[2.4]	[1.8]	[1.8]
Nitrate	184	197	213	233	213	219
Phosphate	2,213	3,762	3,844	4,161	3,842	3,956
Sulfate	47.4	61.7	73.7	85.3	82.3	97.1

Table G.2 (Contd)

Analyte	Analyte Concentration and Density at Given Time After Cooling to Ambient (~21°C) Temperature; g/mL for Density; µg/mL for Metals and Anions; µCi/mL for Radionuclides					
	0 hr	1 hr	2 hr	4 hr	8 hr	24 hr
^{60}Co						<4.E-6
^{137}Cs						0.29
^{154}Eu			Not Measured			<1.E-5
^{155}Eu						<1.E-4
^{241}Am						<1.E-4
Opportunistic Analytes						
Ag	<0.54	<0.54	<0.55	<0.55	<0.54	<0.54
As	<8.9	<8.9	<9.0	<9.0	[10.5]	<8.9
Ba	<0.43	<0.43	<0.44	<0.44	<0.43	<0.43
Be	<0.02	<0.02	<0.02	<0.02	<0.02	<0.02
Ca	[5.9]	[4.6]	[3.1]	[3.1]	[3.4]	[3.7]
Ce	<1.5	[1.9]	<1.5	<1.5	<1.5	<1.5
Co	<0.49	<0.50	<0.50	<0.50	<0.50	<0.49
Cu	[0.897]	[1.1]	[1.0]	[1.0]	[0.93]	[0.80]
Dy	<0.45	<0.45	<0.45	<0.45	<0.45	<0.45
Eu	<0.14	<0.14	<0.14	<0.14	<0.14	<0.14
K	[49.5]	[46.4]	[50.0]	[24.7]	[31.0]	[34.0]
La	<0.17	<0.17	[0.275]	<0.17	<0.17	<0.17
Li	<0.70	[0.712]	<0.70	<0.70	<0.70	<0.70
Mg	<0.90	<0.90	<0.91	<0.91	<0.90	<0.90
Mo	[1.1]	[1.1]	[0.88]	[0.87]	[1.0]	<0.835
Nd	<2.2	<2.2	<2.2	<2.2	<2.2	<2.2
Pb	<4.7	<4.7	<4.8	<4.8	<4.7	<4.7
Pd	<1.6	<1.6	<1.6	<1.6	<1.6	<1.6
Rh	<3.2	<3.2	<3.3	<3.3	<3.2	<3.2
Ru	<1.1	<1.1	<1.1	<1.1	<1.1	<1.1
Sb	<4.0	<4.0	<4.1	<4.1	<4.0	<4.0
Se	[8.0]	[18.0]	[16.6]	[11.9]	<6.3	[14.2]
Sn	<2.6	<2.6	<2.6	<2.6	<2.6	<2.6
Ta	<1.7	<1.7	<1.7	<1.7	<1.7	<1.7
Te	<4.0	<4.0	<4.1	<4.1	<4.0	<4.0
Th	<1.5	<1.5	<1.5	<1.5	<1.5	<1.5
Ti	<0.12	<0.12	<0.13	<0.12	<0.12	<0.12
Tl	<8.3	<8.3	<8.4	<8.4	<8.3	<8.3
V	<0.40	<0.40	<0.41	<0.41	<0.40	<0.40
W	<1.9	<1.9	<1.9	<1.9	<1.9	<1.9
Y	<0.11	<0.11	<0.11	<0.11	<0.11	<0.11

Table G.3. Analyte Concentrations as a Function of Time for Leaching at 80ºC

Analyte	Analyte Concentration and Density at Given Time After Cooling to Ambient (~21°C) Temperature; g/mL for Density; µg/mL for Metals and Anions; µCi/mL for Radionuclides					
	0 hr	1 hr	2 hr	4 hr	8 hr	24 hr
1 M NaOH						
Density	1.05	1.07	1.07	1.08	1.09	1.05
Al	107	294	304	304	312	302
B	[1.7]	[1.8]	[1.7]	[1.8]	[1.9]	[2.0]
Bi	[4.7]	27.2	27.9	30.1	32.1	29.2
Cd	<0.06	<0.06	<0.06	<0.06	<0.06	<0.06
Cr	[0.69]	3.1	4.6	7.0	10.3	16.4
Fe	[3.4]	8.9	8.2	7.9	7.6	5.9
Mn	<0.05	<0.05	<0.05	<0.05	<0.05	<0.05
Na	25,136	26,690	26,937	27,086	27,797	26,901
Ni	<0.15	<0.15	<0.15	<0.15	<0.15	<0.15
P	629	1,161	1,173	1,175	1,192	1,148
S	<8.4	[12.4]	[14.0]	[16.7]	[15.6]	[16.4]
Si	117	459	460	456	465	448
Sr	[0.02]	[0.03]	[0.03]	[0.03]	[0.02]	[0.02]
U	67.9	84.4	85.9	86.7	88.3	83.6
Zn	2.9	3.8	3.9	3.8	3.8	3.5
Zr	<0.21	<0.21	<0.21	<0.21	<0.21	<0.20
Fluoride	278	654	675	707	710	647
Nitrite	[1.8]	<3.0	[1.8]	[1.8]	[1.8]	<2.9
Nitrate	206	189	190	195	196	187
Phosphate	2,373	3,866	3,797	3,893	3,961	3,871
Sulfate	37.3	52.8	56.7	57.4	60.2	55.3
[60]Co						<3.E-6
[137]Cs						0.29
[154]Eu			Not Measured			<7.E-6
[155]Eu						<9.E-5
[241]Am						<1.E-4
Opportunistic Analytes						
Ag	<0.11	<0.11	<0.11	<0.11	<0.11	<0.11
As	<1.8	<1.8	<1.8	<1.8	<1.8	<1.7
Ba	[0.24]	[0.13]	<0.09	[0.13]	<0.09	[0.14]
Be	<0.00	<0.00	<0.00	<0.00	<0.00	<0.00
Ca	<0.54	<0.54	<0.54	<0.55	<0.54	<0.53
Ce	<0.31	<0.31	<0.31	<0.31	<0.31	<0.30
Co	<0.10	<0.10	<0.10	<0.10	<0.10	<0.10
Cu	[0.40]	[0.36]	[0.34]	[0.35]	[0.34]	[0.42]
Dy	<0.09	<0.09	<0.09	<0.09	<0.09	<0.09
Eu	<0.03	<0.03	<0.03	<0.03	<0.03	<0.03
K	[4.36]	[7.60]	[9.64]	[11.94]	[5.30]	[10.60]
La	<0.03	<0.03	<0.03	<0.03	<0.03	<0.03
Li	[0.16]	[0.47]	[0.50]	[0.47]	[0.41]	[0.39]
Mg	<0.18	<0.18	<0.18	<0.18	<0.18	<0.18

Table G.3 (Contd)

Analyte	Analyte Concentration and Density at Given Time After Cooling to Ambient (~21°C) Temperature; g/mL for Density; µg/mL for Metals and Anions; µCi/mL for Radionuclides					
	0 hr	1 hr	2 hr	4 hr	8 hr	24 hr
Mo	<0.17	<0.17	<0.17	<0.17	<0.17	<0.16
Nd	<0.44	<0.44	<0.44	<0.45	<0.44	<0.43
Pb	<0.95	[1.1]	[1.2]	[1.3]	[1.1]	<0.93
Pd	<0.32	<0.32	<0.32	<0.33	<0.32	<0.32
Rh	<0.65	<0.65	<0.65	<0.66	<0.65	<0.63
Ru	<0.21	<0.21	<0.21	<0.21	<0.21	<0.21
Sb	<0.81	<0.81	<0.81	<0.82	<0.81	<0.79
Se	[2.0]	<1.3	[1.7]	<1.3	<1.3	<1.2
Sn	<0.52	<0.52	<0.52	<0.52	<0.52	<0.50
Ta	<0.34	<0.34	<0.34	<0.35	<0.34	<0.33
Te	<0.81	<0.81	<0.81	<0.82	<0.81	<0.79
Th	<0.31	<0.30	<0.30	<0.31	<0.31	<0.30
Ti	<0.02	<0.02	<0.02	<0.03	<0.02	<0.02
Tl	<1.7	<1.7	<1.7	<1.7	<1.7	<1.6
V	<0.08	<0.08	<0.08	<0.08	<0.08	<0.08
W	<0.39	[0.41]	<0.39	<0.39	<0.39	<0.38
Y	<0.02	<0.02	<0.02	<0.02	<0.02	<0.02
3 M NaOH						
Density	1.13	1.14	1.15	1.15	1.17	1.14
Al	123	319	329	331	337	333
B	<2.3	[2.6]	[2.3]	<2.3	<2.4	[2.4]
Bi	34.0	152	113	96.4	81.0	82.2
Cd	<0.31	<0.31	<0.31	<0.31	<0.31	<0.31
Cr	[3.4]	9.0	13.6	19.1	25.1	32.1
Fe	26.0	28.8	[25.2]	[23.2]	[21.2]	[16.5]
Mn	[0.31]	<0.26	<0.26	<0.26	<0.26	<0.26
Na	72,211	74,808	74,959	75,369	76,650	74,822
Ni	<0.73	<0.74	<0.74	<0.74	<0.75	<0.73
P	542	1,119	1,115	1,106	1,137	1,118
S	<41.4	<41.4	<41.5	<41.7	<42.1	<41.3
Si	112	518	519	525	542	531
Sr	[0.07]	[0.10]	[0.10]	[0.10]	[0.09]	[0.06]
U	[61.2]	[104]	[101]	[98.8]	[99.7]	[91.6]
Zn	[4.0]	[5.8]	[5.5]	[5.6]	[5.6]	[5.5]
Zr	<1.0	<1.0	<1.0	<1.0	<1.0	<1.0
Fluoride	282	719	711	687	730	711
Nitrite	[1.8]	[1.8]	[1.8]	[1.8]	[1.8]	[1.8]
Nitrate	191	219	213	209	224	219
Phosphate	1,791	3,956	3,858	3,827	4,006	3,957
Sulfate	42.7	72.5	75.3	74.8	91.4	83.4

Table G.3 (Contd)

Analyte	Analyte Concentration and Density at Given Time After Cooling to Ambient (~21°C) Temperature; g/mL for Density; µg/mL for Metals and Anions; µCi/mL for Radionuclides					
	0 hr	1 hr	2 hr	4 hr	8 hr	24 hr
^{60}Co						<3.E-6
^{137}Cs			Not Measured			0.30
^{154}Eu						<1.E-5
^{155}Eu						<8.E-5
^{241}Am						<4.E-5
Opportunistic Analytes						
Ag	<0.54	<0.54	<0.54	<0.54	<0.55	<0.53
As	<8.8	<8.8	<8.9	<8.9	<9.0	<8.8
Ba	<0.43	<0.43	<0.43	<0.43	<0.44	<0.43
Be	<0.02	<0.02	<0.02	<0.02	<0.02	<0.02
Ca	<2.7	<2.7	<2.7	<2.7	<2.7	<2.7
Ce	<1.5	<1.5	<1.5	<1.5	<1.5	<1.5
Co	<0.49	<0.49	<0.49	<0.49	<0.50	<0.49
Cu	[0.67]	[0.86]	[0.80]	[0.68]	[0.75]	[0.76]
Dy	<0.44	<0.44	<0.45	<0.45	<0.45	<0.44
Eu	<0.14	<0.14	<0.14	<0.14	<0.14	<0.14
K	[22.3]	[26.4]	[29.8]	[25.9]	[34.3]	[30.5]
La	<0.17	<0.17	<0.17	<0.17	<0.17	<0.17
Li	<0.69	[0.71]	[0.77]	[0.74]	[0.72]	<0.69
Mg	<0.89	<0.89	<0.89	<0.90	<0.90	<0.89
Mo	<0.83	<0.83	<0.83	[1.1]	<0.84	<0.82
Nd	<2.2	<2.2	<2.2	<2.2	<2.2	<2.2
Pb	<4.7	<4.7	<4.7	<4.7	<4.8	<4.7
Pd	<1.6	<1.6	<1.6	<1.6	<1.6	<1.6
Rh	<3.2	<3.2	<3.2	<3.2	<3.3	<3.2
Ru	<1.0	<1.0	<1.0	<1.1	<1.1	<1.0
Sb	<4.0	<4.0	<4.0	<4.0	<4.1	<4.0
Se	<6.2	<6.2	[7.7]	<6.3	<6.3	<6.2
Sn	<2.5	<2.5	<2.5	<2.6	<2.6	<2.5
Ta	<1.7	<1.7	<1.7	<1.7	<1.7	<1.7
Te	<4.0	<4.0	<4.0	<4.0	<4.1	<4.0
Th	<1.5	<1.5	<1.5	<1.5	<1.5	<1.5
Ti	<0.12	<0.12	<0.12	<0.12	<0.12	<0.12
Tl	<8.2	<8.2	<8.2	<8.3	<8.4	<8.2
V	<0.40	<0.40	<0.40	<0.40	<0.41	<0.40
W	<1.9	<1.9	<1.9	[2.3]	<1.9	<1.9
Y	<0.11	<0.11	<0.11	<0.11	<0.11	<0.11

Table G.4. Analyte Concentrations for Composite Wash Solution for Wash of Samples Leached at 40ºC in 3 M NaOH

Analyte	Concentration (µg/mL)	Opportunistic Analytes	Concentration (µg/mL)
Al	[4.73]	Ag	<0.103
B	<0.446	As	<1.70
Bi	[1.83]	Ba	<0.083
Cd	<0.059	Be	<0.003
Cr	1.23	Ca	<0.514
Fe	[0.561]	Ce	<0.292
Mn	<0.050	Co	<0.095
Na	1,542	Cu	[0.413]
Ni	<0.142	Dy	<0.086
P	[5.61]	Eu	<0.027
S	<7.98	K	<2.97
Si	6.32	La	<0.032
Sr	[0.010]	Li	<0.133
U	<2.05	Mg	<0.171
Zn	[0.679]	Mo	<0.159
Zr	<0.198	Nd	<0.419
Fluoride	2.33	Pb	<0.904
Nitrite	<1.49	Pd	<0.307
Nitrate	86.6	Rh	<0.617
Phosphate	16.1	Ru	<0.201
Sulfate	[2.75]	Sb	<0.768
		Se	[2.72]
		Sn	<0.490
		Ta	<0.325
		Te	<0.771
		Th	<0.289
		Ti	<0.024
		Tl	<1.59
		V	<0.077
		W	<0.366
		Y	<0.021

Appendix H

Duplicate Sample Differential Particle Size Plots
for the Initial Group 2 Sample

Appendix H: Duplicate Sample Differential Particle Size Plots for the Initial Group 2 Sample

Figures H.1, H.2, and H.3 show show the differential volume distribution as a function of particle diameter for the duplicate Group 2 initial characterization sample, TI517-G2-S-WL-PSD-2. Specifically, Figure H.1 shows the pre-sonication PSDs as a function of pump speed, Figure H.2 shows the PSDs as a function of sonication, and Figure H.3 shows the post-sonication PSDs as a function of pump speed.
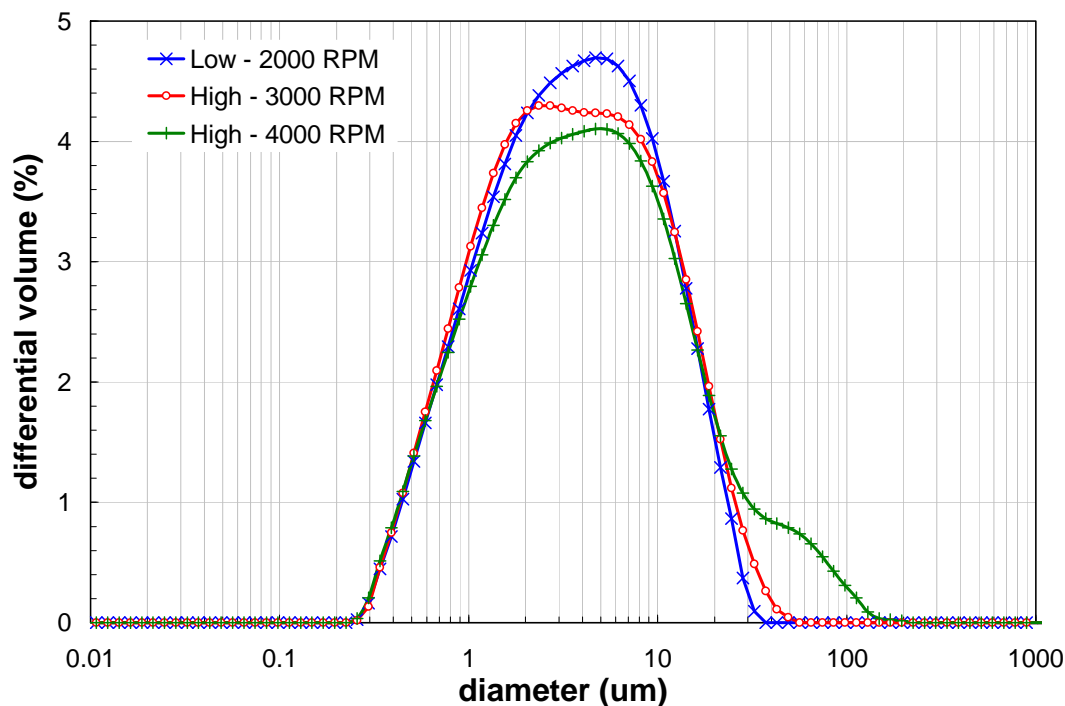
Figure H.1. Pre-Sonication Volume Distribution Result for the Duplicate Group 2 Initial Characterization Sample as a Function of Pump Speed
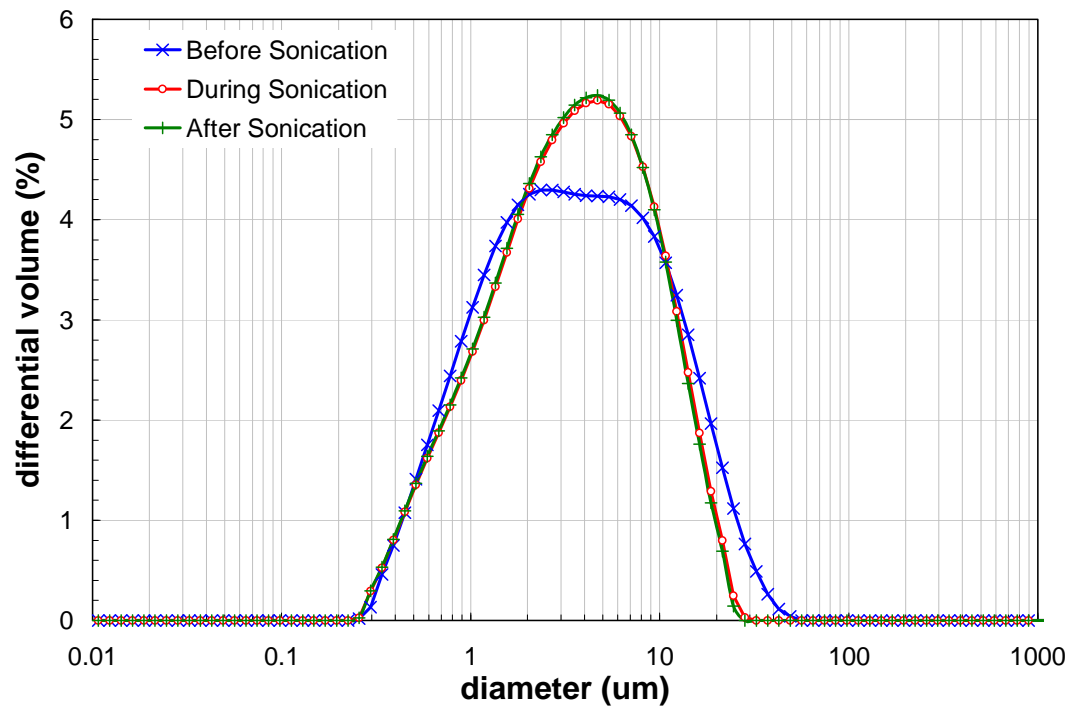
Figure H.2. Volume Distribution Result for the Duplicate Group 2 Initial Characterization Sample as a Function of Sonication (75% power)
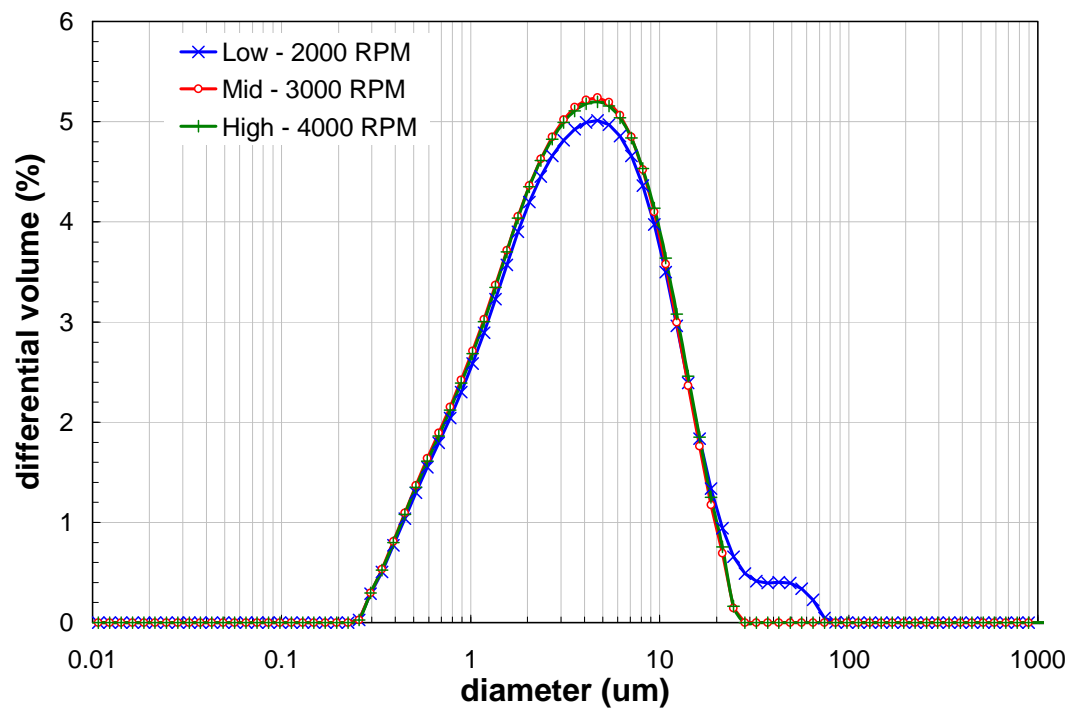
Figure H.3. Post-Sonication Volume Distribution Result for the Duplicate Group 2 Initial Characterization Sample as a Function of Pump Speed

Appendix I

Detailed Cumulative PSD for the Initial Group 2 Sample

Appendix I: Detailed Cumulative PSD for the Initial Group 2 Sample

Tables I.1 and I.2 present detailed cumulative oversize distributions (by volume/weight) for Group 2 Initial Characterization samples TI517-G2-S-WL-PSD-1 and -2, respectively. The results are reported as a function of test condition. This appendix does not provide discussion of the detailed distributions; however, a portion of these results (specifically, the 10th, 50th, and 90th diameter percentiles) are presented and discussed in the main body of the report.

Table I.1. Cumulative Oversize Diameter Distributions for the Primary Group 2 Initial Characterization Sample, TI517-G2-S-WL-PSD-1

Test Condition	Volume/Weight Cumulative Oversize Diameter (μm)														
	1%	5%	10%	20%	25%	30%	40%	50%	60%	70%	75%	80%	90%	95%	99%
1 - 3000/pre-sonic	0.42	0.64	0.86	1.3	1.5	1.8	2.4	3.2	4.2	5.7	6.6	7.7	11	14	20
2 - 4000/pre-sonic	0.41	0.64	0.87	1.4	1.6	1.9	2.6	3.5	4.6	6.2	7.2	8.5	13	17	190
3 - 2000/pre-sonic	0.42	0.65	0.88	1.3	1.6	1.8	2.4	3.2	4.2	5.5	6.4	7.4	10	13	19
4 - 3000/25%	0.38	0.57	0.79	1.2	1.5	1.7	2.3	3.1	4.1	5.4	6.2	7.2	10	13	19
5 - 3000/50%	0.36	0.56	0.77	1.2	1.5	1.8	2.4	3.1	4.0	5.3	6.1	7.1	10	13	18
6 - 3000/75%	0.36	0.55	0.77	1.2	1.5	1.8	2.4	3.1	4.0	5.2	5.9	6.9	9.7	12	17
7 - 3000/post-sonic	0.36	0.55	0.77	1.2	1.5	1.8	2.4	3.1	4.0	5.1	5.9	6.8	9.6	12	17
8 - 4000/post-sonic	0.38	0.59	0.84	1.4	1.7	1.9	2.6	3.4	4.3	5.6	6.4	7.3	10	13	18
9 - 2000/post-sonic	0.36	0.56	0.78	1.3	1.5	1.8	2.4	3.1	4.0	5.2	5.9	6.8	9.6	12	17

Table I.2. Cumulative Oversize Diameter Distributions for the Duplicate Group 2 Initial Characterization Sample, TI517-G2-S-WL-PSD-2

Test Condition	Volume / Weight Cumulative Oversize Diameter (μm)														
	1%	5%	10%	20%	25%	30%	40%	50%	60%	70%	75%	80%	90%	95%	99%
1 - 3000/pre-sonic	0.39	0.60	0.83	1.3	1.5	1.8	2.5	3.5	4.8	6.7	7.9	9.4	14	19	30
2 - 4000/pre-sonic	0.38	0.60	0.84	1.4	1.7	2.0	2.8	4.0	5.6	7.9	9.5	12	21	38	82
3 - 2000/pre-sonic	0.39	0.61	0.85	1.3	1.6	1.9	2.6	3.6	4.8	6.5	7.5	8.8	13	17	24
4 - 3000/25%	0.39	0.62	0.86	1.4	1.7	2.0	2.7	3.6	4.8	6.4	7.4	8.6	12	16	23
5 - 3000/50%	0.38	0.60	0.86	1.4	1.7	2.0	2.7	3.6	4.8	6.3	7.3	8.4	12	15	22
6 - 3000/75%	0.38	0.60	0.85	1.4	1.7	2.0	2.7	3.6	4.6	6.1	7.0	8.1	11	14	20
7 - 3000/post-sonic	0.37	0.59	0.84	1.4	1.7	2.0	2.7	3.5	4.6	6.0	6.8	7.9	11	14	19
8 - 4000/post-sonic	0.37	0.60	0.85	1.4	1.7	2.0	2.7	3.5	4.6	6.0	6.9	8.0	11	14	20
9 - 2000/post-sonic	0.38	0.61	0.87	1.4	1.7	2.1	2.8	3.7	4.9	6.5	7.5	8.8	13	18	46

Table I.3 shows the absolute relative percent difference (RPD) between primary and duplicate results, which is calculated as:

$$RPD = \left| \frac{d_d(n) - d_p(n)}{d_p(n)} \right|$$ (I.1)

where $d_p(n)$ and $d_d(n)$ are the primary and duplicate cumulative oversize diameters corresponding to the nth percentile. As before, this appendix does not provide discussion of the RPD results; however, the RPD for the 10th, 50th, and 90th diameter percentiles are presented and discussed in the main body of this interim report.

Table I.3. Relative Percent Difference Between Primary and Duplicate Group 2 Initial Characterization Samples (TI517-G2-S-WL-PSD-1 and -2, respectively) as a Function of Test Condition

Test Condition	Absolute RPD (%)														
	1%	5%	10%	20%	25%	30%	40%	50%	60%	70%	75%	80%	90%	95%	99%
1 - 3000/pre-sonic	5.5	5.6	4.4	1.2	0.33	2.0	5.7	9.8	14	18	20	22	28	34	50
2 - 4000/pre-sonic	6.6	6.1	4.3	0.30	2.7	5.1	10	15	21	27	31	36	63	120	57
3 - 2000/pre-sonic	6.2	5.3	3.4	0.52	2.5	4.4	8.0	11	14	17	18	20	24	26	29
4 - 3000/25%	3.5	7.3	9.8	12	13	14	16	17	18	19	19	19	20	21	22
5 - 3000/50%	3.8	7.9	11	13	14	14	16	17	18	19	19	19	19	19	19
6 - 3000/75%	3.9	7.8	10	12	13	13	14	16	17	18	18	18	17	16	15
7 - 3000/post-sonic	3.6	7.2	9.6	11	11	12	13	14	15	16	16	16	15	14	13
8 - 4000/post-sonic	0.27	0.34	0.59	0.80	1.1	1.5	2.9	4.7	6.6	8.3	9.0	9.5	10	10	10
9 - 2000/post-sonic	3.6	8.4	12	14	15	15	17	20	23	26	27	29	36	51	170

Appendix J

Group 2 Analytical Results
from Parametric Leaching

Appendix J: Group 2 Analytical Results from Parametric Leaching

Table J.1 provides information about analyte concentrations during leaching at various hour increments at 60ºC, Table J.2 at 80ºC, and Table J.3 at 100°C.

Table J.1. Analyte Concentrations as a Function of Time for Leaching at 60ºC

Analyte	Analyte Concentration and Density at Given Time After Cooling to Ambient (~21°C) Temperature; g/mL for Density; µg/mL for Metals and Anions; µCi/mL for Radionuclides					
	0 hr	1 hr	2 hr	4 hr	8 hr	24 hr
3 M NaOH						
Density	1.14	1.14	1.16	1.17	1.15	1.13
Al	188	736	921	1,095	1,191	1,256
B	[2.6]	<2.4	[2.6]	<2.4	[2.4]	<2.3
Bi	<3.0	[4.1]	<2.931	[3.8]	[3.2]	[3.0]
Cd	<0.31	<0.31	<0.31	<0.31	<0.32	<0.30
Cr	[1.3]	6.1	8.6	12.6	18.1	36.4
Fe	<2.6	<2.6	[2.7]	[2.9]	[3.1]	[3.3]
Mn	<0.27	<0.26	<0.26	<0.27	<0.27	<0.26
Na	71,486	73,253	75,369	75,707	71,854	73,400
P	[24.8]	[9.7]	<7.0	<7.1	[11.35]	<6.9
S	<42.4	<42.1	[43.4]	[43.8]	<42.6	<41.0
Si	64.9	186	189	183	170	162
Sr	[0.13]	[0.10]	[0.11]	[0.09]	[0.09]	[0.08]
U	<10.9	[15.0]	[12.7]	<10.8	[17.3]	[12.7]
Zn	[1.0]	[1.2]	[1.3]	[1.6]	[1.7]	[1.5]
Zr	<1.1	<1.0	<1.0	<1.0	<1.1	<1.0
Fluoride	10.3	12.6	13.0	12.7	12.1	12.1
Nitrite	<1.4	<1.4	[1.5]	[1.7]	[1.7]	[1.7]
Nitrate	501	553	555	551	554	531
Phosphate	64.3	59.1	59.3	57.2	54.6	54.7
Sulfate	[1.1]	[0.97]	[0.98]	[1.1]	[0.87]	[0.89]
^{54}Mn						<1E-5
^{60}Co						<3E-6
^{137}Cs						0.809
^{152}Eu			Not Measured			<1E-5
^{154}Eu						<2E-5
^{155}Eu						<1E-4
^{241}Am						<6E-5
Opportunistic Analytes						
Ag	<0.55	<0.55	<0.54	<0.55	<0.55	<0.53
As	<9.05	<8.99	<8.95	<9.03	<9.09	<8.75
Ba	<0.44	<0.44	<0.43	<0.44	<0.44	<0.42
Be	<0.02	<0.02	<0.02	0.02	0.02	0.02
Ca	2.9	2.7	2.7	2.7	2.7	2.6

Table J.1 (Contd)

Analyte	Analyte Concentration and Density at Given Time After Cooling to Ambient (~21°C) Temperature; g/mL for Density; µg/mL for Metals and Anions; µCi/mL for Radionuclides					
	0 hr	1 hr	2 hr	4 hr	8 hr	24 hr
Ce	1.6	2.0	2.0	1.5	1.6	1.5
Co	<0.50	<0.50	<0.50	<0.50	<0.50	<0.49
La	<0.17	<0.17	<0.17	<0.17	0.2	<0.17
Li	<0.71	<0.70	<0.70	<0.70	<0.71	<0.68
Mg	<0.91	<0.90	<0.90	<0.91	<0.91	<0.88
Mo	<0.85	<0.84	<0.84	<0.84	<0.85	<0.82
Nd	<2.2	<2.2	<2.2	<2.2	<2.2	<2.2
Pb	5.6	8.4	8.7	5.3	7.2	7.6
Pd	<1.6	<1.6	<1.6	<1.6	<1.6	<1.6
Rh	<3.3	<3.3	<3.2	<3.3	<3.3	<3.2
Ru	<1.1	<1.1	<1.1	1.6	<1.1	<1.0
Sb	<4.1	<4.1	<4.0	<4.1	<4.1	<3.9
Se	<6.3	14.7	9.0	16.3	<6.4	<6.1
Sn	3.8	3.1	2.6	5.6	3.0	2.5
Ta	<1.7	<1.7	<1.7	<1.7	2.0	<1.7
Te	<4.1	<4.1	<4.0	<4.1	<4.1	<4.0
Th	<1.5	1.7	2.6	<1.5	<1.5	<1.5
Ti	<0.13	<0.12	<0.12	<0.13	<0.13	<0.12
Tl	<8.4	<8.4	<8.3	<8.4	<8.5	<8.1
V	<0.41	<0.41	<0.40	<0.41	<0.41	<0.39
W	2.0	1.9	1.9	1.9	2.8	1.9
Y	<0.11	<0.11	<0.11	<0.11	<0.11	<0.11

Table J.2. Analyte Concentrations as a Function of Time for Leaching at 80ºC

Analyte	Analyte Concentration and Density at Given Time After Cooling to Ambient (~21°C) Temperature; g/mL for Density; µg/mL for Metals and Anions; µCi/mL for Radionuclides					
	0 hr	**1 hr**	**2 hr**	**4 hr**	**8 hr**	**24 hr**
1 M NaOH						
Density	1.05	1.05	1.05	1.05	1.04	1.06
Al	90	691	866	964	1,142	1,261
B	[0.73]	[0.76]	[1.3]	[1.2]	[2.2]	[2.7]
Bi	[0.67]	<0.57	[1.1]	[1.1]	[2.8]	<2.89
Cd	<0.06	<0.06	<0.06	<0.06	[0.30]	<0.31
Cr	[0.64]	5.1	8.4	12.8	24.6	57.4
Fe	<0.5	[1.1]	[1.5]	[1.9]	<2.5	<2.6
Mn	<0.05	<0.05	<0.05	<0.05	<0.25	<0.26
Na	24,147	24,217	24,356	24,142	24,652	24,952
P	[13.4]	[11.6]	[12.9]	[12.3]	[16.9]	[13.7]
S	[8.54]	<8.2	<8.1	<8.1	<40.0	<41.3
Si	29.7	90.1	79.7	73.6	60.1	53.4
Sr	[0.02]	[0.01]	[0.02]	[0.02]	[0.04]	[0.05]
U	[4.0]	[8.8]	[11.7]	[14.7]	[16.6]	[15.0]
Zn	[0.67]	[1.03]	[1.20]	[1.14]	[1.54]	[1.92]
Zr	<0.20	<0.20	<0.20	<0.20	<0.99	<1.02
Fluoride	8.8	10.8	11.4	11.5	12.3	11.7
Nitrite	<1.4	<14	<1.4	[1.5]	[1.8]	[1.7]
Nitrate	465	505	499	487	551	490
Phosphate	43.6	43.2	42.8	41.7	52.0	41.3
Sulfate	[3.2]	[2.0]	[2.0]	[1.6]	<0.66	[0.91]
^{54}Mn						<9E-6
^{60}Co						<3E-6
^{137}Cs						0.509
^{152}Eu			Not Measured			<1E-5
^{154}Eu						<2E-5
^{155}Eu						<1E-4
^{241}Am						<5E-5
Opportunistic Analytes						
Ag	<0.11	<0.11	<0.11	<0.11	<0.52	<0.53
As	<1.8	<1.8	<1.7	<1.7	<8.5	<8.8
Ba	<0.09	<0.09	[0.24]	[0.10]	<0.41	<0.43
Be	[0.00]	[0.01]	[0.01]	[0.01]	<0.01	<0.02
Ca	0.5	<0.53	<0.52	<0.52	[2.7]	<2.7
Ce	[0.37]	<0.30	<0.30	<0.30	<1.5	<1.5
Co	<0.10	<0.10	<0.10	<0.10	<0.47	<0.49
Cu	1.7	1.8	1.7	1.8	[1.7]	1.7
Dy	<0.09	<0.09	<0.09	<0.09	<0.43	<0.44
Eu	<0.03	<0.03	<0.03	[0.04]	<0.13	<0.14
K	[3.4]	[3.7]	<3.028	3.3	<14.9	<15.4
La	<0.03	<0.03	<0.03	<0.03	<0.16	<0.17
Li	<0.14	[0.30]	[0.33]	[0.36]	<0.67	<0.69

Table J.2 (Contd)

Analyte	Analyte Concentration and Density at Given Time After Cooling to Ambient (~21°C) Temperature; g/mL for Density; µg/mL for Metals and Anions; µCi/mL for Radionuclides					
	0 hr	**1 hr**	**2 hr**	**4 hr**	**8 hr**	**24 hr**
Mg	<0.18	<0.18	<0.17	<0.17	<0.86	<0.89
Mo	<0.16	<0.16	<0.16	<0.16	<0.80	<0.82
Nd	<0.43	<0.43	<0.43	<0.43	<2.10	<2.17
Ni	<0.15	<0.15	<0.14	<0.14	<0.71	<0.73
Pb	[2.0]	[4.3]	[3.9]	[4.5]	[5.6]	[5.2]
Pd	<0.32	<0.32	<0.31	<0.31	<1.5	<1.6
Rh	<0.64	<0.64	<0.63	<0.63	<3.1	<3.2
Ru	<0.21	<0.21	<0.20	<0.20	<1.0	<1.0
Sb	<0.79	<0.79	<0.78	<0.78	<3.8	<4.0
Se	[2.2]	[2.1]	[1.2]	<1.216	<6.0	[11.0]
Sn	[1.2]	[1.1]	[0.75]	[0.90]	<2.5	<2.5
Ta	<0.34	<0.33	<0.33	[0.36]	<1.6	<1.7
Te	<0.80	<0.79	<0.78	<0.78	<3.9	<4.0
Th	<0.30	<0.30	<0.29	<0.29	<1.5	<1.5
Ti	<0.02	<0.02	<0.02	<0.02	<0.12	<0.12
Tl	<1.6	<1.6	<1.6	<1.6	<7.9	<8.2
V	[0.15]	[0.19]	[0.15]	[0.19]	<0.38	<0.40
W	<0.38	<0.38	<0.37	<0.37	<1.8	<1.9
Y	<0.02	<0.02	<0.02	<0.02	<0.10	<0.11
3 M NaOH, Trial a						
Density	1.12	1.12	1.12	1.13	1.13	1.13
Al	144	969	1,120	1,246	1,272	1,331
B	<2.3	<2.3	<2.2	<2.3	<3.3	<2.3
Bi	<2.9	[3.4]	[3.0]	[3.3]	<6.0	[5.2]
Cd	<0.30	<0.30	[0.36]	<0.30	<0.33	[0.46]
Cr	[0.94]	10.0	17.8	28.2	53.4	91.6
Fe	<2.6	[3.4]	[4.8]	[4.5]	[5.4]	[6.7]
Mn	<0.26	<0.26	[0.25]	[0.28]	<0.25	<0.26
Na	70,740	70,729	69,514	69,801	71,995	72,653
P	[17.5]	[22.0]	[18.7]	[14.1]	[16.8]	[22.6]
S	<40.9	<41.2	<40.1	<40.7	<40.5	<41.3
Si	57.4	163	153	153	155	158
Sr	[0.11]	[0.08]	[0.08]	[0.09]	[0.13]	[0.18]
U	<10.5	[11.9]	[11.3]	[13.8]	[21.9]	[20.8]
Zn	[0.85]	[1.4]	[1.4]	[2.0]	[1.9]	[2.0]
Zr	<1.0	<1.0	<1.00	<1.0	<1.0	<1.0
Fluoride	9.7	10.9	11.4	12.1	11.8	12.2
Nitrite	<1.3	<1.4	[1.6]	[1.6]	<1.3	[1.8]
Nitrate	481	490	522	532	483	534
Phosphate	49.8	47.6	50.3	51.1	42.0	49.1
Sulfate	[2.8]	[1.0]	[1.0]	[1.1]	[1.6]	[0.7]

Table J.2 (Contd)

Analyte	Analyte Concentration and Density at Given Time After Cooling to Ambient (~21°C) Temperature; g/mL for Density; μg/mL for Metals and Anions; μCi/mL for Radionuclides					
	0 hr	1 hr	2 hr	4 hr	8 hr	24 hr
^{54}Mn						<6E-6
^{60}Co						<4E-6
^{137}Cs						0.794
^{152}Eu			Not Measured			<2E-5
^{154}Eu						<1E-5
^{155}Eu						<2E-4
^{241}Am						<2E-4
Opportunistic Analytes						
Ag	<0.53	<0.53	<0.52	<0.53	<0.52	<0.53
As	<8.7	<8.8	<8.6	<8.7	<8.7	<8.8
Ba	<0.42	<0.43	<0.42	<0.42	<0.42	<0.43
Be	<0.02	<0.02	<0.01	<0.02	<0.01	[0.02]
Ca	<2.6	<2.7	<2.6	<2.6	<2.6	<2.7
Ce	<1.5	<1.5	<1.5	<1.5	<1.5	<1.5
Co	<0.48	<0.49	<0.48	<0.48	<0.48	<0.49
Cu	[1.7]	[2.0]	[2.1]	[2.0]	[2.2]	[2.1]
Dy	<0.44	<0.44	<0.43	<0.44	<0.43	<0.44
Eu	<0.14	<0.14	<0.13	<0.14	<0.13	<0.14
K	<15.2	<15.3	<15.4	[17.1]	<15.1	[17.4]
La	<0.17	<0.17	<0.16	<0.17	<0.16	<0.17
Li	<0.68	<0.69	<0.67	<0.68	<0.67	<0.69
Mg	<0.88	<0.88	<0.86	<0.87	<0.87	<0.89
Mo	<0.82	<0.82	<0.80	<0.81	<0.81	<0.82
Nd	<2.1	<2.2	<2.1	<2.1	<2.1	<2.2
Ni	<0.73	<0.73	<0.71	<0.72	<0.72	<0.73
Pb	4.6	4.7	[6.8]	[8.7]	[8.1]	[7.6]
Pd	<1.6	<1.6	<1.5	<1.6	<1.6	<1.6
Rh	<3.2	<3.2	<3.1	<3.1	<3.1	<3.2
Ru	<1.0	<1.0	<1.0	<1.0	<1.0	<1.0
Sb	<3.9	<4.0	<3.9	<3.9	<3.9	<4.0
Se	<6.1	<6.2	<6.0	<6.1	<6.1	[11.9]
Sn	<2.5	<2.5	<2.5	<2.5	<2.5	2.5
Ta	[1.7]	<1.7	<1.6	<1.7	<1.6	[1.8]
Te	<3.9	<4.0	<3.9	<3.9	<3.9	<4.0
Th	<1.5	<1.5	<1.5	<1.5	<1.5	<1.5
Ti	<0.12	<0.12	<0.12	<0.12	<0.12	<0.12
Tl	<8.1	<8.2	<8.0	<8.1	<8.1	<8.2
V	<0.39	<0.40	<0.39	<0.39	<0.39	<0.40
W	<1.9	<1.9	<1.8	<1.9	<1.9	<1.9
Y	<0.11	<0.11	<0.10	<0.11	<0.10	<0.11

Table J.2 (Contd)

Analyte	Analyte Concentration and Density at Given Time After Cooling to Ambient (~21°C) Temperature; g/mL for Density; µg/mL for Metals and Anions; µCi/mL for Radionuclides					
	0 hr	1 hr	2 hr	4 hr	8 hr	24 hr
3 M NaOH, Trial b						
Density	1.13	1.13	1.13	1.13	1.13	1.13
Al	138	954	1,171	1,273	1,284	1,281
B	<2.3	<2.3	<2.3	<2.3	<2.3	<2.3
Bi	<2.9	[4.0]	[2.9]	<2.9	<2.9	<2.8
Cd	<0.30	<0.31	<0.30	<0.31	<0.30	[0.39]
Cr	[0.94]	9.6	17.7	27.1	50.5	88.1
Fe	<2.6	[3.1]	[4.3]	[4.6]	[5.4]	[6.3]
Mn	<0.26	<0.26	<0.26	[0.27]	<0.26	<0.26
Na	70,781	72,487	72,681	72,818	72,818	71,279
P	[21.2]	[22.9]	[18.9]	[13.8]	[14.5]	[10.8]
S	<40.9	<41.9	<41.1	<41.4	<40.8	<40.6
Si	58.1	162	159	156	156	154
Sr	[0.11]	[0.09]	[0.09]	[0.10]	[0.12]	[0.17]
U	<10.5	[13.9]	[14.9]	[18.1]	[19.6]	[18.9]
Zn	[0.91]	[1.6]	[1.4]	[1.7]	[1.8]	[1.7]
Zr	<1.0	<1.0	<1.0	<1.0	<1.0	<1.0
Fluoride	9.3	12.3	11.8	11.9	12.6	12.3
Nitrite	<1.4	[1.5]	[1.5]	<1.4	<1.4	[1.8]
Nitrate	484	550	508	577	518	534
Phosphate	46.2	54.4	51.6	51.3	51.3	49.0
Sulfate	[0.90]	[3.4]	<2.0	[0.89]	[0.83]	[0.72]
^{54}Mn						<6E-6
^{60}Co						<4E-6
^{137}Cs						0.796
^{152}Eu			Not Measured			<2E-5
^{154}Eu						<1E-5
^{155}Eu						<2E-4
^{241}Am						<2E-4
Opportunistic Analytes						
Ag	<0.53	<0.54	<0.53	<0.54	<0.53	<0.53
As	<8.7	<8.9	<8.8	<8.8	<8.7	<8.7
Ba	<0.42	<0.43	<0.43	<0.43	<0.42	<0.42
Be	<0.02	<0.02	<0.02	<0.02	<0.02	[0.02]
Ca	<2.6	<2.7	<2.6	<2.7	<2.6	<2.6
Ce	<1.5	<1.5	<1.5	<1.5	<1.5	<1.5
Co	<0.48	<0.50	<0.49	<0.49	<0.48	<0.48
Cu	[1.6]	[1.9]	[2.0]	[2.1]	[2.1]	[2.1]
Dy	<0.44	<0.45	<0.44	<0.44	<0.44	<0.44
Eu	<0.14	<0.14	[0.16]	<0.14	<0.14	<0.14
K	[17.8]	[23.5]	<15.3	<15.4	<15.2	[19.8]
La	<0.17	<0.17	<0.17	<0.17	<0.17	<0.17
Li	<0.68	<0.70	<0.68	<0.69	<0.68	<0.68

Table J.2 (Contd)

Analyte	Analyte Concentration and Density at Given Time After Cooling to Ambient (~21°C) Temperature; g/mL for Density; µg/mL for Metals and Anions; µCi/mL for Radionuclides					
	0 hr	**1 hr**	**2 hr**	**4 hr**	**8 hr**	**24 hr**
Mg	<0.88	<0.90	<0.88	<0.89	<0.88	<0.87
Mo	<0.82	<0.84	<0.82	<0.83	<0.82	<0.81
Nd	<2.1	<2.2	<2.2	<2.2	<2.1	<2.1
Ni	<0.73	<0.74	<0.73	<0.73	<0.73	<0.72
Pb	<4.6	[5.6]	[7.9]	[7.3]	[5.1]	[7.2]
Pd	<1.6	<1.6	<1.6	<1.6	<1.6	<1.6
Rh	<3.2	<3.2	<3.2	<3.2	<3.2	<3.1
Ru	<1.0	<1.1	<1.0	<1.0	<1.0	<1.0
Sb	<3.9	<4.0	<4.0	<4.0	<3.9	<3.9
Se	<6.1	[12.4]	[9.4]	<6.2	<6.1	<6.1
Sn	<2.5	[2.7]	<2.5	[2.6]	<2.5	[2.6]
Ta	<1.7	<1.7	[3.0]	<1.7	[1.8]	[2.7]
Te	<3.9	<4.0	<4.0	<4.0	<3.9	<3.9
Th	<1.5	<1.5	<1.5	<1.5	<1.5	<1.5
Ti	<0.12	<0.12	<0.12	<0.12	<0.12	<0.12
Tl	<8.1	<8.3	<8.2	<8.2	<8.1	<8.1
V	<0.39	<0.40	<0.40	<0.40	<0.39	<0.39
W	<1.9	<1.9	<1.9	<1.9	<1.9	<1.9
Y	<0.11	<0.11	<0.11	<0.11	<0.11	<0.11
3 M NaOH, Trial c						
Density	1.13	1.14	1.13	1.12	1.14	1.12
Al	132	849	1,076	1,240	1,360	1,323
B	<2.3	<2.2	<2.2	<2.3	<2.3	<2.2
Bi	[4.6]	[5.1]	[5.9]	[3.6]	[5.8]	[4.6]
Cd	<0.31	<0.30	<0.30	<0.30	[0.40]	<0.29
Cr	[0.61]	8.8	15.5	24.6	47.7	83.0
Fe	<2.6	[2.8]	[3.9]	[4.2]	[5.2]	[6.1]
Mn	<0.26	<0.25	<0.25	<0.26	<0.26	<0.25
Na	72,755	70,629	71,129	71,491	72,134	69,642
P	[19.6]	[16.1]	[21.3]	[18.1]	[18.3]	[16.2]
S	<41.3	<40.3	<40.1	<40.8	<41.3	<39.2
Si	61.4	156	152	151	150	142
Sr	[0.10]	[0.08]	[0.08]	[0.09]	[0.13]	[0.17]
U	<10.6	[11.3]	[12.4]	[18.7]	[15.0]	[16.0]
Zn	[0.98]	[2.0]	[1.6]	[1.8]	[1.6]	[2.1]
Zr	<1.0	<1.00	<0.99	<1.0	<1.0	<1.0
Fluoride	9.6	12.0	12.5	12.1	10.5	12.3
Nitrite	<1.34	[1.4]	[1.6]	<1.4	<1.4	[2.0]
Nitrate	516	540	547	548	582	545
Phosphate	47.0	51.9	51.9	50.3	55.0	50.8
Sulfate	[0.85]	[0.96]	[1.0]	[0.96]	<0.68	<0.66

Table J.2 (Contd)

Analyte	Analyte Concentration and Density at Given Time After Cooling to Ambient (~21°C) Temperature; g/mL for Density; µg/mL for Metals and Anions; µCi/mL for Radionuclides					
	0 hr	**1 hr**	**2 hr**	**4 hr**	**8 hr**	**24 hr**
^{54}Mn						<1E-5
^{60}Co						<3E-6
^{137}Cs						0.810
^{152}Eu			Not Measured			<1E-5
^{154}Eu						<2E-5
^{155}Eu						<1E-4
^{241}Am						<6E-5
Opportunistic Analytes						
Ag	<0.53	<0.52	<0.52	<0.53	<0.53	<0.51
As	<8.8	<8.6	<8.6	<8.7	<8.8	<8.4
Ba	<0.43	<0.42	<0.41	<0.42	<0.43	<0.41
Be	<0.02	<0.01	<0.01	<0.02	[0.02]	[0.02]
Ca	<2.7	<2.6	<2.6	<2.6	<2.7	<2.5
Ce	<1.5	<1.5	<1.5	<1.5	<1.5	<1.4
Co	<0.49	<0.48	<0.47	<0.48	<0.49	<0.46
Cu	[1.7]	[3.0]	[2.0]	[2.1]	[2.0]	[2.1]
Dy	<0.44	<0.43	<0.43	<0.44	<0.44	<0.42
Eu	<0.14	<0.13	<0.13	<0.14	<0.14	<0.13
K	[22.0]	[18.8]	[21.9]	[25.9]	[25.1]	[22.1]
La	<0.17	<0.16	<0.16	<0.17	<0.17	<0.16
Li	<0.69	<0.67	<0.67	<0.68	<0.69	<0.65
Mg	<0.89	<0.86	<0.86	<0.87	<0.89	<0.84
Mo	<0.83	<0.80	<0.80	<0.81	<0.83	<0.78
Nd	<2.2	<2.1	<2.1	<2.1	<2.2	<2.1
Ni	<0.73	<0.72	<0.71	<0.72	<0.73	<0.70
Pb	<4.7	[6.3]	[6.2]	[6.3]	[7.3]	[8.4]
Pd	<1.6	<1.5	<1.5	<1.6	<1.6	<1.5
Rh	<3.2	<3.1	<3.1	<3.2	<3.2	<3.0
Ru	<1.04	<1.01	<1.01	<1.03	<1.04	<0.99
Sb	<4.0	<3.9	<3.9	<3.9	<4.0	[3.8]
Se	<6.2	<6.0	<6.0	<6.1	<8.9	<5.9
Sn	<2.5	[3.6]	<2.5	<2.5	<2.5	<2.4
Ta	[3.4]	<1.6	[2.4]	<1.7	[1.9]	<1.6
Te	<4.0	<3.9	<3.9	<3.9	<4.0	<3.8
Th	<1.5	<1.5	<1.5	<1.5	<1.5	<1.4
Ti	<0.12	<0.12	<0.12	<0.12	<0.12	<0.12
Tl	<8.2	<8.0	<8.0	<8.1	<8.2	<7.8
V	<0.40	<0.39	<0.39	<0.39	<0.40	<0.38
W	<1.9	<1.8	<1.8	<1.9	<1.9	<1.8
Y	<0.11	<0.10	<0.10	<0.11	<0.11	<0.10

Table J.2 (Contd)

Analyte	Analyte Concentration and Density at Given Time After Cooling to Ambient (~21°C) Temperature; g/mL for Density; µg/mL for Metals and Anions; µCi/mL for Radionuclides					
	0 hr	**1 hr**	**2 hr**	**4 hr**	**8 hr**	**24 hr**
5 NaOH						
Density	1.20	1.19	1.19	1.20	1.20	1.19
Al	276	940	1,182	1,304	1,364	1,349
B	<2.3	<2.3	<2.3	<2.3	<2.3	<2.3
Bi	[6.0]	[3.3]	[5.8]	<2.8	[7.8]	[6.1]
Cd	<0.30	[0.33]	<0.30	[0.54]	[0.60]	[0.82]
Cr	[2.50]	10.6	20.4	31.8	61.9	87.3
Fe	<2.5	[5.5]	[7.9]	[8.4]	[15.0]	[9.5]
Mn	[0.26]	[0.48]	[0.91]	[1.35]	[0.36]	<0.259
Na	116,147	116,378	114,536	115,747	116,897	115,021
P	[22.6]	[25.8]	[20.6]	[18.9]	[17.4]	[24.4]
S	<40.8	<41.0	<41.0	<40.5	<40.6	<41.2
Si	87.2	171	185	190	205	207
Sr	0.5	0.4	0.4	0.3	0.3	0.5
U	[11.5]	<10.5	[10.9]	[16.5]	[17.7]	[18.6]
Zn	[1.1]	[1.7]	[2.2]	[2.3]	[2.4]	[2.5]
Zr	<1.0	<1.0	<1.0	<1.0	<1.0	<1.0
Fluoride	16.8	7.2	13.6	[13.3]	13.4	14.1
Nitrite	<1.4	<1.4	<1.4	<1.4	<1.34	<1.4
Nitrate	542	597	554	577	574	573
Phosphate	66.6	65.0	62.8	63.6	64.8	66.3
Sulfate	<0.67	<0.66	[0.95]	[1.1]	[0.96]	[1.0]
^{54}Mn						<7E-6
^{60}Co						<4E-6
^{137}Cs						0.939
^{152}Eu			Not Measured			<2E-5
^{154}Eu						<1E-5
^{155}Eu						<2E-4
^{241}Am						<2E-4
Opportunistic Analytes						
Ag	<0.53	<0.53	<0.53	<0.52	<0.53	<0.53
As	<8.7	<8.7	<8.7	<8.7	<8.7	<8.8
Ba	<0.42	<0.42	<0.42	<0.42	<0.42	<0.43
Be	<0.02	<0.02	<0.02	<0.01	<0.02	[0.02]
Ca	[6.9]	[5.2]	[11.5]	[8.4]	[6.3]	[4.3]
Ce	<1.5	<1.5	<1.5	<1.5	<1.5	<1.5
Co	<0.48	<0.48	<0.48	<0.48	<0.48	<0.49
Cu	[1.8]	[2.1]	[2.2]	[2.2]	[2.3]	[2.4]
Dy	<0.44	<0.44	<0.44	<0.43	<0.44	<0.44
Eu	<0.14	<0.14	<0.14	<0.13	<0.14	<0.14
K	[19.6]	[27.6]	[36.4]	[42.0]	[48.1]	[51.9]
La	<0.17	<0.17	<0.17	<0.16	<0.17	<0.17

Table J.2 (Contd)

Analyte	Analyte Concentration and Density at Given Time After Cooling to Ambient (~21°C) Temperature; g/mL for Density; µg/mL for Metals and Anions; µCi/mL for Radionuclides					
	0 hr	**1 hr**	**2 hr**	**4 hr**	**8 hr**	**24 hr**
Li	<0.68	<0.68	<0.68	<0.67	<0.68	<0.69
Mg	<0.87	<0.88	<0.88	<0.87	<0.87	<0.88
Mo	<0.81	<0.82	<0.82	<0.81	<0.81	<0.82
Nd	<2.1	<2.2	<2.2	<2.1	<2.1	<2.2
Ni	<0.72	<0.73	<0.73	<0.72	<0.72	<0.73
Pb	<4.6	[7.0]	[7.3]	[5.7]	[8.7]	[8.2]
Pd	<1.6	<1.6	<1.6	<1.6	<1.6	<1.6
Rh	<3.2	<3.2	<3.2	<3.1	<3.1	<3.2
Ru	<1.0	<1.0	<1.0	<1.0	<1.0	<1.0
Sb	<3.9	<3.9	<3.9	[5.7]	<3.9	[4.6]
Se	<6.1	[11.8]	<6.1	<6.1	[6.3]	[9.2]
Sn	<2.5	2.5	[3.6]	[2.5]	<2.5	<2.5
Ta	<1.7	<1.7	<1.7	<1.6	<1.7	[2.7]
Te	<3.9	<4.0	<4.0	<3.9	<3.9	<4.0
Th	<1.5	<1.5	<1.5	<1.5	<1.5	<1.5
Ti	<0.12	<0.12	<0.12	<0.12	<0.12	<0.12
Tl	<8.1	<8.1	<8.1	<8.1	<8.1	<8.2
V	<0.39	<0.39	<0.39	<0.39	<0.39	<0.40
W	<1.9	<1.9	<1.9	<1.9	<1.9	<1.9
Y	<0.11	<0.11	<0.11	<0.10	<0.11	<0.11

Table J.3. Analyte Concentrations as a Function of Time for Leaching at 100ºC

Analyte	Analyte Concentration and Density at Given Time After Cooling to Ambient (~21°C) Temperature; g/mL for Density; µg/mL for Metals and Anions; µCi/mL for Radionuclides					
	0 hr	**1 hr**	**2 hr**	**4 hr**	**8 hr**[(a)]	**24 hr**
3 M NaOH						
Density	1.13	1.16	1.16	1.17	1.17	1.18
Al	111	1,324	1,451	1,472	1,908	1,515
B	<2.4	<2.4	<2.4	<2.4	<3.0	<2.3
Bi	<3.0	[7.3]	[6.4]	[8.3]	[6.3]	[7.7]
Cd	<0.32	<0.32	[0.45]	[0.57]	[0.95]	[0.59]
Cr	[0.82]	21.2	37.0	65.8	120.2	107.4
Fe	<2.7	[6.4]	[7.1]	[7.9]	[11.4]	[8.6]
Mn	<0.27	[1.3]	[1.2]	[0.76]	<0.34	<0.26
Na	72,985	75,613	75,943	74,704	97,382	75,615
P	[22.7]	[21.1]	[16.4]	[19.7]	[19.7]	[20.7]
S	<42.7	<43.1	<43.5	<43.0	<53.3	<41.7
Si	53.7	175	175	179	233	186
Sr	[0.13]	[0.10]	[0.13]	[0.17]	0.3	0.3
U	<10.9	[24.9]	[22.5]	[20.7]	[24.8]	[17.6]
Zn	[1.5]	[2.2]	[2.3]	[2.7]	[3.9]	[3.1]
Zr	<1.1	<1.1	<1.1	<1.1	<1.3	<1.0
Fluoride	13.1	13.0	11.5	13.8	14.0	14.1
Nitrite	<1.4	[1.7]	<0.72	[2.2]	[2.3]	[2.2]
Nitrate	503	560	327	613	591	568
Phosphate	52.8	52.3	50.8	52.2	51.7	49.3
Sulfate	<0.69	[1.0]	[0.56]	[0.74]	<0.69	[0.80]
^{54}Mn						<6E-6
^{60}Co						<4E-6
^{137}Cs						0.905
^{152}Eu			Not Measured			<2E-5
^{154}Eu						<1E-5
^{155}Eu						<2E-4
^{241}Am						<2E-4
Opportunistic Analytes						
Ag	<0.55	<0.56	<0.56	<0.56	<0.69	<0.54
As	<9.1	<9.2	<9.3	<9.2	<11.4	<8.9
Ba	<0.44	<0.45	<0.45	<0.45	<0.55	<0.43
Be	<0.02	<0.02	[0.02]	<0.02	[0.02]	<0.02
Ca	[2.9]	[3.8]	[3.0]	[3.0]	[4.7]	[3.1]
Ce	<1.6	<1.6	<1.6	<1.6	<2.0	<1.5
Co	<0.51	<0.51	<0.51	<0.51	<0.63	<0.49
Cu	[1.8]	[2.3]	[2.2]	[2.2]	[3.0]	[2.4]
Dy	<0.46	<0.46	<0.47	<0.46	<0.57	<0.45
Eu	<0.14	<0.14	<0.14	<0.14	<0.18	<0.14
K	[37.9]	[38.3]	[41.8]	[41.3]	[24.4]	[23.1]
La	<0.17	<0.18	<0.18	<0.17	<0.22	<0.17
Li	<0.71	<0.72	<0.72	<0.72	<0.89	<0.69

Table J.3 (Contd)

Analyte	Analyte Concentration and Density at Given Time After Cooling to Ambient (~21°C) Temperature; g/mL for Density; μg/mL for Metals and Anions; μCi/mL for Radionuclides					
	0 hr	1 hr	2 hr	4 hr	8 hr[a]	24 hr
Mg	<0.92	<0.93	<0.93	<0.92	<1.14	<0.90
Mo	<0.85	<0.86	<0.87	<0.86	<1.06	<0.83
Nd	<2.2	<2.3	<2.3	<2.3	<2.8	<2.2
Ni	<0.76	<0.77	<0.77	<0.76	<0.95	<0.74
Pb	<4.8	[7.3]	[7.1]	[7.9]	[11.0]	[9.3]
Pd	<1.6	<1.7	<1.7	<1.7	<2.1	<1.6
Rh	<3.3	<3.3	<3.4	<3.3	<4.1	<3.2
Ru	<1.1	<1.1	<1.1	<1.1	<1.3	<1.0
Sb	<4.1	<4.1	<4.2	<4.1	<5.1	<4.0
Se	<6.4	<6.5	<6.5	<6.4	[8.3]	[7.4]
Sn	<2.6	<2.6	<2.7	<2.6	[4.3]	2.6
Ta	<1.7	<1.8	<1.8	<1.7	<2.2	<1.7
Te	<4.1	<4.2	<4.2	<4.1	<5.1	<4.0
Th	<1.5	<1.6	<1.6	<1.6	<1.9	<1.5
Ti	<0.13	<0.13	<0.13	<0.13	<0.16	<0.12
Tl	<8.5	<8.6	<8.6	<8.5	<10.6	<8.3
V	<0.41	<0.41	<0.42	<0.41	<0.51	<0.40
W	<2.0	<2.0	<2.0	<2.0	<2.4	<1.9
Y	<0.11	<0.11	<0.11	<0.11	<0.14	<0.11

(a) The accuracy of the 8-h leachate concentrations is suspect because the analyte values appear to be biased high even though the mass of the aliquot added was lower than expected.

Table J.4. Analyte Concentrations for Composite Wash Solution for Wash of Samples Leached at 80ºC in 3 M NaOH

Analyte	Concentration (µg/mL)	Opportunistic Analytes	Concentration (µg/mL)
Al	103	Ag	<0.112
B	<0.485	As	<1.85
Bi	<0.607	Ba	[0.212]
Cd	<0.064	Be	<0.003
Cr	7.30	Ca	<0.559
Fe	<0.543	Ce	<0.318
Mn	<0.055	Co	<0.103
Na	5,399	Cu	1.79
S	<8.69	Dy	<0.093
Si	13.6	Eu	<0.029
Sr	[0.016]	K	<3.236
U	<2.23	La	<0.035
Zn	[0.836]	Li	<0.145
Zr	<0.215	Mg	<0.186
Fluoride	[0.812]	Mo	<0.174
Nitrite	<1.56	Nd	<0.456
Nitrate	470	Ni	<0.154
Phosphate	[4.50]	P	[2.09]
Sulfate	[0.812]	Pb	<0.983
		Pd	<0.334
		Rh	<0.672
		Ru	<0.219
		Sb	<0.836
		Se	<1.30
		Sn	[0.546]
		Ta	[0.354]
		Te	<0.839
		Th	<0.315
		Ti	<0.026
		Tl	<1.73
		V	<0.084
		W	<0.399
		Y	<0.022

Appendix K

CUF Filtration/Leaching Experimental Methods and Analyses

Appendix K: CUF Filtration/Leaching Experimental Methods and Analyses

This appendix describes the experimental equipment and analyses used to perform the bench top filtration and leaching tests with both the Group 1 and 2 composite waste samples using the CUF filtration skid, described in Section 5 of this report.

K.1 Filtration/Leaching Apparatus

The testing apparatus is a bench top skid that allows up to 4-liters of a waste solution to be circulated through a tubular filter. The apparatus can simultaneously measure the filter feed flow rates, filtrate flow rates, system pressures, and temperatures. The testing skid uses a heat exchanger on the main flow loop to cool the feed solution during filtration operations, and it has a heater on the main holding tank to perform leaching at elevated temperatures.

K.1.1 Cell Unit Filter

The WTP Pre-Treatment facility will use cross flow ultrafiltration to separate the LAW liquid streams from the HLW slurry streams. The filter elements to be used are called CUFs and are simply porous sintered metal tubes that the filter feed flows through axially while the permeate passes through the tube walls radially. Filtration occurs when sufficient pressure is applied to the filter feed flowing through the element to drive the slurry permeate through the tubular walls. Because the filter feed is flowing across the filter walls, solid buildup is minimized allowing filtration to occur continuously with minimal downtime for back-pulsing.

The filters used in this testing work were obtained from the Mott Corporation,[a] using the same specifications[b] for the filters being purchased for the WTP-Pretreatment Facility. The dimensions of the filter element used in this test are shown in Figure K.1.
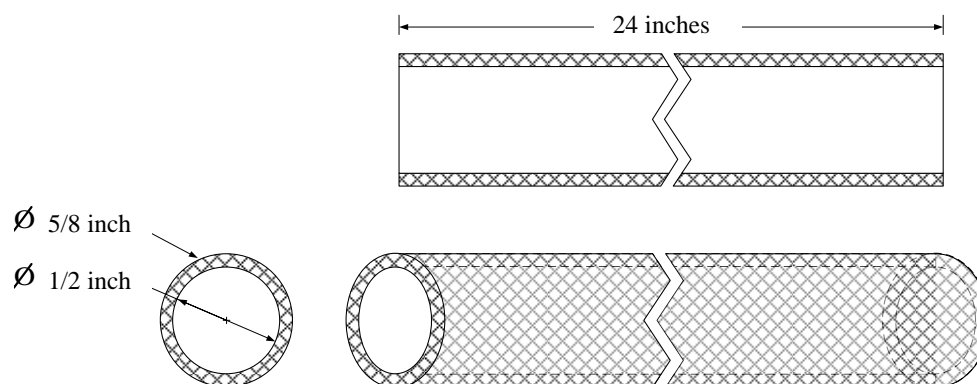
Figure K.1. Illustration of the Filter Element

The as-received filter element was installed in a shell-in-tube configuration with an outer tube surrounding the filter element to capture the filtrate while the inlet and outlet of the filter were welded to steel tubing of the matching outer/inner diameter that extends past the shell, and this provides access to the inside diameter of the filter. The shell side had two $^3/_8$-inch stainless tubes exiting from the filter assembly; one is in the center to collect filtrate from the filter, and the other is near the inlet of the filter to function as a drain. Pressure ports (¼-inch stainless tubing) were installed on the inlet and outlet connections to the assembly to measure the pressure inside the filter. VCO Swagelok fittings were also placed on the inlet and outlet filter feed tube connections for easy installation to the filtration/leaching skid. Figure K.2 and Figure K.3 show the filter assembly tested.
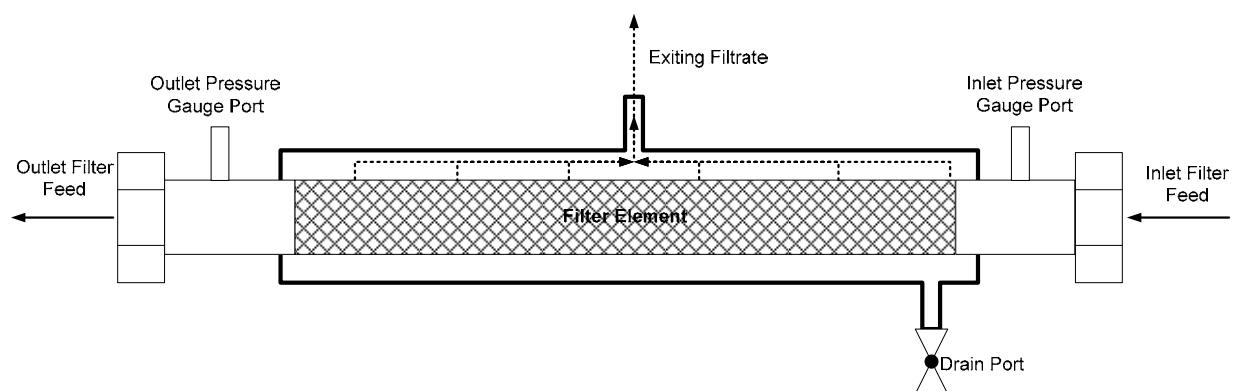
Figure K.2. Illustration of the Filter Assembly Sketch (*Not to Scale*)

Figure K.3. Photograph of the Filter Assembly

K.1.1.1 Filtration/Leaching Skid

The filter described in the section above is installed in a bench top skid that circulates the test waste slurries through the inside of the filter and diverts the filter permeate to a collection bottle or recycles it back into the slurry. Figure K.4 shows a piping diagram of the testing skid. Figure K.5 and Figure K.6 are electronic photographs of the assembled system before and after installation into a hot cell in the Shielded Analytical Laboratory where the testing was performed.
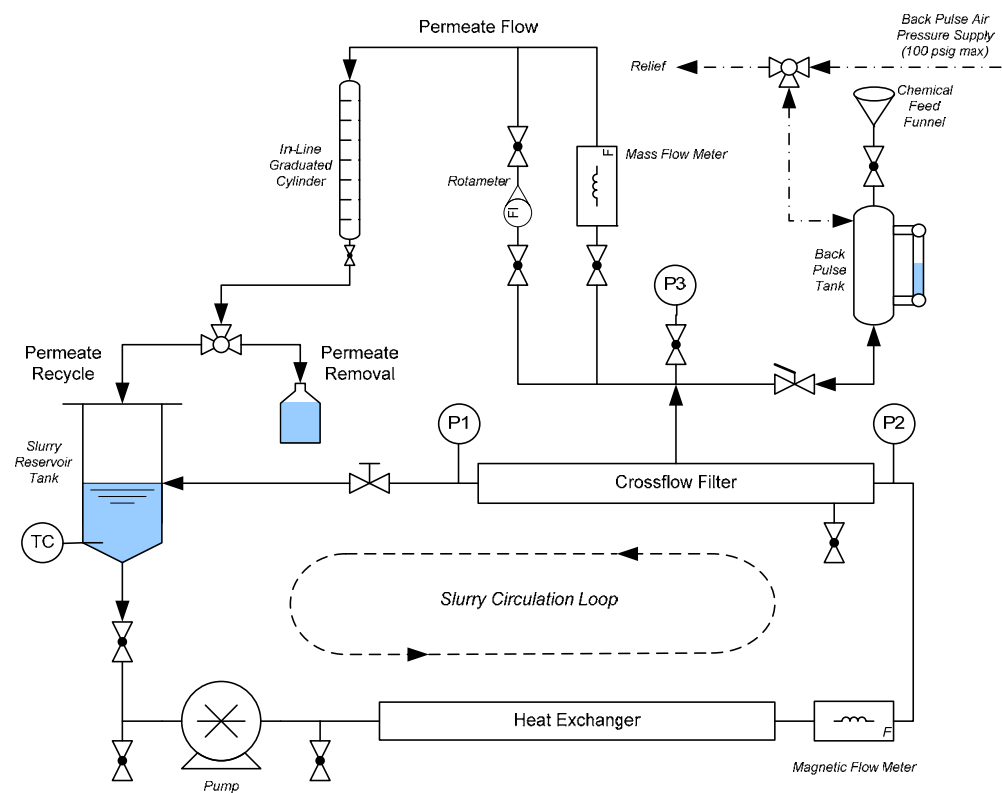
Figure K.4. Piping Diagram of CUF Skid
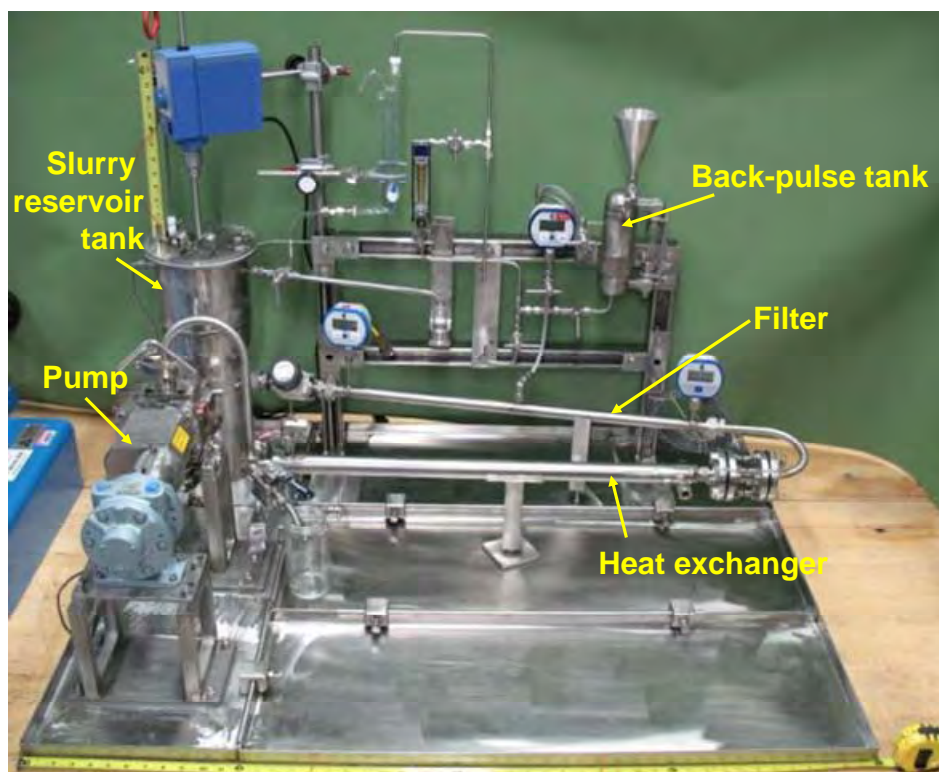
Figure K.5. Photograph of the CUF Testing Skid Prior to Hot Cell Installation
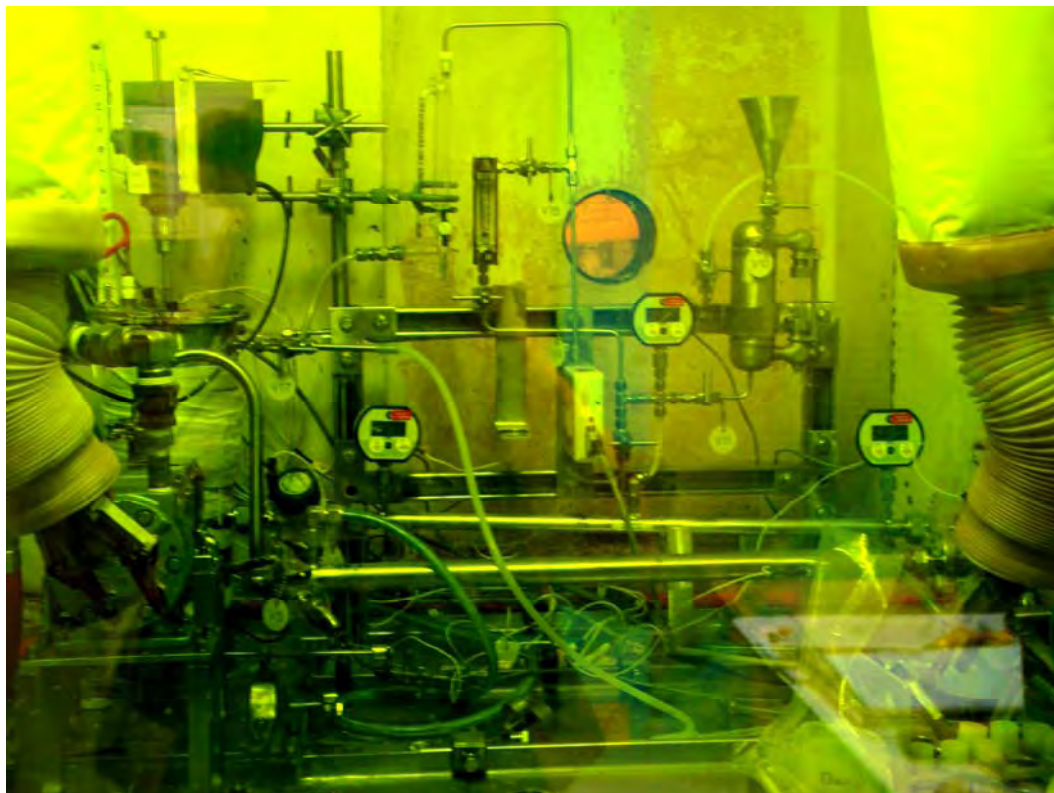
Figure K.6. Picture of Test Skid Installed in Cell 5 of the Shielded Analytical Laboratory

The CUF skid has four main parts:

- Slurry reservoir tank

- Slurry recirculation loop

- Permeate flow loop

- Permeate back pulse chamber.

The *slurry reservoir* is a cylindrical stainless steel tank with a 4-L capacity. Agitation in the tank is provided from an overhead mixer using a 2-inch diameter 3-blade marine propeller. Baffles are also installed inside the tank wall to make sure that the slurry is mixed homogenously. Heat tape is installed around the walls of the tank for leaching at elevated temperatures. The heat tape is connected to a temperature controller that adjusts the electrical load to the heat tape based on a thermocouple input. A duel Type-K thermocouple is installed inside the reservoir tank (extruding just below the overhead mixing impeller) to measure the temperature of the slurry inside the reservoir. One of the thermocouple elements is connected to the heat tape's temperature controller and the other to a data-collection system. To allow the system to be easily drained, the bottom of the vessel is sloped at a 15° angle.

The *slurry recirculation loop* directs slurry flow from the slurry reservoir, through the CUF filter assembly, and back into the reservoir for filtration operations. The bottom of the slurry reservoir feeds into the connection piping for the slurry recirculation pump—a positive displacement rotary lobe pump. The pump is driven with an air motor that is supplied with compressed air from an exterior air

compressor. The speed of the pump is controlled by an exterior air regulator controlling the pressure of the compressed air feed to the air motor. An optical tachometer measures the speed of the pump by measuring the rotational speed of the connection coupling between the air motor and the pump, which had a piece of reflective tape placed on it. The discharge of the pump flows through a single-pass shell-and-tube heat exchanger used to remove excess heat from the system because of frictional flow.

An exterior chiller circulates chilled fluid (water/anti-freeze mixture) through the exterior shell of the heat exchanger to pull heat away from the circulating slurry on the tube side of the heat exchanger. The chiller controllers the chilling fluid temperature by monitor the temperature of the slurry exiting the heat exchanger via a resistance temperature device installed in the discharge line.

The slurry then flows through a magnetic flow sensor that monitors the volumetric flow of the slurry inside the slurry recirculation loop. The sensor's output is displayed on an external panel meter that generates an analog output signal monitored by a data-collection system. The data from this device are used to calculate the axial velocity inside the filter element.

The flowing slurry then enters the filter assembly. Digital pressure gauges are installed on the inlet and outlet port of the filter, which displays the pressure at both locations in pounds per inch squared, gauge (psig). The gauges also transmit analog output signals monitored by a data-collection system. The data from these devices are used to calculate the average pressure inside the filter and the axial pressure drop across the element.

At the discharge of the filter is a manual pinch valve. The valve is used to adjust the pressure inside the filter to drive permeate flow through the filter membrane wall. It is also connected to the slurry reservoir tank and is closed completely when the tank is isolated for leaching.

The *permeate flow loop* begins at the center of the filter assembly where a poly-line connects the filter to a manifold of ¼-inch stainless steel piping that directs the filter permeate through a series of measurement devices before either returning to the slurry reservoir tank, or to a sample container to capture dewatered permeate. A digital pressure gauge is installed at this point to measure the pressure on the permeate side of the filter in psig. Like the other two digital gauges, this instrument transmits an analog output to a data-collection system. The pressure drop across the filter is then calculated by subtracting the pressure on the permeate side of the filter from the average pressure of the slurry inside the filter. This term is called the transmembrane pressure.

Flow from the filter is either diverted through a mass flow meter calibrated up to 180 mL/min or to a user-calibrated rotometer that can measure flow up to 30 mL/s. The mass flow meter also can measure the density of the permeate flow and sends two analog output signals to the data-collection system for the volumetric flow rate and the density. The rotometer is a manual read-out device that is user calibrated. To confirm the volumetric flow rate, an in-line glass cylinder was installed on the discharge of both meters to take manual measurements of the permeate flow. Measurements are taken by closing a valve at the bottom of the cylinder and allowing the permeate to fill the vessel. The volume of the glass vessel is marked on the outside, so the change in permeate volume in the cylinder can be quantified over a time interval.

Flow from the glass cylinder goes through a 3-way valve. This valve directs flow either back to the slurry reservoir tank to be mixed back to the slurry or to a sampling hose that is used to transfer the permeate into a sample container.

The *permeate back pulse chamber* is to the right of the permeate flow loop and is connected to the filter at the same location as the permeate pressure gauge. The chamber is an approximately 500-mL steel vessel with a sight-glass to track the volume inside the chamber. The vessel has three entry ports, a ¼-inch port on the bottom from the permeate side of the filter, a ¼-inch line from a funnel on top, and a ¼-inch line from a compressed air line on the side of the vessel. The bottom line is used to fill the chamber with permeate from the filter and also to send pressurized permeate backwards to the filter as a back pulse. The funnel on the top of the chamber is used to introduce cleaning and rinse solutions directly to the vessel. The compressed gas line is the source of the pressure for the back pulse. Once the chamber is half full of permeate, compressed gas is introduced to the chamber to pressurize the fluid. The chamber is then isolated, and the slurry pressure drops below the pressure of the compressed gas line. The valve at the bottom of the tank is opened, and the pressurized permeate inside the chamber is allowed to flow backwards through the filter. After the back pulse is completed, the chamber is vented to atmospheric pressure through a 3-way valve that either sends compressed gas to the chamber or to a vent line inside the slurry reservoir tank.

K.1.1.2 Instrumentation and Data-Acquisition System

Because the system was to be operated in a hot cell, one of the design goals of the skid was to minimize the number of manual measurements during testing and record the data in an electronic format that could be analyzed readily with other approved software. Most of the sensors on the skid transmit analog data to an external data acquisition collection system (DACS), manufactured by National Instruments. This system relayed the analog data to a LabView data-collection program operating on a computer desktop system using Windows XP, service pack 2. The software program scales the analog data and simultaneously records the data electronically and displays it on the computer's monitor. The performance of the software was verified by test plan RPP-WTP-QA-010, and all reportable data are measured on calibrated instrumentation, including the external DACS board. Figure K.7 shows a diagram of the electronic sensors attached to the DACS, and Figure K.8 displays the screen windows from the data-collection program.

K.1.1.3 Operations of CUF Skid and Sampling

The CUF skid was developed to operate in several different operational modes to simulate the filtration and leaching processes of the WTP Pre-treatment system. The slurry can be filtered with two methods—recycle and dewatering. During recycling operations, permeate is returned to the slurry reservoir tank to maintain a steady-state UDS. The slurry is operated in this mode to understand how the effects of time, pressure, and axial velocity impact filtration of the slurry while maintaining its physical properties. During dewatering operations, permeate from the filter is diverted to a collection vessel, usually operating the system at a constant pressure and flow rate. Removing permeate from the slurry increases the UDS concentration and can change the rheological and filtration properties.
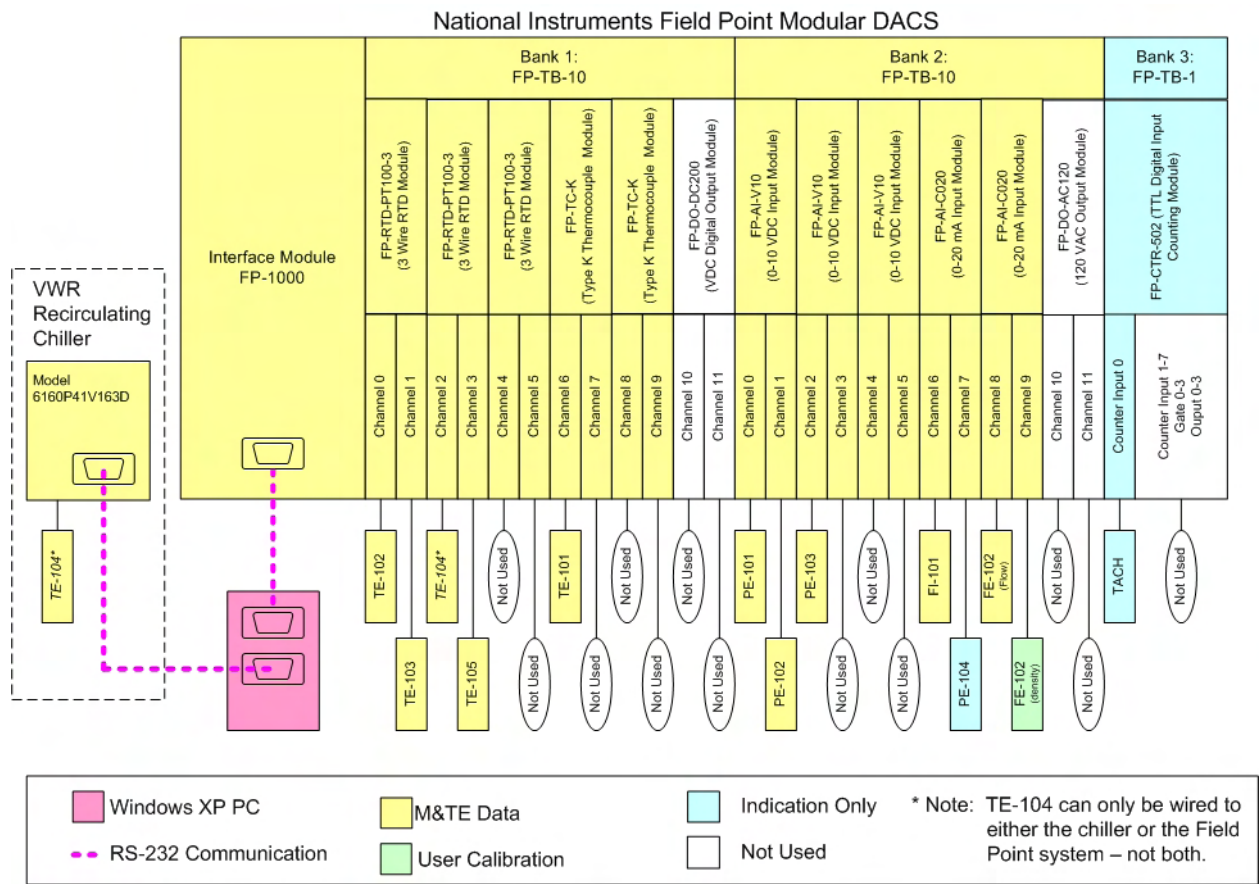
Figure K.7. Diagram of DACS System

Chemical leaching can occur in the slurry reservoir tank when the slurry circulation lines are isolated from the tank. However, to place the slurry in the tank with the valves to the piping closed requires that the slurry and permeate inside the skid be drained first. Once the waste slurry has been removed, the tank is then isolated, and the drained slurry/permeate is returned to the slurry reservoir tank. When the leach is to occur at elevated temperatures, the temperature controller is programmed to create a heating profile to simulate the heat ramp, soak, and cool down of the reaction vessel.

Samples are collected throughout testing to measure the physical and chemical properties of the waste slurry or permeate. Slurry samples are collected from two separate locations on the system. Small slurry samples (20-mL) are collected from the top of the slurry reservoir with the mixer operating using either a polymer or glass pipette 18 inches long, depending on the slurry temperature. The tips of the pipettes are cut at an angle to allow slurry to flow into the pipette to prevent being plugged. Larger samples (100 mL), such as rheology, can be captured using the drain valve on the pump discharge while the pump is running. Permeate samples are collected during dewatering operations directly from the dewatering sample hose. However, permeate collected during leaching operations is more difficult. A slurry sample is initially collected from the slurry reservoir using a pipette described earlier. Next, the sample is filtered through a 0.45-µm nylon or polytetraflouroethylene syringe filter. Permeate samples such as these are collected to measure the kinetics during leaching operations, which requires removing the leaching solution from the solids in the slurry.
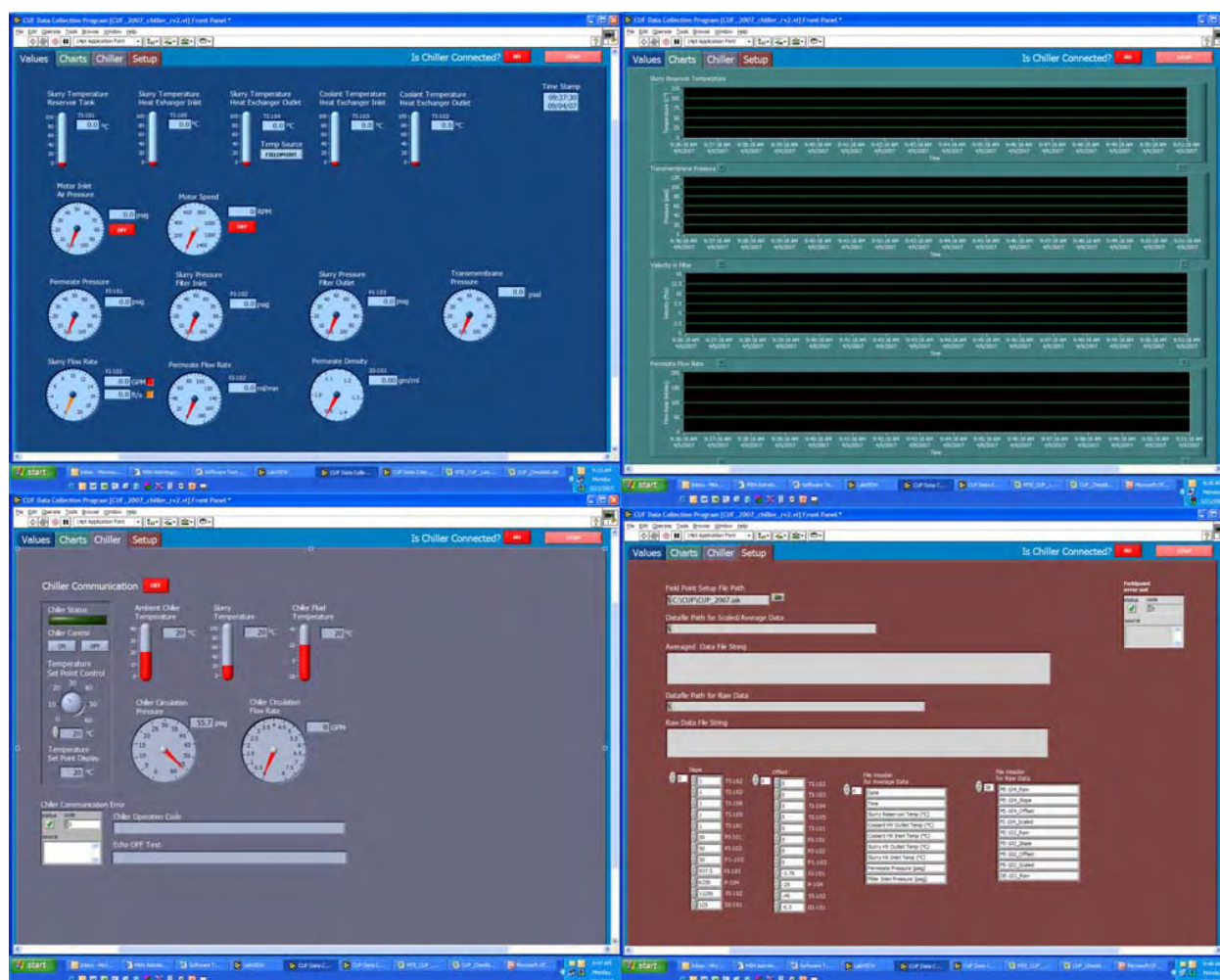
Figure K.8. Digital Images of DACS Display Windows

K.1.1.4 Baseline Testing of Filter

Before testing with HLW composite waste, the skid and the filter were initially cleaned with a laboratory cleaning solution (Alconox[a] at 1:100 dilution) and rinsed with DI water to remove cutting oils and soils from the skid fabrication process and shipping from the manufacturer. After cleaning, the filter flux was measured with a solution of 0.01 M NaOH—this is referred to as the *clean water flux*. Testing was performed at 10, 15, and 20 transmembrane pressure (TMP) at an axial velocity of 11 fps. Each pressure condition was held for 20 minutes, with a single back-pulse performed before changing the pressure. Next, a strontium carbonate ($SrCO_3$) slurry was prepared to test the filter flux with a slurry solution. As before, the $SrCO_3$ slurry was placed in the filtration skid and was operated with the permeate recycling back into the slurry reservoir. Testing was performed at 10, 20, and 30 TMP at an axial velocity of 11 fps. A single back pulse was performed between each test condition. Afterwards, the slurry was removed

---

(a) Alconox, Inc., 30 Glenn Street, Suite 309, White Plains, NY 10603 USA.

and rinsed out with DI water (approximately 10 L). The clean water flux was again tested with a solution of 0.01 M NaOH to verify that the filter was clean before testing with HLW slurries.

The results of the baseline filter flux testing are shown in Figure K.9. Overall, the baseline flux for the filter was demonstrated to be considerably higher than the predicted flux for the waste slurries to be tested (e.g., 0.04 gpm/ft^2 for dewatering operations). No solids were evident in the permeate during filtration of the strontium carbonate slurry, and the density of the permeate was measured at 1.12 g/mL by the mass flow meter. A sample of the permeate was taken, and its density was measured as 1.11 g/mL using a calibrated balance and a 50-mL volumetric flask. While the density could be measured, the volumetric flow of the permeate was beyond the range of the mass flow meter for all three tests. After a density check, permeate flow was diverted through the skid's rotometer. For the SrCO$_3$ flux measurements, the flow was slow enough to verify the flow rate using the in-line volumetric cylinder to measure the permeate flow.
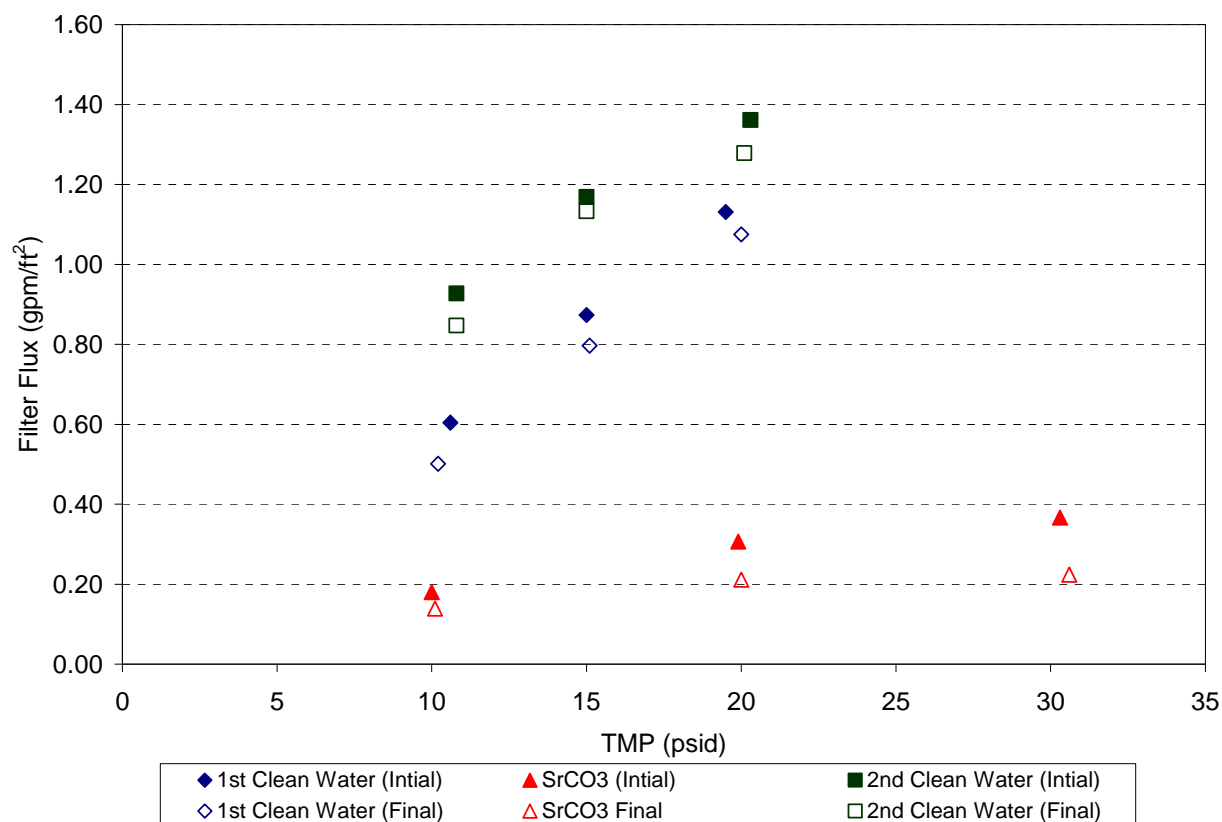
Figure K.9. Initial Clean Water/SrCO$_3$ Flux Measurements of Filter

K.1.2 Filtration Data Analysis

K.1.2.1 Filtration Terms and Equations

Filtration is examined in this report as a filter flux defined as:

$$J = \frac{Q_{permeate}}{A_{filter}} \tag{K.1}$$

where J is the filter flux (gpm/ft^2), $Q_{permeate}$ is the volumetric permeate flow, and A_{filter} is the filtration surface area.

In this study, the filter area is assumed as the inside area of the filter element which is defined as:

$$A_{filter} = \pi Di_{filter} L_{filter} \tag{K.2}$$

where Di_{filter} is the filter element inside diameter, and L_{filter} is the filter element length.

The permeate volumetric flow rate is also corrected for viscosity and surface tension effects because the permeate temperature deviated from 25°C. For a temperature T, the corrected permeate flow rate and filter flux are given as:

$$Q_{25°C} = Q_T e^{2500\left[\frac{1}{T+273} - \frac{1}{298}\right]}$$
$$J_{25°C} = J_T e^{2500\left[\frac{1}{T+273} - \frac{1}{298}\right]} \tag{K.3}$$

The pressure drop across the filter (i.e., the TMP) is calculated in this test to be:

$$TMP = \Delta P_m = \frac{(P_{inlet} + P_{outlet})}{2} - P_{permeate} \tag{K.4}$$

where P_{inlet} is the pressure at the filter inlet, P_{outlet} is the pressure at the filter outlet, and $P_{permeate}$ is the pressure at the permeate side of the filter.

The axial velocity inside the filter is calculated by dividing the volumetric slurry flow of the filter by the cross section area of the inside diameter of filter:

$$AV = \frac{Q_{slurry}}{S_a} = \frac{Q_{slurry}}{\frac{\pi}{4}Di_{filter}^2} \qquad (K.5)$$

where S_a is the cross sectional area of axial flow, and Q_{slurry} is the volumetric slurry flowrate in the axial direction.

The Darcy equation describes filter flux as:

$$J = \frac{\Delta P_m}{\mu_{permeate} R_m} \qquad (K.6)$$

where ΔP_m is the pressure drop across the filter membrane, $\mu_{permeate}$ is the viscosity of the permeate, and R_m is the overall resistance of the filter membrane.

The filter resistance term is considered a more complicated term, which is a sum of the resistance of the actual filter, the resistance of the filter cake that forms on the surface of the filter surface, and the resistance due to fouling of the filter. For cross flow filtration, the overall resistance of the filter membrane for low concentrated slurries is usually constant, and turbulent flow conditions exist inside the filter. The transmembrane pressure and permeate viscosity are the controlling operation parameters. During dewatering, the slurry's flow properties change, and the filter resistance becomes more significant. When the slurry's UDS concentration begins to approach a maximum limit, known as the gel concentration, the filter flux can be described as

$$J = k \cdot \ln\left[\frac{C_s}{C_g}\right] \qquad (K.7)$$

where C_s is the slurry UDS concentration, and C_g is the slurry gel concentration.

When the flux is impacted by the UDS concentration, the impact of axial velocity becomes significant as well. This is due to how the axial velocity affects the thickness of the filter cake inside the filter.

K.1.2.2 Filtration Test Matrix

To understand the impact of the transmembrane pressure and axial velocity on the filter flux of the waste slurry, a filtration test matrix was developed to understand their individual effects. Like the clean water and $SrCO_3$ slurry flux testing described in section K.1.1.4, the waste slurry is circulated through the filtration skid while the slurry permeate leaving the filter is recycled back to the slurry reservoir. By recycling permeate in this way, the UDS concentration of the slurry stays constant. Using a TMP of 40 psid and an AV of 13 fps as the baseline condition, the testing conditions are varied to demonstrate how the flux varies as TMP and AV change from the center condition. Table K.1 and Figure K.9 outline the conditions for the testing performed.

Each filtration condition is maintained for at least an hour while permeate is recycled back to the slurry reservoir tank. Before the test condition is changed, a back-pulse on the filter is performed to provide the same starting conditions for each test. The initial test performed at the baseline condition is performed for a minimum of 3 hours to track how the filter flux varies with time to track possible fouling due to the waste. If needed, the test matrix can be reduced in size by starting at Test 6 in Table K.1 and running this test for a 2-hour period.

Table K.1. Filtration Test Matrix Operating Conditions

Test number	Duration (hours)	Target TMP[a] (psid)	Target AV* (fps)
1	3 (min)	40	13
2	1	30	11
3	1	30	15
4	1	50	15
5	1	50	11
6	1	40	13
7	1	40	9
8	1	40	17
9	1	20	13
10	1	60	13
11	1	40	13
(a) Actual conditions may vary based upon slurry volume and rheology. All conditions may not be obtainable.			
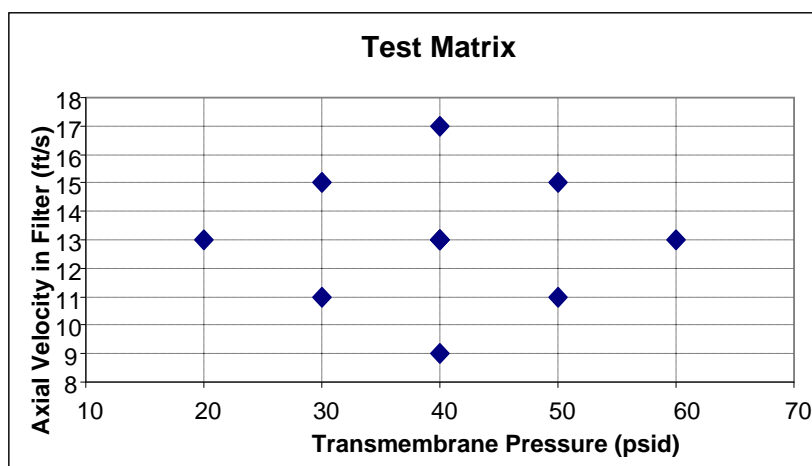
Figure K.9. Filtration Test Matrix Chart

Table K.2. Abridged Filter Test Matrix

Test number	Duration (hrs)	Target TMP (psid)	Target AV (fps)
1	2 (min)	40	13
2	1	40	17 (or max)
3	1	40	9
4	1	40	13
5	1	20	13
6	1	60	13
7	1	40	13

When the slurry is at low concentrations, the system is expected to be controlled by the transmembrane pressure (Equation K.6), with little impact from the axial velocity. However, once the slurry is concentrated and the flow properties change, it is expected that the axial velocity will have some effect on the filtration of the system.

K.1.2.3 Dewatering Operation Analysis

During dewatering operations of the waste slurries, the transmembrane pressure and axial velocity are maintained at the baseline condition of 40 psid and 13 fps. By maintaining the operating conditions of the filtration, the only effect on filtration should be the slurry concentration. As the slurry's UDS changes, the filter flux can be monitored and graphically charted, as shown in Figure K.10. As discussed earlier, the filter flux is initially expected to follow Equation K-6 for low-solids concentrations, which will appear as a horizontal line on the chart when the TMP is held constant. But as the slurry begins to concentrate, the filtration behavior of the slurry is expected to change and begin to follow Equation K.7. With graphic analysis, the transition in filtration behavior can be understood.

$$J = \frac{\Delta P_m}{\mu_{permeate} R_m}$$

$$J = k \cdot \ln\left[\frac{C_s}{C_g}\right]$$

Filter Flux

C_g

Ln (C_s)
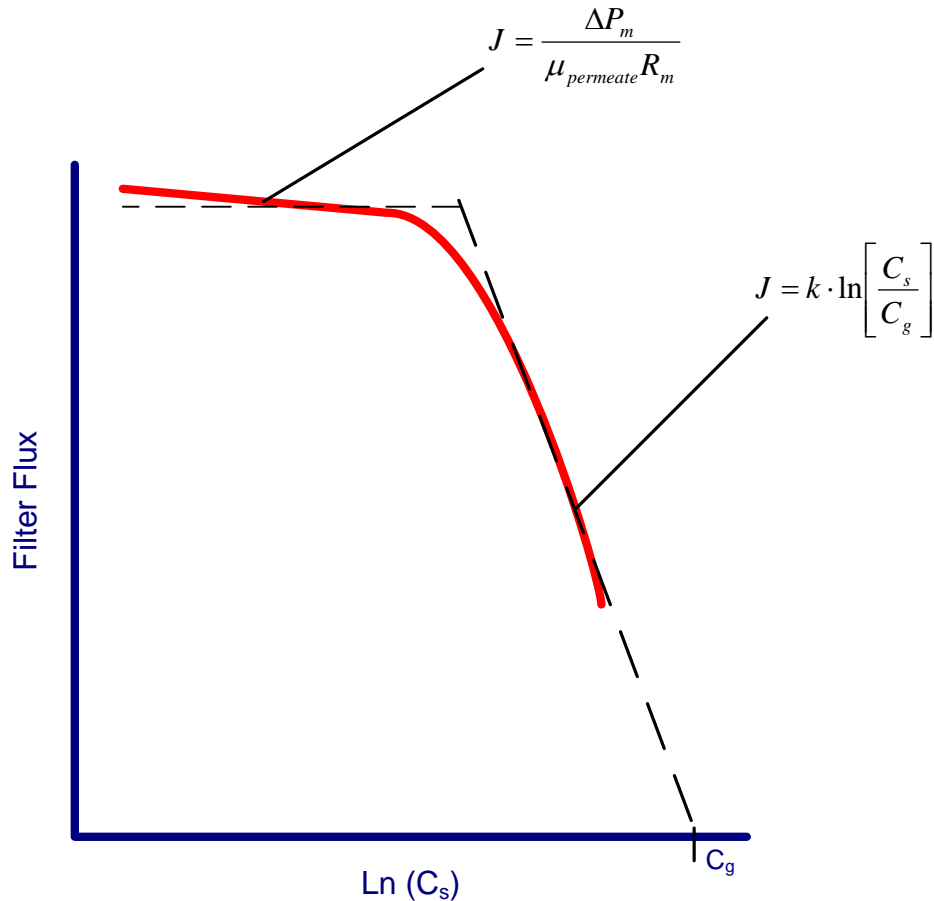
Figure K.10. Example of a Dewatering Curve

K.1.2.4 Effects of Rheology and Particle Size

During testing operations, rheology and particle-size samples are collected to characterize the solids in the slurry and their impact on flow and filtration behavior. As slurries concentrate, their flow behavior changes and becomes more viscous and less Newtonian. This directly impacts the cross-flow behavior of the filter and the formation of filter cake. Particle size also can have an impact by affecting the gel concentration of the slurry and possibly impact fouling. Because the slurries are sheared during filtration, the particle size of the slurry can change—especially if the initial solids are agglomerated. Chemical leaching has a similar impact as well.

K.1.3 Chemical Data Analysis

During the test, the mass of material placed inside the skid and removed is constantly measured to perform an overall mass balance of the slurry during the test. Two main goals are to be achieved from this analysis: 1) verification that transuranic (TRU) material stays in the HLW stream and 2) calculation of the chemical leach factors of glass-limiting compounds of interest.

K.1.3.1 Validation of Filtration Separation of TRU Material

The main goal of the chemical and physical separation processes tested in this report is to demonstrate the effectiveness of removing load-limiting glass compounds (e.g., phosphorus and chromium) from the HLW stream while not introducing TRU material into the LAW waste stream. This is examined during filtration and leaching processes. During filtration, it is important to verify that TRU materials present in the waste slurry do not pass through the filtration media as a colloid or as a particle <0.1 mm. During leaching, it is also important to verify that TRU compounds are not chemically dissolved during operations designed only to remove glass-limiting compounds for the LAW stream. This is achieved by performing radiochemical analysis on permeate and slurry samples throughout the test to verify that the permeate streams contain minimal TRU compounds and that a mass balance on the system shows that almost all the TRU stays in the HLW slurry stream.

K.1.3.2 Chemical Leach Factors for Caustic and Oxidative Leaching

In this report, the chemical leach factor is defined as the percentage difference in mass of a solid component in the waste after chemical leaching.

$$f_i = 1 - \frac{m_i^{final}}{m_i^{initial}} \tag{K.8}$$

where f_i is the leach factor for component i, $m_i^{initial}$ is the initial solid mass of component i, and m_i^{final} is the final solid mass of component i.

The following methods are used to derive the initial and final mass of the components:

- Overall mass balance of the system along with physical property measurement of the solids fraction of the slurry

- Mass balance of the slurry before and after leaching using insoluble components, such as uranium, to trace the fractional change in mass

- Mass balance of the liquid permeate before and after leaching to measure the change of mass in the solids.

K.1.3.3 Physical Examination of Final Leach Material

The chemical characterization and physical morphology are examined after leaching. While most of the analyses used are qualitative, they can show:

- If particles are crystal, agglomerates, or amorphous

- Whether TRU and glass-limiting compounds (like aluminum or chromium) are blends of different phases or single compounds

- What is the crystal phase of the remaining glass-limiting compound (e.g., boehmite for aluminum).

Appendix L

**Group 1/2 Analytical Results
from Parametric Leaching**

Appendix L: Group 1/2 Analytical Results from Parametric Leaching

Table L.1 provides information about analyte concentrations at various time intervals during oxidative leaching of the caustic-leached Group 1/2 solids at 45°C.

Table L.1. Analyte Concentrations as a Function of Time for Leaching at 45ºC

Analyte	Analyte Concentration and Density at Given Time After Cooling to Ambient (~21°C) Temperature; g/mL for Density; µg/mL for Metals; µCi/mL for Radionuclides						
	0 hr	0.5 hr	1 hr	2 hr	4 hr	6 hr	24 hr
0.25 M NaOH, Mn/Cr = 0.59							
Density	1.02	1.02	1.03	1.03	1.02	1.02	1.03
Total Cr	8.57	90.4	90.1	90.6	89.6	95.8	95.6
Cr (VI)	7.75	81.4	84.1	84.6	82.0	85.5	85.0
% Diff	9.6	9.9	6.7	6.6	8.5	10.8	11.0
Al	23.9	56.8	76.7	95.8	103.9	113.0	116.7
B	[0.544]	[0.652]	[0.609]	[0.622]	[0.498]	[0.437]	[0.563]
Bi	[1.5]	<0.93	[1.0]	[1.0]	<0.93	[1.1]	[0.94]
Cd	<0.106	<0.106	<0.104	<0.106	<0.106	<0.106	<0.106
Fe	[0.777]	[0.932]	[0.792]	[0.840]	[0.902]	[1.155]	[0.938]
Mn	<0.007	<0.007	<0.007	<0.007	<0.007	<0.007	<0.007
Na	7,183	7,361	7,429	7,561	7,343	7,741	7,663
Ni	<0.075	<0.075	<0.073	[0.087]	<0.075	[0.078]	<0.075
P	178.5	189.5	187.0	192.3	187.9	199.5	200.5
S	[8.9]	[9.9]	[9.1]	[7.8]	[6.8]	[13.1]	[5.3]
Si	8.1	31.7	45.7	59.1	61.9	66.2	62.6
Sr	[0.03]	[0.02]	[0.02]	[0.02]	[0.02]	[0.01]	[0.02]
U	[2.705]	[4.35]	[2.710]	[3.42]	[2.769]	[3.43]	[2.002]
U by KPA	NM	NM	NM	NM	NM	NM	2.73
Zn	[0.72]	[0.50]	[0.58]	[0.47]	[0.90]	[0.66]	[0.63]
Zr	<0.04	<0.03	<0.03	<0.03	<0.03	<0.03	<0.03
$^{239+240}$Pu	1.54E-06	1.11E-05	4.70E-06	2.69E-06	2.02E-06	2.42E-06	1.93E-06
^{238}Pu	1.11E-06	5.25E-07	6.43E-07	3.90E-07	5.71E-07	9.25E-07	8.53E-07
Opportunistic Analytes							
Ag	<0.07	<0.07	<0.06	<0.07	<0.07	<0.07	<0.07
As	<1.4	<1.3	<1.3	<1.3	<1.3	<1.3	<1.3
Ba	<0.15	[0.06]	0.19	[0.11]	[0.13]	[0.15]	0.319
Be	<0.00	[0.002]	[0.002]	<0.002	[0.003]	[0.002]	[0.002]
Ca	<0.64	[0.53]	[0.67]	[0.59]	[0.65]	[1.03]	[0.75]
Ce	<0.31	<0.31	<0.30	<0.31	<0.31	<0.31	<0.31
Co	[0.09]	<0.07	[0.09]	<0.07	<0.07	<0.07	<0.08
Cu	[0.05]	<0.04	[0.05]	[0.07]	[0.31]	[0.07]	<0.04
Dy	[0.10]	[0.11]	<0.09	[0.11]	<0.09	<0.09	<0.09

Table L.1 (contd)

Analyte	Analyte Concentration and Density at Given Time After Cooling to Ambient (~21°C) Temperature; g/mL for Density; μg/mL for Metals; μCi/mL for Radionuclides						
	0 hr	**0.5 hr**	**1 hr**	**2 hr**	**4 hr**	**6 hr**	**24 hr**
Eu	[0.05]	[0.04]	<0.03	<0.03	<0.03	<0.03	<0.03
K	[0.96]	[2.1]	[1.2]	[1.6]	[2.7]	[1.4]	[1.5]
La	<0.09	<0.09	<0.09	<0.09	<0.09	<0.09	<0.09
Li	[0.20]	[0.27]	[0.21]	[0.20]	[0.15]	[0.18]	[0.19]
Mg	[0.11]	[0.16]	<0.07	<0.07	<0.07	<0.07	<0.07
Mo	[0.28]	<0.16	<0.16	<0.16	[0.19]	<0.16	[0.44]
Nd	[0.18]	<0.17	<0.16	<0.17	<0.17	<0.17	<0.17
Pb	<1.0	<0.99	<0.97	<1.0	<1.0	[1.1]	<1.0
Pd	[0.27]	<0.20	<0.19	<0.20	<0.20	<0.20	<0.20
Rh	[0.42]	[0.50]	<0.37	<0.37	<0.37	<0.37	<0.38
Ru	<0.26	<0.26	<0.26	<0.26	<0.26	<0.27	<0.27
Sb	[0.90]	[1.0]	<0.61	[1.7]	<0.62	<0.62	<0.63
Se	<2.2	<2.2	<2.1	<2.2	<2.2	<2.2	<2.2
Sn	<0.84	<0.84	<0.82	<0.84	<0.84	<0.84	<0.84
Ta	<0.53	<0.53	<0.52	<0.53	<0.53	<0.53	<0.53
Te	[0.95]	<0.81	[0.85]	<0.81	<0.81	<0.81	[0.91]
Th	[0.43]	[0.68]	[0.33]	[0.37]	<0.30	<0.31	<0.31
Ti	[0.02]	[0.02]	<0.01	<0.01	<0.01	<0.01	<0.01
Tl	<1.2	<1.2	<1.2	<1.2	<1.2	<1.2	<1.2
V	[0.07]	[0.12]	[0.16]	[0.15]	[0.18]	[0.17]	[0.18]
W	[0.73]	[0.71]	<0.58	[0.68]	[0.75]	<0.59	<0.59
Y	<0.01	[0.02]	<0.01	<0.01	<0.01	<0.01	<0.01
0.25 M NaOH, Mn/Cr = 0.79, Trial a							
Density	1.02	1.02	1.02	1.02	1.02	1.02	1.02
Total Cr	8.80	108.	111.8	114.1	113.4	115.9	115.7
Cr (VI)	9.23	101.0	103.2	105.1	105.7	107.1	109.7
% Diff	-4.9	7.2	7.7	7.8	6.7	7.6	5.1
Al	23.8	56.6	76.1	96.2	105.6	112.4	115.3
B	[0.340]	[0.560]	[0.457]	[0.462]	[0.532]	[0.502]	[0.534]
Bi	[1.6]	<0.93	[1.0]	<0.92	<0.94	[1.3]	<0.94
Cd	<0.105	<0.106	<0.104	<0.105	<0.106	<0.107	<0.107
Fe	[0.648]	2.27	[0.731]	[1.140]	[0.908]	[0.848]	[0.943]
Mn	<0.007	1.36	<0.007	<0.007	<0.007	<0.007	<0.007
Na	7,315	7,433	7,582	7,675	7,611	7,755	7,543
Ni	<0.074	<0.075	<0.073	[0.099]	<0.075	[0.126]	<0.075
P	181.8	194.1	195.2	193.3	194.5	200.6	198.9
S	[5.9]	[6.5]	[13.7]	[4.3]	[13.2]	[16.0]	[15.7]
Si	8.06	32.3	46.0	58.9	63.9	65.9	61.9
Sr	[0.01]	[0.02]	[0.02]	[0.02]	[0.01]	[0.01]	[0.01]

Table L.1 (contd)

Analyte	Analyte Concentration and Density at Given Time After Cooling to Ambient (~21°C) Temperature; g/mL for Density; µg/mL for Metals; µCi/mL for Radionuclides						
	0 hr	**0.5 hr**	**1 hr**	**2 hr**	**4 hr**	**6 hr**	**24 hr**
U	[1.57]	[4.98]	[3.35]	[3.02]	[2.41]	[2.86]	[2.42]
U by KPA	NM	NM	NM	NM	NM	NM	2.46
Zn	[0.59]	[0.59]	[0.52]	[0.65]	[0.75]	[0.44]	[0.57]
Zr	<0.03	<0.03	<0.03	<0.03	<0.03	<0.03	<0.03
$^{239+240}$Pu	6.13E-07	4.08E-06	3.08E-06	2.27E-06	1.16E-06	4.76E-07	3.46E-07
^{238}Pu	6.90E-07	2.48E-04	2.12E-04	1.44E-04	6.65E-05	3.54E-05	4.85E-06
Opportunistic Analytes							
Ag	<0.06	<0.06	<0.06	<0.06	<0.06	<0.06	<0.06
As	<1.3	<1.3	<1.3	<1.3	<1.3	<1.4	<1.4
Ba	[0.08]	[0.11]	[0.14]	[0.10]	[0.06]	[0.05]	[0.10]
Be	[0.00]	[0.00]	<0.002	[0.00]	[0.00]	<0.002	[0.00]
Ca	[0.46]	[0.56]	[0.64]	[0.52]	[0.69]	[0.91]	[0.79]
Ce	<0.06	<0.06	<0.06	<0.06	<0.06	<0.06	<0.06
Co	<0.06	<0.06	<0.06	[0.09]	<0.06	<0.06	<0.06
Cu	<0.06	[0.06]	<0.06	[0.06]	<0.06	<0.06	<0.06
Dy	<0.06	[0.11]	<0.06	<0.06	<0.06	<0.06	<0.06
Eu	<0.06	[0.04]	<0.06	<0.06	<0.06	<0.06	<0.06
K	<0.06	[2.6]	[2.1]	[1.7]	[3.1]	[3.0]	[2.7]
La	<0.06	<0.06	<0.06	<0.06	<0.06	<0.06	<0.06
Li	[0.16]	[0.20]	[0.20]	[0.21]	[0.20]	[0.22]	[0.17]
Mg	<0.06	<0.06	<0.06	<0.06	<0.06	<0.06	<0.06
Mo	[0.16]	<0.06	[0.33]	[0.17]	[0.44]	[0.23]	[0.35]
Nd	<0.06	<0.06	<0.06	<0.06	<0.06	<0.06	<0.06
Pb	<0.06	<0.06	<0.06	<0.06	<1.0	<1.0	<1.0
Pd	<0.06	<0.06	<0.06	<0.06	<0.06	<0.06	<0.06
Rh	<0.06	<0.06	<0.06	<0.06	<0.06	<0.06	<0.06
Ru	<0.06	[0.31]	[0.30]	<0.06	<0.06	<0.06	<0.06
Sb	[0.96]	[1.2]	[1.0]	[1.2]	[0.91]	<0.628	[1.4]
Se	<2.2	2.2	<2.1	<4.6	<2.2	<2.2	<2.2
Sn	<0.06	<0.06	<0.06	<0.06	<0.06	<0.06	<0.06
Ta	<0.06	<0.06	<0.06	<0.06	<0.06	<0.06	<0.06
Te	<0.06	[1.2]	<0.06	<0.06	<0.06	<0.06	[0.91]
Th	[0.34]	[0.47]	[0.43]	[0.43]	[0.41]	<0.06	<0.06
Ti	<0.06	[0.02]	<0.06	<0.06	<0.06	<0.06	[0.014]
Tl	[1.5]	[1.6]	<1.2	<1.2	<1.2	<1.2	<1.2
V	[0.09]	[0.16]	[0.16]	[0.18]	[0.21]	[0.23]	[0.19]
W	<0.06	[0.65]	<0.06	[1.4]	[0.69]	[0.91]	[1.1]
Y	<0.06	<0.06	<0.06	<0.06	<0.06	<0.06	<0.06
0.25 M NaOH, Mn/Cr = 0.79, Trial b							
Density	1.02	1.02	1.02	1.02	1.02	1.02	1.01

Table L.1 (contd)

Analyte	Analyte Concentration and Density at Given Time After Cooling to Ambient (~21°C) Temperature; g/mL for Density; µg/mL for Metals; µCi/mL for Radionuclides						
	0 hr	**0.5 hr**	**1 hr**	**2 hr**	**4 hr**	**6 hr**	**24 hr**
Total Cr	8.56	104.6	108.9	107.8	111.5	111.0	112.2
Cr (VI)	8.20	99.6	98.3	98.5	99.5	100.7	102.1
% Diff	4.2	4.8	9.7	8.6	10.7	9.2	9.0
Al	23.2	59.3	78.6	95.4	106.5	109.7	114.3
B	[0.372]	0.403	[0.339]	[0.424]	[0.621]	[0.527]	[0.490]
Bi	[1.3]	0.96	[1.0]	<0.91	[0.99]	<0.93	<0.92
Cd	<0.105	0.106	<0.105	<0.103	<0.106	<0.105	<0.104
Fe	[0.651]	0.714	[0.709]	[0.697]	[0.870]	[0.899]	[0.920]
Mn	<0.007	1.92	[0.046]	<0.007	<0.007	<0.007	<0.007
Na	7,225	7,324	7,402	7,389	7,485	7,500	7,602
Ni	<0.074	0.074	<0.074	<0.073	[0.099]	<0.074	<0.074
P	178.0	186.2	188.4	186.6	191.3	190.9	188.2
S	[11.2]	6.207	[2.2]	[10.6]	[6.8]	[4.0]	[11.0]
Si	8.06	35.4	48.7	60.0	65.2	65.7	62.2
Sr	[0.02]	0.02	[0.02]	[0.01]	[0.02]	[0.01]	[0.01]
U	[2.108]	3.72	[2.621]	[3.03]	[3.42]	[2.417]	[2.146]
U by KPA	NM	NM	NM	NM	NM	NM	2.35
Zn	[0.71]	0.56	[0.52]	[0.58]	[0.56]	[0.65]	[0.58]
Zr	<0.03	0.03	<0.03	<0.03	<0.03	<0.03	<0.03
$^{239+240}$Pu	6.78E-07	3.61E-06	2.03E-06	2.14E-06	1.36E-06	6.08E-07	2.89E-07
^{238}Pu	6.30E-07	2.45E-04	2.14E-04	1.22E-04	8.73E-05	4.64E-05	6.67E-06
Opportunistic Analytes							
Ag	<0.07	<0.07	<0.06	<0.06	<0.07	<0.07	<0.06
As	<1.3	<1.3	<1.3	<1.3	<1.3	<1.3	[2.3]
Ba	0.180	[0.09]	[0.08]	[0.08]	[0.08]	[0.11]	[0.09]
Be	<0.002	<0.002	[0.00]	<0.002	[0.00]	[0.00]	[0.00]
Ca	[0.50]	[0.59]	[0.52]	[0.55]	[0.84]	[0.90]	[0.83]
Ce	<0.31	<0.31	<0.31	<0.30	<0.31	<0.31	<0.31
Co	<0.07	[0.11]	<0.07	[0.08]	[0.08]	[0.08]	[0.10]
Cu	[0.05]	[0.14]	<0.04	[0.04]	<0.04	<0.04	[0.04]
Dy	[0.10]	<0.09	<0.09	[0.11]	<0.09	<0.09	<0.09
Eu	<0.03	<0.03	<0.03	<0.03	[0.06]	<0.03	<0.03
K	<0.62	[2.1]	[4.6]	[3.9]	[0.6]	[1.7]	[1.1]
La	<0.09	<0.09	<0.09	<0.08	<0.09	<0.09	<0.09
Li	[0.17]	[0.16]	[0.19]	[0.21]	[0.22]	[0.22]	[0.21]
Mg	<0.07	<0.07	<0.07	<0.07	[0.08]	<0.07	<0.07
Mo	[0.17]	<0.16	[0.21]	[0.19]	[0.21]	[0.43]	[0.18]
Nd	<0.17	[0.18]	<0.17	<0.16	<0.17	<0.17	<0.17
Pb	<0.99	<0.99	<0.99	<0.97	<0.99	<0.99	<0.98
Pd	<0.20	<0.20	<0.19	<0.19	<0.20	<0.20	<0.19

Table L.1 (contd)

Analyte	Analyte Concentration and Density at Given Time After Cooling to Ambient (~21°C) Temperature; g/mL for Density; µg/mL for Metals; µCi/mL for Radionuclides						
	0 hr	**0.5 hr**	**1 hr**	**2 hr**	**4 hr**	**6 hr**	**24 hr**
Rh	<0.37	<0.37	<0.37	<0.36	<0.37	<0.37	<0.37
Ru	<0.26	<0.26	<0.26	<0.26	<0.26	<0.26	<0.26
Sb	[2.3]	<0.62	<0.62	<0.61	<0.62	<0.62	<0.61
Se	<2.2	[2.3]	[2.5]	<2.1	<2.2	[3.1]	<2.1
Sn	<0.84	<0.84	<0.83	<0.82	<0.84	<0.84	<0.83
Ta	<0.53	[0.5]	<0.52	<0.51	<0.53	<0.53	<0.52
Te	<0.81	[1.6]	<0.80	<0.79	[1.3]	[2.0]	[1.0]
Th	<0.30	[0.34]	<0.30	<0.30	[1.0]	[0.53]	<0.30
Ti	<0.01	<0.01	[0.02]	<0.01	[0.03]	[0.02]	[0.02]
Tl	[1.5]	<1.2	<1.2	<1.2	<1.2	<1.2	<1.2
V	[0.05]	[0.18]	[0.18]	[0.19]	[0.21]	[0.21]	[0.22]
W	<0.59	[0.74]	[0.99]	[0.58]	<0.59	[0.93]	<0.58
Y	<0.01	<0.01	<0.01	[0.01]	<0.01	<0.01	<0.01
0.25 M NaOH, Mn/Cr = 0.79, Trial c							
Density	1.02	1.02	102	1.02	1.02	1.03	1.02
Total Cr	8.44	103.2	104.6	105.8	106.6	112.0	113.5
Cr (VI)	8.25	95.5	100.7	98.2	100.8	102.7	100.4
% Diff	2.3	7.5	3.8	7.3	5.4	8.3	11.5
Al	22.5	58.6	76.6	95.0	103.8	111.6	117.9
B	[0.403]	[0.338]	[0.370]	[0.374]	[0.310]	[0.314]	[0.568]
Bi	[1.1]	[1.0]	<0.93	<0.93	<0.93	[1.2]	[1.2]
Cd	<0.106	<0.104	<0.105	<0.106	<0.105	<0.109	<0.107
Fe	[0.652]	[0.676]	[0.741]	[0.716]	[0.775]	[0.832]	[0.914]
Mn	<0.007	1.20	<0.007	<0.007	<0.007	<0.007	<0.007
Na	6,859	6,909	6,945	7,004	7,033	7,326	7,220
Ni	<0.074	<0.074	<0.074	<0.075	[0.133]	<0.077	[0.082]
P	172.6	179.6	184.3	185.5	182.8	194.2	191.1
S	[6.5]	[6.8]	[5.2]	[10.0]	[4.6]	[10.9]	[10.1]
Si	7.67	33.8	47.54	58.	63.2	66.9	64.3
Sr	[0.01]	[0.01]	[0.02]	[0.02]	[0.01]	[0.01]	[0.01]
U	[2.173]	[3.38]	[3.70]	[2.615]	[2.478]	[2.399]	[4.41]
U by KPA	NM	NM	NM	NM	NM	NM	2.45
Zn	[0.78]	[0.52]	[0.68]	[0.53]	[0.56]	[0.64]	[0.79]
Zr	<0.03	<0.03	<0.03	<0.03	<0.03	<0.04	<0.03
$^{239+240}$Pu	3.30E-07	3.87E-06	3.39E-06	1.38E-06	1.59E-06	4.46E-07	1.15E-06
^{238}Pu	5.13E-07	2.13E-04	1.88E-04	1.38E-04	7.72E-05	3.68E-05	5.73E-06
Opportunistic Analytes							
Ag	<0.07	<0.06	<0.06	<0.07	<0.07	<0.07	<0.07
As	<1.3	[2.7]	<1.3	<1.3	<1.3	<1.4	<1.4
Ba	0.214	[0.05]	[0.10]	[0.10]	[0.11]	[0.11]	[0.09]

Table L.1 (contd)

Analyte	Analyte Concentration and Density at Given Time After Cooling to Ambient (~21°C) Temperature; g/mL for Density; µg/mL for Metals; µCi/mL for Radionuclides						
	0 hr	**0.5 hr**	**1 hr**	**2 hr**	**4 hr**	**6 hr**	**24 hr**
Be	[0.00]	[0.00]	[0.00]	[0.00]	[0.00]	[0.00]	[0.00]
Ca	[0.37]	[0.58]	[0.40]	[0.47]	[0.81]	[0.93]	[1.3]
Ce	<0.31	<0.31	<0.31	<0.31	<0.31	<0.32	<0.32
Co	<0.07	[0.12]	[0.10]	[0.11]	<0.07	<0.08	<0.08
Cu	<0.04	<0.04	<0.04	<0.04	<0.04	<0.04	[0.08]
Dy	<0.09	<0.09	<0.09	<0.09	<0.09	<0.09	[0.11]
Eu	<0.03	<0.03	<0.03	<0.03	<0.03	<0.04	<0.03
K	[2.0]	[1.7]	[3.0]	[2.8]	[3.1]	[3.8]	[3.2]
La	<0.09	<0.09	<0.09	<0.09	<0.09	<0.09	<0.09
Li	[0.15]	[0.18]	[0.18]	[0.21]	[0.20]	[0.20]	[0.22]
Mg	<0.07	<0.07	<0.07	<0.07	<0.07	<0.07	<0.07
Mo	<0.16	<0.16	<0.16	<0.16	[0.28]	[0.29]	[0.22]
Nd	<0.17	<0.17	<0.17	<0.17	<0.17	<0.17	<0.17
Pb	<0.99	<0.98	<0.99	<1.00	<0.99	<1.02	<1.01
Pd	<0.20	<0.19	<0.19	<0.20	<0.20	<0.20	<0.20
Rh	<0.37	<0.37	<0.37	<0.37	<0.37	<0.38	<0.38
Ru	<0.26	[0.28]	<0.26	<0.26	<0.26	<0.27	<0.27
Sb	[0.93]	[0.89]	<0.62	<0.62	<0.62	<0.64	<0.63
Se	<2.2	<2.1	<2.2	<2.2	<2.2	<2.2	<2.2
Sn	<0.84	<0.83	[0.83]	<0.84	<0.84	<0.86	<0.85
Ta	<0.53	<0.52	<0.52	<0.53	<0.53	<0.54	<0.54
Te	<0.81	<0.80	[0.96]	<0.81	[0.84]	<0.83	[1.0]
Th	<0.30	<0.30	<0.30	<0.31	<0.30	<0.31	[0.69]
Ti	<0.01	[0.01]	<0.01	[0.01]	[0.02]	<0.01	<0.01
Tl	<1.2	<1.2	<1.2	<1.2	<1.2	<1.2	<1.2
V	[0.10]	[0.17]	[0.21]	[0.20]	[0.21]	[0.22]	[0.22]
W	<0.59	[0.61]	[0.80]	<0.59	[0.68]	[0.99]	[0.73]
Y	<0.01	<0.01	<0.01	<0.01	<0.01	<0.01	<0.01
0.25 M NaOH, Mn/Cr = 0.98							
Density	1.02	1.02	1.01	1.02	1.02	1.02	1.02
Total Cr	8.56	105.4	112.8	112.8	114.2	118.4	122.8
Cr (VI)	8.61	93.4	99.4	98.9	101.3	107.2	108.2
% Diff	-0.6	11.4	11.9	12.3	11.3	9.5	11.9
Al	22.8	49.2	91.2	72.5	101.8	108.5	116.7
B	[0.740]	[0.815]	[0.563]	[0.531]	[0.572]	[0.540]	[0.577]
Bi	<0.91	<0.91	<0.89	<0.94	<0.90	<0.90	<0.91
Cd	<0.103	<0.103	<0.101	<0.106	<0.102	<0.102	<0.103
Fe	[0.740]	[0.755]	27.036	[0.750]	[0.723]	[0.779]	[1.398]
Mn	<0.007	31.7	12.79	22.010	4.37	0.995	<0.007
Na	7,199	7,367	7,462	7,438	7,441	7,615	7,626

Table L.1 (contd)

Analyte	Analyte Concentration and Density at Given Time After Cooling to Ambient (~21°C) Temperature; g/mL for Density; µg/mL for Metals; µCi/mL for Radionuclides						
	0 hr	**0.5 hr**	**1 hr**	**2 hr**	**4 hr**	**6 hr**	**24 hr**
Ni	<0.072	<0.072	<0.071	<0.075	<0.072	<0.072	<0.073
P	171.9	181.8	185.7	184.7	183.8	191.0	191.7
S	[8.6]	[9.1]	[7.7]	[5.3]	<2.2	<2.2	[7.3]
Si	7.5	27.1	56.6	42.8	61.8	64.8	62.6
Sr	[0.01]	[0.02]	[0.01]	[0.01]	[0.01]	[0.01]	[0.01]
U	[3.17]	[4.53]	[3.26]	[4.06]	[4.22]	[3.30]	[3.34]
U by KPA	NM	NM	NM	NM	NM	NM	2.73
Zn	[0.88]	[0.63]	[0.56]	[0.47]	[0.36]	[0.45]	[0.46]
Zr	[0.05]	[0.04]	[0.04]	[0.04]	[0.05]	<0.03	<0.03
$^{239+240}$Pu	5.47E-07	4.29E-06	4.24E-06	4.03E-06	4.11E-06	4.22E-06	1.97E-06
^{238}Pu	1.15E-06	2.72E-04	2.57E-04	2.74E-04	2.47E-04	2.54E-04	1.42E-04
Opportunistic Analytes							
Ag	<0.06	<0.06	<0.06	<0.07	<0.06	<0.06	<0.06
As	[1.3]	[1.5]	<1.273	<1.344	<1.295	<1.289	<1.306
Ba	0.200	0.234	[0.09]	0.184	[0.11]	0.174	[0.09]
Be	<0.002	<0.002	<0.002	<0.002	<0.002	<0.002	<0.002
Ca	[0.95]	[1.2]	[0.255]	[0.406]	[0.283]	[0.282]	[0.486]
Ce	<0.30	<0.30	<0.30	<0.31	<0.30	<0.30	<0.30
Co	<0.07	[0.07]	<0.07	<0.08	<0.07	<0.07	[0.09]
Cu	<0.04	<0.04	<0.04	<0.04	<0.04	<0.04	<0.04
Dy	<0.09	<0.09	<0.09	<0.09	<0.09	<0.09	<0.09
Eu	<0.033	<0.03	<0.03	<0.03	<0.03	<0.03	<0.03
K	[1.1]	[3.6]	[4.1]	[2.2]	[3.6]	[3.3]	[2.6]
La	<0.08	<0.08	<0.08	<0.09	<0.08	<0.08	<0.09
Li	[0.08]	[0.11]	[0.17]	[0.12]	[0.14]	[0.11]	[0.14]
Mg	<0.07	<0.07	<0.07	<0.07	<0.07	<0.07	<0.07
Mo	[0.23]	[0.22]	[0.36]	[0.38]	<0.16	<0.16	<0.16
Nd	<0.16	<0.16	<0.16	<0.17	<0.16	<0.16	<0.16
Pb	<0.97	<0.97	<0.95	<1.00	<0.96	<0.96	<0.97
Pd	<0.19	<0.19	<0.19	<0.20	[0.292]	<0.19	[0.207]
Rh	<0.36	<0.36	<0.36	<0.38	<0.36	<0.36	<0.36
Ru	<0.26	<0.26	<0.25	<0.27	<0.26	<0.25	<0.26
Sb	[1.1]	[1.4]	[0.6]	[2.7]	[1.1]	[1.1]	[1.2]
Se	[3.6]	<2.1	<2.1	<2.2	<2.1	<2.1	<2.1
Sn	<0.81	<0.82	<0.80	<0.84	<0.81	<0.81	<0.82
Ta	<0.51	<0.51	<0.50	<0.53	<0.51	<0.51	<0.52
Te	<0.78	<0.79	<0.77	<0.81	<0.78	<0.78	<0.79
Th	<0.30	<0.30	<0.29	<0.31	<0.30	<0.29	<0.30
Ti	<0.01	<0.01	<0.01	<0.01	<0.01	<0.01	<0.01
Tl	[1.3]	<1.1	[2.9]	<1.2	[2.0]	[2.3]	[1.2]

Table L.1 (contd)

Analyte	Analyte Concentration and Density at Given Time After Cooling to Ambient (~21°C) Temperature; g/mL for Density; µg/mL for Metals; µCi/mL for Radionuclides						
	0 hr	**0.5 hr**	**1 hr**	**2 hr**	**4 hr**	**6 hr**	**24 hr**
V	[0.04]	[0.14]	[0.15]	[0.14]	[0.17]	[0.20]	0.230
W	[0.60]	<0.57	<0.56	<0.59	[0.57]	<0.57	<0.58
Y	<0.01	<0.01	<0.01	<0.01	<0.01	<0.01	<0.01
0.25 M NaOH, Mn/Cr = 1.19							
Density	1.02	1.02	1.02	1.02	1.02	1.02	1.02
Total Cr	8.47	109.9	115.1	114.4	116.0	117.4	123.3
Cr (VI)	8.44	100.6	110.	106.9	110.3	112.7	114.8
% Diff	0.3	8.5	4.3	6.6	4.9	4.1	6.9
Al	22.90	52.7	94.0	74.3	104.0	107.0	114.9
B	[0.359]	[0.521]	[0.483]	[0.362]	[0.361]	[0.509]	[0.541]
Bi	<0.90	<0.92	<0.91	<0.91	<0.90	<0.90	<0.90
Cd	<0.102	<0.104	<0.103	<0.103	<0.102	<0.102	<0.102
Fe	[0.659]	[0.735]	[0.755]	[0.755]	[0.721]	[0.749]	[1.113]
Mn	<0.007	60.3	36.3	48.6	23.5	16.57	<0.007
Na	6,975	7,349	7,341	7,247	7,271	7,339	7,339
Ni	<0.072	<0.073	<0.073	<0.072	<0.072	<0.072	<0.072
P	170.6	183.1	188.2	183.3	182.7	184.5	185.9
S	[5.7]	[7.3]	[9.7]	[13.6]	[9.9]	[4.2]	<2.2
Si	7.69	28.3	58.6	43.8	62.8	63.8	62.0
Sr	[0.01]	[0.01]	[0.01]	[0.01]	[0.01]	[0.01]	[0.01]
U	[1.98]	[3.67]	[4.23]	[3.62]	[3.91]	[3.59]	[4.51]
U by KPA	NM	NM	NM	NM	NM	NM	3.23
Zn	[0.66]	[0.49]	[0.69]	[0.42]	[0.39]	[0.51]	[0.54]
Zr	<0.03	[0.05]	[0.04]	[0.04]	[0.04]	[0.04]	[0.05]
$^{239+240}$Pu	2.91E-07	5.10E-06	4.71E-06	4.77E-06	4.89E-06	4.45E-06	4.22E-06
^{238}Pu	5.41E-07	2.78E-04	2.63E-04	2.81E-04	2.58E-04	2.62E-04	2.68E-04
Opportunistic Analytes							
Ag	<0.06	<0.06	<0.06	<0.06	<0.06	<0.06	<0.06
As	[1.4]	[3.0]	<1.30	<1.30	<1.29	<1.29	[2.3]
Ba	[0.10]	0.195	0.207	[0.08]	[0.07]	[0.10]	[0.16]
Be	<0.002	<0.002	[0.00]	<0.002	<0.002	<0.002	<0.002
Ca	[0.28]	[0.25]	[0.36]	[0.28]	[0.20]	[0.30]	[0.45]
Ce	<0.30	<0.31	<0.30	<0.30	<0.30	<0.30	<0.30
Co	<0.07	<0.07	<0.07	<0.07	[0.078]	<0.07	<0.07
Cu	<0.04	<0.04	<0.04	<0.04	<0.04	<0.04	<0.04
Dy	<0.09	<0.09	<0.09	<0.09	<0.09	<0.09	<0.09
Eu	<0.03	<0.03	<0.03	<0.03	<0.03	<0.03	<0.03
K	[0.78]	[3.67]	[3.32]	[2.446]	[3.61]	[2.187]	[3.31]
La	<0.08	<0.09	<0.08	<0.08	<0.08	<0.08	<0.08
Li	[0.07]	[0.14]	[0.16]	[0.12]	[0.12]	[0.16]	[0.19]

Table L.1 (contd)

Analyte	Analyte Concentration and Density at Given Time After Cooling to Ambient (~21°C) Temperature; g/mL for Density; µg/mL for Metals; µCi/mL for Radionuclides						
	0 hr	0.5 hr	1 hr	2 hr	4 hr	6 hr	24 hr
Mg	<0.07	<0.07	<0.07	<0.07	<0.07	<0.07	<0.07
Mo	<0.16	[0.31]	[0.19]	[0.20]	[0.51]	[0.23]	[0.18]
Nd	<0.16	<0.17	<0.16	<0.16	<0.16	<0.16	<0.16
Pb	<0.96	<0.98	<0.97	<0.97	<0.96	[0.99]	<0.96
Pd	<0.19	<0.19	<0.19	<0.19	[0.28]	<0.19	[0.19]
Rh	<0.36	<0.37	<0.36	<0.36	<0.36	<0.36	<0.36
Ru	<0.25	<0.26	<0.26	<0.26	<0.26	<0.25	<0.26
Sb	[0.63]	<0.61	[1.4]	[1.8]	[1.9]	[0.9]	<0.60
Se	<2.10	<2.14	<2.11	<2.11	[4.2]	<2.10	<2.11
Sn	<0.81	<0.83	[1.2]	<0.82	<0.81	<0.81	<0.81
Ta	<0.51	<0.52	<0.51	<0.51	<0.51	<0.51	<0.51
Te	<0.78	<0.80	<0.79	<0.79	<0.78	<0.78	<0.78
Th	<0.29	<0.30	<0.30	<0.30	<0.29	<0.29	<0.29
Ti	<0.01	<0.01	<0.01	<0.01	<0.01	<0.01	<0.01
Tl	<1.14	[3.4]	[3.3]	[1.5]	[1.7]	[2.6]	[2.3]
V	[0.04]	[0.13]	[0.17]	[0.15]	[0.18]	[0.16]	[0.20]
W	<0.57	<0.58	[0.97]	<0.57	<0.57	<0.57	<0.57
Y	<0.01	<0.01	<0.01	<0.01	<0.01	<0.01	<0.01
1.25 M NaOH, Mn/Cr = 0.98							
Density	1.06	1.07	1.06	1.07	1.06	1.06	1.07
Total Cr	8.93	108.5	119.4	113.8	119.7	118.7	124.2
Cr (VI)	8.01	96.7	103.4	99.3	105.1	105.4	107.3
% Diff	10.2	10.9	13.4	12.8	12.3	11.2	13.6
Al	32.5	148.5	201.7	188.8	204.3	202.9	205.5
B	[0.439]	[0.563]	[0.522]	[0.508]	[0.390]	[0.639]	[0.449]
Bi	[12.9]	[3.3]	[4.6]	[3.6]	[4.2]	[4.6]	[6.3]
Cd	<0.199	<0.202	<0.209	<0.203	<0.204	<0.207	<0.203
Fe	[0.966]	[0.978]	[1.044]	[1.016]	[1.050]	[1.095]	[1.257]
Mn	<0.013	26.15	7.86	15.98	1.48	[0.076]	<0.014
Na	31,321	31,424	32,232	32,258	32,707	32,552	33,209
Ni	<0.141	<0.142	<0.147	<0.143	<0.144	<0.146	<0.144
P	174.8	181.4	192.5	184.6	190.8	188.9	194.5
S	[27.8]	[27.6]	[11.7]	[16.1]	[5.7]	<4.381	[19.4]
Si	14.93	123.6	165.8	155.9	162.9	159.1	155.9
Sr	[0.02]	[0.01]	[0.01]	[0.01]	[0.01]	[0.02]	[0.02]
U	[5.27]	[10.67]	[7.06]	[8.96]	[8.10]	[7.91]	[8.08]
U by KPA	NM	NM	NM	NM	NM	NM	7.46
Zn	[1.0]	[1.1]	[1.1]	[1.5]	[1.3]	[1.5]	[1.4]
Zr	[0.08]	[0.12]	[0.12]	[0.12]	<0.07	[0.10]	<0.07
$^{239+240}$Pu	3.30E-07	2.05E-05	2.24E-05	2.23E-05	2.38E-05	2.29E-05	1.34E-05

Table L.1 (contd)

Analyte	Analyte Concentration and Density at Given Time After Cooling to Ambient (~21°C) Temperature; g/mL for Density; µg/mL for Metals; µCi/mL for Radionuclides						
	0 hr	**0.5 hr**	**1 hr**	**2 hr**	**4 hr**	**6 hr**	**24 hr**
^{238}Pu	6.24E-06	1.29E-03	1.55E-03	1.45E-03	1.48E-03	1.54E-03	8.14E-04
Opportunistic Analytes							
Ag	<0.12	<0.12	<0.13	<0.13	<0.13	<0.13	<0.13
As	<2.5	<2.5	[4.9]	<2.6	<2.6	<2.6	<2.6
Ba	[0.26]	[0.11]	[0.11]	[0.12]	[0.10]	[0.18]	[0.14]
Be	[0.003]	<0.003	[0.004]	<0.003	[0.004]	<0.003	[0.004]
Ca	[1.7]	[2.2]	[0.52]	[0.96]	[0.66]	[0.55]	[1.3]
Ce	<0.59	<0.59	<0.61	<0.60	<0.60	<0.61	<0.60
Co	<0.14	[0.26]	<0.15	<0.14	<0.14	<0.15	<0.14
Cu	<0.08	<0.08	<0.09	[0.10]	<0.08	<0.09	<0.08
Dy	<0.17	<0.17	<0.18	<0.17	<0.17	<0.18	<0.17
Eu	<0.06	<0.07	<0.07	<0.07	<0.07	<0.07	<0.07
K	<1.17	[5.0]	[8.0]	[6.0]	[8.4]	[7.3]	[7.2]
La	<0.16	<0.17	<0.17	<0.17	<0.17	<0.17	<0.17
Li	[0.12]	[0.21]	[0.24]	[0.18]	[0.22]	[0.21]	[0.23]
Mg	<0.13	<0.14	<0.14	<0.14	<0.14	<0.14	<0.14
Mo	<0.30	[0.53]	[0.49]	[0.42]	<0.31	<0.32	<0.31
Nd	<0.32	<0.32	<0.33	<0.32	<0.32	<0.33	<0.32
Pb	<1.9	[3.3]	[4.3]	[3.3]	[4.2]	[3.3]	[2.4]
Pd	<0.37	<0.37	<0.39	<0.38	<0.38	<0.38	<0.38
Rh	<0.70	<0.71	<0.74	<0.72	<0.72	<0.73	<0.72
Ru	<0.50	<0.50	<0.52	<0.51	<0.51	<0.52	<0.51
Sb	[2.9]	[3.0]	[4.0]	[2.8]	[1.5]	[2.3]	[2.1]
Se	<4.1	<4.2	<4.3	<4.182	[6.9]	<4.3	<4.2
Sn	<1.6	<1.6	<1.7	[2.2]	[1.7]	<1.6	<1.6
Ta	<1.0	<1.0	<1.0	<1.0	<1.0	<1.0	<1.0
Te	<1.5	<1.5	<1.6	<1.6	<1.6	<1.6	<1.6
Th	<0.57	<0.58	<0.60	<0.59	<0.59	<0.60	<0.59
Ti	<0.03	<0.03	<0.03	<0.03	<0.03	<0.03	<0.03
Tl	[3.8]	[2.8]	[3.1]	[3.9]	[4.5]	[3.7]	[4.2]
V	[0.10]	[0.28]	[0.26]	[0.22]	[0.27]	[0.29]	[0.26]
W	<1.1	<1.1	<1.2	<1.1	<1.1	<1.2	<1.1
Y	<0.03	<0.03	<0.03	<0.03	<0.03	<0.03	<0.03
NM = not measured							

Table L.2. Analyte Concentrations for Composite Wash Solution for Wash of Samples Oxidatively-Leached in 0.25 M NaOH with a Mn/Cr ratio of 0.79

Analyte	Concentration (μg/mL)	Opportunistic Analytes	Concentration (μg/mL)
Al	62.0	Ag	<0.065
B	[0.496]	As	<1.33
Bi	<0.930	Ba	0.171
Cd	<0.105	Be	<0.002
Cr	6.17	Ca	2.73
Fe	[1.40]	Ce	<0.310
Mn	[0.034]	Co	<0.074
Na	747	Cu	<0.043
Ni	[0.118]	Dy	<0.090
P	15.8	Eu	[0.037]
S	<2.23	K	[1.18]
Si	55.5	La	<0.087
Sr	0.574	Li	[0.071]
U	[2.64]	Mg	[0.146]
Zn	[0.744]	Mo	[0.372]
Zr	[0.093]	Nd	[0.183]
		Pb	<0.992
		Pd	<0.195
		Rh	<0.372
		Ru	<0.264
		Sb	[1.40]
		Se	<2.17
		Sn	<0.837
		Ta	<0.527
		Te	<0.806
		Th	[0.434]
		Ti	[0.015]
		Tl	[1.55]
		V	[0.084]
		W	[0.930]
		Y	<0.014

Appendix M

Group 1/2 CUF Analytical Results

Appendix M: Group 1/2 CUF Analytical Results

Special Instructions for the
CUF Group 1/2 Bismuth Phosphate Sludge/Saltcake and
CUF Group 5/6 Redox Sludge/Saltcake Treatablility Studies
Analysis Requirements

A blend of two composite materials containing liquid and sludge from Hanford waste tanks was subjected to CUF process as per TI-RPP-WTP-572. The first composite blend was from tanks B-104, BX-112, and T-104, representing waste described as Bismuth Phosphate Sludge (Group 1). The second composite blend was comprised of material from tanks BX-110, BX-111, BY-104, BY-105, BY-107, BY-108, BY-109, BY-110, BY-112, T-108, T-109, TX-104 and SX-103, representing tank waste described as Bismuth Phosphate Saltcake (Group 2). The start date for this treatability study is January 7th, 2008. Color code: Fluorescent Pink.

In addition to these samples, additional samples are to be analyzed from the CUF Group 5/6 CUF treatability study started on November 5th, 2007 as per TI-RPP-WTP-552 and ASR 8055. In this case, two archive slurry samples are to be analyzed as a verification of result provided from ASR 8055. Along with those samples, an archive permeate sample from the run will be analyzed along with a filtered sample of a 2M nitric solution used to clean the system. The color code for these samples is: Brilliant Lime.

The processing and analysis schematic is shown by Figure 1, Figure 2, and Table 1. The aqueous samples are ready to directly sub-sample for analysis and acid digestion. The solid slurry samples have yet to be split into aliquots and prepped for fusion or HF-assisted acid digestion.

SAL Preparation/Analysis

Please record observations associated with the dissolution preparations. If any residual solids remain after any of the fusion and acid digestions, note on the bench sheet (include estimated quantity, color, texture, etc.) and contact RW Shimskey or MK Edwards for further instruction prior to distribution.

Archive of SAL Fusion Preparation Samples

The fusion preparations will result in a 100-mL volume. This solution will be apportioned to the laboratory as needed to conduct work-station-specific analyses. Please prepare a 15-mL aliquot from each preparation as an archive sample. The vials need to be labeled with the following: date, ASO-ID, matrix, treatablility study, hazard, fusion prep (if applicable) and their tare, gross masses, and IDs provided to RW Shimskey or MK Edwards. The vials may be removed from the hot cells for storage. The remaining portions of the fusion preparations may be disposed of.

Quality Control

All work is to be conducted according to RPP-WTP-QA-005, Rev. 2.

Preparative or sample analysis QC includes a preparation blank, sample, sample duplicate, matrix spike, and a LCS or BS. The samples submitted for fusion are sub-aliquoted into fusion vessels in duplicate (sample, sample duplicate). If possible, the matrix spike and LCS/BS need to include all the analytes of interest to be reported for the specific analysis.

The duplicate, LCS/BS, and MS QC acceptance criteria for the aqueous phases and solid phases are provided in Table 4. The preparation blank (PB) analyte concentration shall be less than the estimated quantitation limit (EQL) or the minimum detectable activity (MDA) of the associated sample. When the PB concentration is equal to or exceeds the EQL, then the PB concentration shall not exceed 5% of the measured concentration present in the sample. Failure of the PB, and/or duplicates, and/or LCS/BS to meet the acceptance criteria requires that affected samples in the processing batch be re-prepared and re-analyzed for the failed analytes, availability of samples permitting, at ASO expense.

In the case of multi-elemental methods (IC and ICP-OES), isolated QC failure(s) may be communicated to RW Shimskey or MK Edwards for an assessment of the impact on data interpretation. If the data are acceptable, RW Shimskey or MK Edwards will indicate, in writing, that the data may be reported, and the resulting limitations on the data from the QC sample failure(s) shall be included in the final report.

When the MS fails to meet the acceptance criteria, the results shall be investigated for potential sources of error. When the sources of error cannot be identified, the failure of the MS and any resulting limitations on the data shall be included in the report.

Note that in some cases BS and MS are requested for U/KPA as well as ICP metals in solution analysis. Because the broad suite of ICP BS metals will interfere with the U KPA analysis, two MS and BS samples (one supporting each technique) will need to be prepared as part of the acid digestion.

Reporting Units

Report aqueous sample results in units of ug/mL or uCi/mL. Report solids sample results as ug/g or uCi/g; the initial dry mass of solids (as measured in each fusion crucible) will be provided. For radiochemistry, the reference date shall be November 5, 2007 for samples from TI-RPP-WTP-552 and January 7th, 2008 for samples from TI-RPP-WTP-572. Report the hydroxide concentration in units of molarity and ug/mL.

Reporting

Please prepare the analytical data report in accordance with PNL-ASO-058, Rev. 0, Section 5.3, Comprehensive Data Report. Please be sure to include action taken with respect to any identified unexpected results and discrepancies.

The following elements may be included in the final report or be traceable to the test results (usually by entry in the LRB, Test Instruction, or data sheet) and be maintained as lifetime records:
- identification of standards used
- identification of M&TE used
- reference to the Test Plan (identified on page 1 of the ASR)
- signature and date of person who performed the test and recorded the data

- hand calculation review documentation.

Analytical results shall be reported both in hard copy and electronically. Preliminary data reports and electronic files shall be provided as soon as practical after completion of analysis. **The final ASR data report shall be provided no later than the commitment date on the ASR.**
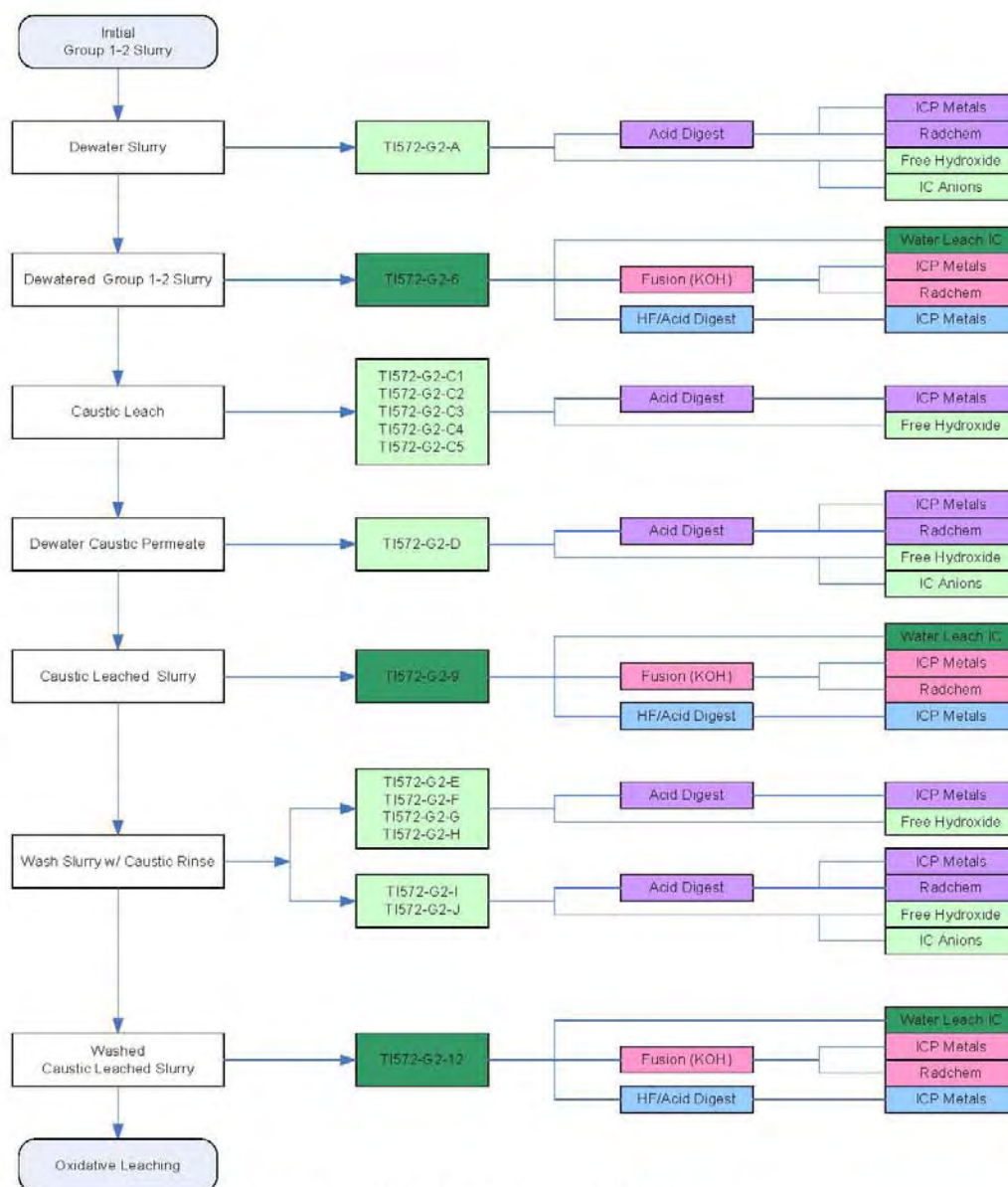
Figure 1: TI-RPP-WTP-572 Process Sampling Plan
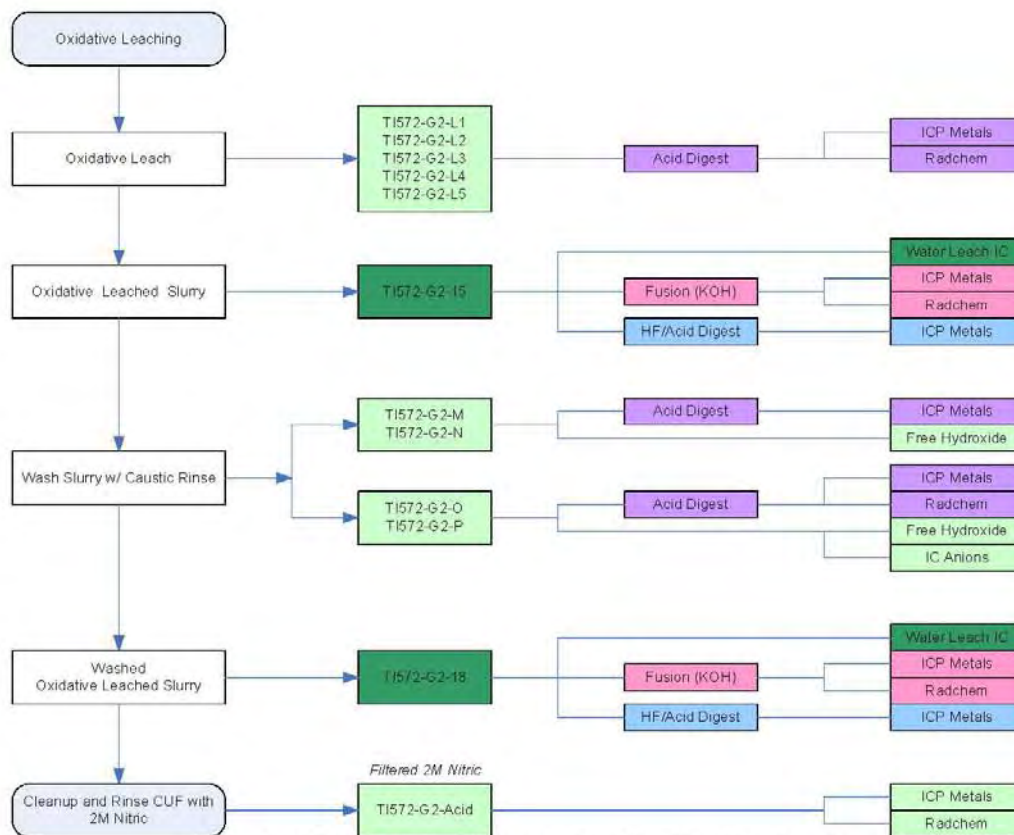
Figure 1: TI-RPP-WTP-572 Process Sampling Plan (Continued)
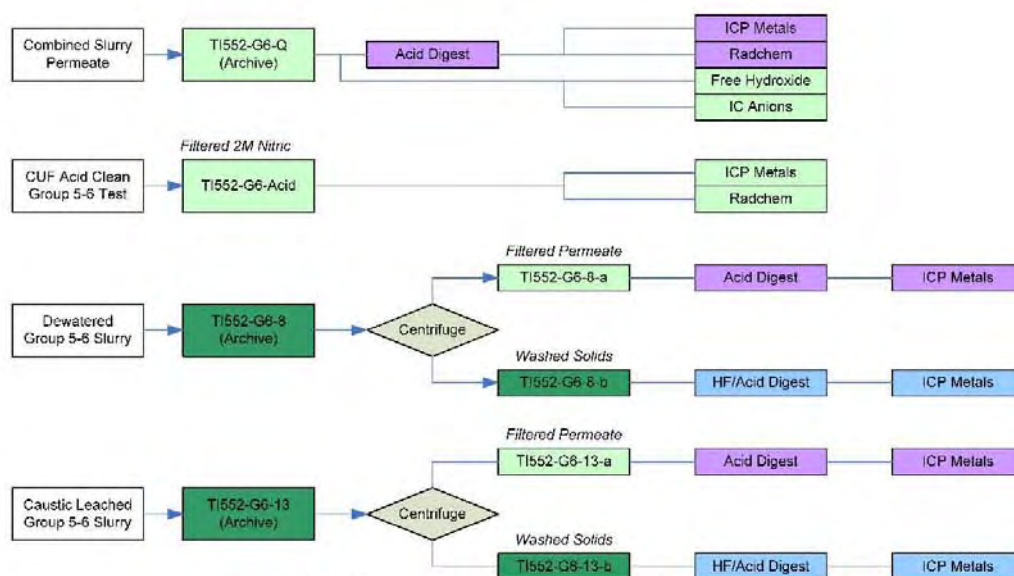
Figure 2: TI-RPP-WTP-552 Additional Sampling Plan

Table 1. Cross-Reference of Process component, Sample ID, and RPL ID

Component	Sample ID	ASO ID
TI-RPP-WTP-572: Group 1/2 CUF Test and TI-RPP-WTP-552: Group 5/6 CUF Test		
Dewater filtrate	TI572-G2-A	08-01290
Leach permeate	TI572-G2-D	08-01291
wash 5 permeate	TI572-G2-I	08-01292
Combined permeate	TI572-G2-J	08-01293
Oxidative wash 3 permeate	TI572-G2-O	08-01294
Combined wash	TI572-G2-P	08-01295
Final Slurry Permeate from TI552	TI**552**-G6-Q	08-01296
0.5 hr oxidative leach	TI572-G2-L1	08-01297
1 hr oxidative leach	TI572-G2-L2	08-01298
2 hr oxidative leach	TI572-G2-L3	08-01299
4 hr oxidative leach	TI572-G2-L4	08-01300
6 hr oxidative leach	TI572-G2-L5	08-01301
2M Nitric Acid Wash Solution	TI572-G2-Acid	08-01302
2M Nitric Acid Wash Solution	TI**552**-G6-Acid	08-01303
Caustic leach filtrate, 1 hour heat up	TI572-G2-C1	08-01304
Caustic leach filtrate, 3 hour heat up	TI572-G2-C2	08-01305
Caustic leach filtrate, 0 hour leach	TI572-G2-C3	08-01306
Caustic leach filtrate, 4 hour leach	TI572-G2-C4	08-01307
Caustic leach filtrate, 8 hour leach	TI572-G2-C5	08-01308
wash 1 permeate	TI572-G2-E	08-01309
wash 2 permeate	TI572-G2-F	08-01310
wash 3 permeate	TI572-G2-G	08-01311
wash 4 permeate	TI572-G2-H	08-01312
Oxidative wash 1 permeate	TI572-G2-M	08-01313
Oxidative wash 2 permeate	TI572-G2-N	08-01314
Group 5/6 Slurry Permeate	TI**552**-G6-8-a	08-01315
Leached 5/6 Slurry Permeate	TI**552**-G6-13-a	08-01316
20 wt% slurry	TI572-G2-6	08-01317
Leach slurry	TI572-G2-9	08-01318
Leached and washed slurry	TI572-G2-12	08-01319
Leached and washed slurry	TI572-G2-15	08-01320
Leached and washed slurry	TI572-G2-18	08-01321
Group 5/6 Slurry Washed Solids	TI**552**-G6-8-b	08-01322
Leached 5/6 Slurry Washed Solids	TI**552**-G6-13-b	08-01323

Laboratory Analysis

The required sample analyses are shown in **Table 2.** Filtration and Leach Testing Characterization Plan.

Table 2. Filtration and Leach Testing Characterization Plan

Process Step	Analyte	
TI-RPP-WTP-572		
Dewatered slurry **(TI572-G2-6)**	HF assisted Acid digestion • ICP metals (**Table 3**)	
	KOH fusion • ICP metals (**Table 3**) • GEA • Total alpha • ^{238}Pu, $^{239+240}$Pu • U/KPA • ^{90}Sr • Total beta	
	Water Leach • Anions (**Table 3**)	
Dewater filtrate **(TI572-G2-A)**	Direct distribution • Anions (**Table 3**) • Free hydroxide	
	Acid digestion • ICP metals (**Table 3**) • GEA • Total alpha • ^{238}Pu, $^{239+240}$Pu • U/KPA • ^{90}Sr • Total beta	
Time interval Caustic Leach filtrates **(TI572-G2-C1, TI572-G2-C2, TI572-G2-C3,** **TI572-G2-C4, TI572-G2-C5)**	Direct distribution • Free hydroxide	
	Acid digestion • ICP metals (**Table 3**)	
Caustic-leached permeate **(TI572-G2-D)**	Direct distribution • Anions (**Table 3**) • Free hydroxide	
	Acid digestion • ICP metals (**Table 3**) • GEA • Total alpha • ^{238}Pu, $^{239+240}$Pu • U/KPA • ^{90}Sr • Total beta	

Process Step	Analyte	
Caustic-leached slurry **(TI572-G2-9)**	HF assisted Acid digestion • ICP metals (Table 3)	
	KOH fusion • ICP metals (Table 3) • GEA • Total alpha • ^{238}Pu, $^{239+240}$Pu • U/KPA • ^{90}Sr • Total beta	
	Water Leach • Anions (Table 3)	
First through fourth washes **following caustic leach** **(TI572-G2-E, TI572-G2-F, TI572-G2-G,** **TI572-G2-H)**	Direct distribution • Free hydroxide	
	Acid digestion • ICP metals (Table 3)	
Fifth wash and combined washes **following caustic leach** **(TI572-G2-I, TI572-G2-J)**	Direct distribution • Anions (Table 3) • Free hydroxide	
	Acid digestion • ICP metals (Table 3) • GEA • Total alpha • ^{238}Pu, $^{239+240}$Pu • U/KPA • ^{90}Sr • Total beta	
Caustic-leached and washed slurry **(TI572-G2-12)**	HF assisted Acid digestion • ICP metals (Table 3)	
	KOH fusion • ICP metals (Table 3) • GEA • Total alpha • ^{238}Pu, $^{239+240}$Pu • U/KPA • ^{90}Sr • Total beta	
	Water Leach • Anions (Table 3)	
Time interval Oxidative Leach filtrates **(TI572-G2-L1, TI572-G2-L2, TI572-G2-L3,** **TI572-G2-L4, TI572-G2-L5)**	Acid digestion • ICP metals (Table 3) • GEA • Total alpha • ^{238}Pu, $^{239+240}$Pu • U/KPA • ^{90}Sr • Total beta	

Process Step	Analyte	
Oxidative leach slurry **(TI572-G2-15)**	HF assisted Acid digestion • ICP metals (Table 3)	
	KOH fusion • ICP metals (Table 3) • GEA • Total alpha • ^{238}Pu, $^{239+240}$Pu • U/KPA • ^{90}Sr • Total beta	
	Water Leach • Anions (Table 3)	
First and second washes **following oxidative leach** **(TI572-G2-M, TI572-G2-N)**	Direct distribution • Free hydroxide	
	Acid digestion • ICP metals (Table 3)	
Third wash and combined washes **following oxidative leach** **(TI572-G2-O, TI572-G2-P)**	Direct distribution • Anions (Table 3) • Free hydroxide	
	Acid digestion • ICP metals (Table 3) • GEA • Total alpha • ^{238}Pu, $^{239+240}$Pu • U/KPA • ^{90}Sr • Total beta	
Oxidative leached and washed slurry **(TI572-G2-18)**	HF assisted Acid digestion • ICP metals (Table 3)	
	KOH fusion • ICP metals (Table 3) • GEA • Total alpha • ^{238}Pu, $^{239+240}$Pu • U/KPA • ^{90}Sr • Total beta	
	Water Leach • Anions (Table 3)	
Nitric Acid Wash Sample **(TI572-G2-Acid)**	Direct distribution • ICP metals (Table 3) • GEA • Total alpha • ^{238}Pu, $^{239+240}$Pu • U/KPA • ^{90}Sr • Total beta	

Process Step		Analyte	
TI-RPP-WTP-552			
Combined Slurry Permeate (TI552-G6-Q)		Direct distribution • Anions (Table 3) • Free Hydroxide	
		Acid digestion • ICP metals (Table 3) • GEA • Total alpha • ^{238}Pu, $^{239+240}$Pu • U/KPA • ^{90}Sr • Total beta	
Nitric Acid Wash Sample (TI552-G6-Acid)		Direct distribution • ICP metals (Table 3) • GEA • Total alpha • ^{238}Pu, $^{239+240}$Pu • U/KPA • ^{90}Sr • Total beta	
Permeate from Dewatered Slurry Archive (TI552-G6-8-a)		Acid digestion • ICP metals (Table 3)	
Washed Solids from Dewatered Slurry Archive (TI552-G6-8-b)		HF assisted Acid digestion • ICP metals (Table 3)	
Permeate from Leached Slurry Archive (TI552-G6-13-a)		Acid digestion • ICP metals (Table 3)	
Washed Solids from Leached Slurry Archive (TI552-G6-13-b)		HF assisted Acid digestion • ICP metals (Table 3)	

All analyses are to be conducted per approved PNNL procedures or test plans with the QC defined in the QC information Section. Table 3 defines the analytes of interest, the required detection limits, and analysis methods.

Table 3. Method Detection Limits for Solids and Supernatants

Analyte	Solids	Solutions	Analysis Method
	$\mu Ci/g^{(a)}$	$\mu Ci/ml$	
^{137}Cs	6.0E-02	1.0E-02	
^{60}Co	3.0E-02	1.0E-02	
^{154}Eu	5.0E-03	4.0E-04	GEA
^{155}Eu	8.0E-03	4.0E-04	
^{241}Am	3.0E-03	2.0E-03	
Pu	1.0E-03	1.0E-04	$^{239+240}Pu$ and ^{238}Pu by AEA
Total alpha	1.0E-02	4.0E-03	Proportional counting
Total beta	1.0E-02	1.0E-03	Proportional counting
^{90}Sr	1.0E-02	1.0E-03	Separation and proportional counting
	$\mu g/g$	$\mu g/ml$	
Al	3.0E+02	7.5E+01	
B	2.0E+02	7.5E+01	
Bi	4.0E+02	3.0E+01	
Cd	7.5E+01	7.5E+01	
Cr	1.2E+02	1.5E+01	
Fe	3.0E+02	7.5E+01	
K	1.0E+03[b]	5.0E+01	
Mn	3.0E+02	1.5E+01	
Na	3.0E+03	7.5E+01	ICP-OES
Ni	1.6E+02[b]	3.0E+01	
P	2.0E+02	1.0E+01	
S	1.5E+03	2.0E+2	
Si	3.0E+03	7.5E+01	
Sr	3.0E+02	7.5E+01	
Zn	3.0E+02	7.5E+01	
Zr	3.0E+02	7.5E+01	
U	2.5E+03	7.5E+01	
U	6.0E+01	6.0E+01	Kinetic Phosphorescence
Fluoride	2.5E+02	1.2E+02	
Nitrite	2.5E+02	1.2E+02	
Nitrate	2.5E+02	1.2E+02	Ion Chromatography
Phosphate	2.5E+02	1.2E+02	(water-soluble species)
Sulfate	2.5E+02	1.2E+02	
Oxalate	8.0E+02	4.0E+02	
Hydroxide	NA	1E-01 M	Titration
Total organic carbon	NA	4.0E+02 (as C)	Hot persulfate method
Total inorganic carbon	NA	2.0E+02 (as C)	

(a) KOH fusion for solid samples.
(b) The Ni and K cannot be measured from the KOH fusion which uses a Ni crucible. The Ni and K will be assessed from a separate HF-assisted acid digestion.

Table 4. Analytical Quality Control Parameters

Analyte	Analytical Technique	Liquids			Solids		
		LCS or BS % Recovery[a]	Matrix Spike % Recovery[b]	Duplicate RPD[c]	LCS or BS % Recovery[a]	Matrix or Post Spike % Recovery[b]	Duplicate RPD[c]
As identified in Table 3	ICP-OES	80 - 120%	75 - 125%	<20%	80 - 120%	70 - 130%	<25%
Pu	AEA	80 - 120%	75 - 125%	<20%	80 - 120%	70 - 130%	<25%
Total alpha	Proportional counting	80 - 120%	75 - 125%	<20%	80 - 120%	70 - 130%	<25%
Total beta	Proportional counting	80 - 120%	75 - 125%	<20%	80 - 120%	70 - 130%	<25%
^{90}Sr	Proportional counting	80 - 120%	75 - 125%	<20%	80 - 120%	70 - 130%	<25%
U	KPA	80 - 120%	75 - 125%	<20%	NA[d]	NA[d]	<25%
Anions	Ion chromatography	80 - 120%	75 - 125%	<20%	80 - 120%	70 - 130%	<25%
OH⁻	Potentiometric titration	80 - 120%	N/A	<20%	NA	N/A	NA
As identified in Table 3	GEA	N/A	N/A	<20%	N/A	N/A	<25%
Density	Gravimetry	N/A	N/A	<20%	N/A	N/A	<25%

N/A – not applicable
Footnotes:

(a) LCS = Laboratory Control Standard; BS = Blank Spike A laboratory control sample (LCS) or blank spike (BS) sample is used to monitor the effectiveness of the sample preparation process and is a good measure of method accuracy. Ideally, the LCS is a material similar to the sample being processed, containing the analytes of interest (e.g., standard reference material). An LCS, if available, shall be prepared with each batch of samples processed at the same time. When an appropriate LCS is not available, a BS shall be used in lieu of the LCS. A BS is distilled or deionized water or another suitable matrix spiked with the analytes of interest. It may not be possible to prepare a single BS that contains all analytes of interest (e.g., chemical incompatibility). In such cases, an agreement with the client shall be made to identify the analytes of interest used to prepare the BS, and more than one BS may be used. The BS result is expressed as percent recovery; i.e., the amount measured, divided by the known concentration, multiplied by 100.

(b) For some methods, the sample accuracy is expressed as the percent recovery of a matrix spike sample. Post spikes and analytical spikes are also included under these acceptance criteria. The spiked sample result is expressed as percent recovery; i.e., the amount measured less the amount in the sample, divided by the spike added, times 100. One matrix spike (or post spike or analytical spike) is performed per analytical batch. Samples are batched with similar matrices. For other analytes, the accuracy can be determined based on use of serial dilutions.

(c) RPD = Relative Percent Difference between the samples. Sample precision is estimated by analyzing replicates taken separately through preparation and analysis. Acceptable sample precision for liquids is usually <15% RPD if the sample result is at least 10 times the instrument detection limit. Solids RPDs are generally higher because of the difficulty associated with obtaining homogonously represented samples.
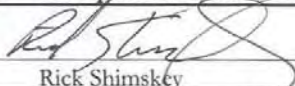
(d) The LCS used to support fusion preparations is SRM2710 (Montana soil). It contains a subset of the analyte list: Al, Ba. Ca, Cu, Fe, Mg, Mn, Na, Si, Sr, Ti, and Zn. It does not contain U.

Analytical Service Request (ASR)

ASR-FY2007-RPP-WTP Tasks Rev. 1.doc

(Information on this COVER PAGE is applicable to all samples submitted under this ASR)

Requestor --- Complete all fields on this COVER PAGE, unless specified as optional or ASR is a revision

Requestor:
Signature _Rick Shimskey_
Print Name _____Rick Shimskey_____
Phone _____376-3183_____ MSIN __P7-27__

Project Number: _____52964_____

Work Package: _____F99189_____

Matrix Type Information

- ◆ **Liquids:** X Aqueous ☐ Organic ☐ Multi-phase
- ◆ **Solids:** ☐ Soil X Sludge ☐ Sediment
  ☐ Glass ☐ Filter ☐ Metal
  ☐ Smear ☐ Organic ☐ Other
- ◆ **Other:** ☐ Solid/Liquid Mixture, Slurry
  ☐ Gas ☐ Biological Specimen

(If sample matrices vary, specify on Request Page)

Disposal Information

- ◆ **Disposition of Virgin Samples:**
  Virgin samples are returned to requestor unless archiving provisions are made with receiving group!

  If archiving, provide:
  Archiving Reference Doc: _____

- ◆ **Disposition of Treated Samples:**
  X Dispose ☐ Return

QA/Special Requirements

- ◆ **QA Plan:**
  X ASO-QAP-001, Rev. 6 (Equivalent to HASQARD)
  X Additional QA Requirements, List Document Below:
  Reference Doc Number:_RPP_WTP-QA-005, Rev. 2_
- ◆ **Field COC Submitted?** X No ☐ Yes
- ◆ **Lab COC Required?** X No ☐ Yes
- ◆ **Sample/Container Inspection Documentation Required?**
  X No ☐ Yes
- ◆ **Hold Time:** X No ☐ *Yes*
  If Yes, ☐ Use SW 846 (PNL-ASO-071, identify
  Contact ASO analytes/methods where holding times apply)
  Lead before
  submitting ☐ Other? Specify: _____
  Samples
- ◆ **Special Storage Requirements:**
  X None ☐ Refrigerate ☐ Other, Specify: _____
- ◆ **Data Requires ASO Quality Engineer Review?** X No ☐ Yes

Data Reporting Information

- ◆ **Is Work Associated with a Fee-Based Milestone?** X No ☐ Yes
  If yes, milestone due date:
  _____

- ◆ **Preliminary Results Requested, As Available?** ☐ No X Yes

- ◆ **Data Reporting Level**
  X ASO-QAP-001 (Equivalent to HASQARD).
  ☐ Minimum data report.
  ☐ Project Specific Requirements:
  Contact ASO Lead or List Reference
  Document:_____

- ◆ **Requested Analytical Work Completion Date:**
  _____
  (Note: Priority rate charge for < 10 business day turn-around time)
- ◆ **Negotiated Commitment Date:**
  _____5/26/08_____
  (To be completed by ASO Lead)
  KNP, LRG, CZS LPD, KJC
  BHO, PKB, IEB, RGG, MTS
  KCT

Waste Designation Information

- ◆ **Sample Information Check List Attached?** X No ☐ Yes
  If no, Reference Doc Attached: _____
  or, Previous ASR Number: ____7985_____
  or, Previous RPL Number: _____

Does the Waste Designation Documentation Indicate Presence of PCBs?
X No ☐ Yes

Send Report To: _____Rick Shimskey_____ MSIN _____P7-27_____

_____Matt Edwards_____ MSIN _____P7-25_____

Additional or Special Instructions _The requirements of Statement of Work, RPP-WTP-QA-005, Rev. 2, apply to this work. Task-specific Quality Control criteria are attached. Reference Document (i.e., TP-RPP-WTP-____):____

Receiving and Login Information *(to be completed by ASO staff)*

Date Delivered: _In SAL 3/17/08_	Received By: _____
Delivered By (optional) _____	
Time Delivered (optional) _____	**ASR Number:** _____8113_____ Rev.: __00__
Group ID (optional) _RPP-WTP/Task No: [ ]_	
CMC Waste Sample? X No ☐ Yes	**RPL Numbers:** _____08-01290 to 08-01323_____
(first and last)

ASO Work Accepted By: _KN. Pool_ **Signature/Date:** _____ 4/15/08

Analytical Service Request (ASR)

(REQUEST PAGE —— Information Specific to Individual Samples)

Provide Analytes of Interest and required Detection limits - ☐ Below   X Attached

ASO Staff Use Only — RPL Number	Client Sample ID	Sample Description (& Matrix, If Varies)	Analysis Requested	ASO Staff Use Only — Test	Library
08-01290	TI572-G2-A	Dewater Filtrate	*Direct Analyses* 1) OH 2) IC-Anions	OH IC	Lab Analyses
08-01291	TI572-G2-D	Leach Permeate			
08-01292	TI572-G2-I	Wash 5 Permeate		Prep -128 ICP	Lab Analysis
08-01293	TI572-G2-J	Combined Permeate	*Acid Digest – 128 (Prep Lab)*	GEA	Radchem
08-01294	TI572-G2-O	Oxidative Wash 3 Permeate	1) ICP/OES 2) GEA	Alpha	
08-01295	TI572-G2-P	Combined Wash	3) Total Alpha 4) Total Beta	Beta	
08-01296	TI552-G2-Q	Final Slurry Permeate form TI552	5) ^{238}Pu, $^{239+240}$Pu	Pu-AEA	
08-01297	TI572-G2-L1	0.5 hr Oxidative Leach	6) ^{90}Sr	Sr-90	
08-01298	TI572-G2-L2	1 hr Oxidative Leach	7) U/KPA (Separate BS & MS needed using U spike only)	U-KPA	
08-01299	TI572-G2-L3	2 hr Oxidative Leach			
08-01300	TI572-G2-L4	4 hr Oxidative Leach	**No OH or IC**		
08-01301	TI572-G2-L5	6 hr Oxidative Leach			
08-01302	TI572-G2-Acid	2M Nitric acid Wash Soln			
08-01303	TI552-G6-Acid	2M Nitric acid Wash Soln			
08-01304	TI572-G2-C1	Caustic Leached Filtrate, 1 hr heat up	*Direct Analyses* 1) OH	OH	Lab Analyses
08-01305	TI572-G2-C2	Caustic Leached Filtrate, 3 hr heat up			
08-01306	TI572-G2-C3	Caustic Leached Filtrate, 0 hr heat up		Prep -128 ICP	Lab Analysis
08-01307	TI572-G2-C4	Caustic Leached Filtrate, 4 hr heat up			
08-01308	TI572-G2-C5	Caustic Leached Filtrate, 8 hr heat up	*Acid Digest – 128 (Prep Lab)*		
08-01309	TI572-G2-E	Wash 1 Permeate	1) ICP/OES		
08-01310	TI572-G2-F	Wash 2 Permeate			
08-01311	TI572-G2-G	Wash 3 Permeate			
08-01312	TI572-G2-H	Wash 4 Permeate			
08-01313	TI572-G2-M	Oxidative Wash 1 Permeate			
08-01314	TI572-G2-N	Oxidative Wash 2 Permeate			
08-01315	TI552-G6-8-a	*Group 5/6 Slurry Permeate*	**No OH**		
08-01316	TI552-G6-13-a	*Group 5/6 Slurry Permeate*			

ASR # 8113   Rev: 00   Page 1 of 2

ASR 8113 - Group 1-2 CUF ASR.doc

M.13

Analytical Service Request (ASR)

(REQUEST PAGE ---- Information Specific to Individual Samples)

Provide Analytes of Interest and required Detection limits - ☐ Below X Attached

ASO Staff Use Only				ASO Staff Use Only	
RPL Number	Client Sample ID	Sample Description (& Matrix, If Varies)	Analysis Requested	Test	Library
08-01317	TI572-G2-6	~20 wt% Slurry	KOH Fusion – 115 (SAL) 1) ICP/OES 2) GEA 3) Total Alpha 4) Total Beta 5) ^{238}Pu, $^{239+240}$Pu 6) ^{90}Sr 7) U/KPA	Prep – 115 ICP GEA Alpha Beta Pu-AEA Sr-90 U-KPA	Lab Analysis Radchem ↓
08-01318	TI572-G2-9	Leach Slurry			
08-01319	TI572-G2-12	Leached and Washed Slurry			
08-01320	TI572-G2-15	Leached and Washed Slurry			
08-01321	TI572-G2-18	Leached and Washed Slurry	Acid Digest – 138 (SAL) 1) ICP/OES	Prep – 138 ICP	Lab Analysis
08-01322	TI552-G6-8-b	Group 5/6 Slurry Permeate	Water Leach – 103 (SAL) 1) IC – Anions	Prep – 103 IC	Lab Analysis
08-01323	TI552-G6-13-b	Group 5/6 Slurry Permeate	Acid Digest – 138 (SAL) ICP/OES Only		

M.14

ASR # ____ 8113 ____ Rev.: ___ 00 ___

Page ____ 2 ____ of ____ 2 ____

ASR 8113 - Group 1-2 CUF ASR.doc

Battelle PNNL/RPG/Inorganic Analysis:
ICP-OES Data Report for KOH Fusions

		Run Date >	4/23/2008	4/23/2008	4/23/2008	4/23/2008	4/23/2008	4/23/2008	4/23/2008
		Multiplier >	2967.1	2598.8	2655.3	3617.9	3138.7	2997.6	3010.2
		RPL/LAB >	08-01317-115-B @5	08-01317-115-S @5	08-01317-115-D @5	08-01318-115-S @5	08-01319-115-S @5	08-01320-115-S @5	08-01321-115-S @5
Instr. Det. Limit (IDL)	Est. Quant. Limit (EQL)	Client ID >	Prep Blank	TI572-G2-6		TI572-G2-9	TI572-G2-12	TI572-G2-15	TI572-G2-18
(µg/mL)	(µg/mL)	(Analyte)	(µg/g)	(µg/g)	(µg/g)	(µg/g)	(µg/g)	(µg/g)	(µg/g)
0.2900	2.900	Al	--	37,300	37,600	30,500	83,900	56,500	75,100
0.0077	0.077	B	--	[97]	[92]	--	--	--	--
0.0240	0.240	Bi	--	19,100	19,200	26,500	84,500	57,800	78,300
0.0029	0.029	Cd	--	[18]	[13]	[20]	128	[82]	108
0.0024	0.024	Cr	[17]	3,790	3,750	4,930	13,900	11,400	7,250
0.1800	1.800	Fe	--	23,600	23,400	33,100	111,000	71,200	101,000
4.0000	40.000	K	na	na	na	na	na	na	na
0.0011	0.011	Mn	[8.1]	347	348	529	1,730	11,600	10,700
1.9000	19.000	Na	--	260,000	258,000	314,000	177,000	194,000	121,000
0.0400	0.400	Ni	na	na	na	na	na	na	na
0.0540	0.540	P	[280]	37,700	37,100	42,200	24,300	30,900	14,100
0.1600	1.600	S	--	8,120	7,650	[3,900]	[2,000]	[2,800]	[590]
0.2300	2.300	Si	--	18,500	18,600	25,000	84,700	56,200	78,600
0.0003	0.005	Sr	[1.5]	1,300	1,290	1,820	6,280	4,280	5,700
0.0410	0.820	U	--	5,820	5,760	8,290	28,100	19,200	25,900
0.0032	0.064	Zn	[53]	202	199	290	546	391	470
0.0035	0.035	Zr	--	[49]	[42]	[65]	751	468	570
Other Analytes									
0.0015	0.015	Ag	--	--	[4.5]	--	[21]	[16]	[13]
0.0390	0.390	As	--	--	--	--	--	--	--
0.0005	0.010	Ba	[5.4]	77.6	77.6	113	374	253	344
0.0000	0.000	Be	--	[0.46]	[0.53]	[0.25]	[0.82]	[0.53]	[0.69]
1.1000	11.000	Ca	--	--	--	[4,100]	[13,000]	[9,200]	[13,000]
0.0083	0.083	Ce	--	[72]	[48]	[86]	331	[220]	321
0.0027	0.027	Co	--	[18]	[20]	[20]	[58]	[44]	[58]
0.0020	0.020	Cu	--	[43]	[47]	97.7	125	93.5	113
0.0029	0.029	Dy	--	--	--	--	--	--	--
0.0004	0.004	Eu	--	--	--	--	--	--	--
0.0027	0.027	La	--	[11]	[12]	[21]	[58]	[39]	[44]
0.0019	0.019	Li	[6.4]	[29]	[28]	[39]	98.7	72.3	83.9
0.0052	0.052	Mg	423	492	578	716	2,390	1,690	2,210
0.0072	0.072	Mo	[45]	[32]	[38]	[65]	[53]	[63]	[53]
0.0062	0.062	Nd	--	--	[19]	--	[75]	[52]	[77]
0.0320	0.320	Pb	--	[460]	[480]	[590]	2,050	1,470	1,870
0.0064	0.064	Pd	--	--	[21]	--	--	--	--
0.0130	0.130	Rh	--	--	--	--	--	--	--
0.0067	0.067	Ru	--	--	[24]	--	[38]	[42]	[25]
0.0310	0.310	Sb	[120]	--	[150]	--	--	--	--
0.1100	1.100	Se	--	--	--	--	--	--	--
0.0250	0.250	Sn	--	--	--	--	--	--	--
0.0200	0.200	Ta	--	--	--	--	--	--	--
0.0260	0.260	Te	--	--	--	--	[88]	--	--
0.0084	0.084	Th	--	--	--	--	[47]	[60]	[31]
0.0005	0.005	Ti	--	56.1	52.9	82.5	259	165	236
0.0300	0.300	Tl	--	[84]	--	--	--	--	--
0.0032	0.032	V	--	[14]	[12]	[14]	[38]	[21]	[28]
0.0210	0.210	W	--	--	--	--	--	--	--
0.0003	0.003	Y	--	[2.6]	[2.2]	[3.2]	11.3	[7.1]	10.5

1) "--" indicates the value is < MDL. The method detection limit (MDL) = IDL times the "multiplier"
near the top of each column. The estimated sample quantitation limit = EQL (in Column 2)
times the "multiplier". Overall error for values ≥ EQL is estimated to be within ±15%.

2) Values in brackets [ ] are ≥ MDL but < EQL, with errors likely to exceed 15%.

na = not applicable; KOH flux and Ni crucible or Na $_2$O $_2$ flux and Zr crucible for fusion preparations, or Si for HF assisted digests.

Battelle PNNL/RPG/Inorganic Analysis:
ICP-OES Data Report for Acid Digestions

		Run Date >	5/2/2008	5/2/2008	5/2/2008	5/2/2008	5/2/2008	5/2/2008	5/2/2008	5/2/2008	5/2/2008	5/2/2008
		Multiplier >	24.9	611.4	617.7	607.2	613.4	627.4	123.8	119.3	122.8	125.0
		RPL/LAB >	PB-08-01304	08-01304 @25 m	08-01305 @25	08-01306 @25	08-01307 @25	08-01308 @25	08-01309 @5	08-01309-DUP @5	08-01310 @5	08-01311 @5
Instr. Det. Limit (IDL)	Est. Quant. Limit (EQL)	Client ID >	Prep Blank	TI572-G2-C1	TI572-G2-C2	TI572-G2-C3	TI572-G2-C4	TI572-G2-C5	TI572-G2-E	TI572-G2-E	TI572-G2-F	TI572-G2-G
(µg/mL)	(µg/mL)	(Analyte)	(µg/mL)	(µg/mL)	(µg/mL)	(µg/mL)	(µg/mL)	(µg/mL)	(µg/mL)	(µg/mL)	(µg/mL)	(µg/mL)
0.0060	0.060	Al	--	1,610	4,150	8,650	5,600	5,660	2,290	2,290	1,260	444
0.0048	0.096	B	[0.30]	[47]	[39]	64.6	[44]	[44]	15.5	16.4	[10]	[4.9]
0.0300	0.300	Bi	--	--	[180]	654	188	210	45.2	44.7	[18]	[8.9]
0.0034	0.034	Cd	--	[2.8]	--	--	--	[4.2]	[0.57]	--	--	[0.49]
0.0017	0.017	Cr	[0.064]	263	197	377	223	229	121	123	72.4	29.3
0.0024	0.048	Fe	[0.34]	[1.8]	[20]	[28]	[12]	[13]	[1.9]	[1.8]	[3.1]	--
0.0720	0.720	K	--	[310]	[230]	[400]	[320]	[270]	130	113	[66]	[20]
0.0002	0.005	Mn	--	--	[0.20]	--	[0.26]	[0.35]	[0.043]	[0.042]	[0.12]	--
0.0160	0.320	Na	[1.2]	211,000	148,000	238,000	157,000	160,000	74,700	74,800	47,800	29,200
0.0024	0.024	Ni	--	--	--	--	[1.9]	--	--	--	[0.31]	--
0.0500	0.500	P	--	[99]	691	918	726	723	571	580	1,530	4,870
0.0720	2.160	S	[14]	[680]	1,600	[790]	1,470	1,620	1,260	1,260	635	288
0.0056	0.056	Si	--	447	48.6	216	218	264	93.4	87.3	56.5	22.6
0.0001	0.002	Sr	[0.0071]	[0.15]	[0.33]	[0.16]	[0.23]	[0.30]	[0.063]	[0.055]	[0.056]	[0.041]
0.0320	0.320	U	--	[180]	[71]	[66]	[21]	[45]	[9.2]	[12]	[8.3]	--
0.0028	0.056	Zn	[0.29]	[16]	[17]	37.0	[23]	[21]	[6.8]	7.14	[5.3]	[1.3]
0.0011	0.011	Zr	--	--	[1.7]	[2.3]	[2.1]	[1.8]	--	--	--	--
Other Analytes												
0.0021	0.021	Ag	--	--	--	--	--	--	--	--	--	--
0.0430	0.430	As	--	[47]	--	--	--	--	--	--	--	--
0.0003	0.005	Ba	[0.13]	[0.62]	[0.55]	[0.65]	[0.77]	[0.46]	[0.22]	[0.21]	[0.22]	[0.21]
0.0001	0.001	Be	--	[0.055]	[0.065]	[0.15]	[0.11]	[0.12]	[0.035]	[0.034]	[0.022]	[0.0074]
0.0061	0.061	Ca	[0.73]	[21]	[7.2]	[17]	[11]	[19]	[1.4]	--	12.0	[0.85]
0.0100	0.100	Ce	--	--	--	--	--	--	--	--	--	--
0.0024	0.024	Co	[0.15]	[1.5]	[2.6]	[4.7]	[1.6]	[2.0]	[1.2]	--	[0.53]	--
0.0014	0.014	Cu	--	[1.0]	[3.9]	[8.4]	[6.0]	[4.3]	[0.74]	[0.57]	[0.45]	[0.27]
0.0029	0.029	Dy	--	--	--	--	--	--	--	--	--	--
0.0011	0.011	Eu	--	--	--	--	--	--	--	--	--	--
0.0028	0.028	La	--	--	--	--	--	--	--	--	--	--
0.0006	0.012	Li	--	[4.3]	[4.3]	[5.3]	[4.2]	[3.8]	[0.75]	[0.79]	[0.99]	[0.70]
0.0023	0.023	Mg	--	--	--	--	--	--	--	--	--	--
0.0052	0.052	Mo	--	--	--	--	--	--	--	[1.2]	--	--
0.0054	0.054	Nd	--	--	--	--	--	--	--	--	--	--
0.0320	0.320	Pb	--	[32]	[21]	[52]	[37]	[22]	--	[6.5]	--	--
0.0063	0.063	Pd	[0.25]	[5.6]	[9.0]	--	--	[4.2]	[1.2]	[1.4]	--	[1.5]
0.0120	0.120	Rh	--	[8.9]	--	--	--	--	[2.2]	--	--	--
0.0085	0.085	Ru	--	--	--	--	--	--	--	--	--	--
0.0200	0.200	Sb	[0.64]	[37]	--	--	--	--	[6.3]	--	--	--
0.0700	0.700	Se	[5.8]	--	[76]	[130]	[180]	[110]	[40]	[29]	[34]	[40]
0.0270	0.270	Sn	[0.90]	[17]	[42]	[51]	[51]	[40]	[14]	[8.4]	[8.5]	[5.6]
0.0170	0.170	Ta	--	--	--	--	--	--	--	--	--	--
0.0260	0.260	Te	--	--	--	--	--	--	--	--	--	--
0.0098	0.098	Th	--	--	--	--	[6.2]	--	[1.5]	--	[1.9]	[1.4]
0.0004	0.004	Ti	--	--	--	--	--	--	--	--	[0.073]	--
0.0380	0.380	Tl	--	--	--	--	--	--	--	--	--	--
0.0007	0.007	V	[0.057]	[1.2]	[2.0]	[1.4]	[1.9]	[2.1]	[0.34]	[0.46]	[0.30]	[0.55]
0.0190	0.190	W	--	--	--	--	--	--	--	[3.1]	--	--
0.0004	0.004	Y	--	--	--	--	--	--	--	--	--	--

1) "--" indicates the value is < MDL. The method detection limit (MDL) = IDL times the "multiplier" near the top of each column. The estimated sample quantitation limit = EQL (in Column 2) times the "multiplier". Overall error for values ≥ EQL is estimated to be within ±15%.

2) Values in brackets [ ] are ≥ MDL but < EQL, with errors likely to exceed 15%.

e-report_(17).xls
Worksheet: ASR 8113 Batch 1 Final

Battelle PNNL/RPG/Inorganic Analysis:
ICP-OES Data Report for Acid Digestions

5/2/2008	5/2/2008	5/2/2008	5/2/2008	5/2/2008	5/2/2008
24.5	24.4	24.5	122.6	122.7	613.7
08-01312	08-01313	08-01314	08-01315 @5	08-01316 @5	08-01316 @25 rr
TI572-G2-H	TI572-G2-M	TI572-G2-N	TI552-G6-8-a	TI552-G6-13-a	
(µg/mL)	(µg/mL)	(µg/mL)	(µg/mL)	(µg/mL)	(µg/mL)
215	138	172	3,530	15,600	
[1.5]	[1.0]	[1.1]	46.1	30.6	
[4.0]	[2.4]	[1.1]	--	--	
--	[0.10]	[0.11]	[0.43]	[0.67]	
14.3	337	271	1,260	1,660	
[0.087]	[0.43]	[1.1]	[1.4]	14.9	
[12]	[13]	[10]	1,030	576	
[0.032]	[0.0088]	[0.0062]	[0.11]	0.645	
18,700	6,380	5,880	113,000	over-range	214,000
--	--	--	[2.6]	[0.31]	
4,240	1,120	971	2,490	678	
123	[51]	58.5	2,330	1,180	
45.6	27.9	33.8	50.1	49.9	
[0.023]	[0.012]	[0.016]	[0.057]	[0.11]	
[1.8]	[0.81]	[1.8]	--	[8.0]	
[0.42]	--	[0.22]	--	[6.6]	
--	[0.042]	--	[0.24]	[0.68]	

--	--	--	--	--	
--	--	--	--	--	
0.143	[0.088]	0.166	[0.27]	[0.34]	
[0.0018]	[0.0033]	[0.0017]	[0.014]	0.0800	
[0.24]	[0.80]	3.31	21.1	[2.9]	
--	--	--	--	--	
--	[0.14]	--	[0.54]	--	
--	[0.047]	[0.060]	[0.28]	2.74	
--	--	--	--	--	
--	--	--	--	--	
[0.25]	[0.29]	0.318	[0.60]	3.19	
--	--	--	--	--	
--	--	--	30.1	16.2	
--	--	--	--	--	
--	--	--	--	[36]	
[0.38]	[0.20]	--	[3.1]	[2.7]	
--	--	--	[3.6]	[2.7]	
--	--	--	[4.7]	[2.7]	
--	--	--	--	--	
[5.9]	[4.0]	[8.8]	[27]	[29]	
--	[2.4]	[1.4]	[15]	[14]	
--	--	--	--	--	
--	--	--	--	--	
--	[0.43]	[0.43]	[2.7]	[1.9]	
--	--	[0.015]	--	--	
--	--	--	--	--	
0.185	0.244	0.208	1.74	[0.80]	
--	[0.47]	--	56.5	30.6	
--	--	--	--	--	

Battelle PNNL/RPG/Inorganic Analysis:
ICP-OES Data Report for Acid Digestions

QC Performance 5/2/2008

Criteria >	≤ 20%	80%-120%	75%-125%	75%-125%	75%-125%	≤ 10%
QC ID >	08-01309 Dup	LCS/BS	08-01309 MS	08-1309 + PS-A	08-1309 + PS-B	08-01304 5-fold Serial Dil
Analytes	RPD (%)	%Rec	%Rec	%Rec	%Rec	%Diff
Al	0.0	98	102	104		3.2
B	5.6	104	103	103		
Bi	1.3	96	91	96		
Cd		98	99	97		
Cr	1.0	98	102	104		0.9
Fe		97	101	100		
K	13.9	99	102	101		
Mn		99	98	101		
Na	0.2	97	nr	nr		2.0
Ni		97	99	102		
P	1.6	100	99	101		
S	0.0	97	101		101	
Si	6.7	96	97	107		9.2
Sr		100	100	103		
U		95	96		97	
Zn		99	111	105		
Zr		89	87	100		
Other Analytes						
Ag				96		
As				103		
Ba		97	99	99		
Be		95	98	100		
Ca		98	98	101		
Ce		92	91		95	
Co				102		
Cu		96	98	101		
Dy					97	
Eu					97	
La		93	92		84	
Li		99	100	101		
Mg		98	98	100		
Mo		100	102	102		
Nd		94	93		95	
Pb		100	101	102		
Pd					92	
Rh					98	
Ru					97	
Sb				98		
Se				107		
Sn				97		
Ta				103		
Te					97	
Th		61	74		95	
Ti		100	98	98		
Tl				96		
V		91	92	96		
W		96	102	97		
Y				96		

Shaded results are outside the acceptance criteria.

nr = not recovered; spike concentration less than 25% of sample concentration.

e-report_(17).xls
Worksheet: ASR 8113 Batch 1 Final

Battelle PNNL/RPG/Inorganic Analysis:
ICP-OES Data Report for Acid Digestions

		Run Date >	5/5/2008	5/5/2008	5/5/2008	5/5/2008	5/5/2008	5/5/2008	5/5/2008	5/5/2008	5/5/2008	5/5/2008
		Multiplier >	19.9	118.2	124.1	122.7	613.4	24.5	24.2	121.1	123.0	19.7
		RPL/LAB >	PB-08-01290	08-01290-128 @5 m	08-01290-DUP-128 @5	08-01291-128 @5	08-01291-128 @25	08-01292-128	08-01293-128	08-01293-128 @5	08-01294-128 @5	08-01295-128
Instr. Det. Limit (IDL)	Est. Quant. Limit (EQL)	Client ID >	Prep Blank	TI572-G2-A		TI572-G2-D		TI572-G2-I	TI572-G2-J		TI572-G2-O	TI572-G2-P
(µg/mL)	(µg/mL)	(Analyte)	(µg/mL)	(µg/mL)	(µg/mL)	(µg/mL)	(µg/mL)	(µg/mL)	(µg/mL)	(µg/mL)	(µg/mL)	(µg/mL)
0.0060	0.060	Al	--	952	931	5,070		115	802		841	123
0.0048	0.096	B	[1.0]	63.2	65.4	33.9		[1.1]	5.38		[7.5]	[0.73]
0.0300	0.300	Bi	--	--	--	157		--	13.1		[9.1]	--
0.0034	0.034	Cd	--	--	--	--		--	--		--	--
0.0017	0.017	Cr	[0.063]	486	473	206		7.65	45.1		47.2	231
0.0024	0.048	Fe	[0.075]	[5.6]	[5.0]	8.24		[0.16]	[0.77]		[0.75]	[0.74]
0.0720	0.720	K	--	557	547	286		[5.4]	46.1		[42]	[7.8]
0.0002	0.005	Mn	--	[0.093]	[0.086]	1.20		[0.012]	[0.053]		--	[0.011]
0.0160	0.320	Na	--	100,000	100,000	over-range	142,000	9,540	over-range	36,300	36,500	4,840
0.0024	0.024	Ni	--	--	--	--		--	--		--	--
0.0500	0.500	P	--	1,010	1,040	309		2,130	2,890		3,000	819
0.0720	2.160	S	--	5,360	5,240	1,800		63.1	448		446	42.6
0.0056	0.056	Si	--	[5.9]	15.3	215		16.5	80.2		20.0	24.6
0.0001	0.002	Sr	[0.0034]	0.226	0.230	[0.095]		[0.011]	[0.022]		[0.042]	[0.0096]
0.0320	0.320	U	--	107	109	[7.6]		--	[1.8]		--	--
0.0028	0.056	Zn	[0.68]	[0.54]	[0.53]	17.5		[0.50]	2.24		[2.9]	[0.61]
0.0011	0.011	Zr	--	--	--	[0.49]		--	--		--	--
Other Analytes												
0.0021	0.021	Ag	--	--	--	--		--	--		--	[0.059]
0.0430	0.430	As	--	--	--	--		--	--		--	--
0.0003	0.005	Ba	[0.031]	[0.31]	[0.30]	[0.23]		[0.12]	0.175		[0.22]	0.247
0.0001	0.001	Be	--	--	--	[0.062]		[0.0018]	[0.0071]		[0.0078]	[0.0012]
0.0061	0.061	Ca	[0.82]	--	[2.8]	--		[0.60]	--		[2.5]	[0.52]
0.0100	0.100	Ce	--	--	--	--		--	--		--	--
0.0024	0.024	Co	--	--	--	--		--	--		--	--
0.0014	0.014	Cu	--	--	--	3.32		--	[0.098]		[0.20]	--
0.0029	0.029	Dy	--	--	--	--		--	--		--	--
0.0011	0.011	Eu	--	--	--	--		--	--		--	--
0.0028	0.028	La	--	--	--	--		--	--		--	--
0.0006	0.012	Li	--	[0.89]	[1.1]	[0.61]		[0.21]	0.347		[0.64]	0.239
0.0023	0.023	Mg	--	--	--	--		--	--		--	--
0.0052	0.052	Mo	--	7.02	7.19	[3.6]		[0.18]	[0.72]		--	[0.23]
0.0054	0.054	Nd	--	--	--	--		--	[0.18]		--	--
0.0320	0.320	Pb	--	--	--	[22]		--	[2.0]		[5.5]	--
0.0063	0.063	Pd	--	--	[1.2]	--		--	[0.16]		--	--
0.0120	0.120	Rh	--	[2.1]	--	[2.3]		[0.32]	[0.31]		[2.6]	[0.24]
0.0085	0.085	Ru	--	--	[1.1]	--		--	--		--	--
0.0200	0.200	Sb	[1.2]	[5.5]	[3.2]	--		[0.92]	--		[7.7]	--
0.0700	0.700	Se	--	[16]	[21]	[16]		[2.7]	--		--	--
0.0270	0.270	Sn	--	--	[5.6]	[11]		--	[2.1]		--	--
0.0170	0.170	Ta	--	--	--	--		--	--		--	--
0.0260	0.260	Te	[0.58]	[3.5]	[6.8]	--		[0.90]	[0.75]		[5.2]	[0.59]
0.0098	0.098	Th	--	--	[1.4]	--		--	--		--	[0.31]
0.0004	0.004	TI	--	[0.053]	--	--		--	[0.017]		--	[0.012]
0.0380	0.380	TI	--	--	--	--		--	--		--	--
0.0007	0.007	V	--	[0.092]	--	--		[0.058]	[0.091]		[0.21]	[0.14]
0.0190	0.190	W	--	[14]	[13]	[7.0]		[0.54]	[1.5]		--	--
0.0004	0.004	Y	--	--	--	--		--	--		--	--

1) "--" indicates the value is < MDL. The method detection limit (MDL) = IDL times the "multiplier" near the top of each column. The estimated sample quantitation limit = EQL (in Column 2) times the "multiplier". Overall error for values ≥ EQL is estimated to be within ±15%.

2) Values in brackets [ ] are ≥ MDL but < EQL, with errors likely to exceed 15%.

e-report_(17).xls
Worksheet: ASR 8113 Batch 2 Final

Battelle PNNL/RPG/Inorganic Analysis:
ICP-OES Data Report for Acid Digestions

5/5/2008	5/5/2008	5/5/2008	5/5/2008	5/5/2008	5/5/2008	5/5/2008	5/5/2008
24.9	126.2	24.9	24.1	24.6	25.1	23.9	24.8
08-01296-128	08-01297-128 @5	08-01298-128	08-01299-128	08-01300-128	08-01301-128	08-01302-128	08-01303-128
TI552-G6-Q	TI572-G2-L1	TI572-G2-L2	TI572-G2-L3	TI572-G2-L4	TI572-G2-L5	TI572-G2-Acid	TI552-G6-Acid
(µg/mL)	(µg/mL)	(µg/mL)	(µg/mL)	(µg/mL)	(µg/mL)	(µg/mL)	(µg/mL)
1,170	316	111	170	158	243	40.3	111
[1.7]	[3.7]	[0.89]	[1.4]	[1.2]	[1.8]	[0.16]	[0.26]
--	--	--	--	--	[0.82]	--	149
--	--	--	--	--	--	--	[0.16]
284	1,500	329	710	713	1,050	4.08	14.3
[0.082]	[0.42]	[0.17]	[0.25]	[0.26]	1.32	31.2	142
32.0	[46]	[11]	29.7	17.9	27.5	[2.8]	[2.0]
3.98	340	112	850	39.7	[0.098]	9.02	7.59
10,300	25,400	7,350	11,600	10,300	15,300	187	383
--	--	--	--	--	--	2.97	8.29
28.0	5,250	1,550	2,300	2,100	3,180	--	59.3
[12]	[220]	56.9	99.6	72.9	115	[5.6]	[3.9]
5.86	15.5	9.31	21.1	15.8	28.4	21.5	59.6
[0.0043]	[0.029]	[0.0059]	--	[0.0054]	0.0596	9.42	8.56
--	--	--	--	--	--	48.7	38.0
[0.62]	--	[0.49]	[0.64]	--	--	1.45	1.66
[0.047]	--	--	--	[0.066]	[0.076]	[0.26]	0.632
--	--	--	--	[0.071]	[0.063]	[0.060]	--
--	--	[1.5]	--	--	--	--	--
[0.13]	[0.16]	[0.099]	[0.098]	[0.13]	[0.13]	0.647	0.721
[0.0016]	--	--	[0.0037]	[0.0059]	[0.0080]	[0.0015]	[0.0021]
[0.74]	[0.94]	[0.72]	--	[0.62]	[0.77]	6.52	20.5
--	--	--	--	--	--	--	[0.62]
--	--	--	--	--	--	4.67	1.08
--	--	--	--	--	--	0.399	[0.18]
--	--	--	--	--	--	--	--
--	--	--	--	--	--	--	--
--	--	--	--	--	--	[0.071]	--
[0.078]	[0.79]	[0.18]	[0.23]	[0.28]	0.408	[0.063]	[0.12]
--	--	--	--	--	--	1.24	3.05
[0.63]	[1.1]	[0.53]	[0.42]	[0.42]	[0.84]	--	[0.31]
--	[1.0]	[0.17]	--	[0.16]	--	[0.39]	[0.18]
[1.5]	[4.8]	[1.2]	[2.1]	[1.3]	[2.2]	[0.93]	[2.9]
--	--	--	--	--	--	--	--
--	--	--	--	[0.40]	--	[0.36]	--
[0.31]	--	--	--	--	--	--	--
--	[3.5]	[1.4]	--	--	--	--	[1.4]
--	[19]	[5.1]	[3.0]	[4.2]	[5.0]	--	--
--	--	--	--	--	--	--	--
--	--	--	--	--	--	--	--
[0.83]	[5.8]	--	[1.1]	--	[0.67]	[1.0]	--
[0.41]	[1.7]	[0.61]	[1.2]	[0.97]	[1.5]	[0.26]	--
[0.013]	--	--	[0.019]	[0.018]	[0.035]	0.120	0.259
--	--	--	--	--	--	--	--
[0.15]	[0.52]	[0.13]	0.180	[0.18]	[0.18]	[0.032]	0.207
--	--	--	[0.52]	--	[0.48]	--	--
--	--	--	--	--	--	[0.040]	[0.018]

e-report_(17).xls
Worksheet: ASR 8113 Batch 2 Final

Battelle PNNL/RPG/Inorganic Analysis:
ICP-OES Data Report for Acid Digestions

QC Performance 5/5/2008

Criteria >	≤ 20%	80%-120%	75%-125%	75%-125%	75%-125%	≤ 10%
QC ID >	08-01290 Dup	LCS/BS	08-01290 MS	08-01290 + PS-A	08-01290 + PS-B	08-01290 5-fold Serial Dil
Analytes	RPD (%)	%Rec	%Rec	%Rec	%Rec	%Diff
Al	2.2	96	98	102		1.8
B	3.3	101	105	103		2.5
Bi		95	90	97		
Cd		97	98	97		
Cr	2.8	97	nr	101		3.5
Fe		97	104	104		
K	1.8	98	103	101		6.2
Mn		97	99	101		
Na	0.3	97	nr	nr		2.6
Ni		97	101	104		
P	2.9	99	98	100		0.7
S	2.2	88	92		100	1.1
Si		96	102	102		
Sr	1.8	99	101	102		
U	1.6	95	98		96	
Zn		97	101	104		
Zr		89	93	102		
Other Analytes						
Ag				94		
As				100		
Ba		98	100	102		
Be		94	99	100		
Ca		96	99	100		
Ce		92	93		95	
Co				101		
Cu		96	101	104		
Dy					98	
Eu					98	
La		93	95		95	
Li		97	101	101		
Mg		99	101	102		
Mo	2.4	98	98	101		
Nd		94	97		95	
Pb		98	100	101		
Pd					94	
Rh					99	
Ru					98	
Sb				99		
Se				107		
Sn				99		
Ta				100		
Te					99	
Th		63	20		98	
Tl		100	102	102		
Ti				95		
V		92	95	98		
W		96	117	102		
Y				99		

Shaded results are outside the acceptance criteria.
nr = not recovered; spike concentration less than 25% of sample concentration.

e-report_(17).xls
Worksheet: ASR 8113 Batch 2 Final

M.21

Battelle PNNL/RPG/Inorganic Analysis:
ICP-OES Data Report for HF-Assisted Acid Digestions

		Run Date >	4/24/2008	4/24/2008	4/24/2008	4/24/2008	4/24/2008	4/24/2008
		Multiplier >	784.5	716.8	711.2	749.6	874.1	4370.6
		RPL/LAB >	08-01317-138-B	08-01317-138-S	08-01317-138-D	08-01318-138-S	08-01319-138-S	08-01319-138-S @5
Instr. Det. Limit (IDL)	Est. Quant. Limit (EQL)	Client ID >	Prep Blank	TI572-G2-6		TI572-G2-9	TI572-G2-12	TI572-G2-12
(µg/mL)	(µg/mL)	(Analyte)	(µg/g)	(µg/g)	(µg/g)	(µg/g)	(µg/g)	(µg/g)
0.0060	0.060	Al	[30]	40,900	40,500	32,800	76,600	
0.0048	0.096	B	--	[54]	[53]	--	--	
0.0300	0.300	Bi	--	20,700	20,600	27,900	75,900	
0.0034	0.034	Cd	--	30.3	29.7	42.7	121	
0.0017	0.017	Cr	--	4,080	4,040	5,120	12,700	
0.0024	0.048	Fe	[24]	25,400	25,100	35,300	99,700	
0.0720	0.720	K	[25]	934	970	[400]	[140]	
0.0002	0.005	Mn	[0.93]	362	358	535	1,520	
0.0160	0.320	Na	[50]	268,000	266,000	327,000	153,000	
0.0024	0.024	Ni	--	1,460	1,450	2,060	5,690	
0.0500	0.500	P	[62]	40,300	40,200	45,700	21,600	
0.0720	2.160	S	[100]	8,450	8,440	4,250	[1,300]	
0.0056	0.056	Si	na	na	na	na	na	
0.0001	0.002	Sr	[0.58]	1,410	1,390	1,980	over-range	5,780
0.0320	0.320	U	--	6,360	6,290	8,960	25,600	
0.0028	0.056	Zn	54.9	207	201	208	468	
0.0011	0.011	Zr	[2.0]	106	106	147	408	
Other Analytes								
0.0021	0.021	Ag	--	[4.4]	[5.0]	[7.7]	19.2	
0.0430	0.430	As	--	--	--	--	--	
0.0003	0.005	Ba	8.19	109	90.0	132	340	
0.0001	0.001	Be	[0.051]	0.431	0.397	[0.25]	0.858	
0.0061	0.061	Ca	110	3,190	3,130	4,450	12,600	
0.0100	0.100	Ce	--	84.1	83.3	119	335	
0.0024	0.024	Co	--	[15]	[12]	19.6	53.7	
0.0014	0.014	Cu	[3.2]	39.7	39.6	43.2	101	
0.0029	0.029	Dy	--	--	--	--	--	
0.0011	0.011	Eu	--	--	--	--	[1.0]	
0.0028	0.028	La	[2.2]	[15]	[16]	[20]	54.0	
0.0006	0.012	Li	--	27.2	26.2	34.1	84.0	
0.0023	0.023	Mg	22.1	546	544	758	2,110	
0.0052	0.052	Mo	--	[18]	[24]	[16]	[36]	
0.0054	0.054	Nd	--	[17]	[17]	[27]	72.0	
0.0320	0.320	Pb	--	578	533	645	1,890	
0.0063	0.063	Pd	--	--	--	--	--	
0.0120	0.120	Rh	--	--	--	--	--	
0.0085	0.085	Ru	--	[7.5]	[6.1]	--	[12]	
0.0200	0.200	Sb	--	--	[33]	--	--	
0.0700	0.700	Se	--	--	--	--	--	
0.0270	0.270	Sn	--	[47]	[21]	--	--	
0.0170	0.170	Ta	--	--	--	--	--	
0.0260	0.260	Te	--	--	--	--	--	
0.0098	0.098	Th	--	--	[9.5]	[12]	[42]	
0.0004	0.004	Ti	[0.74]	63.6	63.4	84.2	239	
0.0380	0.380	Tl	[51]	[55]	[82]	[110]	--	
0.0007	0.007	V	[1.1]	16.9	17.0	18.2	40.6	
0.0190	0.190	W	--	[27]	[31]	--	--	
0.0004	0.004	Y	--	[2.6]	[2.6]	3.60	10.5	

1) "--" indicates the value is < MDL. The method detection limit (MDL) = IDL times the "multiplier" near the top of each column. The estimated sample quantitation limit = EQL (in Column 2) times the "multiplier". Overall error for values ≥ EQL is estimated to be within ±15%.
2) Values in brackets [ ] are ≥ MDL but < EQL, with errors likely to exceed 15%. na indicates that the analyte is not recovered for the preparation procedure.

Battelle PNNL/RPG/Inorganic Analysis:
ICP-OES Data Report for HF-Assisted Acid Digestions

4/24/2008	4/24/2008	4/24/2008	4/24/2008	4/24/2008	4/24/2008
1014.2	988.1	4940.7	763.9	620.7	3103.7
08-01320-138-S	08-01321-138-S	08-01321-138-S @5	08-01322-138-S	08-01323-138-S	08-01323-138-S @5
TI572-G2-15	TI572-G2-18	TI572-G2-18	TI552-G6-8-b	TI552-G6-13-b	TI552-G6-13-b
(µg/g)	(µg/g)	(µg/g)	(µg/g)	(µg/g)	(µg/g)
61,800	80,800		357,000	over-range	368,000
--	--		--	--	
62,000	84,600		308	334	
99.2	132		56.0	67.8	
12,700	8,020		31,200	33,500	
77,300	107,000		10,800	14,300	
[330]	[170]		[99]	--	
12,400	11,200		6,360	7,870	
201,000	125,000		21,200	17,400	
4,650	6,420		735	1,050	
32,800	14,700		1,300	403	
[1,600]	[1,300]		--	[210]	
na	na		na	na	
4,630	over-range	6,250	1,200	1,790	
21,300	28,600		24,000	35,400	
396	520		146	125	
339	464		340	430	
[17]	[19]		[14]	17.2	
--	--		--	--	
302	378		146	207	
0.655	0.660		0.964	0.392	
10,300	14,000		3,100	4,170	
274	365		146	204	
41.5	57.8		[8.3]	15.0	
82.3	114		69.3	49.5	
--	--		--	[1.9]	
--	--		[3.8]	[5.4]	
41.9	57.4		124	158	
70.0	88.4		78.2	42.9	
1,710	2,350		501	709	
[16]	[28]		[12]	[11]	
57.9	79.7		271	370	
1,510	2,020		1,100	898	
--	--		--	--	
--	--		--	--	
[18]	[8.6]		--	[7.3]	
--	--		--	--	
--	--		--	--	
--	--		--	--	
--	--		--	--	
--	--		--	--	
[26]	[22]		133	149	
178	260		51.4	67.3	
[69]	[110]		[37]	--	
28.6	41.4		8.57	6.15	
--	--		[55]	[15]	
8.31	11.3		37.5	52.0	

Battelle PNNL/RPG/Inorganic Analysis:
ICP-OES Data Report for HF-Assisted Acid Digestions

QC Performance 4/24/2008

Criteria >	≤ 25%	80%-120%	70%-130%	70%-130%	70%-130%	≤ 10%
QC ID >	08-01317 Dup	LCS/BS	MS (none)	08-01317 + AS-A	08-01317 + AS-B	08-01317 5-fold Serial Dil
Analytes	RPD (%)	%Rec	%Rec	%Rec	%Rec	%Diff
Al	0.9	102		100		0.5
B				102		
Bi	0.1			96		1.7
Cd	2.0	94		99		
Cr	1.1			99		3.0
Fe	1.2	101		99		1.7
K	3.9			101		
Mn	1.2	102		99		3.1
Na	0.8	100		97		0.2
Ni	0.6	nr		100		2.6
P	0.1	91		nr		1.1
S	0.1	104			96	5.6
Si	na	na	na	na	na	na
Sr	1.0			100		1.0
U	1.2				99	0.2
Zn	3.0	102		104		4.0
Zr	0.0			100		2.2
Other Analytes						
Ag		103		96		
As		99		101		
Ba	19.1	101		100		1.0
Be	8.3			99		
Ca	1.8	103		102		3.8
Ce	0.9				97	
Co				102		
Cu	0.3	99		100		
Dy					99	
Eu					97	
La					99	
Li	3.8			101		
Mg	0.5	97		101		0.4
Mo				103		
Nd					99	
Pb	8.2	103		103		
Pd					94	
Rh					97	
Ru					96	
Sb				100		
Se				100		
Sn				98		
Ta				103		
Te					97	
Th					97	
Ti	0.2	97		99		4.7
Tl				96		
V	1.0	96		97		
W				100		
Y				98		

Shaded results are outside the acceptance criteria.

nr = not recovered; spike concentration less than 25% of sample concentration.

na indicates that the analyte is not recovered for the preparation procedure.

Direct Liquid Sample Results ASR 8113

RPL Number	Client Sample ID	F MDL µg/mL	F Result µg/mL	DF	NO₂ MDL µg/mL	NO₂ Result µg/mL	DF	SO₄ MDL µg/mL	SO₄ Result µg/mL	DF
08-01290	TI572-G2-A	82	3,970		130	7,800		200	14,700	
08-01291	TI572-G2-D	16	1,520		26	3,130		40	5,090	
08-01292	TI572-G2-I	16	860		5.3	57.5		7.9	156	
08-01293	TI572-G2-J	16	2,330		5.3	493		7.9	1,280	
08-01294	TI572-G2-O	3.3	224		1.1	25.2		1.6	83.1	
08-01295	TI572-G2-P	3.3	378		1.1	42.9		1.6	111	
08-01296	TI552-G6-Q	0.66	1.50	J	5.3	1,070		1.6	37.8	
Dilution Blank	DB 5/12/08	0.031	0.031	U	0.050	0.050	U	0.076	0.076	U

RPL Number	Client Sample ID	C₂O₂ MDL µg/mL	C₂O₂ Result µg/mL	DF	NO₃ MDL µg/mL	NO₃ Result µg/mL	DF	PO₄ MDL µg/mL	PO₄ Result µg/mL	DF
08-01290	TI572-G2-A	26	1,430		1,300	191,000		31	3,070	
08-01291	TI572-G2-D	26	432		1,300	74,900		31	982	
08-01292	TI572-G2-I	5.2	197		11	1,490		31	6,690	
08-01293	TI572-G2-J	5.2	957		53	12,100		160	9,110	
08-01294	TI572-G2-O	1.0	73.7		11	709		6.3	1,510	
08-01295	TI572-G2-P	1.0	1.0	U	11	1,150		31	2,570	
08-01296	TI552-G6-Q	1.0	98.4		53	4,310		1.3	85.4	
Dilution Blank	DB 5/12/08	0.050	0.050	U	0.10	0.100	U	0.060	0.060	U

Direct Liquid Sample QC Results ASR 8113

Sample/Replicate Precision Results [a]

RPL Number	Sample ID	F µg/mL	%RSD	NO₂ µg/mL	%RSD	SO₄ µg/mL	%RSD	C₂O₄ µg/mL	%RSD	NO₃ µg/mL	%RSD	PO₄ µg/mL	%RSD
08-01296	Sample	J	--	1070	--	37.8	--	98.4	--	4310	--	85.4	--
	Duplicate | RPD	J	N/A	1070	0	37.9	0	95.9	3	4320	0	84.5	1

Sample Spike Results - At IC Workstation

RPL Number	Sample ID	F µg/mL	%Rec	NO₂ µg/mL	%Rec	SO₄ µg/mL	%Rec	C₂O₄ µg/mL	%Rec	NO₃ µg/mL	%Rec	PO₄ µg/mL	%Rec
08-01290	Sample	3970	--	7800	--	14700	--	1430	--	191000	--	3070	--
	AS Sample	1.75	99	3.97	100	6.57	100	U	N/A	40.9	103	6	99

Nitrate spike sample results were slightly above the highest calibration standandard

LCS Results - IC System

RPL Number	Run ID	F %Rec	NO₂ %Rec	SO₄ %Rec	C₂O₂ %Rec	NO₃ %Rec	PO₄ %Rec
LCS	5/13/2008 10:15	101	101	101	105	103	102

AS = Analytical Spike: Spike performed at IC Workstation on liquid Sample.
LCS = Laboratory Control Sample (Standard analyzed at IC Workstation)
RPD = Relative Percent Difference
%Rec = Percent Recovery
U = Not Detected Above Method Detection Limit
J = Detected, Result are Qualitative: Result >MDL but <EQL (estimated quantitation limit)
-- = Value Not Calculated, place holder for blank cell
a = %RPD is not calculated for results which are below the EQL

Leached Dry Solids Sample Results ASR 8113

RPL Number	Client Sample ID	F MDL µg/g	F Result µg/g	DF	NO_2 MDL µg/g	NO_2 Result µg/g	DF	SO_4 MDL µg/g	SO_4 Result µg/g	DF
08-01317-103-S	TI572-G2-6	360	26,000		203	11,600		297	23,500	
08-01318-103-S	TI572-G2-9	293	28,700		32	3,730		48	11,000	
08-01319-103-S	TI572-G2-12	124	6,000		8.0	528		12	1,320	
08-01320-103-S	TI572-G2-15	151	11,400		9.7	804		15	2,550	
08-01321-103-S	TI572-G2-18	31	2,200		9.8	328		15	1,340	

		µg/mL	µg/mL	DF	µg/mL	µg/mL	DF	µg/mL	µg/mL	DF
Process Blank		23	23	U	38	38	U	57	57	U
Dilution Blank 5/12/08		0.031	0.031	U	0.050	0.050	U	0.076	0.076	U

RPL Number	Client Sample ID	C_2O_4 MDL µg/g	C_2O_4 Result µg/g	DF	NO_3 MDL µg/g	NO_3 Result µg/g	DF	PO_4 MDL µg/g	PO_4 Result µg/g	DF
08-01317-103-S	TI572-G2-6	39	39	U	1,174	286,000	U	704	92,000	
08-01318-103-S	TI572-G2-9	153	11,500	J	957	91,400		574	133,000	
08-01319-103-S	TI572-G2-12	40	1,850	J	80	16,400		239	33,300	
08-01320-103-S	TI572-G2-15	48	3,860	J	483	25,100		58	58	U
08-01321-103-S	TI572-G2-18	9.8	1,200	J	98	12,100		59	12,100	

		µg/mL	µg/mL	DF	µg/mL	µg/mL	DF	µg/mL	µg/mL	DF
Process Blank		37	37	U	75	75	U	45	45	U
Dilution Blank 5/12/08		0.050	0.050	U	0.10	0.10	U	0.060	0.060	U

Leached Dry Solids Sample Results ASR 8113

Sample/Replicate Precision Results [a]

RPL Number	Sample ID	F µg/g	%RSD	NO_2 µg/g	%RSD	SO_4 µg/g	%RSD	NO_3 µg/g	%RSD	C_2O_4 µg/g	%RSD	PO_4 µg/g	%RSD
08-01317-103-S	Sample	26,000	--	11,600	--	23,500	--	286,000	--	U	--	92,000	--
	Dup (RPD)	25,800	1	11,600	0	23,500	0	287,000	0	10,200	N/A	91,000	1

Sample Spike Results – At IC Workstation

RPL Number	Sample ID	F µg/mL	%Rec	NO_2 µg/mL	%Rec	SO_4 µg/mL	%Rec	NO_3 µg/mL	%Rec	C_2O_4 µg/mL	%Rec	PO_4 µg/mL	%Rec
08-01317-103-BS	Process Leach Blank	U	--	U	--	U	--	U	--	U	--	U	--
	LCS/BS Sample	5.33	104	9.25	104	15.7	102	18.3	102	2.81	27	12.8	100
08-01319-103-S	Sample	376	--	33.1	--	82.7	--	1030	--	116	--	2090	--
	PS Sample	1.73	98	4.23	98	7.82	98	14.9	105	3.76	104	7.27	99

Results E-file 8113 Shimskey.xls
Worksheet: ASR 8113 leached solids

LCS Results – IC System

RPL Number	Run ID	F %Rec	NO₂ %Rec	SO₄ %Rec	C₂O₂ %Rec	NO₃ %Rec	PO₄ %Rec
LCS	5/13/2008 10:15	101	101	101	105	103	102

AS = Analytical Spike: Spike performed at IC Workstation on liquid Sample.

LCS = Laboratory Control Sample (Standard analyzed at IC Workstation)

RPD = Relative Percent Difference

%Rec = Percent Recovery

U = Not Detected Above Method Detection Limit

J = Detected, Result are Qualitative: Result >MDL but <EQL (estimated quantitation limit)

– = Value Not Calculated, place holder for blank cell

▭ = QC recovery did not meet QA Plan or client specifications

Results E-file 8113 Shimskey.xls
Worksheet: ASR 8113 leached solids

M.27

Battelle

. . . Putting Technology To Work

Client:	Rick Shimskey		Report Date:	5/5/2008
			Analysis Date:	5/2/2008

Subject:	Hydroxide Analyses for:	**CUF Group 1/2 Bi-Phosphate Sludge and**	
		Group 5/6 Redox Sludge/Saltcake Treatability	

ASR:	**8113**	Rev-0		Procedure: RPG-CMC-228-Rev 1
Sample ID.	08-01290	thru	08-01296	
and	08-01304	thru	08-01314	

Direct sample aliquots of CUF Group 1/2 Bi-Phosphate Sludge/Saltcake , and CUF Group 5/6 REDOX Sludge Treatability samples (see above assigned RPL Sample #'s), 18 samples total were analyzed in duplicate for the base constituents content following procedure RPG-CMC-228, and using a Brinkman 636 Auto-Titrator. The titrant used was 0.1016 M HCl and the base standard, 0.1118 M NaOH was used for QC verification standards and matrix spike. -- See Chemrec_139 pdf imbedded in the result report.

The hydroxide Standard recovery was 100%, well within the allowed ± 20% recovery range. Although not required in this ASR, three matrix spikes were analyzed with recoveries of 96%, 99%, and 97%. No hydroxide was detected in the reagent blank.

The initial pH is reported on attached Report Summary along with the free hydroxide molarities (generally the 1st inflection point whenever the initial pH is 12 or more). In such cases, generally the 2nd inflection point around pH 7-8, indicates the total hydroxide molarity. Generally, the analysis used very small volumes (0.05ml) due to high caustic, yet surprisingly these results showed excellent Relative Percent Deviation (RPD) for the first inflection point, well within ± 20% allowed range. Many of the samples also indicated a third inflection point around pH 4-5, and   most RPD's for 2nd and third points were within ± 20% allowed range even though this is not a requirement. Again this data is very acceptable considering the small sample size, undissolved species in some samples, and the fact that other base constituent molarities were very miminal compared to the hydroxide.

The best estimate of the MDL for this method is obtained from the reagent blank which did not show any inflection points and is consistent with a value of 0 within our measurement sensitivity. All samples molarities were well above the MDL (0.1M) for this analysis. The results are accepted based on the QC data meeting the acceptance criteria as specified in the ASR.

Following is the report summary, the sample results calculated from the raw data, and the record file for the standardized acid and base used. The entire sample fractions supplied for hydroxide analysis were consumed in the analysis.

Copies of the titration curves are available upon request.

Battelle Pacific Northwest Laboratory
Radiochemical Processing Group-325 Building
Chemical Measurements Center

ASR # **8113**

WP# F99189

Hydroxide and Alkalinity Determination
   Procedure: RPG-CMC-228-Rev 1   Equip # WB76843

Report Summary for ASR # -- 8113   Report Date: 5/5/2008
                      Revision # Rev-0   Analysis Date: 5/2/2008

| RPG # | Client ID | Initial pH | OH conc ug/mL | Concentration, moles / Liter | | | | | |
| | | | | First Point | | Second Point | | Third Point | |
				Molarity	RPD	Molarity	RPD	Molarity	RPD
08-01290	TI-572-G2-A	10.95	1.16E+03	0.07		0.39		0.40	
08-01290-Dup	TI-572-G2-A	11.24	1.18E+03	0.07	2.0%	0.37	5.7%	0.41	1.4%
08-01291	TI-572-G2-D	12.75	6.99E+04	4.11		0.43		0.26	
08-01291-Dup	TI-572-G2-D	12.45	7.18E+04	4.22	2.7%	0.46	5.9%	0.20	25.0%
08-01292	TI-572-G2-I	11.92	3.23E+03	0.19		0.10			
08-01292-Dup	TI-572-G2-I	12.01	3.32E+03	0.20	2.6%	0.10	7.0%		
08-01293	TI-572-G2-J	12.33	1.58E+04	0.93		0.10		0.18	
08-01293-Dup	TI-572-G2-J	12.29	1.55E+04	0.91	2.2%	0.12	15.2%	0.18	2.5%
08-01294	TI-572-G2-O	10.83	5.61E+02	0.03		0.02		0.05	
08-01294-Dup	TI-572-G2-O	10.72	5.18E+02	0.03	8.0%	0.02	11.8%	0.05	2.0%
08-01295	TI-572-G2-P	11.12	1.27E+03	0.07		0.03		0.06	
08-01295-Dup	TI-572-G2-P	11.15	1.23E+03	0.07	3.5%	0.02	24.7%	0.07	8.4%
08-01296	TI-552-G6-Q	11.89	4.28E+03	0.25		0.08		0.03	
08-01296-Dup	TI-552-G6-Q	11.54	4.27E+03	0.25	0.2%	0.09	1.8%	0.03	14.2%

			µg/ml or mg/L MDL	Molarity MDL	Required RPD
OH conc (mg/L) = M (g/L) * 17,000					
free OH as specified in ASR			1.70E+03	0.100	+/- 20%

					Allowed Recovery Range
Reag. Blk.1				0	
Standard 1		12.53		99.6%	+/- 20%
08-01291MS	Matrix spike	12.49		96.4%	N/A

Note: Results are presented for the first, second, and third inflection points on the titration curves, as applicable. The first inflection point is generally associated with the free hydroxide concentration. The second inflection point generally represents total hydroxide, or carbonate or a combination of aluminate and carbonate. The third inflection point is usually indicative of bicarbonate or other weak acids or possibly the continued protonation of alumina.

Battelle Pacific Northwest Laboratory
Radiochemical Processing Group-325 Building
Chemical Measurements Center

ASR #	8113
WP#	F99189

Hydroxide and Alkalinity Determination
Procedure: RPG-CMC-228-Rev 1   Equip #   WB76843

Report Summary for ASR # -- | **8113**   Report Date: | 5/5/2008
Revision # | **Rev-0**   Analysis Date: | 5/2/2008

RPG #	Client ID	Initial pH	OH conc ug/mL	First Point Molarity	RPD	Second Point Molarity	RPD	Third Point Molarity	RPD
08-01304	TI-572-G2-C1	12.60	1.14E+05	6.73		0.50		---	
08-01304-Dup	TI-572-G2-C1	12.55	1.17E+05	6.88	2.1%	0.48	4.6%	0.73	---
08-01305	TI-572-G2-C2	12.71	8.20E+04	4.83		0.36		0.26	
08-01305-Dup	TI-572-G2-C2	12.56	8.18E+04	4.81	0.3%	0.39	7.0%	0.24	4.9%
08-01306	TI-572-G2-C3	12.61	1.26E+05	7.40		0.63		0.24	
08-01306-Dup	TI-572-G2-C3	12.60	1.19E+05	6.98	5.9%	0.68	8.0%	0.30	23.6%
08-01307	TI-572-G2-C4	12.50	8.07E+04	4.75		0.55		0.25	
08-01307-Dup	TI-572-G2-C4	12.52	7.99E+04	4.70	1.1%	0.62	12.1%	0.32	25.9%
08-01308	TI-572-G2-C5	12.50	7.88E+04	4.63		0.48		0.18	
08-01308-Dup	TI-572-G2-C5	12.33	7.16E+04	4.21	9.5%	0.44	7.9%	0.16	10.8%
08-01309	TI-572-G2-E	12.08	3.78E+04	2.22		0.23		0.18	
08-01309-Dup	TI-572-G2-E	12.28	3.72E+04	2.19	1.5%	0.26	12.2%	0.30	49.0%
08-01310	TI-572-G2-F	12.29	2.20E+04	1.29		0.15		0.24	
08-01310-Dup	TI-572-G2-F	12.25	2.20E+04	1.29	0.1%	0.16	5.8%	0.25	4.1%

OH conc (mg/L) = M (g/L) * 17,000

		μg/ml or mg/L MDL	Molarity MDL	Required RPD
free OH as specified in ASR		1.70E+03	0.100	+/- 20%

				Allowed Recovery Range
Reag. Blk.1			0	
Standard 1		12.53	99.6%	+/- 20%
08-01309MS	Matrix spike	12.53	98.8%	N/A

Note: Results are presented for the first, second, and third inflection points on the titration curves, as applicable. The first inflection point is generally associated with the free hydroxide concentration. The second inflection point generally represents total hydroxide, or carbonate or a combination of aluminate and carbonate. The third inflection point is usually indicative of bicarbonate or other weak acids or possibly the continued protonation of alumina.

Battelle Pacific Northwest Laboratory
Radiochemical Processing Group-325 Building
Chemical Measurements Center

ASR # 8113

WP# F99189

Hydroxide and Alkalinity Determination
    Procedure: RPG-CMC-228-Rev 1   Equip # WB76843

Report Summary for ASR # -- 8113   Report Date: 5/5/2008
                   Revision # Rev-0   Analysis Date: 5/2/2008

| | | | | Concentration, moles / Liter | | | | | |
| | | | | First Point | | Second Point | | Third Point | |
RPG #	Client ID	Initial pH	OH conc ug/mL	Molarity	RPD	Molarity	RPD	Molarity	RPD
08-01311	TI-572-G2-G	12.00	1.01E+04	0.59		0.06		0.04	
08-01311-Dup	TI-572-G2-G	12.24	1.04E+04	0.61	3.2%	0.08	26.2%	0.04	18.1%
08-01312	TI-572-G2-H	12.03	6.37E+03	0.37		0.19			
08-01312-Dup	TI-572-G2-H	11.99	6.30E+03	0.37	1.2%	0.20	1.3%		
08-01313	TI-572-G2-M	11.75	2.34E+03	0.14		0.07			
08-01313-Dup	TI-572-G2-M	11.70	2.37E+03	0.14	1.1%	0.07	0.0%		
08-01314	TI-572-G2-N	10.25	8.12E+02	0.05		0.14			
08-01314-Dup	TI-572-G2-N	10.29	7.51E+02	0.04	7.7%	0.14	4.3%		

		μg/ml or mg/L MDL	Molarity MDL	Required RPD
OH conc (mg/L) = M (g/L) * 17,000				
free OH as specified in ASR		1.70E+03	0.100	+/- 20%

				Allowed Recovery Range
Reag. Blk.1			0	
Standard 1		12.53	99.6%	+/- 20%
08-01311MS	Matrix spike	12.10	96.7%	N/A

Note: Results are presented for the first, second, and third inflection points on the titration curves, as applicable. The first inflection point is generally associated with the free hydroxide concentration. The second inflection point generally represents total hydroxide, or carbonate or a combination of aluminate and carbonate. The third inflection point is usually indicative of bicarbonate or other weak acids or possibly the continued protonation of alumina.

Battelle Pacific Northwest Laboratory
Radiochemical Processing Group-325 Building

ASR # and Rev # **8113** Rev-0
Client: **Rick Shimskey**
WP# **F99189**

File: R:\radchem\hydroxide\asr **8113**
Report Date: **5/5/2008**
Analysis Date: **5/2/2008**

Procedure: **RPG-CMC-228-Rev 1** — Determination of Hydroxyl (OH-) and Alkalinity of Aqueous Solutions, Leachates and Supernates

Spreadsheet: OH-TemplateLocked07.xls 4/1/2007

using a Brinkman 636 Auto Titrator Equip # WB76843 Lab Loc. 525

Chem Rec# **139**

Analyst: _____

Titrant	Molarity
HCl	**0.1016**

Std. & Spike Molarity	
NaOH	**0.1118**

R:\CHEMREC\C-rec_139.XLS

RPG #	Sample ID		Dilution Factor	Sample Vol. (mL)	Sample Wt. (g)	Density g/mL	Titrator Routine #	Diluted Initial pH reading	OH 1st Equivalence Point Titrant Vol. (mL)	pH	Found millimoles base	Molarity base	millimole RPD
08-01290	TI-572-G2-A		na	0.100	na		3	10.946	0.067	10.624	0.007	0.068	
08-01290-Dup	TI-572-G2-A	Replicate	na	0.300	na		4	11.240	0.205	10.624	0.021	0.069	2.0%
08-01291	TI-572-G2-D		na	0.200	na		5,6	12.749	8.092	10.221	0.822	4.111	
08-01291-Dup	TI-572-G2-D	Replicate	na	0.050	na		7	12.451	2.078	10.039	0.211	4.222	2.7%
08-01292	TI-572-G2-I		na	0.300	na		8	11.917	0.561	9.481	0.057	0.190	
08-01292-Dup	TI-572-G2-I	Replicate	na	0.400	na		9	12.008	0.768	9.155	0.078	0.195	2.6%
08-01293	TI-572-G2-J		na	0.200	na		10	12.330	1.833	9.812	0.186	0.931	
08-01293-Dup	TI-572-G2-J	Replicate	na	0.200	na		11	12.294	1.793	9.901	0.182	0.911	2.2%
08-01294	TI-572-G2-O		na	0.200	na		12	10.834	0.065	9.218	0.007	0.033	
08-01294-Dup	TI-572-G2-O	Replicate	na	0.200	na		13	10.717	0.060	9.233	0.006	0.030	8.0%
08-01295	TI-572-G2-P		na	0.200	na		14	11.119	0.147	9.083	0.015	0.075	
08-01295-Dup	TI-572-G2-P	Replicate	na	0.200	na		15	11.147	0.142	9.143	0.014	0.072	3.5%
08-01296	TI-552-G6-Q		na	0.200	na		16	11.892	0.496	9.932	0.050	0.252	
08-01296-Dup	TI-552-G6-Q	Replicate	na	0.200	na		17	11.540	0.495	9.941	0.050	0.251	0.2%

		OH vol 2.0	OH Wt.									OH % Recovery	
Reag. Blk.1				0.100		na	1	7.848					
Standard 1	0.1118 M NaOH		2.0116	2.000	na		2	12.525	2.108	8.698	0.2142	95.8%	

		OH vol 2.0	OH Wt.										
08-01291MS	+ 2mL 0.1118 M NaOH		2.0190	0.050	na		18	12.490	4.122	9.814	0.4188	94.1%	MS

Slope **98.5%**
init.pH 7 check 7.025

verif. pH reading
start **7.018**
end **6.998**

Instrument Calibration

Buffer	VWR Lot #	CMS#	Expire Date
4	6350	275295	31-Dec-08
7	6325	275294	30-Nov-08
10	6303	275293	30-Nov-08

2-nd Verif	Fisher Lot #	CMS#	Expire Date
7	68198	275346	31-Mar-09

Performance checks using Balance # 360-01-06-037

Pipet #	Vol.	Wt.	Pipet #	Vol.	Wt.
92501	0.100	0.101	00545	0.0500	0.0494
		0.1002			0.0495
		0.0998			0.0492
		0.1001			0.0501
		0.0995			0.0503
Ave		0.1003	Ave		0.0497
Std. Dev.		0.0006	Std. Dev.		0.0005
% eror		0.61%	% eror		0.95%

OH ASR8113-rs-rev-0.xls
Worksheet: Data

Page 5 of10

Battelle Pacific Northwest Laboratory
Radiochemical Processing Group-325 Building

ASR # and [8113]   File: R:\radchem\hydroxide\asr

Procedure: Alkalinity of Aqueous Solutions, Leachates and Supernates

WP# [F99189]   0

using a Brinkman 636 Auto Titrator   Equip # WB76843

Titrant	Molarity
HCl	0.1016 0

RPG #		Sample Vol. (mL)	2nd Equivalence Point Titrant Vol. (mL)	pH	Found millimoles base	Molarity base	millimole RPD	3rd Equivalence Point Titrant Vol. (mL)	pH	Found millimoles base	Molarity base	millimole RPD
08-01290	0	0.100	0.455	7.641	0.039	0.394		0.852	4.682	0.040	0.403	
08-01290-Dup	Replicat	0.300	1.304	8.048	0.112	0.372	5.7%	2.512	4.755	0.123	0.409	1%
08-01291	0	0.200	8.937	7.776	0.086	0.429		9.446	4.349	0.052	0.259	
08-01291-Dup	Replicat	0.050	2.302	7.382	0.023	0.455	5.9%	2.401	4.553	0.010	0.201	25%
08-01292	0	0.300	0.869	4.424	0.031	0.104						
08-01292-Dup	Replicat	0.400	1.151	4.474	0.039	0.097	7.0%					
08-01293	0	0.200	2.034	7.702	0.020	0.102		2.388	4.566	0.036	0.180	
08-01293-Dup	Replicat	0.200	2.027	7.580	0.024	0.119	15.2%	2.390	4.236	0.037	0.184	3%
08-01294	0	0.200	0.105	7.356	0.004	0.020		0.206	3.922	0.010	0.051	
08-01294-Dup	Replicat	0.200	0.105	7.211	0.005	0.023	11.8%	0.208	3.855	0.010	0.052	2%
08-01295	0	0.200	0.197	6.968	0.005	0.025		0.323	3.500	0.013	0.064	
08-01295-Dup	Replicat	0.200	0.181	7.469	0.004	0.020	24.7%	0.318	3.634	0.014	0.070	8%
08-01296	0	0.200	0.662	6.652	0.017	0.084		0.721	4.410	0.006	0.030	
08-01296-Dup	Replicat	0.200	0.664	6.627	0.017	0.086	1.8%	0.732	4.088	0.007	0.035	14%
							2-nd Recovered					
Standard 1		2.000	2.191	4.471	0.2226		99.6%					
							Total OH recovery					
08-01291MS		0.050	4.331	7.184	0.4400	93.7%	MS	4.503	3.961	0.4575	96.4%	

Matrix spike recovery is calculated as follows:

Spike = 2.00 mL 0.1023 N NaOH was added to the 0.100-mL of sample for each matrix spike.

SpikeTitrant vol. (sample @ .1mL + spike) - SampleTitrant vol. (average sample only equated to .1mL) * 0.2176 N (HCl titrant) = meq. OH

meq OH / 2.00 mL added = meq OH/mL found / 0.1023 N OH added * 100 = % recovered.

OH ASR8113-rs-rev-0.xls
Worksheet: Data

Battelle Pacific Northwest Laboratory
Radiochemical Processing Group-325 Building

ASR # and Rev #: **8113** Rev-0
Client: **Rick Shimskey**
WP#: **F99189**

File: R:\radchem\hydroxide\asr **8113**
Report Date: **5/5/2008**
Analysis Date: **5/2/2008**

Procedure: **RPG-CMC-228-Rev 1** — Determination of Hydroxyl (OH-) and Alkalinity of Aqueous Solutions, Leachates and Supernates using a Brinkman 636 Auto Titrator

Spreadsheet: OH-TemplateLocked07.xls 4/1/2007

Equip # WB76843   Lab Loc. 525

Chem Rec# **139**   R:\CHEMREC\C-rec_139.XLS

Analyst: _____

Titrant	Molarity
HCl	**0.1016**

		Std. & Spike	Molarity
		NaOH	**0.1118**

RPG #	Sample ID		Dilution Factor	Sample Vol. (mL)	Sample Wt. (g)	Density g/mL	Titrator Routine #	Diluted Initial pH reading	OH 1st Equivalence Point Titrant Vol. (mL)	pH	Found millimoles base	Molarity base	millimole RPD
08-01304	TI-572-G2-C1		na	0.050	na		19	12.596	3.314	10.620	0.337	6.734	
08-01304-Dup	TI-572-G2-C1	Replicate	na	0.050	na		20	12.552	3.385	10.773	0.344	6.878	2.1%
08-01305	TI-572-G2-C2		na	0.100	na		21,22	12.708	4.750	9.800	0.483	4.826	
08-01305-Dup	TI-572-G2-C2	Replicate	na	0.050	na		23	12.556	2.368	9.753	0.241	4.812	0.3%
08-01306	TI-572-G2-C3		na	0.050	na		24	12.605	3.643	10.155	0.370	7.403	
08-01306-Dup	TI-572-G2-C3	Replicate	na	0.050	na		25	12.604	3.434	10.269	0.349	6.978	5.9%
08-01307	TI-572-G2-C4		na	0.050	na		26	12.504	2.337	10.092	0.237	4.749	
08-01307-Dup	TI-572-G2-C4	Replicate	na	0.050	na		27	12.523	2.312	10.359	0.235	4.698	1.1%
08-01308	TI-572-G2-C5		na	0.050	na		28	12.499	2.280	10.149	0.232	4.633	
08-01308-Dup	TI-572-G2-C5	Replicate	na	0.050	na		29	12.326	2.073	10.157	0.211	4.212	9.5%
08-01309	TI-572-G2-E		na	0.050	na		30	12.079	1.094	9.547	0.111	2.223	
08-01309-Dup	TI-572-G2-E	Replicate	na	0.050	na		31	12.282	1.078	9.626	0.110	2.190	1.5%
08-01310	TI-572-G2-F		na	0.100	na		32	12.289	1.271	9.439	0.129	1.291	
08-01310-Dup	TI-572-G2-F	Replicate	na	0.100	na		33	12.250	1.272	9.534	0.129	1.292	0.1%
Reag. Blk.1		OH vol 2.0	na		na		1	7.848					
Standard 1	0.1118 M NaOH		na	2.000	na		2	12.525	2.108	8.698	0.2142	95.8% OH % Recovery	
08-01309MS	+ 2mL 0.1118 M NaOH	OH vol 2.0	2.0104	0.050	na		34	12.529	3.173	9.078	0.3224	94.8%	MS

OH Wt. 2.0104

Slope: **98.5%**
init.pH 7 check: 7.025
verif. pH reading: start **7.018** end **6.998**

Instrument Calibration

Buffer	VWR Lot #	CMS#	Expire Date
4	6350	275295	31-Dec-08
7	6325	275294	30-Nov-08
10	6303	275293	30-Nov-08

2-nd Verif	Fisher Lot #	CMS#	Expire Date
7	68198	275346	31-Mar-09

Performance checks using Balance # 360--01-06-037

Pipet #	Vol.	Wt.	Pipet #	Vol.	Wt.
92501	0.100	0.101	00545	0.0500	0.0494
		0.1002			0.0495
		0.0998			0.0492
		0.1001			0.0501
		0.0995			0.0503
	Ave	0.1003		Ave	0.0497
	Std. Dev.	0.0006		Std. Dev.	0.0005
	% eror	0.61%		% eror	0.95%

Battelle Pacific Northwest Laboratory
Radiochemical Processing Group-325 Building   ASR # and 8113   File: R:\radchem\hydroxide\asr

WP# F99189   0

Procedure: Alkalinity of Aqueous Solutions, Leachates and Supernates

using a Brinkman 636 Auto Titrator   Equip # WB76843

Titrant	Molarity	
HCl	0.1016	0

RPG #		Sample Vol. (mL)	2nd Equivalence Point Titrant Vol. (mL)	pH	Found millimoles base	Molarity base	millimole RPD	3rd Equivalence Point Titrant Vol. (mL)	pH	Found millimoles base	Molarity base	millimole RPD
08-01304	0	0.050	3.559	7.421	0.025	0.498			4.196			
08-01304-Dup	Replicat	0.050	3.619	8.766	0.024	0.475	4.6%	3.979	3.951	0.037	0.732	
08-01305	0	0.100	5.108	7.313	0.036	0.364		5.360	3.943	0.026	0.256	
08-01305-Dup	Replicat	0.050	2.560	6.948	0.020	0.390	7.0%	2.680	4.411	0.012	0.244	5%
08-01306	0	0.050	3.953	6.590	0.031	0.630		4.069	3.653	0.012	0.236	
08-01306-Dup	Replicat	0.050	3.770	6.891	0.034	0.683	8.0%	3.917	3.698	0.015	0.299	24%
08-01307	0	0.050	2.609	6.996	0.028	0.553		2.730	4.253	0.012	0.246	
08-01307-Dup	Replicat	0.050	2.619	7.082	0.031	0.624	12.1%	2.776	4.059	0.016	0.319	26%
08-01308	0	0.050	2.516	7.031	0.024	0.480		2.604	4.672	0.009	0.179	
08-01308-Dup	Replicat	0.050	2.291	6.914	0.022	0.443	7.9%	2.370	4.578	0.008	0.161	11%
08-01309	0	0.050	1.209	7.428	0.012	0.234		1.300	4.515	0.009	0.185	
08-01309-Dup	Replicat	0.050	1.208	7.011	0.013	0.264	12.2%	1.358	3.645	0.015	0.305	49%
08-01310	0	0.100	1.422	7.227	0.015	0.153		1.662	3.909	0.024	0.244	
08-01310-Dup	Replicat	0.100	1.432	7.338	0.016	0.163	5.8%	1.682	4.103	0.025	0.254	4%
							2-nd Recovered					
Standard 1		2.000	2.191	4.471	0.2226		99.6%					
						Total OH recovery						
08-01309MS		0.050	3.282	7.423	0.3335	MS 94.2%		3.503	3.621	0.3559	98.8%	

Matrix spike recovery is calculated as follows:

Spike = 2.00 mL 0.1023 N NaOH was added to the 0.100-mL of sample for each matrix spike.

SpikeTitrant vol. (sample @ .1mL + spike) - SampleTitrant vol. (average sample only equated to .1mL) * 0.2176 N (HCl titrant) = meq. OH

meq OH / 2.00 mL added = meq OH/mL found / 0.1023 N OH added * 100 = % recovered

OH ASR8113-rs-rev-0.xls
Worksheet: Data (2)

M.35

Battelle Pacific Northwest Laboratory
Radiochemical Processing Group-325 Building

ASR # and Rev #	8113	Rev-0

File: R:\radchem\hydroxide\asr **8113**

Client: **Rick Shimskey**
Report Date: 5/5/2008
WP#: F99189
Analysis Date: 5/2/2008

Procedure: **RPG-CMC-228-Rev 1** Determination of Hydroxyl (OH-) and Alkalinity of Aqueous Solutions, Leachates and Supernates

Spreadsheet: OH-TemplateLocked07.xls 4/1/2007

using a Brinkman 636 Auto Titrator

Equip # WB76843   Lab Loc. 525

Analyst: _____

Chem Rec#: **139**

Titrant	Molarity		Std. & Spike	Molarity
HCl	0.1016		NaOH	0.1118

OH

RPG #	Sample ID	Dilution Factor	Sample Vol. (mL)	Sample Wt. (g)	Density g/mL	Titrator Routine #	Diluted Initial pH reading	1st Equivalence Point Titrant Vol. (mL)	pH	Found millimoles base	Molarity base	millimole RPD
08-01311	TI-572-G2-G	na	0.100	na		35	11.995	0.585	9.226	0.059	0.594	
08-01311-Dup	TI-572-G2-G	Replicate na	0.200	na		36	12.241	1.208	9.700	0.123	0.614	3.2%
08-01312	TI-572-G2-H	na	0.200	na		37	12.034	0.738	9.395	0.075	0.375	
08-01312-Dup	TI-572-G2-H	Replicate na	0.200	na		38	11.985	0.729	9.260	0.074	0.370	1.2%
08-01313	TI-572-G2-M	na	0.200	na		40	11.745	0.271	8.119	0.028	0.138	
08-01313-Dup	TI-572-G2-M	Replicate na	0.200	na		41	11.695	0.274	7.961	0.028	0.139	1.1%
08-01314	TI-572-G2-N	na	0.200	na		42	10.253	0.094	8.450	0.010	0.048	
08-01314-Dup	TI-572-G2-N	Replicate na	0.200	na		43	10.288	0.087	8.727	0.009	0.044	7.7%
		na		na								
		Replicate na		na								
		na		na								
		Replicate na		na								
		na		na								
		Replicate na		na								
Reag. Blk.1	OH vol 2.0	na		na		1	7.848					
Standard 1	0.1118 M NaOH	OH Wt. 2.000		na		2	12.525	2.108	8.698	0.2142	95.8%	OH % Recovery
08-01311MS	+ 2mL 0.1118 M NaOH	OH vol 2.0	0.100	na		44	12.102	2.720	8.905	0.2764	96.6%	MS

Slope **98.5%**
init.pH 7 check 7.025

verif. pH reading
start 7.018
end 6.998

Instrument Calibration

Buffer	VWR Lot #	CMS#	Expire Date
4	6350	275295	31-Dec-08
7	6325	275294	30-Nov-08
10	6303	275293	30-Nov-08

2-nd Verif	Fisher Lot #	CMS#	Expire Date
7	68198	275346	31-Mar-09

Performance checks using Balance # 360-01-06-037

Pipet #	Vol.	Wt.	Pipet #	Vol.	Wt.
92501	0.100	0.101	00545	0.0500	0.0494
		0.1002			0.0495
		0.0998			0.0492
		0.1001			0.0501
		0.0995			0.0503
Ave		0.1003	Ave		0.0497
Std. Dev.		0.0006	Std. Dev.		0.0005
% eror		0.61%	% eror		0.95%

OH ASR8113-rs-rev-0.xls
Worksheet: Data (3)

Battelle Pacific Northwest Laboratory
Radiochemical Processing Group-325 Building

ASR # and 8113
File: R:\vadchem\hydroxide\asr

WP# F99189
0

Procedure: Alkalinity of Aqueous Solutions, Leachates and Supernates

using a Brinkman 636 Auto Titrator Equip # WB76843

Titrant	Molarity	
HCl	0.1016	0

RPG #		Sample Vol. (mL)	2nd Equivalence Point Titrant Vol. (mL)	pH	Found millimoles base	Molarity base	millimole RPD	3rd Equivalence Point Titrant Vol. (mL)	pH	Found millimoles base	Molarity base	millimole RPD
08-01311	0	0.100	0.643	7.914	0.006	0.059		0.902	4.072	0.026	0.045	
08-01311-Dup	Replicat	0.200	1.359	7.723	0.015	0.077	26.2%	1.805	4.509	0.045	0.038	18.1%
08-01312	0	0.200	1.120	4.341	0.039	0.194						
08-01312-Dup	Replicat	0.200	1.116	4.680	0.039	0.197	1.3%					
08-01313	0	0.200	0.400	4.114	0.013	0.066						
08-01313-Dup	Replicat	0.200	0.403	4.161	0.013	0.066	0.0%					
08-01314	0	0.200	0.366	3.820	0.028	0.138						
08-01314-Dup	Replicat	0.200	0.371	3.796	0.029	0.144	4.3%					
							2-nd Recovered					
Standard 1		2.000	2.191	4.471	0.2226		99.6%					
						Total OH recovery						
08-01311MS		0.100	2.790	7.652	0.2835		96.7%	MS				

Matrix spike recovery is calculated as follows:

Spike = 2.00 mL 0.1023 N NaOH was added to the 0.100-mL of sample for each matrix spike.

SpikeTitrant vol. (sample @ .1mL + spike) - SampleTitrant vol. (average sample only equated to .1mL) * 0.2176 N (HCl titrant) = meq. OH

meq OH / 2.00 mL added = meq OH/mL found / 0.1023 N OH added * 100 = % recovered.

OH ASR8113-rs-rev-0.xls
Worksheet: Data (3)

Filename: 08-0

Report date:

Battelle, Pacific Northwest National Laboratory
PO Box 999, Richland, WA 99354 USA

Client: R. Shimskey
Project 52964, charge code F99189
ASR 8113, 19 Samples

Samples processed between April-May, 2008

RPG-CMC-128, Rev 0, HNO$_3$-HCl Acid Extraction of Liquids for Metals Analysis using a Dry-Block Heater
RPG-CMC-450 Rev 1, Gamma Energy Analysis (GEA) and Low-Energy Photon Spectroscopy (LEPS)
RPG-CMC-4001 Rev 1, Source Preparation for Gross Alpha and Gross Beta Analysis
RPG-CMC-408 Rev 2, Total Alpha and Beta Analysis
RPG-CMC-476 Rev 0, Strontium-90 Separation using Eichrom Strontium Resin
RPG-CMC-474 Rev 1, Measurement of Alpha and Beta Activity by Liquid Scintillation Spectrometry
RPG-CMC-4017 Rev 0, Analysis of Environmental Water Samples for Actinides and Strontium-90
RPG-CMC-496 Rev 0, Coprecipitation Mounting of Actinides for Alpha Spectroscopy
RPG-CMC-422 Rev 2, Solutions Analysis: Alpha Spectrometry
RPG-CMC-4014 Rev 1, Uranium by Kinetic Phosphorescence Analysis

M&TE:
Gamma detectors C,D,E,G, & K (gamma emitters)
Alpha spectrometry counting system (Pu-238, Pu-239+240 analysis)
Ludlum alpha counters (gross alpha)
LB4100 proportional counter (gross beta)
Perkin Elmer TriCarb model 3100 liquid scintillation spectrometer (Sr-90)
Chem Chek Instruments model KPA-11R uranium analyzer
See the M&TE summary sheet in the file for cross references to property numbers.

Reference date November 5, 2007 from TI-RPP-WTP-552
Reference date January 7, 2008 from TI-RPP-WTP-572

08-01290_Shimskey.xls
Worksheet: Cover Page

M.38

Battelle, Pacific Northwest National Laboratory
PO Box 999, Richland, WA 99354 USA

Filename: 08-0

Report date:

Sample:	Lab ID:
TI572-G2-A	08-01290
TI572-G2-D	08-01291
TI572-G2-I	08-01292
TI572-G2-J	08-01293
TI572-G2-O	08-01294
TI572-G2-P	08-01295
TI552-G6-Q	08-01296

Sample:	Lab ID:
TI572-G2-L1	08-01297
TI572-G2-L2	08-01298
TI572-G2-L3	08-01299
TI572-G2-L4	08-01300
TI572-G2-L5	08-01301
TI572-G2-Acid	08-01302
TI552-G6-Acid	08-01303
TI572-G2-6	08-01317
TI572-G2-9	08-01318
TI572-G2-12	08-01319
TI572-G2-15	08-01320
TI572-G2-18	08-01321

08-01290_Shimskey.xls
Worksheet: Cover Page

Battelle, Pacific Northwest National Laboratory
Richland, WA
Radiochemical Sciences and Engineering Group

filename   08-01290_Shimskey
5/20/2008

Client: R. Shimskey
ASR 8113

The Samples

These samples were delivered to the analytical lab in late March 2008. The samples required analysis of metals by ICPOES, hydroxide, anions, and several radionuclides. Only the radiochemistry data is reported here; the inorganic analytes are reported separately.

Sample Preparation

The aqueous samples were digested in dilute nitric acid (procedure RPG-CMC-128), and the digestions were used for all the subsequent radiochemistry. The solid samples were fused with potassium hydroxide (procedure PNL-ALO-115). The fusion solutions were used for radiochemical analysis.

Quality Control Results

All of the quality control results fell well within the limits prescribed by the project, with the exception of detection limits for some of the gamma emitters. The high Compton background from Cs-137 made it impossible to reach the detection limits requested for Eu-154 and Eu-155 on some of the samples. All of the blanks were negligible compared to the samples.

All pairs of duplicates agree closely, within two standard deviations in every case. All of the spike recoveries fell within the limits prescribed by the project, and within expected uncertainty.

Gamma Emitters (procedure RPG-CMC-450)

Gamma emitters were measured by counting 2-mL aliquots of the acid digestions and potassium hydroxide fusions. All gamma emitters that were detected were reported, except for potassium-40. Because no sample preparation or separation is done for gamma counting, no spikes are prepared.

The Compton background from the high Cs-137 in the solid samples made it impossible to reach the requested detection limit for Eu-155.

Gross Alpha and Gross Beta (procedures RPG-CMC-4001 and -408)

To measure gross alpha, a small volume of each sample solution (the acid digestion or fusion solution) was dried onto a steel disk and counted on a Ludlum solid scintillation alpha counter.

To measure gross beta, a small volume of each sample solution was evaporated onto a planchet and counted on a gas proportional counter . Nearly all the activity is beta, not alpha, and crosstalk corrections were not necessary. Solids loading on the counting planchets was too small to affect the data.

Battelle, Pacific Northwest National Laboratory
Richland, WA
Radiochemical Sciences and Engineering Group

filename   08-01290_Shimskey
5/20/2008

Client: R. Shimskey
ASR 8113

The aqueous samples have too little alpha to measure accurately by gross alpha counting. The sum of Pu-239+240, Pu-238, and Am-241 is a more accurate and sensitive estimate of the gross alpha activity of these samples. (Uranium contributes only a small part of the alpha activity.) The solid samples have enough alpha activity to measure by gross alpha count, but the uncertainty is high. Only a small amount of the fusion solution can be evaporated onto a counting disk without compromising the accuracy from mass loading.

The gross beta activity agrees reasonably well with the sum of Cs-137, Sr-90, and Y-90.

Strontium-90 (procedures RPG-CMC-476 and -474)

Strontium was chemically separated from the acid digestion preparations, then measured by liquid scintillation. Some of the aqueous samples have little Sr-90. The solid samples have very high Sr-90 activity.

Plutonium (procedures RPG-CMC-4017, -496, and -422)

Plutonium was separated from the sample solutions by anion exchange in hydrochloric acid, then mounted for alpha spectroscopy by coprecipitation, then measured using alpha spectrometry.

Uranium (procedures RPG-CMC-4017 and -4014)

Uranium was chemically separated from the samples by anion exchange in hydrochloric acid, then measured by kinetic phosphorescence. All of the samples have easily measurable uranium, well above the blanks.

Battelle, Pacific Northwest National Laboratory
Richland, WA
Radiochemical Sciences and Engineering Group

Client: R. Shimskey
ASR 8113

Procedures: RPG-CMC-450, Gamma counting

M&TE: Detectors C,D,E,G & K
Reference date November 5, 2007 from TI-RPP-WTP-552
Reference date January 7, 2008 from TI-RPP-WTP-572

filename   08-01290_Shimskey
5/20/2008

Measured Activity, **µci per mL** ± 1s counting error

Sample	Lab ID	Co-60	Cs-137	Eu-154	Eu-155	Am-241
TI572-G2-A	08-01290	< 4.E-5	**1.22E+1 ± 4%**	< 2.E-4	< 2.E-3	< 2.E-3
	08-01290DUP	< 4.E-5	**1.20E+1 ± 4%**	< 2.E-4	< 2.E-3	< 2.E-3
	RPD	--	2%	--	--	--
TI572-G2-D	08-01291	< 3.E-5	**8.46E+0 ± 4%**	< 1.E-4	< 2.E-3	< 2.E-3
TI572-G2-I	08-01292	< 2.E-5	**2.17E-1 ± 4%**	< 4.E-5	< 2.E-4	< 4.E-4
TI572-G2-J	08-01293	< 2.E-5	**1.42E+0 ± 3%**	< 8.E-5	< 7.E-4	< 1.E-3
TI572-G2-O	08-01294	< 2.E-5	**2.10E-1 ± 5%**	< 6.E-5	< 2.E-4	< 1.E-4
TI572-G2-P	08-01295	< 1.E-5	**3.56E-1 ± 4%**	< 4.E-5	< 3.E-4	< 5.E-4
TI552-G6-Q	08-01296	< 2.E-5	**7.41E-1 ± 3%**	< 6.E-5	< 5.E-4	< 1.E-3
TI572-G2-L1	08-01297	< 2.E-5	**7.90E-1 ± 3%**	< 5.E-5	< 5.E-4	< 8.E-4
TI572-G2-L2	08-01298	< 2.E-5	**2.45E-1 ± 3%**	< 4.E-5	< 3.E-4	< 9.E-4
TI572-G2-L3	08-01299	< 2.E-5	**3.96E-1 ± 5%**	< 6.E-5	< 3.E-4	< 2.E-4
TI572-G2-L4	08-01300	< 2.E-5	**3.63E-1 ± 3%**	< 5.E-5	< 3.E-4	< 7.E-4
TI572-G2-L5	08-01301	< 2.E-5	**5.61E-1 ± 4%**	< 5.E-5	< 4.E-4	< 7.E-4
TI572-G2-Acid	08-01302	**3.96E-4 ± 3%**	**1.01E-1 ± 3%**	**3.01E-4 ± 7%**	< 3.E-4	**1.10E-3 ± 26%**
TI552-G6-Acid	08-01303	< 3.E-5	**1.52E-1 ± 5%**	< 8.E-5	< 2.E-4	**8.13E-4 ± 8%**
Acid digestion blank		< 2.E-5	< 2.E-5	< 4.E-5	< 4.E-5	< 2.E-5
Requested detection limit		1.0E-2	1.0E-2	4.0E-4	4.0E-4	2.0E-3

08-01290_Shimskey.xls
Worksheet: Gamma

M.42

Battelle, Pacific Northwest National Laboratory
Richland, WA
Radiochemical Sciences and Engineering Group

filename 08-01290_Shimskey
5/20/2008

Measured Activity, **μci per g ± 1s counting error**

Sample	Lab ID	Co-60	Cs-137	Eu-154	Eu-155	Am-241
TI572-G2-6	08-1317	4.42E-3 ± 12%	6.41E+1 ± 6%	< 7.E-3	< 3.E-2	1.18E-1 ± 7%
	08-1317 Dup	< 2.E-3	6.16E+1 ± 6%	< 7.E-3	< 3.E-2	1.21E-1 ± 7%
	RPD	--	4%	--	--	3%
TI572-G2-9	08-1318	5.71E-3 ± 15%	4.79E+1 ± 4%	2.52E-2 ± 8%	< 4.E-2	1.71E-1 ± 14%
TI572-G2-12	08-1319	1.19E-1 ± 3%	1.30E+2 ± 4%	9.07E-2 ± 3%	< 6.E-2	5.40E-1 ± 11%
TI572-G2-15	08-1320	9.06E-3 ± 9%	8.78E+1 ± 3%	5.69E-2 ± 5%	< 5.E-2	4.14E-1 ± 9%
TI572-G2-18	08-1321	8.71E-3 ± 12%	1.14E+2 ± 3%	8.61E-2 ± 4%	< 7.E-2	4.92E-1 ± 7%
KOH fusion blank		< 2.E-3	1.47E-1 ± 6%	< 5.E-3	< 5.E-3	< 3.E-3
Requested detection limit		3.0E-2	6.0E-2	5.0E-3	8.0E-3	3.0E-3

08-01290_Shimskey.xls
Worksheet: Gamma

M.43

filename 08-01290_Shimskey
5/20/2008

Battelle, Pacific Northwest National Laboratory
Richland, WA
Radiochemical Sciences and Engineering Group

Client: R. Shimskey
ASR 8113
Reference date November 5, 2007 from TI-RPP-WTP-552
Reference date January 7, 2008 from TI-RPP-WTP-572

Sample	Lab ID	Measured Activity, µci per mL ± 1s total uncertainty					Total Uranium, µg/mL
		Gross Alpha	Gross Beta	Sr-90	Pu-239+240	Pu-238	
TI572-G2-A	08-01290	< 6.E-4	1.13E+1 ± 4%	9.48E-3 ± 2%	3.09E-5 ± 5%	2.04E-5 ± 7%	9.96E+1 ± 4%
	08-01290DUP	7.32E-4 ± 30%	1.15E+1 ± 4%	9.91E-3 ± 2%	3.40E-5 ± 4%	1.77E-5 ± 6%	1.01E+2 ± 4%
	RPD	--	2%	4%	9%	14%	2%
TI572-G2-D	08-01291	< 7.E-4	7.83E+0 ± 4%	4.03E-3 ± 2%	7.75E-6 ± 10%	< 1.E-6	7.33E+0 ± 4%
TI572-G2-I	08-01292	< 6.E-4	2.10E-1 ± 4%	2.62E-4 ± 5%	< 1.E-6	< 8.E-7	2.42E-1 ± 2%
TI572-G2-J	08-01293	< 7.E-4	1.27E+0 ± 4%	1.11E-3 ± 2%	6.07E-6 ± 15%	< 1.E-6	2.13E+0 ± 2%
TI572-G2-O	08-01294	< 7.E-4	1.81E-1 ± 3%	1.90E-4 ± 7%	< 3.E-6	< 3.E-6	2.12E-1 ± 2%
TI572-G2-P	08-01295	< 5.E-4	2.94E-1 ± 4%	2.32E-4 ± 4%	< 3.E-6	< 2.E-6	3.64E-1 ± 2%
TI552-G6-Q	08-01296	< 8.E-4	6.30E-1 ± 4%	1.09E-4 ± 11%	3.24E-4 ± 2%	4.87E-5 ± 5%	8.79E-1 ± 2%
TI572-G2-L1	08-01297	< 7.E-4	7.26E-1 ± 4%	6.12E-4 ± 3%	4.17E-4 ± 4%	9.14E-6 ± 20%	1.47E+0 ± 3%
TI572-G2-L2	08-01298	< 6.E-4	2.21E-1 ± 4%	8.89E-5 ± 13%	1.41E-4 ± 4%	2.05E-6 ± 32%	5.18E-1 ± 5%
TI572-G2-L3	08-01299	< 6.E-4	3.32E-1 ± 4%	1.29E-4 ± 9%	1.84E-4 ± 3%	3.45E-6 ± 23%	5.53E-1 ± 4%
TI572-G2-L4	08-01300	< 7.E-4	3.17E-1 ± 4%	1.19E-4 ± 10%	1.44E-4 ± 5%	4.45E-6 ± 24%	1.59E+0 ± 3%
TI572-G2-L5	08-01301	< 7.E-4	5.05E-1 ± 4%	2.38E-3 ± 2%	1.46E-4 ± 5%	5.97E-6 ± 22%	1.06E+0 ± 3%
TI572-G2-Acid	08-01302	4.01E-3 ± 11%	3.46E+0 ± 4%	1.51E+0 ± 2%	2.02E-3 ± 2%	1.99E-4 ± 5%	4.51E+1 ± 4%
TI552-G6-Acid	08-01303	1.78E-3 ± 17%	8.36E-1 ± 4%	3.80E-1 ± 2%	9.75E-4 ± 3%	3.89E-5 ± 14%	3.63E+1 ± 4%
Acid digestion blank		< 5.E-4	8.57E-3 ± 4%	< 3.E-5	< 7.E-7	< 7.E-7	5.05E-2 ± 4%
Requested detection limit		4.0E-3	1.0E-3	1.0E-3	1.0E-4	1.0E-4	6.0E+1
Lab blank		< 2.E-6	6.69E-7 ± 24%	< 2.E-6	< 3.E-8	< 3.E-8	2.15E-3 ± 4%
Reagent spike		99%	92%	96%	93%	--	94%
Matrix spike		100%	78%	95%	97%	--	[spike was too small]

08-01290_Shimskey.xls
Worksheet: AB, Pu, Sr, U

Page 7 of 8

M.44

Battelle, Pacific Northwest National Laboratory
Richland, WA
Radiochemical Sciences and Engineering Group

filename 08-01290_Shimskey
5/20/2008

Sample	Lab ID	Gross Alpha	Gross Beta	Sr-90	Pu-239+240	Pu-238	Total Uranium, µg/g
			Measured Activity, µci per g ± 1s total uncertainty				
TI572-G2-6	08-1317	2.74E-1 ± 21%	1.51E+2 ± 4%	5.74E+1 ± 2%	1.38E-1 ± 4%	< 4.E-3	
	08-1317 Dup	2.31E-1 ± 23%	1.38E+2 ± 4%	5.48E+1 ± 2%	1.30E-1 ± 3%	3.74E-3 ± 24%	
	RPD	17%	9%	5%	6%		
TI572-G2-9	08-1318	5.07E-1 ± 17%	2.18E+2 ± 4%	8.28E+1 ± 2%	2.01E-1 ± 3%	6.25E-3 ± 18%	
TI572-G2-12	08-1319	1.38E+0 ± 9%	7.23E+2 ± 4%	2.89E+2 ± 2%	6.96E-1 ± 3%	1.17E-2 ± 16%	
TI572-G2-15	08-1320	9.57E-1 ± 11%	5.06E+2 ± 4%	2.00E+2 ± 2%	4.83E-1 ± 3%	9.75E-3 ± 19%	
TI572-G2-18	08-1321	1.00E+0 ± 11%	6.27E+2 ± 4%	2.66E+2 ± 2%	6.59E-1 ± 3%	1.10E-2 ± 18%	
KOH fusion blank		<1.E-2	2.51E-1 ± 4%	6.52E-3 ± 5%	4.57E-4 ± 25%	9.76E-4 ± 15%	
Requested detection limit		1.0E-2	1.0E-2	1.0E-2	1.0E-3	1.0E-3	6.0E+1
Lab blank		<2.E-6	6.69E-7 ± 24%	<2.E-6	<3.E-8	<3.E-8	
Reagent spike		99%	92%	98%	92%	--	
Matrix spike		100%	78%	97%	92%	--	

Potassium hydroxide fusion sample preparations were used for the analyses on this page.

08-01290_Shimskey.xls
Worksheet: AB, Pu, Sr, U

M.45

Distribution

No. of
Copies

ONSITE

4	Bechtel National, Inc.	
	WTP R&T Docs (2)	H4-02
	P. S. Sundar	H4-02
	S. Barnes	H4-02
16	Pacific Northwest National Laboratory	
	EC Buck	P7-27
	RC Daniel	P7-22
	K. Draper	K6-75
	MK Edwards	P7-25
	SK Fiskum	P7-25
	RT Hallen	P8-60
	LK Jagoda	K6-24
	AE Kozelisky	P7-25
	DE Kurath	K3-52
	GJ Lumetta	P7-25
	RA Peterson	P7-22
	RW Shimskey	P7-27
	SI Sinkov	P7-25
	LA Snow	P7-25
	Information Release	P8-55
	Project File	K3-52